Detonations in H_2-N_2O-CH_4-NH_3-O_2-N_2 Mixtures

Raza Akbar, Michael Kaneshige, Eric Schultz, Joseph Shepherd

Graduate Aeronautical Laboratories
California Institute of Technology
Pasadena, CA 91125

Explosion Dynamics Laboratory Report FM97-3

July 24, 1997
Revised January 17, 2000

Prepared for Los Alamos National Laboratory under
Contract 929Q0015-3A, DOE W-7405-ENG-36

Abstract

This report describes experimental studies and analyses on the detonation properties of flammable gases that may be present in the waste storage tanks at Hanford, WA. These studies were carried out in the Explosion Dynamics Laboratory, part of the the Graduate Aeronautical Laboratories of the California Institute of Technology (GALCIT). Detonation cell sizes and pressures were measured in the GALCIT detonation tube facility for mixtures of hydrogen, ammonia, methane, nitrous oxide, oxygen and nitrogen. Measurements were made as a function of nitrogen and air dilution for stoichiometric mixtures of fuels and oxidizers and also specific retained gas compositions of tanks such as SY-101. Chemical kinetic modeling of these mixtures has been performed using the idealized ZND model. Existing reaction mechanisms and rate constant sets were benchmarked against shock tube data available in the literature. Correlations between reaction zone length and detonation cell width were developed that can be used to correlate and extrapolate the existing experimental data base.

Contents

Executive Summary

This report provides fundamental data and analyses needed to evaluate possible detonation hazards that may result from flammable gases within the waste storage tanks located at Hanford, WA. The emphasis is on the measurement and correlation of detonation cell widths. Cell-width information can be used through generally accepted correlations (Lee 1984) to predict more direct indicators of detonation hazards, such as critical-initiation energy or the critical-tube diameter for transmission of a detonation to an unconfined space. By measuring cell widths in some representative gas mixtures, a basis for one or more correlations is made. The cell-width data can be correlated to some other length scale, for instance the reaction-zone thickness, which can be computed directly.

Experiments have been performed in the GALCIT detonation tube for the following mixtures:

- Stoichiometric hydrogen and nitrous oxide diluted by nitrogen and air.
- Stoichiometric methane and oxygen diluted by nitrogen.
- Stoichiometric methane and nitrous oxide diluted by nitrogen and air.
- Stoichiometric ammonia and oxygen diluted by nitrogen.
- Stoichiometric ammonia and nitrous oxide diluted by nitrogen and air.
- Various model tank mixtures for tanks SY-101, AW-101, AN-105, AN-104, AN-103, and A-101 diluted by air.

Detonation velocities have also been measured and found in good agreement with equilibrium thermochemical calculations. Our measured cell widths agree with data from the literature where available, but most of the mixtures we have examined have not been studied before. The oxy-acetylene driver has been studied and found to be capable of providing 10-120 kJ of initiation energy in a repeatable fashion.

Reaction zone calculations have the advantage of being generally faster and cheaper than experiments and also of being capable of a larger range of conditions and mixtures. However, a number of difficulties prevent the calculations from being straightforward. The first problem is the lack of a comprehensive reaction mechanism for the most general mixtures. In an effort to find or create such a mechanism, we have collected several mechanisms from the literature, and a large amount of experimental data for validation.

The most successful mechanism for the model tank mixtures found so far is a modified version of the the mechanism of Miller and Bowman (1989), although it is not as successful at methane oxidation as the GRI-Mech 2.11 (Frenklach et al. 1995), which can not be used for ammonia oxidation. The mechanisms of Miller et al. (1983) and Miller and Bowman (1989) can be used for ammonia combustion but are not as useful for hydrocarbon combustion.

Two analysis tools are available for performing chemical kinetics calculations under constant-volume conditions or during steady, one-dimensional, compressible flow behind a shock. The constant-volume calculations are used for validation comparisons with shock tube induction time data, and the one-dimensional dynamical calculations are used to compute the reaction zone thickness in idealized planar detonation waves.

Using the experimental data mentioned above and reaction-zone thickness calculations performed with appropriate mechanisms, cell-width correlations have been created for several mixtures. For limited conditions involving fixed fuel-oxidizer stoichiometry, with variations in initial pressure or dilution, a power law correlation between cell size and reaction zone thickness appears to be very useful. A more general correlation applicable to various fuel-oxidizer systems is more elusive but currently under development.

1 Introduction

Detonation hazards are typically characterized by several detonability parameters (critical energy, critical tube diameter, minimum tube diameter) that can each be related to the detonation cell width (Lee 1984), which provides a convenient measurable length scale. The novel mixtures encountered in the Hanford waste tanks provide a challenge because cell-width data are scarce and the mixtures are sensitive to small changes in some variables (e.g. N_2O and O_2 concentrations). One approach to determining the detonability of the mixtures of interest is to measure cell widths under a range of possible conditions. Another, complementary approach, is to compute reaction zone thicknesses behind idealized detonation waves, derive a correlation between measured cell widths and these computed reaction zone thicknesses, and use the correlation to predict cell widths at untested conditions. Reaction zone calculations rely on detailed reaction rate mechanisms, so some effort is required to ensure that the calculations are meaningful. However, the empirical correlation to cell width masks some uncertainty in the reaction zone calculations. Following this combined approach, cell-width data of direct usefulness to hazard analysis are generated and a rational means of interpolating and extrapolating these data is developed.

2 Experiments

2.1 Apparatus and Procedure

The experimental apparatus used was the GALCIT Detonation Tube (Figs. 1, 2, and 3), first described in a previous report (Akbar and Shepherd 1996). The tube is constructed of three cast stainless steel (304) sections joined together by flanges and high-strength fasteners. The assembly is 7.3-m long and has a 280-mm inside diameter. A vacuum system is used to evacuate the tube to less than 50 mTorr before each test. A gas handling system can supply H_2, N_2O, N_2, NH_3, CH_4, O_2, Ar, and He from a cylinder farm located outside the building. Gas composition is controlled by the method of partial pressures using an electronic Heise 901a gauge, accurate to $\pm$ 0.18 kPa. Before a test, the test mixture is circulated through the tube volume with a bellows pump to ensure homogeneity.

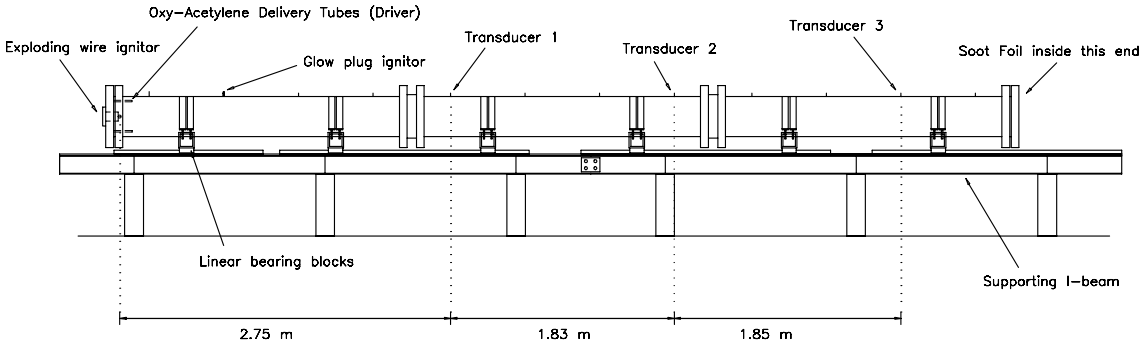

Figure 1: Elevation schematic of GALCIT Detonation Tube.

An oxy-acetylene driver is used to reliably initiate mixtures with a wide range of sensitivities. The driver gas is injected through a distribution manifold (4 tubes, 150-mm long) located at one end of the tube, and is a slightly lean mixture of acetylene and oxygen. Partial pressure of the driver gas is about 2 kPa, and can be controlled by varying the injection time. Initiation of the driver is achieved by a capacitor discharge through an exploding copper wire (30-mm long). A study has been carried out to measure the equivalent energy of the driver (see Appendix B). The results of this study allow control of the detonation wave strength, and a close approximation of the Chapman-Jouguet condition at the downstream end of the tube.

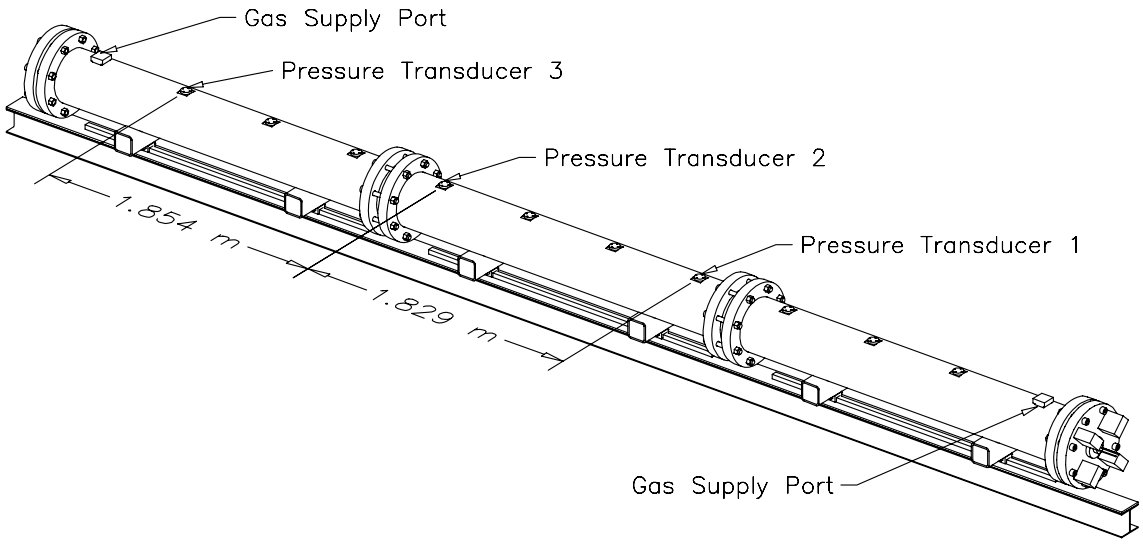

Figure 2: Oblique schematic of GALCIT Detonation Tube.

Table 1 summarizes the mixtures tested so far. For all mixtures except mixture 1, air was made from bottled O_2 and N_2. Tests with mixture 1 (H_2+N_2O+β(O_2+3.76N_2)) used atmospheric air. We use a simplified representation of air composition as O_2 + 3.76N_2; the complete specification of all compositions used in this study are given in Table 1. Note that the mixture numbers do not correspond to the mixture numbers in the previous report (Ross and Shepherd 1996). To simplify the presentation, N_2 and air are treated as diluents even though air is an effective oxidizer. The amount of diluent was specified in terms of the fraction (percentage) in the figures rather than in terms of the parameter β given in Table 1 and Appendix A. For the case of nitrogen dilution, the fraction of diluent is β/N where N is the total number of moles in the mixture formula in Table 1 and in the case of air, the fraction is $4.76\beta/N$.

Mixtures 2 to 11 represent simple mixtures of one fuel and one oxidizer that have been used to characterize the behavior of each substance individually. Mixtures 12 through 17 are best estimates of the retained gas composition in the waste tank as determined by recent tests at Hanford. A small percentage of the gas sample was not identified in those cases and was simply stated as "unknown." In those cases, we have increased the amount of N_2 to preserve the actual percentages of the other species. For instance, mixture 12 was originally specified with 2% unknown, so the original 33% N_2 was replaced with 35% N_2. In each series, as the dilution was increased, the initial pressure was increased such that predicted detonation pressures were just below the tube design limit, up to 1 atm initial pressure. The purpose of this strategy was to acquire as much data at 1 atm initial pressure (field conditions) as possible while deviating as little as possible when required by structural limitations. The largest cell sizes possible are about 50% to 100% of the tube diameter (280 mm). Only one test was carried out for each mixture type 3 and 4 and no cell data were obtained.

Detonation cell widths are measured by the soot foil technique. The cell width is determined by physical measurements of the spacing, transverse to the detonation propagation direction, between triple point tracks inscribed on soot foils placed within the detonation tube. The foils are 61 cm x 91.4 cm x 0.5 mm aluminum sheets, rolled into cylinders to conform to the detonation tube inner diameter. Soot is deposited on the inside surface of each foil by burning a kerosene-soaked cloth strip inside a closed vertical tube containing the foil. Each foil is normally sooted twice, in both vertical orientations, to cancel convection-induced gradients. The upstream edge of the foil is riveted to an aluminum ring (3-mm thick by 51-mm wide) to secure it as the detonation passes. The downstream end (adjacent to the end flange) is clamped at two points to the tube wall. The cell widths are measured on flattened foils, as the transverse distance between triple point tracks. Since this distance can vary significantly over a foil,

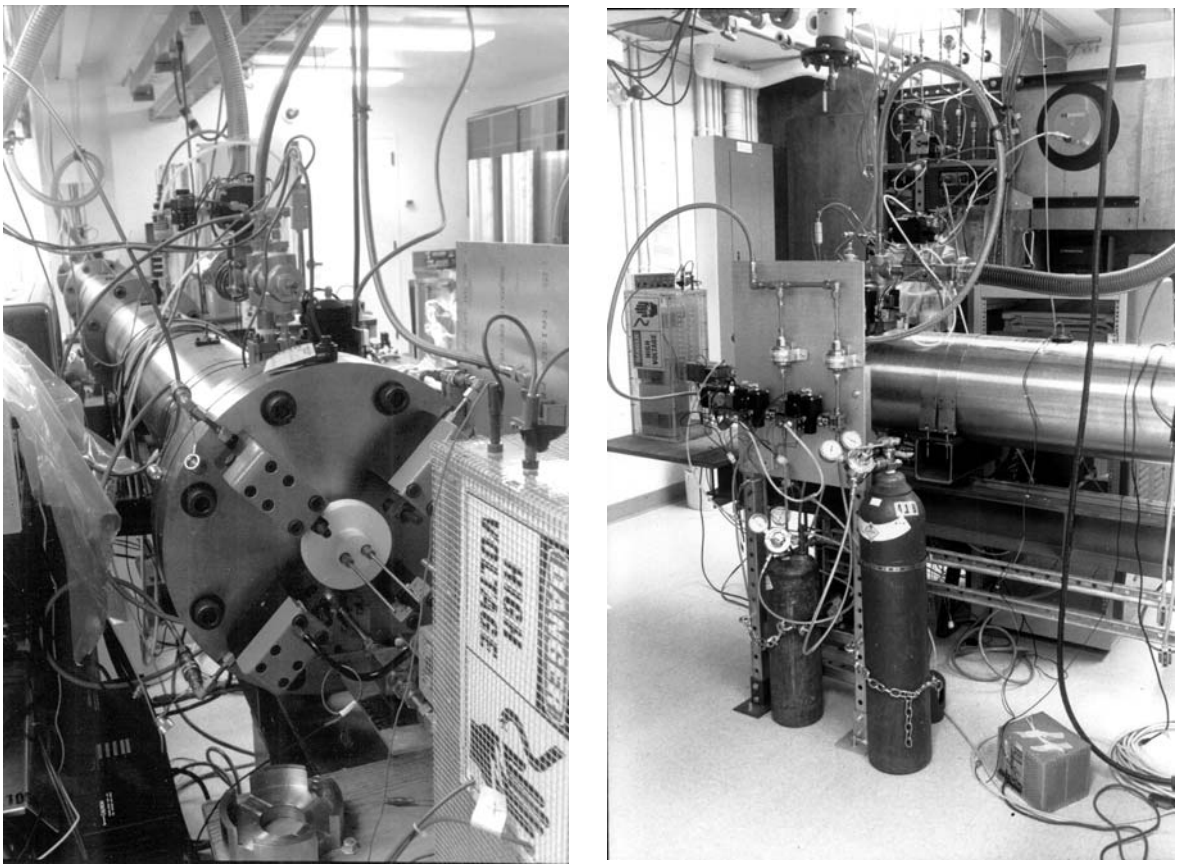

(a) (b)

Figure 3: GALCIT Detonation Tube facility. a) View along tube from driver end. b) Side view of driver end.

minimum and maximum values are reported. Note that for small cells (relative to the tube diameter), this is a unique measure of the cell width, but for cell widths on the order of the tube diameter, this measure may not be comparable to measurements in other facilities or by other techniques. In this case, the effect of the tube geometry on the cells should be considered. Currently, cell widths are measured manually. The inherent variation of cell size across the foil and the difficulty of identifying cell boundaries are significant sources of uncertainty and impose serious limitations on efforts to characterize and predict cell size. Typically, 10 cell-width measurements are made and representative minimum and maximum values are reported. In general, the uncertainty in cell-width measurements, reflected in the reported ranges, can be up to 50%.

2.2 Results

Appendix A summarizes the results of tests involving the mixtures listed in Table 1. The initial pressure listed for each shot includes the pressure added by the driver gas. Detonation initiation or failure of each shot is recorded under "Go". Chapman-Jouguet detonation speeds, as predicted by STANJAN (Reynolds 1986), are reported under D_{CJ} while the measured (average) wave speeds between pressure transducers 1 and 2, and 2 and 3 are reported under D_{1-2} and D_{2-3}, respectively. λ_{min} and λ_{max} represent the range of cell widths recorded by the soot foil technique for shots where cells were measurable. One conclusion to be reached from the data in Appendix A is that equilibrium predictions of detonation speed are quite

Table 1: Experimentally Studied Mixtures

Mixture	Composition	Initial Pressure	Note
1	H_2+N_2O+β(O_2 + 3.76N_2)	100 kPa	
2	H_2+N_2O+βN_2	100 kPa	
3	14H_2+14N_2O+71N_2+O_2	100 kPa	
4	H_2+4O_2	98 kPa	
5	CH_4+2O_2+βN_2	72-102 kPa	
6	CH_4+4N_2O+βN_2	57-102 kPa	
7	CH_4+4N_2O+β(O_2 + 3.76N_2)	86-97 kPa	
8	NH_3+0.75O_2+βN_2	66-91 kPa	
9	NH_3+1.5N_2O+βN_2	56-81 kPa	
10	NH_3+1.5N_2O+β(O_2 + 3.76N_2)	61-101 kPa	
11	42H_2+21NH_3+36N_2O+CH_4+β(O_2 + 3.76N_2)	76-101 kPa	SY-101[1]
12	29H_2+11NH_3+24N_2O+35N_2+CH_4+β(O_2 + 3.76N_2)	94-101 kPa	SY-101
13	31H_2+0.02NH_3+4.3N_2O+63.08N_2+1.6CH_4+β(O_2 + 3.76N_2)	101 kPa	AW-101
14	63H_2+0.02NH_3+11N_2O+25.28N_2+0.7CH_4+β(O_2 + 3.76N_2)	101 kPa	AN-105
15	47H_2+0.02NH_3+19N_2O+33.08N_2+0.9CH_4+β(O_2 + 3.76N_2)	101 kPa	AN-104
16	61H_2+0.05NH_3+3.8N_2O+35.14N_2+0.01CH_4+β(O_2 + 3.76N_2)	101 kPa	AN-103
17	75H_2+2.4NH_3+5.6N_2O+16.3N_2+0.7CH_4+β(O_2 + 3.76N_2)	101 kPa	A-101

[1]Mixture 26 from Ross and Shepherd (1996), see Appendix D

accurate. This relates to the performance of the driver (Section B) as well as the accuracy and relevance of equilibrium calculations. Of the shots with promptly initiated detonations, the apparent velocity between pressure transducers 1 and 2 was slightly above the CJ velocity (0.14% on average), and the apparent velocity between transducers 2 and 3 exhibited a slight velocity deficit (0.27% on average). The average drop in velocity was 7.92 m/s. Several photographic examples of soot foils are given in Appendix F and a number of pressure traces are provided in Appendix G.

Figures 4 through 11 show the cell-width measurements along with data from the literature. These data are also shown in different form in Section 3.3. Figure 4 shows cell-width measurements of H_2-N_2O-diluent mixtures from the present work and from a previous report (Akbar and Shepherd 1993). Cases with dilution by air and N_2 are presented together. Figure 5 shows cell-width measurements of CH_4-O_2-N_2 from the present work and a number of other publications (Moen et al. (1984), Manzhalei et al. (1974), Knystautas et al. (1984), Beeson et al. (1991)). Note that the data points around 0% N_2 have been artificially spread out so they are distinguishable, but they all represent the undiluted case. The data points at 71.5% N_2 also represent stoichiometric CH_4-air. As described in Section 2.1, higher initial pressures were generally used at higher dilutions, but some data points at low pressure (70 kPa) are shown for both low and high dilution. Figure 6 shows cell-width measurements of CH_4-N_2O-diluent mixtures from the present work only. No comparable data have been found in the published literature. Five of the tests shown in Fig. 6 used air dilution and the rest were with N_2 dilution. Within the range of dilution studied experimentally, little difference is seen between N_2 and air dilution. Again, data from a number of initial pressures are shown together.

Some data were available from unpublished sources for cell widths in stoichiometric NH_3-O_2 mixtures diluted by N_2 (Bennett 1986) and these data are shown along with some from the current work in Fig. 7. Figure 8 shows data for stoichiometric NH_3-N_2O mixtures diluted with N_2 and air. As seen in the CH_4-N_2O data (Fig. 6), little difference is apparent between N_2 and air dilution at the levels tested.

A large number of tests were performed with two versions of SY-101 model tank mixtures with variable air dilution, and these results are shown in Fig. 9. At the lower dilution levels, the initial pressure varied below 1 atm. These data are interesting for the slow increase (and slight decrease for mixture 12) of cell width with increasing air concentration at low dilution. A selection of air dilution

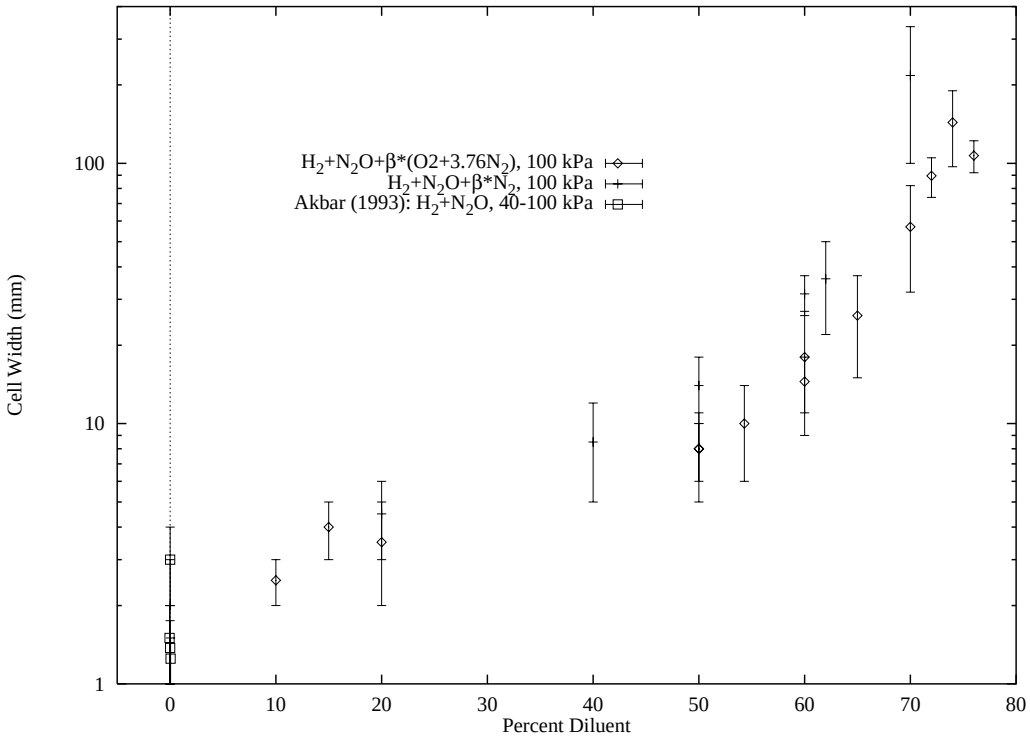

Figure 4: Cell width vs. percent dilution for stoichiometric H_2-N_2O-diluent mixtures.

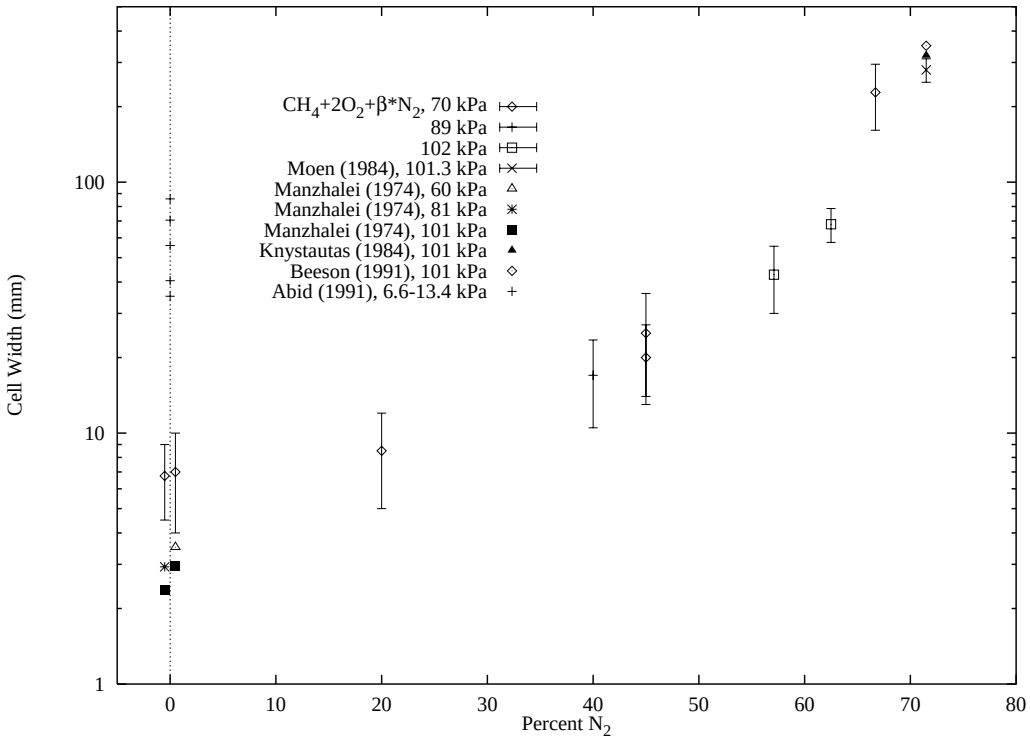

Figure 5: Cell width vs. percent N_2 for stoichiometric CH_4-O_2-N_2 mixtures.

cases were tested in other model tank mixtures, and these data are shown together in Fig. 10.

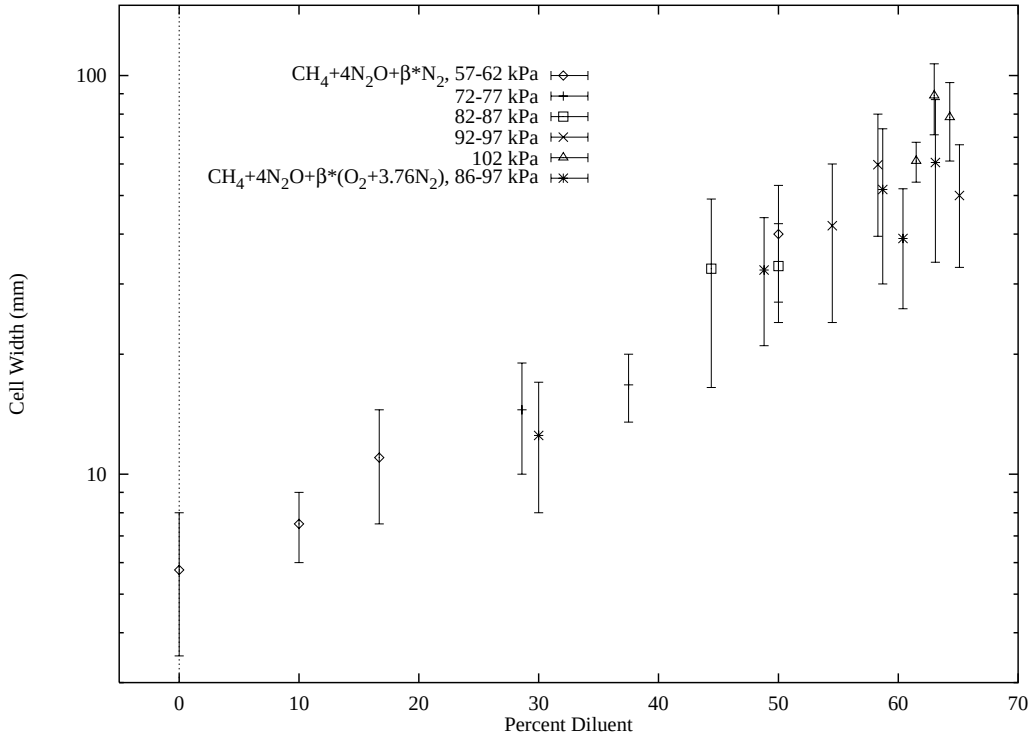

Figure 6: Cell width vs. percent dilution for stoichiometric CH_4-N_2O-diluent mixtures.

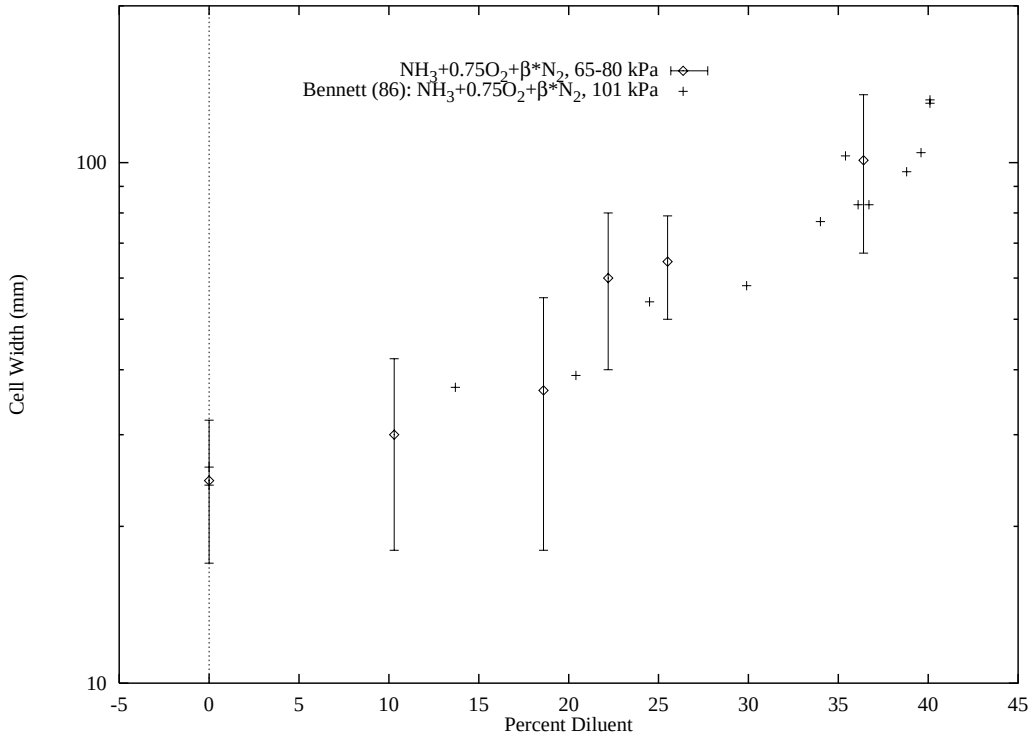

Figure 7: Cell width vs. percent dilution for stoichiometric NH_3-O_2-N_2 mixtures.

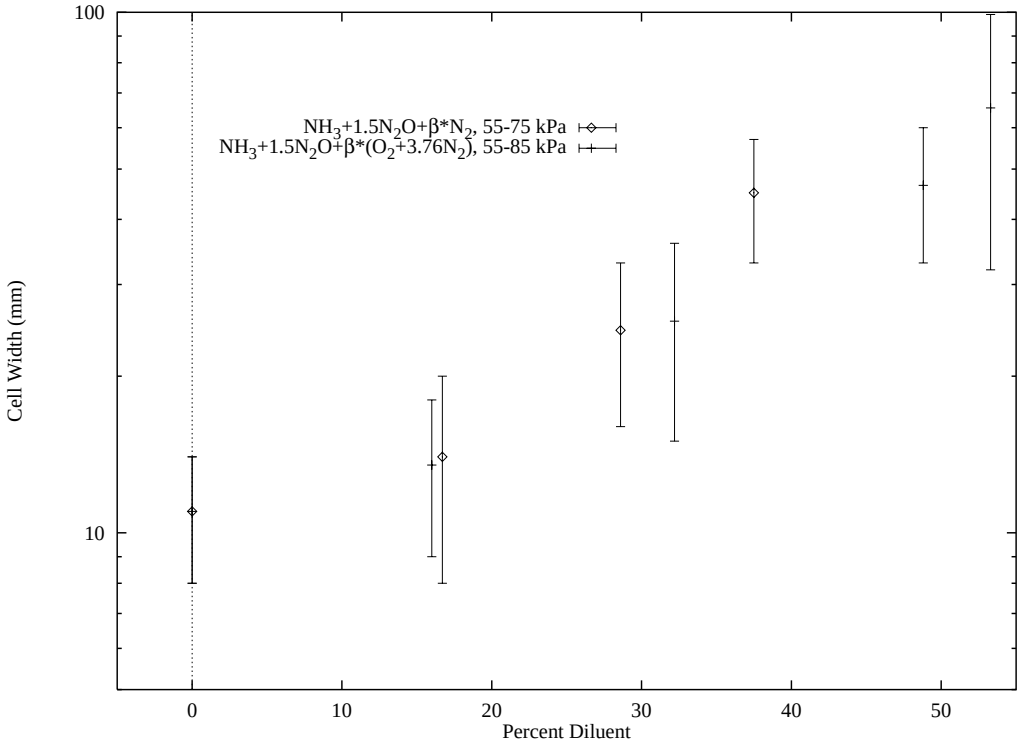

Figure 8: Cell width vs. percent dilution for stoichiometric NH_3-N_2O-Diluent mixtures.

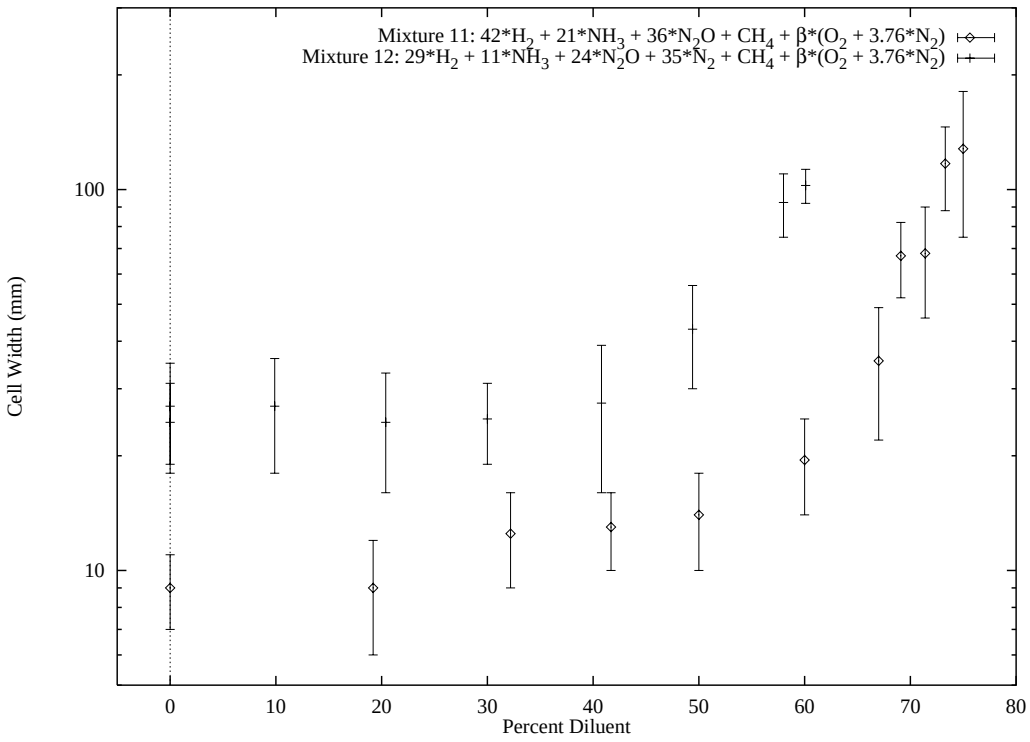

Figure 9: Cell width vs. percent air dilution for model SY-101 mixtures.

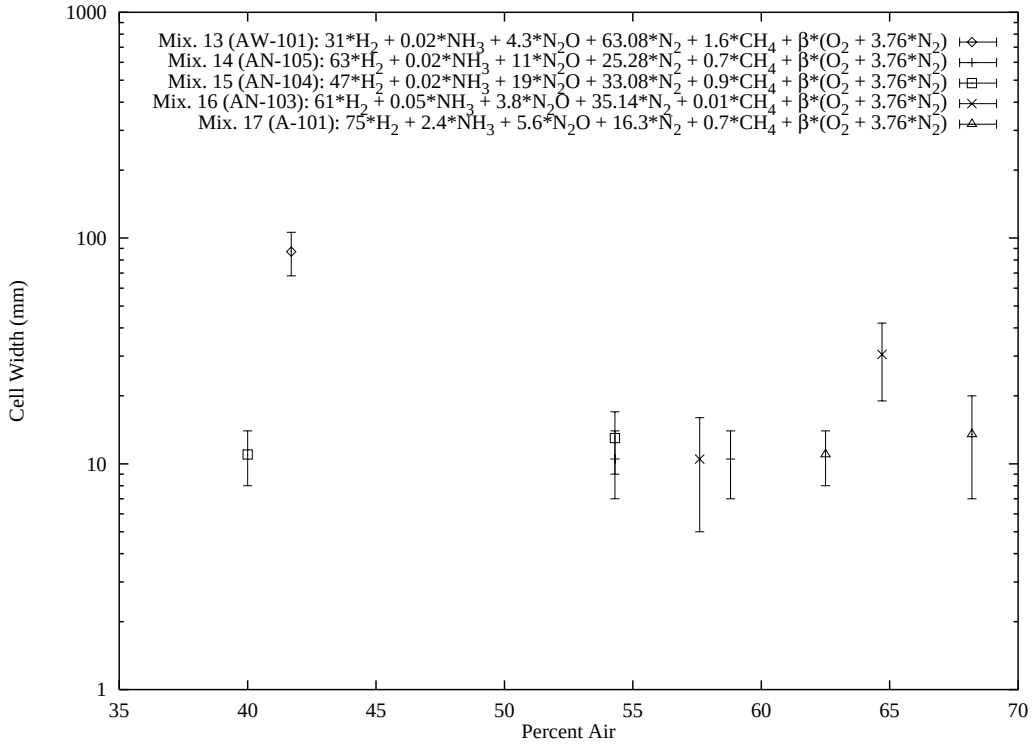

Figure 10: Cell width vs. percent air dilution for model tank mixtures.

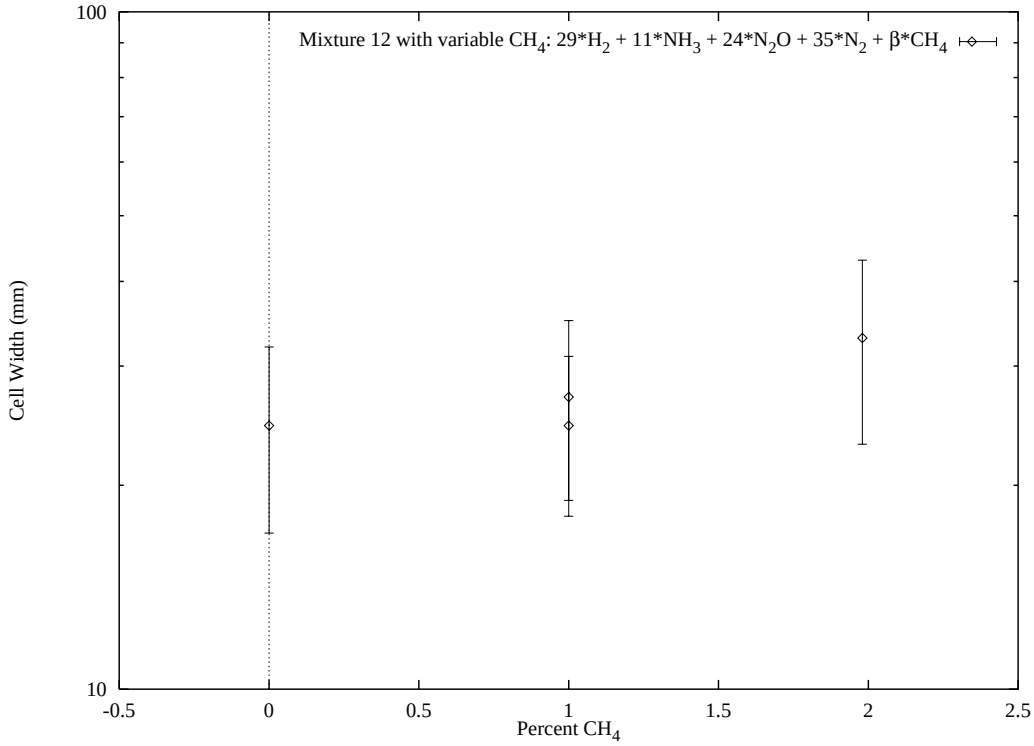

Figure 11: Cell width vs. percent CH_4 for mixture 12.

A notable feature of the model tank mixtures under study is the small concentrations of CH_4 present. In all experiments and calculations performed so far, the CH_4 has been included as specified. However, analysis of the mixtures would be greatly simplified if it were omitted, particularly for chemical kinetics calculations. The number of reactions to be considered could be dramatically reduced (79 reactions and 20 species vs 201 reactions and 45 species) for one standard mechanism. Possible strategies for omitting CH_4 from the study include ignoring it, replacing it with a comparable species, or developing some correction scheme based on modeling results. Considering this, a set of experiments with one of the model tank mixtures were performed (without air) with various CH_4 concentrations. These results are shown in Fig. 11 which shows a slight increase in cell width with methane concentration in the range of 0-2% CH_4.

Some of the model tank mixtures contain very small quantities of NH_3, which may be insignificant. However, since some mixtures do contain substantial concentrations of NH_3, any gains made by omitting it would be limited.

2.3 Summary of Experimental Data

Experimental data have been obtained on detonations for mixtures that have not been previously studied. For convenience, we summarize these data in Table 2. The diluent amount required to reach a cell width of 100 mm has been estimated by interpolating or extrapolating the experimental data.

Table 2: Summary of measured cell width data (initial pressure of 100 kPa).

Mixture	Diluent	(%)	λ (mm)
$H_2 + 1/2O_2$	-	0	1.3-2.0
	N_2	55	10-15
H_2+N_2O	-	0	1.5
	N_2	62	36
	air	65	26
CH_4+2O_2	-	0	3
	N_2	72	300
CH_4+4N_2O	-	0	3(*)
	N_2	64	80
	air	60	50
$NH_3+ 3/4O_2$	-	0	16-25
	N_2	35	100
$NH_3+ 3/2N_2O$	-	0	6(*)
	N_2	38	34(*)
	air	53	64(*)

(*) Extrapolated from lower pressure.

Comparison of results without dilution show that cell widths for H_2 and CH_4 are slightly smaller with O_2 as the oxidizer than with N_2O. The situation is reversed in NH_3, which has a smaller cell width (24 mm vs 40 mm) with N_2O as an oxidizer than with O_2.

All of the mixtures with the exception of the model SY-101 composition demonstrate increasing cell widths with increasing diluent concentration. The SY-101 mixtures show a constant or slightly decreasing cell width with increasing air concentration up to about 40% dilution, then the cell width rises sharply with increasing dilution. This is a consequence of these mixtures being fuel rich.

Air dilution results in slightly smaller cell widths than N_2 dilution for both H_2 and CH_4 mixtures. This effect is not discernible in the NH_3–N_2O data. The amount of diluent required to obtain a cell width of 100 mm is about 60 to 70% in all cases except for the NH_3-O_2 mixture which only requires

about 35% N_2. The ammonia mixture has substantially (one order-of-magnitude) larger cell widths than either the H_2 or CH_4 mixtures. Using N_2O instead of O_2 results in substantially smaller cell widths for NH_3, suggesting a direct channel of reaction that is not present in either H_2 or CH_4.

The original SY-101 mixture has a cell width of 100 mm at a dilution of about 75% air, however the revised composition only requires 60% dilution to reach a the same cell width.

3 Chemical Reaction Kinetics

Many parameters of interest for detonation and high pressure combustion (cell width, critical energy, etc.) can be measured experimentally. For the sake of detonation hazard analysis, cell width is the most convenient characteristic parameter, because it is easy to measure and can be related to the other dynamic parameters (Lee 1984). A limited predictive capability can be obtained by using computations based on detailed chemical reaction mechanisms to extrapolate and interpolate experimental data. In the context of the present study, we have explored the potential for using existing mechanisms for this purpose. The first task before using the reaction mechanisms is to benchmark the performance of these mechanisms and rate constant sets against standard shock-tube induction time measurements available in the literature.

Predicting cell size from chemical kinetics calculations is based on the concept of the finite reaction-zone thickness of a detonation wave. Historically, the relationship between reaction zone thickness and cell size has often been taken to be a simple linear proportionality (Westbrook and Urtiew 1983), although this is valid only within limited ranges of conditions. An empirically based extension of this theory suggests that the ratio of cell size to reaction zone thickness is a function of equivalence ratio (Shepherd 1986). While this theory is more successful at describing observed trends, it is still limited to specific mixtures and conditions, and does not address the functional form of the relationship.

Two steps are critical in developing reliable predictions of cell size from chemical kinetics calculations: 1) developing a validated reaction mechanism for the compositions of interest, and 2) correlating the computed reaction zone lengths to the cell size. Our validation testing is described in Section 3.1 and the correlations are presented in Sections 3.2 and 3.3.

For this report, two classes of chemical kinetics calculations were performed: constant volume explosion, and one-dimensional steady flow. In addition, purely equilibrium calculations were performed with a thermochemical solver (STANJAN, Reynolds (1986)). Numerically, the kinetics calculations consist of integrating forward in time the appropriate ordinary differential equations. The initial conditions were obtained by using STANJAN to solve the frozen shock jump conditions.

Reaction rate and property calculations were performed with the Sandia gas phase chemical kinetics subroutine library (Kee et al. 1989). The primary limitation on the accuracy of these calculations is the reaction mechanism and rate constants. We tested several different published mechanisms as part of our study. Thermodynamic data for all kinetics calculations were taken from the thermodynamic database distributed with the Sandia chemical kinetics package. The thermodynamic database distributed with the GRI mechanism (Frenklach et al. 1995) was not used except where data were not available in the Sandia database.

Modeling of finite-rate chemical reactions is a standard practice, but compiling a list of the relevant elementary reactions and corresponding rate parameters is still a challenge for novel mixtures. Much published work in this area is aimed at finding the most important elementary reactions and parameters to allow stripped down or *reduced* (and therefore computationally faster) mechanisms to yield accurate solutions. This is generally successful only for simple reactions and within limited ranges of conditions. Since our mixtures of interest involve many reactants, we are focusing on comprehensive, rather than fast, mechanisms. The mechanisms listed in Appendix E have been selected to be as comprehensive as possible. For calculations that do not use some of the reactions in these mechanisms, the unnecessary reactions can be removed to reduce solution time.

Furthermore, while there are mechanisms available containing all the elementary reactions we need, they are tuned for conditions quite different from ours. Namely, atmospheric flame modeling is more common than detonation modeling, and hydrocarbon combustion in air is far more studied than oxidation of NH_3 or by N_2O.

The reactions of interest in this study involve the oxidation of H_2, CH_4, and NH_3 by N_2O and air. The chemistry of the individual fuel-oxidizer combinations have been studied and reported in some detail in the literature, but few studies are available with combinations of these fuels and oxidizers. The number of relevant studies is further reduced by the limited conditions considered in each. Generally, mechanisms can be built and expanded from the simpler and better understood reactions to the more complicated systems of interest. However, an assembly of simpler mechanisms may omit reactions that are not important in the constituent mechanisms but that become important in the mixture. Also, some reactions may proceed through various sequences of elementary reactions, and the importance of each path may vary with the addition of other reactants. A mechanism that successfully models a simple mixture while ignoring certain routes will perform poorly when those routes become important.

3.1 Validation of Reaction Mechanisms

Currently, no known published mechanism is capable of accurately modeling mixtures containing all of the chemical species of interest to this study. Computational requirements and limitations cause most mechanisms to be designed for a particular application, and they are of uncertain value under off-design conditions. To evaluate the usefulness of the collected mechanisms under a variety of conditions, simulations using the mechanisms have been compared to experimental data from the literature. Data suitable for comparison with chemical kinetics computational results include shock tube induction times, flame induction distances, stirred reactor induction times, and flame species concentration profiles. To simplify the analysis, and because a large portion of the available data is in the form of shock tube induction time, we concentrated on comparisons with induction time measurements. For the sake of numerical analysis, the chemical reactions behind both incident and reflected shocks are modeled as constant-volume processes. This is a good approximation in most cases since the shocked mixtures are typically highly diluted with Argon and there is relatively weak coupling between the chemical reactions and the fluid motion.

In general, induction times are straightfoward to measure and there are abundant data in the published literature. However, there are a number of difficulties that we encountered:

1. Induction time can be defined in a number of different ways for the purposes of both experimental measurement and numerical modeling (see Section 3.1.1).

2. Data from different reactant concentrations are sometimes presented together without individual identification, making proper modeling difficult.

3. Most validated reaction mechanisms are most accurate at lower pressures and higher temperatures than those encountered in detonations (within the induction zone).

4. Each validation data set or each set of reaction rate parameters is useful for limited ranges of temperature, pressure, and species concentrations.

5. Many investigators plot induction time data in such a way as to remove the pressure dependence (i.e. τ[X]), and then plot data for a variety of pressures together. This makes it difficult to precisely compare experimental and computational results.

In Sections 3.1.3 to 3.1.9 below, a brief review of the validation effort is given for each simple fuel-oxidizer mixture. In some instances, different dilutions are examined separately. Each section consists of a list of references containing reaction mechanism or induction time data, discussion of these references, a description of the results of the validation study, and recommendations of appropriate conditions for

use of the studied mechanisms. These recommendations are summarized in Table 11 and supporting figures are provided in Appendix C. These reviews are not exhaustive.

The thermodynamic condition within a fuel-air detonation typically varies from 1500 K and 40 atm (von Neumann state) to 3000 K and 20 atm (Chapman-Jouguet state). Since the conditions within the induction zone are approximately the von Neumann condition and primarily determine the length of the reaction zone, accurate modeling of this condition is most important.

3.1.1 Experimental Data

Many experimental studies of reactions behind reflected shocks in shock tubes have been performed. In these experiments, the region near the shock-tube end wall is monitored, usually by pressure transducers or spectroscopically, and one or more thermodynamic or species variables is measured over time. The definition of induction time varies considerably throughout the literature, but most of the data are comparable. An advantage of shock-tube induction time data for validation of detonation chemistry mechanisms (over flame or flow reactor data) is that the postshock conditions more closely resemble the conditions within a detonation. Many shock tube studies obtain typical detonation temperatures (1500 - von Neumann, 3000 - Chapman-Jouguet), but pressures above 5 atm are rare. High argon dilution is frequently used to increase induction times, but unfortunately nitrogen dilution is uncommon.

Induction Time Definitions The concept of induction time presupposes that the shocked-heated reactants will have a well-defined period of nearly isothermal reaction followed by a very rapid exothermal event (explosion). The end of the induction period is typically marked by a very sharp increase in pressure, temperature, and product species. This supposition is reasonable for most cases because almost all combustion reactions initially consist of thermally-neutral, chain-branching processes that create the intermediate and radical species that ultimately combine to form products. Under some conditions, for instance at very high or very low temperature, an induction time does not exist. At low temperature, it may be effectively infinite. At high temperature, the equilibrium state may not contain significant quantities of product, but rather may be largely dissociated. At some intermediate conditions, the induction time may be weakly defined, because the transition from reactants to products may be smooth and continuous.

Supposing that an induction time can be used to characterize a combustion event, the question arises of exactly how to define it. The definition is unimportant if all variables (temperature, pressure, reactant, product, and species concentrations) change rapidly at the same time. This is not always the case for the mixtures of interest to the present study. We generally use the definition that the end of the induction zone is the point where the rate of increase of temperature is maximum. This is convenient because it does not involve arbitrary reactant consumption fractions (for instance when 50% of reactant A is consumed), and it coincides with the point of maximum heat release. Table 3 gives a list of measures used in the literature to indicate the end of the induction zone.

3.1.2 Numerical Technique

The numerical model used to simulate the shock tube data is an adiabatic, constant-volume process with finite rate chemical kinetics. The initial conditions are the pre-shock chemical concentrations and the post-shock thermal conditions. This model isolates the chemical kinetics from fluid dynamical considerations. The appropriateness of the constant volume approximation is limited to reflected shock experiments and compositions with small heat release (effectively high dilution). Another limitation of the constant-volume analysis is that the fluid between the reflected shock and the endwall can be nonuniform due to shock-wave boundary layer interaction (Bradley 1962). Neither of these effects are considered in the present study.

Some published mechanisms specify pressure fall-off relations that are not standard within the Sandia package (Kee et al. 1989). In some cases, the published relation is found to be a special case of a Sandia

Table 3: Induction time definitions used in the literature

Asaba et al. (1963)	Sudden end wall pressure rise.
Bhaskaran et al. (1973)	Large increase in optical emission (photomultiplier) and end wall pressure.
Blumenthal et al. (1996)	Multiple induction time definitions were used, and two events were sometimes observed: an initial small change ("first kernel") followed by a more rapid change (DDT). The "first kernel" was variably measured by detection of a density gradient (shadowgraph), sudden OH emission, or a slight pressure rise. A sudden pressure jump defined the DDT. In cases where no detonation occurred, a first kernel was reported by the shadowgraph technique.
Borisov et al. (1977) and Borisov et al. (1978)	In "static experiments", induction time was defined as the delay between stopping the flow and the observation of a sharp pressure increase. In shock tube experiments, absorption spectroscopy of N_2O at 253.6 nm was used to detect a sudden decrease in N_2O concentration.
Bradley et al. (1968)	Appearance of OH by absorption at 306.7 nm and NH_3 emission at 3000 nm.
Burcat et al. (1971)	Sudden level or slope change in pressure and heat flux.
Cheng and Oppenheim (1984)	Extrapolated from reflected wave trajectories (pressure increase).
Craig (1966)	Sudden pressure rise.
Drummond (1969)	Maximum OH absorption at 307 nm and end wall pressure rise.
Drummond (1972b)	Absorption by OH at 307 nm, NH_2 at 570 nm, and NH at 336 nm.
Hidaka et al. (1985b)	t_m was defined by the point of maximum OH emission intensity at 305.5 nm.
Hidaka et al. (1985a)	t_{20}, t_{50}, and t_{80} are times to 20, 50, and 80 percent consumption of N_2O measured by infrared emission at 4.68 μm. τ indicates a rapid decrease in N_2O concentration.
Miyama and Endoh (1967a)	Appearance of nitric oxide emission at 430.5 nm.
Miyama and Endoh (1967b)	Variation of NH_3 absorption at 224.5 nm.
Miyama (1968b)	Variation of NH_3 absorption at 224.5, 230, and 240 nm.
Miyama (1968a)	Variation in nitric oxide emission at 430.5 nm.
Pamidimukkala and Skinner (1982)	Induction time was defined at maximum O concentration by atomic resonance absorption spectroscopy. Another time was reported as the point where the reaction was 65% complete, by an unknown method.
Petersen et al. (1996)	Time of maximum rate of OH formation as indicated by absorption spectroscopy.
Seery and Bowman (1970)	Most rapid increase in pressure, OH absorption, and emission of OH (306.7 nm), CH (431.5 nm), CO (220.0 nm) and C_2 (516.5 nm).
Skinner and Ringrose (1966)	Time of maximum OH emission.
Soloukhin (1971)	Interferograms, emission of N_2O at 4.5 μ, and of OH at around 300 nm were interpreted to derive induction times.
Takeyama and Miyama (1967)	Variation in NH_3 absorption at 224.5 nm.
Takeyama and Miyama (1965)	Variation in OH emission.

relation, but in others, an approximation is the best that can be achieved. In the Sandia package, the rate constant for a reaction that includes fall-off effects is given by a function that blends a low pressure

limit to a high pressure limit:

$$k = k_\infty \left(\frac{P_r}{1 + P_r} \right) F$$

where

$$P_r = \frac{k_0[M]}{k_\infty}$$

The Lindemann form results when F is unity, and the code then requires 6 rate parameters - three for the low pressure limit and three for the high pressure limit. In the Troe form, F is a function of P_r and F_{cent}, where

$$F_{cent} = (1 - a) \exp\left(-\frac{T}{T^{***}} \right) + a \exp\left(-\frac{T}{T^{*}} \right) + \exp\left(-\frac{T^{**}}{T} \right)$$

and the code then uses the four additional parameters a, T^{***}, T^{*}, and T^{**}, where T^{**} is optional. In the SRI form, F is a function of P_r and 5 additional parameters:

$$F = \left[a \exp\left(\frac{-b}{T} \right) + \exp\left(\frac{-T}{c} \right) \right]^X dT^e$$

$$X = \frac{1}{1 + \log^2 P_r}$$

Where fall-off relations are specified in a published mechanism but are not standard relations in the Sandia code, approximations have been made (see Appendix E).

3.1.3 H_2 - O_2 - N_2 (- Ar)

Table 4: H_2 - O_2 - N_2 (- Ar) References

Reaction Mechanism	Experimental Data
Allen et al. (1995), Baulch et al. (1992), Baulch et al. (1994a), Baulch et al. (1994b), Cobos et al. (1985), Dean et al. (1978) (with CO), Frank and Just (1985), Miller and Bowman (1989), Frenklach and Bornside (1984), Frenklach et al. (1995), Frenklach et al. (1992), Zuev and Starikovskii (1992)	Blumenthal et al. (1996), Bollinger (1964), Bollinger et al. (1961), Cheng and Oppenheim (1984), Craig (1966), Dean et al. (1978), Frank and Just (1985), Petersen et al. (1996), Schott and Kinsey (1958), Skinner and Ringrose (1966), White and Moore (1965)

Reaction Mechanisms Mechanisms from four of the references listed above have been compared to the available shock tube data: Allen et al. (1995), Baulch et al. (1994a), Miller and Bowman (1989), and Frenklach et al. (1995). These were selected for evaluation because they are more comprehensive than the others. Baulch et al. (1994a) is a supplement to and includes all the data of Baulch et al. (1992), and is apparently identical to Baulch et al. (1994b). Cobos et al. (1985) contains some fall-off data. Dean et al. (1978) gives data on some important O_2 reactions involving H_2 and CO. Frank and Just (1985) provides a reduced mechanism for H_2-O_2-N_2O reactions. Frenklach and Bornside (1984) and Frenklach et al. (1992) seem to be forerunners of Frenklach et al. (1995) and do not include nitrogen. Zuev and Starikovskii (1992) contains a mechanism for H_2-N_2O reactions. The modified form of the Miller and Bowman (1989) mechanism (see Section 3.1.7) was also evaluated.

Induction Time Data Data from Craig (1966), Petersen et al. (1996), and Skinner and Ringrose (1966) were used to evaluate H_2-O_2-Ar data (high dilution). Data from Blumenthal et al. (1996), and Bhaskaran et al. (1973) were used to evaluate H_2-air data. Of the Blumenthal et al. (1996) data, only "first kernel" data was considered appropriate, and DDT times were discarded for the purpose of validation.

Induction distance data in Bollinger (1964) and Bollinger et al. (1961) are less directly useful. Cheng and Oppenheim (1984), Schott and Kinsey (1958), and White and Moore (1965) have good induction time data but were omitted because they were largely redundant. Frank and Just (1985) contains time history data but no tabulated induction times.

Results Results of H_2 - O_2 - Ar constant volume simulations using the Allen et al. (1995), Baulch et al. (1994a), Frenklach et al. (1995) (GRI), Miller and Bowman (1989), and modified Miller and Bowman (1989) mechanisms, and data from Petersen et al. (1996) and Skinner and Ringrose (1966) are shown in Figs. 18, 19, 20, 21, and 22. Results of H_2 - air constant volume simulations using the same mechanisms and, data from Bhaskaran et al. (1973) and Blumenthal et al. (1996) are shown in Figs. 23, 24, 25, 27, and 26. Reasonable comparison is achieved in all cases, although the H_2-air data exhibit quite a bit of scatter.

Recommendations

H_2-O_2-Ar The temperature and pressure range of the validation study was 870-2000 K and 1-87 atm. The equivalence ratio was always near unity and the dilution was 90-97%. The Miller and Bowman (1989) mechanism performed marginally better than the others.

H_2-Air The temperature and pressure range of the validation study was 950-1330 K and 2.5-15.0 atm. The concentration of H_2 in air was 15% and 30%. The Baulch et al. (1994a) mechanism matched the data best overall. More data are needed to support the existing data and extend the validation to higher pressures and temperatures.

3.1.4 H_2 - N_2O (- Ar)

Table 5: H_2 - N_2O (- Ar) References

Reaction Mechanism	Experimental Data
Allen et al. (1995), Balakhnine et al. (1977), Borisov et al. (1978), Dean et al. (1978) (with CO), Drummond (1972a), Frank and Just (1985), Frenklach et al. (1995), Hidaka et al. (1985a), Miller et al. (1983), Miller and Bowman (1989), Pamidimukkala and Skinner (1982), Sausa et al. (1993), Zuev and Starikovskii (1992)	Allen et al. (1995), Balakhnine et al. (1977), Bollinger et al. (1962), Borisov et al. (1978), Dean et al. (1978), Frank and Just (1985), Hidaka et al. (1985a), Hidaka et al. (1985b), Pamidimukkala and Skinner (1982), Soloukhin (1973)

Reaction Mechanisms All of the primary mechanisms used to model H_2-O_2-N_2 are useful for oxidation by N_2O also except Baulch et al. (1994a). Balakhnine et al. (1977) contains rate constants for a few N_2O reactions. The reaction mechanism in Borisov et al. (1978) is strictly H_2-N_2O. Dean et al. (1978) provides rate constants for some important N_2O reactions (see Section 3.1.3). Drummond (1972a) reports rate constants for some N_2O reactions, among others, from other sources. Frank and Just (1985), Hidaka et al. (1985a), and Pamidimukkala and Skinner (1982) contain mechanisms for H_2-O_2-N_2O reactions. Sausa et al. (1993) contains a mechanism for low pressure H_2-N_2O-Ar flames that includes N_2 and O_2. Zuev and Starikovskii (1992) contains a mechanism for high temperature H_2-N_2O combustion.

Induction Time Data Data in Borisov et al. (1978), Hidaka et al. (1985a), Hidaka et al. (1985b), and Pamidimukkala and Skinner (1982), are accessible. Some of the Borisov et al. (1978) data are not shock tube data, but the shock tube data matches the other data. Soloukhin (1973) presents induction time data combined with molar concentrations, but does not provide enough information to reconstruct the mixtures. Allen et al. (1995), Balakhnine et al. (1977), and Frank and Just (1985) contain time history data but no tabulated induction time data. Bollinger et al. (1962) contains induction distance data. Dean et al. (1978) contains induction time data for diluted mixtures of H_2-N_2O-CO.

Results Results of H_2 - N_2O - Ar simulations using the Allen et al. (1995), Frenklach et al. (1995), Miller and Bowman (1989), and modified Miller and Bowman (1989) mechanisms with comparisons to data from Hidaka et al. (1985a), Hidaka et al. (1985b), and Pamidimukkala and Skinner (1982) are shown in Figs. 28, 29, 30, and 31. All these mechanisms generate comparably decent results, except above about 2200 K. The divergence in this region may be a result of limited precision calculations.

Recommendations The temperature and pressure range of the validation study was 1430-2860 K and 1.5-3.0 atm. The reactants were approximately stoichiometric with high and very high dilution (97-99.98%). More data are needed at higher pressures and temperatures, with lower dilution, and with different dilution (i.e. N_2).

3.1.5 CH_4 - O_2 - N_2 (- Ar)

Table 6: CH_4 - O_2 - N_2 (- Ar) References

Reaction Mechanism	Experimental Data
Baulch et al. (1992), Baulch et al. (1994a), Baulch et al. (1994b), Frenklach and Bornside (1984), Frenklach et al. (1995), Frenklach et al. (1992), Hidaka et al. (1996), Hunter et al. (1994), Miller and Bowman (1989), Seery and Bowman (1970), Starikovskii (1994), Starikovskii (1995)	Asaba et al. (1963), Bollinger et al. (1961), Burcat et al. (1996), Burcat et al. (1971), Cheng and Oppenheim (1984), Frenklach and Bornside (1984), Frenklach et al. (1992), Miyama and Takeyama (1965), Seery and Bowman (1970), Spadaccini and Colket III (1994)

Reaction Mechanisms Baulch et al. (1994a) (see Section 3.1.3), Frenklach et al. (1995), and Miller and Bowman (1989) mechanisms contain appropriate hydrocarbon species to be applied to CH_4-O_2-N_2 reactions. The Hunter et al. (1994) and Seery and Bowman (1970) mechanisms are only good for methane - oxygen reactions (no nitrogen), although Hunter et al. (1994) includes a large number of hydrocarbon reactions. Frenklach and Bornside (1984) and Frenklach et al. (1992) also have a large number of hydrocarbon reactions but no nitrogen chemistry.

Induction Time Data The sources of experimental induction time data listed in Table 6 contain much more data than have been utilized for this study so far. Burcat et al. (1996), Burcat et al. (1971), Cheng and Oppenheim (1984), and Seery and Bowman (1970) data have been used. Asaba et al. (1963) contains CH_4-air data, plus references to other authors. Bollinger et al. (1961) contains only induction distance data, not induction time. Frenklach and Bornside (1984) and Frenklach et al. (1992) contain CH_4-O_2 data but do not directly report the pressure used. Miyama and Takeyama (1965) and Spadaccini and Colket III (1994) contain relevant data, and the latter gives many references to related sources.

Results Results of CH_4 - O_2 - Ar simulations using the Frenklach et al. (1995), Miller and Bowman (1989), and modified Miller and Bowman (1989) mechanisms with comparisons to data from Cheng and Oppenheim (1984), Burcat et al. (1971), and Seery and Bowman (1970) are shown in Figs. 34, 35, 36, 37, 38, and 39. Two figures are used for each mechanism to reduce the clutter on each. The Frenklach et al. (1995) mechanism produced significantly better results.

Recommendations The temperature and pressure range of the validation study was 1300-2100 K and 1.7-13 atm. The equivalence ratio was 0.2-5.0, and the dilution was about 50-90%. The Frenklach et al. (1995) mechanism performed best under these conditions. More data are needed at higher temperatures and pressures, and with other dilution (i.e. N_2). Note that highly dilute methane-oxygen mixtures are difficult to ignite and have very long induction times that may be difficult to model.

3.1.6 CH_4 - N_2O (- Ar)

Reaction Mechanisms The mechanisms of Frenklach et al. (1995), and Miller and Bowman (1989) were used for the validation study. Drummond (1972a) contains a few important rate parameters.

Table 7: CH_4 - N_2O (- Ar) References

Reaction Mechanism	Experimental Data
Drummond (1972a), Frenklach et al. (1995), Hidaka et al. (1996), Miller and Bowman (1989), Starikovskii (1994), Starikovskii (1995)	Borisov et al. (1977), Drummond (1969), Soloukhin (1971)

Hidaka et al. (1996), Starikovskii (1994), and Starikovskii (1995) contain enough hydrocarbon and N_2O data to also be included in the validation study.

Induction Time Data Data from Drummond (1969) and Soloukhin (1971) was used in the validation study. Borisov et al. (1977) contains only flow reactor data that can not easily be used in this study.

Results Results of CH_4 - N_2O - Ar simulations using the Frenklach et al. (1995), Miller and Bowman (1989), and modified Miller and Bowman (1989) mechanisms with comparisons to data from Soloukhin (1971) and Drummond (1969) are shown in Figs. 40, 41, and 42. The predictions of both mechanisms match the experimental data quite well.

Recommendations The temperature and pressure range of the validation study was 1470-2780 K and 1-3.5 atm. All mixtures evaluated were stoichiometric, with dilution of 70-95%. More data are needed at higher pressures and with different dilution (i.e. N_2).

3.1.7 NH_3 - O_2 (- Ar)

Table 8: NH_3 - O_2 (- Ar) References

Reaction Mechanism	Experimental Data
Fujii et al. (1981), Lindstedt et al. (1994), Lindstedt and Selim (1994), Miller and Bowman (1989), Miller et al. (1983)	Bradley et al. (1968), Bull (1968), Drummond (1972b), Fujii et al. (1981), Miyama (1968a), Miyama (1968b), Takeyama and Miyama (1965), Takeyama and Miyama (1967)

Reaction Mechanisms Only one of the mechanisms used for hydrocarbon oxidation could be used for ammonia oxidation without modification, Miller and Bowman (1989). Unfortunately, it did not perform as well as other ammonia mechanisms not capable of hydrocarbon modeling (e.g. Miller et al. (1983)). The mechanism of Fujii et al. (1981) has been tested against shock tube data already, so it was combined with the Miller and Bowman (1989) mechanism. This mechanism performed as well as the Miller et al. (1983) mechanism at ammonia oxidation and as well as the Miller and Bowman (1989) mechanism at hydrocarbon combustion.

Induction Time Data The most useful data for NH_3 - O_2 - Ar validation came from Bull (1968), Drummond (1972b), and Fujii et al. (1981). A number of the other references have applicable data also, but the interesting case of no dilution (Miyama 1968a) currently can not be accurately modeled.

Results Results of the NH_3 - O_2 - Ar simulations using the Miller and Bowman (1989), modified Miller and Bowman (1989), and Miller et al. (1983) mechanisms with comparisons to data from Bull (1968), Fujii et al. (1981), and Drummond (1972b) are shown in Figs. 43, 44, and 45.

Three mechanisms were found to hold promise: Lindstedt et al. (1994), Miller and Bowman (1989), and Miller et al. (1983). The Miller and Bowman (1989) mechanism is actually two mechanisms combined, one for hydrocarbons and one for ammonia oxidation. It was reported to have been validated against flame data, but the comparison with our compilation of shock tube data was found to be poor (Fig. 43). This poor performance is believed to be caused by the lack of a dissociation path for NH_3, which is especially important in high Ar dilution. The apparently earlier version of this ammonia oxidation mechanism, given in Miller et al. (1983), contained a dissociation reaction and performed similarly, and slightly better than, the mechanism given in Lindstedt et al. (1994). This mechanism compared well with the high Ar dilution data (Fig. 45) except for some divergence from the Bull (1968) data at low temperatures.

Recommendations The temperature and pressure range of the validation study was 1450-4000 K and 3.2-35.8 atm. The mixtures evaluated contained approximately equimolar NH_3 and O_2, with 90-98% dilution. The best mechanisms for this reaction appear to be that of Miller et al. (1983) and the modified form of Miller and Bowman (1989).

3.1.8 NH_3 - O_2 - N_2

Table 9: NH_3 - O_2 - N_2 References

Reaction Mechanism	Experimental Data
Fujii et al. (1981), Lindstedt et al. (1994), Lindstedt and Selim (1994), Miller and Bowman (1989), Miller et al. (1983)	Bull (1968), Drummond (1972b), Fujii et al. (1981), Miyama (1968a), Miyama (1968b), Miyama and Endoh (1967a), Miyama and Endoh (1967b)

Reaction Mechanisms The mechanism discussion of Section 3.1.7 applies for NH_3-O_2-N_2.

Induction Time Data For the purpose of calculating post-shock conditions from measured shock parameters (shock speed, pressure), Miyama and Endoh (1967b) performed translational, rotational, and vibrational relaxation calculations. Their results show that relaxation effects are significant. Data from Miyama (1968a) and Miyama (1968b) were used for the validation study. In addition, data from Miyama and Endoh (1967a) and Miyama and Endoh (1967b) may be useful.

Results Results of the NH_3 - O_2 - N_2 simulations using the Miller and Bowman (1989), modified Miller and Bowman (1989), and Miller et al. (1983) mechanisms with comparisons to data from Miyama and Endoh (1967b) and Miyama and Endoh (1967a) are shown in Figs. 46, 47, and 48.

Recommendations The temperature and pressure range of the validation study was 1490-2330 K and about 0.95-3.5 atm. The mechanism of Miller et al. (1983) performed the best.

3.1.9 NH_3 - N_2O (- Ar)

Reaction Mechanisms The set of available mechanisms for NH_3-N_2O reactions (see Table 10) is a subset of those listed for NH_3-O_2-N_2 (Table 9).

Table 10: NH_3 - N_2O References

Reaction Mechanism	Experimental Data
Drummond (1972a), Fujii et al. (1981), Miller and Bowman (1989), Miller et al. (1983)	Drummond (1967), Soloukhin (1971)

Induction Time Data Data from Soloukhin (1971) are difficult to reproduce numerically because the experimental conditions are not clear. Initial pressures are only hinted at and initial concentrations are unclear. The NH_3-N_2O mixtures are said to be stoichiometric, but the meaning of "stoichiometric" is unclear because example figures suggest equimolar mixtures were used.

Results Results of the NH_3 - N_2O - Ar simulations using the Miller and Bowman (1989), modified Miller and Bowman (1989), and Miller et al. (1983) mechanisms with comparisons to data from Drummond (1967) and Soloukhin (1971) are shown in Figs. 49, 50, and 51. All mechanisms yield similarly good matches to the experimental data except at lower temperature.

Recommendations The temperature and pressure range of the validation study was 1540-3030 K and 1-3.9 atm. All mixtures evaluated consisted of "stoichiometric" NH_3-N_2O ratios and 90-95% dilution. More data are needed at higher pressure and with lower dilution.

3.1.10 Summary

Table 11 lists the conditions and summarizes the results of the validation studies. For more detail, see Sections 3.1.3 through 3.1.9. The classifications listed under "Comments" are subjective judgements to be used as a rough guide only for the specific mixture tested. Reference should be made to the orginal citation for a mechanism to determine if it has been tested for other situations.

The most useful mechanisms were the GRI Mech-2.11 (Frenklach et al. 1995) and the modified form of Miller and Bowman (1989). The GRI Mech-2.11 was the most accurate with reactions involving methane, as can be expected since it was designed to model natural gas combustion. However, it could not be used for ammonia combustion. The original form of the Miller and Bowman (1989) mechanism (actually a combination of separate hydrocarbon and ammonia mechanisms) was nearly as accurate for methane combustion but could also nominally be used with ammonia. Unfortunately it was particularly inaccurate with most ammonia tests. The earlier mechanism of Miller et al. (1983) proved better with ammonia but did not incorporate hydrocarbons. Finally, some reactions from Fujii et al. (1981), which were originally tested against shock tube data, were added to the Miller and Bowman (1989) mechanism to produce an overall reasonably accurate mechanism.

3.2 Cell Width and ZND Calculations

The ZND (Zeldovich - von Neumann - Döring) model of a detonation wave decomposes the one-dimensional steady wave into a non-reactive thin shock followed by an exothermic reaction zone (Zeldovich 1950) that terminates at the CJ state. The reaction zone typically consists of an induction zone where non-exothermic dissociation reactions cause radical species to accumulate, followed by a thin recombination zone where the reaction runs to completion and heat is released. The thickness of the reaction zone is determined by the reaction rates, primarily in the induction zone.

Numerically, the shock speed is computed from the Chapman-Jouguet model and equilibrium thermochemistry. The frozen postshock state is the initial condition for a marching solution of a system of ordinary differential equations for the thermal and chemical state. The distance from the shock to the point of maximum heat release normally defines the reaction zone thickness, analogously to the

Table 11: Summary of Validation Results and Recommendations

Mixture	Mechanism	Temperature (K)	Pressure (atm)	Comments
H_2-O_2-Ar	Allen et al. (1995)	870-2000	1-87	Fair
	Baulch et al. (1994a)			Good
	Frenklach et al. (1995)			Good
	Miller and Bowman (1989)			Best
	Miller and Bowman (1989)[1]			Same as above
H_2-Air	Allen et al. (1995)	950-1330	2.5-15	Poor above 2.5 atm
	Baulch et al. (1994a)			Best, but poor at 2.5 atm
	Frenklach et al. (1995)			Poor above 2.5 atm
	Miller and Bowman (1989)			Poor above 2.5 atm
	Miller and Bowman (1989)[1]			Same as above
H_2-N_2O-Ar	Allen et al. (1995)	1430-2860	1.5-3.0	Good below 2000 K
	Frenklach et al. (1995)			Good below 2000 K, worst
	Miller and Bowman (1989)			Good below 2000 K, best
	Miller and Bowman (1989)[1]			Good below 2000 K, best
CH_4-O_2-Ar	Baulch et al. (1994a)	1300-2100	1.7-13	Poor above 3.4 atm
	Frenklach et al. (1995)			Best
	Miller and Bowman (1989)			Poor
	Miller and Bowman (1989)[1]			Same as above
CH_4-N_2O-Ar	Frenklach et al. (1995)	1470-2780	1-3.5	Good
	Miller and Bowman (1989)			Good
	Miller and Bowman (1989)[1]			Same as above
NH_3-O_2-Ar	Miller and Bowman (1989)	1450-4000	3.2-35.8	Poor
	Miller and Bowman (1989)[1]			Good
	Miller et al. (1983)			Good
NH_3-O_2-N_2	Miller and Bowman (1989)	1490-2330	0.95-3.5	Poor
	Miller and Bowman (1989)[1]			Fair
	Miller et al. (1983)			Good
NH_3-N_2O-Ar	Miller and Bowman (1989)	1540-3030	1-3.9	Good
	Miller and Bowman (1989)[1]			Best
	Miller et al. (1983)			Good

[1]Modified version including Fujii et al. (1981) rates.

constant volume induction time. In fact, reaction zone thicknesses have been estimated using a constant volume approximation (Westbrook 1982). Other definitions based on Mach number can be used, and the different definitions provide information about the shape of the reaction zone (Shepherd 1986).

Reaction zone thicknesses (vs percent mixture in air) computed by ZND analysis for mixtures 1-26 of Ross and Shepherd (1996) (see Table 13) and two additional mixtures are presented in Figs. 52-58 in Appendix D. Fig. 59 shows reaction zone thicknesses for mixtures 12-17 from Table 1. These calculations were performed with the modified reaction mechanism of Miller and Bowman (1989).

3.3 Correlations

Cell width can not currently be computed or predicted directly. Current hydrodynamic simulations that attempt to reproduce detonation cellular structure make large sacrifices, usually by using single step, irreversible reactions and constant properties, and are capable of exhibiting qualitatively correct phenomena, but can not be used as engineering predictive tools. Simulations that compute detailed

chemical kinetics generally lack spatial resolution such that the reaction zone structure is meaningless.

Our analysis proceeds along dimensional analysis grounds. The ratio of cell width to reaction zone thickness (λ/Δ) is a function of other nondimensional parameters of the flow. For a system characterized by a single reaction with activation energy E_a, energy release q, ratio of specific heats γ, and detonation Mach number M_{CJ}, we expect that

$$\frac{\lambda}{\Delta} \approx f\left(M_{\mathrm{CJ}}, \gamma, \frac{q}{RT_{vN}}, \frac{E_a}{RT_{vN}}\right)$$

In general, f may include a large number of other parameters, but these are believed to be the most influential. The activation energy and heat release normalization factors include the von Neumann temperature because it is most relevant to the reaction zone behavior. While the general form of this function has not been found, certain useful approximations are possible. For instance, for a given fuel - oxidizer - diluent system at constant equivalence ratio and initial pressure, the function f is generally constant with respect to variation in dilution ratio. A slightly more general approach is illustrated in Figs. 12, 13, 14, and 15. The cell width data from different test conditions are plotted together by using computed reaction zone thickness for each condition as the abscissa.

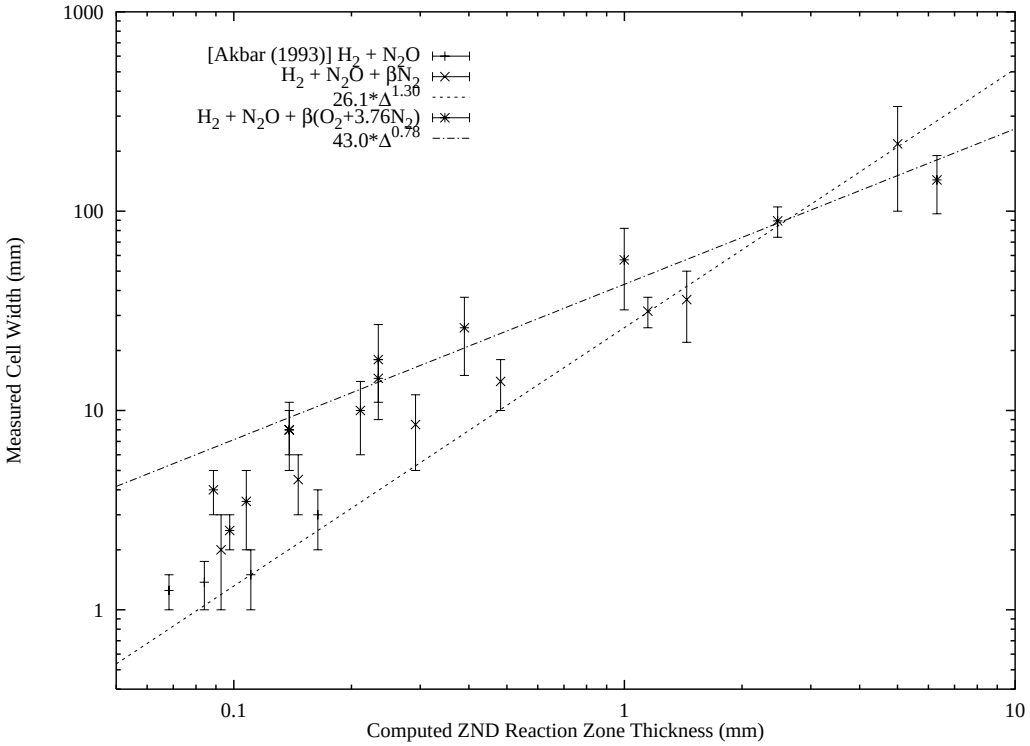

Figure 12: Correlation of cell width measurements with computed ZND reaction zone thicknesses using the modified Miller and Bowman (1989) mechanism for stoichiometric H_2-N_2O mixtures in air and N_2

For each fuel - oxidizer - diluent system, at constant equivalence ratio, cell width is found to obey a power law with respect to ZND reaction zone thickness. Note that while air is presented as a diluent along with N_2 in the H_2-N_2O and CH_4-N_2O mixtures, it acts as an oxidizer also and therefore mixtures with air are unique from N_2 systems. The undiluted H_2-N_2O data are considered to be a subset of the N_2 dilution data but not the air dilution data because O_2 is found to have a significant effect on N_2O mixtures even at very small concentrations.

A power law has been least-squares fit to the available cell width - reaction zone thickness data for each mixture, as shown in Figs. 12, 13, and 14. The data for H_2-N_2O-Air do not correlate well to a

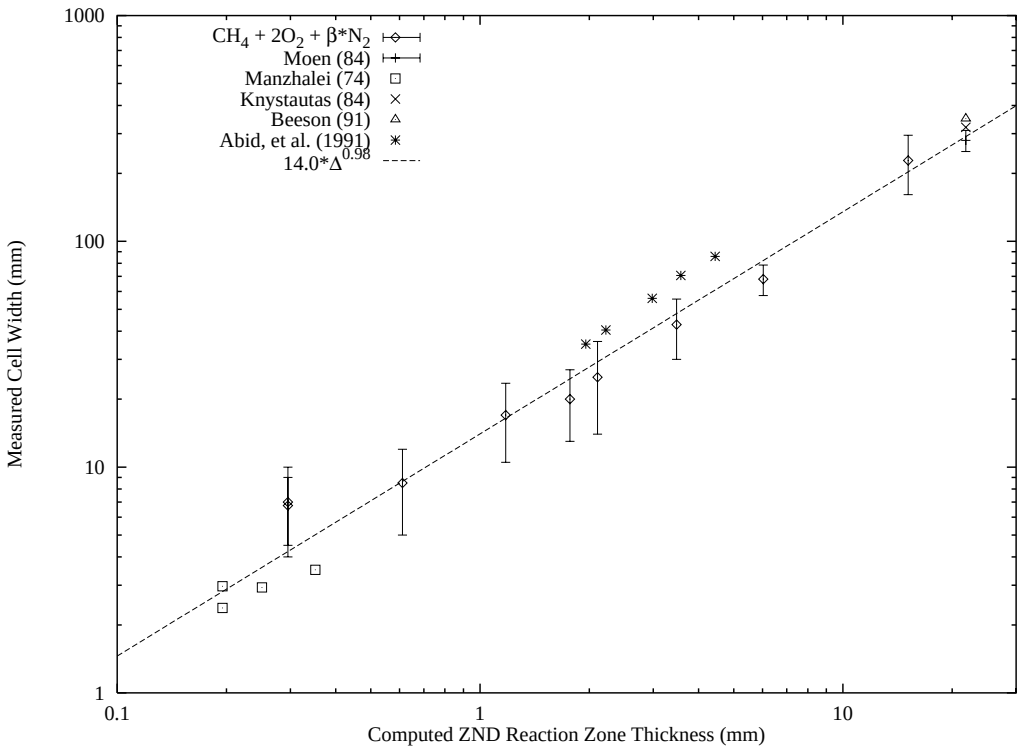

Figure 13: Correlation of cell width measurements with computed ZND reaction zone thicknesses using the modified Miller and Bowman (1989) mechanism for stoichiometric CH_4-O_2 mixtures in N_2

power law. The correlations for CH_4-O_2-N_2, CH_4-N_2O-N_2, and CH_4-N_2O-Air are good, although the number of data points is limited in the N_2O mixtures. A number of initial pressures are represented in the literature CH_4-O_2-N_2 data along with various dilution ratios.

4 Summary and Unresolved Issues

Work reported here has followed two complementary approaches to characterizing the detonation parameters of certain mixtures of H_2-CH_4-NH_3-N_2O-air. Experiments have been performed with mixtures of H_2-N_2O-O_2-N_2, CH_4-O_2-N_2, CH_4-N_2O-O_2-N_2, NH_3-O_2-N_2, NH_3-N_2O-O_2-N_2, and model tank mixtures of all these. Detonation velocities and cell widths have been measured and reported. Detonation velocities have been found to be very predictable by conventional thermochemical calculations.

Chemical kinetic models of the mixtures of interest have been compared to published experimental data and evaluated with respect to limits of validity. No mechanism has been shown to be valid for all the conditions necessary for detonation modeling, although a modified Miller and Bowman (1989) mechanism has been moderately successful. Some correlations between kinetic calculation results and detonation cell widths have been produced from the available cell width data.

Several issues remain unresolved and could benefit from additional attention:

- The performance of the current collection of reaction mechanisms is not as good as desired. More experimental data and validation effort to develop a mechanism specifically for detonation conditions with all the species of interest could make the modeling efforts more robust and reliable.
- The effort to correlate cell width and reaction zone thickness is in its infancy. The key missing element is a physical theory that would suggest a functional relationship between these quantities

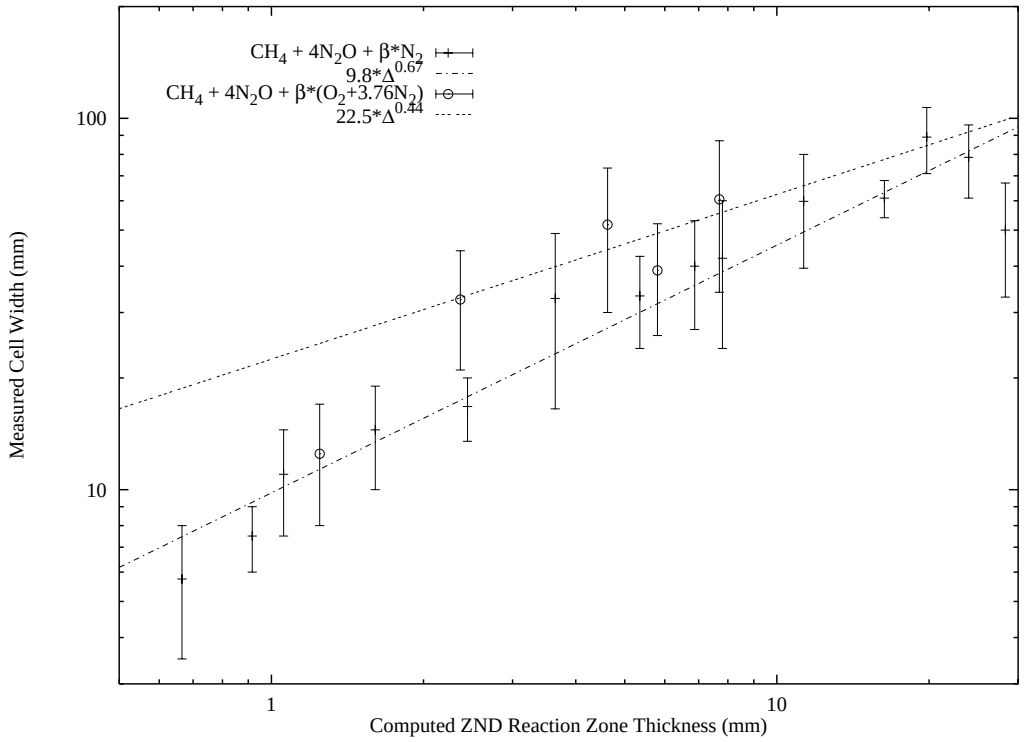

Figure 14: Correlation of cell width measurements with computed ZND reaction zone thicknesses using the modified Miller and Bowman (1989) mechanism for stoichiometric CH_4-N_2O mixtures in air and N_2

and other properties of a mixture. In lieu of such a theory, more analysis of the compiled data may uncover further useful relationships.

- The possibility of omitting hydrocarbons or otherwise simplifying the chemical kinetics calculations would dramatically reduce the time necessary to perform these calculations. However, any simplification must be carefully tested before being trusted.

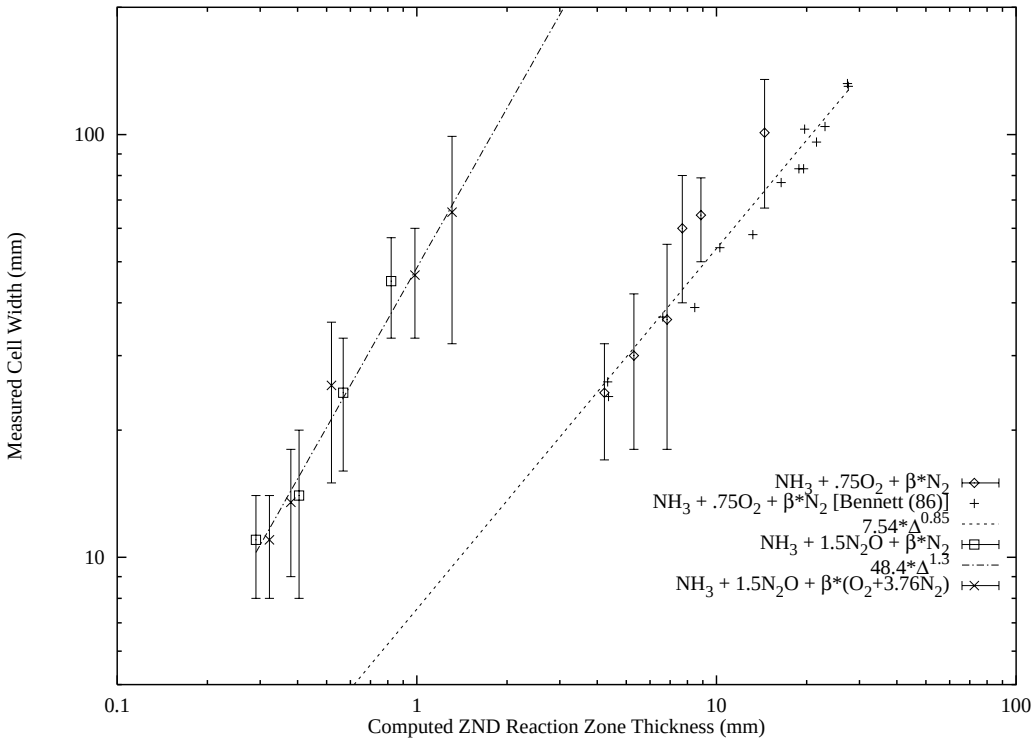

Figure 15: Correlation of cell width measurements with computed ZND reaction zone thicknesses using the modified Miller and Bowman (1989) mechanism for stoichiometric NH_3-O_2 and NH_3-N_2O mixtures in N_2 and air

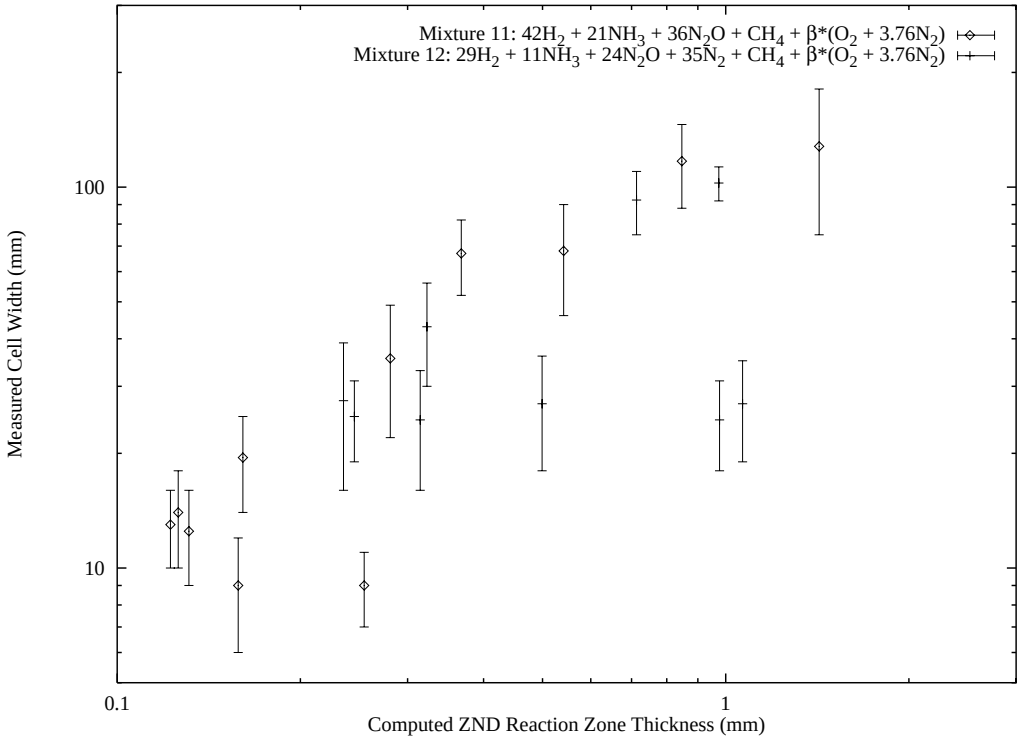

Figure 16: Correlation of cell width measurements with computed ZND reaction zone thicknesses using the modified Miller and Bowman (1989) mechanism for model tank mixtures in air

References

Akbar, R. and J. Shepherd (1993, June). Detonations in N_2O-H_2-N_2-Air mixtures. Prepared for the Los Alamos National Laboratory Under Consultant Agreement C-4836.

Akbar, R. and J. Shepherd (1996, September). Detonations in N_2O-H_2 mixtures diluted with N_2 or air. Prepared for the Los Alamos National Laboratory Under Contract 929Q0015-3A, DOE W-7405-ENG-36.

Allen, M., R. Yetter, and F. Dryer (1995). The decomposition of nitrous oxide at $1.5 \leq P \leq 10.5$ atm and $1103 \leq T \leq 1173$ K. *Int. J. Chem. Kinet. 27*(9), 883–909.

Asaba, T., K. Yoneda, N. Kakihara, and T. Hikita (1963). A shock tube study of ignition of methane-oxygen mixtures. In *9th Symp. Int. Combust. Proc.*, pp. 193–200.

Balakhnine, V., J. Vandooren, and P. V. Tiggelen (1977). Reaction mechanism and rate constants in lean hydrogen-nitrous oxide flames. *Combust. Flame 28*(2), 165–173.

Baulch, D., C. Cobos, R. Cox, C. Esser, P. Frank, T. Just, J. Kerr, M. Pilling, J. Troe, R. Walker, and J. Warnatz (1992). Evaluated kinetic data for combustion modeling. *J. Phys. Chem. Ref. Data 21*(3), 411–736.

Baulch, D., C. Cobos, R. Cox, P. Frank, G. Hayman, T. Just, J. Kerr, T. Murrells, M. Pilling, J. Troe, R. Walker, and J. Warnatz (1994a). Evaluated kinetic data for combustion modeling: Supplement I. *J. Phys. Chem. Ref. Data 23*(6), 847–1033.

Baulch, D., C. Cobos, R. Cox, P. Frank, G. Hayman, T. Just, J. Kerr, T. Murrells, M. Pilling, J. Troe, R. Walker, and J. Warnatz (1994b). Summary table of evaluated kinetic data for combustion modeling: Supplement I. *Combust. Flame 98*(1), 59–79.

Beeson, H., R. McClenagan, C. Bishop, F. Benz, W. J. Pitz, C. Westbrook, and J. Lee (1991). Detonability of hydrocarbon fuels in air. In *Prog. Astronaut. Aeronaut.*, Volume 133, pp. 19–36.

Bennett, C. A. (1986, March). Personal communication. Detonation Test Results and Predictions for NH_3-O_2-N_2 Mixtures.

Bhaskaran, K., M. Gupta, and T. Just (1973). Shock tube study of the effect of unsymmetric dimethyl hydrazine on the ignition characteristics of hydroge-air mixtures. *Combust. Flame 21*, 45–48.

Blumenthal, R., K. Fieweger, K. Komp, G. Adomeit, and B. Gelfand (1996). Self-ignition of H_2-air mixtures at high pressure and low temperature. In *20th Symp. Int. Shock Waves*, pp. 935–940.

Bollinger, L. (1964). Experimental detonation velocities and induction distances in hydrogen-air mixtures. *AIAA J. 2*(1), 131–133.

Bollinger, L., M. Fong, and R. Edse (1961). Experimental measurements and theoretical analysis of detonation induction distances. *Am. Rocket Soc. Pap. 31*, 588–595.

Bollinger, L., J. Laughrey, and R. Edse (1962). Experimental detonation velocities and induction distances in hydrogen-nitrous oxide mixtures. *Am. Rocket Soc. Pap. 32*, 81–82.

Borisov, A., V. Zamanskii, K. Potmishil, G. Skachkov, and V. Foteenkov (1977). The mechanism of methane oxidation with nitrous oxide. *Kinet. Katal. 8*, 307–315.

Borisov, A., V. Zamanskii, and G. Skachkov (1978). Kinetics and mechanism of reaction of hydrogen with nitrous oxide. *Kinet. Katal. 19*(1), 26–32.

Bradley, J. (1962). *Shock Waves in Chemistry and Physics*. Wiley.

Bradley, J., R. Butlin, and D. Lewis (1968). Oxidation of ammonia in shock waves. *Trans. Faraday Soc. 64*, 71–77.

Bull, D. (1968). A shock tube study of the oxidation of ammonia. *Combust. Flame 12*, 603–610.

Burcat, A., M. Dvinyaninov, and A. Lifshitz (1996). The effect of halocarbons on methane ignition. In *20th Symp. Int. Shock Waves*.

Burcat, A., K. Scheller, and A. Lifshitz (1971). Shock-tube investigation of comparative ignition delay times for C_1 - C_5 alkanes. *Combust. Flame 16*(1), 29–33.

Cheng, R. and A. Oppenheim (1984). Autoignition in methane-hydrogen mixtures. *Combust. Flame 58*(2), 125–139.

Cobos, C., H. Hippler, and J. Troe (1985). High pressure falloff curves and specific rate constants for the reactions H+O_2=HO_2=HO+O. *J. Phys. Chem. 89*(1), 342–349.

Craig, R. (1966). A shock tube study of the ignition delay of hydrogen-air mixtures near the second explosion limit. Technical Report AFAPL-TR-66-74, Air Force Aero-Propulsion Lab, Wright-Patterson.

Dean, A., D. Steiner, and E. Wang (1978). A shock tube study of the $H_2/O_2/CO/Ar$ and $H_2/N_2O/CO/Ar$ systems: Measurement of the rate constant for H+N_2O=N_2+OH. *Combust. Flame 32*(1), 73–83.

Drummond, L. (1967). Shock-initiated exothermic reactions III. the oxidation of hydrogen. *Aust. J. Chem. 20*, 2331–2341.

Drummond, L. (1969). Shock-induced reactions of methane with nitrous and nitric oxides. *Bull. Chem. Soc. Japan 42*, 285–289.

Drummond, L. (1972a). Comments upon shock-initiated oxidations by nitrous oxide. *Combust. Sci. Technol. 5*, 183–185.

Drummond, L. (1972b). High temperature oxidation of ammonia. *Combust. Sci. Technol. 5*, 175–182.

Drummond, L. and S. Hiscock (1967). Shock-initiated exothermic reactions II. the oxidation of ammonia. *Aust. J. Chem. 20*, 825–836.

Frank, P. and T. Just (1985). High temperature reaction rate for H+O_2=OH+O and OH+H_2=H_2O+H. *Ber. Bunsenges. Phys. Chem. 89*(1), 181–187.

Frenklach, M. and D. Bornside (1984). Shock-initiated ignition in methane-propane mixtures. *Combust. Flame 56*, 1–27.

Frenklach, M., H. Wang, C. Bowman, R. Hanson, G. Smith, D. Golden, W. Gardiner, and V. Lissianski (1995). An optimized kinetics model for natural gas combustion. Technical report, Gas Research Institute. For more information, see HTTP://www.gri.org.

Frenklach, M., H. Wang, and M. Rabinowitz (1992). Optimization and analysis of large chemical kinetic mechanisms using the solution mapping method - combustion of methane. *Prog. Energy Combust. Sci. 18*, 47–73.

Fujii, N., H. Miyama, M. Koshi, and T. Asaba (1981). Kinetics of ammonia oxidation in shock waves. In *18th Symp. Int. Combust. Proc.*, pp. 873–883.

Hidaka, Y., K. Kimura, K. Hattori, and T. Okuno (1996). Shock tube and modeling study of ketene oxidation. *Combust. Flame 106*(1), 155–167.

Hidaka, Y., H. Takuma, and M. Suga (1985a). Shock-tube studies of N_2O decomposition and N_2O-H_2 reaction. *Bull. Chem. Soc. Japan. 58*(10), 2911–2916.

Hidaka, Y., H. Takuma, and M. Suga (1985b). Shock-tube study of the rate constant for excited OH* ($^2\Sigma^+$) formation in the N_2O-H_2 reaction. *J. Phys. Chem. 89*(23), 4903–4905.

Hunter, T., H. Wang, T. Litzinger, and M. Frenklach (1994). The oxidation of methane at elevated pressures: Experiments and modeling. *Combust. Flame 97*(2), 201–224.

Kee, R., F. Rupley, and J. Miller (1989). Chemkin-II: A fortran chemical kinetics package for the analysis of gas-phase chemical kinetics. Technical Report SAND89-8009, Sandia National Laboratory.

Knystautas, R., C. Guirao, J. Lee, and A. Sulmistras (1984). Measurement of cell size in hydrocarbon-air mixtures and predictions of critical tube diameter, critical initiation energy, and detonability limits. In *Prog. Astronaut. Aeronaut.*, Volume 94, pp. 23–37.

Lee, J. (1984). Dynamic parameters of gaseous detonations. *Ann. Rev. Fluid Mech. 16*, 311–336.

Lindstedt, R., F. Lockwood, and M. Selim (1994). Detailed kinetic modelling of chemistry and temperature effects on ammonia oxidation. *Combust. Sci. Technol. 99*(4-6), 253–276.

Lindstedt, R. and M. Selim (1994). Reduced reaction mechanisms for ammonia oxidation in premixed laminar flames. *Combust. Sci. Technol. 99*(4-6), 277–298.

Manzhalei, V., V. Mitrofanov, and V. Subbotin (1974). Measurement of inhomogeneities of a detonation front in gas mixtures at elevated pressures. *Combust. Explos. Shock Waves (USSR) 10*(1), 89–95.

Miller, J. and C. Bowman (1989). Mechanism and modeling of nitrogen chemistry in combustion. *Prog. Energy Combust. Sci. 15*, 287–338.

Miller, J., M. Smooke, R. Green, and R. Kee (1983). Kinetic modeling of the oxidation of ammonia in flames. *Combust. Sci. Technol. 34*, 149–176.

Miyama, H. (1968a). Ignition of ammonia-oxygen mixtures by shock waves. *J. Chem. Phys. 48*, 1421–1422.

Miyama, H. (1968b). Kinetic studies of ammonia oxidation in shock waves. IV. comparison of induction periods for the ignition of NH_3-O_2-N_2 with thos for NH_3-O_2-Ar mixtures. *Bull. Chem. Soc. Japan 41*, 1761–1765.

Miyama, H. and R. Endoh (1967a). Ignition of ammonia-air mixtures by reflected shock waves. *Combust. Flame 11*, 359–360.

Miyama, H. and R. Endoh (1967b). Vibrational relaxation of nitrogen in shock-heated NH_3- O_2-N_2 mixtures. *J. Chem. Phys. 46*, 2011–2012.

Miyama, H. and T. Takeyama (1965). Kinetics of methane oxidation in shock waves. *Bull. Chem. Soc. Japan 38*(1), 37–43.

Moen, I., J. Funk, S. Ward, G. Rude, and P. Thibault (1984). Detonation length scales for fuel-air explosives. In *Prog. Astronaut. Aeronaut.*, Volume 94, pp. 55–79.

Pamidimukkala, K. and G. Skinner (1982). Resonance absorption measurements of atom concentrations in reacting gas mixtures. VIII. rate constants for O+H_2=OH+H and O+D_2=OD+D from measurements of O atoms in oxidation of H_2 and D_2 by N_2O. *J. Chem. Phys. 76*(1), 311–315.

Petersen, E., D. Davidson, M. Rohrig, and R. Hanson (1996). High-pressure shock-tube measurements of ignition times in stoichiometric H_2/O_2/Ar mixtures. In *20th Symp. Int. Shock Waves*, pp. 941–946.

Reynolds, W. C. (1986, January). *The Element Potential Method for Chemical Equilibrium Analysis: Implementation in the Interactive Program STANJAN* (3rd ed.). Dept. of Mechanical Engineering, Stanford, CA: Stanford University.

Ross, M. and J. Shepherd (1996). Lean combustion characteristics of hydrogen-nitrous oxide-ammonia mixtures in air. Technical Report FM96-4, Graduate Aeronautical Laboratories, California Institute of Technology.

Sausa, R., W. Anderson, D. Dayton, C. Faust, and S. Howard (1993). Detailed structure study of a low pressure, stoichiometric H_2/N_2O/Ar flame. *Combust. Flame 94*(4), 407–425.

Schott, G. and J. Kinsey (1958). Kinetic studies of hydroxyl radicals in shock waves. II. induction times in the hydrogen-oxygen reaction. *J. Chem. Phys. 29*(5), 1177–1182.

Seery, D. and C. Bowman (1970). An experimental and analytical study of methane oxidation behind shock waves. *Combust. Flame 14*(1), 37–48.

Shepherd, J. (1986). Chemical kinetics of hydrogen-air-diluent detonations. In *Prog. Astronaut. Aeronaut.*, Volume 106, pp. 263–293.

Skinner, G. and G. Ringrose (1966). Ignition delays of a hydrogen-oxygen-argon mixture at relatively low temperature. *J. Chem. Phys. 42*(6), 2190–2192.

Soloukhin, R. (1971). High-temperature oxidation of ammonia, carbon monoxide and methane by nitrous oxide in shock waves. In *13th Symp. Int. Combust. Proc.*, pp. 121–128.

Soloukhin, R. (1973). High-temperature oxidation of hydrogen by nitrous oxide in shock waves. In *14th Symp. Int. Combust. Proc.*, pp. 77–82.

Spadaccini, L. and M. Colket III (1994). Ignition delay characteristics of methane fuels. *Prog. Energy Combust. Sci. 20*, 431–460.

Starikovskii, A. (1994). Kinetics and mechanism of reaction in the N_2O - CO system at high temperatures. *Chem. Phys. Reports 13*(1), 151–190.

Starikovskii, A. (1995). Development of flows with exothermic reactions behind reflected shock waves. ignition and detonation in N_2O - CO - H_2 - He mixtures at high temperatures. *Chem. Phys. Reports 13*(8-9), 1422–1474.

Takeyama, T. and H. Miyama (1965). Kinetic studies of ammonia oxidation in shock waves. I. the reaction mechanism for the induction period. *Bull. Chem. Soc. Japan 38*, 1670–1674.

Takeyama, T. and H. Miyama (1967). A shock-tube study of the ammonia-oxygen reaction. In *11th Symp. Int. Comb. Proc.*, pp. 845–852.

Thibault, P., J. Shepherd, W. Benedick, and D. Ritzel (1987). Blast waves generated by planar detonations. In *Proc. 16th Int. Symp. Shock Tubes Waves*, pp. 765–771.

Westbrook, C. (1982). Chemical kinetics of hydrocarbon oxidation in gaseous detonations. *Combust. Flame 46*(2), 191–210.

Westbrook, C. and P. Urtiew (1983). Use of chemical kinetics to predict critical parameters of gaseous detonations. *Fiz. Goreniya Vzryva 19*(6), 65–76.

White, D. and G. Moore (1965). Structure of gaseous detonation. IV. induction zone studies in H_2-O_2 and CO-O_2 mixtures. In *18th Symp. Int. Combust. Proc.*, pp. 785–795.

Zeldovich, Y. (1950). On the theory of the propagation of detonation in gaseous systems. Technical Memorandum 1261, National Advisory Committee for Aeronautics. Translated from "K Teorri Rasprostranenia Detonantsii v Gasoobraznykh Sistremakh", Zhurnal Experimentalnoi i Teoretich-eskoi Fiziki, T. 10, 1940.

Zuev, A. and A. Starikovskii (1992). Reactions in the N_2O - H_2 system at high temperatures. *Sov. J. Chem. Phys. 10*(3), 520–540.

A Experimental Test Matrix

Test	Mix	β	Press. kPa	Go	D_{CJ} m/s	D_{1-2} m/s	D_{2-3} m/s	λ_{min} mm	λ_{max} mm
17	1	0.42	100	Yes	1937	1928	1923	6	10
18	1	0.63	100	Yes	1806	1794	1787	9	27
19	1	0.63	100	Yes	1806	1792	1787	11	18
20	1	0.98	100	Yes	1637	1618	1610	32	82
22	1	1.68	100	No					
23	1	1.19	100	Yes	1554	1546	1521	97	190
24	1	1.33	100	DDT	1521	1807	1440	92	122
25	1	0.42	100	Yes				5	11
26	2	2.0	100	Yes	1962	1947	1947	10	18
27	2	3.0	100	Yes	1839	1812	1814	26	37
28	2	4.7	100	No					
29	2	3.6	100	No					
30	2	3.3	100	Yes	1810	1780	1779		
31	2	3.3	100	DDT	1810				
32	2	3.3	100	Yes	1810	1775	1778		
33	2	3.3	100	Yes	1810	1780	1777	22	50
34	2	3.9	100	Yes	1746	1710	1713		
35	2	4.3	100	Yes	1711	1668	1671		
36	2	4.7	100	Yes	1674	1644	1621		
37	2	5.1	100	No					
38	3		100	Yes	1632	1605	1608		
39	2	5.1	100	Yes	1633	1605	1598		
40	2	4.7	100	No					
41	2	4.7	100	No					
42	2	4.7	100	No					
43	2	4.7	100	No					
44	4		98	Yes	1593	1591	1595		
45	2	4.7	100	No					
46	2	4.7	100	Yes	1674	1649	1637	100	335
51	5	0.0	72.1	Yes	2378	2815	2761	4.5	9
52	5[1]	0.0	72.1	Yes	2378	2440	2434	2.5	5
53	5	0.0	72.2	Yes	2378	2528	2387	4	10
54	5	2.0	89.2	Yes	2109	2125	2117	10.5	23.5
55	5	4.0	102.2	Yes	1969	1978	1979	30	55.5
56	5	5.0	102.19	Yes	1915	1918	1909	57.5	84.5
57	5	6.0	72.16	Yes	1860	1867	1856	161	295
76	6	0.0	57.15	Yes	2178.9	2186.4	2179	3.5	8
77	6	1.0	62.16	Yes	2114.4	2120.5	2119.1	7.5	14.5
78	6	2.0	72.21	Yes	2063	2070.1	2064.7	10	19
79	6	3.0	77.21	Yes	2015.6	2019.9	2017.5	13.5	20
80	6	4.0	82.21	Yes	1974.9	1978.4	1976.5	16.5	49
81	6	5.0	87.21	Yes	1937.6	1940.6	1931.1	24	42.5
85	6	6.0	92.24	Yes	1903.2	1906.3	1901.3	24	60
86	6	7.0	97.23	Yes	1871.2	1873.1	1863	39.5	80
87	6	8.0	102.23	Yes	1899.4	1841.1	1828.1	54	68
88	6	9.0	102.26	Yes	1811.5	1804.7	1784	61	96
90	6	9.0	102.23	No	1811.5	528.3	503.8	-	-
91	6	8.5	102.22	Yes	1826	1828.2	1806.6	71	107
92	7	1.0	86.26	Yes	1936.5	1940.6	1933.1	21	44
93	7	1.5	97.08	Yes	1853.5	1852.2	1846.3	30	73.5
264	7	2.5	99..9	No	1711	515.9	489.9		
265	7	2.0	99.9	No	1779	538.4	511.5		

Test	Mix	β	Press. kPa	Go	D_{CJ} m/s	D_{1-2} m/s	D_{2-3} m/s	λ_{min} mm	λ_{max} mm
266	7	1.6	88.4	Yes	1838	1830	1824	26	52
267	7	1.8	91.2	Yes	1807	1808	1798	34	87
268	1	0.78	99.97	Yes	1727	1710	1705	15	37
269	1	1.08	99.99	Yes	1597	1578	1564	74	105
270	2	0.5	81	Yes	2228	2229	2224	3	6
271	2	1.33	91.2	Yes	2059	2058	2053	5	12
272	1	0.50	69.86	Yes	1884	1873	1869	6	14
273	1	0.105	75.98	Yes	2221.7	2218	2213	2	5
274	1	0.047	76	Yes	2301.8	2301.9	2298.1	2	3
275	2	0.0	72.9	Yes	2380.2	2382.8	2371.8	1	3
276	1	0.228	88.4	Yes	2091.7	2091.4	2083.3	3	5
277	5	0.75	69.96	Yes	2242.9	2264.9	2256.1	5	12
278	5	2.45	69.98	Yes	2063.2	2079.6	2071.7	14	36
279	5	2.45	82.05	Yes	2068.3	2077.2	2074	13	27
280	6	5.0	56.97	Yes	1928	1930	1919	27	53
281	7	0.117	56.09	Yes	2136.8	2147.9	2141.2	6	9
282	7	0.45	64.57	Yes	2046.4	2058.5	2046.5	8	17
283	7	1.96	96.45	Yes	1785.8	1778.4	1765.3	33	67
286	8	0.0	65.87	Yes	2441.2	2453	2450	17	32
287	8	0.5	75.88	No	2260	773.8	696.8		
288	8	0.2	70.99	Yes	2359	2379.7	2362.7	18	42
289	8	0.4	73.94	Yes	2290.4	2304.8	2301	18	55
290	8	0.6	75.98	Yes	2231.3	2237.2	2239.7	50	79
291	8	1.0	81.13	Yes	2135	2137.9	2146.2	67	135
292	8	1.5	91.25	No	2041.1	603.6	568.9		
293	8	1.25	86.13	No	2085.4	621.2	599.1		
294	9	0.0	55.73	Yes	2229.8	2239.9	2231.6	8	14
295	9	0.5	63.79	Yes	2147.9	2152.9	2151.2	8	20
296	9	1.0	71	Yes	2079.7	2091.4	2081	16	33
297	9	1.5	75.98	Yes	2020.3	2026.6	2019.7	33	57
298	9	2.0	80.98	No	1967.6	577.1	542.8		
299	9	1.75	75.98	No	1992.5	579.7	551.9		
300	10	0.50	86.02	Yes	1913.2	1910.2	1905.3	33	60
301	10	1.00	101.4	No	1706.9	855.1	753.6		
302	10	0.75	101.4	No	1801.8	556.4	540.1		
303	10	0.25	70.93	Yes	2048.7	2051.6	2051	15	36
304	11	0.0	75.94	Yes	2521.1	2520.7	2506.8	7	11
305	12^2	0.0	94.34	Yes	2121.4	2120.5	2111.9	18	31
306	11	21.0	91.17	Yes	2084.9	2086.7	2081	10	18
307	11	31.5	101.31	Yes	1959	1957.2	1949.4	14	25
308	11	42.0	101.34	Yes	1847.2	1837.4	1840.8	22	49
309	11	52.5	101.26	Yes	1756.7	1736.2	1735.5	46	90
310	11	63.0	101.37	Yes	1680.4	1677.4	1653.3	75	181
311	12	14.5	101.42	Yes	1939	1930.4	1933.1	16	39
312	12	29.0	101.26	Yes	1730.2	1713.5	1711.4	75	110
313	12	36.2	101.3	No	1649.1	586.2	554.4		
314	10	0.75	101.44	No	1801.8	540.8	522.3		
315	11	5.0	75.96	Yes	2359	2358.3	2350.7	6	12
316	11	10.0	81.11	Yes	2251.7	2256.5	2245.2	9	16
317	11	47.2	101.3	Yes	1800.8	1778.4	1799.6	52	82
318	11	57.5	101.3	Yes	1719.4	1705.5	1700.4	88	146
319	11	15.0	86.19	Yes	2169.2	2165.7	2168.8	10	16
320	11	78.1	101.32	No	1578	892.7	801.6		
321	12	5.4	96.3	Yes	2051.6	2044.7	2039.7	16	33

Test	Mix	β	Press. kPa	Go	D_{CJ} m/s	D_{1-2} m/s	D_{2-3} m/s	λ_{min} mm	λ_{max} mm
322	12	20.5	101.28	Yes	1848.4	1841.1	1840.5	30	56
323	12	0.0	96.29	Yes	2103.1	2101	2095.1	19	35
324	12	2.3	96.16	Yes	2076.9	2084.3	2067	18	36
325	12	9.0	96.24	Yes	2012.4	2004.4	2000	19	31
326	12	31.5	101.31	Yes	1701.7	1683.5	1680.3	92	108
327	10	0.10	60.74	Yes	2148.3	2155.5	2151.2	9	18
328	10	0.60	91.28	Yes	1866.4	1852.2	1859.3	32	99
329	8	0.5	75.87	Yes	2260.2	2267.7	2264.4	40	80
330	8	1.1	86.1	No	2115.5	617	586.4		
331	12[3]	0.0	96.27	Yes	2111.4	2108.3	2099.9	17	32
332	12[3]	0.0	96.36	Yes	2092.1	2093.8	2085.7	23	43
333	13	10.0	101.33	No	1662	915.5	817.5		
334	13	15.0	101.28	Yes	1732.3	1729.7	1708.2	68	106
335	14	25.0	101.32	Yes	1978.4	1980.5	1970.2	7	14
336	14	30.0	101.31	Yes	1922.8	1928.4	1919.1	7	14
337	15	14.0	101.21	Yes	1996.7	1991.3	1985.0	8	14
338	15	25.0	101.33	Yes	1837.0	1839.2	1831.7	9	17
339	16	28.5	101.32	Yes	1893.6	1896.4	1891.6	5	16
340	16	38.5	101.19	Yes	1772.6	1780.2	1773.7	19	42
341	17	35.0	101.31	Yes	1973.9	1969.9	1965.9	8	14
342	17	45.0	101.31	Yes	1860.3	1882.7	1874.4	7	20

[1]Contaminated with about 2% C_2H_2

[2]Mixture 12 with 33 N_2 instead of 35

[3]These shots used a modified mixture 12. Test 331 contained 0 CH_4, test 332 contained 2 CH_4. See text (Section 2.2)

B Driver Calibration

The driver of the GALCIT Detonation Tube is intended to reliably and controllably initiate detonations in any mixture that is detonable in the tube (Akbar and Shepherd 1996). It consists of acetylene and oxygen cylinders, regulators, flash arrestors, and valves, an injection valve, a digital control circuit, and an exploding wire circuit. The control circuit actuates the electropneumatic valves to control the driver injection duration and ignition delay, and triggers the exploding wire. It is interlocked to various gas supply valves and hydraulic closure devices for safety purposes.

A manual fire signal starts the driver sequence. The control circuit opens the acetylene and oxygen valves and the injection valve for a programmed time period and then waits for a programmed delay period. The ratio of acetylene to oxygen is controlled by adjusting the cylinder pressure regulators. A fire signal is then sent to a trigger module that sends a high voltage trigger to the exploding wire spark gap. The spark gap switches the 2 μF capacitor bank (typically charged to 9 kV) through a small copper wire in the tube. The oxy-acetylene mixture is easily initiated by this discharge and transitions to a planar detonation wave which is transmitted to the test mixture.

Tests are periodically performed to verify the overall quantity of driver gas injected with each shot and to measure and adjust its equivalence ratio. To check the amount of gas injection, the driver is triggered several times without the exploding wire and the final pressure is measured after each injection. Measuring the detonation wave speed in this mixture and comparing it to equilibrium calculations (STANJAN) allow an estimate of the equivalence ratio. The driver is kept slightly lean to avoid formation of soot.

A number of tests with the driver transmitting blast waves into air have been performed to evaluate its equivalent energy. A summary of results from these shots is presented in Table 12.

Table 12: Driver Characterization Shot List

Shot	Press.	Flow Duration		Delay		D_{1-2}	D_{2-3}	ΔP_1	ΔP_2	ΔP_3
	(kPa)	(dial)	(s)	(dial)	(s)	(m/s)	(m/s)	(kPa)	(kPa)	(kPa)
48	100.0	560	4.442	200	1.025	712	658	430	330	270
58[1]	100.08	560	4.442	200	1.025	-	-			
59	25.2	560	4.442	200	1.025	-	-	361	210	150
60	25.2	560	4.442	200	1.025	999.5	846.7	305	206	163
61	50.2	560	4.442	200	1.025	823.6	739.1	340	224	185
62	75.2	560	4.442	200	1.025	-	-	434	312	253
63	100.0	560	4.442	200	1.025	711.8	652.1	350	270	230
64[2]	98.9	69	0.440	200	1.025	-	-			
65	99.69	260	1.997	200	1.025	453.5	450.7	95	90	80
66[2]	99.47	137.7	1.000	200	1.025	-	-			
67	100.0	751	6.000	200	1.025	744.8	683.2	500	330	310
68	100.0	628.5	5.000	200	1.025	716.8	663.3	450	340	290
69	100.0	505.8	4.000	200	1.025	689.3	635.3	430	280	240
70	100.0	383.1	3.000	200	1.025	655.2	599.5	350	230	200
71	100.0	560	4.442	200	1.025	705.7	644.4	420	300	240
72	100.0	560	4.442	50	0.500	706.6	651.9	500	330	270
73	100.0	560	4.442	336	1.501	707.9	645.3	400	280	250
74	100.0	560	4.442	479	2.002	696.1	646.6	510	380	280
75	100.0	560	4.442	765.1	3.003	701.1	646.4	350	270	240

[1]Pressure signals too small on CAMAC data; oscilloscope failed to trigger
[2]Driver did not detonate

The injection and delay periods are programmed through dial potentiometers. The relationship between the numerical values on these potentiometers and the actual injection and delay periods has

been measured, and for reference are given below.

$$\text{Injection Period} = 8.1513(\text{Dial Setting}) - 122.26$$

and

$$\text{Ignition Delay} = 3.5(\text{Dial Setting}) + 325$$

where the injection period and ignition delay are in units of milliseconds.

According to the approximate analysis by Thibault et al. (1987), the far field overpressure in a tube subjected to a blast wave at X=0 is a function of γ, X, P_0, and E_c, where E_c is the equivalent energy of the source:

$$\frac{\Delta P}{P_0} = \frac{4\gamma/(\gamma+1)}{\sqrt{1+4\gamma/(\gamma^2-1)\cdot X/L_e}-1}$$

where

$$L_e = \frac{E_c}{P_0}$$

Far field is considered to be $X/L_e > 0.3$.

Solving these relations for E_c in terms of γ, $\Delta P/P_0$, and X allows the data in Table 12 to be used to plot equivalent energy vs injection time. These data, and a semilog curve fit are shown in Fig. 17.

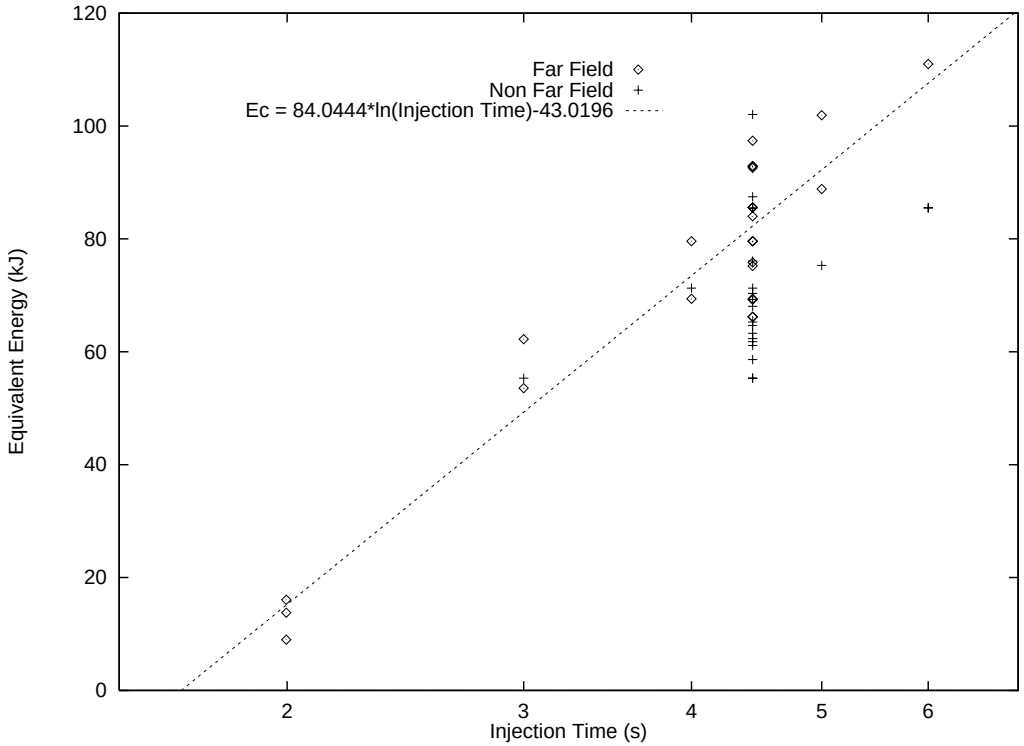

Figure 17: Driver equivalent energy

Each point represents a shock pressure measured at one of the pressure transducers. The equivalent energy computed from the three transducers for each shot were averaged and used to calculate explosion lengths (L_e) and the nondimensional distance to each transducer. Since the nondimensional distance to each transducer was a function of the initial pressure and the injection time, the validity of the far field assumption was checked for each pressure trace and the data points were sorted and plotted accordingly. The "far field" data were found to lie along a linear curve in linear-log coordinates, so a semilog curve fit was made and plotted with the data. The applicability of this fit is limited to the range of injection times investigated. Below about 2 s injection time the driver slug itself will not initiate. Above 6 s,

the equivalent energy begins to plateau and the length of the driver slug begins to become appreciable (especially at low initial pressures). However, the data are useful by demonstrating that the relationship between equivalent energy and injection time is not linear. The effect of varying the delay time has also been investigated but no trend with respect to equivalent energy has been found.

Note that the analysis illustrated here assumes that certain system variables are constant, namely oxygen and acetylene delivery pressures and flow rates. These can be affected by variations in cylinder pressure and in the detonation tube initial pressure. Acetylene delivery pressure depends strongly on the frequency of use since the gas is dissolved in acetone within the cylinder. Furthermore, the specific construction of each cylinder can affect its flow characteristics. Variations in the component flow rates can affect the equivalence ratio and the driver equivalent energy. Efforts have been made to compensate for these variations, and tests are performed periodically to correct them.

C Validation Figures

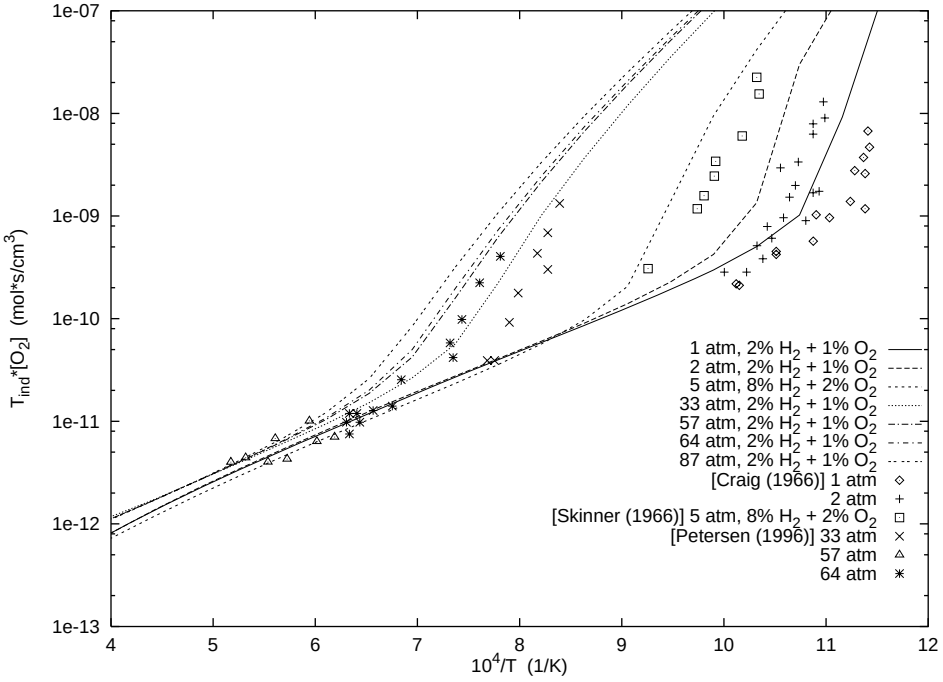

Figure 18: H_2-O_2-Ar Comparison of Allen et al. (1995) Mechanism with Data of Craig (1966), Petersen et al. (1996), and Skinner and Ringrose (1966)

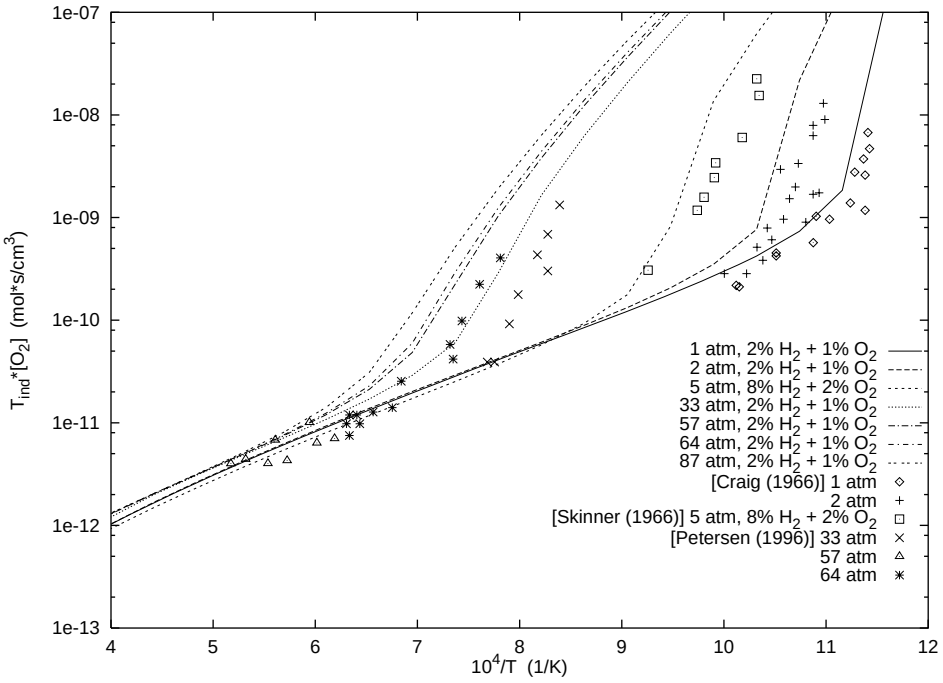

Figure 19: H_2-O_2-Ar Comparison of Baulch et al. (1992) Mechanism with Data of Craig (1966), Petersen et al. (1996), and Skinner and Ringrose (1966)

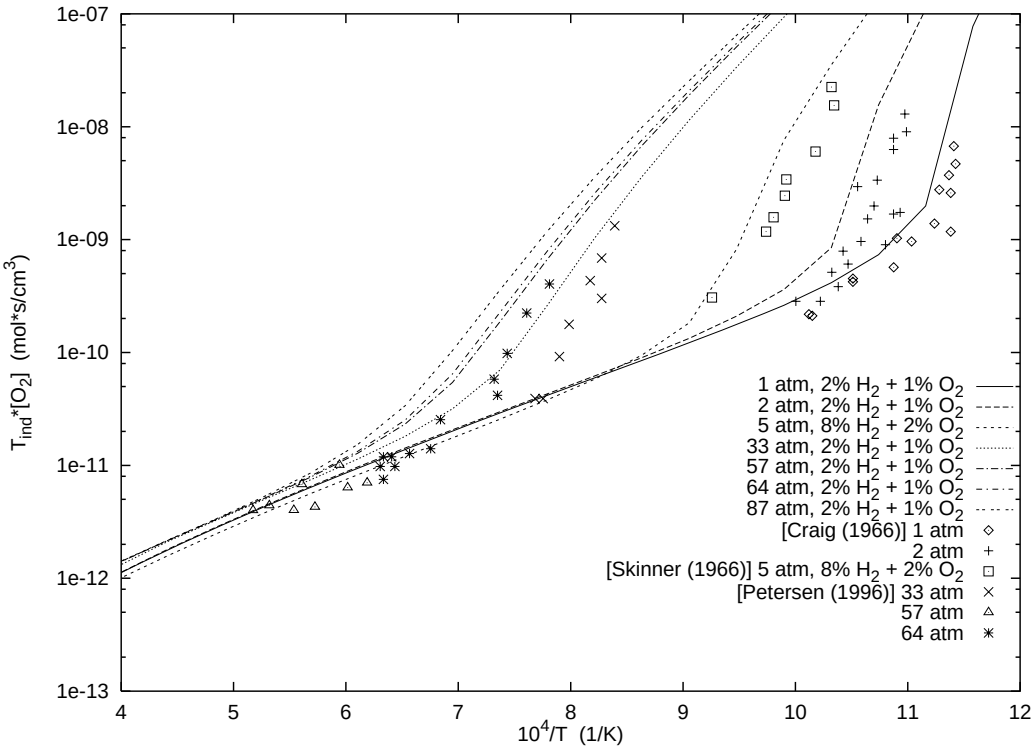

Figure 20: H_2-O_2-Ar Comparison of Frenklach et al. (1995) (GRI) Mechanism with Data of Craig (1966), Petersen et al. (1996), and Skinner and Ringrose (1966)

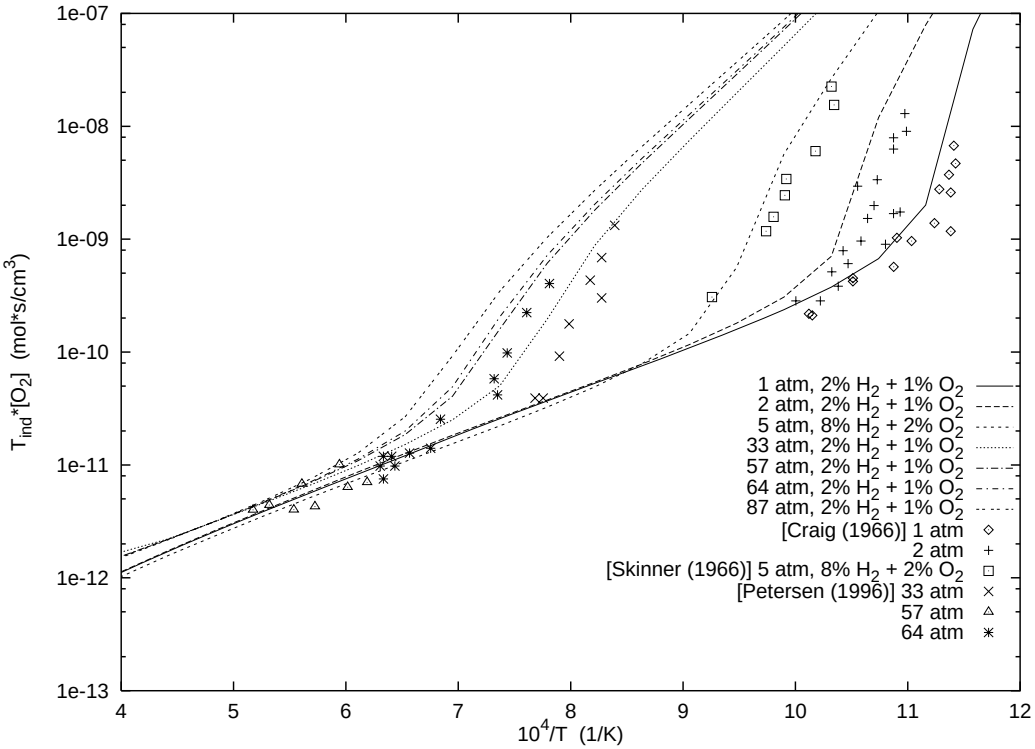

Figure 21: H_2-O_2-Ar Comparison of Miller and Bowman (1989) Mechanism with Data of Craig (1966), Petersen et al. (1996), and Skinner and Ringrose (1966)

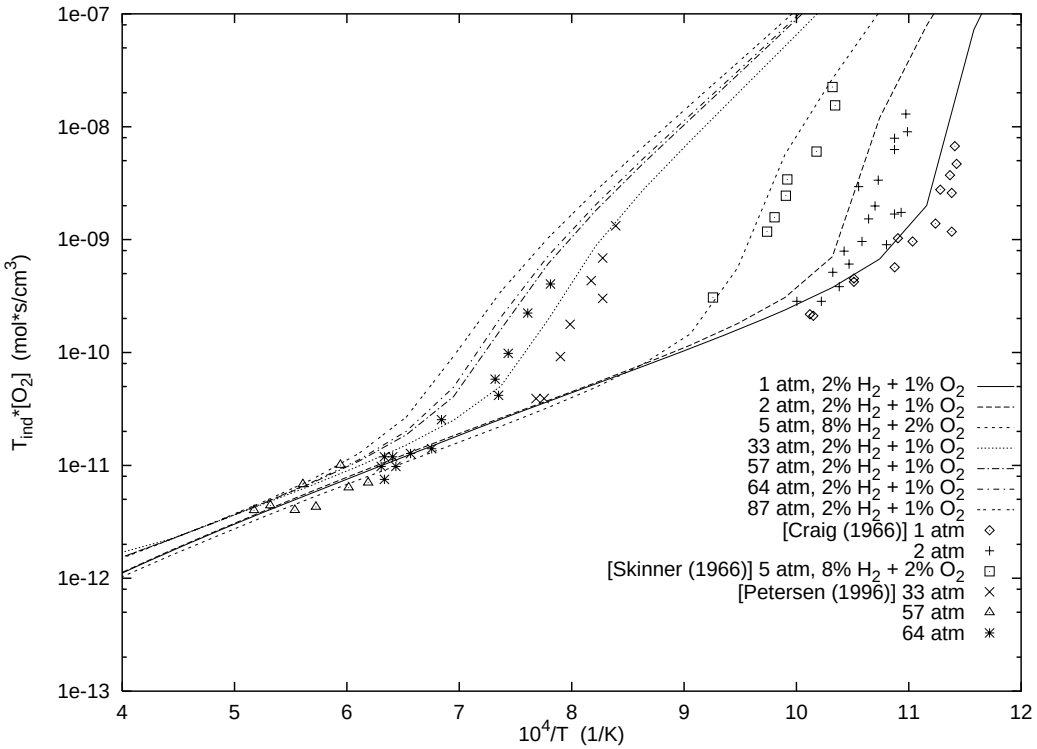

Figure 22: H_2-O_2-Ar Comparison of modified Miller and Bowman (1989) Mechanism with Data of Craig (1966), Petersen et al. (1996), and Skinner and Ringrose (1966)

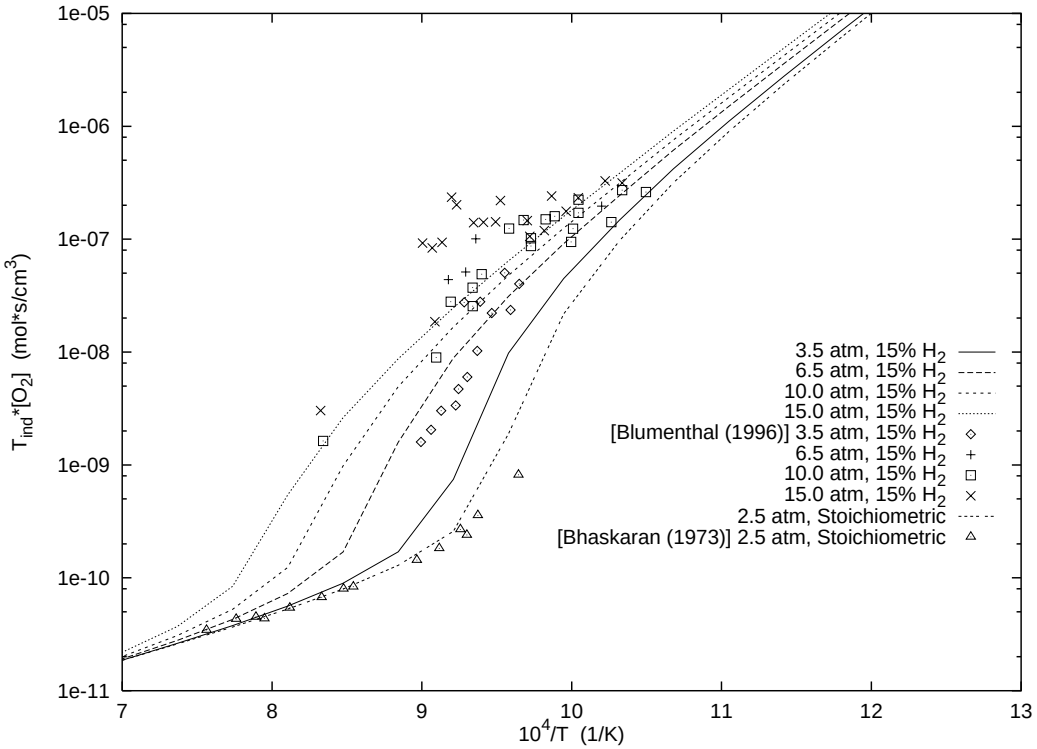

Figure 23: H_2-Air Comparison of Allen et al. (1995) Mechanism with Blumenthal et al. (1996) and Bhaskaran et al. (1973) Data

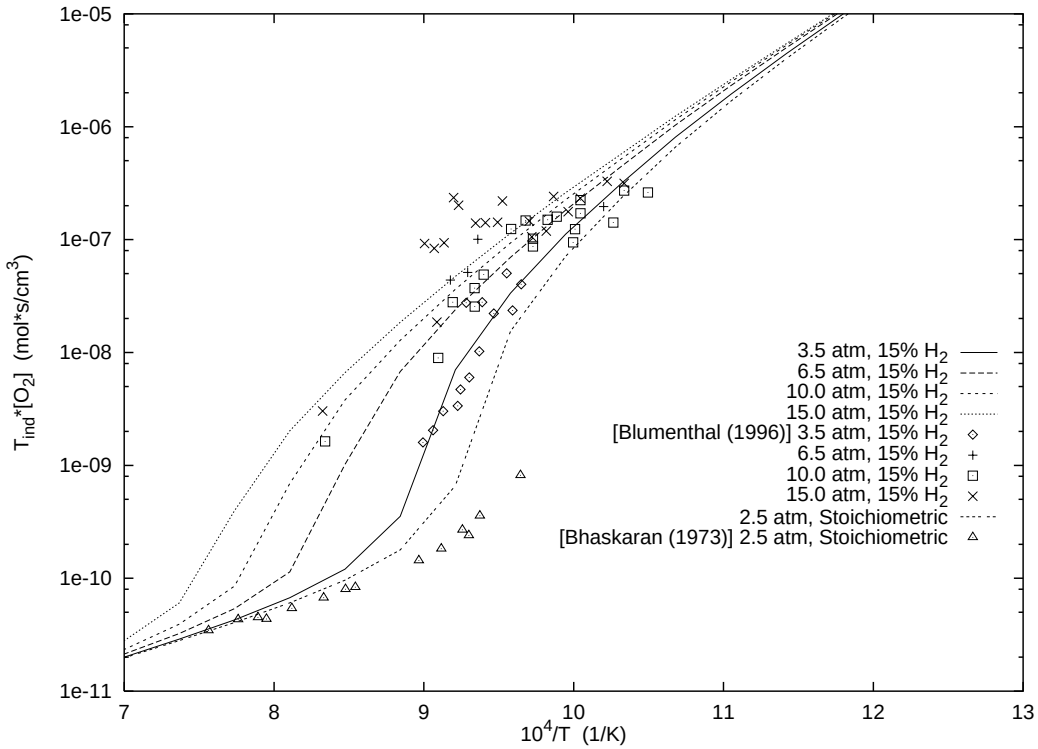

Figure 24: H_2-Air Comparison of Baulch et al. (1992) Mechanism with Blumenthal et al. (1996) and Bhaskaran et al. (1973) Data

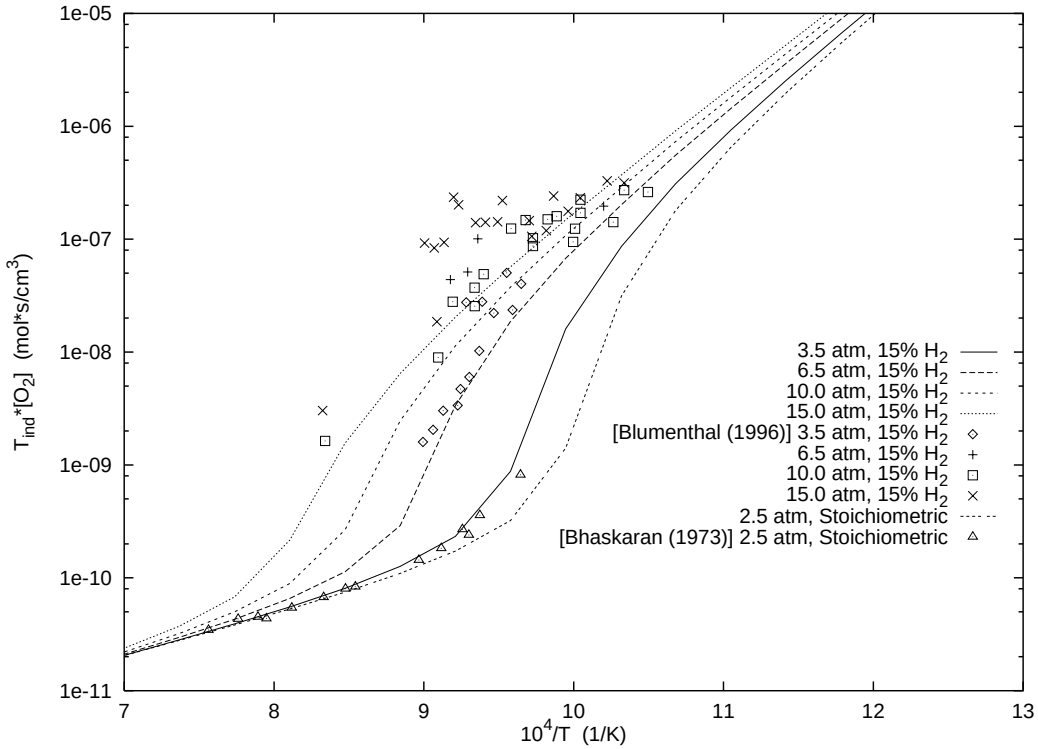

Figure 25: H_2-Air Comparison of Frenklach et al. (1995) (GRI) Mechanism with Blumenthal et al. (1996) and Bhaskaran et al. (1973) Data

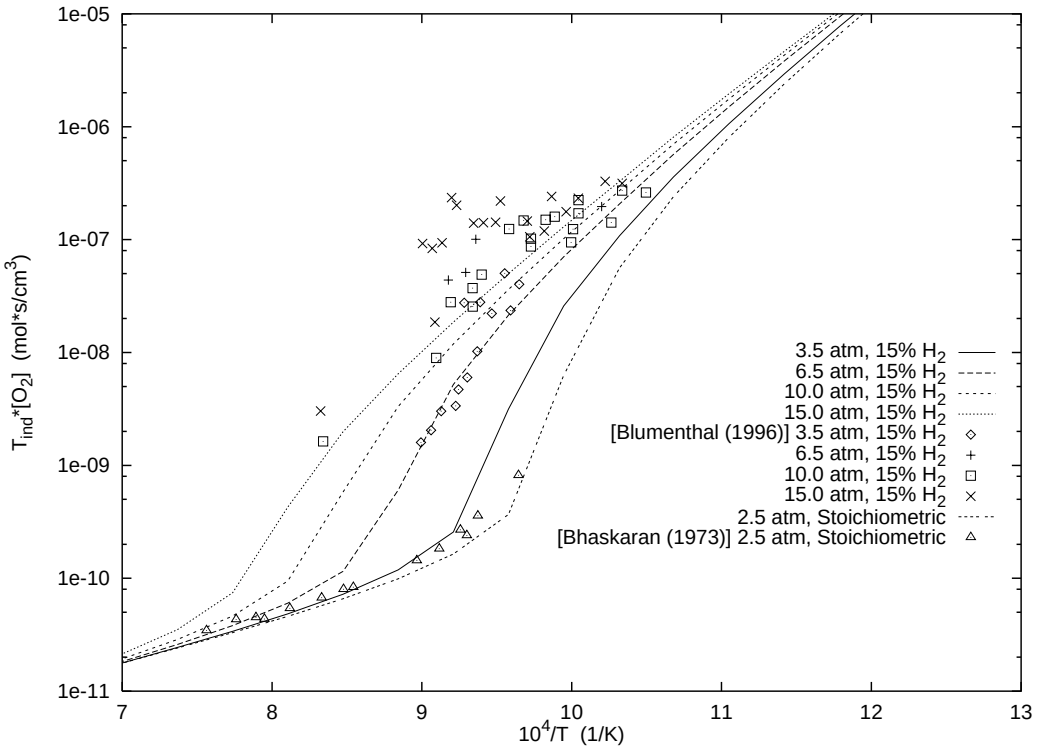

Figure 26: H_2-Air Comparison of Miller and Bowman (1989) Mechanism with Blumenthal et al. (1996) and Bhaskaran et al. (1973) Data

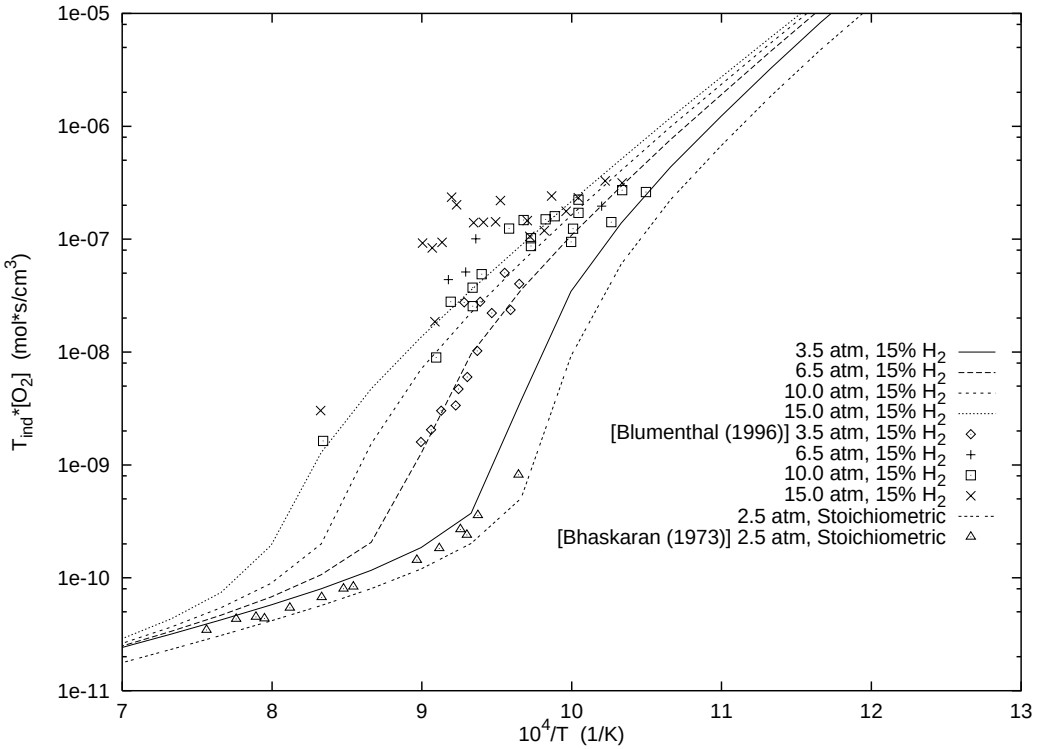

Figure 27: H_2-Air Comparison of modified Miller and Bowman (1989) Mechanism with Blumenthal et al. (1996) and Bhaskaran et al. (1973) Data

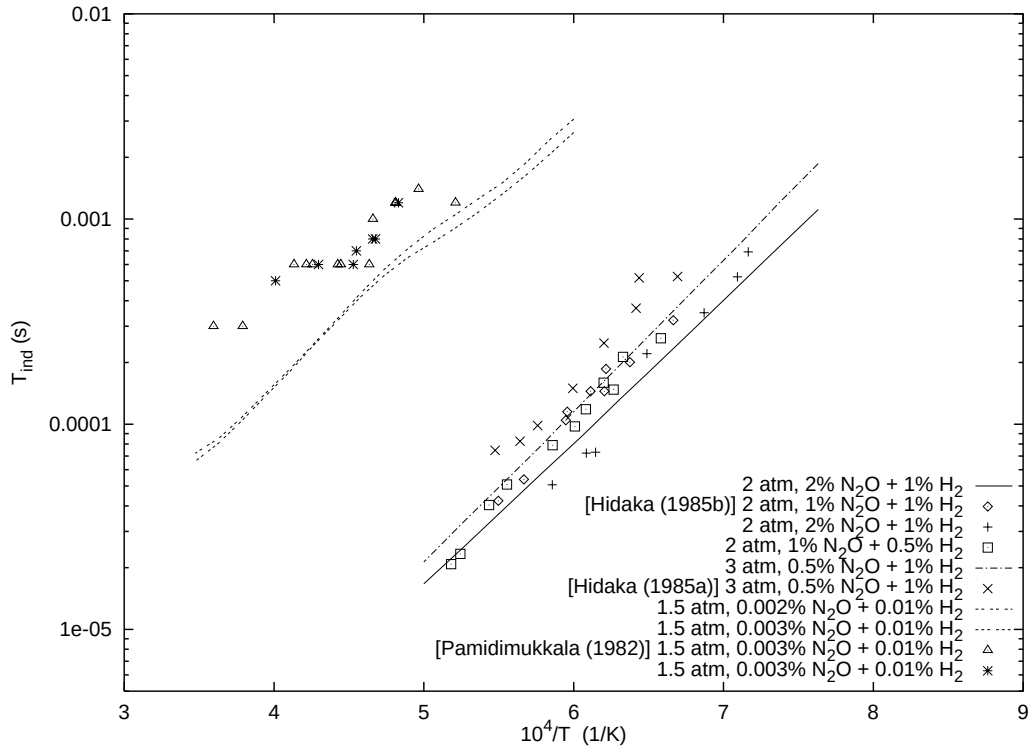

Figure 28: H_2-N_2O-Ar Comparison of Allen et al. (1995) Mechanism with Hidaka et al. (1985a), Hidaka et al. (1985b), and Pamidimukkala and Skinner (1982) Data, at 1.5-3 atm

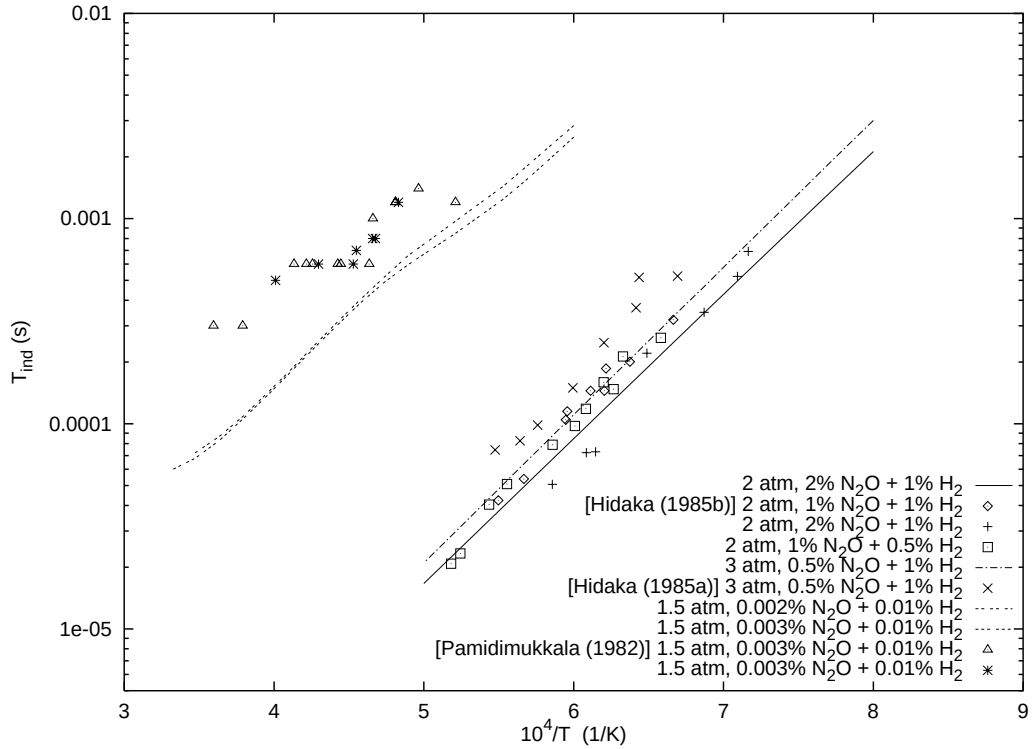

Figure 29: H_2-N_2O-Ar Comparison of Frenklach et al. (1995) Mechanism with Hidaka et al. (1985a), Hidaka et al. (1985b), and Pamidimukkala and Skinner (1982) Data, at 1.5-3 atm

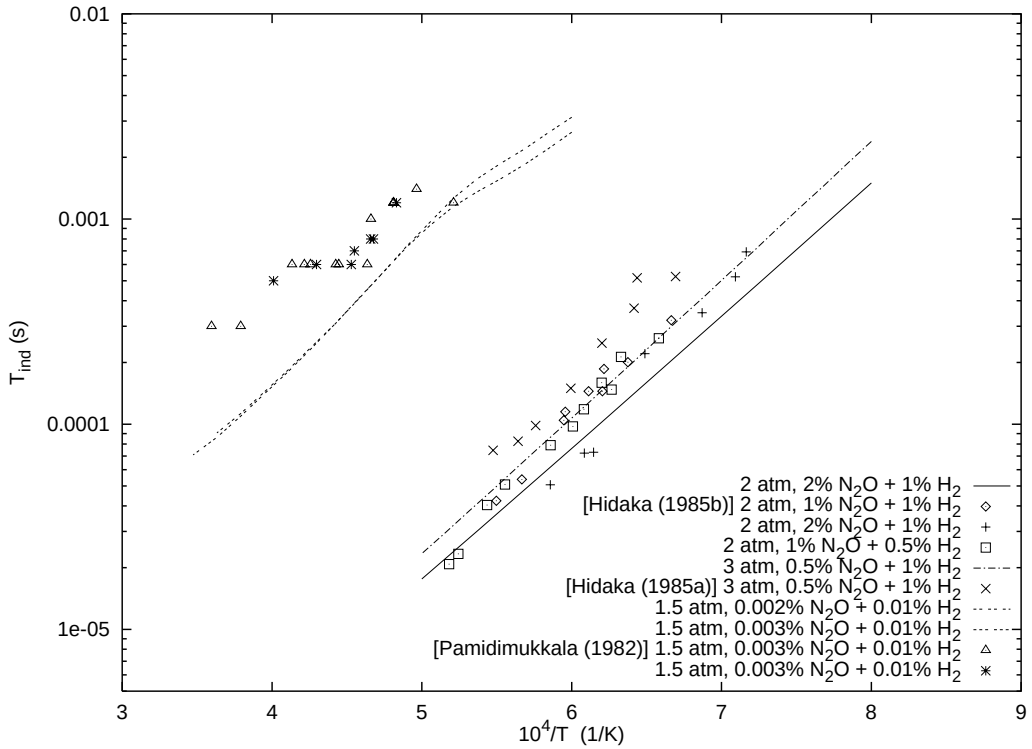

Figure 30: H_2-N_2O-Ar Comparison of Miller and Bowman (1989) Mechanism with Hidaka et al. (1985a), Hidaka et al. (1985b), and Pamidimukkala and Skinner (1982) Data, at 1.5-3 atm

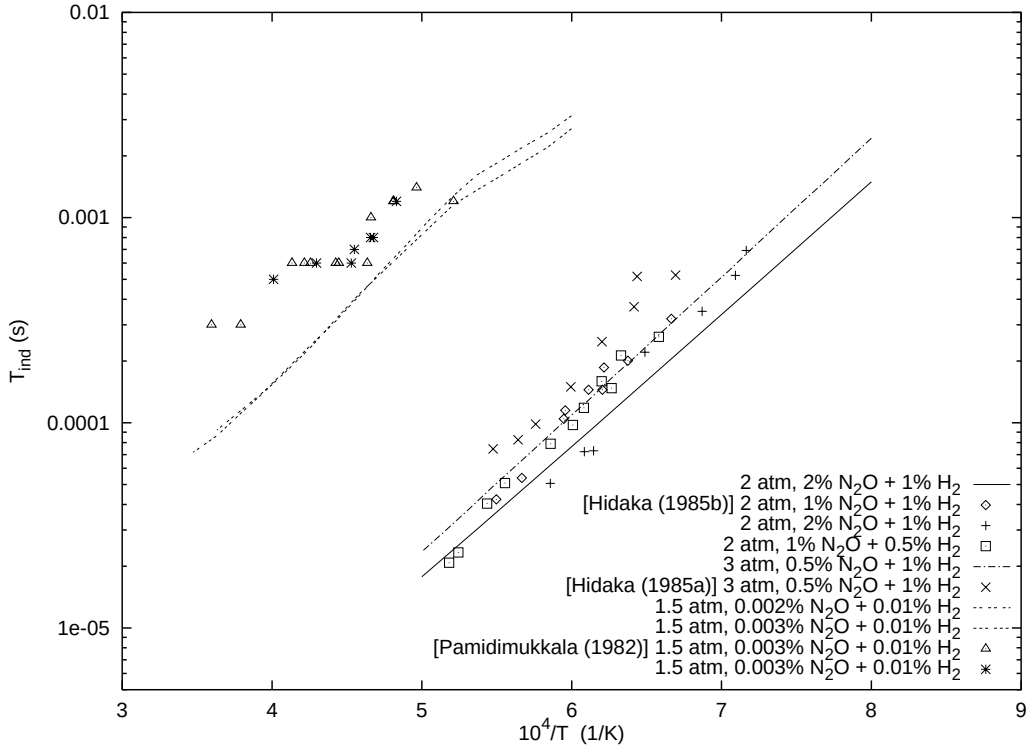

Figure 31: H_2-N_2O-Ar Comparison of modified Miller and Bowman (1989) Mechanism with Hidaka et al. (1985a), Hidaka et al. (1985b), and Pamidimukkala and Skinner (1982) Data, at 1.5-3 atm

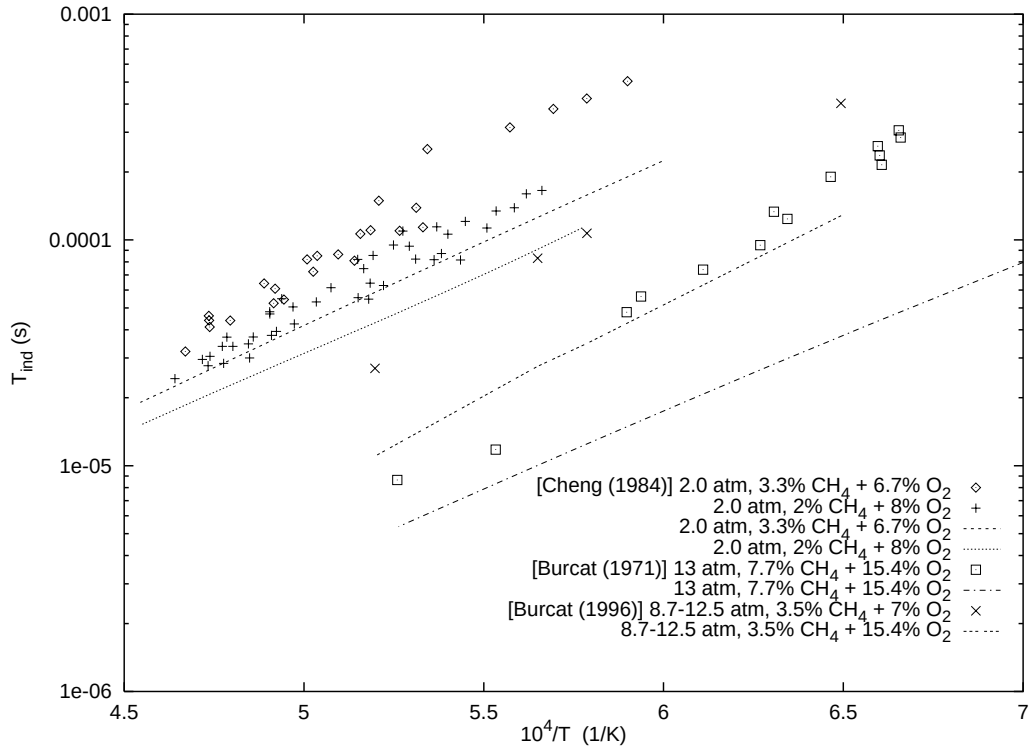

Figure 32: CH_4-O_2-Ar Comparison of Baulch et al. (1994a) Mechanism with Cheng and Oppenheim (1984), Burcat et al. (1971), and Burcat et al. (1996) Data, at 2-13 atm

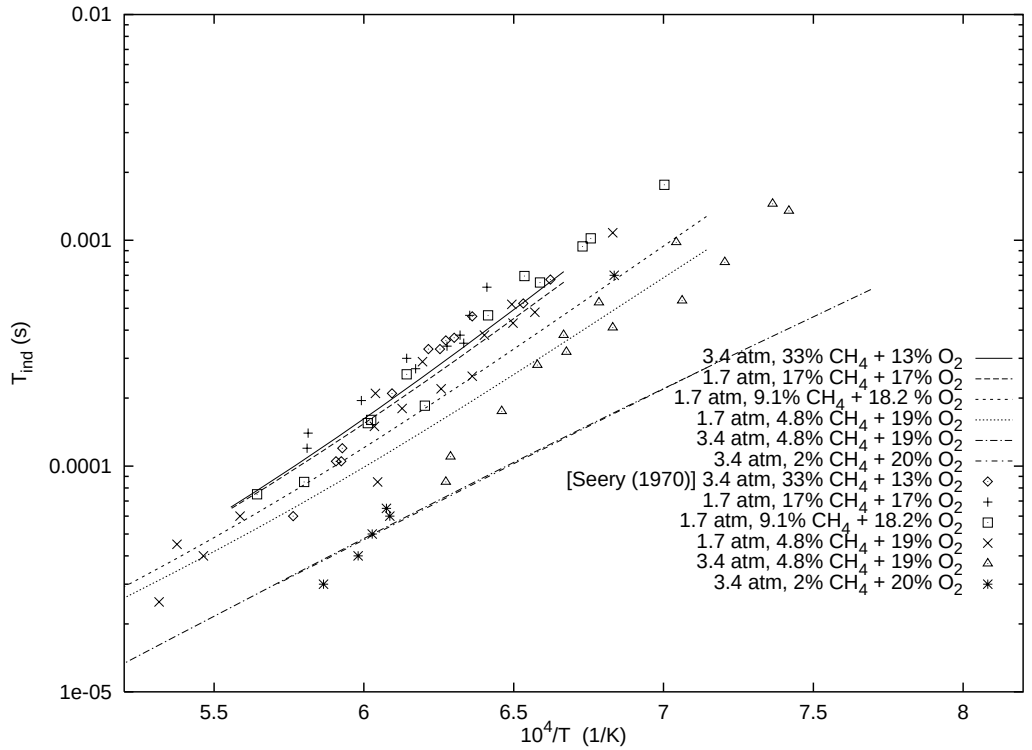

Figure 33: CH_4-O_2-Ar Comparison of Baulch et al. (1994a) Mechanism with Seery and Bowman (1970) Data, at 1.7-3.4 atm

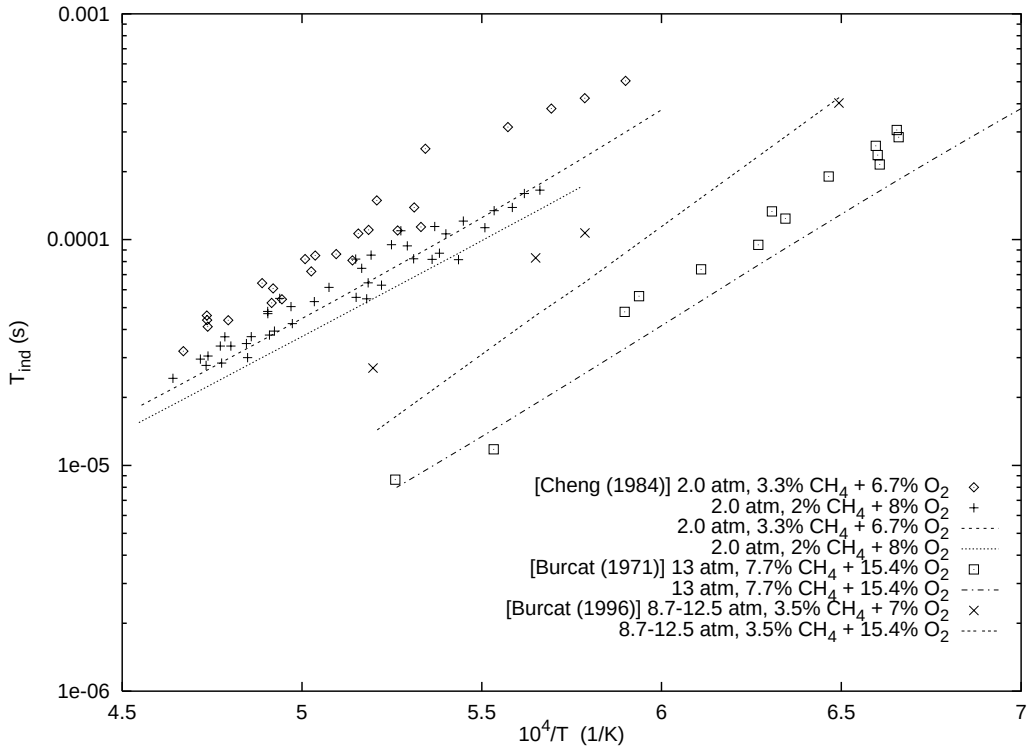

Figure 34: CH_4-O_2-Ar Comparison of Frenklach et al. (1995) Mechanism with Cheng and Oppenheim (1984), Burcat et al. (1971), and Burcat et al. (1996) Data, at 2-13 atm

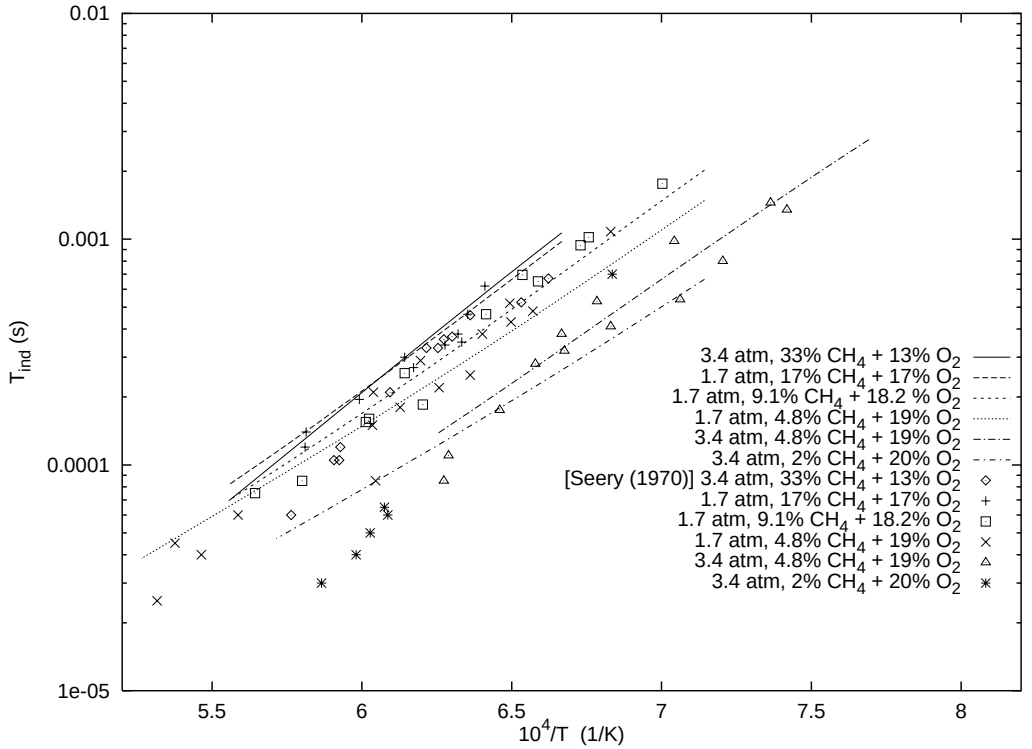

Figure 35: CH_4-O_2-Ar Comparison of Frenklach et al. (1995) Mechanism with Seery and Bowman (1970) Data, at 1.7-3.4 atm

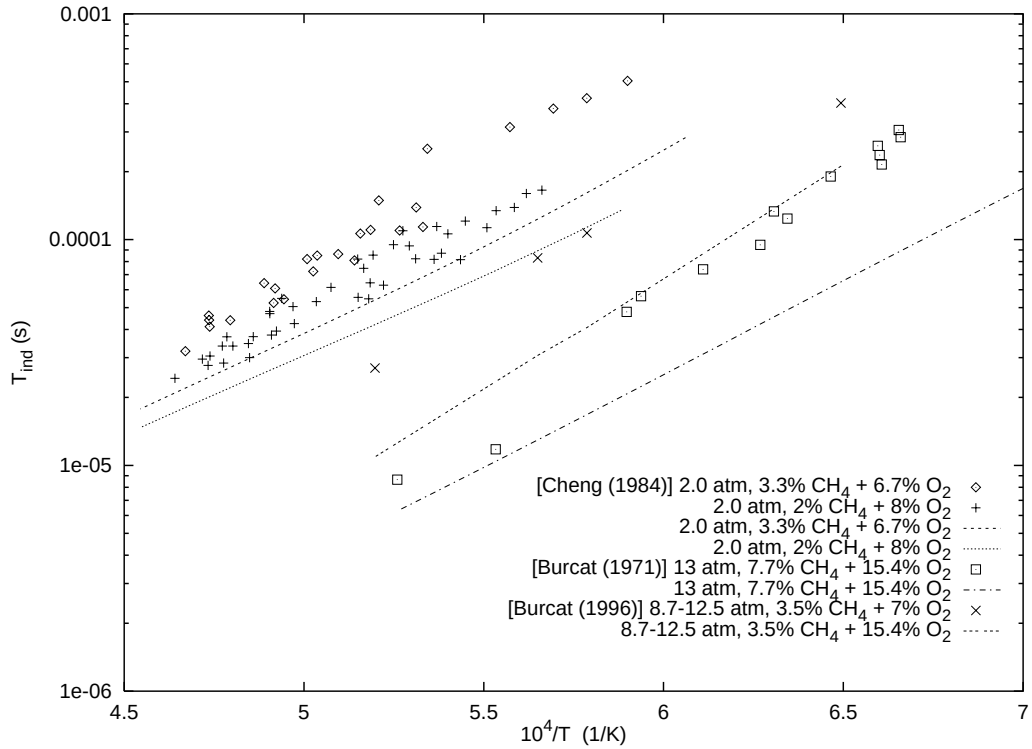

Figure 36: CH_4-O_2-Ar Comparison of Miller and Bowman (1989) Mechanism with Cheng and Oppenheim (1984), Burcat et al. (1971), and Burcat et al. (1996) Data, at 2-13 atm

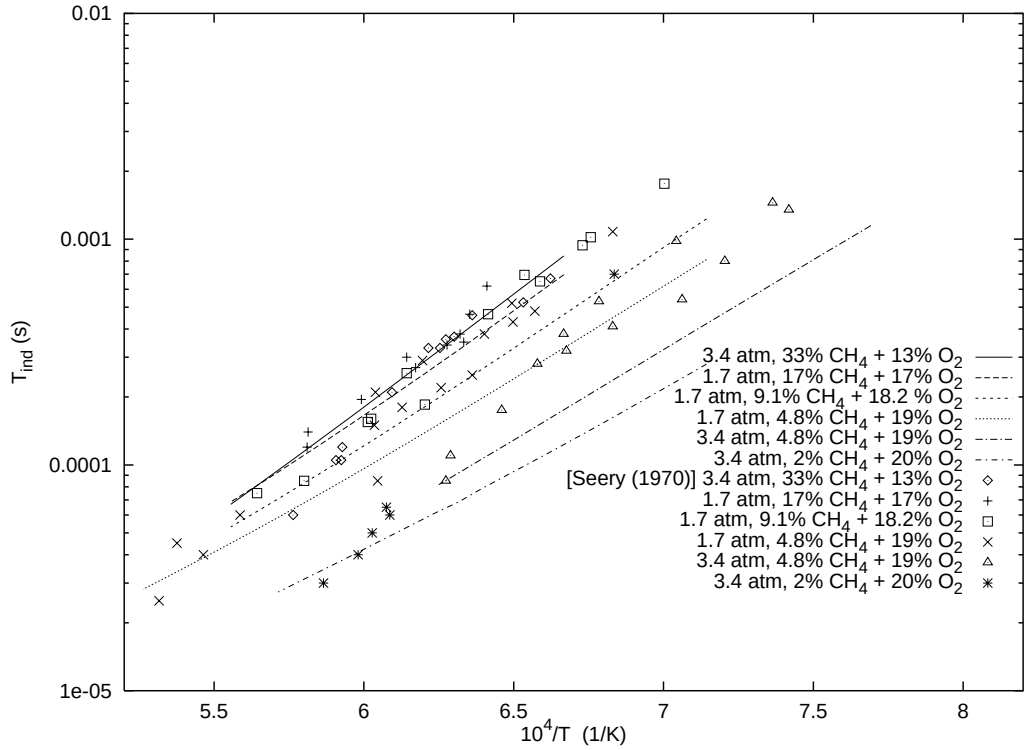

Figure 37: CH_4-O_2-Ar Comparison of Miller and Bowman (1989) Mechanism with Seery and Bowman (1970) Data, at 1.7-3.4 atm

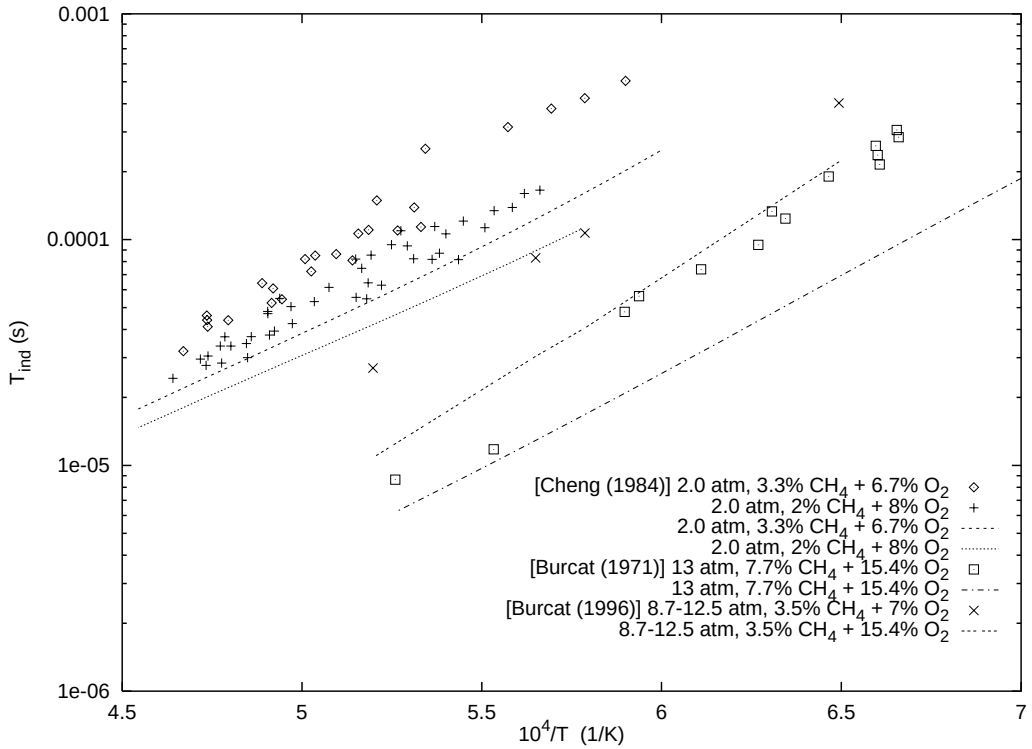

Figure 38: CH_4-O_2-Ar Comparison of modified Miller and Bowman (1989) Mechanism with Cheng and Oppenheim (1984), Burcat et al. (1971), and Burcat et al. (1996) Data, at 2-13 atm

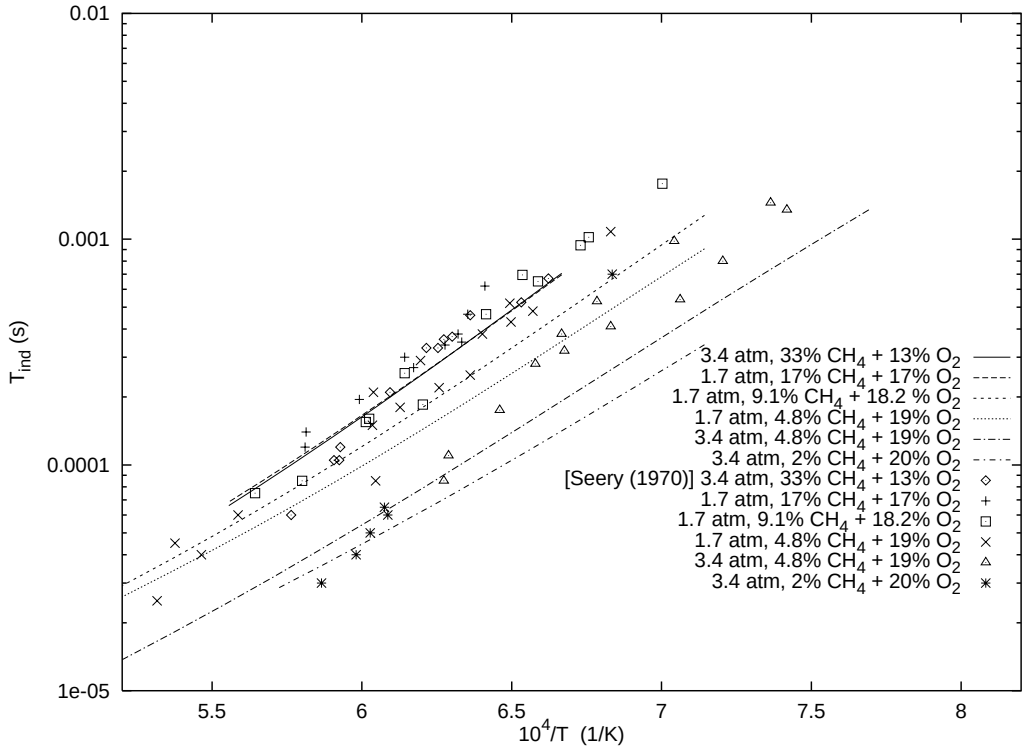

Figure 39: CH_4-O_2-Ar Comparison of modified Miller and Bowman (1989) Mechanism with Seery and Bowman (1970) Data, at 1.7-3.4 atm

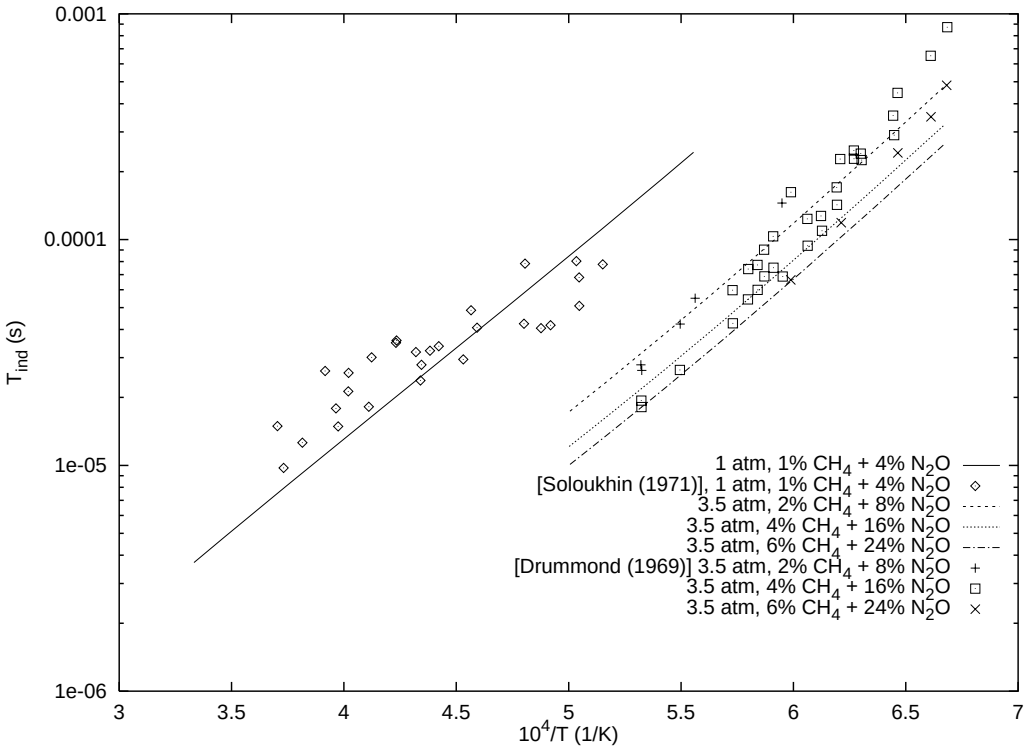

Figure 40: CH_4-N_2O-Ar Comparison of Frenklach et al. (1995) Mechanism with Soloukhin (1971) and Drummond (1969) Data

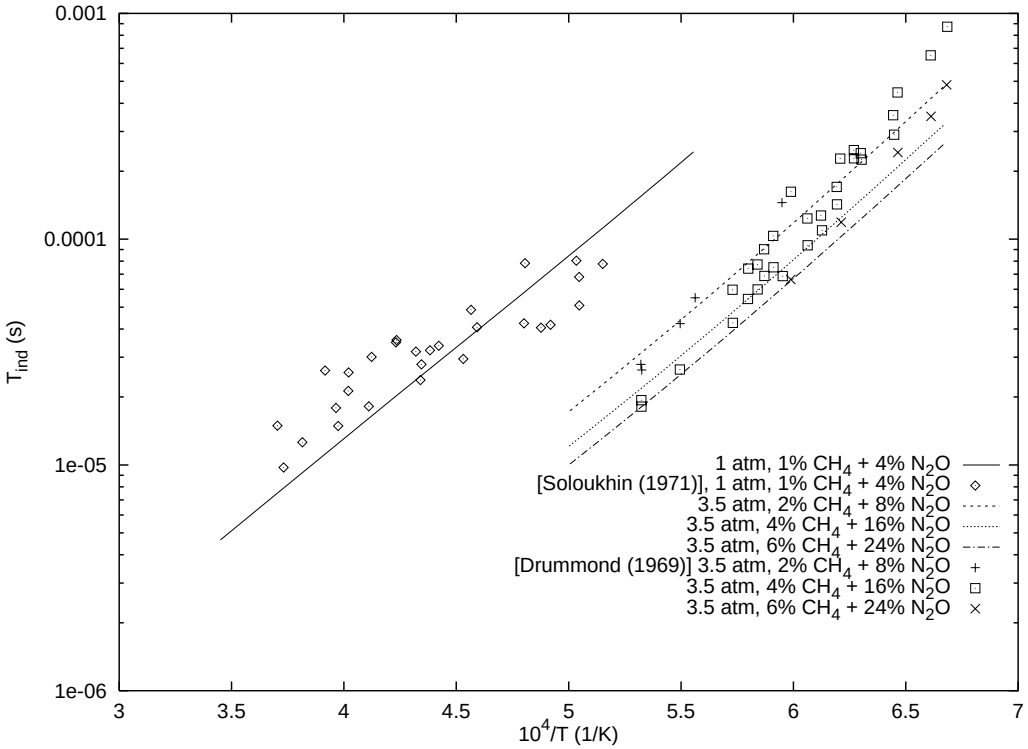

Figure 41: CH_4-N_2O-Ar Comparison of Miller and Bowman (1989) Mechanism with Soloukhin (1971) and Drummond (1969) Data

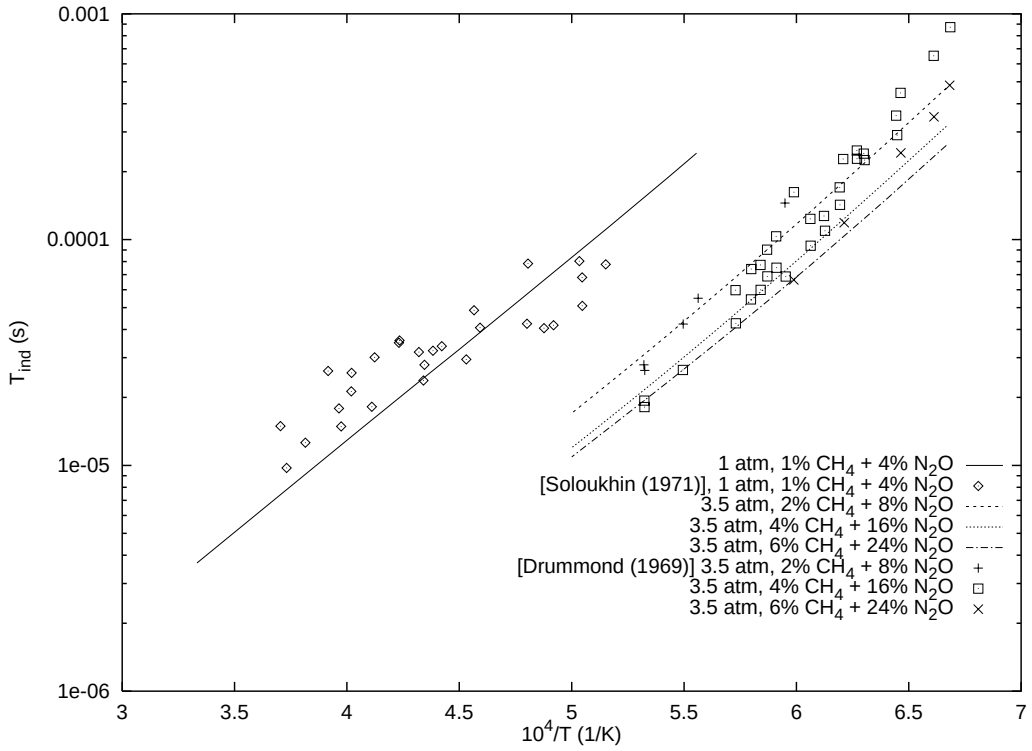

Figure 42: CH_4-N_2O-Ar Comparison of modified Miller and Bowman (1989) Mechanism with Soloukhin (1971) and Drummond (1969) Data

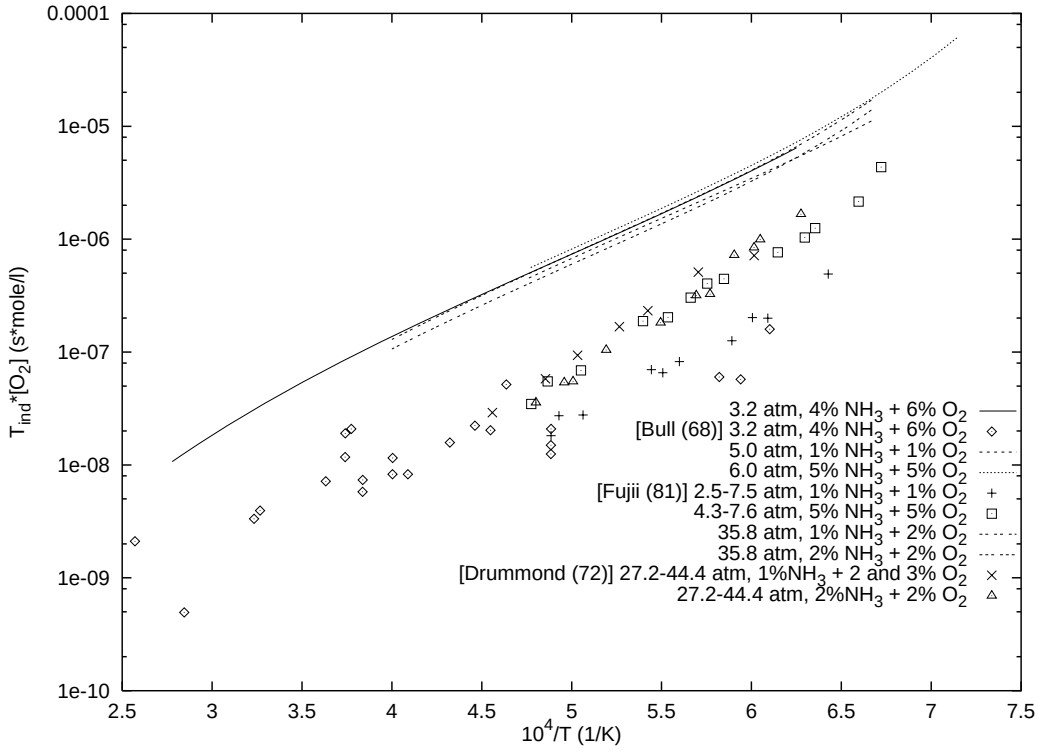

Figure 43: NH_3-O_2-Ar Comparison of Miller and Bowman (1989) Mechanism with Data of Bull (1968), Drummond (1972b), and Fujii et al. (1981)

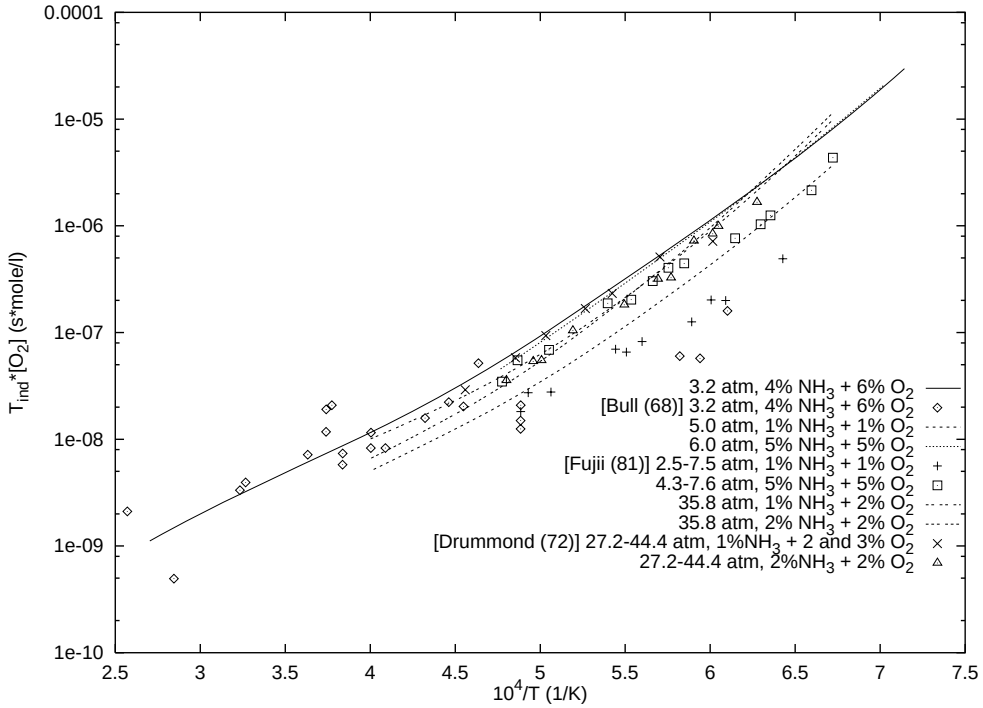

Figure 44: NH_3-O_2-Ar Comparison of modified Miller and Bowman (1989) Mechanism with Data of Bull (1968), Drummond (1972b), and Fujii et al. (1981)

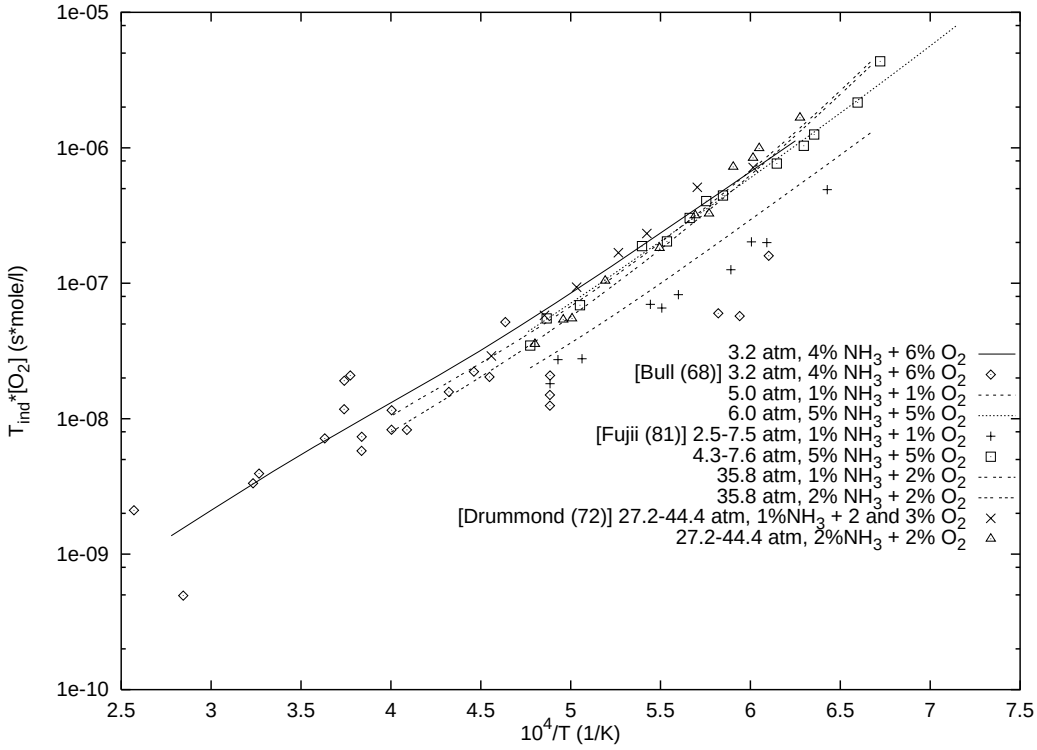

Figure 45: NH_3-O_2-Ar Comparison of Miller et al. (1983) Mechanism with Data of Bull (1968), Drummond (1972b), and Fujii et al. (1981)

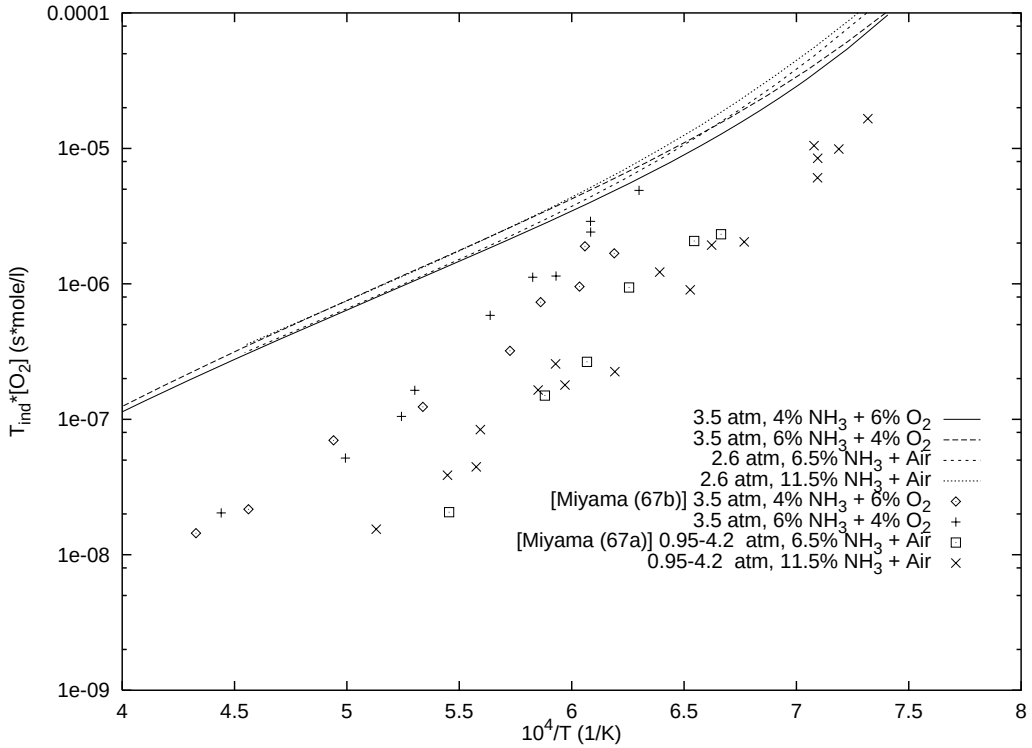

Figure 46: NH_3-O_2-N_2 Comparison of Miller and Bowman (1989) Mechanism with Data of Miyama and Endoh (1967b) and Miyama and Endoh (1967a)

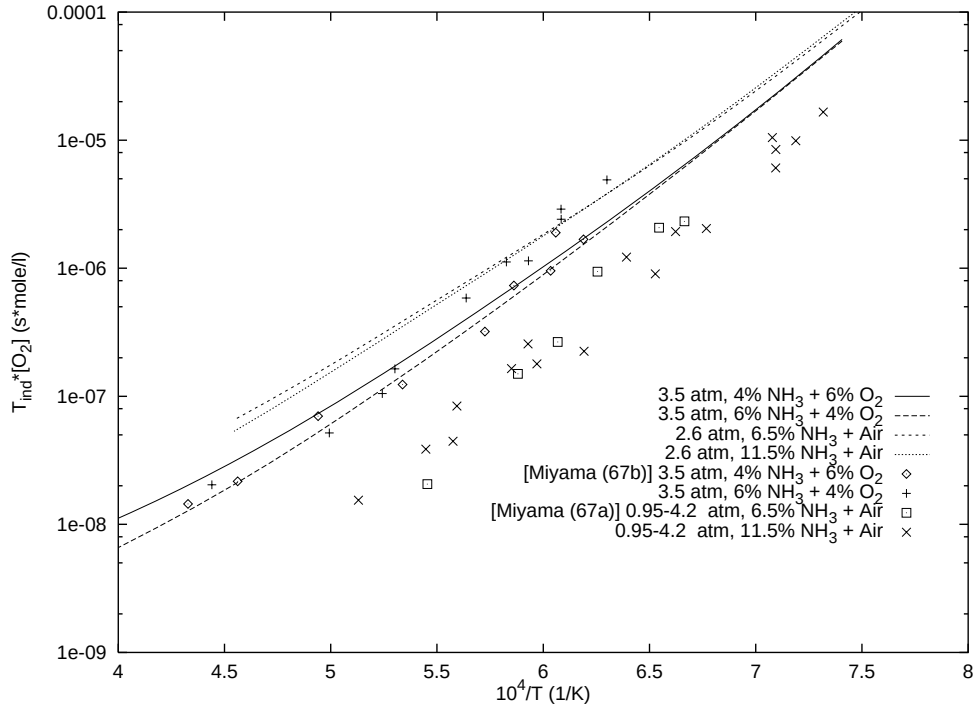

Figure 47: NH_3-O_2-N_2 Comparison of modified Miller and Bowman (1989) Mechanism with Data of Miyama and Endoh (1967b) and Miyama and Endoh (1967a)

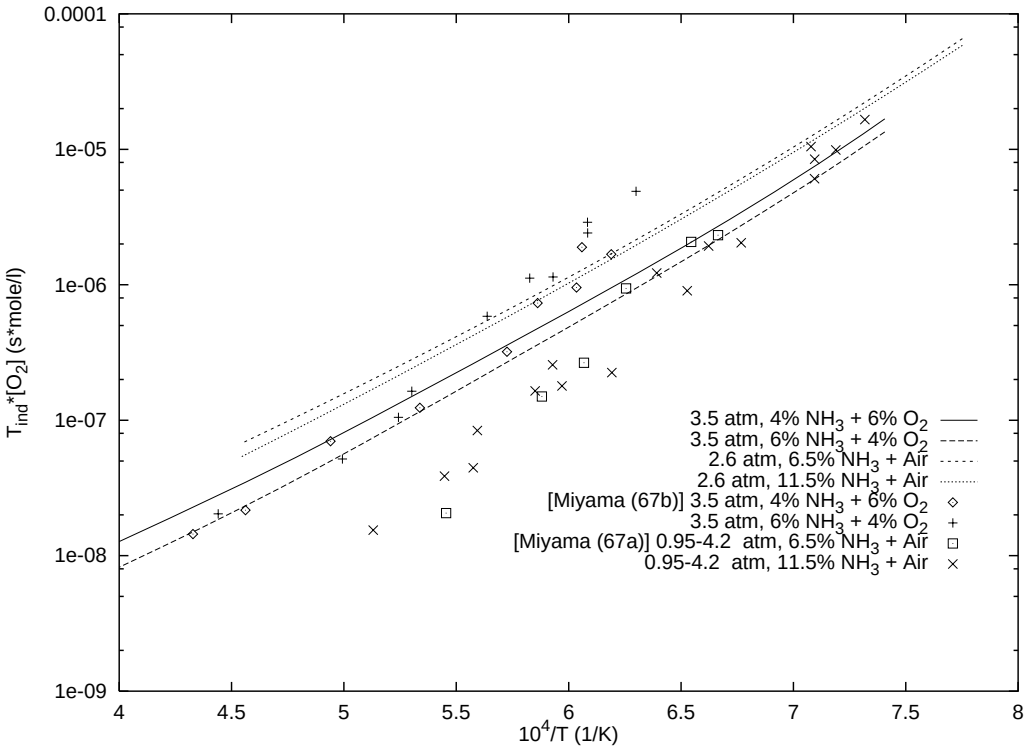

Figure 48: NH_3-O_2-N_2 Comparison of Miller et al. (1983) Mechanism with Data of Miyama and Endoh (1967b) and Miyama and Endoh (1967a)

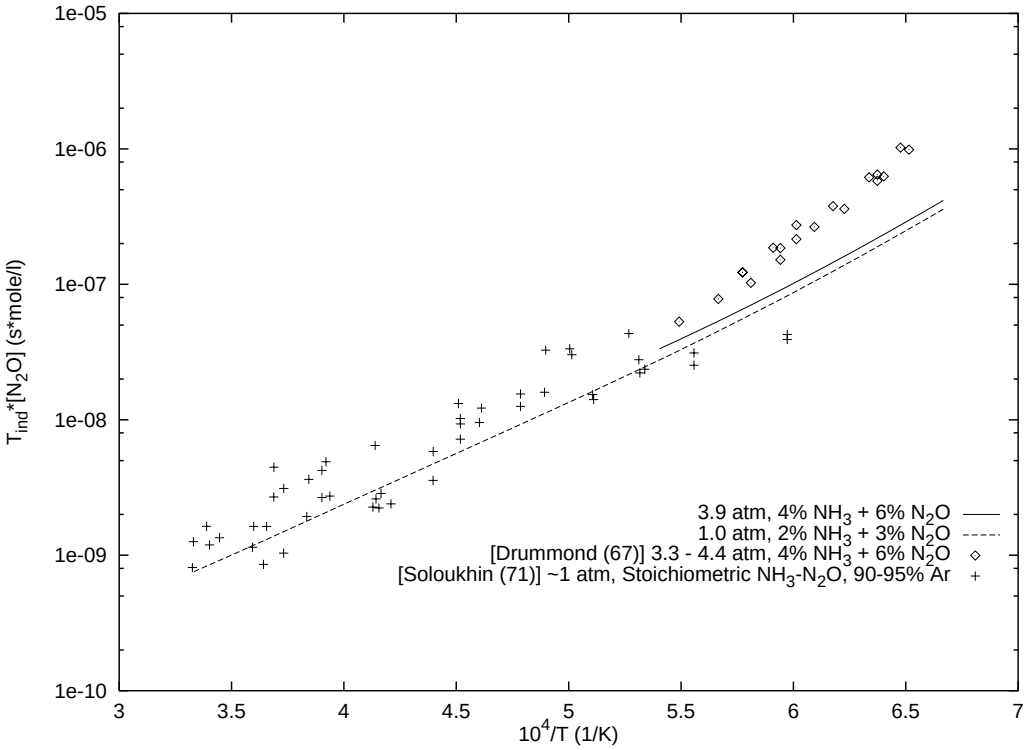

Figure 49: NH_3-N_2O-Ar Comparison of Miller and Bowman (1989) Mechanism with Data of Drummond and Hiscock (1967) and Soloukhin (1971)

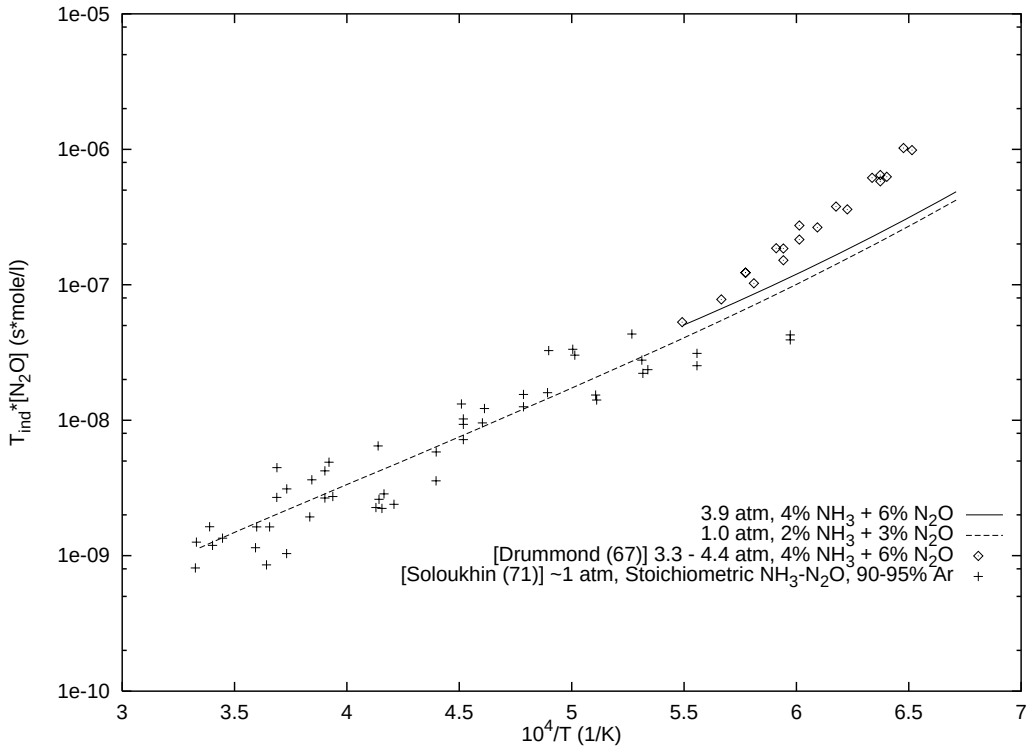

Figure 50: NH_3-N_2O-Ar Comparison of modified Miller and Bowman (1989) Mechanism with Data of Drummond and Hiscock (1967) and Soloukhin (1971)

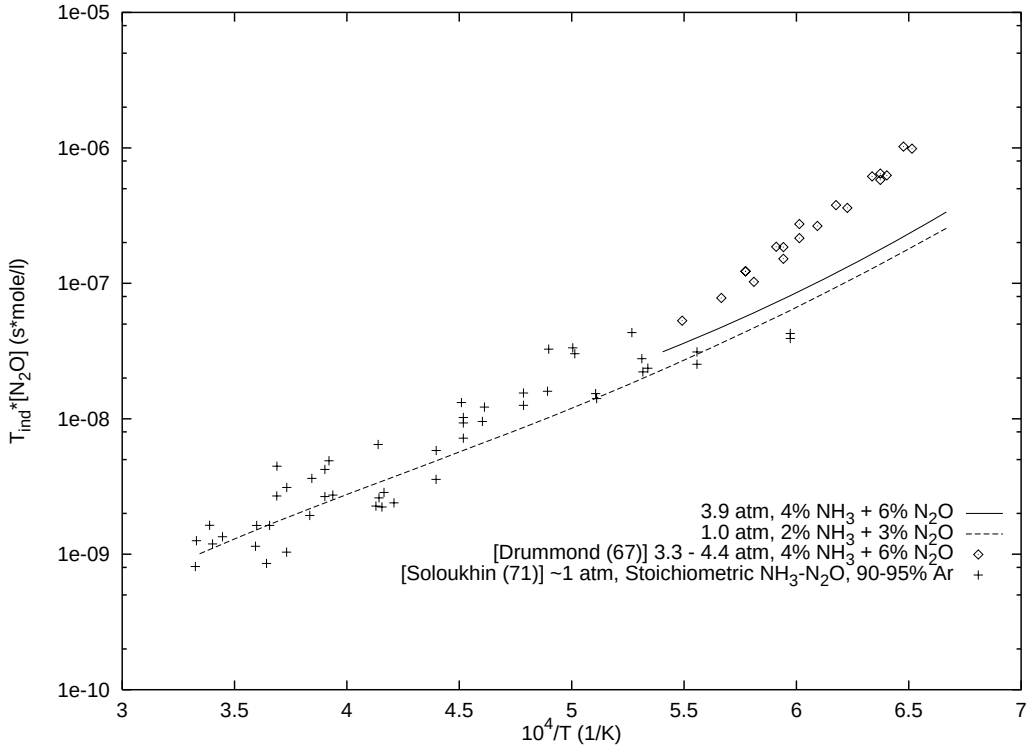

Figure 51: NH_3-N_2O-Ar Comparison of Miller et al. (1983) Mechanism with Data of Drummond and Hiscock (1967) and Soloukhin (1971)

D ZND Calculation Results

No.	H_2 (%)	N_2O (%)	NH_3 (%)	CH_4 (%)
1	100	0	0	0
2	85	0	15	0
3	70	0	30	0
4	50	0	50	0
5	95	0	0	5
6	80	0	15	5
7	65	0	30	5
8	45	0	50	5
9	50	50	0	0
10	42.5	42.5	15	0
11	35	35	30	0
12	25	25	50	0
13	47.5	47.5	0	0
14	40	40	15	5
15	32.5	32.5	30	5
16	22.5	22.5	50	5
17	33.3	66.7	0	0
18	28.3	56.7	15	0
19	23.3	46.7	30	0
20	16.7	33.3	50	0
21	31.7	63.3	0	5
22	26.7	53.3	15	5
23	21.7	43.3	30	5
24	15	30	50	5
25	33	53	14	0
26	42	36	21	1
27	4	4	2	0
28	35	35	10	20

Table 13: Mixture list from Ross and Shepherd (1996), Table E.1, plus two additional mixtures (27 and 28)

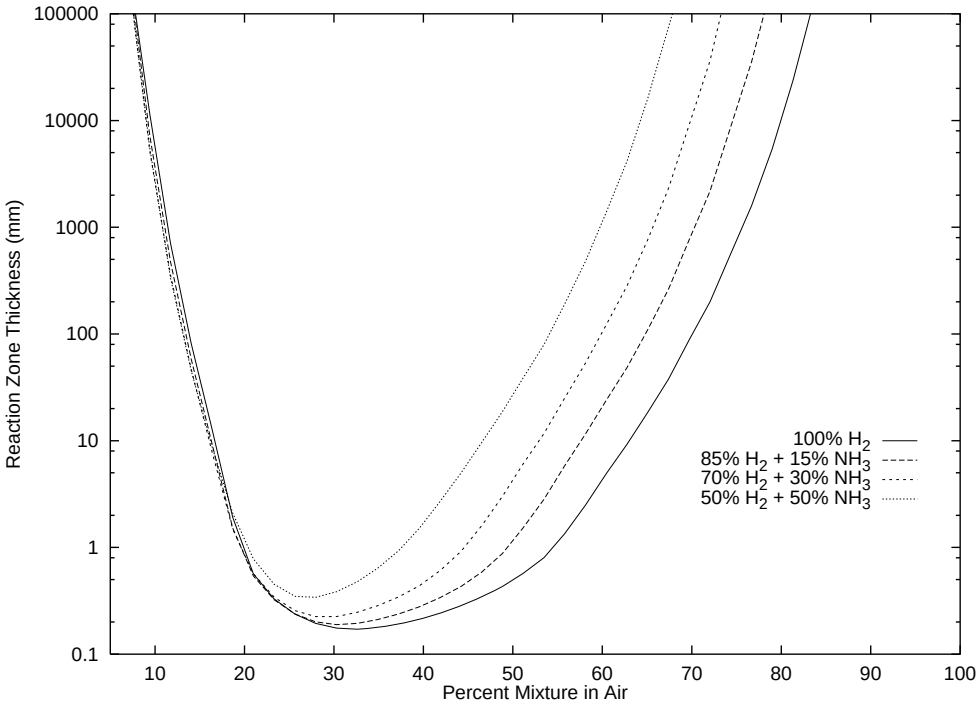

Figure 52: ZND reaction zone thickness calculations for Ross and Shepherd (1996) mixtures 1, 2, 3, and 4

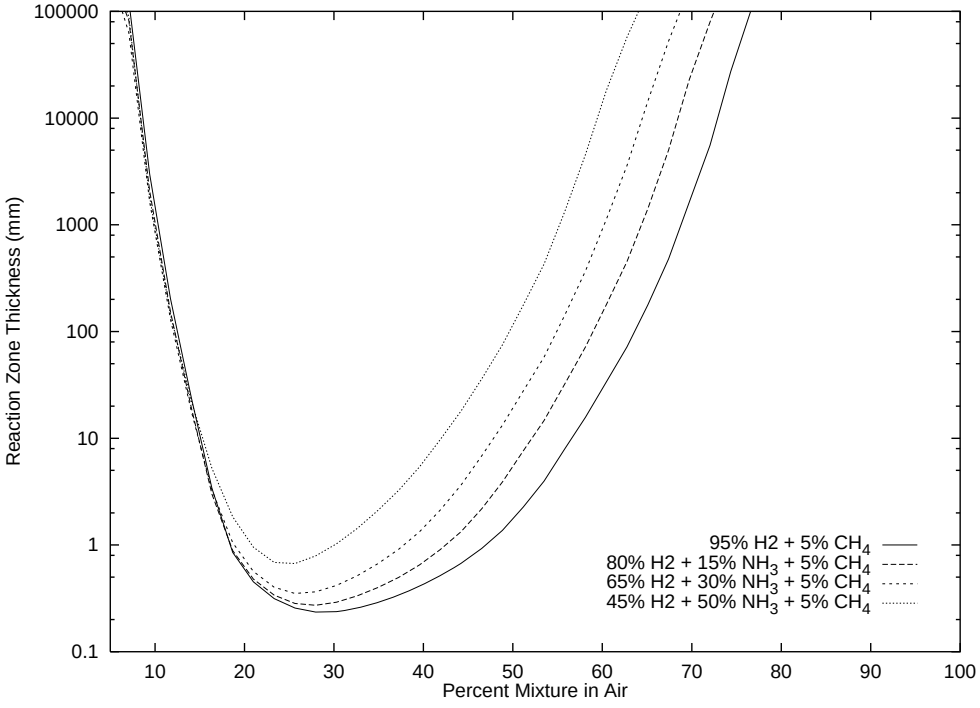

Figure 53: ZND reaction zone thickness calculations for Ross and Shepherd (1996) mixtures 5, 6, 7, and 8

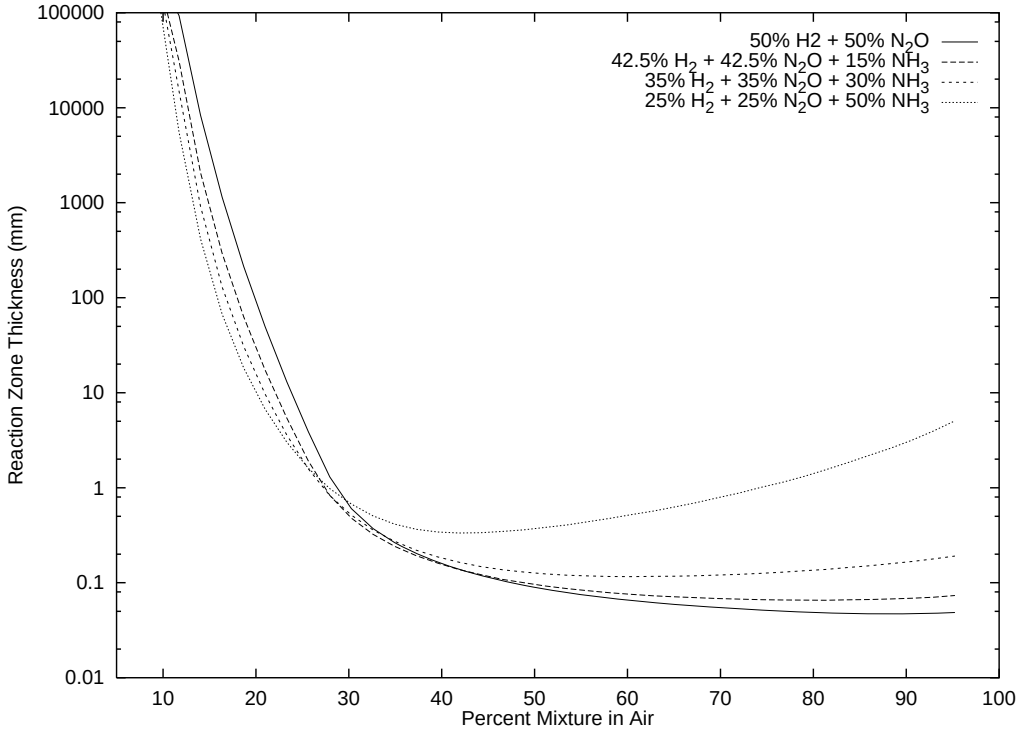

Figure 54: ZND reaction zone thickness calculations for Ross and Shepherd (1996) mixtures 9, 10, 11, and 12

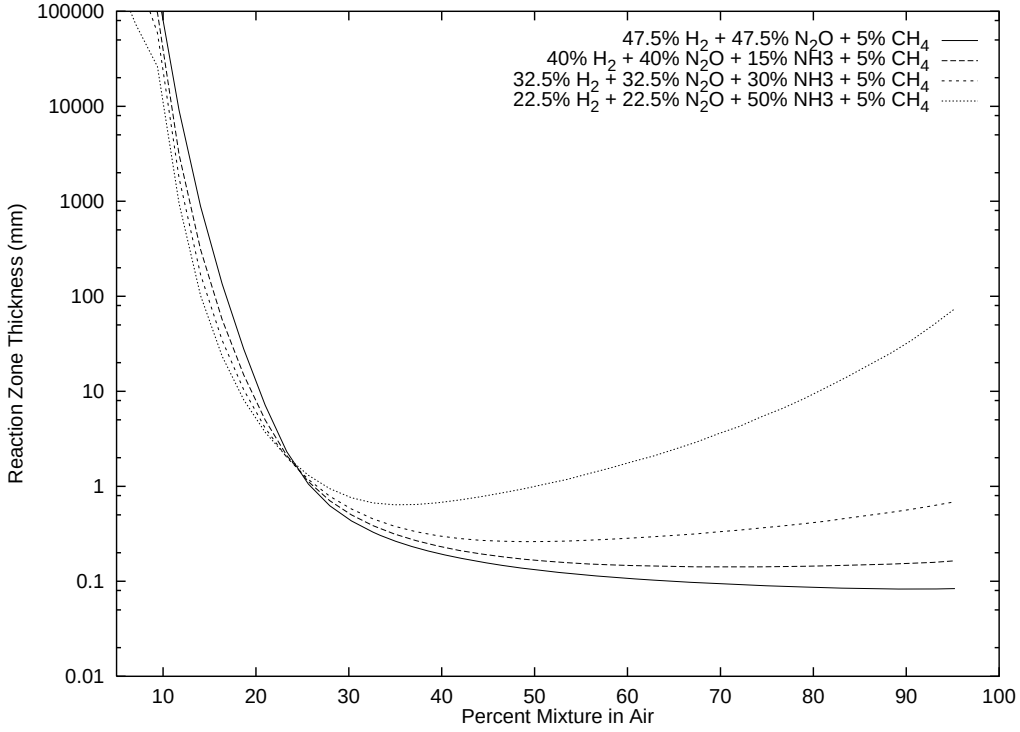

Figure 55: ZND reaction zone thickness calculations for Ross and Shepherd (1996) mixtures 13, 14, 15, and 16

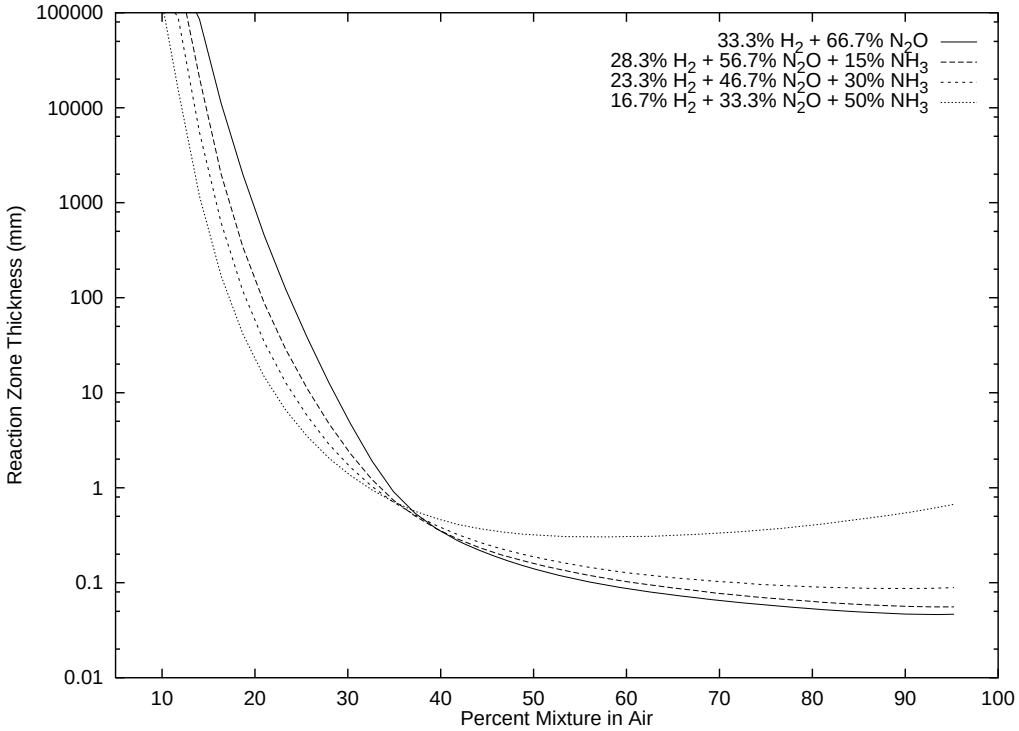

Figure 56: ZND reaction zone thickness calculations for Ross and Shepherd (1996) mixtures 17, 18, 19, and 20

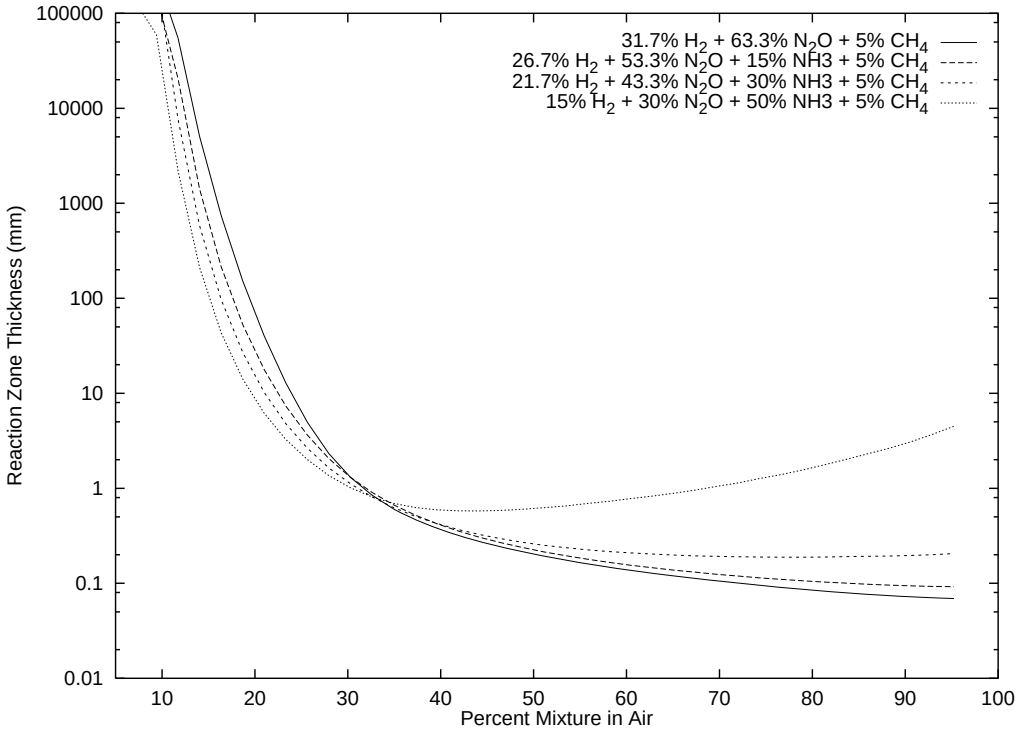

Figure 57: ZND reaction zone thickness calculations for Ross and Shepherd (1996) mixtures 21, 22, 23, and 24

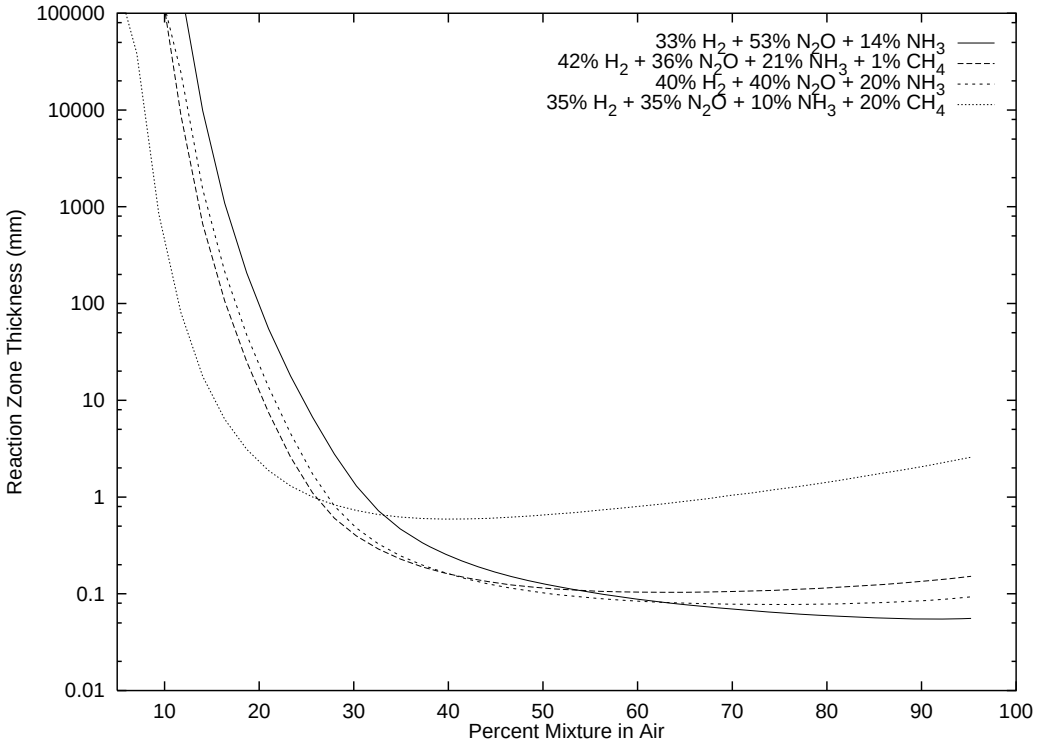

Figure 58: ZND reaction zone thickness calculations for Ross and Shepherd (1996) mixtures 25, 26, 27, and 28

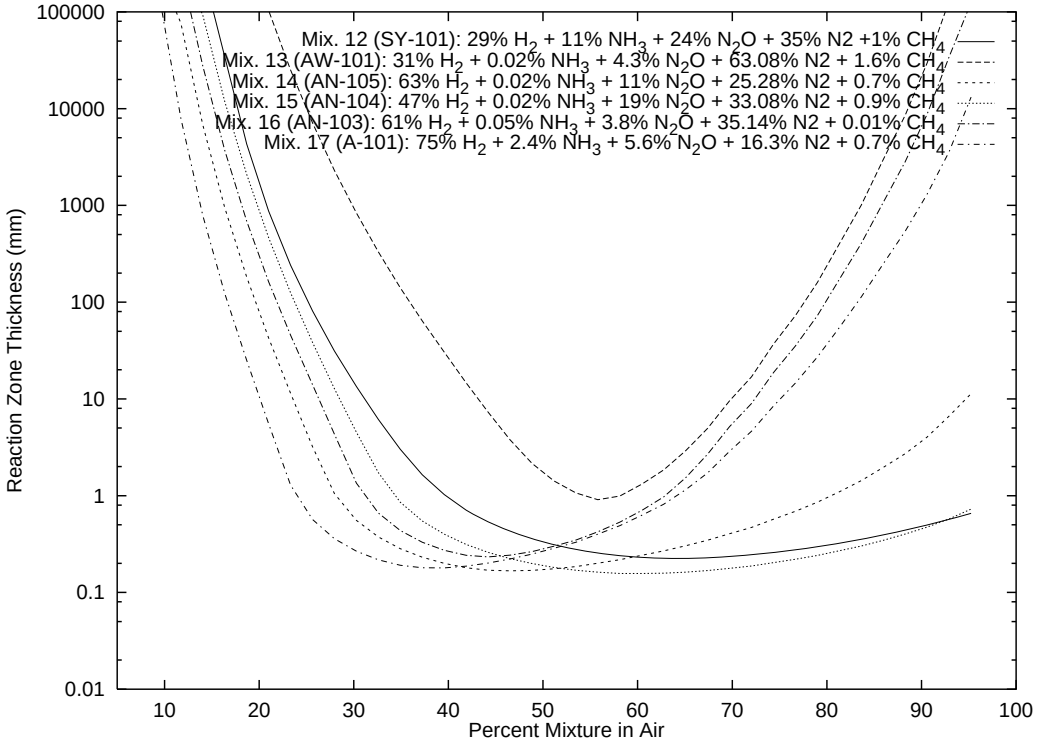

Figure 59: ZND reaction zone thickness calculations for Table 1 mixtures 12, 13, 14, 15, 16, and 17

E Reaction Mechanisms

The core of chemical kinetics calculations is the reaction mechanism, which specifies the set of elementary reactions to be considered and the rate parameters that describe the temperature dependency of the rates of these reactions. The rate equation used is the modified Arrhenius equation, which requires three parameters:

$$k = AT^n \exp(-E/RT)$$

The dimensions of k are $\frac{1}{\text{concentration}^{m-1}\text{time}}$ where m is the order of the reaction. The temperature exponent n is dimensionless while temperature is understood to be in K. The activation energy E has dimensions of energy/mole, although sometimes the ratio E/R is provided instead, which has a dimension of temperature. In the tables of reaction mechanisms below, units have not been used consistently so the units of each table are provided in the header. Most elementary reactions described below are bidirectional, meaning that the rate parameters for one direction are provided, but the reverse rates can be computed through equilibrium considerations. Some reactions are specified as unidirectional (by $\Rightarrow$), generally because rate data are directly available for the reverse reaction. Other annotations are consistent with conventions of the Sandia gas phase chemical kinetics package (Kee et al. 1989). In calculations performed with these mechanisms for this report, thermodynamic data were obtained from the Sandia thermodynamic database whenever possible. Where data were not available from this database, they were taken from the GRI thermodynamic database (Frenklach et al. 1995).

E.1 Allen et al. (1995)

Allen et al. (1995) uses a fall-off relation that is a special case of the SRI form available in the Sandia package, when F_c is constant. In this case, the package parameters are given by $a = F_c$, $b = 0$, $c = 0$, and d and e are not used. A couple of reactions specify temperature dependent F_c that can not be handled exactly by the SRI form. In these cases, any optimum approximate match will be appropriate over a certain temperature range. For lack of a better criteria, an exact match at 0 K has been applied to derive software parameters.

Reaction	A (cm-moles-sec-K)	n	E (cal/mole)
H+O2⇌O+OH	1.910E+14	0.00	16440
O+H2⇌H+OH	5.060E+04	2.67	6290
OH+H2⇌H2O+H	2.160E+08	1.51	3430
H2O+O⇌OH+OH	2.970E+06	2.02	13400
H2+M⇌H+H+M	4.570E+19	-1.40	104400
Enhanced Collision Efficiencies:			
	H2O=12.0, H2=2.5, AR=0.0		
H2+AR⇌H+H+AR	5.840E+18	-1.10	104400
O+O+M⇌O2+M	6.170E+15	-0.50	0
Enhanced Collision Efficiencies:			
	H2O=12.0, H2=2.5, AR=0.0		
O+O+AR⇌O2+AR	1.890E+13	0.00	-1790
H+O+M⇌OH+M	4.720E+18	-1.00	0
Enhanced Collision Efficiencies:			
	H2O=12.0, H2=2.5, AR=0.75		
OH+H+M⇌H2O+M	2.210E+22	-2.00	0
Enhanced Collision Efficiencies:			
	H2O=12.0, H2=2.5, AR=0.0		
OH+H+AR⇌H2O+AR	8.410E+21	-2.00	0
H+O2(+M)⇌HO2(+M)	4.520E+13	0.00	0
Low pressure limit	6.70E+19	-1.42	0.0
SRI parameters: a=1.0, b=0.0, c=0.0			
Enhanced Collision Efficiencies:			
	H2O=12.0, H2=2.5, AR=0.0		
H+O2(+AR)⇌HO2(+AR)	4.520E+13	0.00	0
Low pressure limit	1.49E+15	0.00	-1000.0
SRI parameters: a=1.0, b=0.0, c=0.0			
HO2+H⇌H2+O2	6.620E+13	0.00	2130
HO2+H⇌OH+OH	1.690E+14	0.0	874
HO2+O⇌O2+OH	1.750E+13	0.0	-397
HO2+OH⇌H2O+O2	1.900E+16	-1.0	0
HO2+HO2⇌H2O2+O2	4.200E+14	0.0	11980
Duplicate Reaction			
HO2+HO2⇌H2O2+O2	1.300E+11	0.0	-1629
Duplicate Reaction			
H2O2(+M)⇌OH+OH(+M)	2.950E+14	0.0	48400
Low pressure limit	1.20E+17	0.0	45500
SRI parameters: a=0.5, b=0.0, c=0.0			
Enhanced Collision Efficiencies:			
	H2O=12.0, H2=2.5, AR=0.0		
H2O2(+AR)⇌OH+OH(+AR)	2.950E+14	0.0	48400
Low pressure limit	1.90E+16	0.0	43000
SRI parameters: a=0.5, b=0.0, c=0.0			
H2O2+H⇌H2O+OH	1.000E+13	0.0	3590
H2O2+H⇌HO2+H2	4.820E+13	0.0	7950
H2O2+O⇌OH+HO2	9.640E+06	2.0	3970
H2O2+OH⇌H2O+HO2	1.000E+12	0.0	0
Duplicate Reaction			
H2O2+OH⇌H2O+HO2	5.800E+14	0.0	9560
Duplicate Reaction			
NO+H2⇌HNO+H	1.390E+13	0.0	56530
NO+O(+M)⇌NO2(+M)	1.300E+15	-0.75	0
Low pressure limit	4.720E+24	-2.87	1551
SRI parameters: a=0.95, b=0.0, c=0.0			
Enhanced Collision Efficiencies:			
	AR=0.0		
NO+O(+AR)⇌NO2(+AR)	1.300E+15	-0.75	0

Reaction	A (cm-moles-sec-K)	n	E (cal/mole)
Low pressure limit	7.560E+19	-1.41	0
SRI parameters: a=0.95, b=0.0, c=0.0			
NO+H(+M)⇌HNO(+M)	1.520E+15	-0.41	0
Low pressure limit	8.96E+19	-1.32	735.2
SRI parameters: a=0.82, b=0.0, c=0.0			
Enhanced Collision Efficiencies:			
	AR=0.75		
NO+OH(+M)⇌HONO(+M)	1.990E+12	-0.05	-721
Low pressure limit	5.08E+23	-2.51	-67.6
SRI parameters: a=0.62, b=0.0, c=0.0			
Enhanced Collision Efficiencies:			
	AR=0.75		
NO2+H2⇌HONO+H	3.210E+12	0.0	28810
NO2+O⇌O2+NO	3.910E+12	0.0	-238
NO2+O(+M)⇌NO3(+M)	1.330E+13	0.0	0
Low pressure limit	1.49E+28	-4.08	2467
SRI parameters: a=0.79, b=0.0, c=0.0			
Enhanced Collision Efficiencies:			
	AR=0.75		
NO2+H⇌NO+OH	1.320E+14	0.0	362
NO2+OH(+M)⇌HNO3(+M)	2.410E+13	0.0	0
Low pressure limit	6.42E+32	-5.49	2350
SRI parameters: a=0.725, b=0.0, c=0.0			
Enhanced Collision Efficiencies:			
	AR=0.75		
NO2+OH⇌HO2+NO	1.810E+13	0.0	6676
NO2+NO2⇌NO3+NO	9.640E+09	0.73	20920
NO2+NO2⇌2NO+O2	1.630E+12	0.0	26120
NH+O2⇌HNO+O	3.890E+13	0.0	17890
NH+O2⇌NO+OH	7.600E+10	0.0	1530
NH+O⇌NO+H	5.500E+13	0.0	0
NH+OH⇌HNO+H	2.000E+13	0.0	0
NH+NO⇌N2O+H	2.940E+14	-0.4	0
Duplicate Reaction			
NH+NO⇌N2O+H	-2.160E+13	-0.23	0
Duplicate Reaction			
NH+NO⇌N2+OH	2.160E+13	-0.23	0
NH+NO2⇌NO+HNO	1.000E+11	0.5	4000
NH+NH⇌N2+H+H	5.100E+13	0.0	0
HNO+O⇌OH+NO	1.810E+13	0.0	0
HNO+OH⇌H2O+NO	4.820E+13	0.0	993.5
HNO+NO⇌N2O+OH	2.000E+12	0.0	26000
HNO+NO2⇌HONO+NO	6.020E+11	0.0	1987
HNO+HNO⇌H2O+N2O	8.510E+08	0.0	3080
HONO+O⇌OH+NO2	1.200E+13	0.0	5961
HONO+OH⇌H2O+NO2	1.260E+10	1.0	135.1
N2O(+M)⇌N2+O(+M)	7.910E+10	0.0	56020
Low pressure limit	9.13E+14	0.0	57690
SRI parameters: a=1.0, b=0.0, c=0.0			
Enhanced Collision Efficiencies:			
	AR=0.63, H2O=7.5		
N2O+O⇌O2+N2	1.000E+14	0.0	28000
N2O+O⇌2NO	1.000E+14	0.0	28000
N2O+H⇌N2+OH	2.530E+10	0.0	4550
Duplicate Reaction			
N2O+H⇌N2+OH	2.230E+14	0.0	16750
Duplicate Reaction			

Reaction	A (cm-moles-sec-K)	n	E (cal/mole)
N2O+NO⇌NO2+N2	1.000E+14	0.0	50000

E.2 Baulch et al. (1994a)

The fall-off relation used (typically) in Baulch et al. (1994a) for constant F_c is a special case of the SRI form with $a = F_c$, $b = 0$, and $c = 0$. The data, as published, although intended as such, were not in a convenient form for use in modeling. Many of the rates were stated as unidirectional for consumption of the reactants, sometimes with a list of possible products, but often without detailed branching information. Naturally, a complete mechanism requires detailed accounting of all species. Where a choice of products was given without proportioning data, the overall rate was divided equally among the products. Unidirectional rates were used wherever reverse rates were independently provided. Only reactions considered pertinent to the current work have been included. More hydrocarbon rates (for molecules larger than CH_4) are available from the original publication.

Reaction	A (cm-molecules-sec-K)	n	E (K)
O+H2⇌OH+H	8.500E-20	2.67	3160
O+OH⇒O2+H	2.400E-11	0.00	353
O+HO2⇌OH+O2	5.300E-11	0.00	0
O+H2O2⇌OH+HO2	1.100E-12	0.00	2000
O+NO⇒O2+N	1.140E-15	1.13	19200
O+N2⇒N+NO	3.000E-10	0.00	38300
O+NH⇌NO+H	0.750E-10	0.00	0
O+NH⇌N+OH	0.750E-10	0.00	0
O+NH3⇒OH+NH2	1.600E-11	0.00	3670
O+CH⇌CO+H	6.600E-11	0.00	0
O+CH2⇌CO+2H	1.200E-10	0.00	0
O+CH2⇌CO+H2	0.800E-10	0.00	0
O+CH3⇌CH2O+H	1.400E-10	0.00	0
O+CH4⇌OH+CH3	1.200E-15	1.56	4270
O+HCO⇌OH+CO	5.000E-11	0.00	0
O+HCO⇌CO2+H	5.000E-11	0.00	0
O+CH2O⇌OH+HCO	6.900E-13	0.57	1390
O+CH3O⇒O2+CH3	2.200E-11	0.00	0
O+CH3O⇌OH+CH2O	0.300E-11	0.00	0
O+CN⇒CO+N	1.700E-11	0.00	0
O+NCO⇌NO+CO	3.500E-11	0.00	0
O+NCO⇒O2+CN	3.500E-11	0.00	0
O+HCN⇒NCO+H	0.767E-18	2.10	3075
O+HCN⇌CO+NH	0.767E-18	2.10	3075
O+HCN⇒OH+CN	0.767E-18	2.10	3075
O+C2H⇌CO+CH	0.360E-11	0.00	0
O+C2H2⇌CO+CH2	0.840E-17	2.10	790
O+C2H2⇌HCCO+H	1.200E-17	2.10	790
O+HCCO⇌2CO+H	1.600E-10	0.00	0
O2+CH4⇌HO2+CH3	6.600E-11	0.00	28630
O2+CH2O⇌HO2+HCO	1.000E-10	0.00	20460
H+O2⇒OH+O	1.620E-10	0.00	7470
H+O2+M⇌HO2+M	1.700E-30	-0.80	0
Enhanced Collision Efficiencies:			
	H2=3.41, N2=2.29		
H+H+M⇒H2+M	1.800E-30	-1.00	0
Enhanced Collision Efficiencies:			
	H2=0.00		
H+H+H2⇒H2+H2	2.700E-31	-0.60	0
H+OH+M⇒H2O+M	2.300E-26	-2.00	0
Enhanced Collision Efficiencies:			
	H2O=16.96, N2=2.65		
H+HO2⇌H2+O2	7.100E-11	0.00	710
H+HO2⇌2OH	2.800E-10	0.00	440
H+HO2⇌H2O+O	5.000E-11	0.00	866
H+H2O⇒OH+H2	7.500E-16	1.6	9270
H+H2O2⇌H2+HO2	2.800E-12	0.00	1890
H+H2O2⇌OH+H2O	1.700E-11	0.00	1800
H+NO⇒OH+N	3.600E-10	0.00	24910
H+NH⇌H2+N	1.700E-11	0.00	0
H+NH2⇌H2+NH	1.000E-11	0.00	0
H+CO+M⇒HCO+M	5.300E-34	0.00	370
H+CH2⇒H2+CH	1.000E-11	0.00	-900
H+CH3⇒H2+CH2(S)	1.000E-10	0.00	7600
H+CH3(+M)⇒CH4(+M)	3.500E-10	0.00	0
Low pressure limit	1.700E-24	-1.80	0.0
Troe parameters: a=0.37, T^{***}=3315, T^{*}=61			

Reaction	A (cm-molecules-sec-K)	n	E (K)
H+CH4⇒H2+CH3	2.200E-20	3.00	4045
H+HCO⇌H2+CO	1.500E-10	0.00	0
H+CH2O⇌H2+HCO	2.100E-16	1.62	1090
H+CH3O⇌H2+CH2O	3.000E-11	0.00	0
H+HNCO⇌H2+NCO	3.400E-10	-0.27	10190
H+NCO⇌NH+CO	4.350E-11	0.00	0
H+NCO⇒HCN+O	4.350E-11	0.00	0
H+C2H2⇒H2+C2H	1.100E-10	0.00	14000
H+HCCO⇌CH2+CO	0.833E-10	0.00	0
H+HCCO⇌H2+C2O	0.833E-10	0.00	0
H+CH2CO⇌CH3+CO	3.000E-11	0.00	1700
H2+M⇒2H+M	3.700E-10	0.00	48350
Enhanced Collision Efficiencies:			
	H2=4.05		
OH+H2⇒H2O+H	1.700E-16	1.60	1660
2OH⇌H2O+O	2.500E-15	1.14	50
OH+OH(+M)⇒H2O2(+M)	1.200E-10	-0.37	0
Low pressure limit	6.1E-29	-0.76	0.0
SRI parameters: a=0.5, b=0.0, c=0.0			
Enhanced Collision Efficiencies:			
	H2O=0.0		
OH+OH(+H2O)⇒H2O2(+H2O)	1.200E-10	-0.37	0
Low pressure limit	4.0E-30	0.0	0.0
OH+HO2⇌H2O+O2	4.800E-11	0.00	-250
OH+H2O2⇌H2O+HO2	1.300E-11	0.00	670
OH+NH⇌NO+H2	4.000E-11	0.00	0
OH+NH⇌H2O+N	4.000E-11	0.00	0
OH+NH2⇒O+NH3	3.300E-14	0.405	250
OH+CO⇌H+CO2	1.050E-17	1.50	-250
OH+CH3⇌H2O+CH2(S)	1.200E-11	0.00	1400
OH+CH3(+M)⇌CH3OH(+M)	1.000E-10	0.00	0
Low pressure limit	4.40E-04	-8.2	0.0
Troe parameters: a=0.82, T^{***}=200, T^{*}=1438			
OH+CH4⇌H2O+CH3	2.600E-17	1.83	1400
OH+HCO⇌H2O+CO	1.700E-10	0.00	0
OH+CH2O⇌H2O+HCO	5.700E-15	1.18	-225
OH+CN⇒O+HCN	0.500E-10	0.00	0
OH+CN⇌NCO+H	0.500E-10	0.00	0
OH+HCN⇒H2O+CN	1.500E-11	0.00	5400
OH+C2H2⇌H2O+C2H	0.500E-10	0.00	6500
OH+C2H2⇌H+CH2CO	0.500E-10	0.00	6500
OH+CH2CO⇌CH2OH+CO	0.850E-11	0.00	0
OH+CH2CO⇌CH2O+HCO	0.850E-11	0.00	0
H2O+M⇒H+OH+M	5.800E-09	0.00	52920
HO2+HO2⇌H2O2+O2	7.000E-10	0.00	6030
HO2+NH2⇌NH3+O2	1.300E-11	0.00	0
HO2+NH2⇌HNO+H2O	1.300E-11	0.00	0
HO2+CH3⇌OH+CH3O	3.000E-11	0.00	0
HO2+CH4⇌H2O2+CH3	1.500E-11	0.00	12440
HO2+CH2O⇌H2O2+HCO	5.000E-12	0.00	6580
H2O2(+M)⇒OH+OH(+M)	3.000E+14	0.00	24400
Low pressure limit	3.000E-08	0.00	21600
SRI parameters: a=0.5, b=0.0, c=0.0			
Enhanced Collision Efficiencies:			
	N2=0.00		
H2O2(+N2)⇒OH+OH(+N2)	3.000E+14	0.00	24400
Low pressure limit	2.000E-07	0.00	22900

Reaction	A (cm-molecules-sec-K)	n	E (K)
SRI parameters: a=0.5, b=0.0, c=0.0			
N+O2⇒NO+O	1.500E-14	1.00	3270
N+OH⇒NO+H	4.700E-11	0.00	0
N+NO⇒N2+O	7.100E-11	0.00	790
N+CN⇒N2+C	3.000E-10	0.00	0
N+NCO⇌N2+CO	3.300E-11	0.00	0
NH+O2⇌NO+OH	0.650E-13	0.00	770
NH+O2⇌NO2+H	0.650E-13	0.00	770
NH+O2⇌HNO+O	6.500E-11	0.00	9000
NH+NO⇌N2O+H	0.933E-10	0.00	6400
NH+NO⇌NNH+O	0.933E-10	0.00	6400
NH+NO⇌N2+OH	0.933E-10	0.00	6400
NH2+NO⇌N2+H2O	0.792E-12	0.00	-650
NH2+NO⇌N2+H+OH	0.108E-12	0.00	-650
NH2+NO⇌NNH+OH	0.108E-12	0.00	-650
NH2+NO⇌N2O+H2	0.792E-12	0.00	-650
NH3(+M)⇌NH2+H(+M)	8.300E+15	0.00	55170
Low pressure limit	7.400E-9	0.0	41560
Troe parameters: a=0.42, T^{***}=4581, T^{*}=102			
C+N2⇒CN+N	8.700E-11	0.00	22600
C+NO⇌CN+O	3.200E-11	0.00	0
C+NO⇒CO+N	4.800E-11	0.00	0
CH+O2⇌HCO+O	2.750E-11	0.00	0
CH+O2⇌CO+OH	2.750E-11	0.00	0
CH+H2⇒CH2+H	2.400E-10	0.00	1760
CH+N2⇌HCN+N	2.600E-12	0.00	9030
CH+NO⇌CO+NH	0.667E-10	0.00	0
CH+NO⇌CN+OH	0.667E-10	0.00	0
CH+NO⇌HCN+O	0.667E-10	0.00	0
CH2+O2⇌CO+H+OH	0.820E-11	0.00	750
CH2+O2⇌CO2+H+H	0.820E-11	0.00	750
CH2+O2⇌CO+H2O	0.820E-11	0.00	750
CH2+O2⇌CO2+H2	0.820E-11	0.00	750
CH2+O2⇌CH2O+O	0.820E-11	0.00	750
CH2+CH2⇌C2H2+H2	0.200E-10	0.00	400
CH2+CH2⇌C2H2+2H	1.800E-10	0.00	400
CH2(S)+AR⇌CH2+AR	6.000E-12	0.00	0
CH2(S)+N2⇌CH2+N2	1.000E-11	0.00	0
CH2(S)+CH4⇌CH2+CH4	1.200E-11	0.00	0
CH2(S)+C2H2⇌CH2+C2H2	8.000E-11	0.00	0
CH2(S)+O2⇌CO+H+OH	1.300E-11	0.00	0
CH2(S)+O2⇌CO2+H2	1.300E-11	0.00	0
CH2(S)+O2⇌CO+H2O	1.300E-11	0.00	0
CH2(S)+O2⇌CH2+O2	1.300E-11	0.00	0
CH2(S)+H2⇒CH3+H	1.200E-10	0.00	0
CH3+M⇌CH2+H+M	1.700E-08	0.00	45600
CH3+O2⇒CH3O+O	2.200E-10	0.00	15800
CH3+O2⇌CH2O+OH	5.500E-13	0.00	4500
CH3+H2⇒CH4+H	1.140E-20	2.74	4740
CH3+CH2O⇌CH4+HCO	1.300E-31	6.10	990
CH4(+M)⇒CH3+H(+M)	2.400E+16	0.00	52800
Low pressure limit	7.8E+23	-8.2	59200
Troe parameters: a=1.0, T^{***}=0.0, T^{*}=1350, T^{**}=7830			
Enhanced Collision Efficiencies:			
	CH4=0.0		
CH4(+CH4)⇒CH3+H(+CH4)	2.400E+16	0.00	52800
Low pressure limit	1.4E-06	0.0	45700

Reaction	A (cm-molecules-sec-K)	n	E (K)
Troe parameters: a=0.69, T^{***}=90, T^{*}=2210			
HCO+M⇒H+CO+M	2.600E-10	0.00	7930
HCO+O2⇌CO+HO2	2.500E-12	0.00	0
HCO+O2⇌OH+CO2	2.500E-12	0.00	0
HCO+HCO⇌CH2O+CO	5.000E-11	0.00	0
CH2O+M⇌H+HCO+M	0.810E+12	-5.54	48660
CH2O+M⇌H2+CO+M	1.890E+12	-5.54	48660
CH2OH+O2⇌CH2O+HO2	2.600E-09	-1.00	0
Duplicate Reaction			
CH2OH+O2⇌CH2O+HO2	1.200E-10	0.00	1800
Duplicate Reaction			
CH3O+M⇌CH2O+H+M	9.000E-11	0.00	6790
CH3O+O2⇌CH2O+HO2	3.600E-14	0.00	880
CN+O2⇒NCO+O	1.200E-11	0.00	-210
CN+H2⇌HCN+H	3.200E-20	2.87	820
CN+H2O⇒HCN+OH	0.650E-11	0.00	3750
CN+H2O⇌HOCN+H	0.650E-11	0.00	3750
CN+CH4⇌HCN+CH3	1.500E-19	2.64	-150
NCO+M⇌N+CO+M	1.700E-09	0.00	23500
NCO+NO⇌N2O+CO	0.767E-06	-1.73	380
NCO+NO⇌N2+CO2	0.767E-06	-1.73	380
NCO+NO⇌N2+CO+O	0.767E-06	-1.73	380
C2H+O2⇌CO2+CH	0.750E-11	0.00	0
C2H+O2⇌2CO+H	0.750E-11	0.00	0
C2H+O2⇌CO+HCO	0.750E-11	0.00	0
C2H+H2⇒C2H2+H	1.800E-11	0.00	1090
HCCO+O2⇌CO2+HCO	0.675E-12	0.00	430
HCCO+O2⇌2CO+OH	0.675E-12	0.00	430
HCCO+O2⇌C2O+HO2	0.675E-12	0.00	430

E.3 Frenklach et al. (1995) (GRI-Mech 2.11)

GRI-Mech 2.11 is the latest version of a mechanism created, validated, and maintained by the Gas Research Institute. It and other information are available in electronic form through the World Wide Web at http://www.gri.org and http://www.me.berkeley.edu/gri_mech/.

Reaction	A (cm-moles-sec-K)	n	E (cal/mole)
2O+M⇌O2+M	1.200E+17	-1.000	.00
Enhanced Collision Efficiencies: H2=2.40, H2O=15.40, CH4=2.00, CO=1.75, CO2=3.60, C2H6=3.00, AR=.83			
O+H+M⇌OH+M	5.000E+17	-1.000	.00
Enhanced Collision Efficiencies: H2=2.00, H2O=6.00, CH4=2.00, CO=1.50, CO2=2.00, C2H6=3.00, AR=.70			
O+H2⇌H+OH	5.000E+04	2.670	6290.00
O+HO2⇌OH+O2	2.000E+13	.000	.00
O+H2O2⇌OH+HO2	9.630E+06	2.000	4000.00
O+CH⇌H+CO	5.700E+13	.000	.00
O+CH2⇌H+HCO	8.000E+13	.000	.00
O+CH2(S)⇌H2+CO	1.500E+13	.000	.00
O+CH2(S)⇌H+HCO	1.500E+13	.000	.00
O+CH3⇌H+CH2O	8.430E+13	.000	.00
O+CH4⇌OH+CH3	1.020E+09	1.500	8600.00
O+CO+M⇌CO2+M	6.020E+14	.000	3000.00
Enhanced Collision Efficiencies: H2=2.00, O2=6.00, H2O=6.00, CH4=2.00, CO=1.50, CO2=3.50, C2H6=3.00, AR=.50			
O+HCO⇌OH+CO	3.000E+13	.000	.00
O+HCO⇌H+CO2	3.000E+13	.000	.00
O+CH2O⇌OH+HCO	3.900E+13	.000	3540.00
O+CH2OH⇌OH+CH2O	1.000E+13	.000	.00
O+CH3O⇌OH+CH2O	1.000E+13	.000	.00
O+CH3OH⇌OH+CH2OH	3.880E+05	2.500	3100.00
O+CH3OH⇌OH+CH3O	1.300E+05	2.500	5000.00
O+C2H⇌CH+CO	5.000E+13	.000	.00
O+C2H2⇌H+HCCO	1.020E+07	2.000	1900.00
O+C2H2⇌OH+C2H	4.600E+19	-1.410	28950.00
O+C2H2⇌CO+CH2	1.020E+07	2.000	1900.00
O+C2H3⇌H+CH2CO	3.000E+13	.000	.00
O+C2H4⇌CH3+HCO	1.920E+07	1.830	220.00
O+C2H5⇌CH3+CH2O	1.320E+14	.000	.00
O+C2H6⇌OH+C2H5	8.980E+07	1.920	5690.00
O+HCCO⇌H+2CO	1.000E+14	.000	.00
O+CH2CO⇌OH+HCCO	1.000E+13	.000	8000.00
O+CH2CO⇌CH2+CO2	1.750E+12	.000	1350.00
O2+CO⇌O+CO2	2.500E+12	.000	47800.00
O2+CH2O⇌HO2+HCO	1.000E+14	.000	40000.00
H+O2+M⇌HO2+M	2.800E+18	-.860	.00
Enhanced Collision Efficiencies: O2=.00, H2O=.00, CO=.75, CO2=1.50, C2H6=1.50, N2=.00, AR=.00			
H+2O2⇌HO2+O2	3.000E+20	-1.720	.00
H+O2+H2O⇌HO2+H2O	9.380E+18	-.760	.00
H+O2+N2⇌HO2+N2	3.750E+20	-1.720	.00
H+O2+AR⇌HO2+AR	7.000E+17	-.800	.00
H+O2⇌O+OH	8.300E+13	.000	14413.00
2H+M⇌H2+M	1.000E+18	-1.000	.00
Enhanced Collision Efficiencies: H2=.00, H2O=.00, CH4=2.00, CO2=.00, C2H6=3.00, AR=.63			
2H+H2⇌2H2	9.000E+16	-.600	.00
2H+H2O⇌H2+H2O	6.000E+19	-1.250	.00
2H+CO2⇌H2+CO2	5.500E+20	-2.000	.00
H+OH+M⇌H2O+M	2.200E+22	-2.000	.00
Enhanced Collision Efficiencies: H2=.73, H2O=3.65, CH4=2.00, C2H6=3.00, AR=.38			
H+HO2⇌O+H2O	3.970E+12	.000	671.00
H+HO2⇌O2+H2	2.800E+13	.000	1068.00

Reaction	A (cm-moles-sec-K)	n	E (cal/mole)
H+HO2⇌2OH	1.340E+14	.000	635.00
H+H2O2⇌HO2+H2	1.210E+07	2.000	5200.00
H+H2O2⇌OH+H2O	1.000E+13	.000	3600.00
H+CH⇌C+H2	1.100E+14	.000	.00
H+CH2(+M)⇌CH3(+M)	2.500E+16	-.800	.00
Low pressure limit	3.200E+27	-3.140	1230.00
Troe parameters: a=.6800, T***=78.00, T*=1995.00, T**=5590.00			
Enhanced Collision Efficiencies:			
H2=2.00, H2O=6.00, CH4=2.00, CO=1.50, CO2=2.00, C2H6=3.00, AR=.70			
H+CH2(S)⇌CH+H2	3.000E+13	.000	.00
H+CH3(+M)⇌CH4(+M)	1.270E+16	-.630	383.00
Low pressure limit	2.477E+33	-4.760	2440.00
Troe parameters: a=.7830, T***=74.00, T*=2941.00, T**=6964.00			
Enhanced Collision Efficiencies:			
H2=2.00, H2O=6.00, CH4=2.00, CO=1.50, CO2=2.00, C2H6=3.00, AR=.70			
H+CH4⇌CH3+H2	6.600E+08	1.620	10840.00
H+HCO(+M)⇌CH2O(+M)	1.090E+12	.480	-260.00
Low pressure limit	1.350E+24	-2.570	1425.00
Troe parameters: a=.7824, T***=271.00, T*=2755.00, T**=6570.00			
Enhanced Collision Efficiencies:			
H2=2.00, H2O=6.00, CH4=2.00, CO=1.50, CO2=2.00, C2H6=3.00, AR=.70			
H+HCO⇌H2+CO	7.340E+13	.000	.00
H+CH2O(+M)⇌CH2OH(+M)	5.400E+11	.454	3600.00
Low pressure limit	1.270E+32	-4.820	6530.00
Troe parameters: a=.7187, T***=103.00, T*=1291.00, T**=4160.00			
Enhanced Collision Efficiencies:			
H2=2.00, H2O=6.00, CH4=2.00, CO=1.50, CO2=2.00, C2H6=3.00			
H+CH2O(+M)⇌CH3O(+M)	5.400E+11	.454	2600.00
Low pressure limit	2.200E+30	-4.800	5560.00
Troe parameters: a=.7580, T***=94.00, T*=1555.00, T**=4200.00			
Enhanced Collision Efficiencies:			
H2=2.00, H2O=6.00, CH4=2.00, CO=1.50, CO2=2.00, C2H6=3.00			
H+CH2O⇌HCO+H2	2.300E+10	1.050	3275.00
H+CH2OH(+M)⇌CH3OH(+M)	1.800E+13	.000	.00
Low pressure limit	3.000E+31	-4.800	3300.00
Troe parameters: a=.7679, T***=338.00, T*=1812.00, T**=5081.00			
Enhanced Collision Efficiencies:			
H2=2.00, H2O=6.00, CH4=2.00, CO=1.50, CO2=2.00, C2H6=3.00			
H+CH2OH⇌H2+CH2O	2.000E+13	.000	.00
H+CH2OH⇌OH+CH3	1.200E+13	.000	.00
H+CH2OH⇌CH2(S)+H2O	6.000E+12	.000	.00
H+CH3O(+M)⇌CH3OH(+M)	5.000E+13	.000	.00
Low pressure limit	8.600E+28	-4.000	3025.00
Troe parameters: a=.8902, T***=144.00, T*=2838.00, T**=45569.00			
Enhanced Collision Efficiencies:			
H2=2.00, H2O=6.00, CH4=2.00, CO=1.50, CO2=2.00, C2H6=3.00			
H+CH3O⇌H+CH2OH	3.400E+06	1.600	.00
H+CH3O⇌H2+CH2O	2.000E+13	.000	.00
H+CH3O⇌OH+CH3	3.200E+13	.000	.00
H+CH3O⇌CH2(S)+H2O	1.600E+13	.000	.00
H+CH3OH⇌CH2OH+H2	1.700E+07	2.100	4870.00
H+CH3OH⇌CH3O+H2	4.200E+06	2.100	4870.00
H+C2H(+M)⇌C2H2(+M)	1.000E+17	-1.000	.00
Low pressure limit	3.750E+33	-4.800	1900.00
Troe parameters: a=.6464, T***=132.00, T*=1315.00, T**=5566.00			
Enhanced Collision Efficiencies:			
H2=2.00, H2O=6.00, CH4=2.00, CO=1.50, CO2=2.00, C2H6=3.00, AR=.70			

Reaction	A (cm-moles-sec-K)	n	E (cal/mole)
H+C2H2(+M)⇌C2H3(+M)	5.600E+12	.000	2400.00
Low pressure limit	3.800E+40	-7.270	7220.00
Troe parameters: a=.7507, T*** =98.50, T* =1302.00, T** =4167.00			
Enhanced Collision Efficiencies:			
H2=2.00, H2O=6.00, CH4=2.00, CO=1.50, CO2=2.00, C2H6=3.00, AR=.70			
H+C2H3(+M)⇌C2H4(+M)	6.080E+12	.270	280.00
Low pressure limit	1.400E+30	-3.860	3320.00
Troe parameters: a=.7820, T*** =207.50, T* =2663.00, T** =6095.00			
Enhanced Collision Efficiencies:			
H2=2.00, H2O=6.00, CH4=2.00, CO=1.50, CO2=2.00, C2H6=3.00, AR=.70			
H+C2H3⇌H2+C2H2	3.000E+13	.000	.00
H+C2H4(+M)⇌C2H5(+M)	1.080E+12	.454	1820.00
Low pressure limit	1.200E+42	-7.620	6970.00
Troe parameters: a=.9753, T*** =210.00, T* =984.00, T** =4374.00			
Enhanced Collision Efficiencies:			
H2=2.00, H2O=6.00, CH4=2.00, CO=1.50, CO2=2.00, C2H6=3.00, AR=.70			
H+C2H4⇌C2H3+H2	1.325E+06	2.530	12240.00
H+C2H5(+M)⇌C2H6(+M)	5.210E+17	-.990	1580.00
Low pressure limit	1.990E+41	-7.080	6685.00
Troe parameters: a=.8422, T*** =125.00, T* =2219.00, T** =6882.00			
Enhanced Collision Efficiencies:			
H2=2.00, H2O=6.00, CH4=2.00, CO=1.50, CO2=2.00, C2H6=3.00, AR=.70			
H+C2H5⇌H2+C2H4	2.000E+12	.000	.00
H+C2H6⇌C2H5+H2	1.150E+08	1.900	7530.00
H+HCCO⇌CH2(S)+CO	1.000E+14	.000	.00
H+CH2CO⇌HCCO+H2	5.000E+13	.000	8000.00
H+CH2CO⇌CH3+CO	1.130E+13	.000	3428.00
H+HCCOH⇌H+CH2CO	1.000E+13	.000	.00
H2+CO(+M)⇌CH2O(+M)	4.300E+07	1.500	79600.00
Low pressure limit	5.070E+27	-3.420	84350.00
Troe parameters: a=.9320, T*** =197.00, T* =1540.00, T** =10300.00			
Enhanced Collision Efficiencies:			
H2=2.00, H2O=6.00, CH4=2.00, CO=1.50, CO2=2.00, C2H6=3.00, AR=.70			
OH+H2⇌H+H2O	2.160E+08	1.510	3430.00
2OH(+M)⇌H2O2(+M)	7.400E+13	-.370	.00
Low pressure limit	2.300E+18	-.900	-1700.00
Troe parameters: a=.7346, T*** =94.00, T* =1756.00, T** =5182.00			
Enhanced Collision Efficiencies:			
H2=2.00, H2O=6.00, CH4=2.00, CO=1.50, CO2=2.00, C2H6=3.00, AR=.70			
2OH⇌O+H2O	3.570E+04	2.400	-2110.00
OH+HO2⇌O2+H2O	2.900E+13	.000	-500.00
OH+H2O2⇌HO2+H2O	1.750E+12	.000	320.00
Duplicate Reaction			
OH+H2O2⇌HO2+H2O	5.800E+14	.000	9560.00
Duplicate Reaction			
OH+C⇌H+CO	5.000E+13	.000	.00
OH+CH⇌H+HCO	3.000E+13	.000	.00
OH+CH2⇌H+CH2O	2.000E+13	.000	.00
OH+CH2⇌CH+H2O	1.130E+07	2.000	3000.00
OH+CH2(S)⇌H+CH2O	3.000E+13	.000	.00
OH+CH3(+M)⇌CH3OH(+M)	6.300E+13	.000	.00
Low pressure limit	2.700E+38	-6.300	3100.00
Troe parameters: a=.2105, T*** =83.50, T* =5398.00, T** =8370.00			
Enhanced Collision Efficiencies:			
H2=2.00, H2O=6.00, CH4=2.00, CO=1.50, CO2=2.00, C2H6=3.00			
OH+CH3⇌CH2+H2O	5.600E+07	1.600	5420.00
OH+CH3⇌CH2(S)+H2O	2.501E+13	.000	.00

Reaction	A (cm-moles-sec-K)	n	E (cal/mole)
OH+CH4⇌CH3+H2O	1.000E+08	1.600	3120.00
OH+CO⇌H+CO2	4.760E+07	1.228	70.00
OH+HCO⇌H2O+CO	5.000E+13	.000	.00
OH+CH2O⇌HCO+H2O	3.430E+09	1.180	-447.00
OH+CH2OH⇌H2O+CH2O	5.000E+12	.000	.00
OH+CH3O⇌H2O+CH2O	5.000E+12	.000	.00
OH+CH3OH⇌CH2OH+H2O	1.440E+06	2.000	-840.00
OH+CH3OH⇌CH3O+H2O	6.300E+06	2.000	1500.00
OH+C2H⇌H+HCCO	2.000E+13	.000	.00
OH+C2H2⇌H+CH2CO	2.180E-04	4.500	-1000.00
OH+C2H2⇌H+HCCOH	5.040E+05	2.300	13500.00
OH+C2H2⇌C2H+H2O	3.370E+07	2.000	14000.00
OH+C2H2⇌CH3+CO	4.830E-04	4.000	-2000.00
OH+C2H3⇌H2O+C2H2	5.000E+12	.000	.00
OH+C2H4⇌C2H3+H2O	3.600E+06	2.000	2500.00
OH+C2H6⇌C2H5+H2O	3.540E+06	2.120	870.00
OH+CH2CO⇌HCCO+H2O	7.500E+12	.000	2000.00
2HO2⇌O2+H2O2	1.300E+11	.000	-1630.00
Duplicate Reaction			
2HO2⇌O2+H2O2	4.200E+14	.000	12000.00
Duplicate Reaction			
HO2+CH2⇌OH+CH2O	2.000E+13	.000	.00
HO2+CH3⇌O2+CH4	1.000E+12	.000	.00
HO2+CH3⇌OH+CH3O	2.000E+13	.000	.00
HO2+CO⇌OH+CO2	1.500E+14	.000	23600.00
HO2+CH2O⇌HCO+H2O2	1.000E+12	.000	8000.00
C+O2⇌O+CO	5.800E+13	.000	576.00
C+CH2⇌H+C2H	5.000E+13	.000	.00
C+CH3⇌H+C2H2	5.000E+13	.000	.00
CH+O2⇌O+HCO	3.300E+13	.000	.00
CH+H2⇌H+CH2	1.107E+08	1.790	1670.00
CH+H2O⇌H+CH2O	1.713E+13	.000	-755.00
CH+CH2⇌H+C2H2	4.000E+13	.000	.00
CH+CH3⇌H+C2H3	3.000E+13	.000	.00
CH+CH4⇌H+C2H4	6.000E+13	.000	.00
CH+CO(+M)⇌HCCO(+M)	5.000E+13	.000	.00
Low pressure limit	2.690E+28	-3.740	1936.00
Troe parameters: a=.5757, T***=237.00, T*=1652.00, T**=5069.00			
Enhanced Collision Efficiencies:			
H2=2.00, H2O=6.00, CH4=2.00, CO=1.50, CO2=2.00, C2H6=3.00, AR=.70			
CH+CO2⇌HCO+CO	3.400E+12	.000	690.00
CH+CH2O⇌H+CH2CO	9.460E+13	.000	-515.00
CH+HCCO⇌CO+C2H2	5.000E+13	.000	.00
CH2+O2⇌OH+HCO	1.320E+13	.000	1500.00
CH2+H2⇌H+CH3	5.000E+05	2.000	7230.00
2CH2⇌H2+C2H2	3.200E+13	.000	.00
CH2+CH3⇌H+C2H4	4.000E+13	.000	.00
CH2+CH4⇌2CH3	2.460E+06	2.000	8270.00
CH2+CO(+M)⇌CH2CO(+M)	8.100E+11	.500	4510.00
Low pressure limit	2.690E+33	-5.110	7095.00
Troe parameters: a=.5907, T***=275.00, T*=1226.00, T**=5185.00			
Enhanced Collision Efficiencies:			
H2=2.00, H2O=6.00, CH4=2.00, CO=1.50, CO2=2.00, C2H6=3.00, AR=.70			
CH2+HCCO⇌C2H3+CO	3.000E+13	.000	.00
CH2(S)+N2⇌CH2+N2	1.500E+13	.000	600.00
CH2(S)+AR⇌CH2+AR	9.000E+12	.000	600.00
CH2(S)+O2⇌H+OH+CO	2.800E+13	.000	.00

Reaction	A (cm-moles-sec-K)	n	E (cal/mole)
CH2(S)+O2⇌CO+H2O	1.200E+13	.000	.00
CH2(S)+H2⇌CH3+H	7.000E+13	.000	.00
CH2(S)+H2O(+M)⇌CH3OH(+M)	2.000E+13	.000	.00
Low pressure limit	2.700E+38	-6.300	3100.00
Troe parameters: a=.1507, T***=134.00, T*=2383.00, T**=7265.00			
Enhanced Collision Efficiencies:			
H2=2.00, H2O=6.00, CH4=2.00, CO=1.50, CO2=2.00, C2H6=3.00			
CH2(S)+H2O⇌CH2+H2O	3.000E+13	.000	.00
CH2(S)+CH3⇌H+C2H4	1.200E+13	.000	-570.00
CH2(S)+CH4⇌2CH3	1.600E+13	.000	-570.00
CH2(S)+CO⇌CH2+CO	9.000E+12	.000	.00
CH2(S)+CO2⇌CH2+CO2	7.000E+12	.000	.00
CH2(S)+CO2⇌CO+CH2O	1.400E+13	.000	.00
CH2(S)+C2H6⇌CH3+C2H5	4.000E+13	.000	-550.00
CH3+O2⇌O+CH3O	2.675E+13	.000	28800.00
CH3+O2⇌OH+CH2O	3.600E+10	.000	8940.00
CH3+H2O2⇌HO2+CH4	2.450E+04	2.470	5180.00
2CH3(+M)⇌C2H6(+M)	2.120E+16	-.970	620.00
Low pressure limit	1.770E+50	-9.670	6220.00
Troe parameters: a=.5325, T***=151.00, T*=1038.00, T**=4970.00			
Enhanced Collision Efficiencies:			
H2=2.00, H2O=6.00, CH4=2.00, CO=1.50, CO2=2.00, C2H6=3.00, AR=.70			
2CH3⇌H+C2H5	4.990E+12	.100	10600.00
CH3+HCO⇌CH4+CO	2.648E+13	.000	.00
CH3+CH2O⇌HCO+CH4	3.320E+03	2.810	5860.00
CH3+CH3OH⇌CH2OH+CH4	3.000E+07	1.500	9940.00
CH3+CH3OH⇌CH3O+CH4	1.000E+07	1.500	9940.00
CH3+C2H4⇌C2H3+CH4	2.270E+05	2.000	9200.00
CH3+C2H6⇌C2H5+CH4	6.140E+06	1.740	10450.00
HCO+H2O⇌H+CO+H2O	2.244E+18	-1.000	17000.00
HCO+M⇌H+CO+M	1.870E+17	-1.000	17000.00
Enhanced Collision Efficiencies:			
H2=2.00, H2O=.00, CH4=2.00, CO=1.50, CO2=2.00, C2H6=3.00			
HCO+O2⇌HO2+CO	7.600E+12	.000	400.00
CH2OH+O2⇌HO2+CH2O	1.800E+13	.000	900.00
CH3O+O2⇌HO2+CH2O	4.280E-13	7.600	-3530.00
C2H+O2⇌HCO+CO	5.000E+13	.000	1500.00
C2H+H2⇌H+C2H2	4.070E+05	2.400	200.00
C2H3+O2⇌HCO+CH2O	3.980E+12	.000	-240.00
C2H4(+M)⇌H2+C2H2(+M)	8.000E+12	.440	88770.00
Low pressure limit	7.000E+50	-9.310	99860.00
Troe parameters: a=.7345, T***=180.00, T*=1035.00, T**=5417.00			
Enhanced Collision Efficiencies:			
H2=2.00, H2O=6.00, CH4=2.00, CO=1.50, CO2=2.00, C2H6=3.00, AR=.70			
C2H5+O2⇌HO2+C2H4	8.400E+11	.000	3875.00
HCCO+O2⇌OH+2CO	1.600E+12	.000	854.00
2HCCO⇌2CO+C2H2	1.000E+13	.000	.00
N+NO⇌N2+O	3.500E+13	.000	330.00
N+O2⇌NO+O	2.650E+12	.000	6400.00
N+OH⇌NO+H	7.333E+13	.000	1120.00
N2O+O⇌N2+O2	1.400E+12	.000	10810.00
N2O+O⇌2NO	2.900E+13	.000	23150.00
N2O+H⇌N2+OH	4.400E+14	.000	18880.00
N2O+OH⇌N2+HO2	2.000E+12	.000	21060.00
N2O(+M)⇌N2+O(+M)	1.300E+11	.000	59620.00
Low pressure limit	6.200E+14	.000	56100.00
Enhanced Collision Efficiencies:			

Reaction	A (cm-moles-sec-K)	n	E (cal/mole)
H2=2.00, H2O=6.00, CH4=2.00, CO=1.50, CO2=2.00, C2H6=3.00, AR=.70			
HO2+NO⇌NO2+OH	2.110E+12	.000	-480.00
NO+O+M⇌NO2+M	1.060E+20	-1.410	.00
Enhanced Collision Efficiencies:			
H2=2.00, H2O=6.00, CH4=2.00, CO=1.50, CO2=2.00, C2H6=3.00, AR=.70			
NO2+O⇌NO+O2	3.900E+12	.000	-240.00
NO2+H⇌NO+OH	1.320E+14	.000	360.00
NH+O⇌NO+H	5.000E+13	.000	.00
NH+H⇌N+H2	3.200E+13	.000	330.00
NH+OH⇌HNO+H	2.000E+13	.000	.00
NH+OH⇌N+H2O	2.000E+09	1.200	.00
NH+O2⇌HNO+O	4.610E+05	2.000	6500.00
NH+O2⇌NO+OH	1.280E+06	1.500	100.00
NH+N⇌N2+H	1.500E+13	.000	.00
NH+H2O⇌HNO+H2	2.000E+13	.000	13850.00
NH+NO⇌N2+OH	2.160E+13	-.230	.00
NH+NO⇌N2O+H	4.160E+14	-.450	.00
NH2+O⇌OH+NH	7.000E+12	.000	.00
NH2+O⇌H+HNO	4.600E+13	.000	.00
NH2+H⇌NH+H2	4.000E+13	.000	3650.00
NH2+OH⇌NH+H2O	9.000E+07	1.500	-460.00
NNH⇌N2+H	3.300E+08	.000	.00
NNH+M⇌N2+H+M	1.300E+14	-.110	4980.00
Enhanced Collision Efficiencies:			
H2=2.00, H2O=6.00, CH4=2.00, CO=1.50, CO2=2.00, C2H6=3.00, AR=.70			
NNH+O2⇌HO2+N2	5.000E+12	.000	.00
NNH+O⇌OH+N2	2.500E+13	.000	.00
NNH+O⇌NH+NO	7.000E+13	.000	.00
NNH+H⇌H2+N2	5.000E+13	.000	.00
NNH+OH⇌H2O+N2	2.000E+13	.000	.00
NNH+CH3⇌CH4+N2	2.500E+13	.000	.00
H+NO+M⇌HNO+M	8.950E+19	-1.320	740.00
Enhanced Collision Efficiencies:			
H2=2.00, H2O=6.00, CH4=2.00, CO=1.50, CO2=2.00, C2H6=3.00, AR=.70			
HNO+O⇌NO+OH	2.500E+13	.000	.00
HNO+H⇌H2+NO	4.500E+11	.720	660.00
HNO+OH⇌NO+H2O	1.300E+07	1.900	-950.00
HNO+O2⇌HO2+NO	1.000E+13	.000	13000.00
CN+O⇌CO+N	7.700E+13	.000	.00
CN+OH⇌NCO+H	4.000E+13	.000	.00
CN+H2O⇌HCN+OH	8.000E+12	.000	7460.00
CN+O2⇌NCO+O	6.140E+12	.000	-440.00
CN+H2⇌HCN+H	2.100E+13	.000	4710.00
NCO+O⇌NO+CO	2.350E+13	.000	.00
NCO+H⇌NH+CO	5.400E+13	.000	.00
NCO+OH⇌NO+H+CO	2.500E+12	.000	.00
NCO+N⇌N2+CO	2.000E+13	.000	.00
NCO+O2⇌NO+CO2	2.000E+12	.000	20000.00
NCO+M⇌N+CO+M	8.800E+16	-.500	48000.00
Enhanced Collision Efficiencies:			
H2=2.00, H2O=6.00, CH4=2.00, CO=1.50, CO2=2.00, C2H6=3.00, AR=.70			
NCO+NO⇌N2O+CO	2.850E+17	-1.520	740.00
NCO+NO⇌N2+CO2	5.700E+18	-2.000	800.00
HCN+M⇌H+CN+M	1.040E+29	-3.300	126600.00
Enhanced Collision Efficiencies:			
H2=2.00, H2O=6.00, CH4=2.00, CO=1.50, CO2=2.00, C2H6=3.00, AR=.70			
HCN+O⇌NCO+H	1.107E+04	2.640	4980.00

Reaction	A (cm-moles-sec-K)	n	E (cal/mole)
HCN+O⇌NH+CO	2.767E+03	2.640	4980.00
HCN+O⇌CN+OH	2.134E+09	1.580	26600.00
HCN+OH⇌HOCN+H	1.100E+06	2.030	13370.00
HCN+OH⇌HNCO+H	4.400E+03	2.260	6400.00
HCN+OH⇌NH2+CO	1.600E+02	2.560	9000.00
H+HCN+M⇌H2CN+M	1.400E+26	-3.400	1900.00
Enhanced Collision Efficiencies: H2=2.00, H2O=6.00, CH4=2.00, CO=1.50, CO2=2.00, C2H6=3.00, AR=.70			
H2CN+N⇌N2+CH2	6.000E+13	.000	400.00
C+N2⇌CN+N	6.300E+13	.000	46020.00
CH+N2⇌HCN+N	2.857E+08	1.100	20400.00
CH+N2(+M)⇌HCNN(+M)	3.100E+12	.150	.00
Low pressure limit	1.300E+25	-3.160	740.00
Troe parameters: a=.6670, T^{***}=235.00, T^{*}=2117.00, T^{**}=4536.00			
Enhanced Collision Efficiencies: H2=2.00, H2O=6.00, CH4=2.00, CO=1.50, CO2=2.00, C2H6=3.00, AR=.70			
CH2+N2⇌HCN+NH	1.000E+13	.000	74000.00
CH2(S)+N2⇌NH+HCN	1.000E+11	.000	65000.00
C+NO⇌CN+O	1.900E+13	.000	.00
C+NO⇌CO+N	2.900E+13	.000	.00
CH+NO⇌HCN+O	5.000E+13	.000	.00
CH+NO⇌H+NCO	2.000E+13	.000	.00
CH+NO⇌N+HCO	3.000E+13	.000	.00
CH2+NO⇌H+HNCO	3.100E+17	-1.380	1270.00
CH2+NO⇌OH+HCN	2.900E+14	-.690	760.00
CH2+NO⇌H+HCNO	3.800E+13	-.360	580.00
CH2(S)+NO⇌H+HNCO	3.100E+17	-1.380	1270.00
CH2(S)+NO⇌OH+HCN	2.900E+14	-.690	760.00
CH2(S)+NO⇌H+HCNO	3.800E+13	-.360	580.00
CH3+NO⇌HCN+H2O	9.600E+13	.000	28800.00
CH3+NO⇌H2CN+OH	1.000E+12	.000	21750.00
HCNN+O⇌CO+H+N2	2.200E+13	.000	.00
HCNN+O⇌HCN+NO	2.000E+12	.000	.00
HCNN+O2⇌O+HCO+N2	1.200E+13	.000	.00
HCNN+OH⇌H+HCO+N2	1.200E+13	.000	.00
HCNN+H⇌CH2+N2	1.000E+14	.000	.00
HNCO+O⇌NH+CO2	9.800E+07	1.410	8500.00
HNCO+O⇌HNO+CO	1.500E+08	1.570	44000.00
HNCO+O⇌NCO+OH	2.200E+06	2.110	11400.00
HNCO+H⇌NH2+CO	2.250E+07	1.700	3800.00
HNCO+H⇌H2+NCO	1.050E+05	2.500	13300.00
HNCO+OH⇌NCO+H2O	4.650E+12	.000	6850.00
HNCO+OH⇌NH2+CO2	1.550E+12	.000	6850.00
HNCO+M⇌NH+CO+M	1.180E+16	.000	84720.00
Enhanced Collision Efficiencies: H2=2.00, H2O=6.00, CH4=2.00, CO=1.50, CO2=2.00, C2H6=3.00, AR=.70			
HCNO+H⇌H+HNCO	2.100E+15	-.690	2850.00
HCNO+H⇌OH+HCN	2.700E+11	.180	2120.00
HCNO+H⇌NH2+CO	1.700E+14	-.750	2890.00
HOCN+H⇌H+HNCO	2.000E+07	2.000	2000.00
HCCO+NO⇌HCNO+CO	2.350E+13	.000	.00
CH3+N⇌H2CN+H	6.100E+14	-.310	290.00
CH3+N⇌HCN+H2	3.700E+12	.150	-90.00
NH3+H⇌NH2+H2	5.400E+05	2.400	9915.00
NH3+OH⇌NH2+H2O	5.000E+07	1.600	955.00
NH3+O⇌NH2+OH	9.400E+06	1.940	6460.00

E.4 Modified Miller and Bowman (1989)

This mechanism is a modified version of the listing published by Miller and Bowman (1989). The separate mechanisms listed in Appendix A and Appendix B of that paper have been combined to handle hydrocarbon and ammonia combustion simultaneously. The original version was found to be deficient for ammonia combustion under highly dilute conditions where thermal dissocation of NH_3 is important. To rectify this difficulty, the mechanism of Fujii et al. (1981) was blended into the Miller and Bowman (1989) mechanism. The Fujii et al. (1981) mechanism was tested against shock tube experiments.

Reaction	A (cm-moles-sec-K)	n	E (cal/mole)
2CH3(+M)⇌C2H6(+M)	9.030E+16	-1.20	654
Low pressure limit	3.180E+41	-7.0	2762
Troe parameters: a=6.04E-1, T***=6927.0, T*=0.0, T**=132.0			
Enhanced Collision Efficiencies:			
H2=2.0, CO=2.0, CO2=3.0, H2O=5.0			
CH3+H(+M)⇌CH4(+M)	6.000E+16	-1.00	0
Low pressure limit	8.000E+26	-3.0	0
SRI parameters: a=4.50E-1, b=797.0, c=979.0, d=1.0, e=0.0			
Enhanced Collision Efficiencies:			
H2=2.0, CO=2.0, CO2=3.0, H2O=5.0			
CH4+O2⇌CH3+HO2	7.900E+13	0.00	56000
CH4+H⇌CH3+H2	2.200E+04	3.00	8750
CH4+OH⇌CH3+H2O	1.600E+06	2.10	2460
CH4+O⇌CH3+OH	1.020E+09	1.50	8604
CH4+HO2⇌CH3+H2O2	1.800E+11	0.00	18700
CH3+HO2⇌CH3O+OH	2.000E+13	0.00	0
CH3+O2⇌CH3O+O	2.050E+19	-1.57	29229
CH3+O⇌CH2O+H	8.000E+13	0.00	0
CH2OH+H⇌CH3+OH	1.000E+14	0.00	0
CH3O+H⇌CH3+OH	1.000E+14	0.00	0
CH3+OH⇌CH2+H2O	7.500E+06	2.00	5000
CH3+H⇌CH2+H2	9.000E+13	0.00	15100
CH3O+M⇌CH2O+H+M	1.000E+14	0.00	25000
CH2OH+M⇌CH2O+H+M	1.000E+14	0.00	25000
CH3O+H⇌CH2O+H2	2.000E+13	0.00	0
CH2OH+H⇌CH2O+H2	2.000E+13	0.00	0
CH3O+OH⇌CH2O+H2O	1.000E+13	0.00	0
CH2OH+OH⇌CH2O+H2O	1.000E+13	0.00	0
CH3O+O⇌CH2O+OH	1.000E+13	0.00	0
CH2OH+O⇌CH2O+OH	1.000E+13	0.00	0
CH3O+O2⇌CH2O+HO2	6.300E+10	0.00	2600
CH2OH+O2⇌CH2O+HO2	1.480E+13	0.00	1500
CH2+H⇌CH+H2	1.000E+18	-1.56	0
CH2+OH⇌CH+H2O	1.130E+07	2.00	3000
CH2+OH⇌CH2O+H	2.500E+13	0.00	0
CH+O2⇌HCO+O	3.300E+13	0.00	0
CH+O⇌CO+H	5.700E+13	0.00	0
CH+OH⇌HCO+H	3.000E+13	0.00	0
CH+CO2⇌HCO+CO	3.400E+12	0.00	690
CH+H⇌C+H2	1.500E+14	0.00	0
CH+H2O⇌CH2O+H	1.170E+15	-0.75	0
CH+CH2O⇌CH2CO+H	9.460E+13	0.00	-515
CH+C2H2⇌C3H2+H	1.000E+14	0.00	0
CH+CH2⇌C2H2+H	4.000E+13	0.00	0
CH+CH3⇌C2H3+H	3.000E+13	0.00	0
CH+CH4⇌C2H4+H	6.000E+13	0.00	0
C+O2⇌CO+O	2.000E+13	0.00	0
C+OH⇌CO+H	5.000E+13	0.00	0
C+CH3⇌C2H2+H	5.000E+13	0.00	0
C+CH2⇌C2H+H	5.000E+13	0.00	0
CH2+CO2⇌CH2O+CO	1.100E+11	0.00	1000
CH2+O⇌CO+2H	5.000E+13	0.00	0
CH2+O⇌CO+H2	3.000E+13	0.00	0
CH2+O2⇌CO2+2H	1.600E+12	0.00	1000
CH2+O2⇌CH2O+O	5.000E+13	0.00	9000
CH2+O2⇌CO2+H2	6.900E+11	0.00	500
CH2+O2⇌CO+H2O	1.900E+10	0.00	-1000

Reaction	A (cm-moles-sec-K)	n	E (cal/mole)
CH2+O2⇌CO+OH+H	8.600E+10	0.00	-500
CH2+O2⇌HCO+OH	4.300E+10	0.00	-500
CH2O+OH⇌HCO+H2O	3.430E+09	1.18	-447
CH2O+H⇌HCO+H2	2.190E+08	1.77	3000
CH2O+M⇌HCO+H+M	3.310E+16	0.00	81000
CH2O+O⇌HCO+OH	1.800E+13	0.00	3080
HCO+OH⇌H2O+CO	1.000E+14	0.00	0
HCO+M⇌H+CO+M	2.500E+14	0.00	16802
Enhanced Collision Efficiencies:			
CO=1.9, H2=1.9, CH4=2.8, CO2=3.0, H2O=5.0			
HCO+H⇌CO+H2	1.190E+13	0.25	0
HCO+O⇌CO+OH	3.000E+13	0.00	0
HCO+O⇌CO2+H	3.000E+13	0.00	0
HCO+O2⇌HO2+CO	3.300E+13	-0.40	0
CO+O+M⇌CO2+M	6.170E+14	0.00	3000
CO+OH⇌CO2+H	1.510E+07	1.30	-758
CO+O2⇌CO2+O	1.600E+13	0.00	41000
HO2+CO⇌CO2+OH	5.800E+13	0.00	22934
C2H6+CH3⇌C2H5+CH4	5.500E-01	4.00	8300
C2H6+H⇌C2H5+H2	5.400E+02	3.50	5210
C2H6+O⇌C2H5+OH	3.000E+07	2.00	5115
C2H6+OH⇌C2H5+H2O	8.700E+09	1.05	1810
C2H4+H⇌C2H3+H2	1.100E+14	0.00	8500
C2H4+O⇌CH3+HCO	1.600E+09	1.20	746
C2H4+OH⇌C2H3+H2O	2.020E+13	0.00	5955
CH2+CH3⇌C2H4+H	3.000E+13	0.00	0
H+C2H4(+M)⇌C2H5(+M)	2.210E+13	0.00	2066
Low pressure limit	6.37E+27	-2.8	-54
Enhanced Collision Efficiencies:			
H2=2.0, CO=2.0, CO2=3.0, H2O=5.0			
C2H5+H⇌2CH3	1.000E+14	0.00	0
C2H5+O2⇌C2H4+HO2	8.430E+11	0.00	3875
C2H2+O⇌CH2+CO	1.020E+07	2.00	1900
C2H2+O⇌HCCO+H	1.020E+07	2.00	1900
H2+C2H⇌C2H2+H	4.090E+05	2.39	864
H+C2H2(+M)⇌C2H3(+M)	5.540E+12	0.00	2410
Low pressure limit	2.67E+27	-3.5	2410
Enhanced Collision Efficiencies:			
H2=2.0, CO=2.0, CO2=3.0, H2O=5.0			
C2H3+H⇌C2H2+H2	4.000E+13	0.00	0
C2H3+O⇌CH2CO+H	3.000E+13	0.00	0
C2H3+O2⇌CH2O+HCO	4.000E+12	0.00	-250
C2H3+OH⇌C2H2+H2O	5.000E+12	0.00	0
C2H3+CH2⇌C2H2+CH3	3.000E+13	0.00	0
C2H3+C2H⇌2C2H2	3.000E+13	0.00	0
C2H3+CH⇌CH2+C2H2	5.000E+13	0.00	0
OH+C2H2⇌C2H+H2O	3.370E+07	2.00	14000
OH+C2H2⇌HCCOH+H	5.040E+05	2.30	13500
OH+C2H2⇌CH2CO+H	2.180E-04	4.50	-1000
OH+C2H2⇌CH3+CO	4.830E-04	4.00	-2000
HCCOH+H⇌CH2CO+H	1.000E+13	0.00	0
C2H2+O⇌C2H+OH	3.160E+15	-0.60	15000
CH2CO+O⇌CO2+CH2	1.750E+12	0.00	1350
CH2CO+H⇌CH3+CO	1.130E+13	0.00	3428
CH2CO+H⇌HCCO+H2	5.000E+13	0.00	8000
CH2CO+O⇌HCCO+OH	1.000E+13	0.00	8000
CH2CO+OH⇌HCCO+H2O	7.500E+12	0.00	2000

Reaction	A (cm-moles-sec-K)	n	E (cal/mole)
CH2CO(+M)⇌CH2+CO(+M)	3.000E+14	0.00	70980
Low pressure limit	3.60E+15	0.0	59270
C2H+O2⇌2CO+H	5.000E+13	0.00	1500
C2H+C2H2⇌C4H2+H	3.000E+13	0.00	0
H+HCCO⇌CH2(S)+CO	1.000E+14	0.00	0
O+HCCO⇌H+2CO	1.000E+14	0.00	0
HCCO+O2⇌2CO+OH	1.600E+12	0.00	854
CH+HCCO⇌C2H2+CO	5.000E+13	0.00	0
2HCCO⇌C2H2+2CO	1.000E+13	0.00	0
CH2(S)+M⇌CH2+M	1.000E+13	0.00	0
Enhanced Collision Efficiencies:			
	H=0.0		
CH2(S)+CH4⇌2CH3	4.000E+13	0.00	0
CH2(S)+C2H6⇌CH3+C2H5	1.200E+14	0.00	0
CH2(S)+O2⇌CO+OH+H	3.000E+13	0.00	0
CH2(S)+H2⇌CH3+H	7.000E+13	0.00	0
CH2(S)+H⇌CH2+H	2.000E+14	0.00	0
C2H+O⇌CH+CO	5.000E+13	0.00	0
C2H+OH⇌HCCO+H	2.000E+13	0.00	0
2CH2⇌C2H2+H2	4.000E+13	0.00	0
CH2+HCCO⇌C2H3+CO	3.000E+13	0.00	0
CH2+C2H2⇌C3H3+H	1.200E+13	0.00	6600
C4H2+OH⇌C3H2+HCO	6.660E+12	0.00	-410
C3H2+O2⇌HCO+HCCO	1.000E+13	0.00	0
C3H3+O2⇌CH2CO+HCO	3.000E+10	0.00	2868
C3H3+O⇌CH2O+C2H	2.000E+13	0.00	0
C3H3+OH⇌C3H2+H2O	2.000E+13	0.00	0
2C2H2⇌C4H3+H	2.000E+12	0.00	45900
C4H3+M⇌C4H2+H+M	1.000E+16	0.00	59700
CH2(S)+C2H2⇌C3H3+H	3.000E+13	0.00	0
C4H2+O⇌C3H2+CO	1.200E+12	0.00	0
C2H2+O2⇌HCCO+OH	2.000E+08	1.50	30100
C2H2+M⇌C2H+H+M	4.200E+16	0.00	107000
C2H4+M⇌C2H2+H2+M	1.500E+15	0.00	55800
C2H4+M⇌C2H3+H+M	1.400E+16	0.00	82360
H2+O2⇌2OH	1.700E+13	0.00	47780
OH+H2⇌H2O+H	1.170E+09	1.30	3626
O+OH⇌O2+H	4.000E+14	-0.50	0
O+H2⇌OH+H	5.060E+04	2.67	6290
H+O2+M⇌HO2+M	3.61E+17	-0.72	0
Enhanced Collision Efficiencies:			
	H2O=18.6, CO2=4.2, H2=2.9, CO=2.1, N2=1.3		
OH+HO2⇌H2O+O2	7.500E+12	0.00	0
H+HO2⇌2OH	1.400E+14	0.00	1073
O+HO2⇌O2+OH	1.400E+13	0.00	1073
2OH⇌O+H2O	6.000E+08	1.30	0
2H+M⇌H2+M	1.000E+18	-1.00	0
Enhanced Collision Efficiencies:			
	H2=0.0, H2O=0.0, CO2=0.0		
2H+H2⇌2H2	9.200E+16	-0.60	0
2H+H2O⇌H2+H2O	6.000E+19	-1.25	0
2H+CO2⇌H2+CO2	5.490E+20	-2.00	0
H+OH+M⇌H2O+M	1.600E+22	-2.00	0
Enhanced Collision Efficiencies:			
	H2O=5.0		
H+O+M⇌OH+M	6.200E+16	-0.60	0
Enhanced Collision Efficiencies:			

Reaction	A (cm-moles-sec-K)	n	E (cal/mole)
	H2O=5.0		
2O+M⇌O2+M	1.890E+13	0.00	-1788
H+HO2⇌H2+O2	1.250E+13	0.00	0
2HO2⇌H2O2+O2	2.000E+12	0.00	0
H2O2+M⇌2OH+M	1.300E+17	0.00	45500
H2O2+H⇌HO2+H2	1.600E+12	0.00	3800
H2O2+OH⇌H2O+HO2	1.000E+13	0.00	1800
CH+N2⇌HCN+N	3.000E+11	0.00	13600
CN+N⇌C+N2	1.040E+15	-0.50	0
CH2+N2⇌HCN+NH	1.000E+13	0.00	74000
H2CN+N⇌N2+CH2	2.000E+13	0.00	0
H2CN+M⇌HCN+H+M	3.000E+14	0.00	22000
C+NO⇌CN+O	6.600E+13	0.00	0
CH+NO⇌HCN+O	1.100E+14	0.00	0
CH2+NO⇌HCNO+H	1.390E+12	0.00	-1100
CH3+NO⇌HCN+H2O	1.000E+11	0.00	15000
CH3+NO⇌H2CN+OH	1.000E+11	0.00	15000
HCCO+NO⇌HCNO+CO	2.000E+13	0.00	0
CH2(S)+NO⇌HCN+OH	2.000E+13	0.00	0
HCNO+H⇌HCN+OH	1.000E+14	0.00	12000
CH2+N⇌HCN+H	5.000E+13	0.00	0
CH+N⇌CN+H	1.300E+13	0.00	0
CO2+N⇌NO+CO	1.900E+11	0.00	3400
HCCO+N⇌HCN+CO	5.000E+13	0.00	0
CH3+N⇌H2CN+H	3.000E+13	0.00	0
C2H3+N⇌HCN+CH2	2.000E+13	0.00	0
C3H3+N⇌HCN+C2H2	1.000E+13	0.00	0
HCN+OH⇌CN+H2O	1.450E+13	0.00	10929
OH+HCN⇌HOCN+H	5.850E+04	2.40	12500
OH+HCN⇌HNCO+H	1.980E-03	4.00	1000
OH+HCN⇌NH2+CO	7.830E-04	4.00	4000
HOCN+H⇌HNCO+H	1.000E+13	0.00	0
HCN+O⇌NCO+H	1.380E+04	2.64	4980
HCN+O⇌NH+CO	3.450E+03	2.64	4980
HCN+O⇌CN+OH	2.700E+09	1.58	26600
CN+H2⇌HCN+H	2.950E+05	2.45	2237
CN+O⇌CO+N	1.800E+13	0.00	0
CN+O2⇌NCO+O	5.600E+12	0.00	0
CN+OH⇌NCO+H	6.000E+13	0.00	0
CN+HCN⇌C2N2+H	2.000E+13	0.00	0
CN+NO2⇌NCO+NO	3.000E+13	0.00	0
CN+N2O⇌NCO+N2	1.000E+13	0.00	0
C2N2+O⇌NCO+CN	4.570E+12	0.00	8880
C2N2+OH⇌HOCN+CN	1.860E+11	0.00	2900
HO2+NO⇌NO2+OH	2.110E+12	0.00	-479
NO2+H⇌NO+OH	3.500E+14	0.00	1500
NO2+O⇌NO+O2	1.000E+13	0.00	600
NO2+M⇌NO+O+M	1.100E+16	0.00	66000
NCO+H⇌NH+CO	5.000E+13	0.00	0
NCO+O⇌NO+CO	2.000E+13	0.00	0
NCO+N⇌N2+CO	2.000E+13	0.00	0
NCO+OH⇌NO+CO+H	1.000E+13	0.00	0
NCO+M⇌N+CO+M	3.100E+16	-0.50	48000
NCO+NO⇌N2O+CO	1.000E+13	0.00	-390
NCO+H2⇌HNCO+H	8.580E+12	0.00	9000
HNCO+H⇌NH2+CO	2.000E+13	0.00	3000
NH+O2⇌NO+OH	7.600E+10	0.00	1530

Reaction	A (cm-moles-sec-K)	n	E (cal/mole)
NH+NO⇌N2O+H	2.400E+15	-0.80	0
N2O+OH⇌N2+HO2	2.000E+12	0.00	10000
N2O+H⇌N2+OH	7.600E+13	0.00	15200
N2O+M⇌N2+O+M	1.600E+14	0.00	51600
N2O+O⇌N2+O2	1.000E+14	0.00	28200
N2O+O⇌2NO	1.000E+14	0.00	28200
NH+OH⇌HNO+H	2.000E+13	0.00	0
NH+OH⇌N+H2O	5.000E+11	0.50	2000
NH+N⇌N2+H	3.000E+13	0.00	0
NH+H⇌N+H2	1.000E+14	0.00	0
NH2+O⇌HNO+H	6.630E+14	-0.50	0
NH2+O⇌NH+OH	6.750E+12	0.00	0
NH2+OH⇌NH+H2O	4.000E+06	2.00	1000
NH2+H⇌NH+H2	6.920E+13	0.00	3650
NH2+NO⇌NNH+OH	6.400E+15	-1.25	0
NH2+NO⇌N2+H2O	6.200E+15	-1.25	0
NNH+M⇌N2+H+M	1.000E+04	0.00	0
NNH+NO⇌N2+HNO	5.000E+13	0.00	0
NNH+H⇌N2+H2	1.000E+14	0.00	0
NNH+OH⇌N2+H2O	5.000E+13	0.00	0
NNH+NH2⇌N2+NH3	5.000E+13	0.00	0
NNH+NH⇌N2+NH2	5.000E+13	0.00	0
NNH+O⇌N2O+H	1.000E+14	0.00	0
HNO+M⇌H+NO+M	1.500E+16	0.00	48680
Enhanced Collision Efficiencies: H2O=10.0, O2=2.0, N2=2.0, H2=2.0			
HNO+OH⇌NO+H2O	3.600E+13	0.00	0
HNO+H⇌H2+NO	5.000E+12	0.00	0
HNO+NH2⇌NH3+NO	2.000E+13	0.0	1000
N+NO⇌N2+O	3.270E+12	0.30	0
N+O2⇌NO+O	6.400E+09	1.00	6280
N+OH⇌NO+H	3.800E+13	0.00	0
NH+O⇌NO+H	2.000E+13	0.00	0
HNO+HNO⇌N2O+H2O	3.950E+12	0.00	5000
HNO+NO⇌N2O+OH	2.000E+12	0.00	26000
NH2+NH⇌N2H2+H	5.000E+13	0.00	0
2NH⇌N2+2H	2.540E+13	0.00	0
NH2+N⇌N2+2H	7.200E+13	0.00	0
N2H2+M⇌NNH+H+M	5.000E+16	0.00	50000
Enhanced Collision Efficiencies: H2O=15.0, O2=2.0, N2=2.0, H2=2.0			
N2H2+H⇌NNH+H2	5.000E+13	0.00	1000
N2H2+O⇌NH2+NO	1.000E+13	0.00	0
N2H2+O⇌NNH+OH	2.000E+13	0.00	1000
N2H2+OH⇌NNH+H2O	1.000E+13	0.00	1000
N2H2+NO⇌N2O+NH2	3.000E+12	0.00	0
N2H2+NH⇌NNH+NH2	1.000E+13	0.00	1000
N2H2+NH2⇌NH3+NNH	1.000E+13	0.00	1000
2NH2⇌N2H2+H2	5.000E+11	0.00	0
NH3+M⇌NH2+H+M	1.778E+16	0.00	92100
NH3+O2⇌NH2+HO2	1.000E+12	0.00	61500
NH3+H⇌NH2+H2	1.259E+14	0.00	22000
NH3+O⇌NH2+OH	1.514E+12	0.00	6000
NH3+OH⇌NH2+H2O	2.512E+12	0.00	2000
NH2+O2⇌HNO+OH	1.5849E+13	0.00	28600
HNO+O2⇌NO+HO2	3.1623E+12	0.00	3000
NH2+O2⇌NH+HO2	1.0000E+14	0.00	50000

Reaction	A (cm-moles-sec-K)	n	E (cal/mole)
NH+O2⇌O+HNO	1.0000E+14	0.00	1000

E.5 Miller et al. (1983)

Reaction	A (cm-moles-sec-K)	n	E (cal/mole)
NH3+M⇌NH2+H+M	1.400E+16	0.00	90600
NH3+H⇌NH2+H2	2.460E+13	0.00	17071
NH3+O⇌NH2+OH	1.500E+12	0.00	6040
NH3+OH⇌NH2+H2O	3.250E+12	0.00	2120
H+NH2⇌NH+H2	6.920E+13	0.00	3650
NH2+OH⇌NH+H2O	4.500E+12	0.00	2200
NH2+O2⇌HNO+OH	4.500E+12	0.00	25000
O+NH2⇌HNO+H	6.630E+14	-0.50	0
O+NH2⇌NH+OH	6.750E+12	0.00	0
H+NH⇌N+H2	3.000E+13	0.00	0
NH+O⇌NO+H	2.000E+13	0.00	0
NH+O⇌N+OH	1.000E+12	0.50	100
NH+OH⇌N+H2O	5.000E+11	0.50	2000
NH+OH⇌H+HNO	2.000E+13	0.00	0
HNO+M⇌H+NO+M	1.500E+16	0.00	48680
Enhanced Collision Efficiencies:			
	H2O=6.0, H2=2.0, O2=2.0, N2=2.0		
HNO+O⇌OH+NO	1.000E+11	0.00	0
HNO+OH⇌NO+H2O	3.600E+13	0.00	0
HNO+H⇌H2+NO	5.000E+12	0.00	0
NH+NO⇌N2O+H	4.330E+14	-0.50	0
N2O+O⇌2NO	1.000E+14	0.00	28200
N2O+O⇌N2+O2	1.000E+14	0.00	28200
N2O+M⇌N2+O+M	1.620E+14	0.00	51600
N2O+H⇌N2+OH	7.600E+13	0.00	15200
N2O+NH⇌N2+HNO	1.000E+11	0.50	3000
N2H3+O⇌N2H2+OH	5.000E+12	0.00	5000
N2H3+O⇌NH2+HNO	1.000E+13	0.00	0
N2H3+OH⇌N2H2+H2O	1.000E+13	0.00	1000
N2H3+H⇌NH2+NH2	1.600E+12	0.00	0
N2H3+M⇌N2H2+H+M	3.500E+16	0.00	46000
N2H3+NH⇌NH2+N2H2	2.000E+13	0.00	0
N2H2+M⇌NNH+H+M	5.000E+16	0.00	50000
N2H2+O⇌NNH+OH	2.000E+13	0.00	1000
N2H2+O⇌NO+NH2	1.000E+13	0.00	0
N2H2+NO⇌N2O+NH2	3.000E+12	0.00	0
NH+NH2⇌N2H2+H	5.000E+13	0.00	0
N2H2+OH⇌NNH+H2O	1.000E+13	0.00	1000
N2H2+H⇌NNH+H2	5.000E+13	0.00	1000
N2H2+NH⇌NNH+NH2	1.000E+13	0.00	1000
N2H2+NH2⇌NH3+NNH	1.000E+13	0.00	1000
NH2+NH2⇌N2H2+H2	5.000E+11	0.00	0
NH2+NH2+M⇌N2H4+M	3.000E+20	-1.00	0
Enhanced Collision Efficiencies:			
	H2O=10.0, N2=2.0		
H+N2H4⇌H2+N2H3	1.300E+13	0.00	2500
NH2+N2H4⇌NH3+N2H3	3.900E+12	0.00	1500
O+N2H4⇌N2H2+H2O	8.500E+13	0.00	1200
OH+N2H4⇌N2H3+H2O	5.000E+12	0.00	1000
N2H3+OH⇌NH3+HNO	1.000E+12	0.00	15000
NH+NH⇌N2+H+H	2.540E+13	0.00	0
NH2+HNO⇌NH3+NO	2.000E+13	0.00	1000
NH+H+M⇌NH2+M	2.000E+16	-0.50	0
NO+NH2⇌HNO+NH	1.000E+13	0.00	40000
NH2+NO⇌NNH+OH	8.820E+15	-1.25	0
NH2+NO⇌N2+H2O	3.780E+15	-1.25	0
NH2+NO⇌HNNO+H	8.000E+13	0.00	28000

Reaction	A (cm-moles-sec-K)	n	E (cal/mole)
HNNO+H⇌N2O+H2	2.000E+13	0.00	0
HNNO+O⇌OH+N2O	2.000E+13	0.00	0
HNNO+OH⇌N2O+H2O	2.000E+13	0.00	0
NH+O2⇌HNO+O	1.000E+13	0.00	12000
NH+O2⇌NO+OH	1.400E+11	0.00	2000
HNO+HNO⇌N2O+H2O	3.950E+12	0.00	5000
HNO+NO⇌N2O+OH	2.000E+12	0.00	26000
HNNO+NO⇌HNO+N2O	2.000E+12	0.00	5000
NNH+NO⇌N2+HNO	5.000E+13	0.00	0
NNH+H⇌N2+H2	3.700E+13	0.00	3000
NNH+O⇌N2+OH	1.000E+13	0.00	5000
NNH+OH⇌N2+H2O	3.000E+13	0.00	0
NNH+O⇌N2O+H	1.000E+13	0.00	3000
OH+N2O⇌N2+HO2	1.000E+12	0.00	10000
NNH+NH2⇌N2+NH3	1.000E+13	0.00	0
NH2+NH2⇌NH3+NH	5.000E+12	0.00	10000
NNH+M⇌N2+H+M	2.000E+14	0.00	20000
NNH+O2⇌N2+HO2	2.000E+12	0.00	9000
NO+HO2⇌HNO+O2	5.000E+11	0.00	15000
H+NO2⇌NO+OH	3.500E+14	0.00	1500
HO2+NO⇌NO2+OH	2.110E+12	0.00	-479
O+NO2⇌NO+O2	1.000E+13	0.00	600
NO2+M⇌NO+O+M	1.100E+16	0.00	66000
H2+O2⇌2OH	1.700E+13	0.00	47780
OH+H2⇌H2O+H	1.170E+09	1.30	3626
H+O2⇌OH+O	5.130E+16	-0.816	16507
O+H2⇌OH+H	1.800E+10	1.00	8826
H+O2+M⇌HO2+M	2.100E+18	-1.00	0
Enhanced Collision Efficiencies:			
	H2O=21.0, H2=3.3		
H+O2+N2⇌HO2+N2	6.700E+19	-1.42	0
H+O2+O2⇌HO2+O2	6.700E+19	-1.42	0
OH+HO2⇌H2O+O2	5.000E+13	0.00	1000
H+HO2⇌2OH	2.500E+14	0.00	1900
O+HO2⇌O2+OH	4.800E+13	0.00	1000
2OH⇌O+H2O	6.000E+08	1.30	0
H2+M⇌H+H+M	2.230E+12	0.50	92600
Enhanced Collision Efficiencies:			
	H2O=6.0, H=20.0, H2=3.0		
O2+M⇌2O+M	1.850E+11	0.50	95560
H+OH+M⇌H2O+M	7.500E+23	-2.60	0
Enhanced Collision Efficiencies:			
	H2O=19.0		
H+HO2⇌H2+O2	2.500E+13	0.00	700
HO2+HO2⇌H2O2+O2	2.000E+12	0.00	0
H2O2+M⇌OH+OH+M	1.300E+17	0.00	45500
H2O2+H⇌HO2+H2	1.600E+12	0.00	3800
H2O2+OH⇌H2O+HO2	1.000E+13	0.00	18000
O+N2⇌NO+N	1.840E+14	0.00	76250
N+O2⇌NO+O	6.400E+09	1.00	6280
H+NO⇌N+OH	2.220E+14	0.00	50500

F Soot Foil Photographs

In the soot foil photographs in this Appendix, the detonation wave propagated from top to bottom.

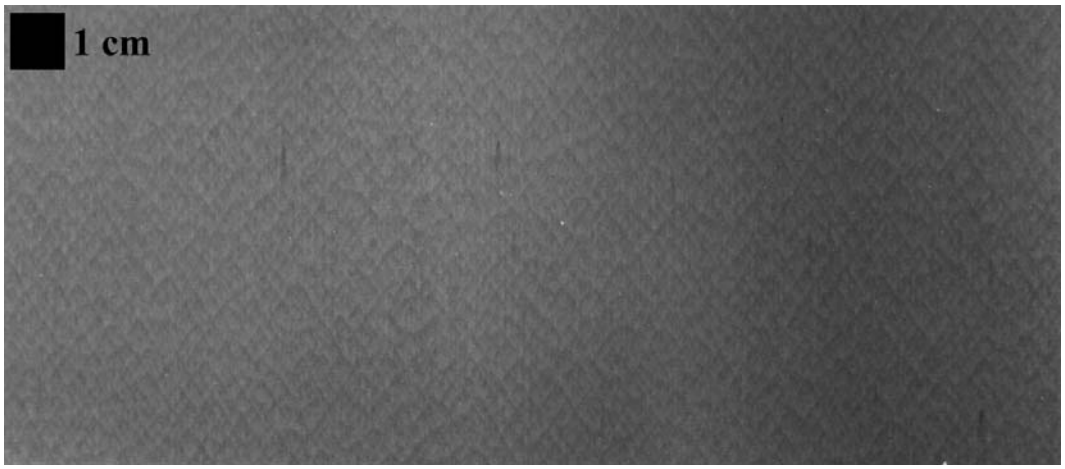

Figure 60: Shot 276: Typical small sized cells

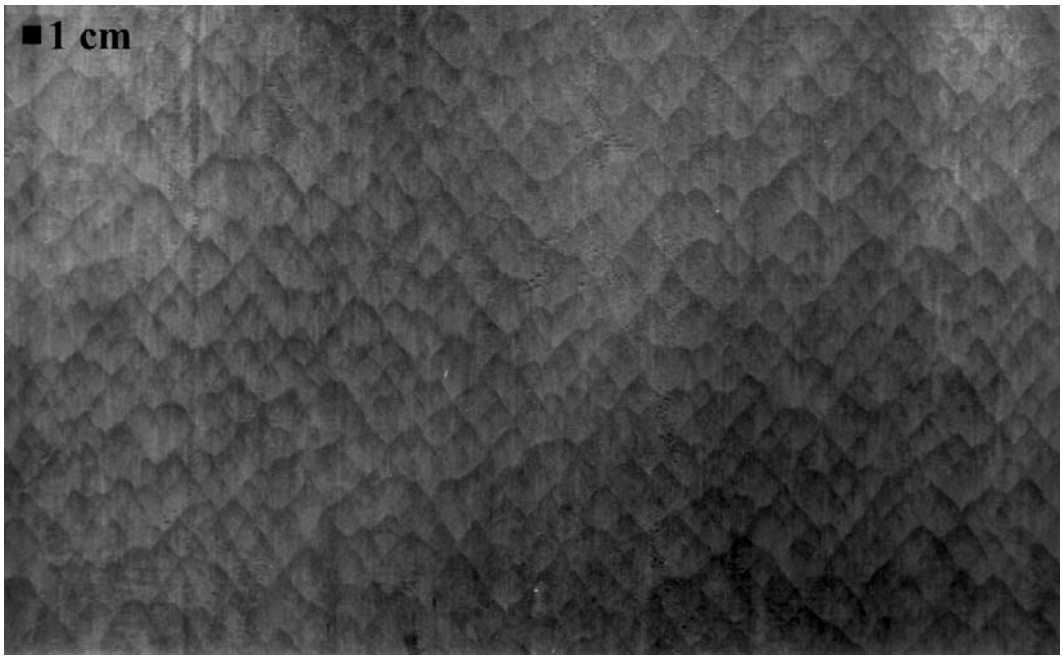

Figure 61: Shot 321: Typical medium sized cells

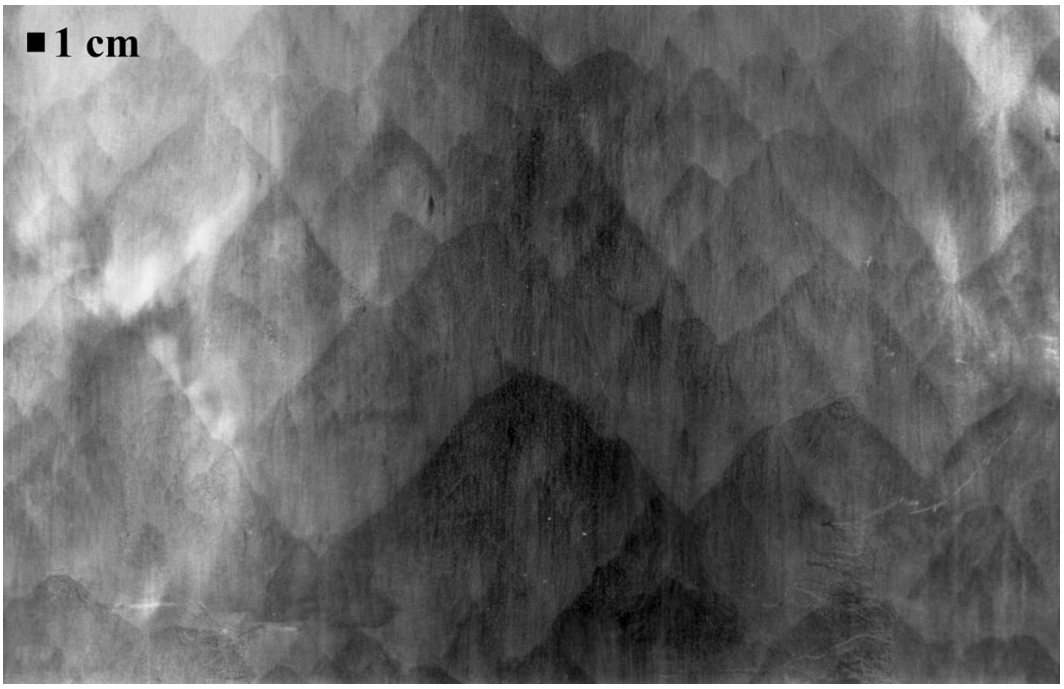

Figure 62: Shot 312: Typical large sized cells

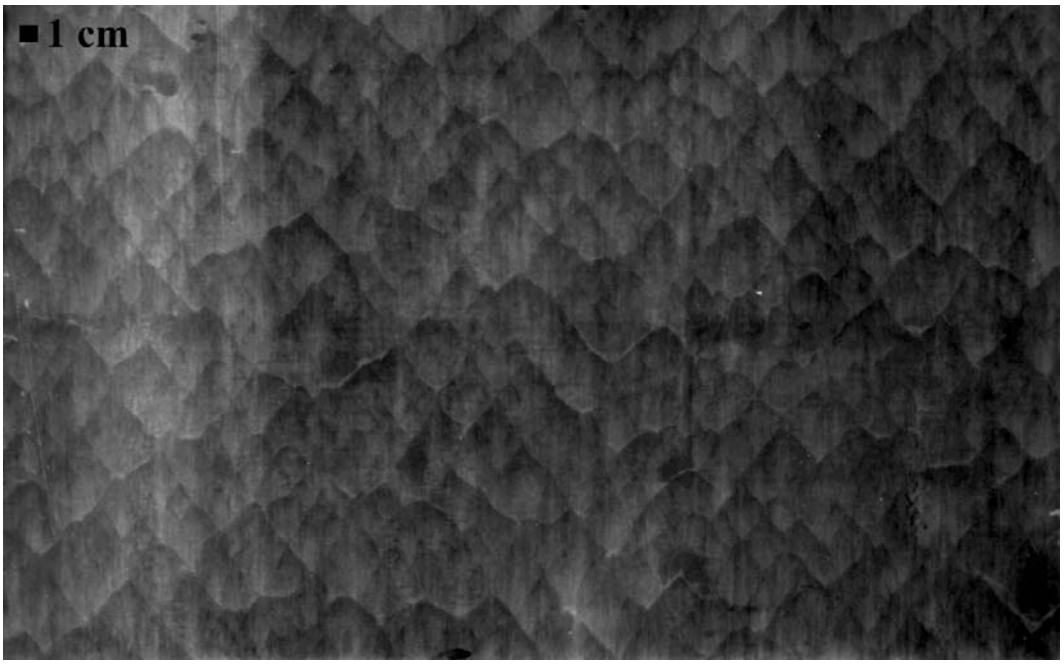

Figure 63: Shot 297: Typical irregular cells

G Pressure Traces

This appendix contains selected pressure traces corresponding to the tests listed in Appendix A. Only traces containing useful information are included, and detailed discussion of each trace is not provided. These data are intended for reference only, and interpretation of them should be made with caution.

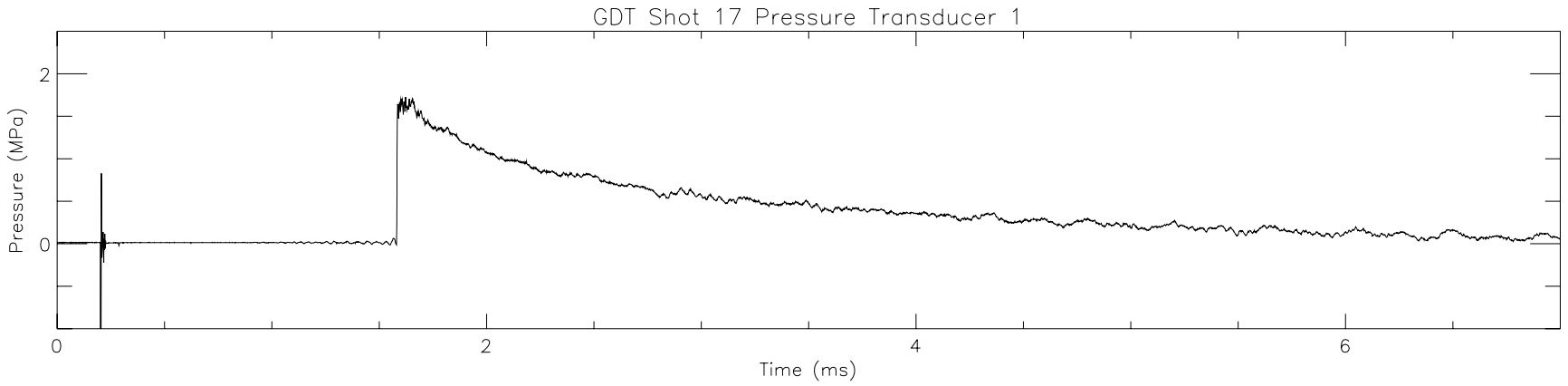
GDT Shot 17 Pressure Transducer 1
Pressure (MPa)
2
0
0
2
4
6
Time (ms)

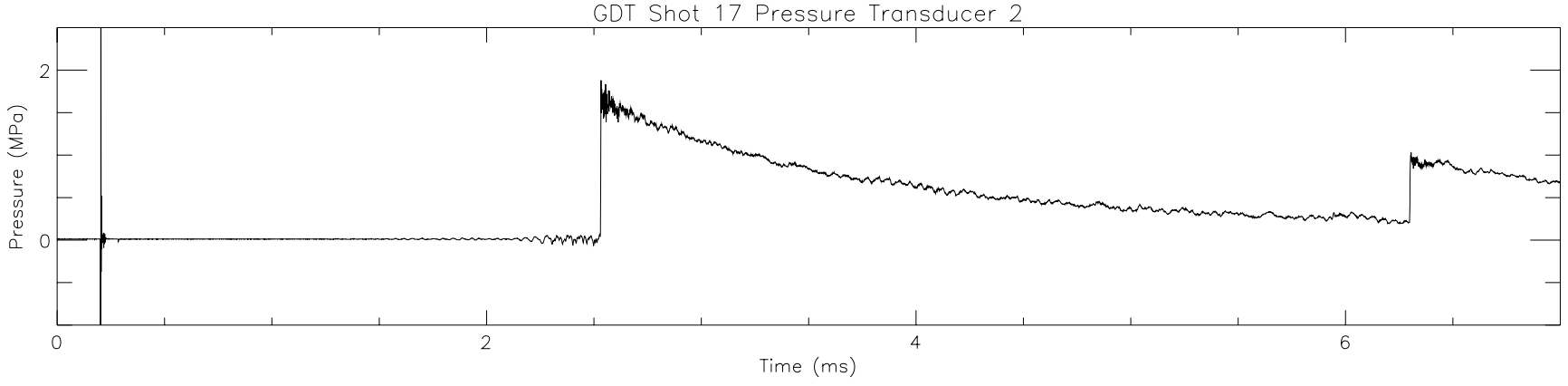
GDT Shot 17 Pressure Transducer 2
Pressure (MPa)
2
0
0
2
4
6
Time (ms)

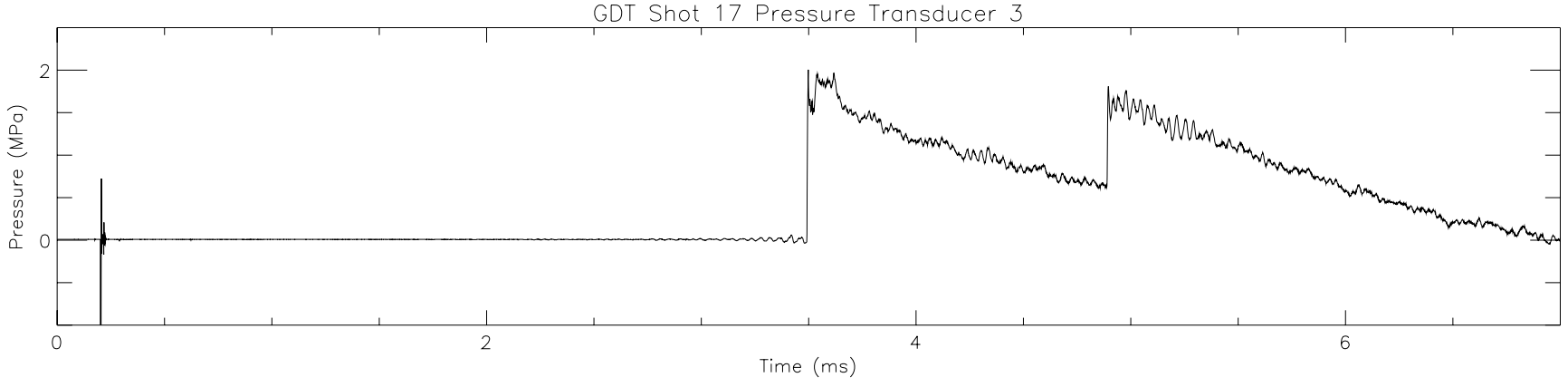
GDT Shot 17 Pressure Transducer 3
Pressure (MPa)
2
0
0
2
4
6
Time (ms)

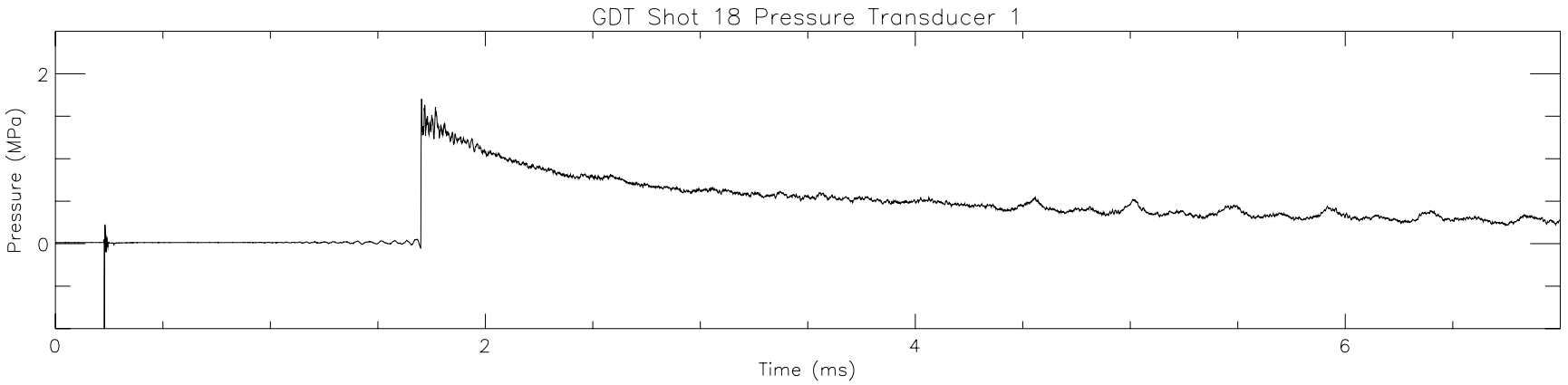
GDT Shot 18 Pressure Transducer 1
Pressure (MPa)
2
0
0
2
4
6
Time (ms)

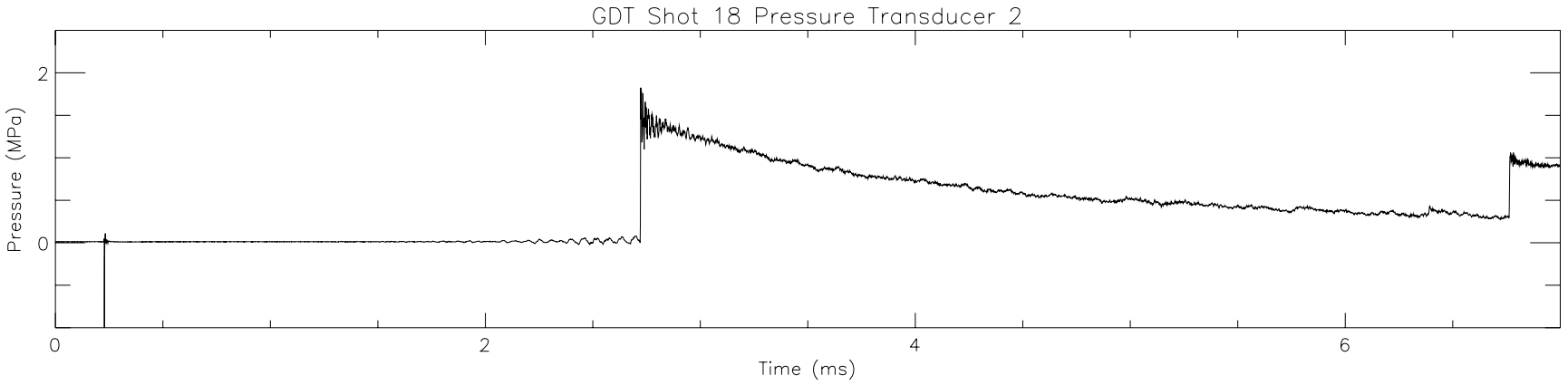
GDT Shot 18 Pressure Transducer 2
Pressure (MPa)
2
0
0
2
4
6
Time (ms)

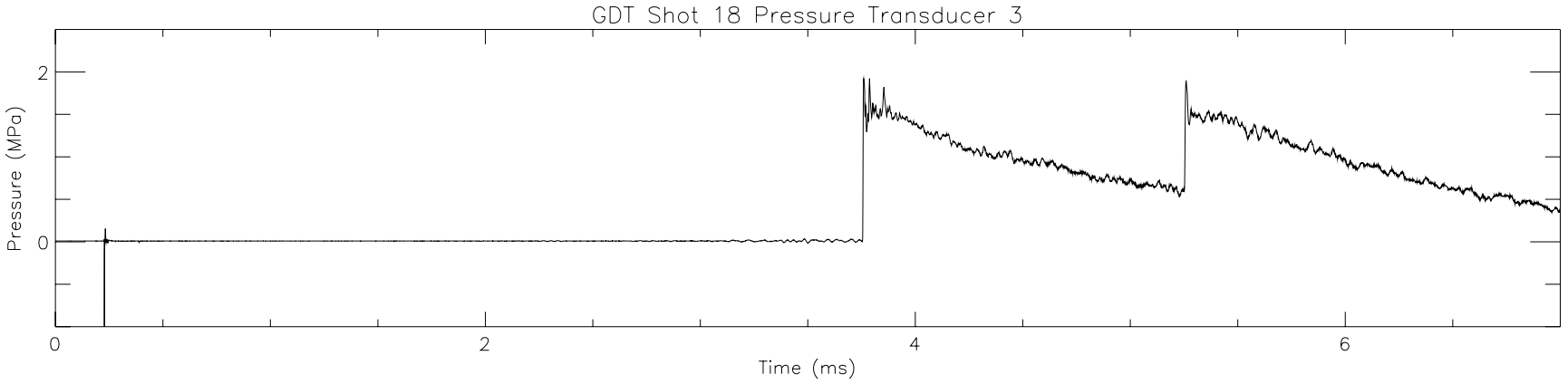
GDT Shot 18 Pressure Transducer 3
Pressure (MPa)
2
0
0
2
4
6
Time (ms)

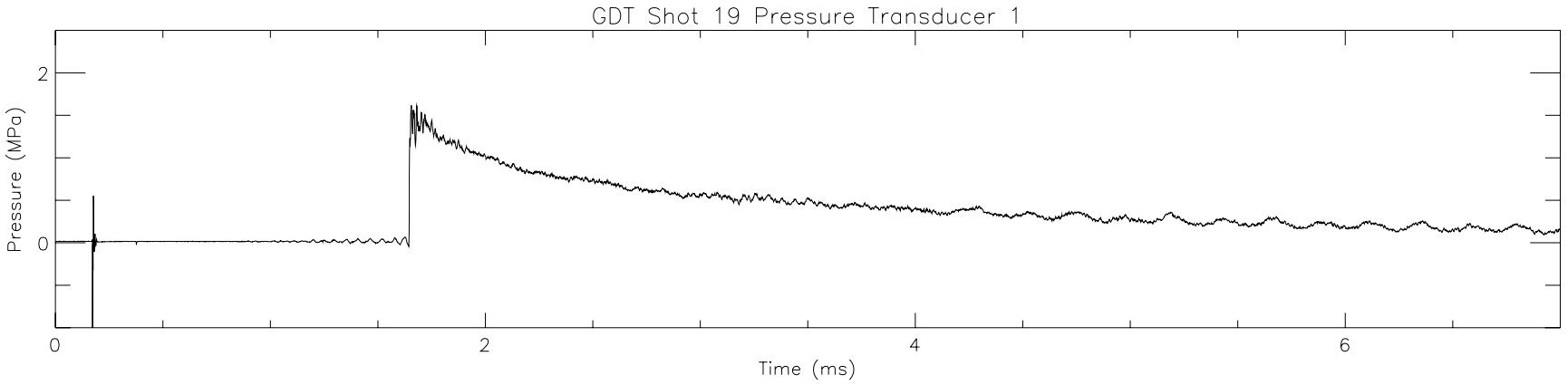
GDT Shot 19 Pressure Transducer 1
Pressure (MPa)
2
0
0
2
4
6
Time (ms)

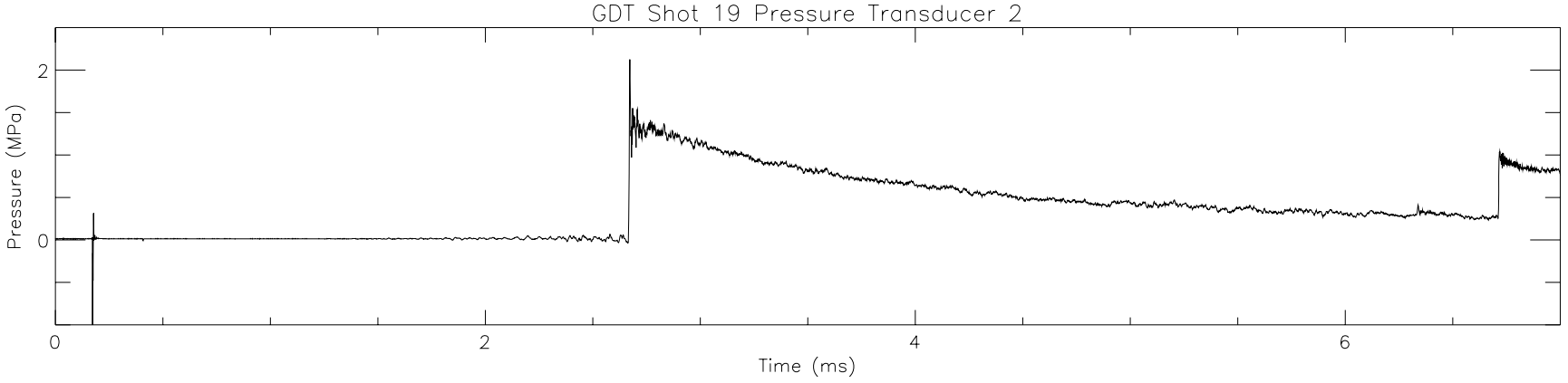
GDT Shot 19 Pressure Transducer 2
Pressure (MPa)
2
0
0
2
4
6
Time (ms)

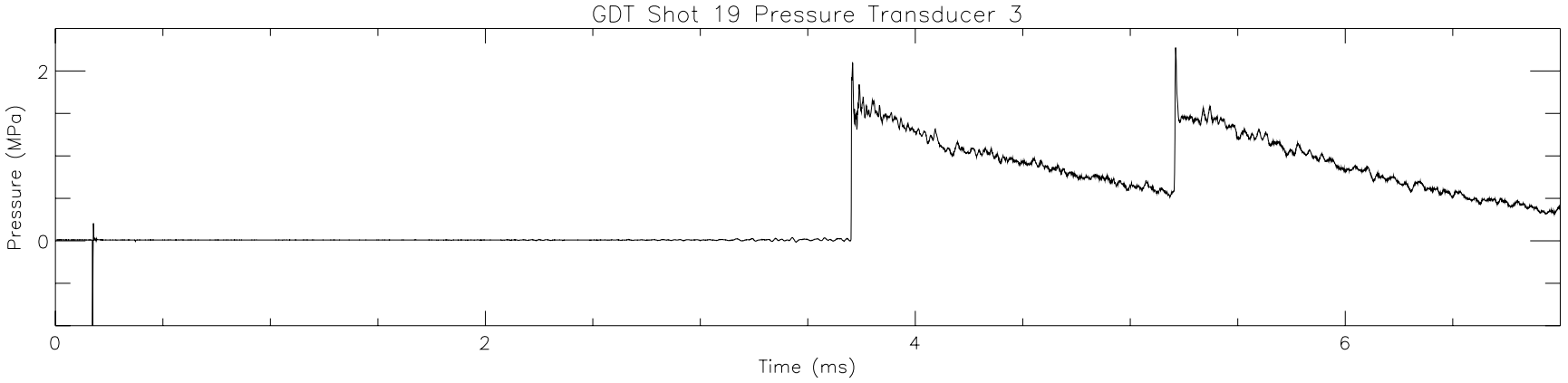
GDT Shot 19 Pressure Transducer 3
Pressure (MPa)
2
0
0
2
4
6
Time (ms)

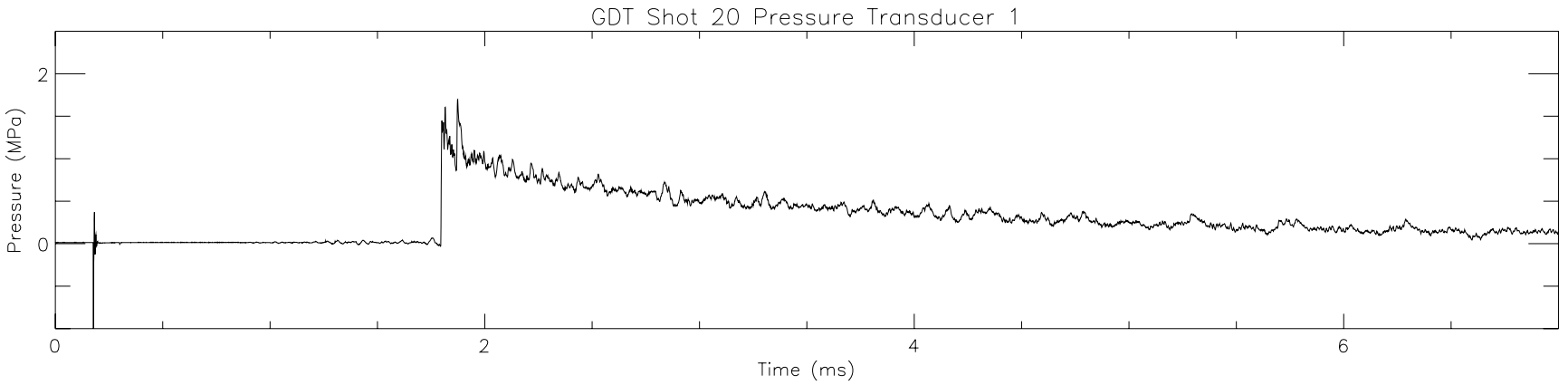
GDT Shot 20 Pressure Transducer 1
Pressure (MPa)
2
0
0
2
4
6
Time (ms)

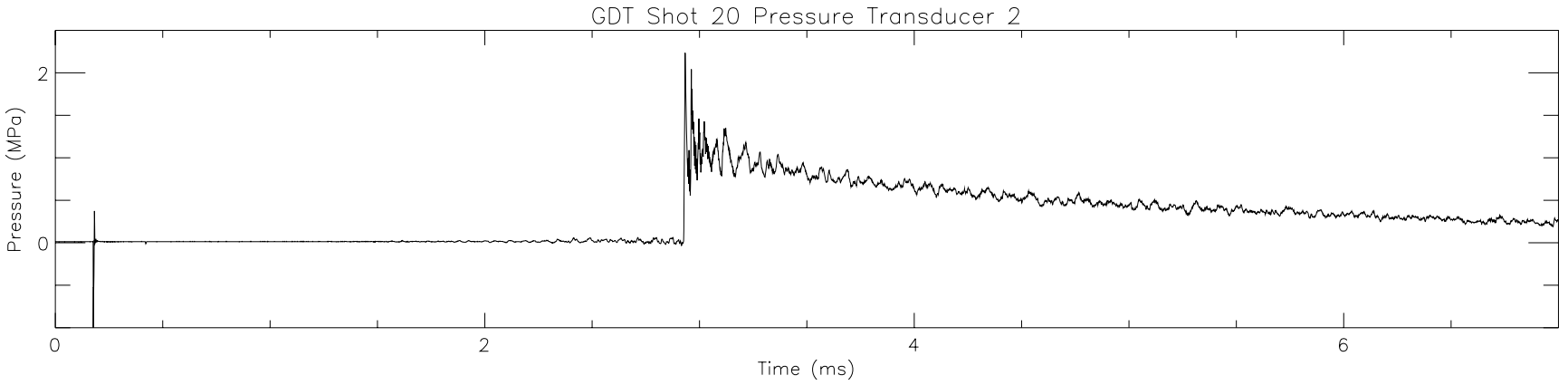
GDT Shot 20 Pressure Transducer 2
Pressure (MPa)
2
0
0
2
4
6
Time (ms)

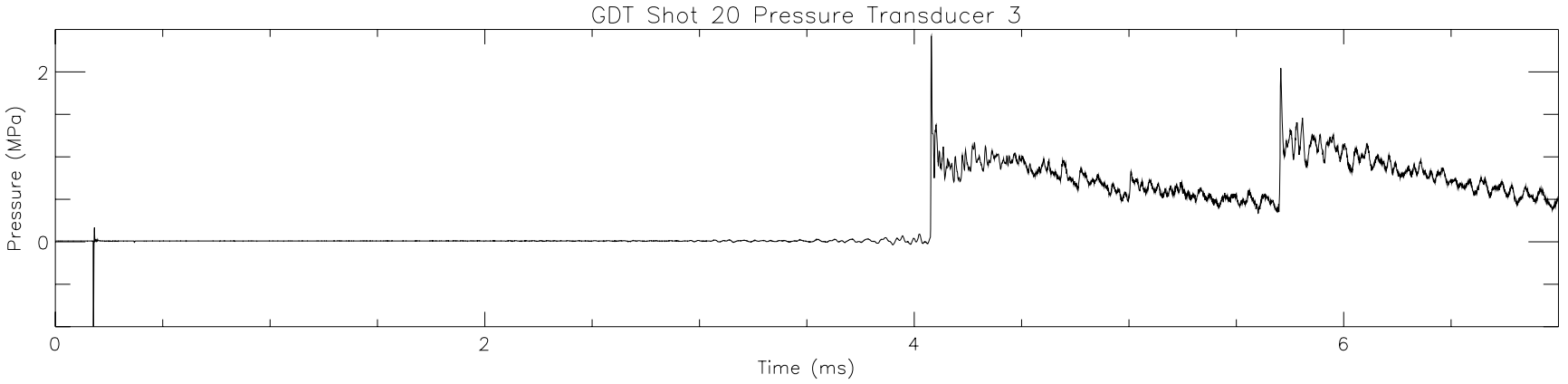
GDT Shot 20 Pressure Transducer 3
Pressure (MPa)
2
0
0
2
4
6
Time (ms)

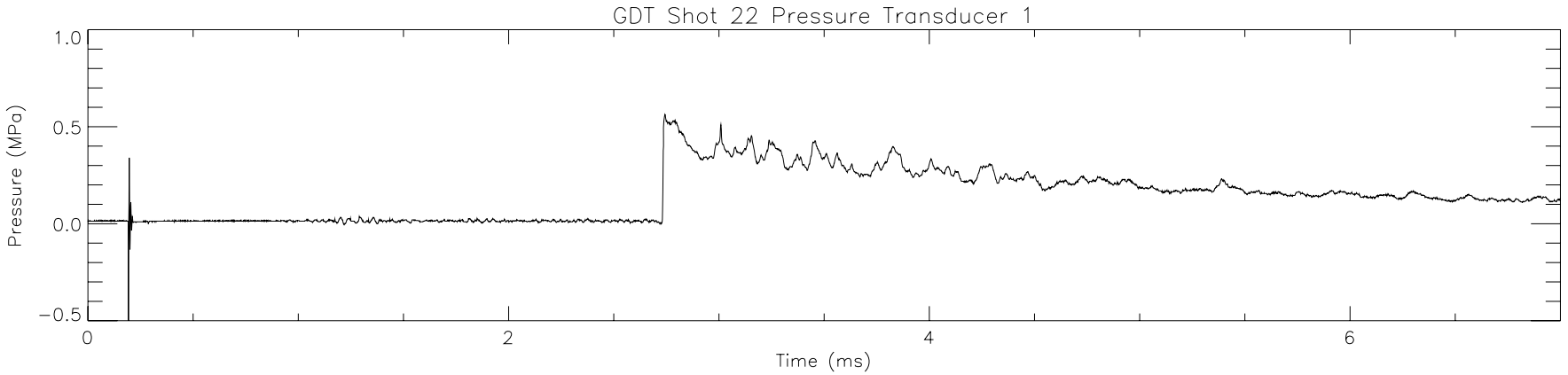
GDT Shot 22 Pressure Transducer 1
Pressure (MPa)
1.0
0.5
0.0
−0.5
0
2
4
6
Time (ms)

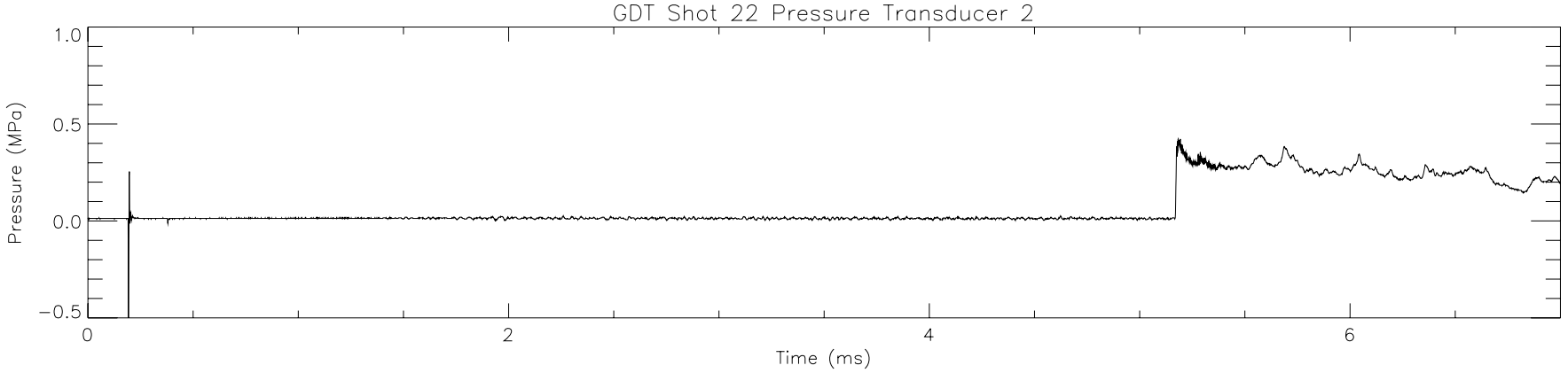
GDT Shot 22 Pressure Transducer 2
Pressure (MPa)
1.0
0.5
0.0
−0.5
0
2
4
6
Time (ms)

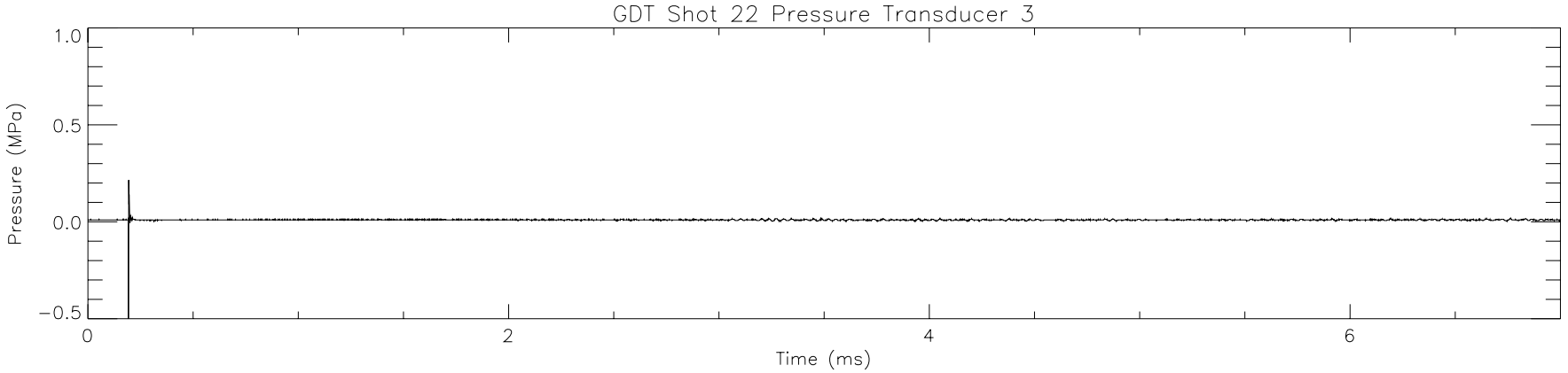
GDT Shot 22 Pressure Transducer 3
Pressure (MPa)
1.0
0.5
0.0
−0.5
0
2
4
6
Time (ms)

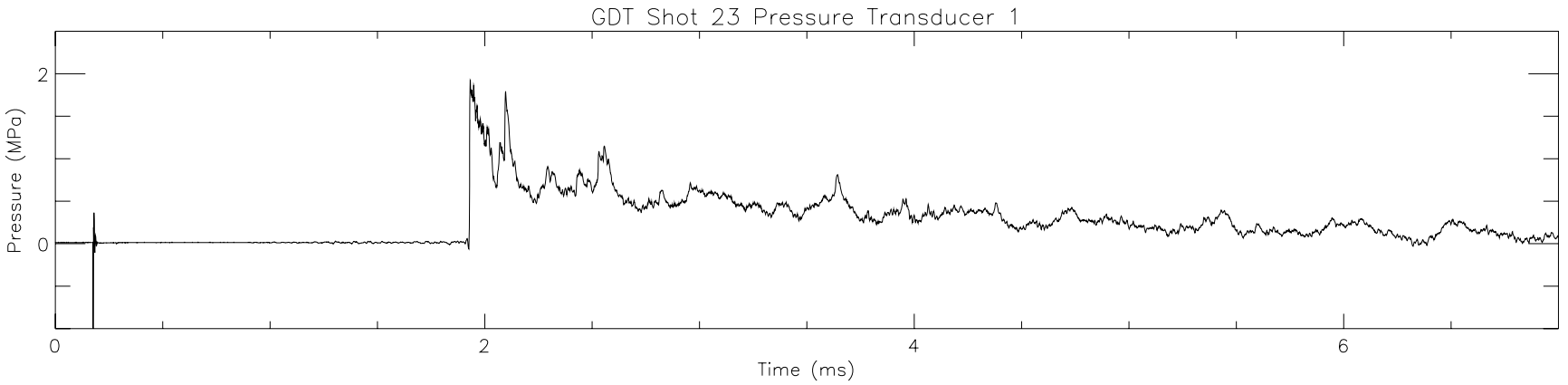
GDT Shot 23 Pressure Transducer 1
Pressure (MPa)
2
0
0
2
4
6
Time (ms)

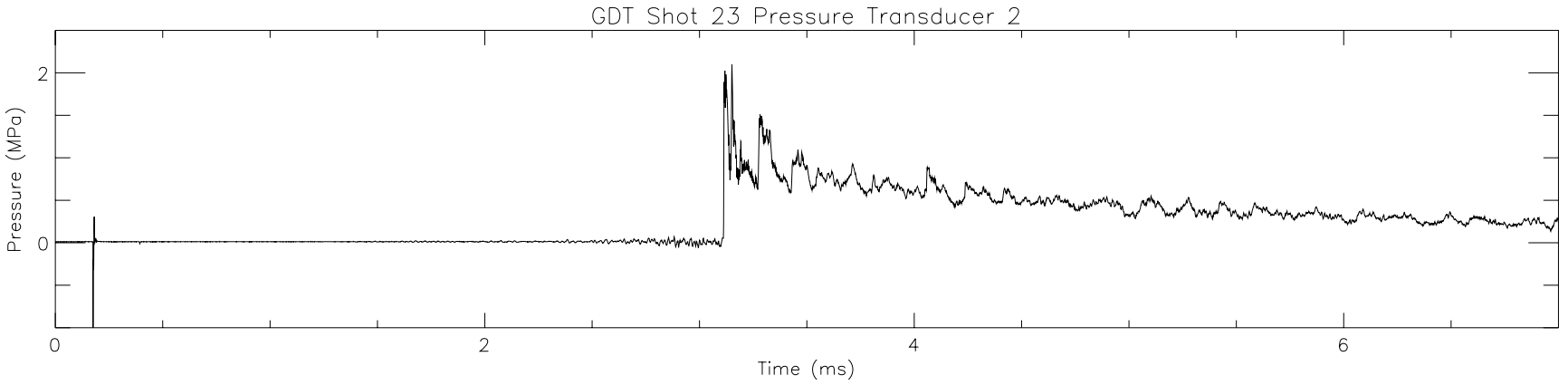
GDT Shot 23 Pressure Transducer 2
Pressure (MPa)
2
0
0
2
4
6
Time (ms)

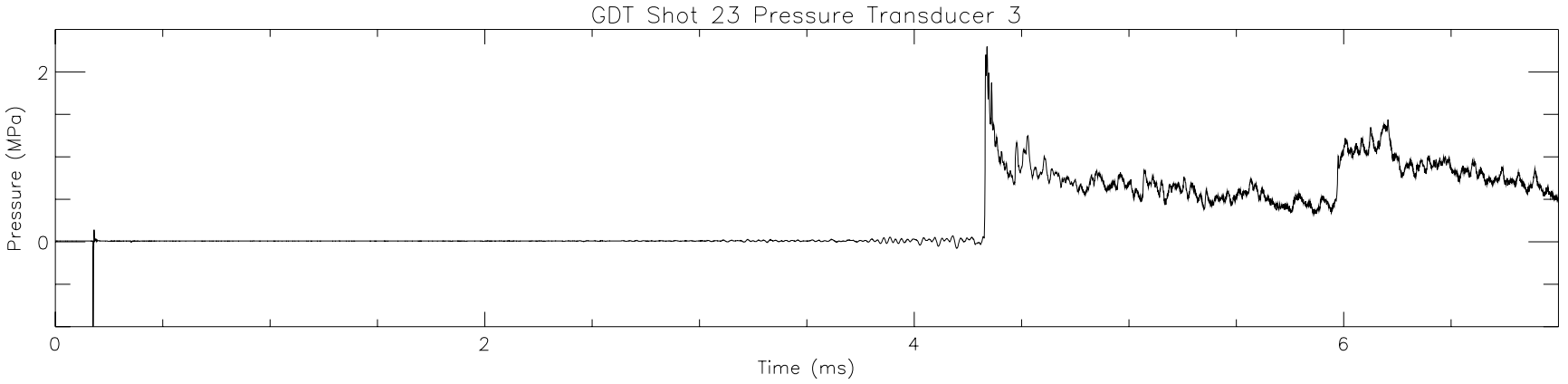
GDT Shot 23 Pressure Transducer 3
Pressure (MPa)
2
0
0
2
4
6
Time (ms)

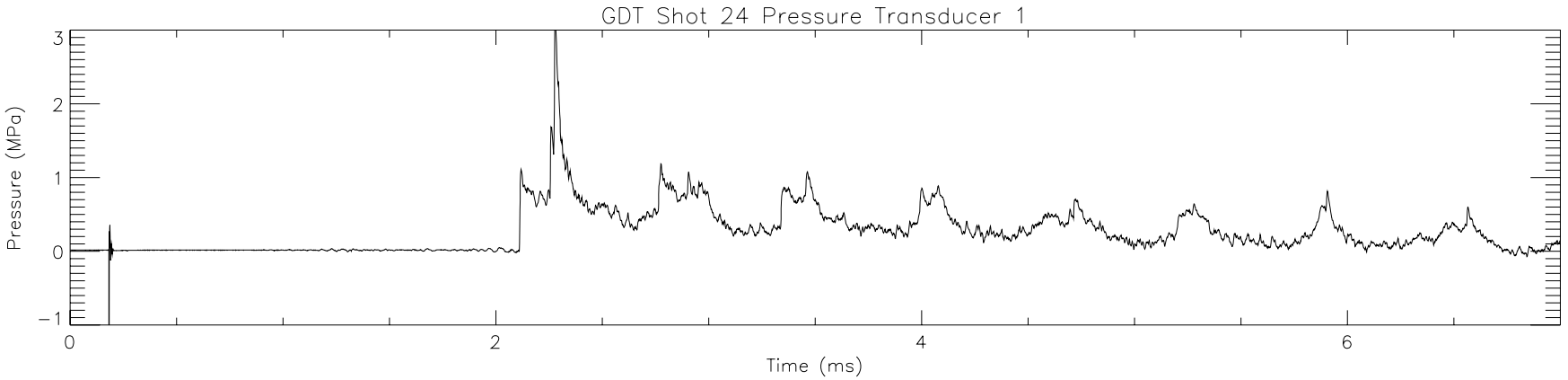
GDT Shot 24 Pressure Transducer 1
Pressure (MPa)
3
2
1
0
−1
0
2
4
6
Time (ms)

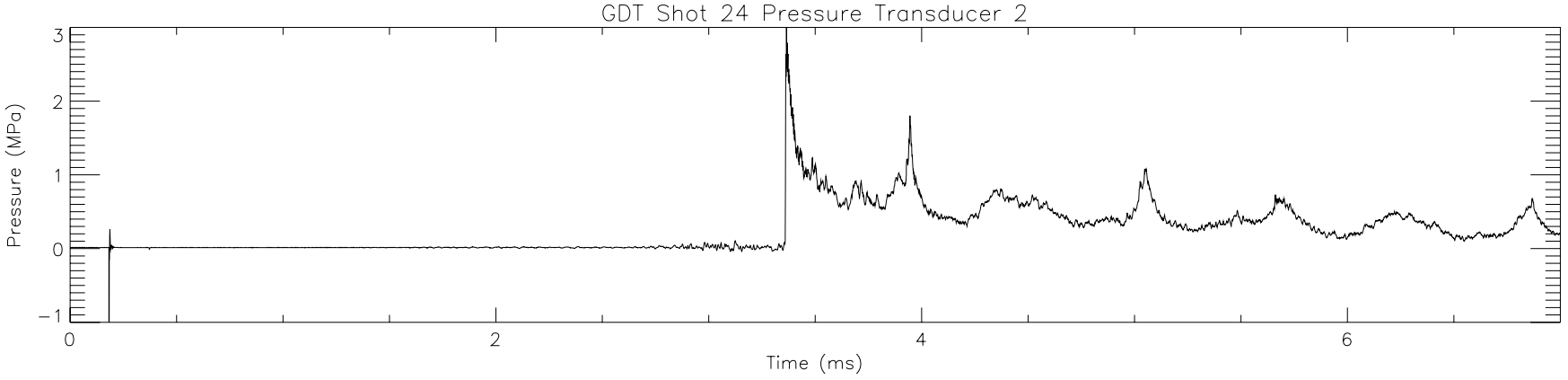
GDT Shot 24 Pressure Transducer 2
Pressure (MPa)
3
2
1
0
−1
0
2
4
6
Time (ms)

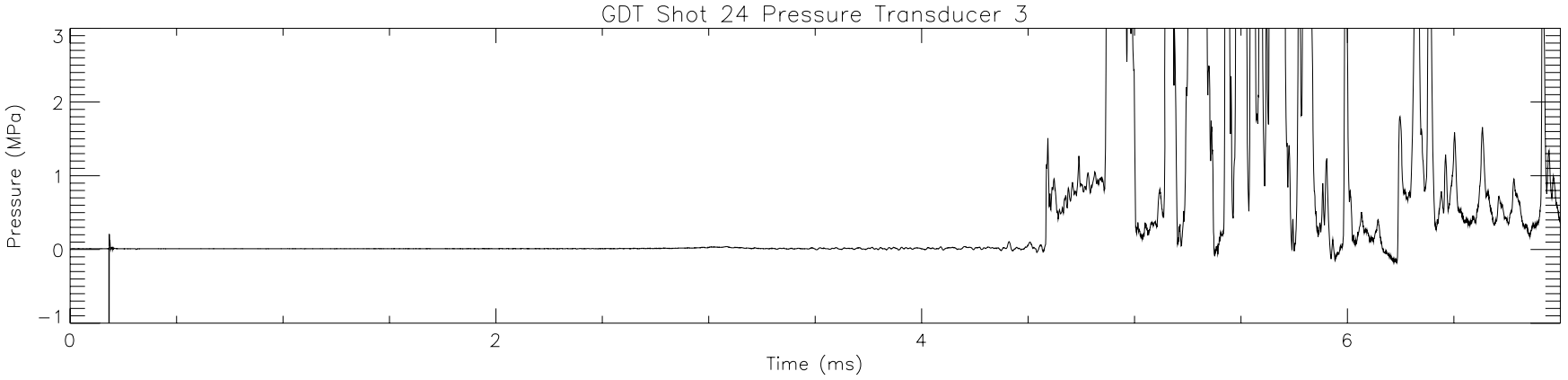
GDT Shot 24 Pressure Transducer 3
Pressure (MPa)
3
2
1
0
−1
0
2
4
6
Time (ms)

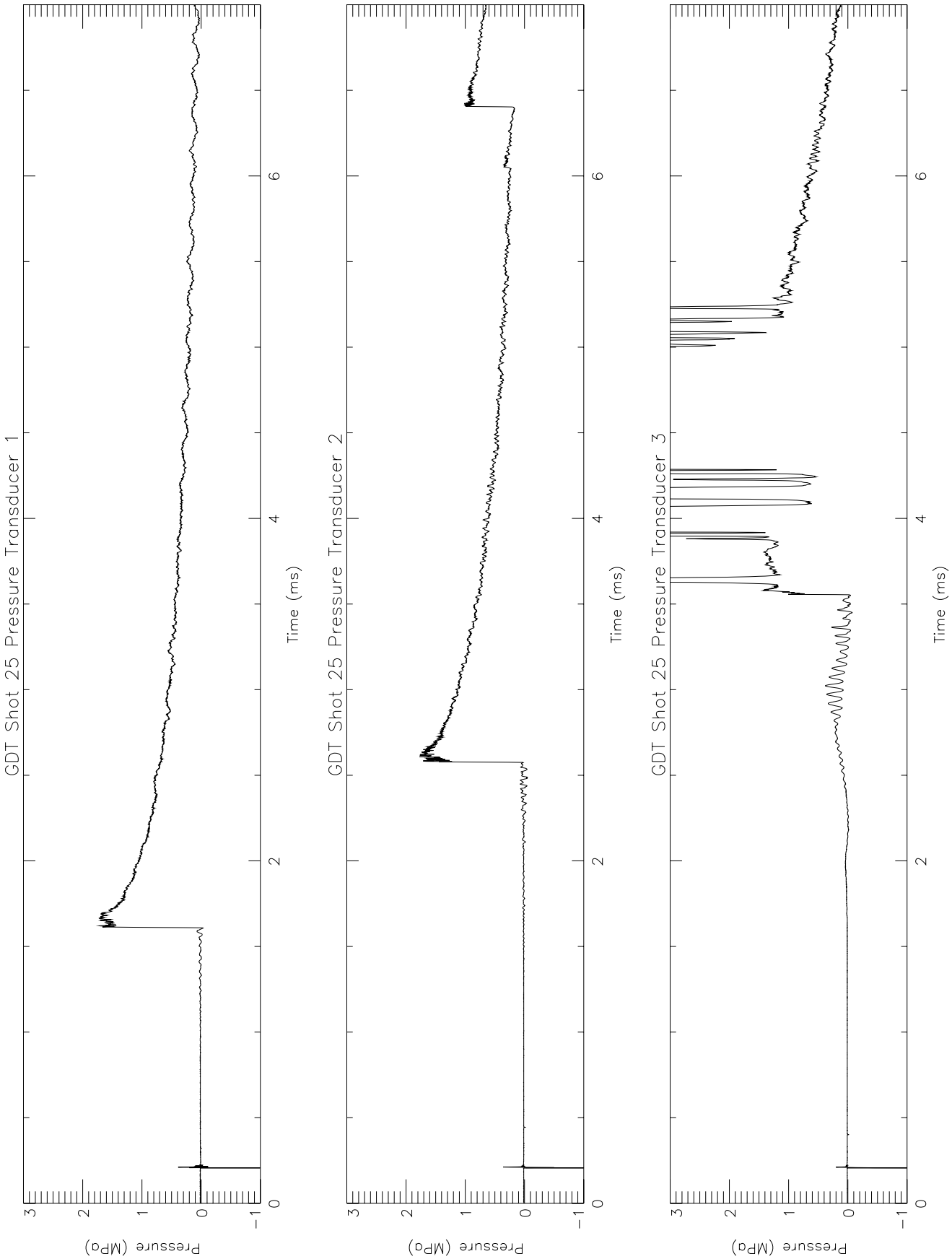
GDT Shot 25 Pressure Transducer 1
Pressure (MPa)
Time (ms)
GDT Shot 25 Pressure Transducer 2
Pressure (MPa)
Time (ms)
GDT Shot 25 Pressure Transducer 3
Pressure (MPa)
Time (ms)

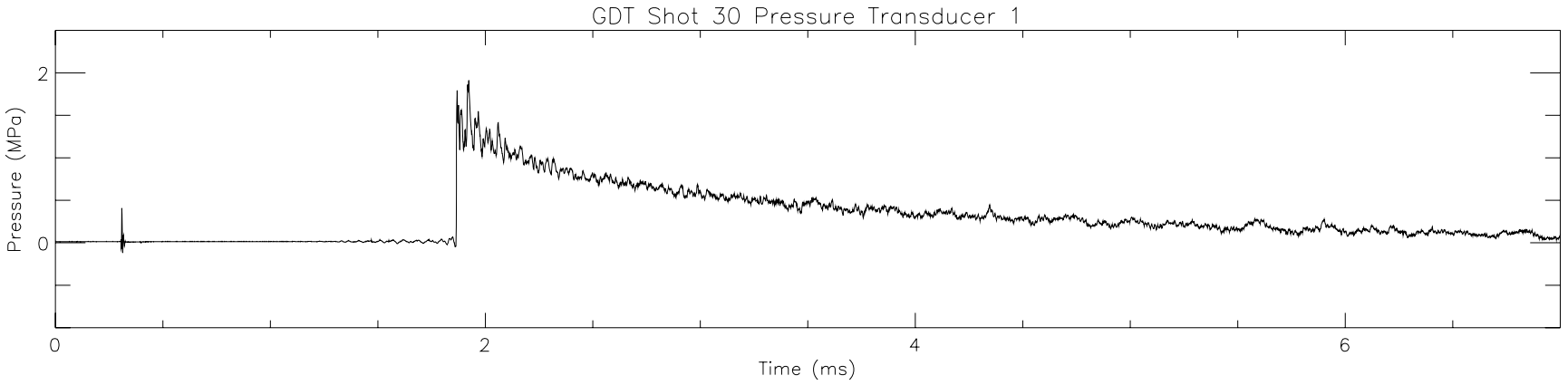
GDT Shot 30 Pressure Transducer 1
Pressure (MPa)
2
0
0
2
4
6
Time (ms)

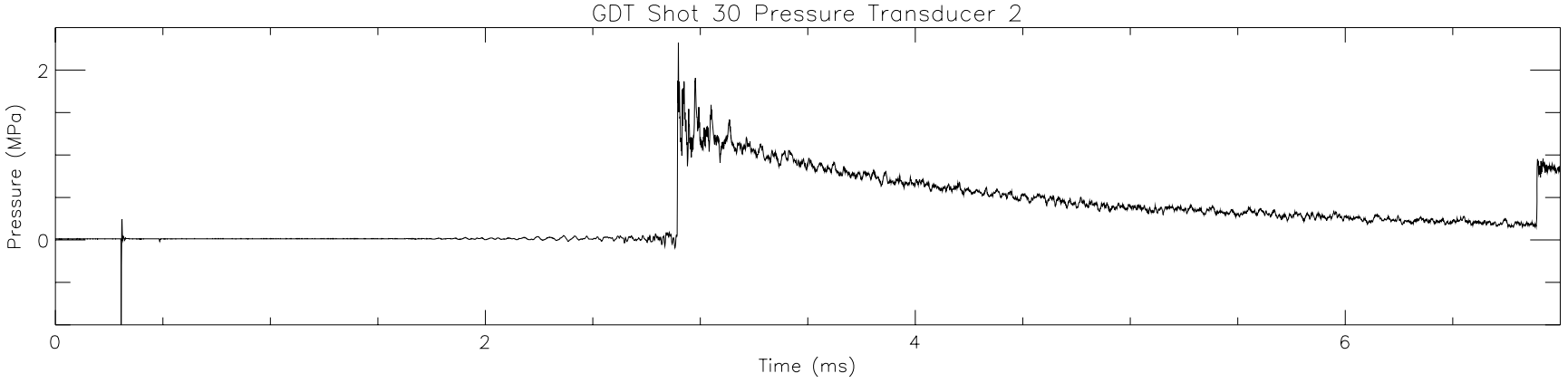
GDT Shot 30 Pressure Transducer 2
Pressure (MPa)
2
0
0
2
4
6
Time (ms)

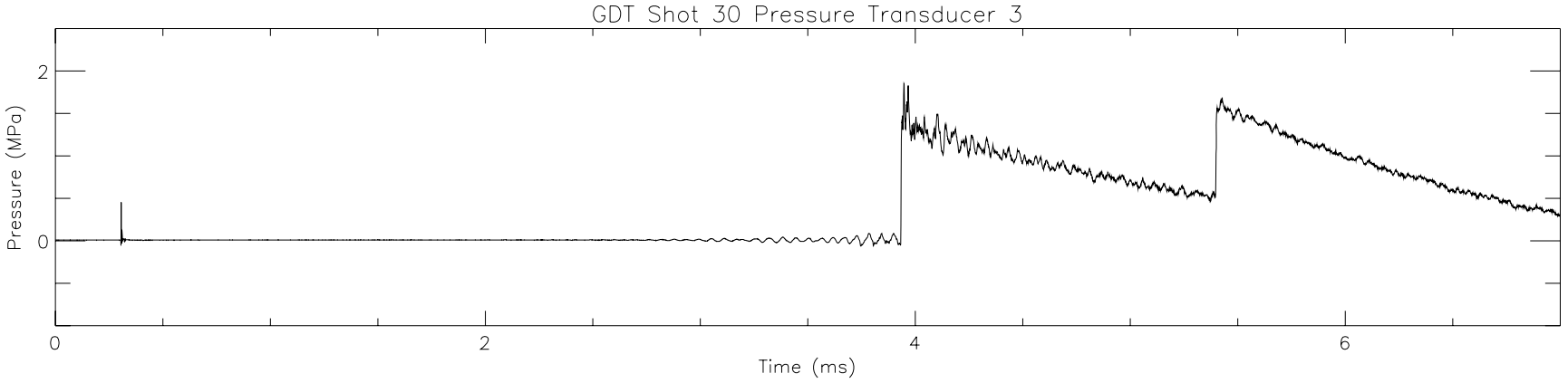
GDT Shot 30 Pressure Transducer 3
Pressure (MPa)
2
0
0
2
4
6
Time (ms)

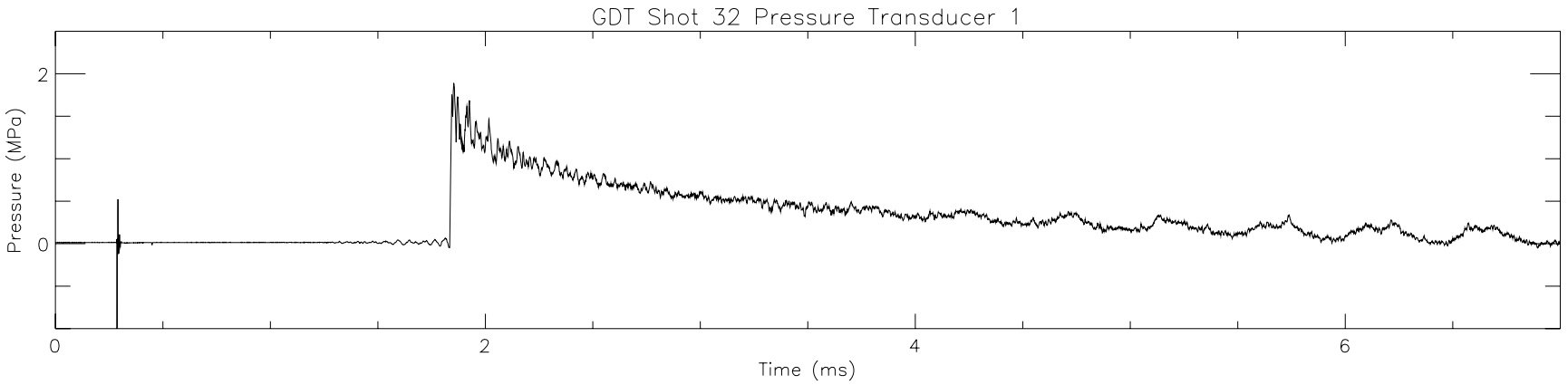
GDT Shot 32 Pressure Transducer 1
Pressure (MPa)
2
0
0
2
4
6
Time (ms)

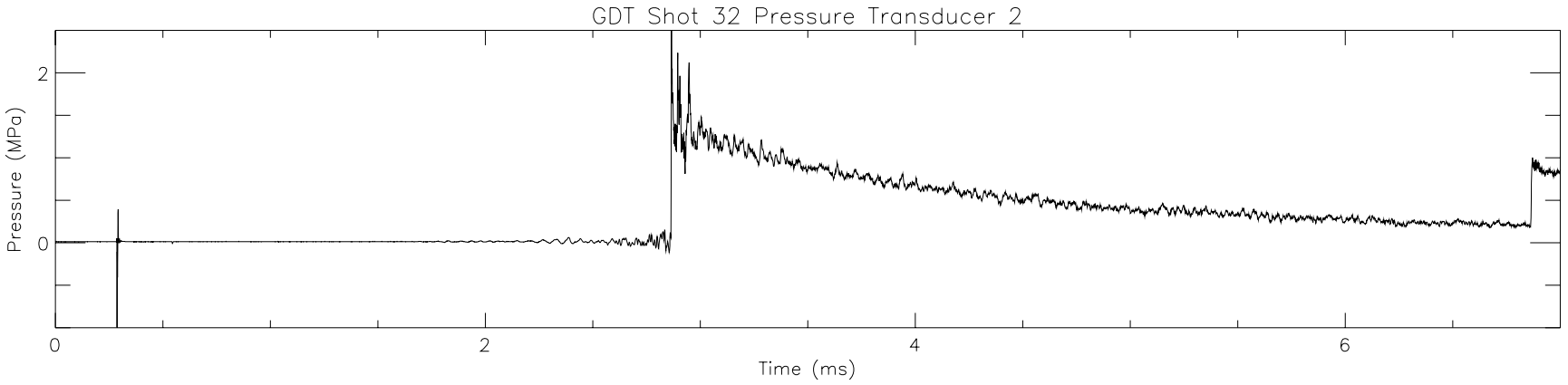
GDT Shot 32 Pressure Transducer 2
Pressure (MPa)
2
0
0
2
4
6
Time (ms)

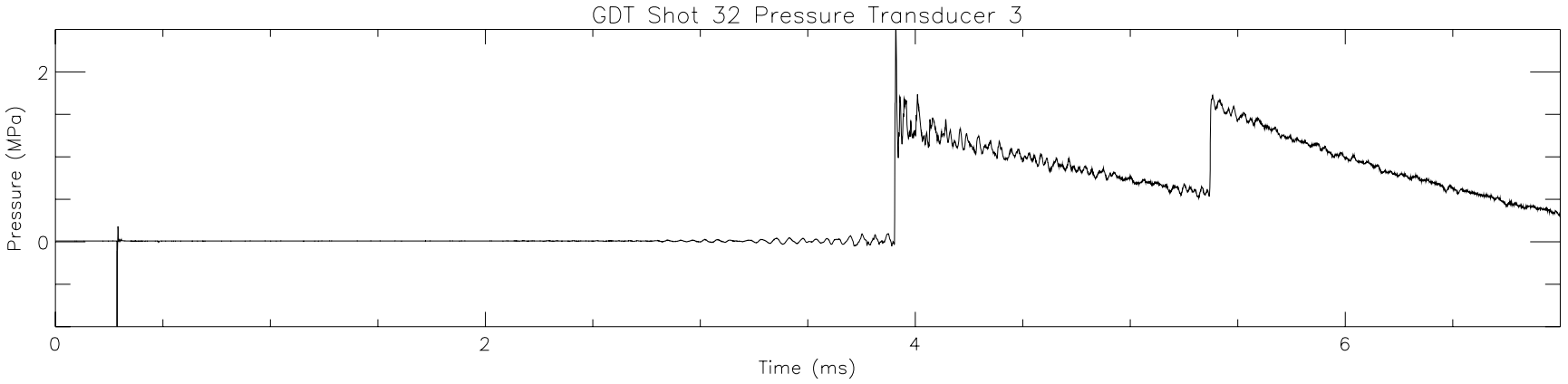
GDT Shot 32 Pressure Transducer 3
Pressure (MPa)
2
0
0
2
4
6
Time (ms)

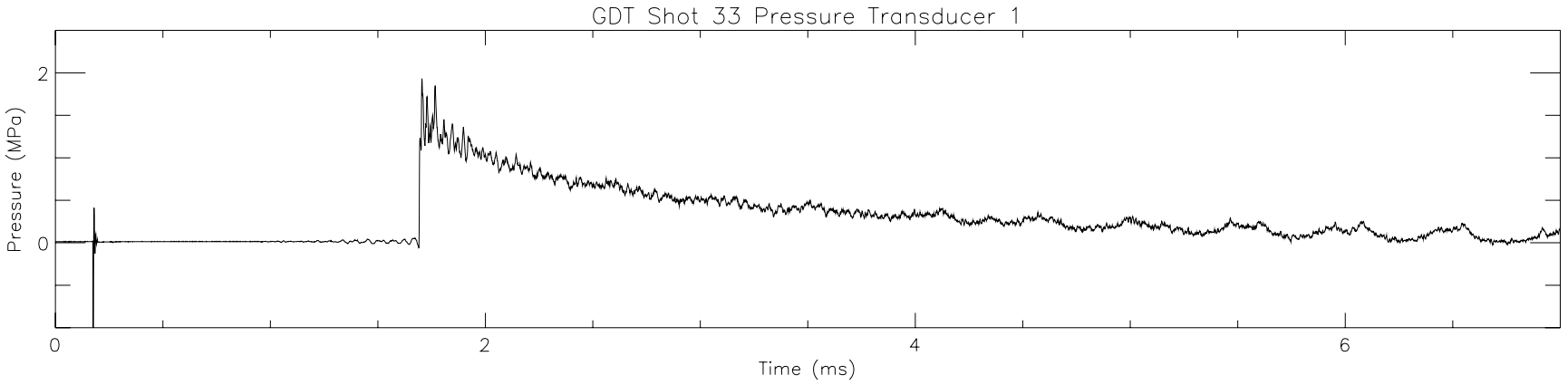
GDT Shot 33 Pressure Transducer 1
Pressure (MPa)
2
0
0
2
4
6
Time (ms)

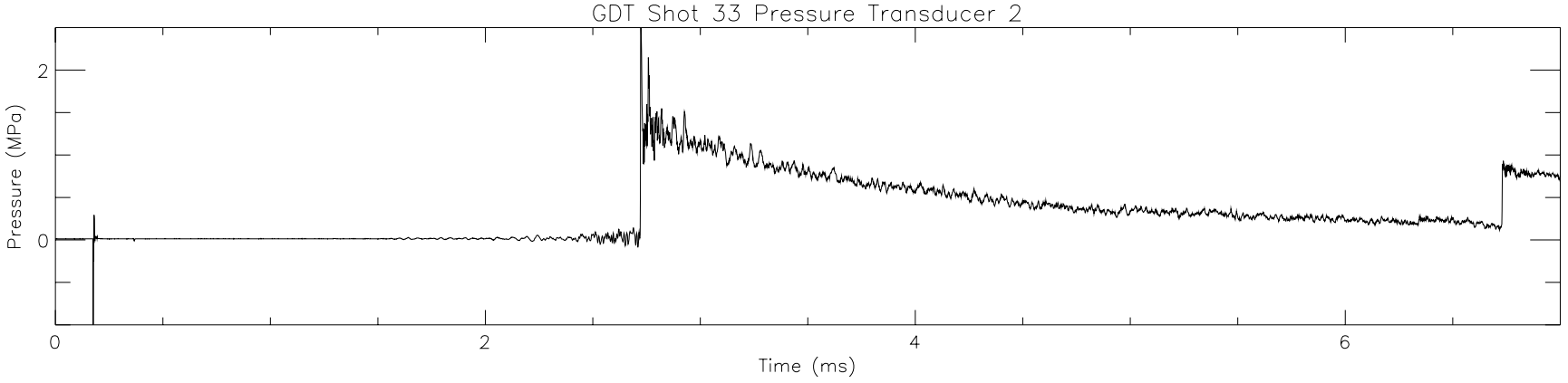
GDT Shot 33 Pressure Transducer 2
Pressure (MPa)
2
0
0
2
4
6
Time (ms)

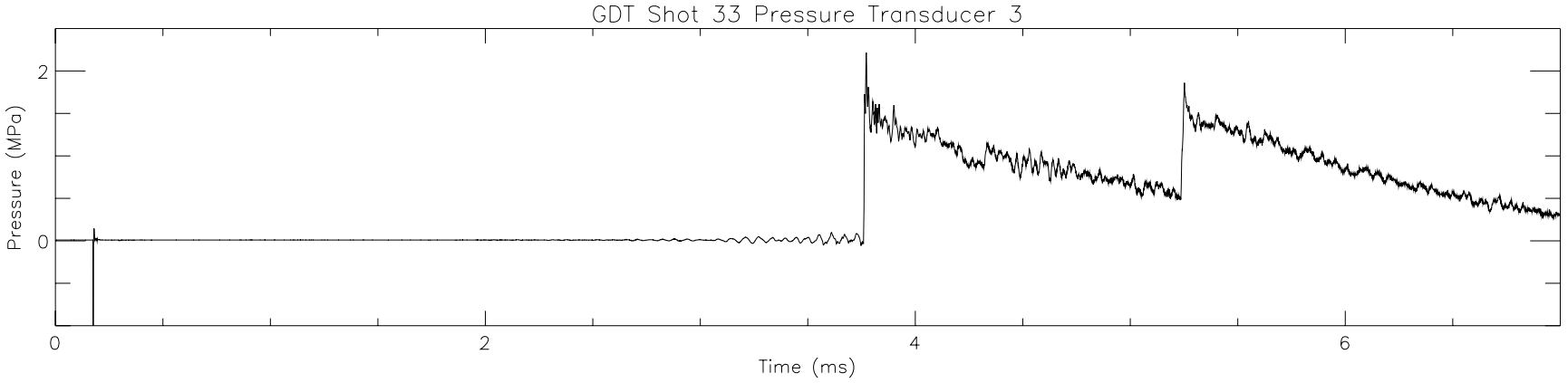
GDT Shot 33 Pressure Transducer 3
Pressure (MPa)
2
0
0
2
4
6
Time (ms)

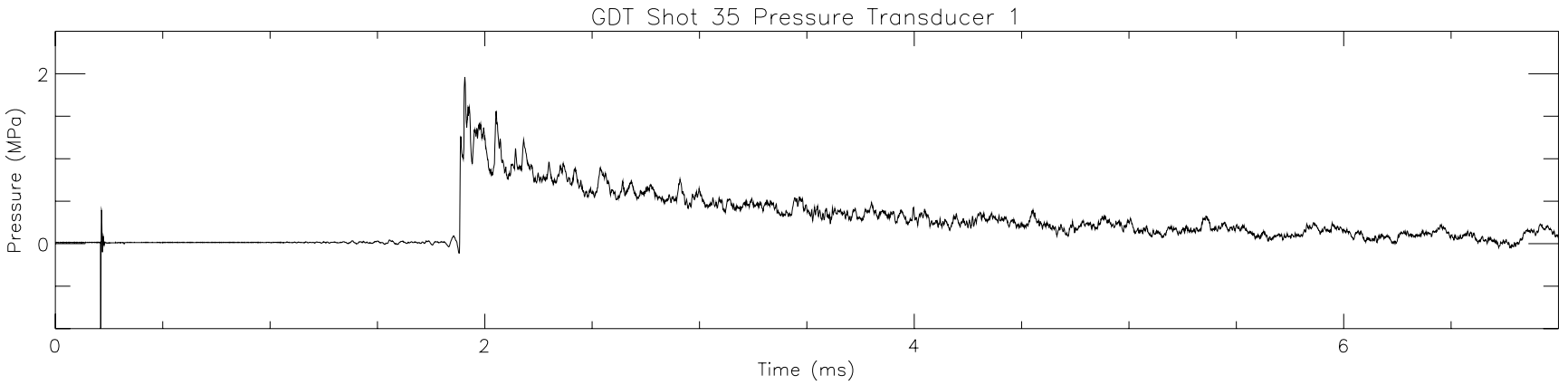
GDT Shot 35 Pressure Transducer 1
Pressure (MPa)
2
0
0
2
4
6
Time (ms)

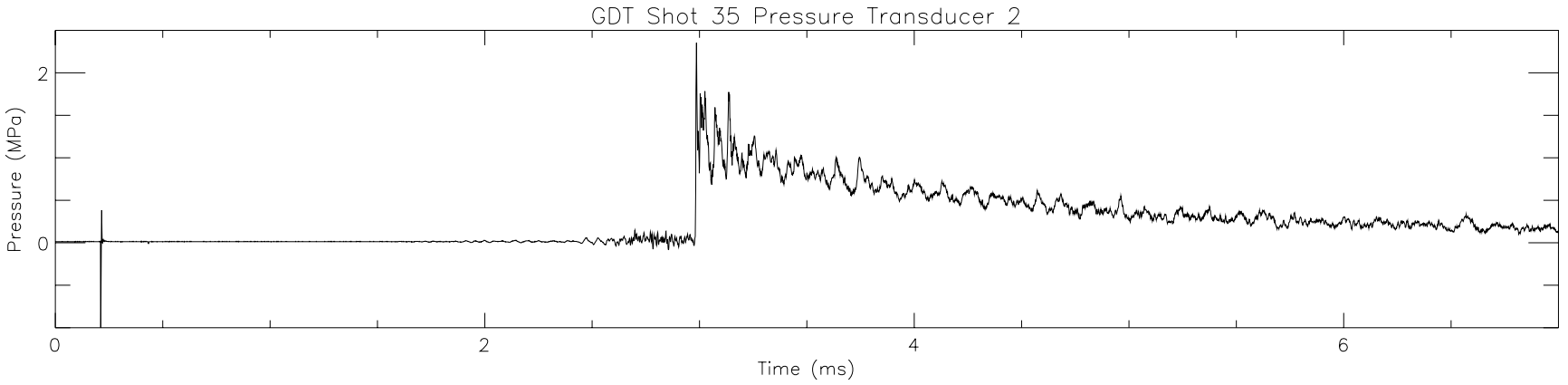
GDT Shot 35 Pressure Transducer 2
Pressure (MPa)
2
0
0
2
4
6
Time (ms)

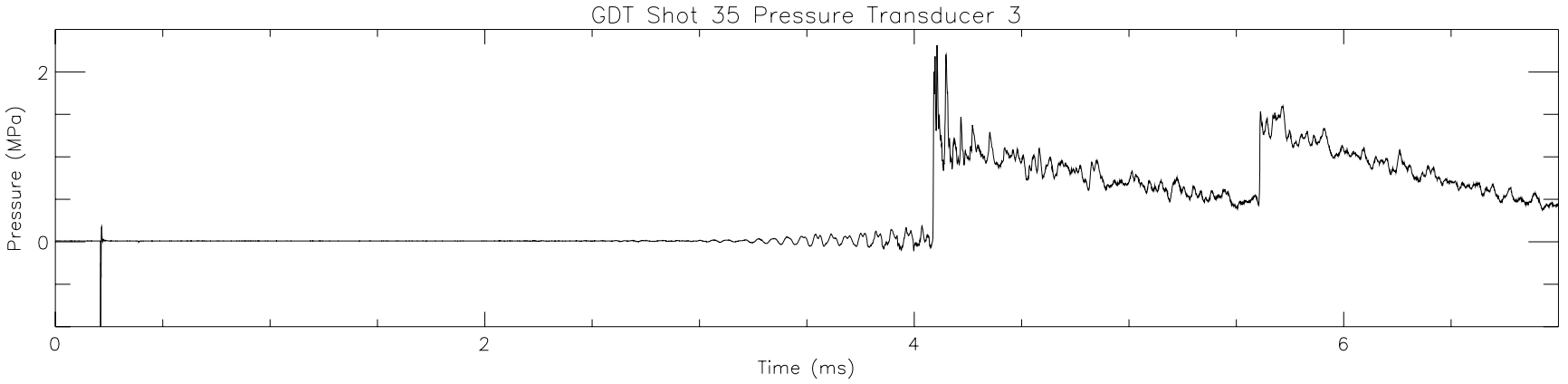
GDT Shot 35 Pressure Transducer 3
Pressure (MPa)
2
0
0
2
4
6
Time (ms)

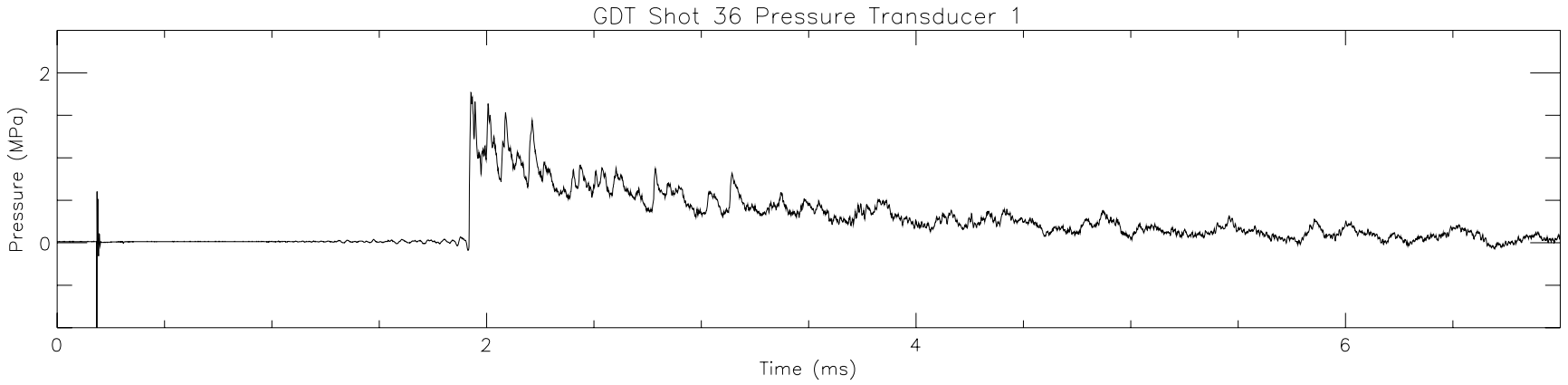
GDT Shot 36 Pressure Transducer 1
Pressure (MPa)
2
0
0
2
4
6
Time (ms)

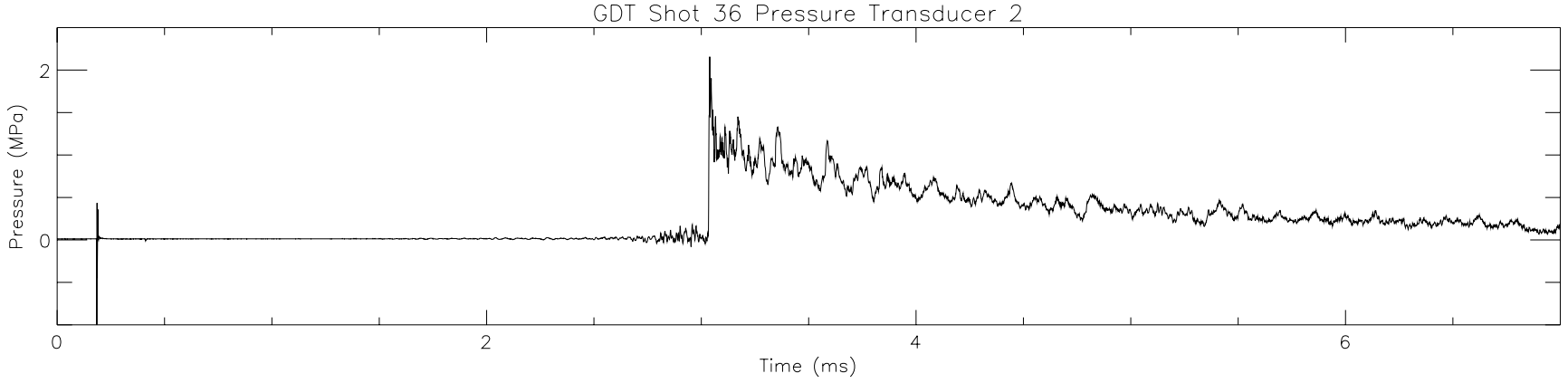
GDT Shot 36 Pressure Transducer 2
Pressure (MPa)
2
0
0
2
4
6
Time (ms)

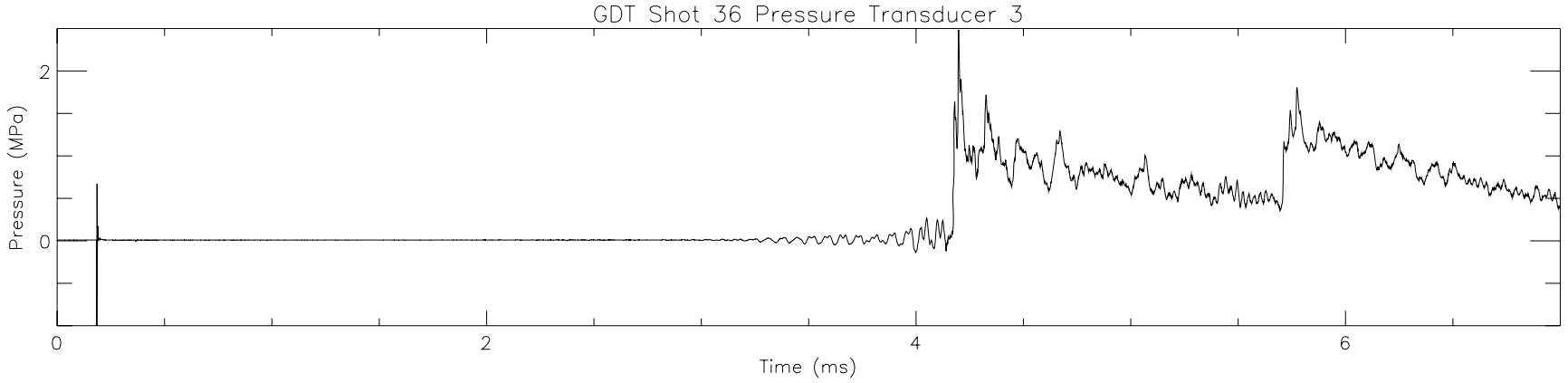
GDT Shot 36 Pressure Transducer 3
Pressure (MPa)
2
0
0
2
4
6
Time (ms)

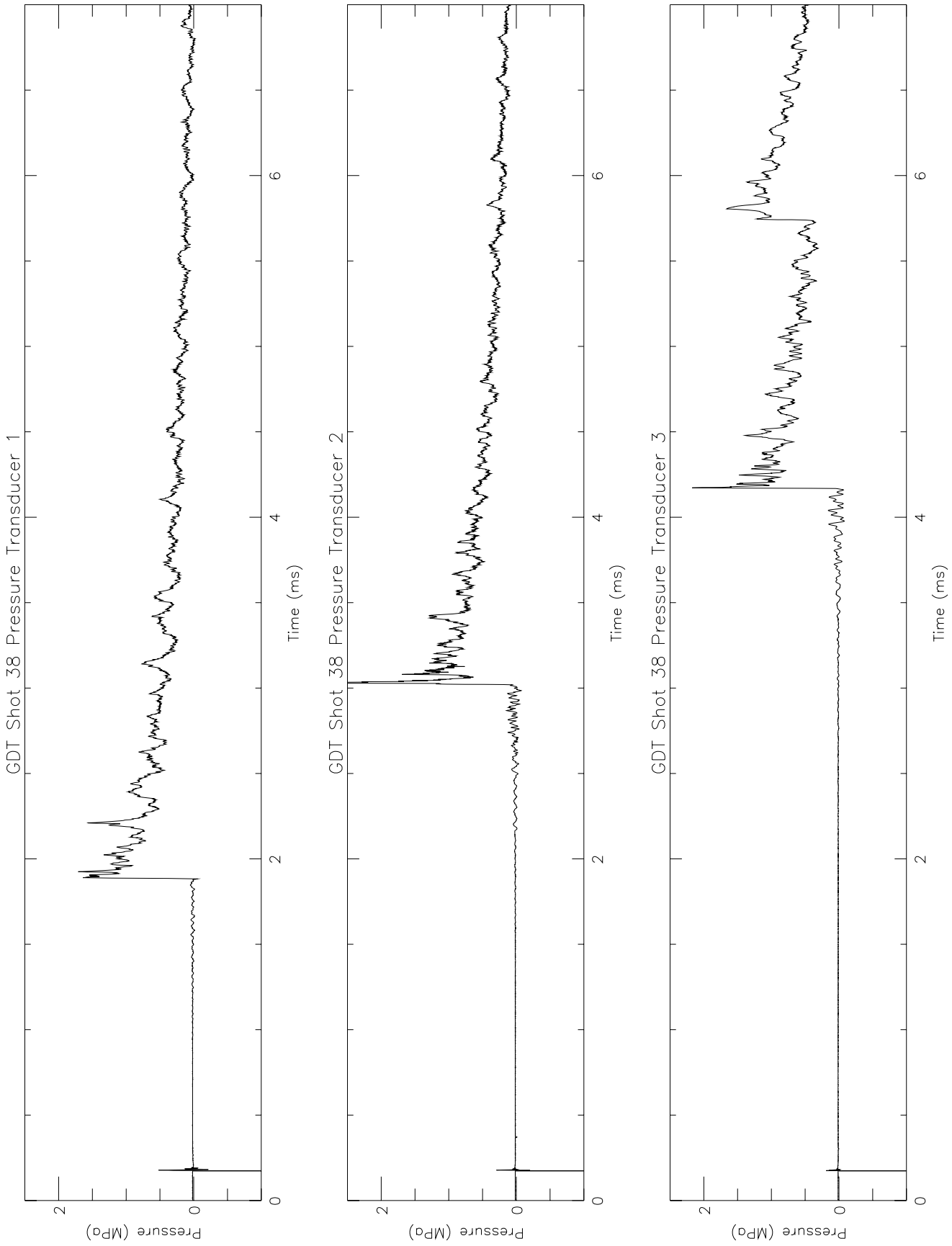
GDT Shot 38 Pressure Transducer 1
Pressure (MPa)
Time (ms)
GDT Shot 38 Pressure Transducer 2
Pressure (MPa)
Time (ms)
GDT Shot 38 Pressure Transducer 3
Pressure (MPa)
Time (ms)

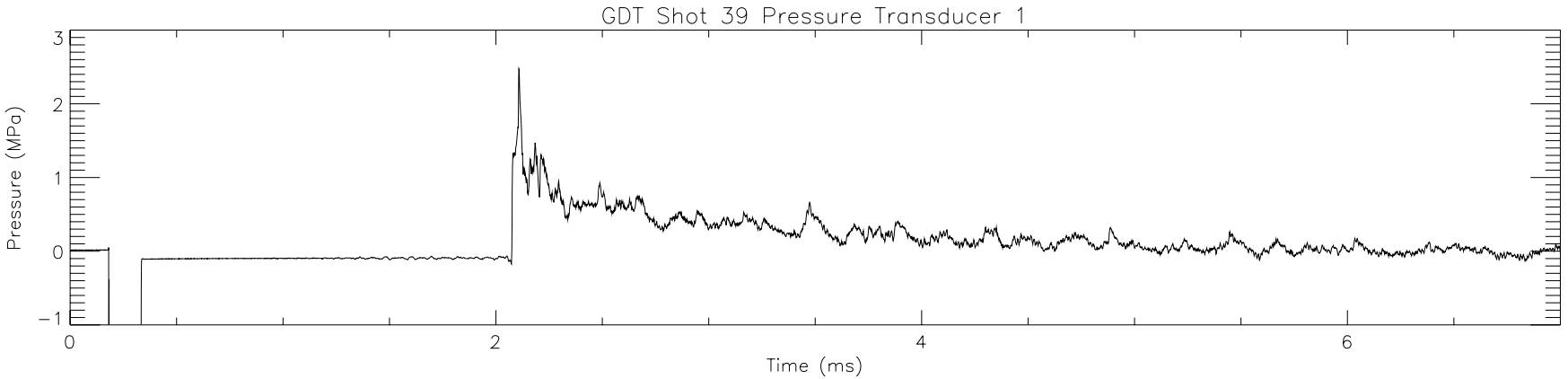
GDT Shot 39 Pressure Transducer 1
Pressure (MPa)
3
2
1
0
−1
0
2
4
6
Time (ms)

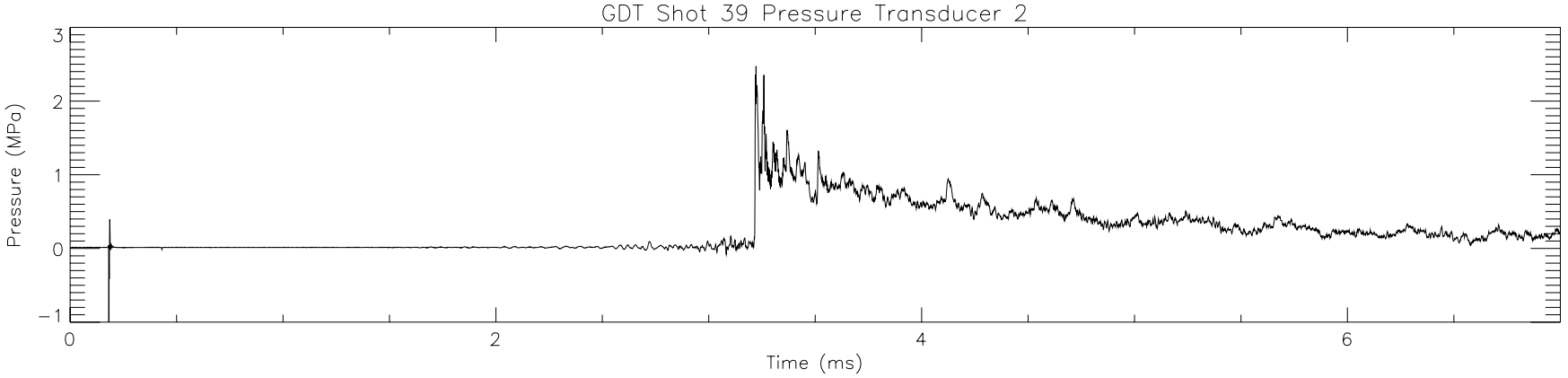
GDT Shot 39 Pressure Transducer 2
Pressure (MPa)
3
2
1
0
−1
0
2
4
6
Time (ms)

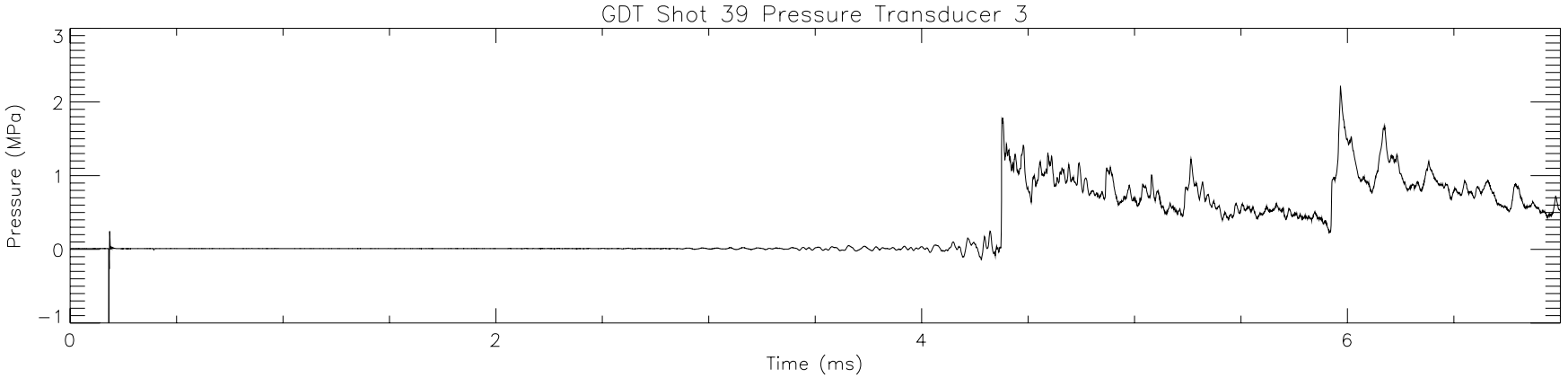
GDT Shot 39 Pressure Transducer 3
Pressure (MPa)
3
2
1
0
−1
0
2
4
6
Time (ms)

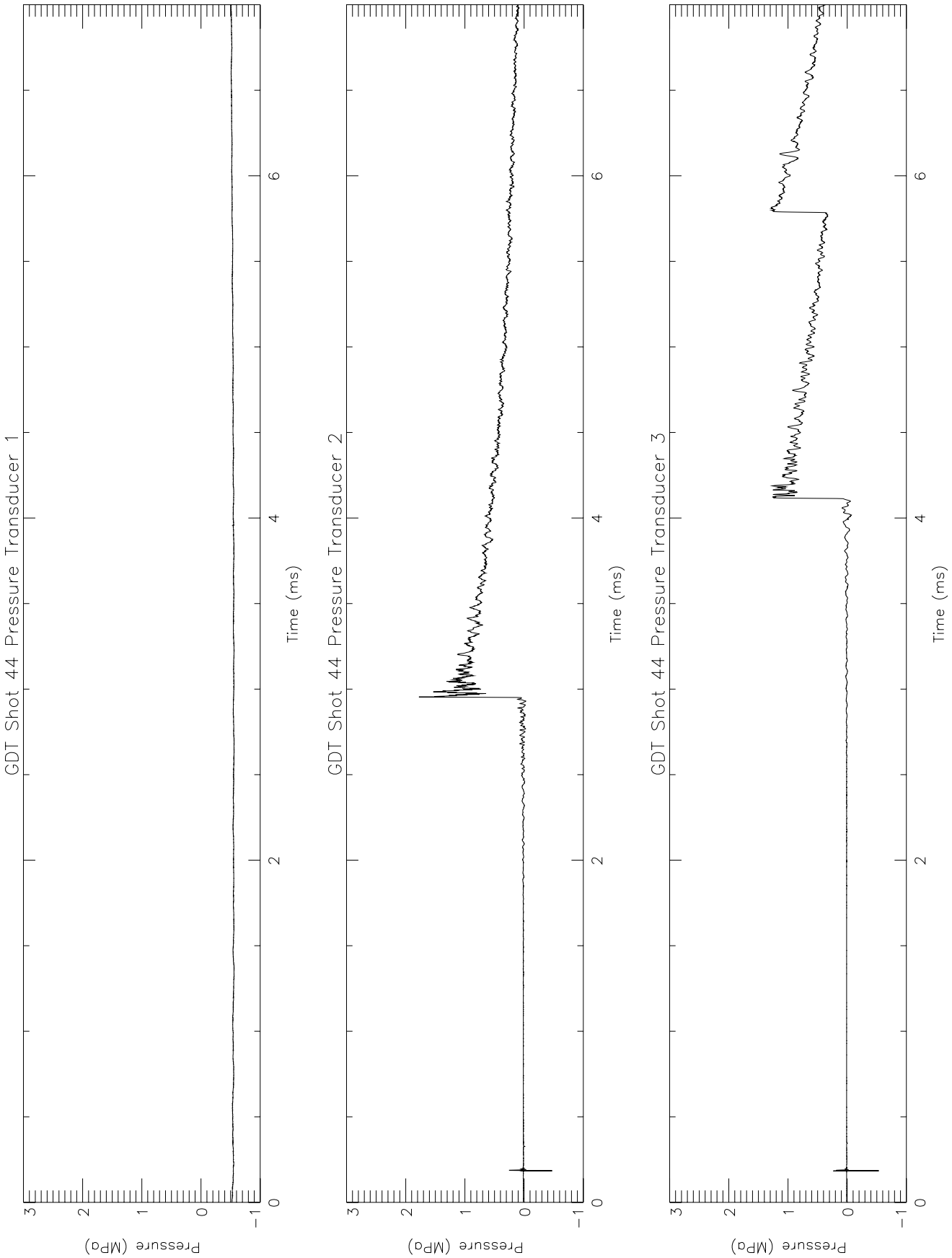
GDT Shot 44 Pressure Transducer 1
Pressure (MPa)
Time (ms)
GDT Shot 44 Pressure Transducer 2
Pressure (MPa)
Time (ms)
GDT Shot 44 Pressure Transducer 3
Pressure (MPa)
Time (ms)

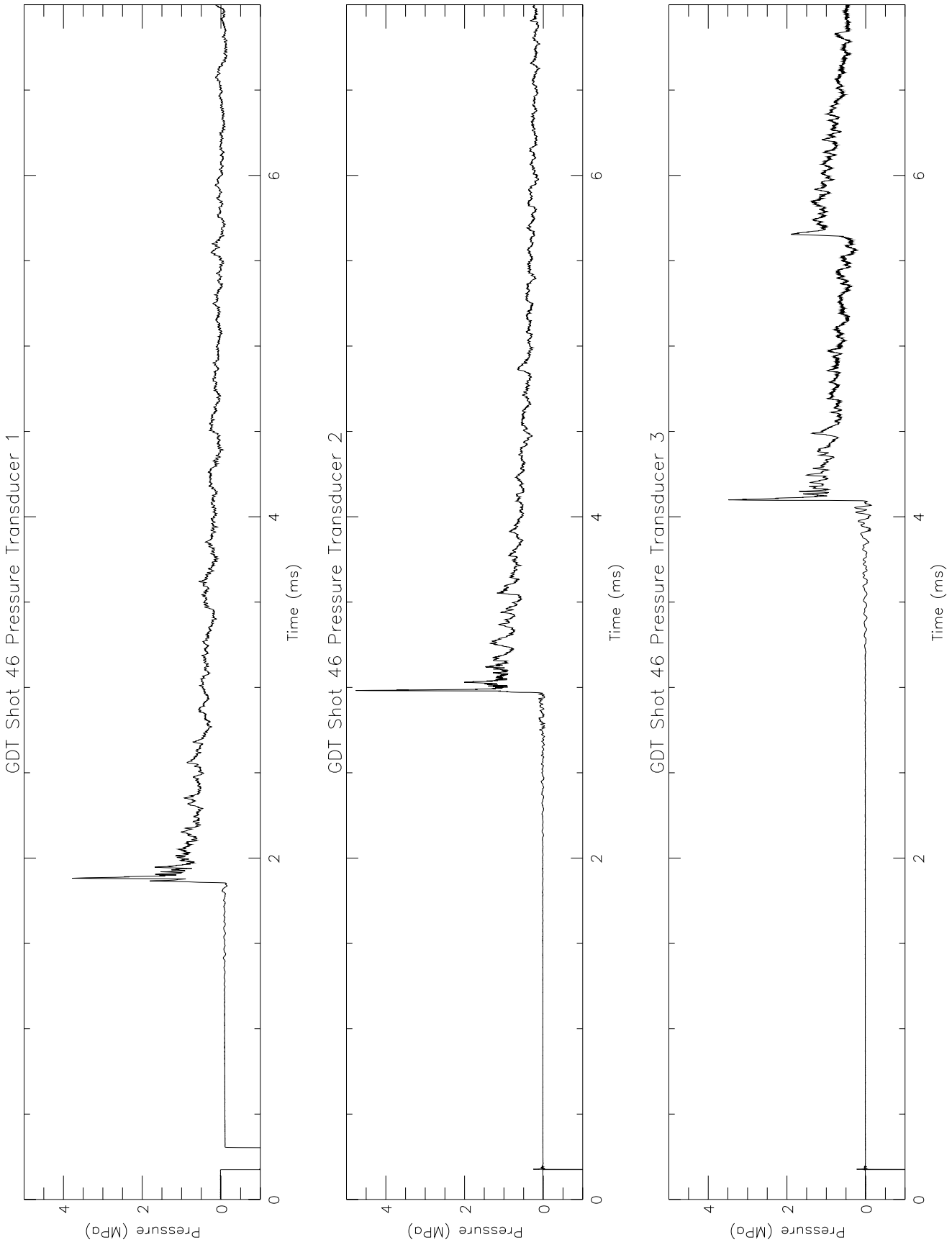
GDT Shot 46 Pressure Transducer 1
Pressure (MPa)
Time (ms)
GDT Shot 46 Pressure Transducer 2
Pressure (MPa)
Time (ms)
GDT Shot 46 Pressure Transducer 3
Pressure (MPa)
Time (ms)

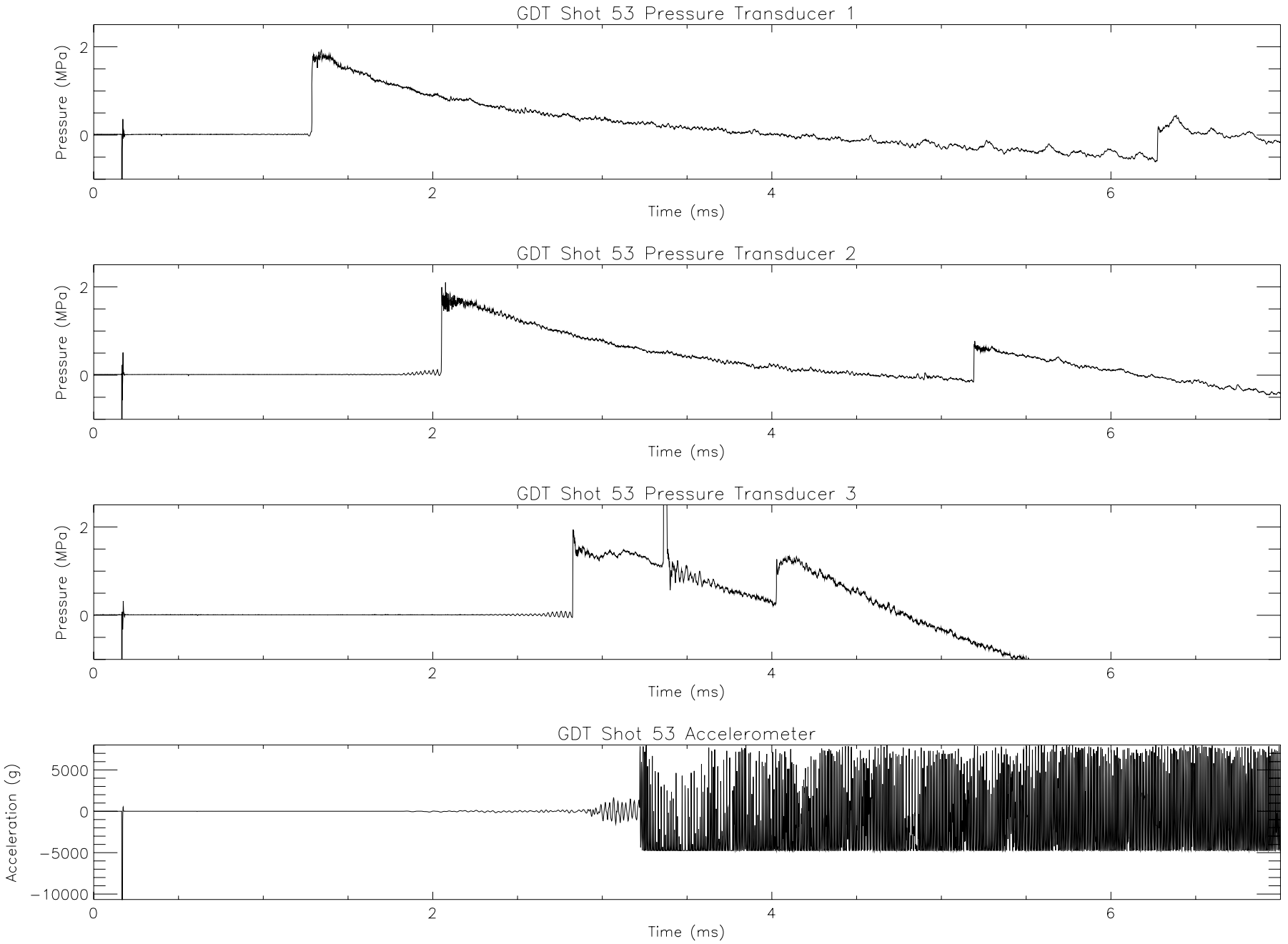
GDT Shot 53 Pressure Transducer 1
Pressure (MPa)
2
0
0
2
4
6
Time (ms)
GDT Shot 53 Pressure Transducer 2
Pressure (MPa)
2
0
0
2
4
6
Time (ms)
GDT Shot 53 Pressure Transducer 3
Pressure (MPa)
2
0
0
2
4
6
Time (ms)
GDT Shot 53 Accelerometer
Acceleration (g)
5000
0
−5000
−10000
0
2
4
6
Time (ms)

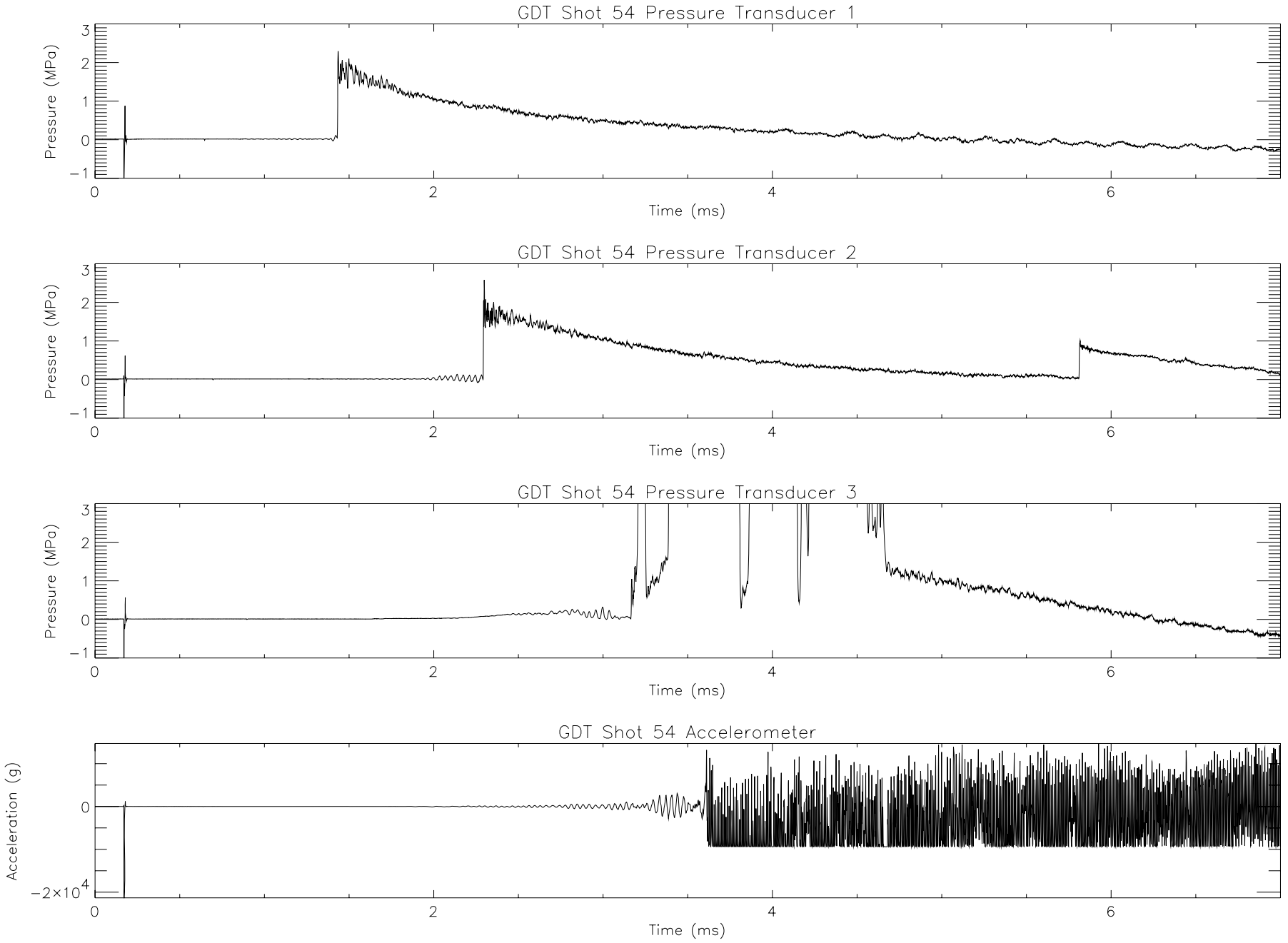
GDT Shot 54 Pressure Transducer 1
Pressure (MPa)
Time (ms)
GDT Shot 54 Pressure Transducer 2
Pressure (MPa)
Time (ms)
GDT Shot 54 Pressure Transducer 3
Pressure (MPa)
Time (ms)
GDT Shot 54 Accelerometer
Acceleration (g)
−2×10^4
Time (ms)

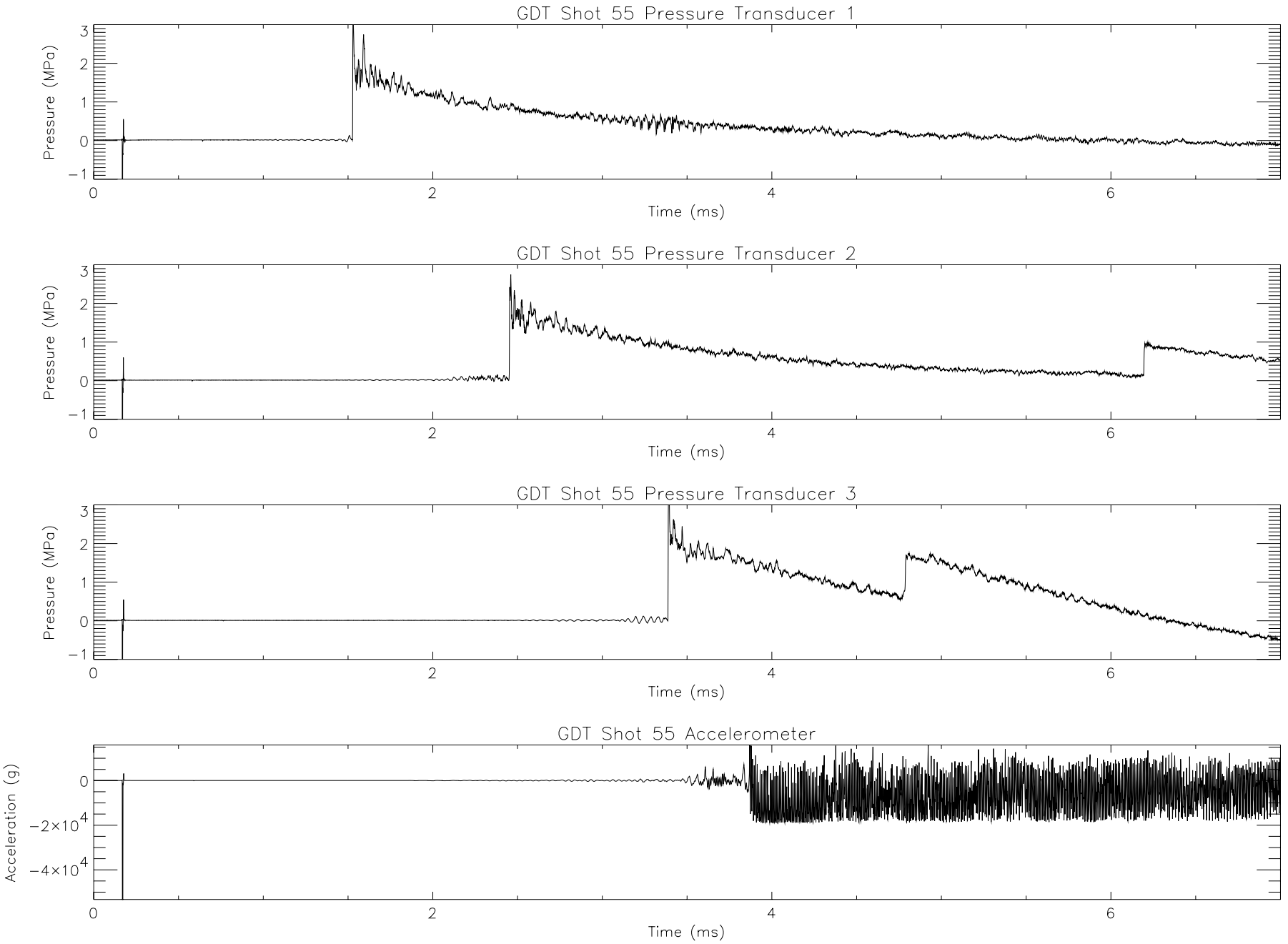
GDT Shot 55 Pressure Transducer 1
Pressure (MPa)
Time (ms)
GDT Shot 55 Pressure Transducer 2
Pressure (MPa)
Time (ms)
GDT Shot 55 Pressure Transducer 3
Pressure (MPa)
Time (ms)
GDT Shot 55 Accelerometer
Acceleration (g)
Time (ms)

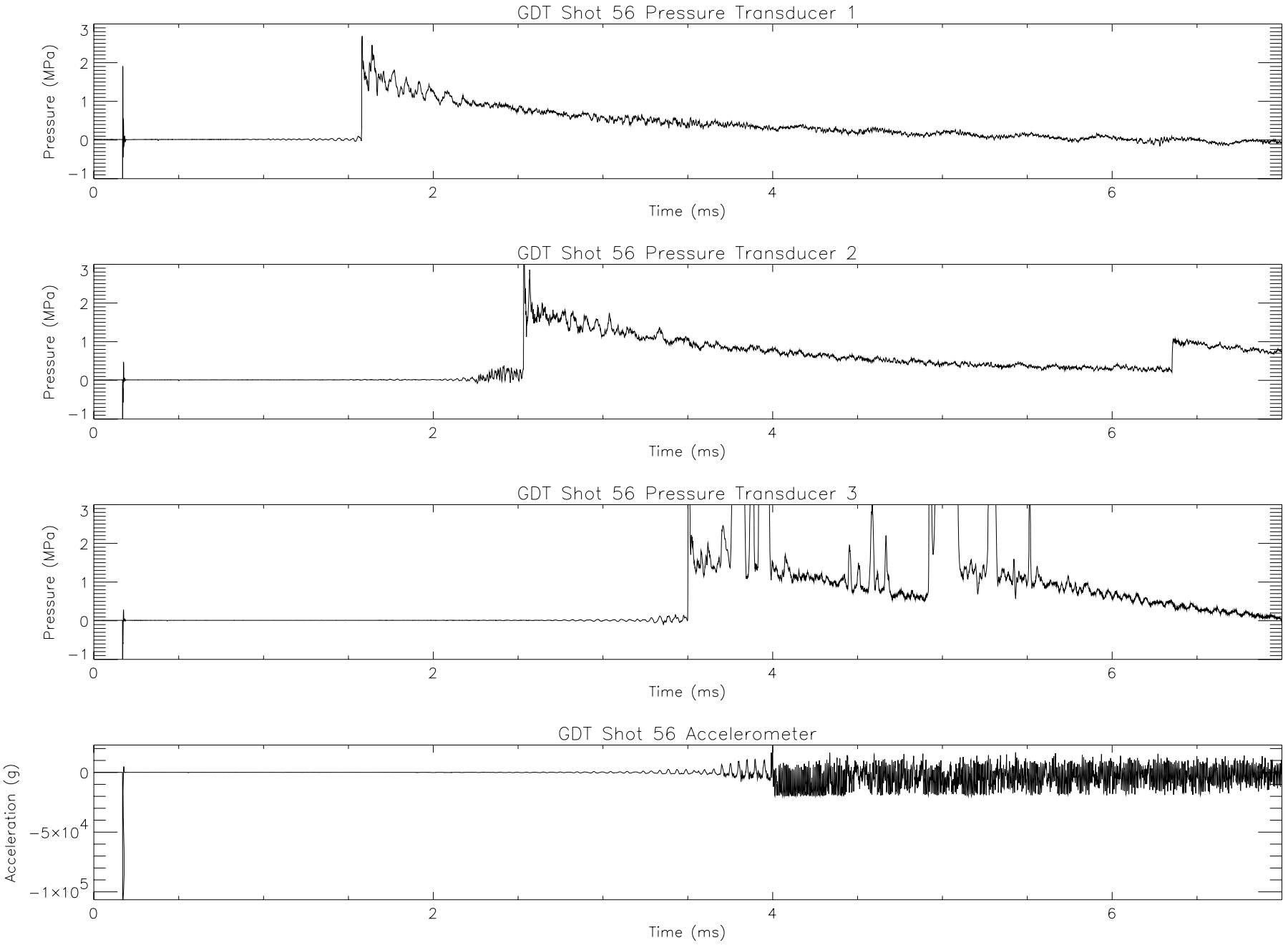
GDT Shot 56 Pressure Transducer 1
Pressure (MPa)
Time (ms)
GDT Shot 56 Pressure Transducer 2
Pressure (MPa)
Time (ms)
GDT Shot 56 Pressure Transducer 3
Pressure (MPa)
Time (ms)
GDT Shot 56 Accelerometer
Acceleration (g)
Time (ms)

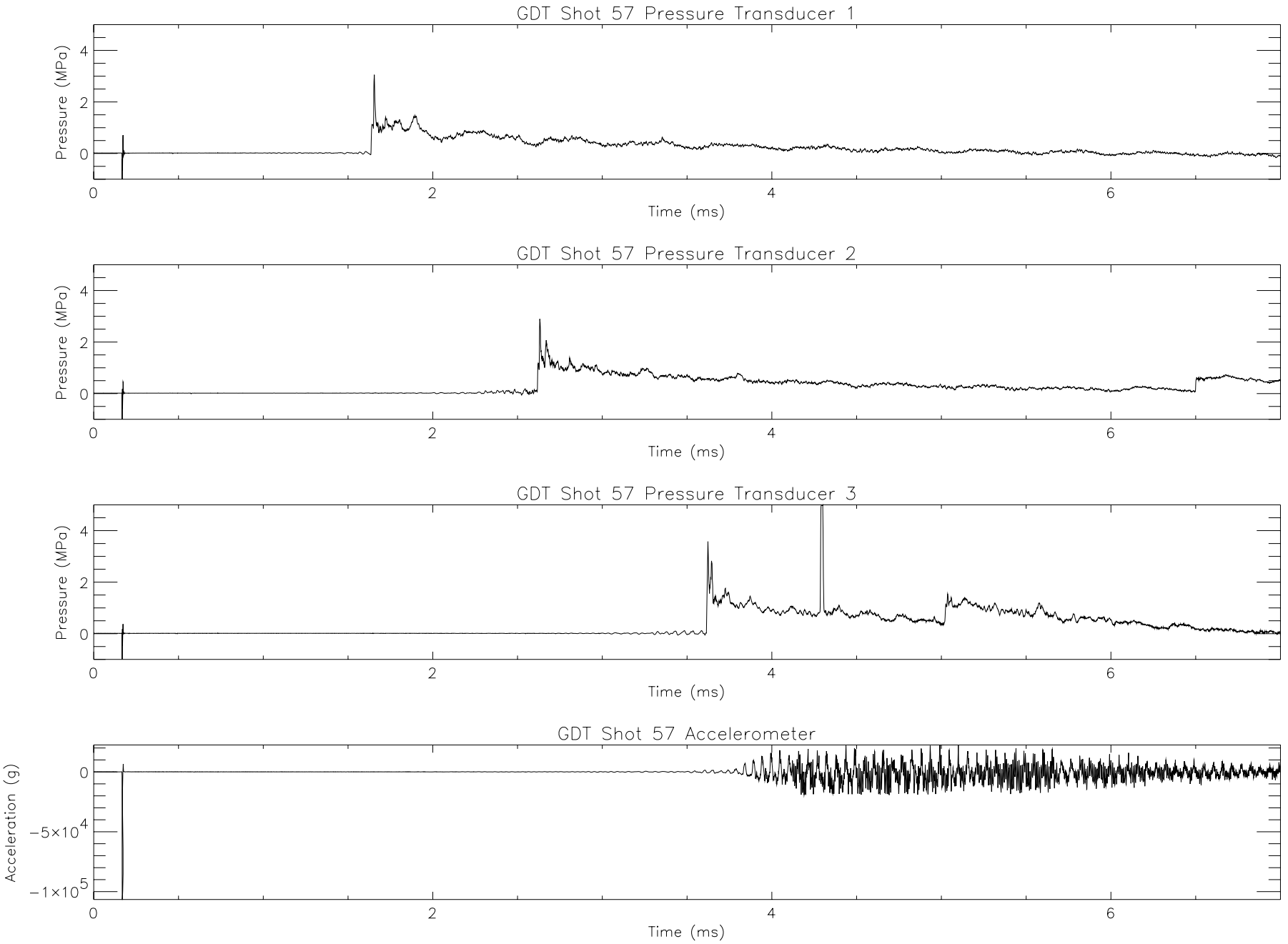
GDT Shot 57 Pressure Transducer 1
Pressure (MPa)
Time (ms)
GDT Shot 57 Pressure Transducer 2
Pressure (MPa)
Time (ms)
GDT Shot 57 Pressure Transducer 3
Pressure (MPa)
Time (ms)
GDT Shot 57 Accelerometer
Acceleration (g)
Time (ms)

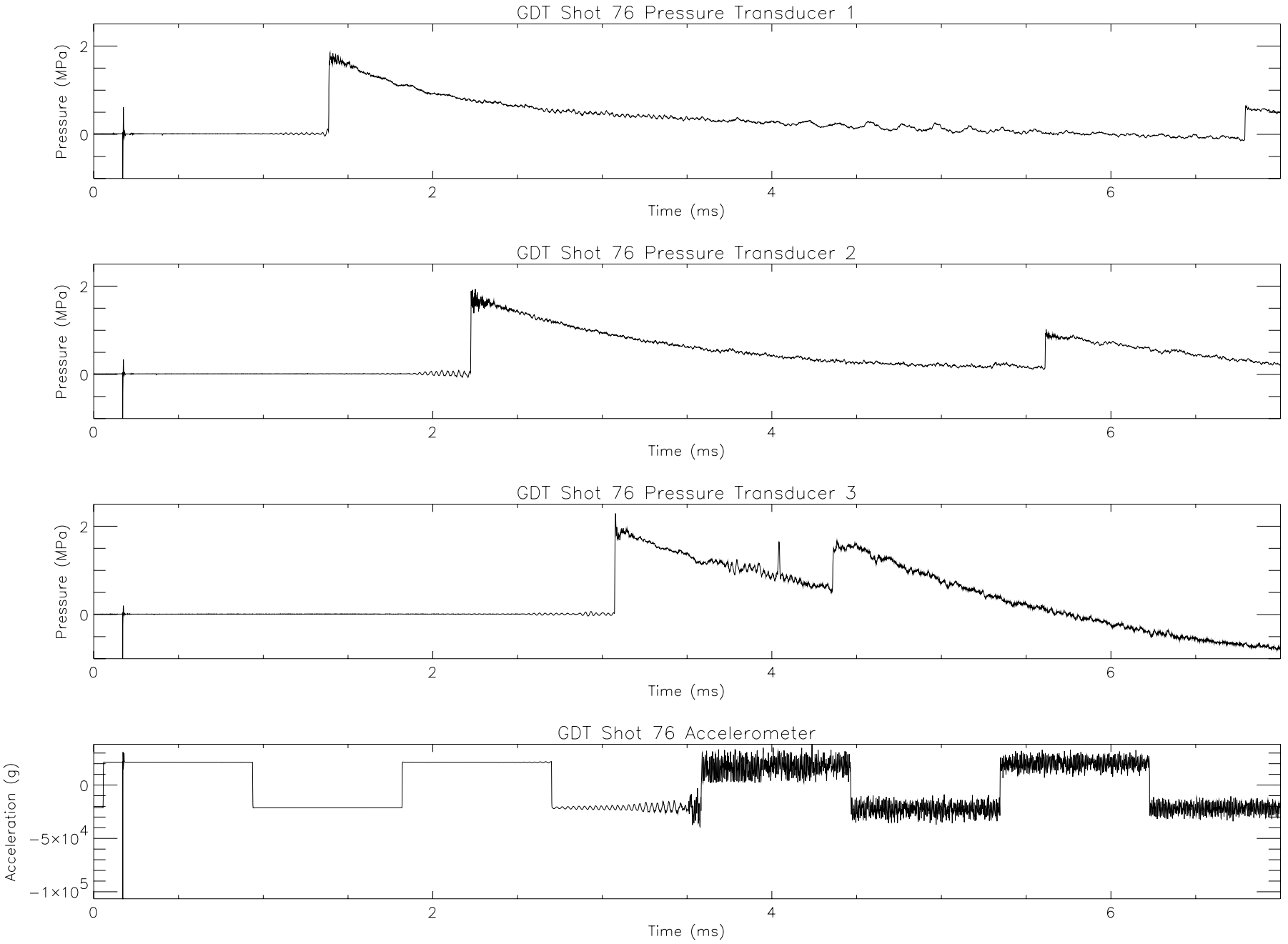
GDT Shot 76 Pressure Transducer 1
Pressure (MPa)
2
0
0
2
4
6
Time (ms)
GDT Shot 76 Pressure Transducer 2
Pressure (MPa)
2
0
0
2
4
6
Time (ms)
GDT Shot 76 Pressure Transducer 3
Pressure (MPa)
2
0
0
2
4
6
Time (ms)
GDT Shot 76 Accelerometer
Acceleration (g)
0
−5×10^4
−1×10^5
0
2
4
6
Time (ms)

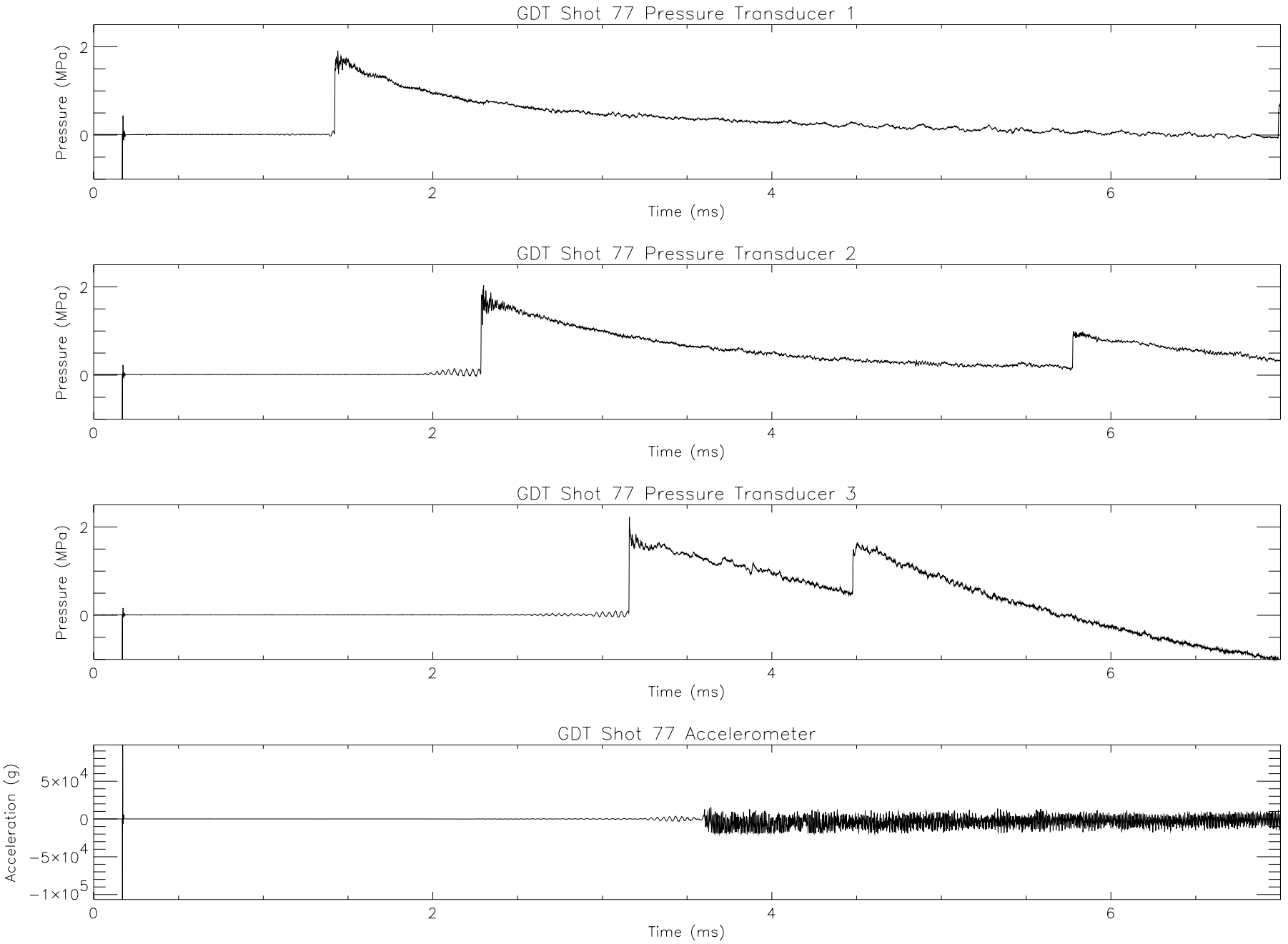
GDT Shot 77 Pressure Transducer 1
Pressure (MPa)
2
0
0
2
4
6
Time (ms)
GDT Shot 77 Pressure Transducer 2
Pressure (MPa)
2
0
0
2
4
6
Time (ms)
GDT Shot 77 Pressure Transducer 3
Pressure (MPa)
2
0
0
2
4
6
Time (ms)
GDT Shot 77 Accelerometer
Acceleration (g)
5×10^4
0
−5×10^4
−1×10^5
0
2
4
6
Time (ms)

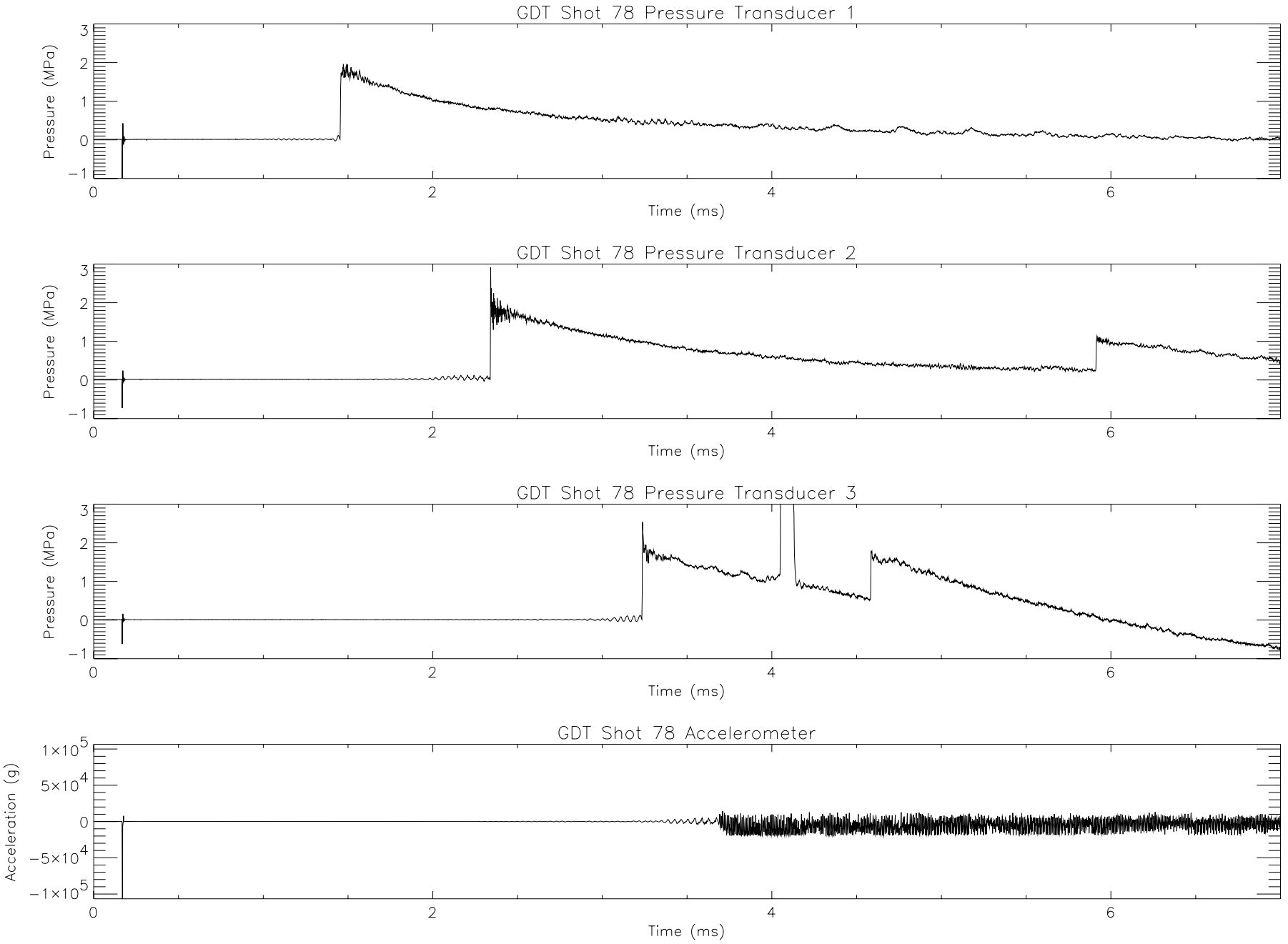
GDT Shot 78 Pressure Transducer 1
Pressure (MPa)
3
2
1
0
−1
0
2
4
6
Time (ms)
GDT Shot 78 Pressure Transducer 2
Pressure (MPa)
3
2
1
0
−1
0
2
4
6
Time (ms)
GDT Shot 78 Pressure Transducer 3
Pressure (MPa)
3
2
1
0
−1
0
2
4
6
Time (ms)
GDT Shot 78 Accelerometer
Acceleration (g)
1×10^5
5×10^4
0
−5×10^4
−1×10^5
0
2
4
6
Time (ms)

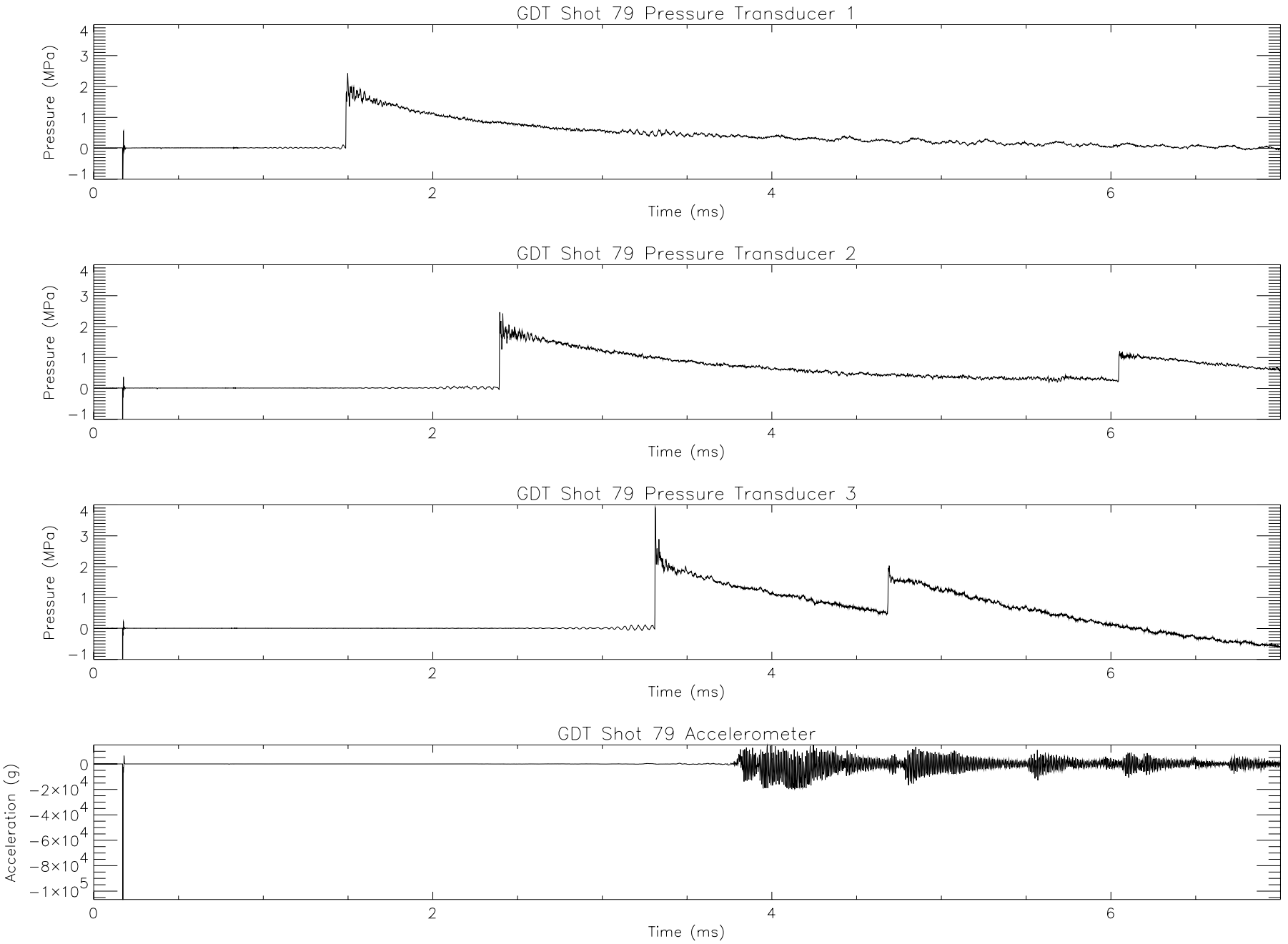
GDT Shot 79 Pressure Transducer 1
Pressure (MPa)
Time (ms)
GDT Shot 79 Pressure Transducer 2
Pressure (MPa)
Time (ms)
GDT Shot 79 Pressure Transducer 3
Pressure (MPa)
Time (ms)
GDT Shot 79 Accelerometer
Acceleration (g)
Time (ms)

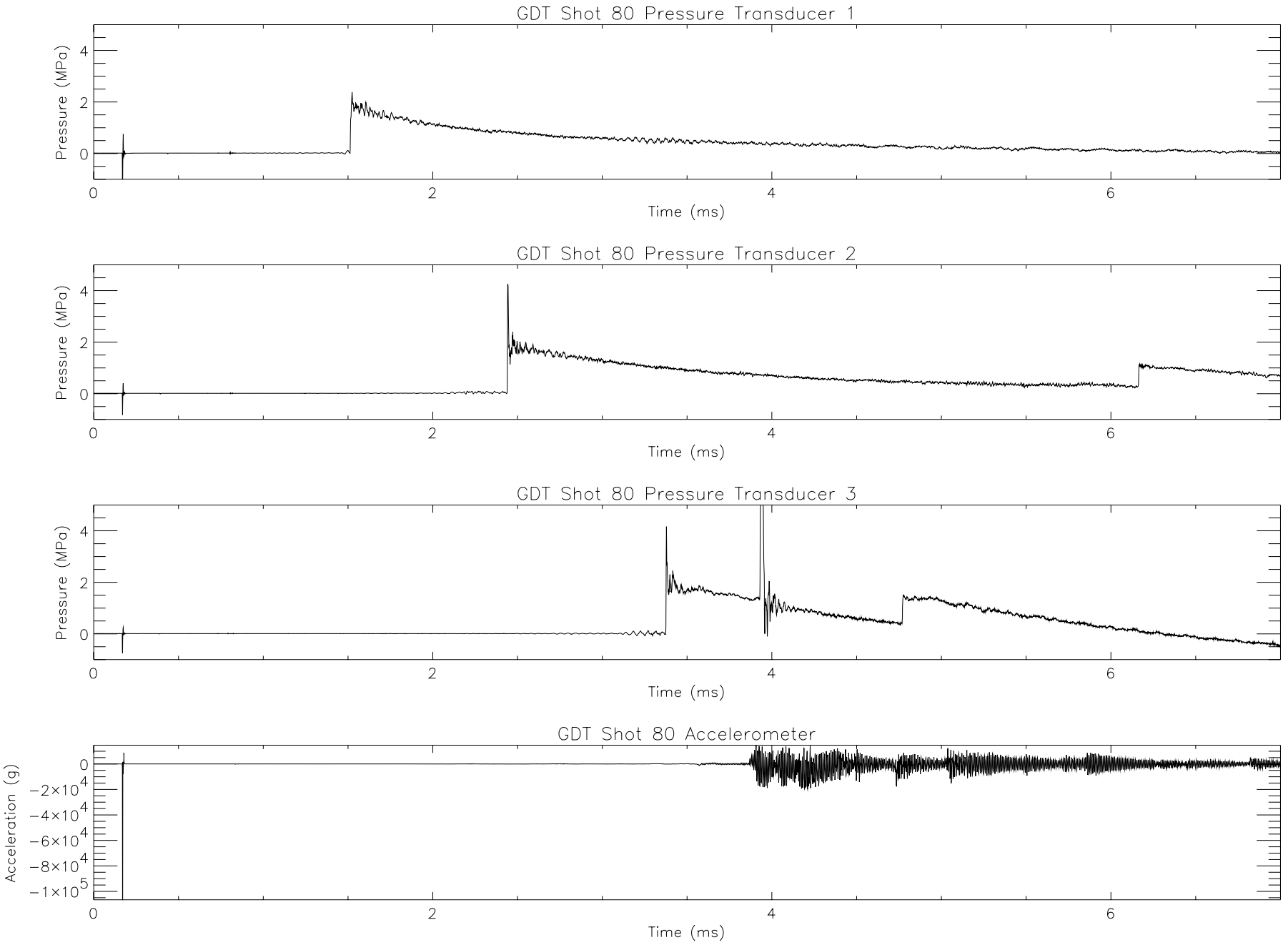
GDT Shot 80 Pressure Transducer 1
Pressure (MPa)
4
2
0
0
2
4
6
Time (ms)
GDT Shot 80 Pressure Transducer 2
Pressure (MPa)
4
2
0
0
2
4
6
Time (ms)
GDT Shot 80 Pressure Transducer 3
Pressure (MPa)
4
2
0
0
2
4
6
Time (ms)
GDT Shot 80 Accelerometer
Acceleration (g)
0
−2×10^4
−4×10^4
−6×10^4
−8×10^4
−1×10^5
0
2
4
6
Time (ms)

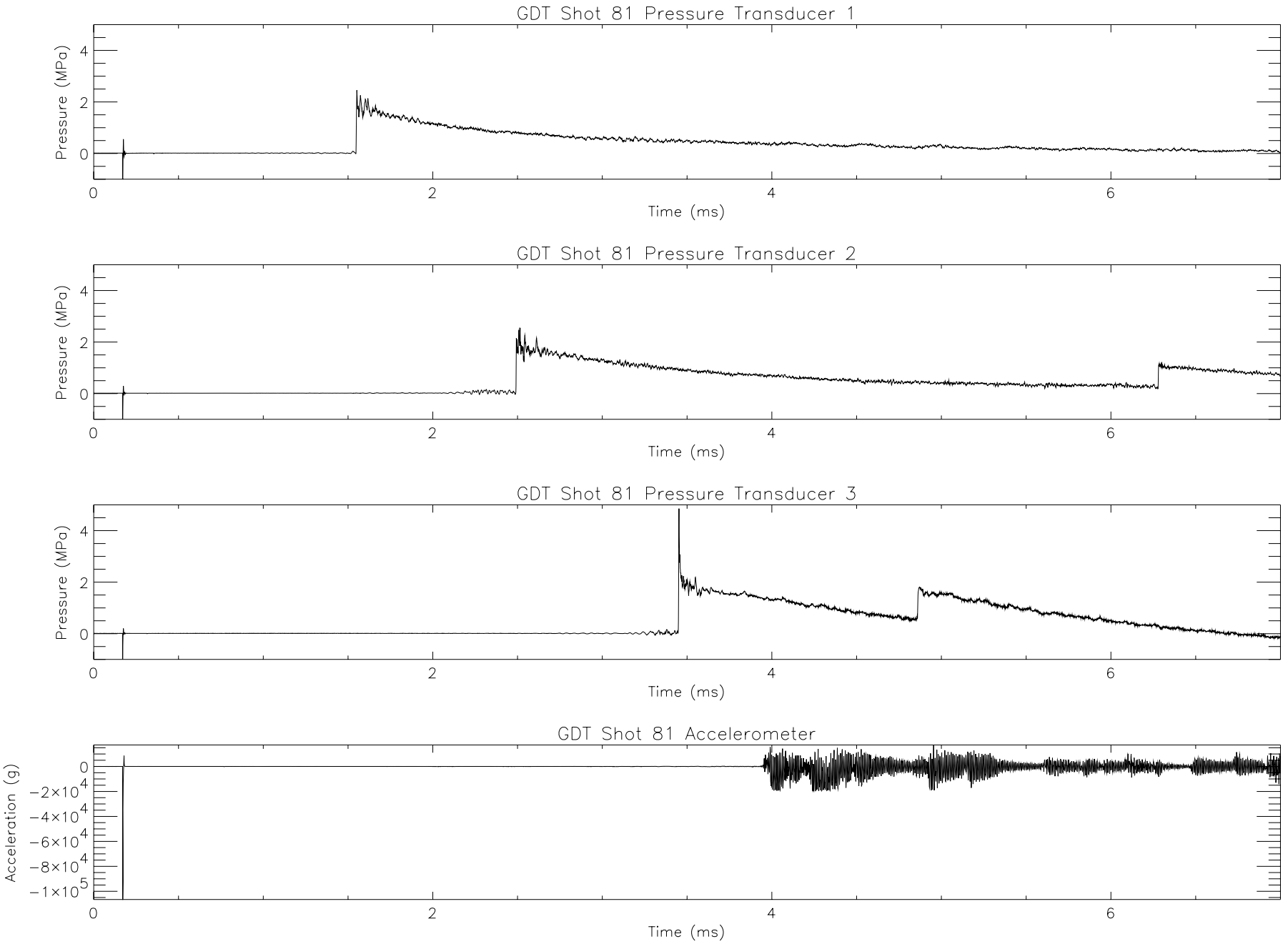
GDT Shot 81 Pressure Transducer 1
Pressure (MPa)
Time (ms)
GDT Shot 81 Pressure Transducer 2
Pressure (MPa)
Time (ms)
GDT Shot 81 Pressure Transducer 3
Pressure (MPa)
Time (ms)
GDT Shot 81 Accelerometer
Acceleration (g)
Time (ms)

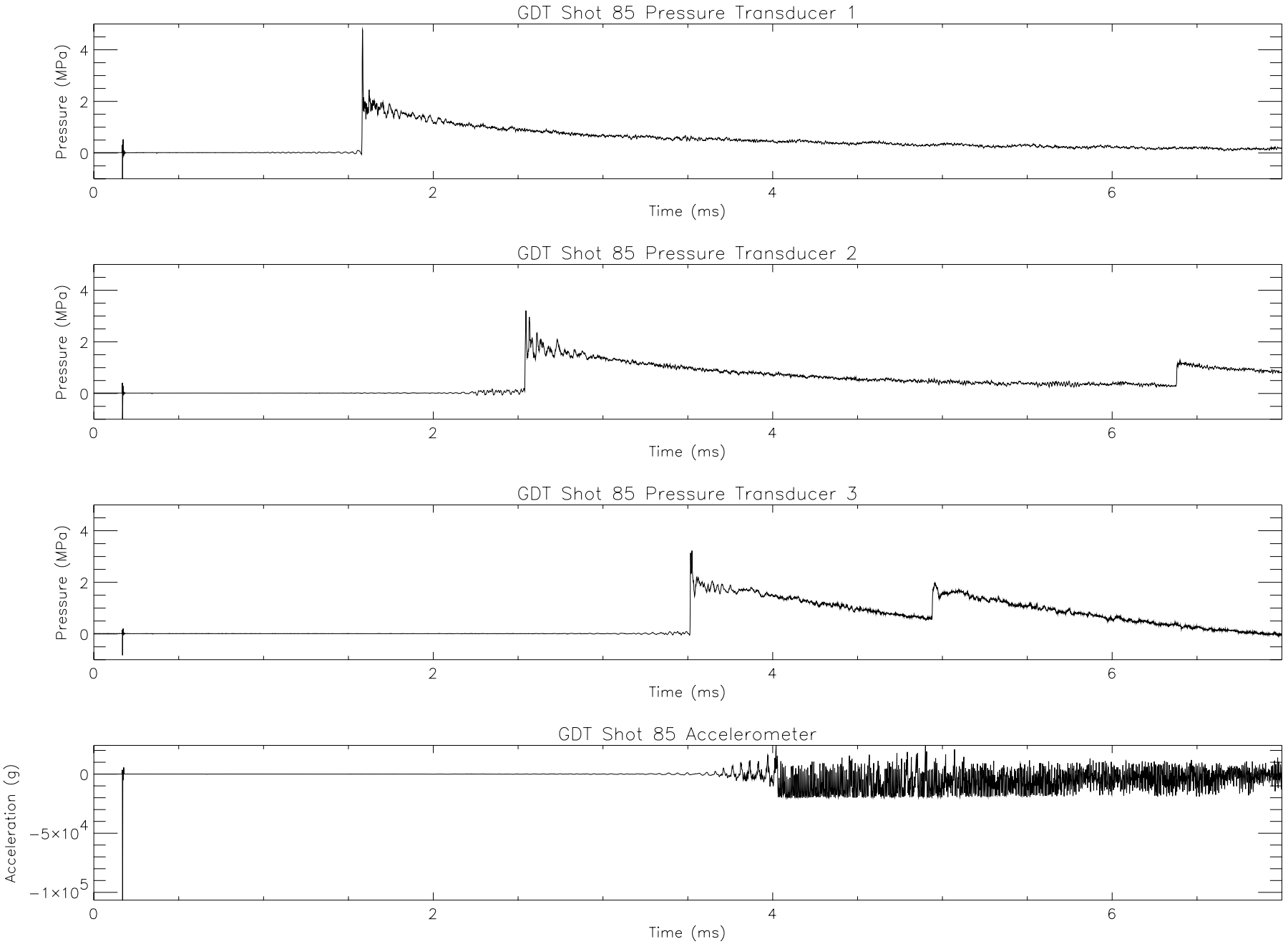
GDT Shot 85 Pressure Transducer 1
Pressure (MPa)
Time (ms)
GDT Shot 85 Pressure Transducer 2
Pressure (MPa)
Time (ms)
GDT Shot 85 Pressure Transducer 3
Pressure (MPa)
Time (ms)
GDT Shot 85 Accelerometer
Acceleration (g)
Time (ms)

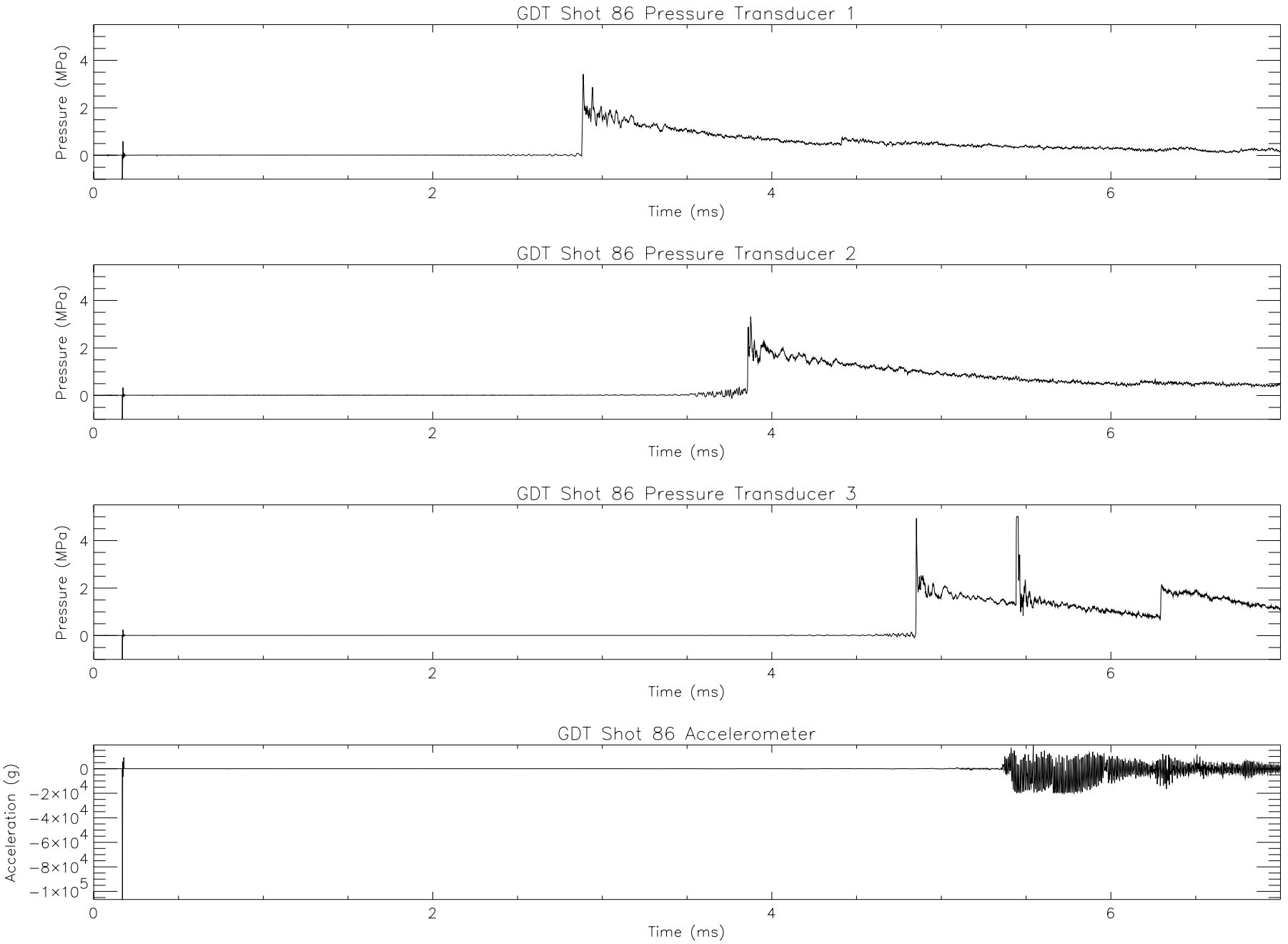
GDT Shot 86 Pressure Transducer 1
Pressure (MPa)
0
2
4
Time (ms)
0
2
4
6
GDT Shot 86 Pressure Transducer 2
Pressure (MPa)
0
2
4
Time (ms)
0
2
4
6
GDT Shot 86 Pressure Transducer 3
Pressure (MPa)
0
2
4
Time (ms)
0
2
4
6
GDT Shot 86 Accelerometer
Acceleration (g)
0
−2×10^4
−4×10^4
−6×10^4
−8×10^4
−1×10^5
Time (ms)
0
2
4
6

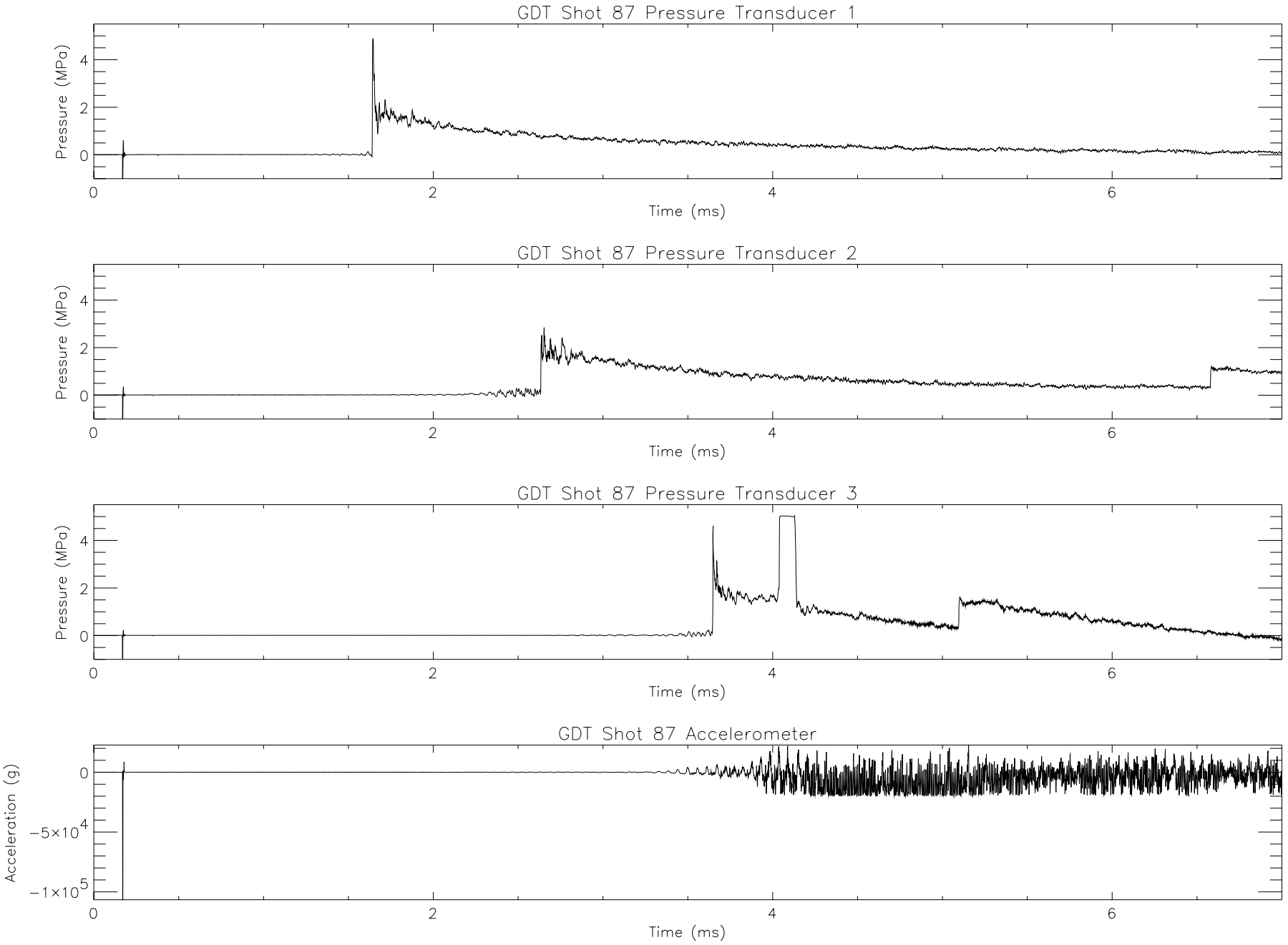
GDT Shot 87 Pressure Transducer 1
Pressure (MPa)
Time (ms)
GDT Shot 87 Pressure Transducer 2
Pressure (MPa)
Time (ms)
GDT Shot 87 Pressure Transducer 3
Pressure (MPa)
Time (ms)
GDT Shot 87 Accelerometer
Acceleration (g)
Time (ms)

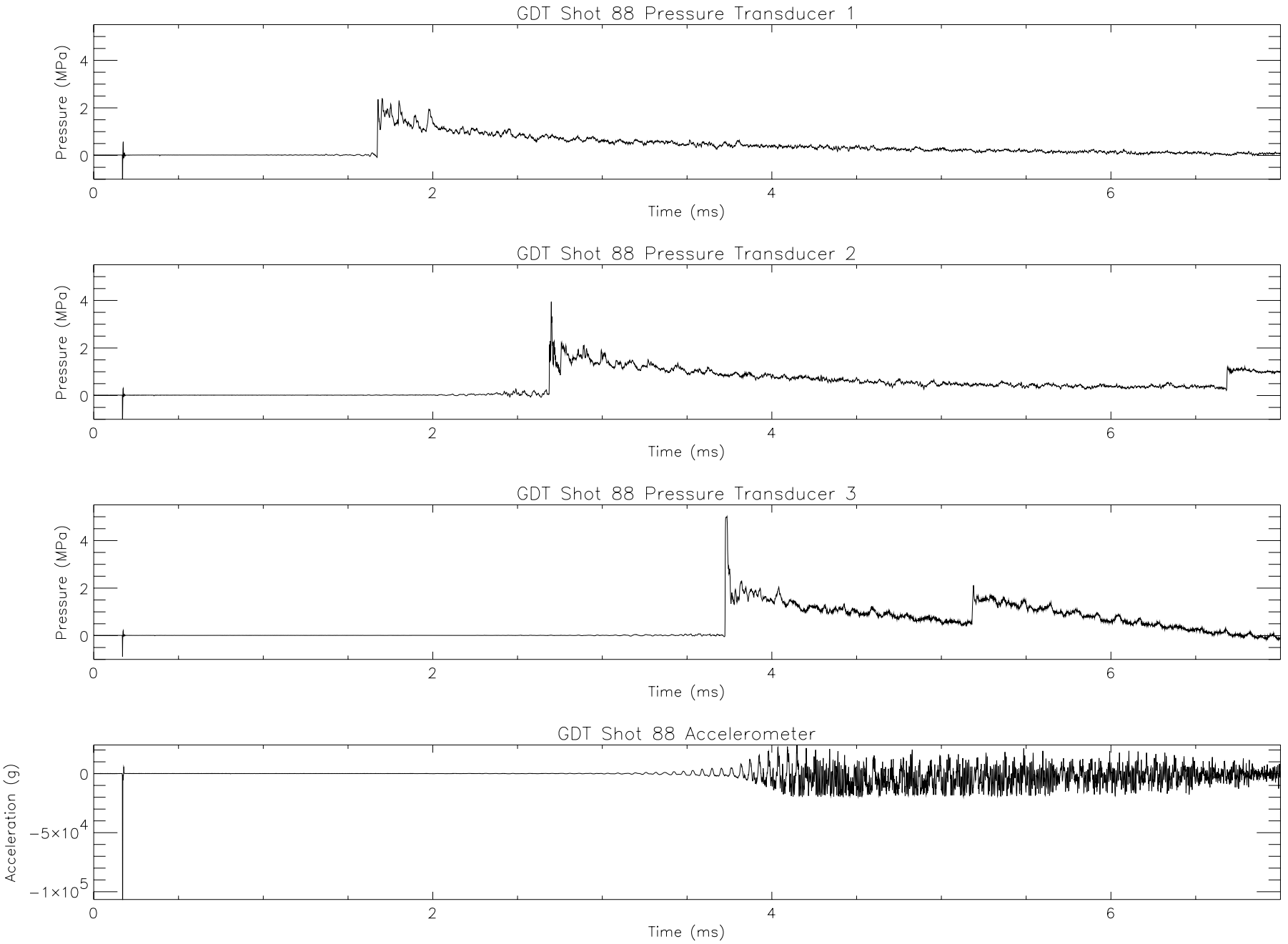
GDT Shot 88 Pressure Transducer 1
Pressure (MPa)
4
2
0
0
2
4
6
Time (ms)
GDT Shot 88 Pressure Transducer 2
Pressure (MPa)
4
2
0
0
2
4
6
Time (ms)
GDT Shot 88 Pressure Transducer 3
Pressure (MPa)
4
2
0
0
2
4
6
Time (ms)
GDT Shot 88 Accelerometer
Acceleration (g)
0
−5×10^4
−1×10^5
0
2
4
6
Time (ms)

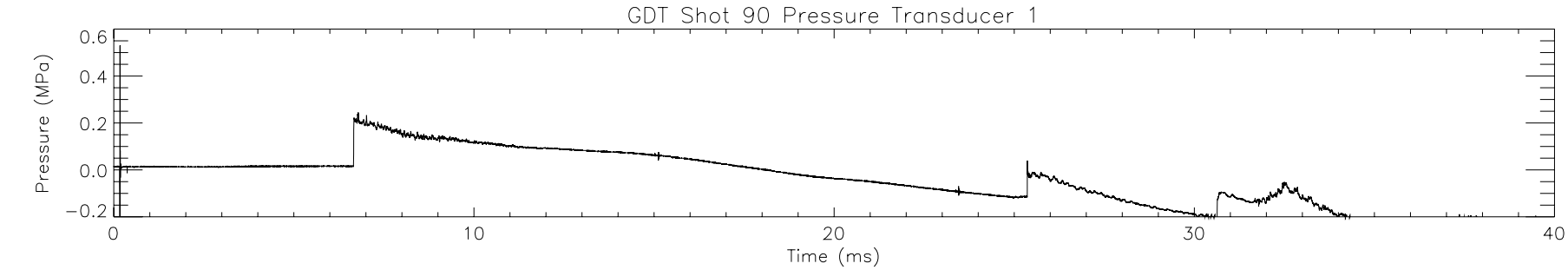
GDT Shot 90 Pressure Transducer 1
Pressure (MPa)
0.6
0.4
0.2
0.0
−0.2
0
10
20
30
40
Time (ms)

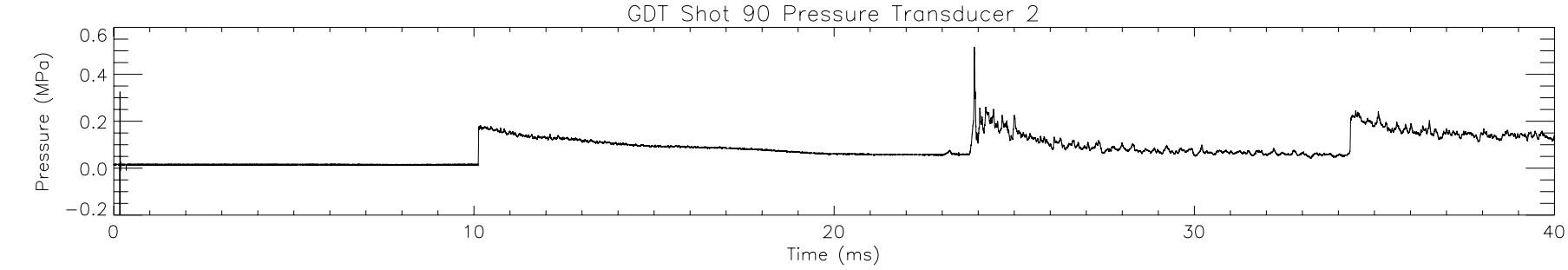
GDT Shot 90 Pressure Transducer 2
Pressure (MPa)
0.6
0.4
0.2
0.0
−0.2
0
10
20
30
40
Time (ms)

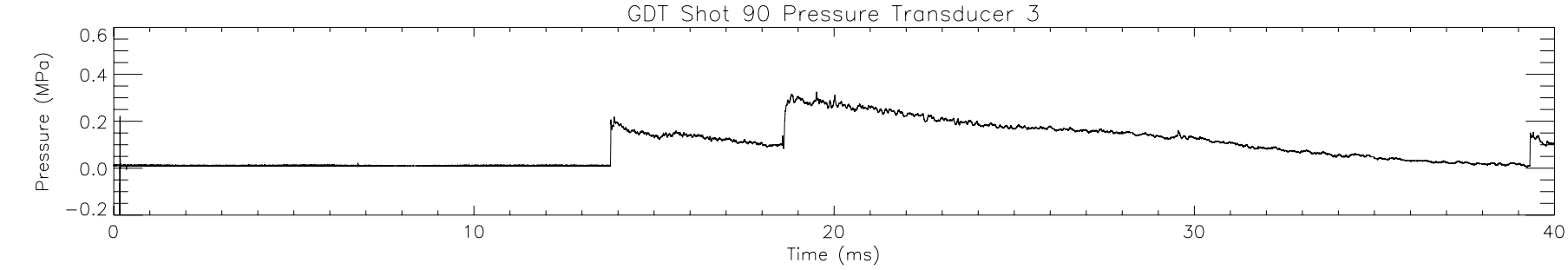
GDT Shot 90 Pressure Transducer 3
Pressure (MPa)
0.6
0.4
0.2
0.0
−0.2
0
10
20
30
40
Time (ms)

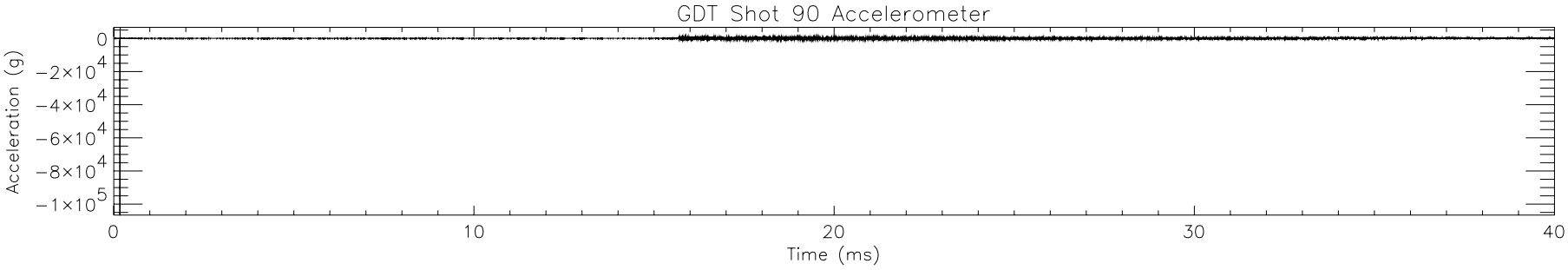
GDT Shot 90 Accelerometer
Acceleration (g)
0
−2×10^4
−4×10^4
−6×10^4
−8×10^4
−1×10^5
0
10
20
30
40
Time (ms)

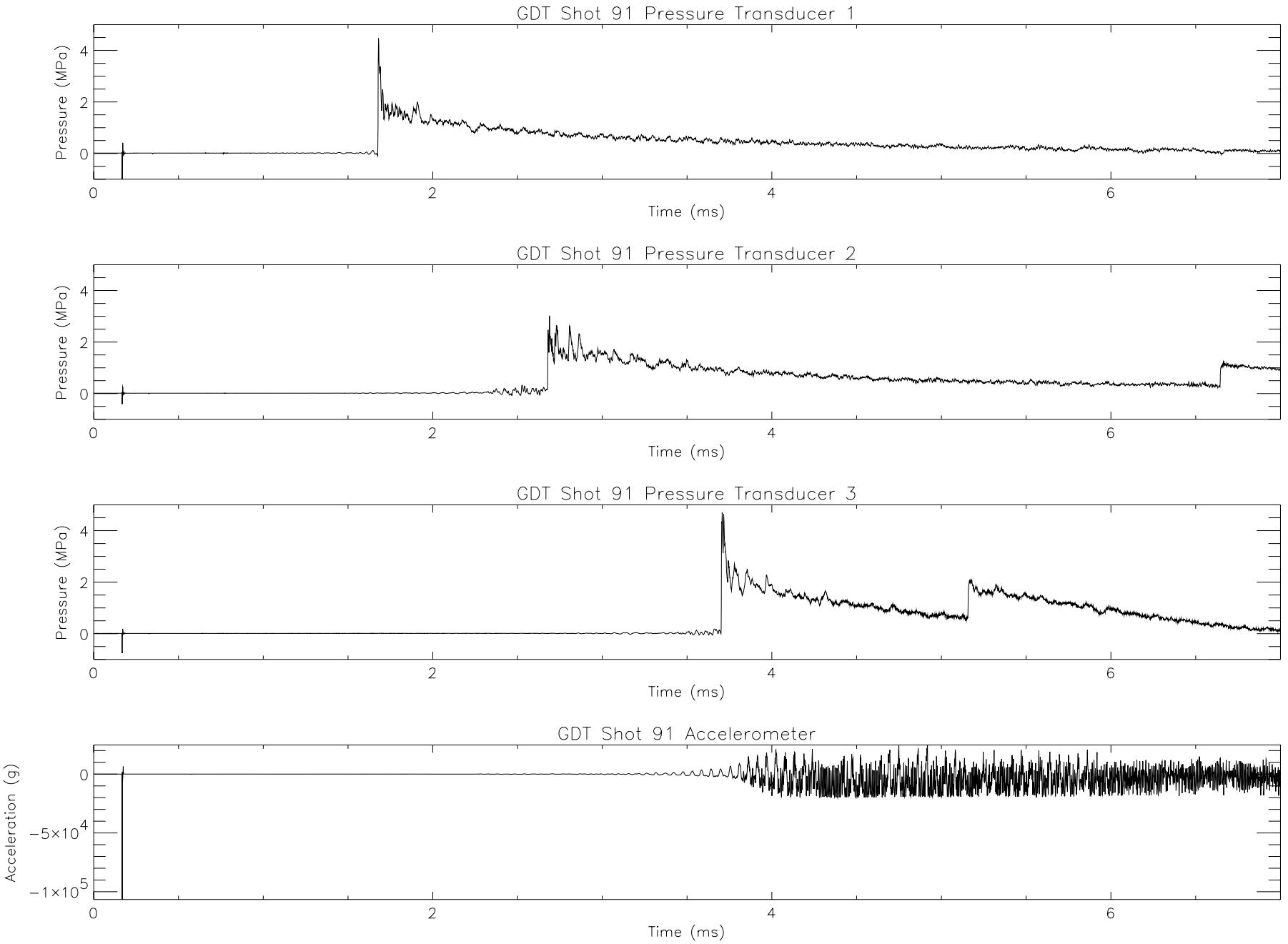
GDT Shot 91 Pressure Transducer 1
Pressure (MPa)
4
2
0
0
2
4
6
Time (ms)
GDT Shot 91 Pressure Transducer 2
Pressure (MPa)
4
2
0
0
2
4
6
Time (ms)
GDT Shot 91 Pressure Transducer 3
Pressure (MPa)
4
2
0
0
2
4
6
Time (ms)
GDT Shot 91 Accelerometer
Acceleration (g)
0
−5×10^4
−1×10^5
0
2
4
6
Time (ms)

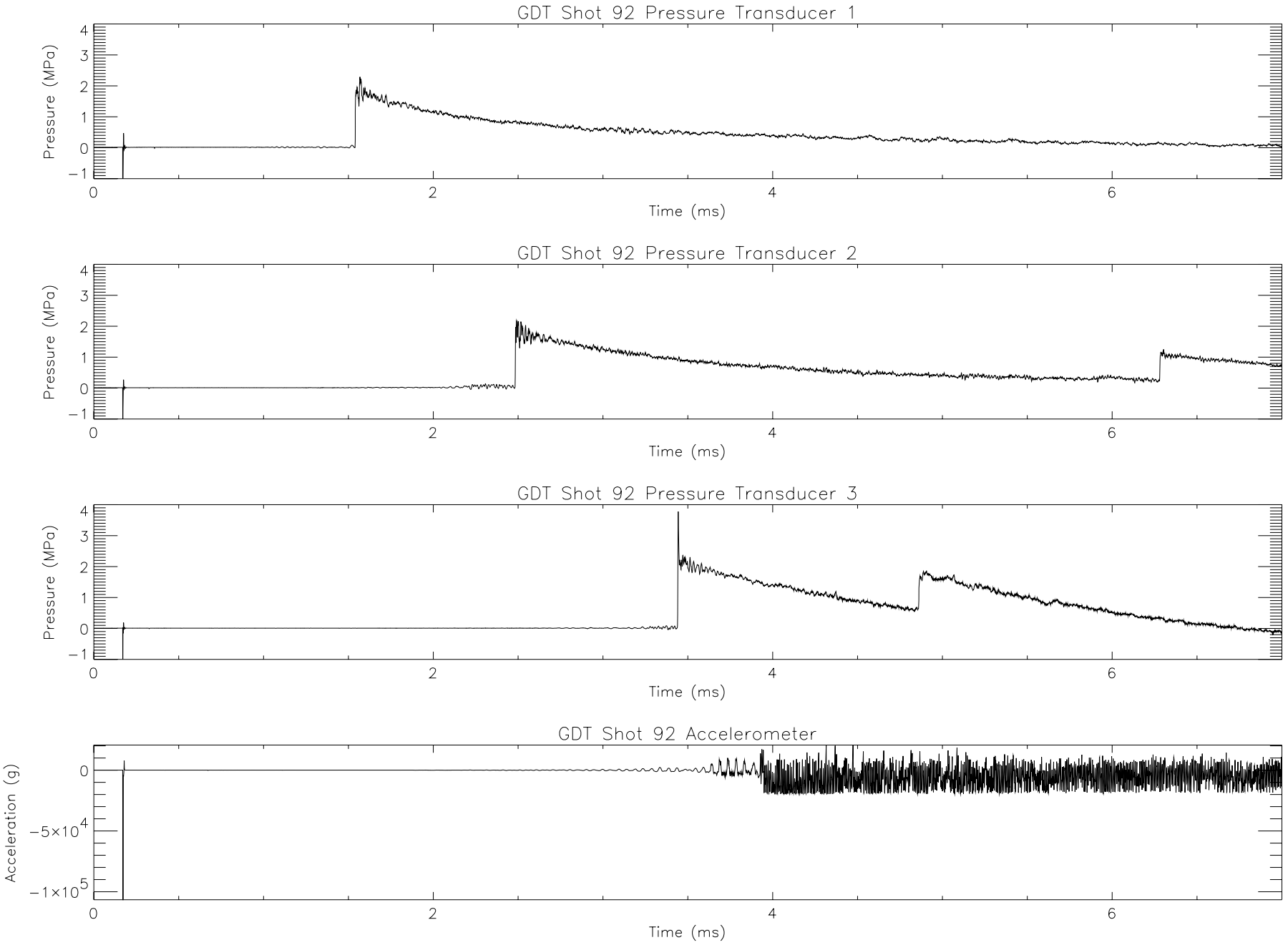
GDT Shot 92 Pressure Transducer 1
Pressure (MPa)
Time (ms)
GDT Shot 92 Pressure Transducer 2
Pressure (MPa)
Time (ms)
GDT Shot 92 Pressure Transducer 3
Pressure (MPa)
Time (ms)
GDT Shot 92 Accelerometer
Acceleration (g)
Time (ms)

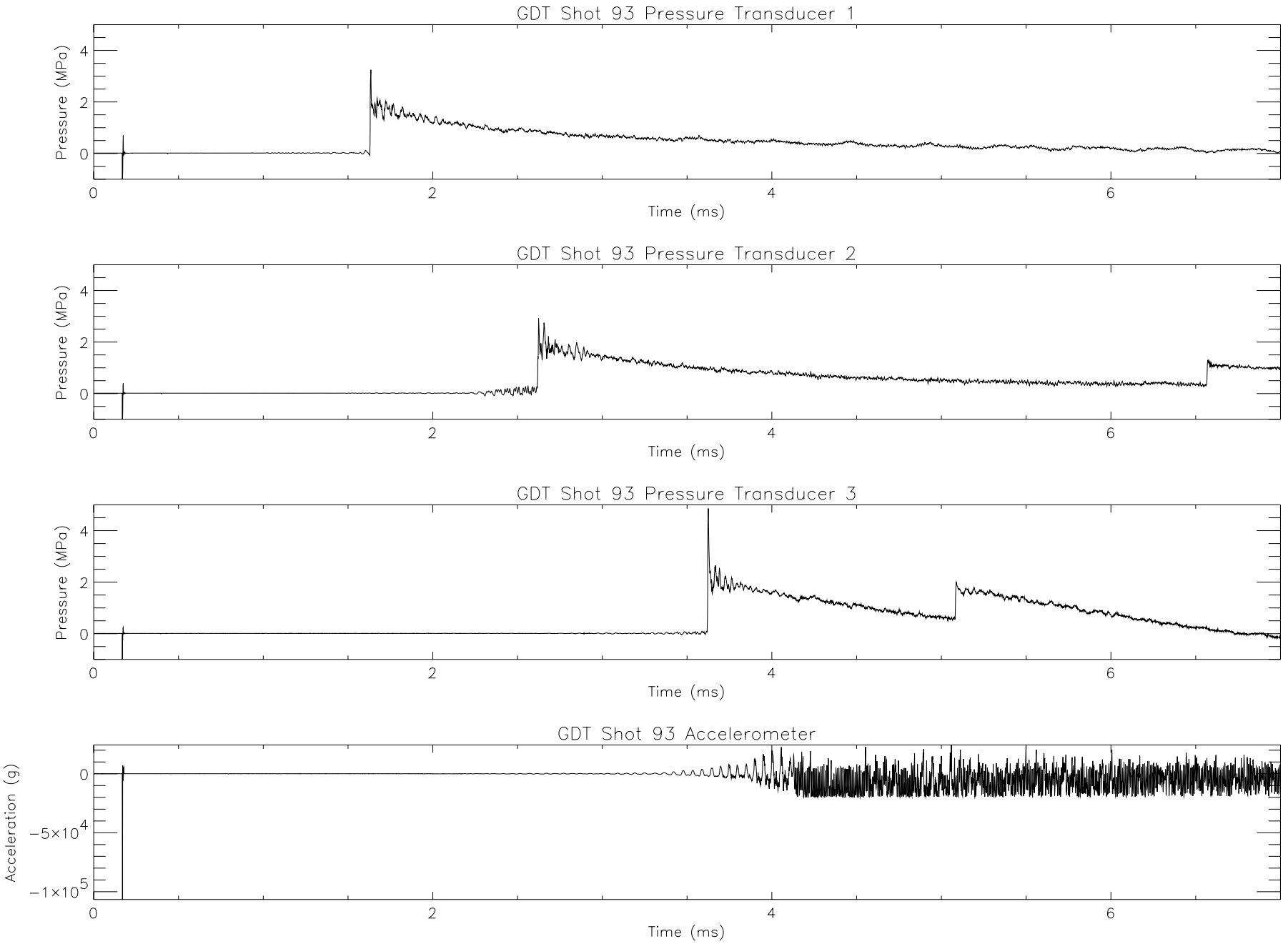
GDT Shot 93 Pressure Transducer 1
Pressure (MPa)
Time (ms)
GDT Shot 93 Pressure Transducer 2
Pressure (MPa)
Time (ms)
GDT Shot 93 Pressure Transducer 3
Pressure (MPa)
Time (ms)
GDT Shot 93 Accelerometer
Acceleration (g)
Time (ms)

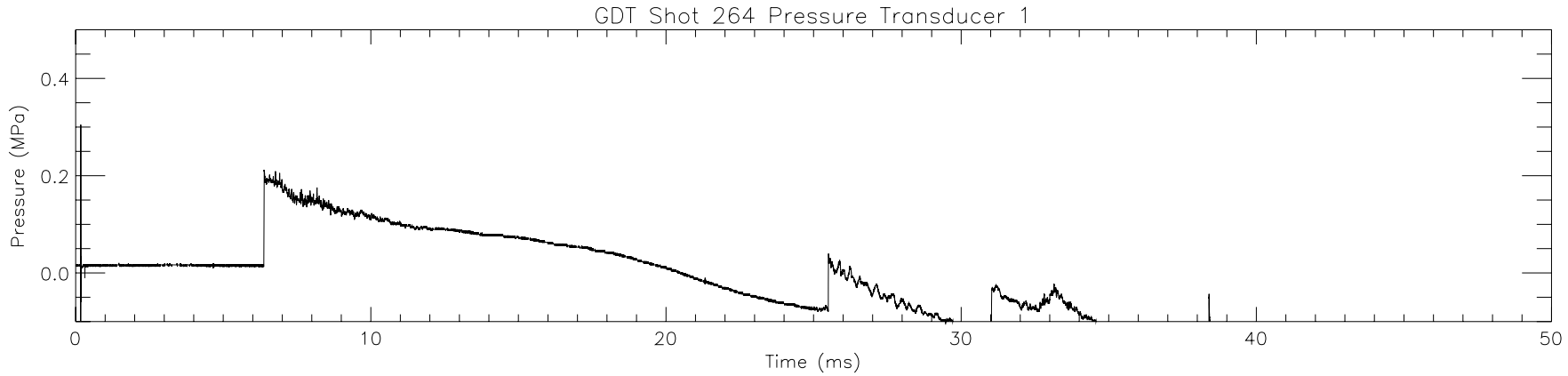
GDT Shot 264 Pressure Transducer 1
Pressure (MPa)
0.4
0.2
0.0
0
10
20
30
40
50
Time (ms)

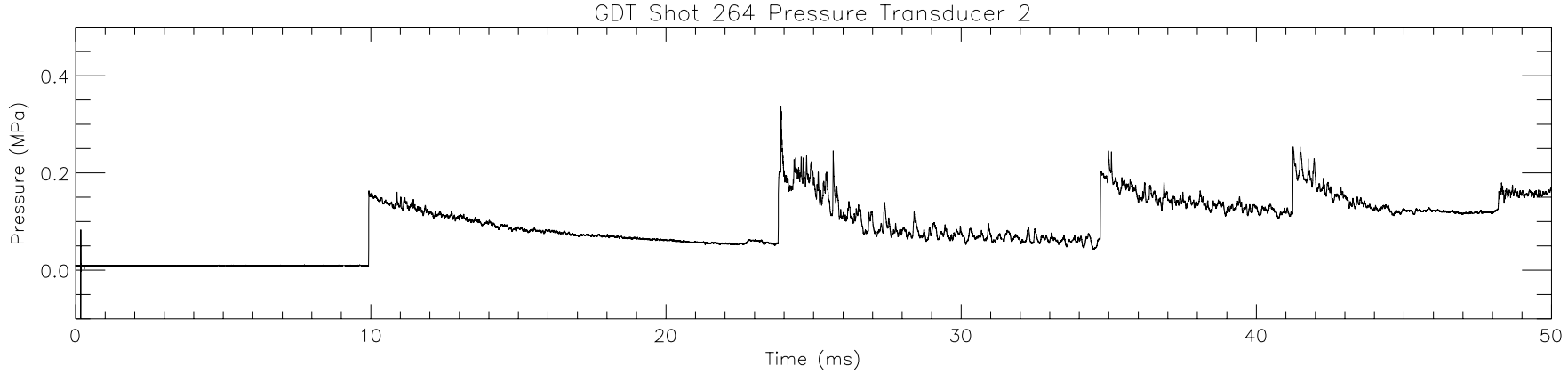
GDT Shot 264 Pressure Transducer 2
Pressure (MPa)
0.4
0.2
0.0
0
10
20
30
40
50
Time (ms)

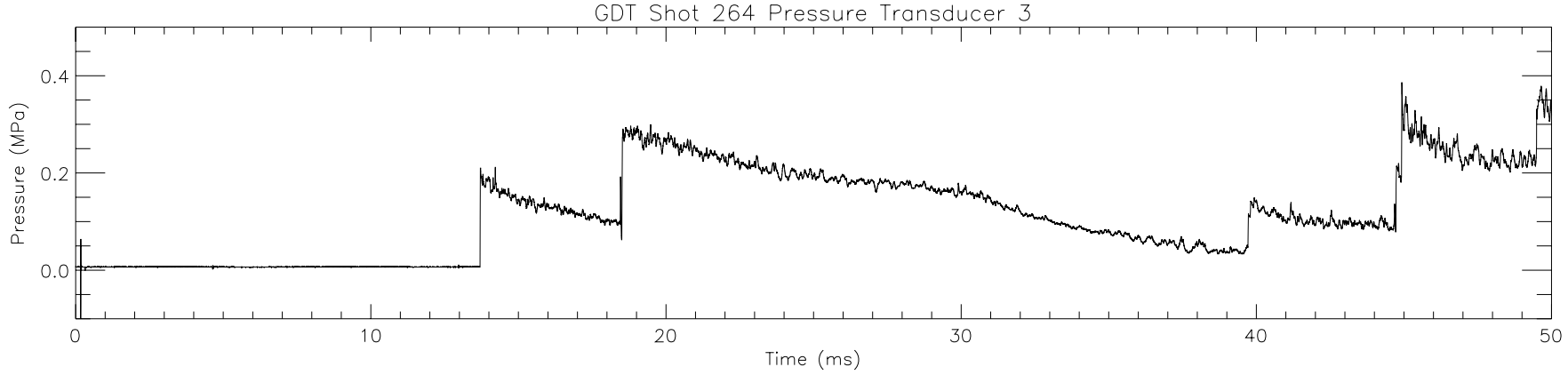
GDT Shot 264 Pressure Transducer 3
Pressure (MPa)
0.4
0.2
0.0
0
10
20
30
40
50
Time (ms)

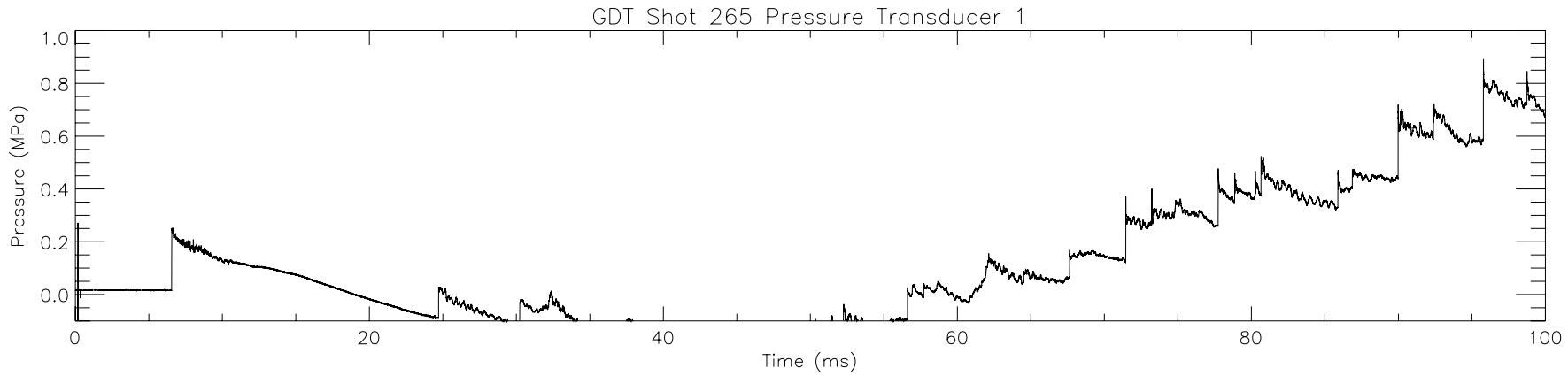
GDT Shot 265 Pressure Transducer 1
Pressure (MPa)
1.0
0.8
0.6
0.4
0.2
0.0
0
20
40
60
80
100
Time (ms)

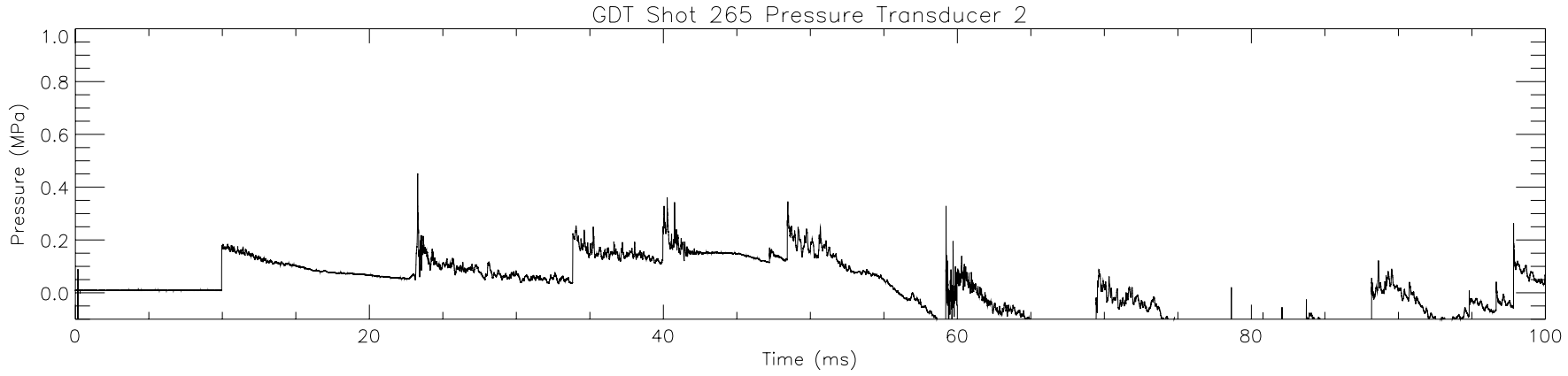
GDT Shot 265 Pressure Transducer 2
Pressure (MPa)
1.0
0.8
0.6
0.4
0.2
0.0
0
20
40
60
80
100
Time (ms)

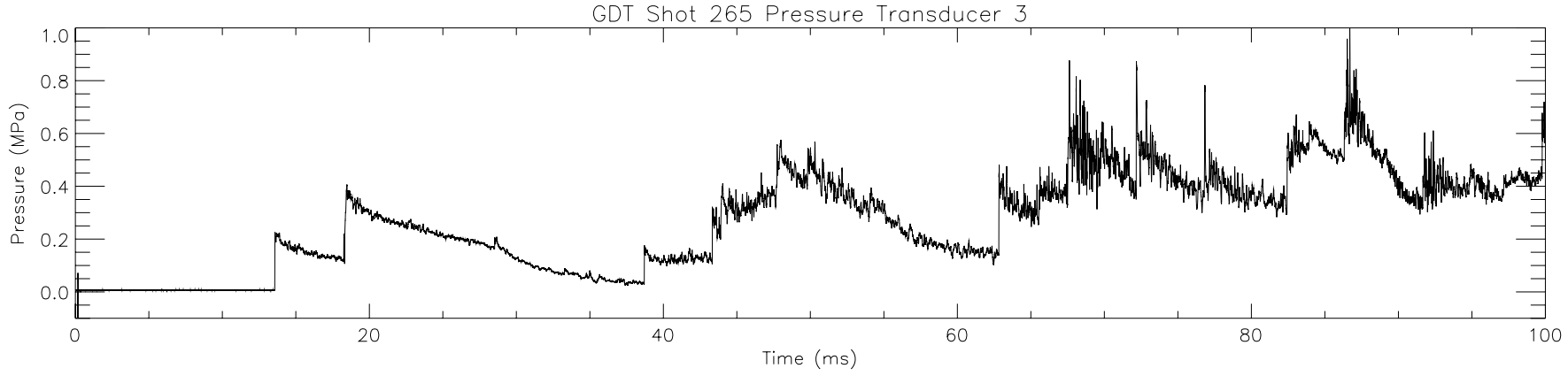
GDT Shot 265 Pressure Transducer 3
Pressure (MPa)
1.0
0.8
0.6
0.4
0.2
0.0
0
20
40
60
80
100
Time (ms)

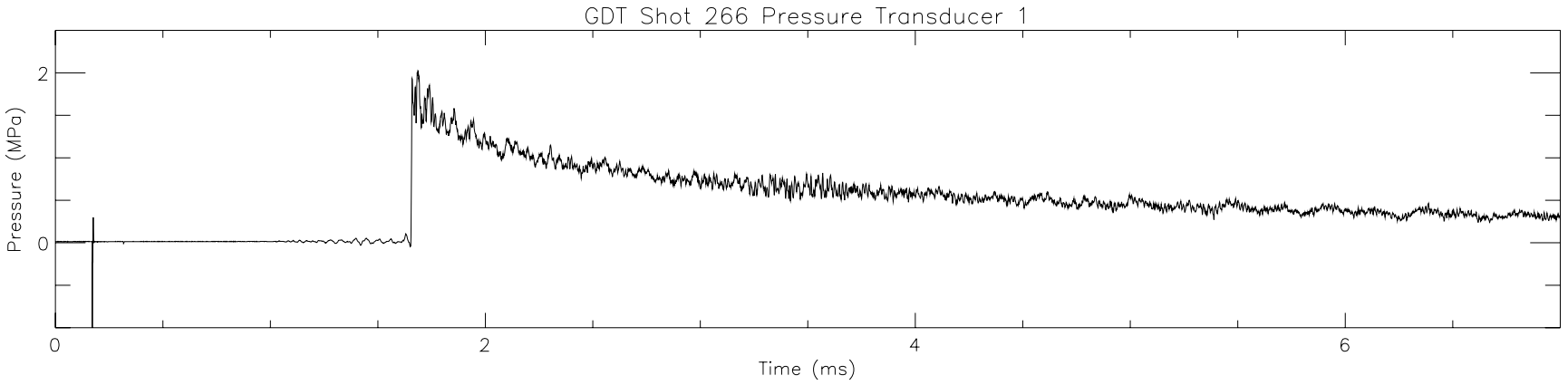
GDT Shot 266 Pressure Transducer 1
Pressure (MPa)
2
0
0
2
4
6
Time (ms)

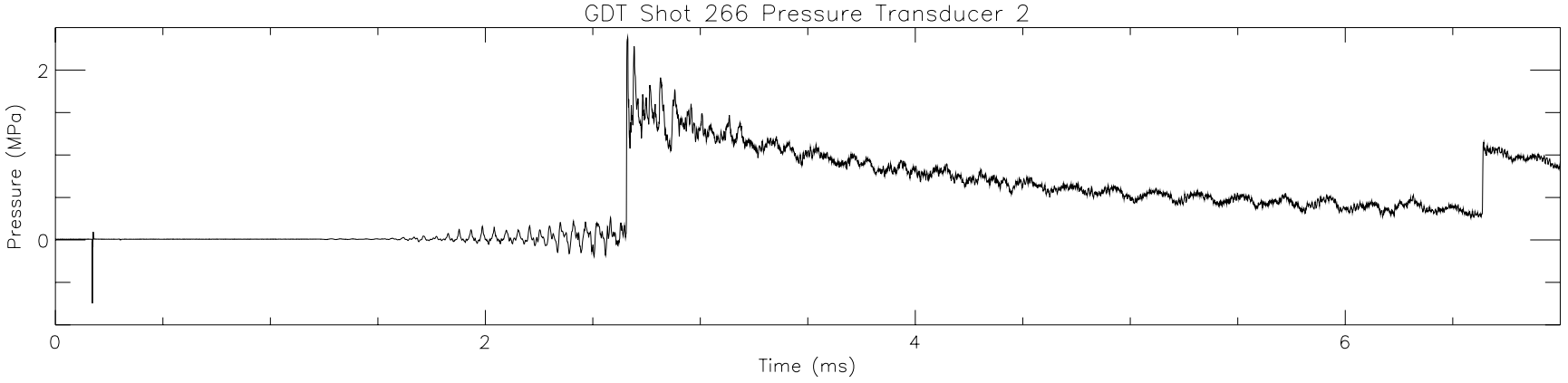
GDT Shot 266 Pressure Transducer 2
Pressure (MPa)
2
0
0
2
4
6
Time (ms)

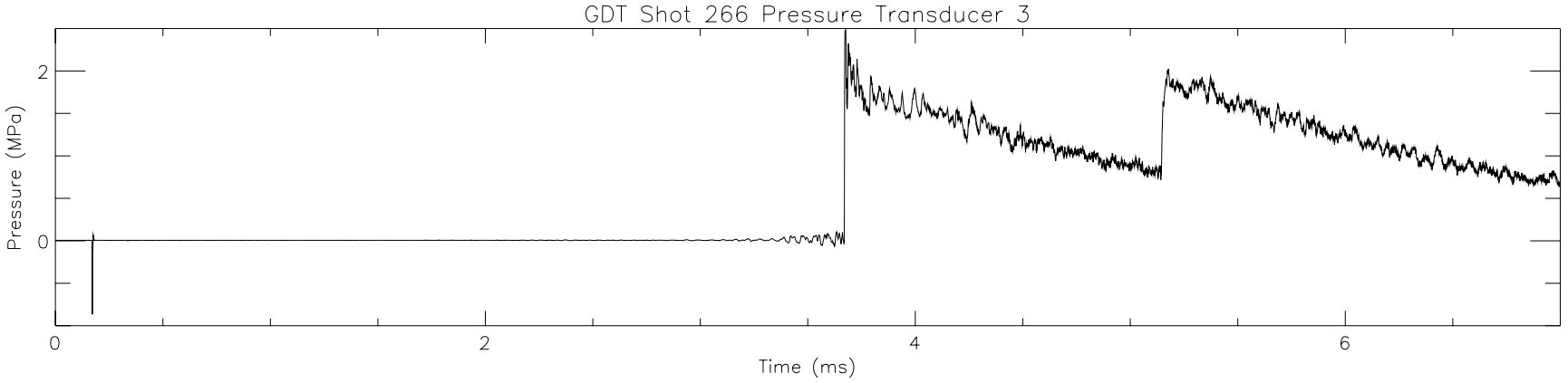
GDT Shot 266 Pressure Transducer 3
Pressure (MPa)
2
0
0
2
4
6
Time (ms)

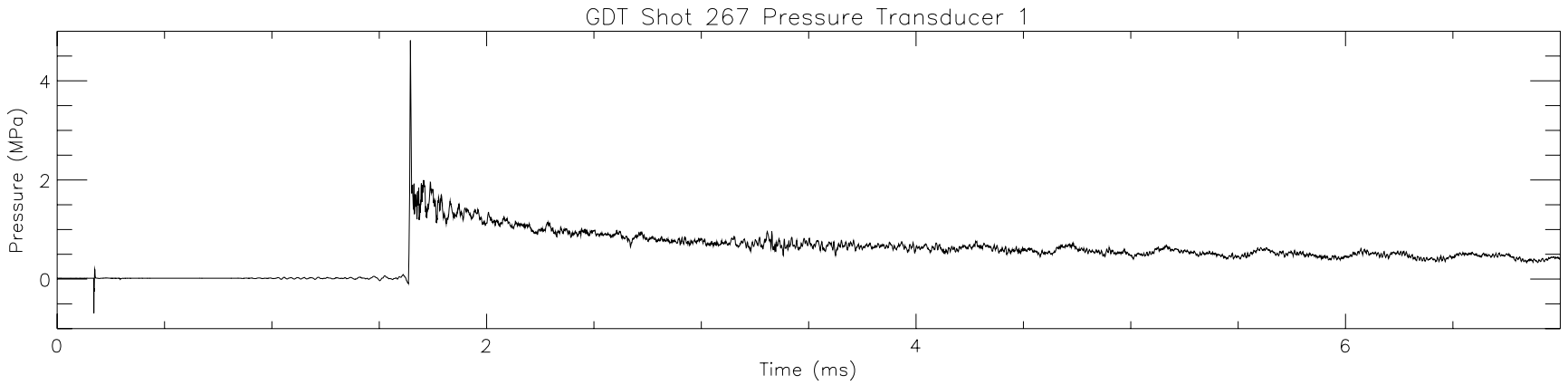
GDT Shot 267 Pressure Transducer 1
Pressure (MPa)
0
2
4
0
2
4
6
Time (ms)

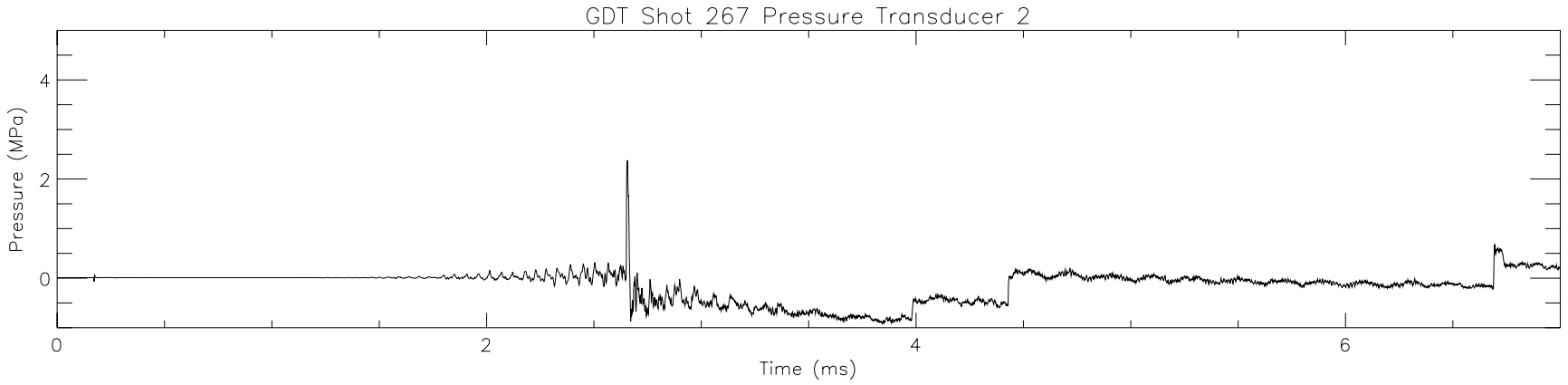
GDT Shot 267 Pressure Transducer 2
Pressure (MPa)
0
2
4
0
2
4
6
Time (ms)

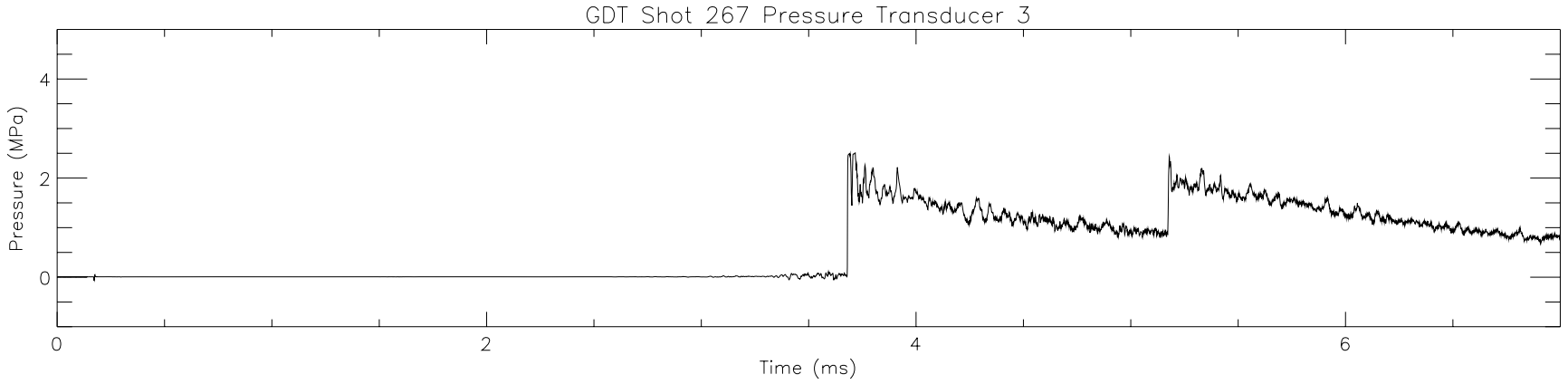
GDT Shot 267 Pressure Transducer 3
Pressure (MPa)
0
2
4
0
2
4
6
Time (ms)

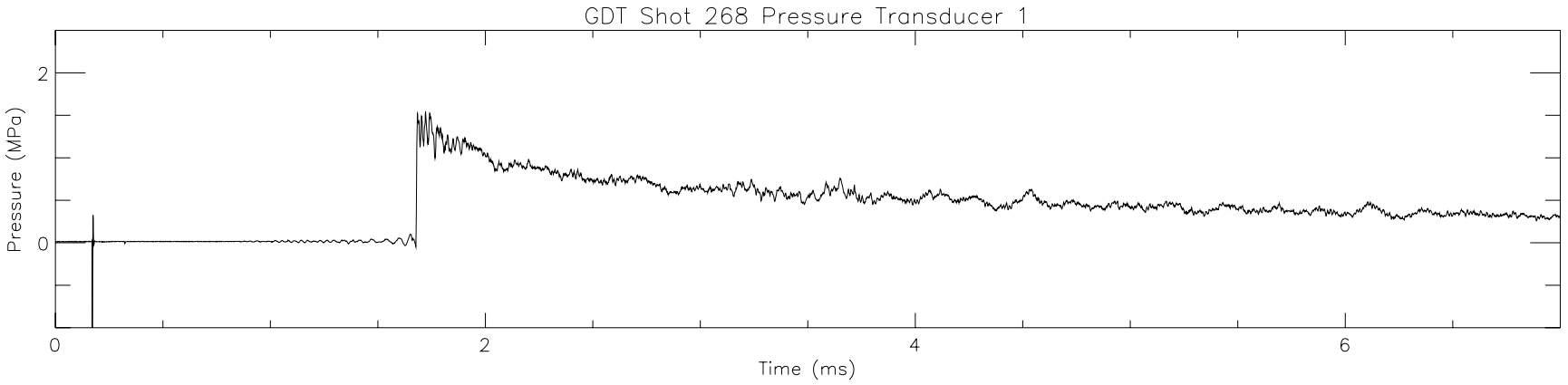
GDT Shot 268 Pressure Transducer 1
Pressure (MPa)
2
0
0
2
4
6
Time (ms)

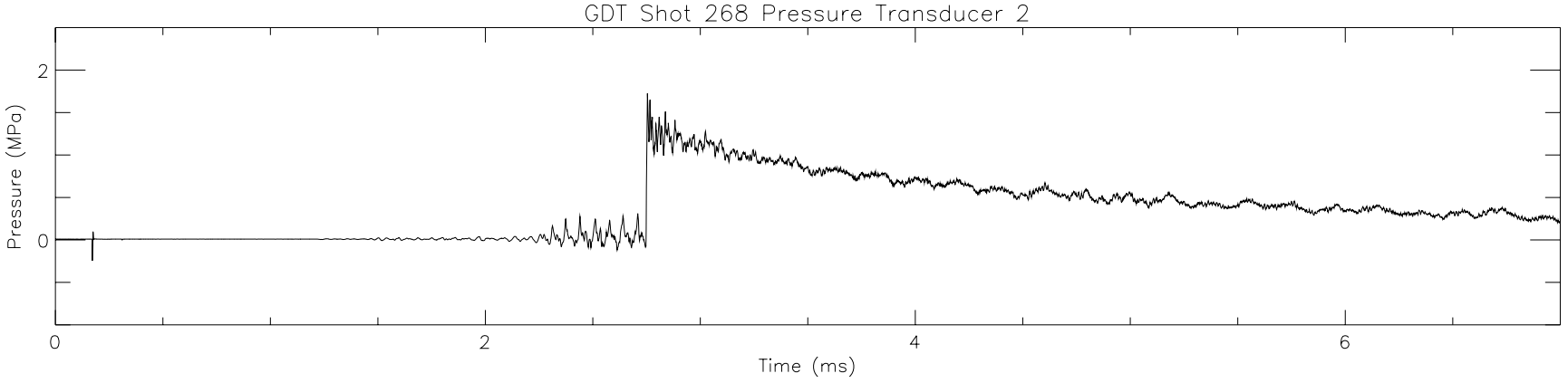
GDT Shot 268 Pressure Transducer 2
Pressure (MPa)
2
0
0
2
4
6
Time (ms)

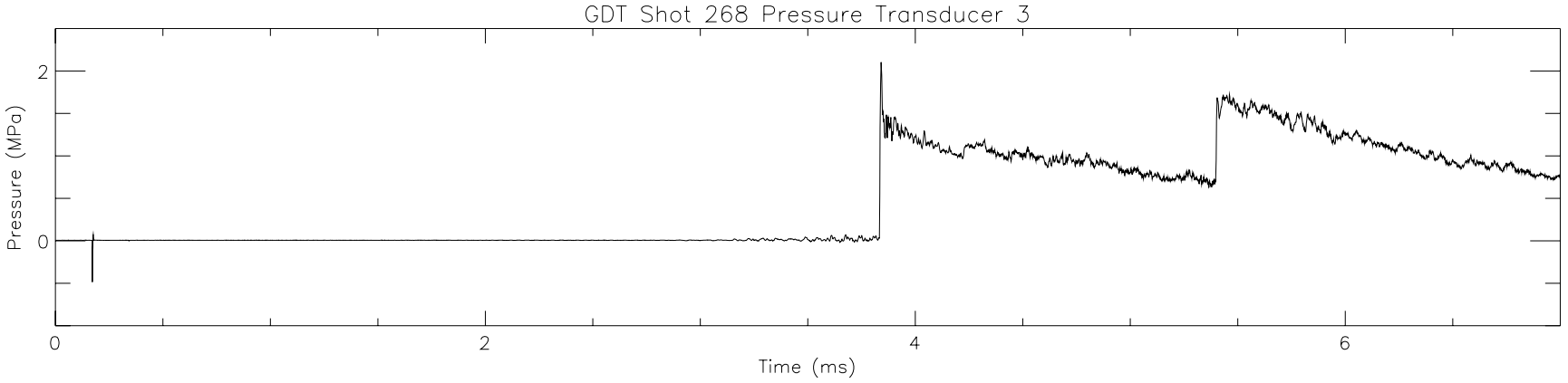
GDT Shot 268 Pressure Transducer 3
Pressure (MPa)
2
0
0
2
4
6
Time (ms)

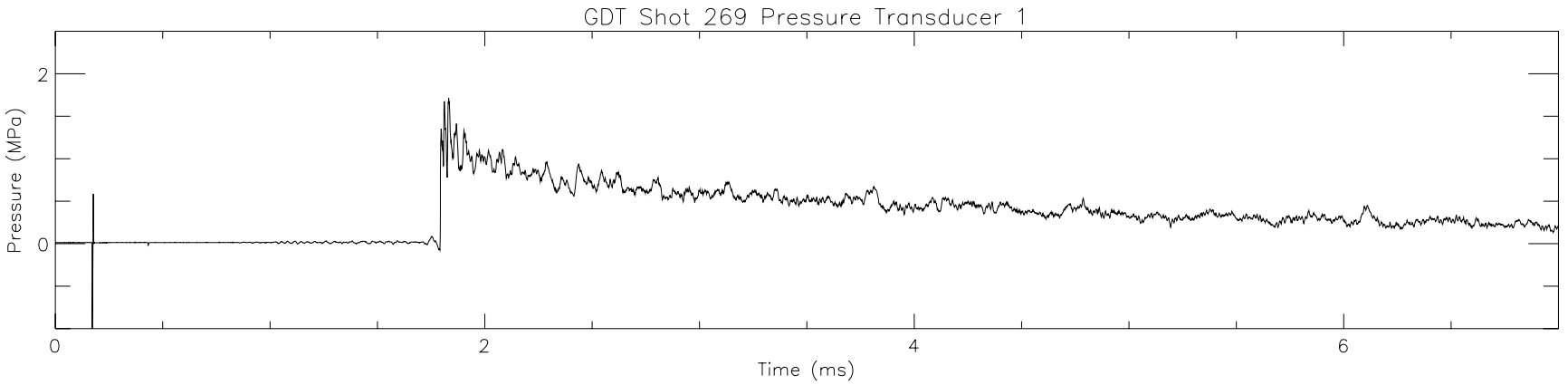
GDT Shot 269 Pressure Transducer 1
Pressure (MPa)
2
0
0
2
4
6
Time (ms)

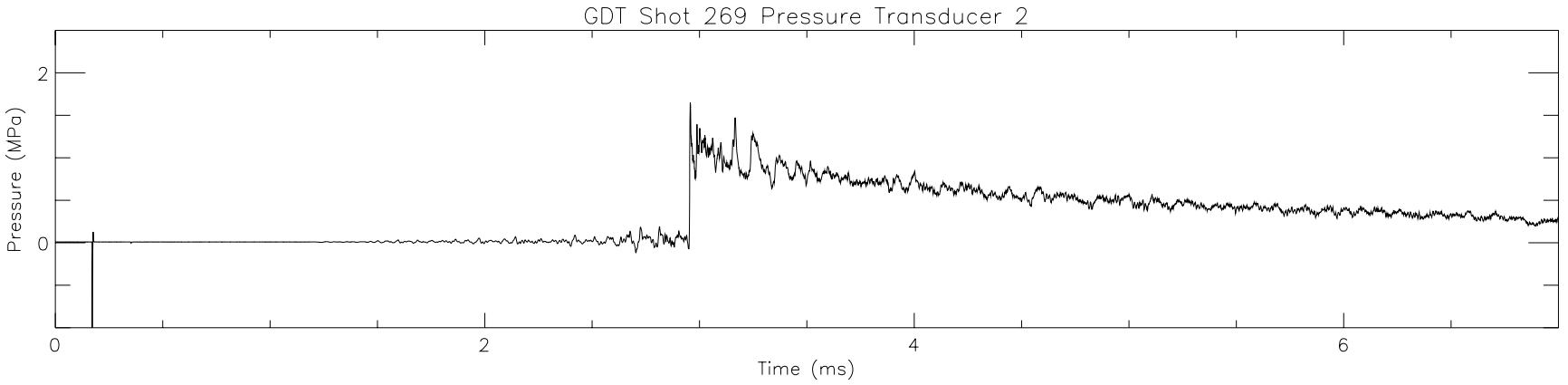
GDT Shot 269 Pressure Transducer 2
Pressure (MPa)
2
0
0
2
4
6
Time (ms)

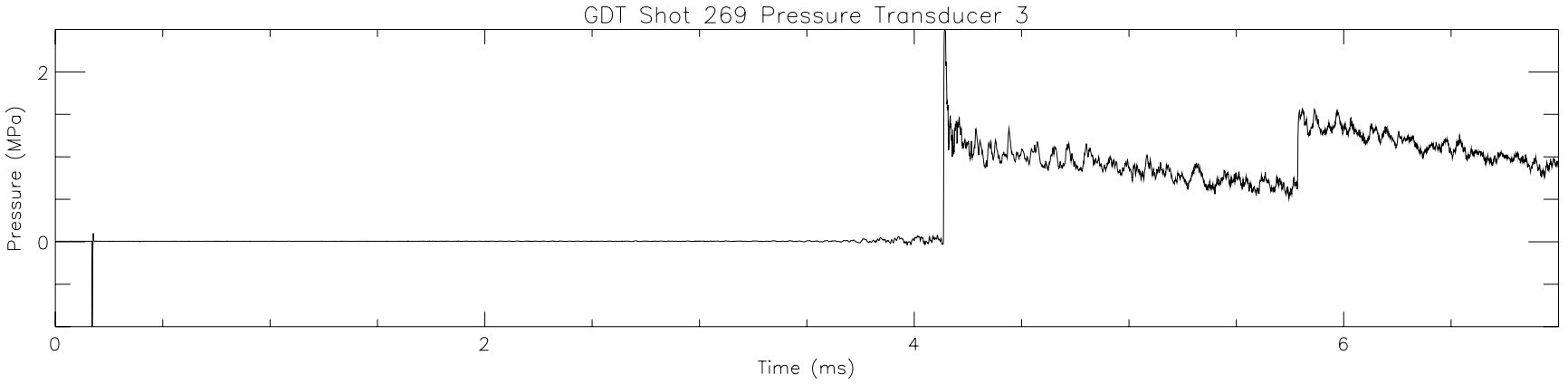
GDT Shot 269 Pressure Transducer 3
Pressure (MPa)
2
0
0
2
4
6
Time (ms)

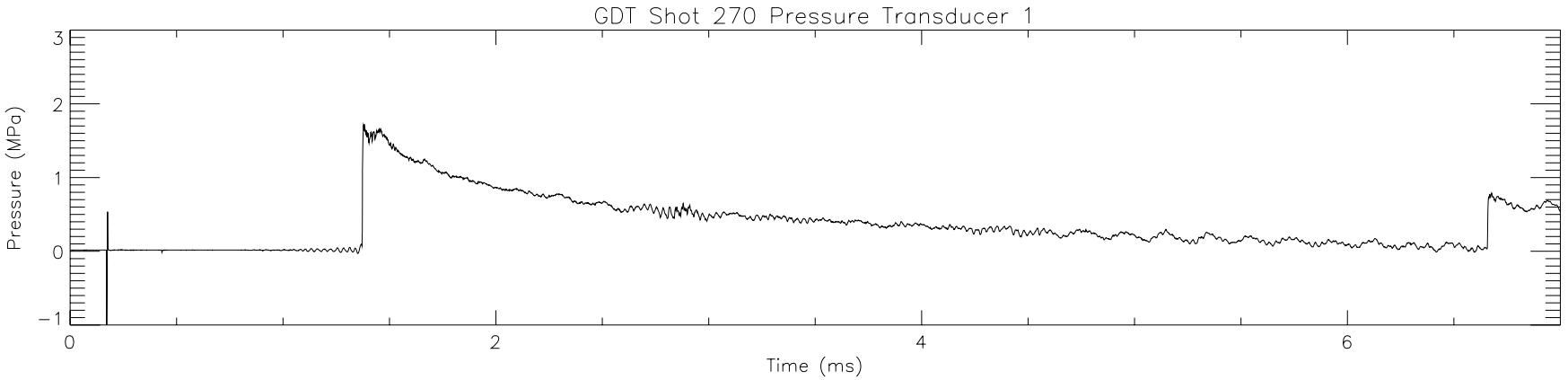
GDT Shot 270 Pressure Transducer 1
Pressure (MPa)
Time (ms)
3
2
1
0
−1
0
2
4
6

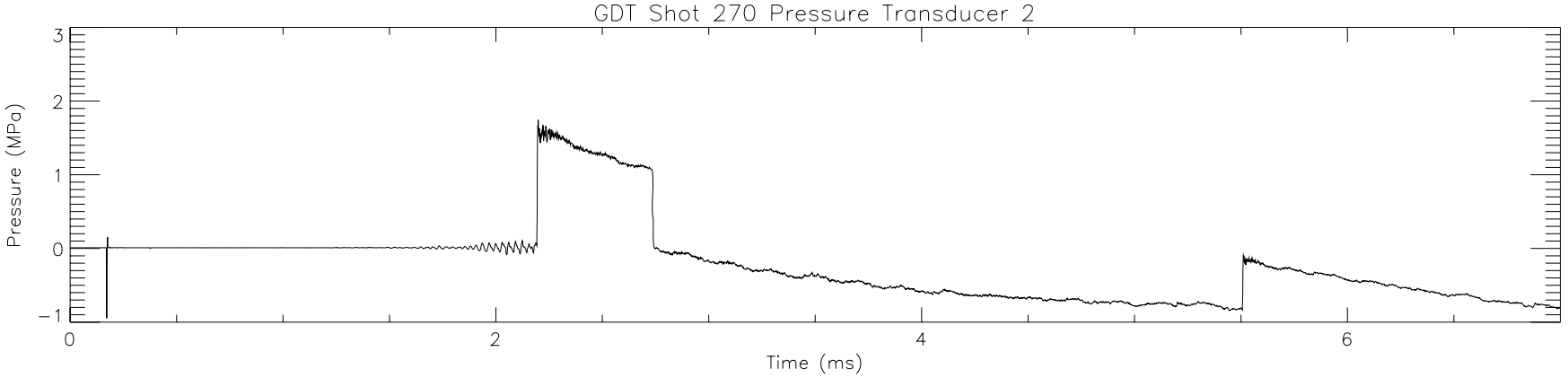
GDT Shot 270 Pressure Transducer 2
Pressure (MPa)
Time (ms)
3
2
1
0
−1
0
2
4
6

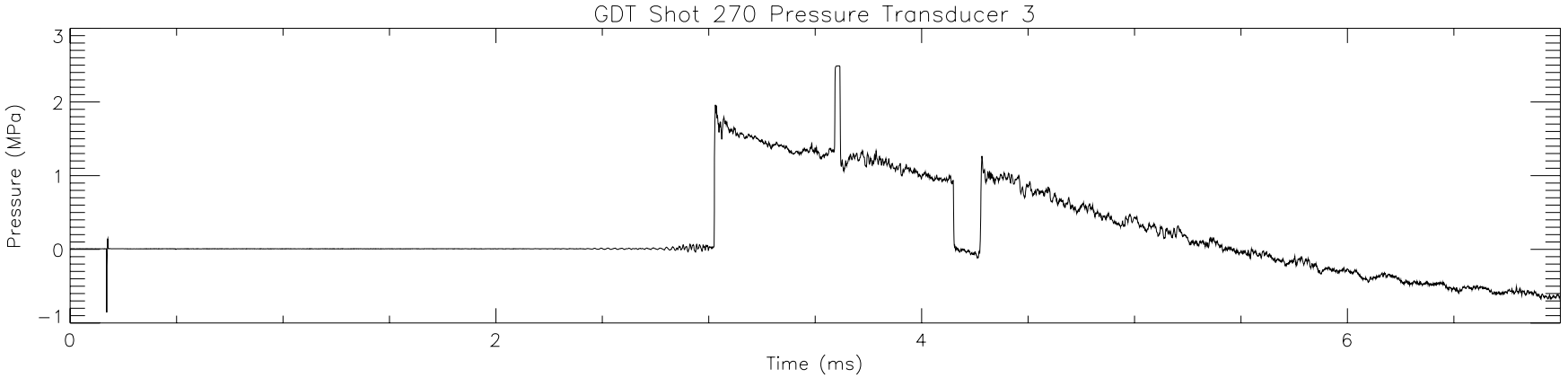
GDT Shot 270 Pressure Transducer 3
Pressure (MPa)
Time (ms)
3
2
1
0
−1
0
2
4
6

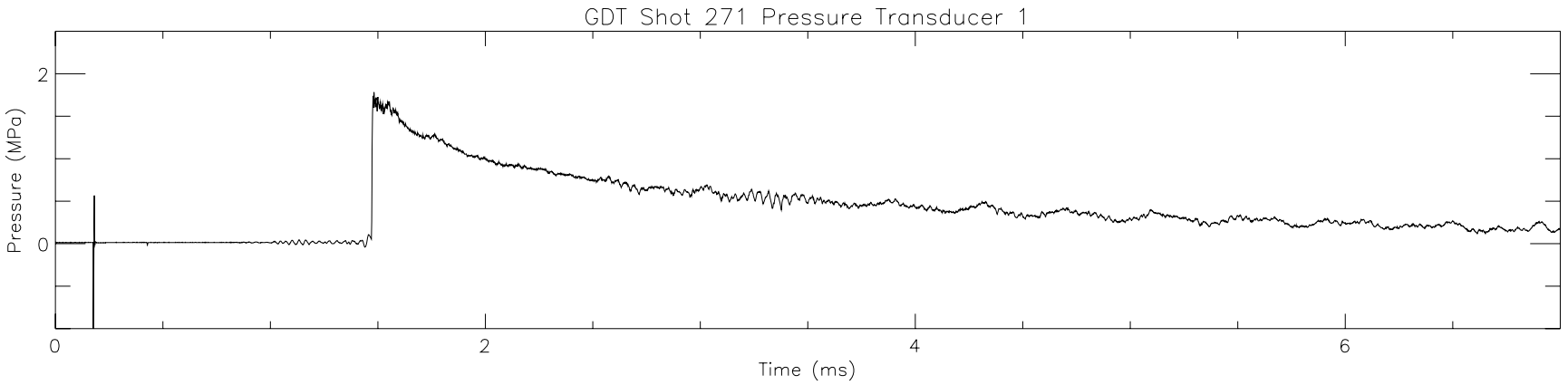
GDT Shot 271 Pressure Transducer 1
Pressure (MPa)
2
0
0
2
4
6
Time (ms)

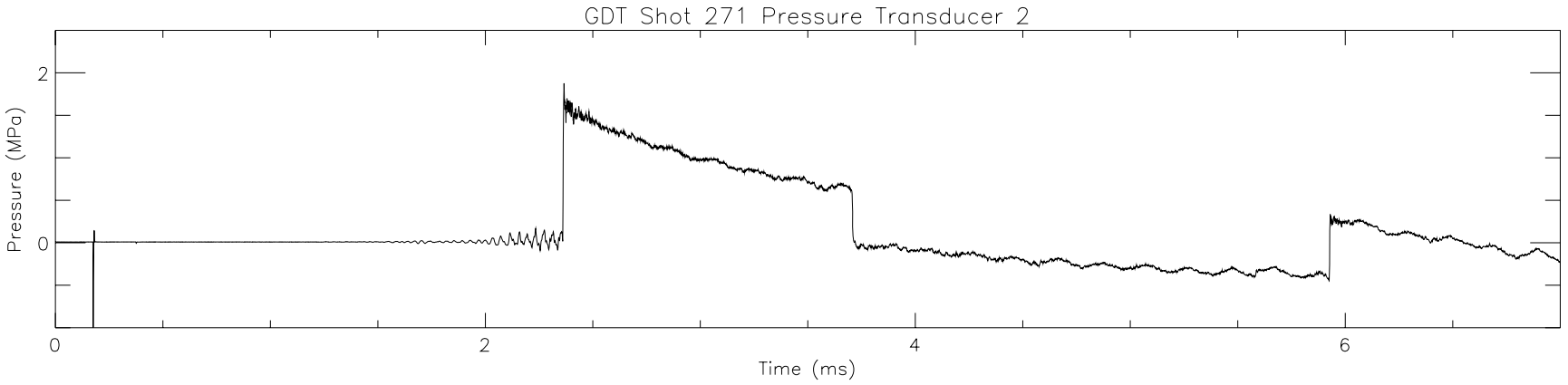
GDT Shot 271 Pressure Transducer 2
Pressure (MPa)
2
0
0
2
4
6
Time (ms)

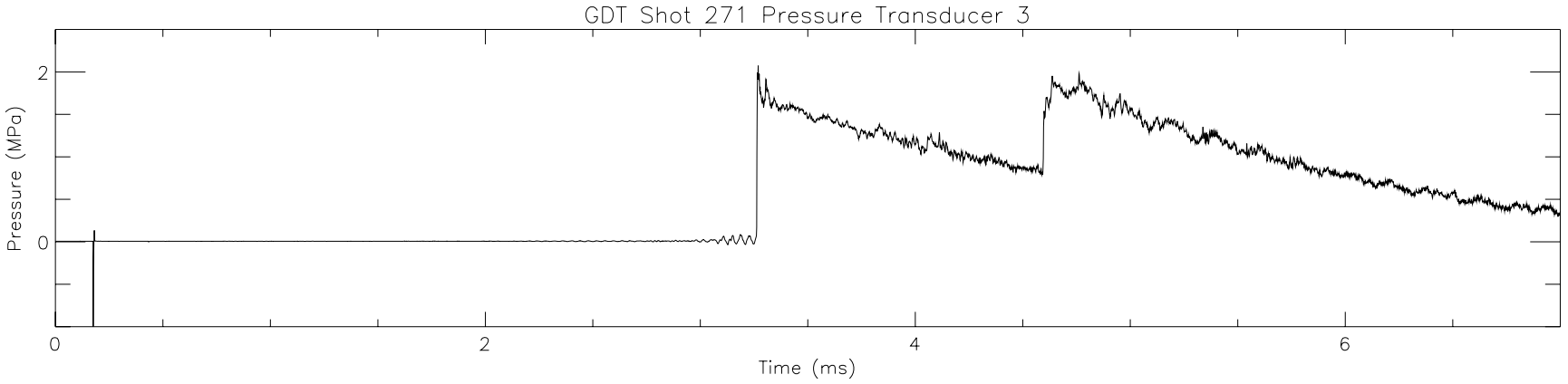
GDT Shot 271 Pressure Transducer 3
Pressure (MPa)
2
0
0
2
4
6
Time (ms)

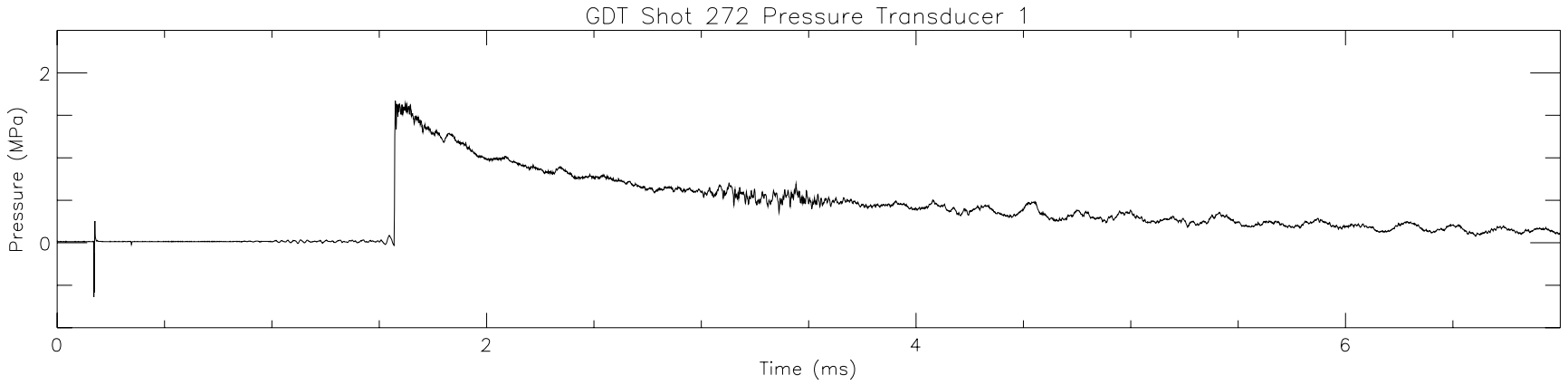
GDT Shot 272 Pressure Transducer 1
Pressure (MPa)
2
0
0
2
4
6
Time (ms)

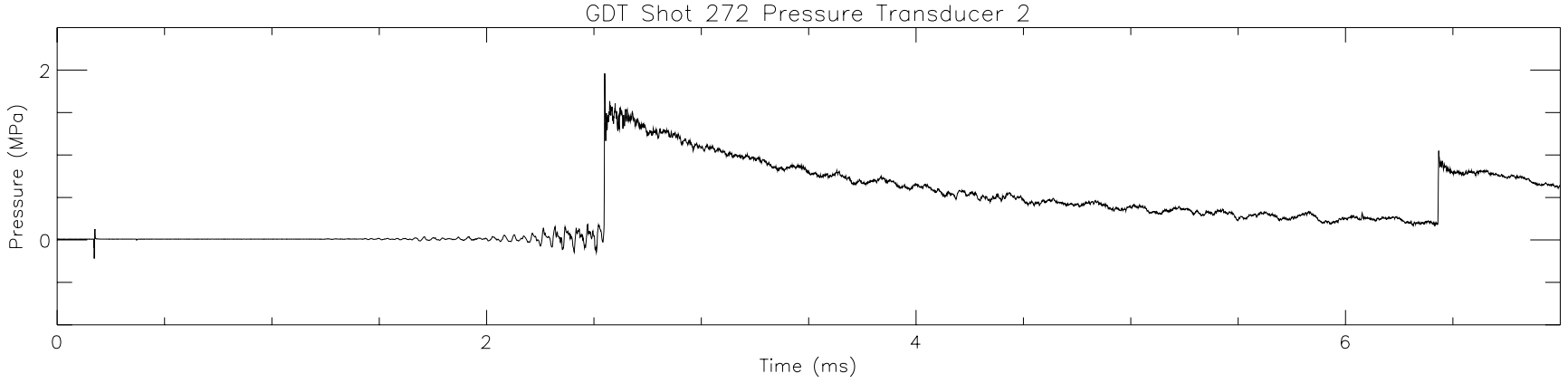
GDT Shot 272 Pressure Transducer 2
Pressure (MPa)
2
0
0
2
4
6
Time (ms)

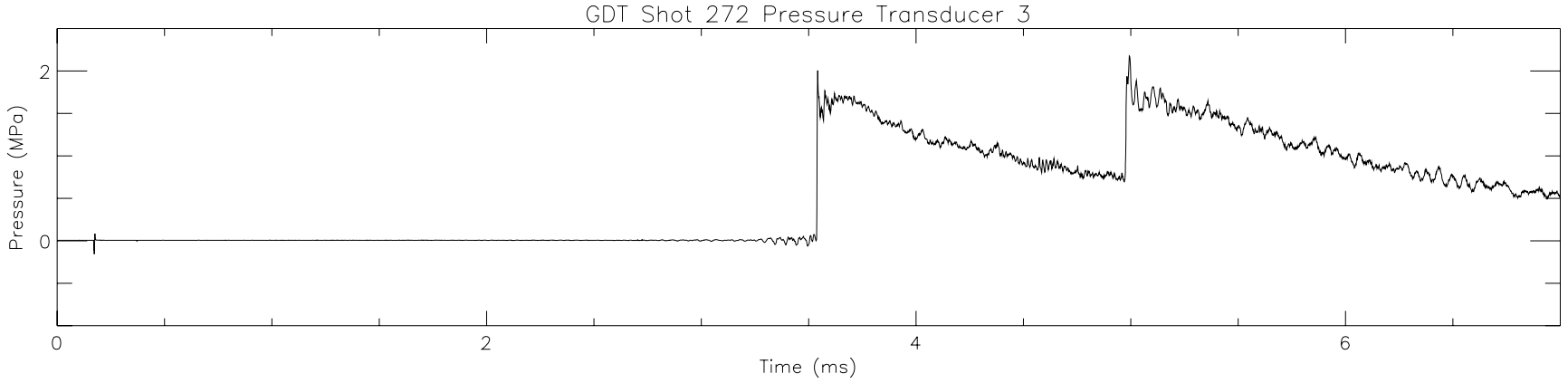
GDT Shot 272 Pressure Transducer 3
Pressure (MPa)
2
0
0
2
4
6
Time (ms)

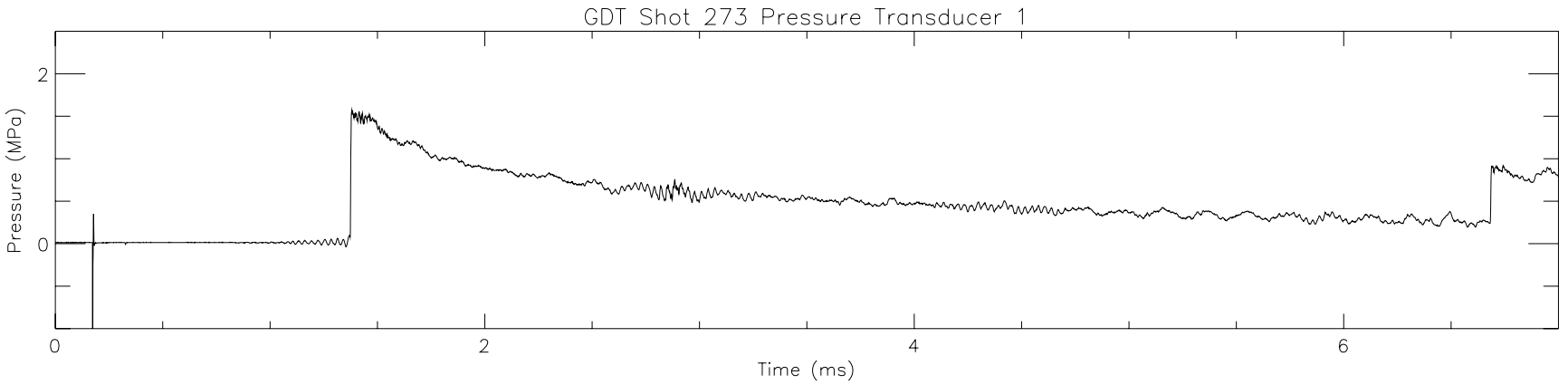
GDT Shot 273 Pressure Transducer 1
Pressure (MPa)
2
0
0
2
4
6
Time (ms)

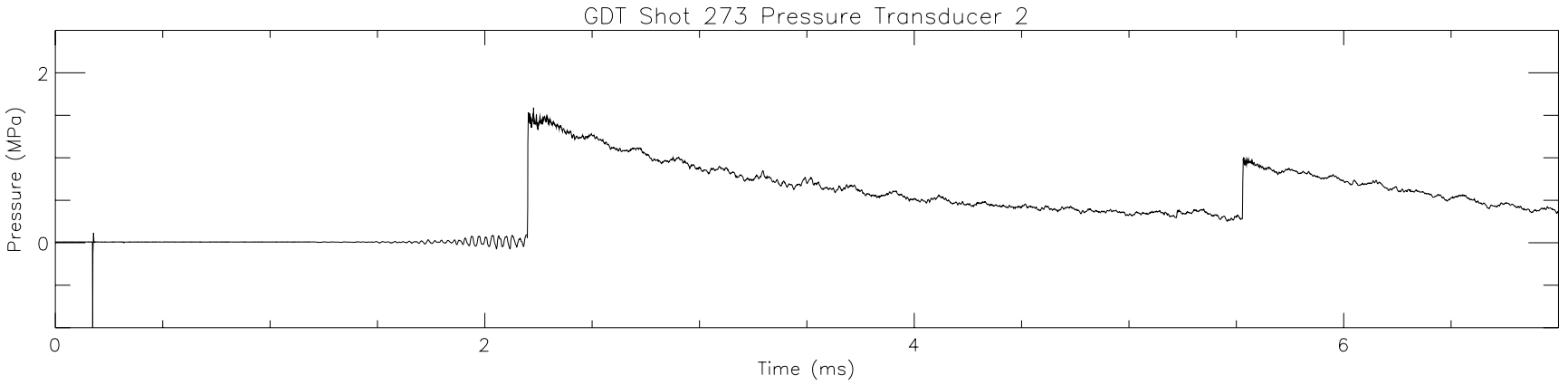
GDT Shot 273 Pressure Transducer 2
Pressure (MPa)
2
0
0
2
4
6
Time (ms)

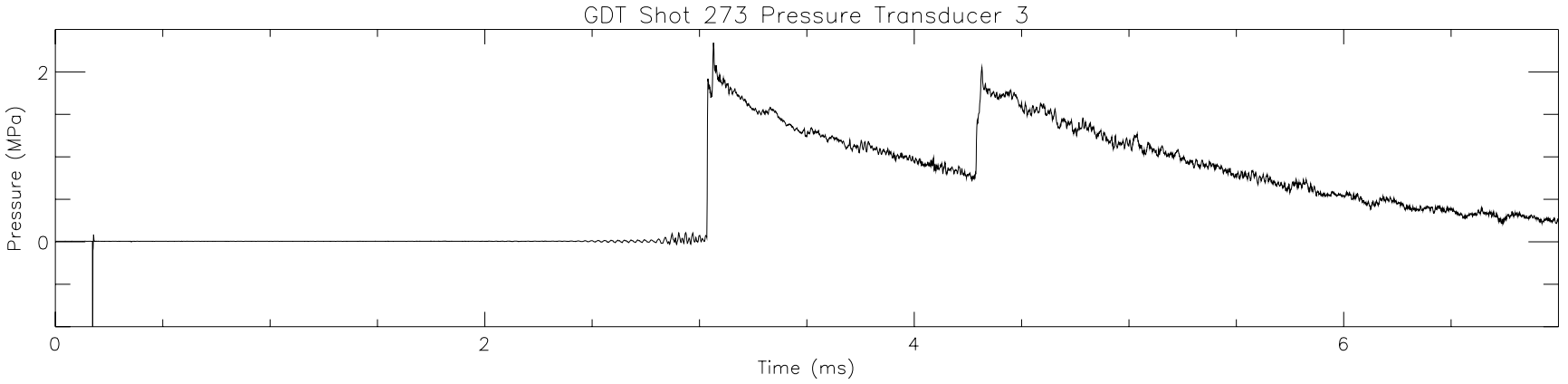
GDT Shot 273 Pressure Transducer 3
Pressure (MPa)
2
0
0
2
4
6
Time (ms)

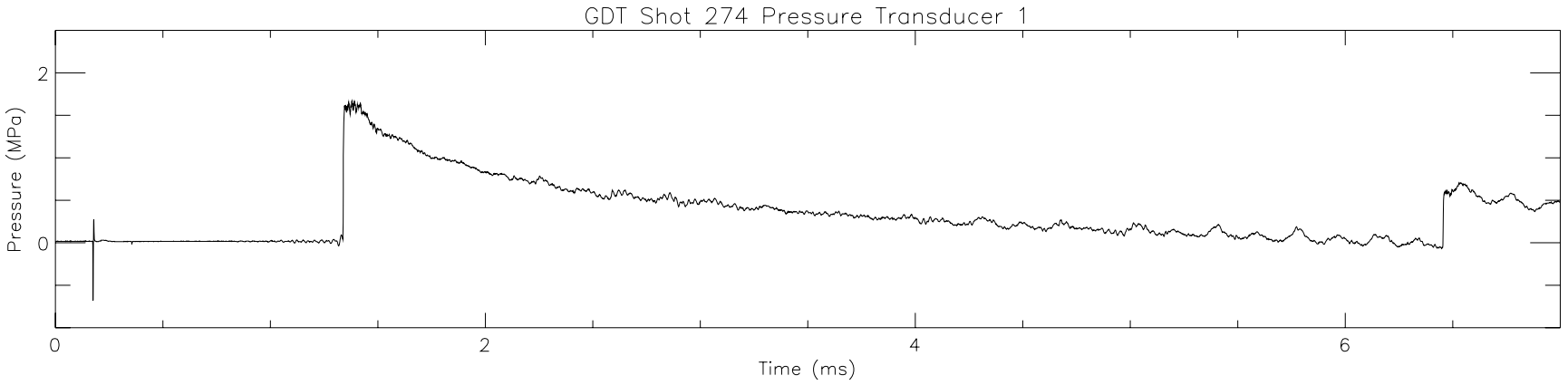
GDT Shot 274 Pressure Transducer 1
Pressure (MPa)
2
0
0
2
4
6
Time (ms)

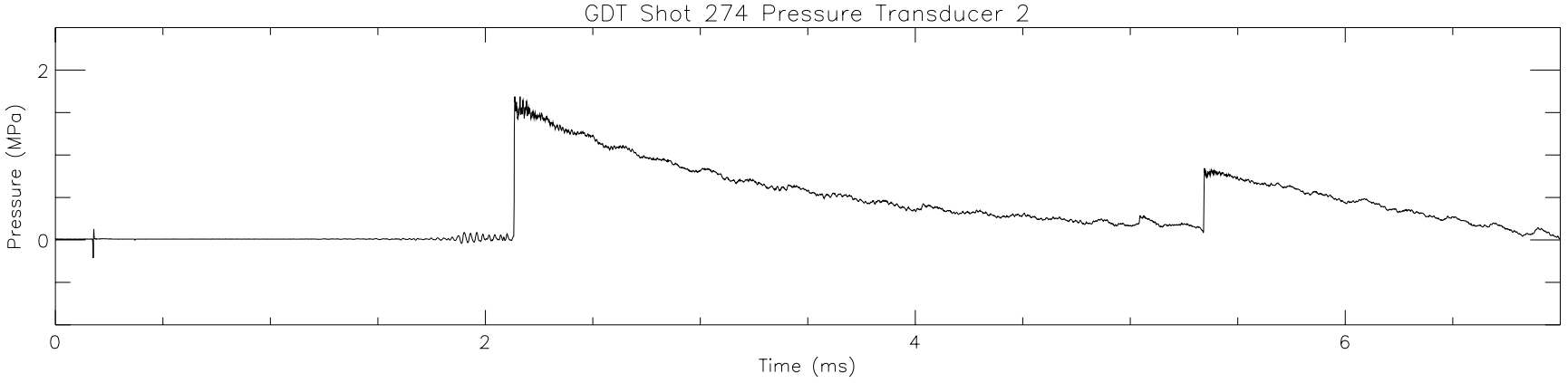
GDT Shot 274 Pressure Transducer 2
Pressure (MPa)
2
0
0
2
4
6
Time (ms)

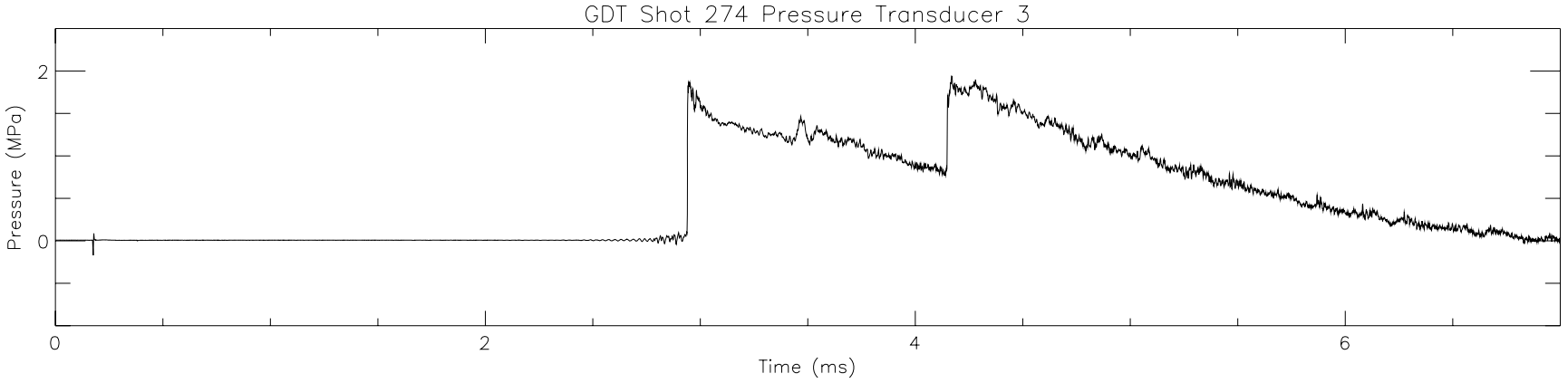
GDT Shot 274 Pressure Transducer 3
Pressure (MPa)
2
0
0
2
4
6
Time (ms)

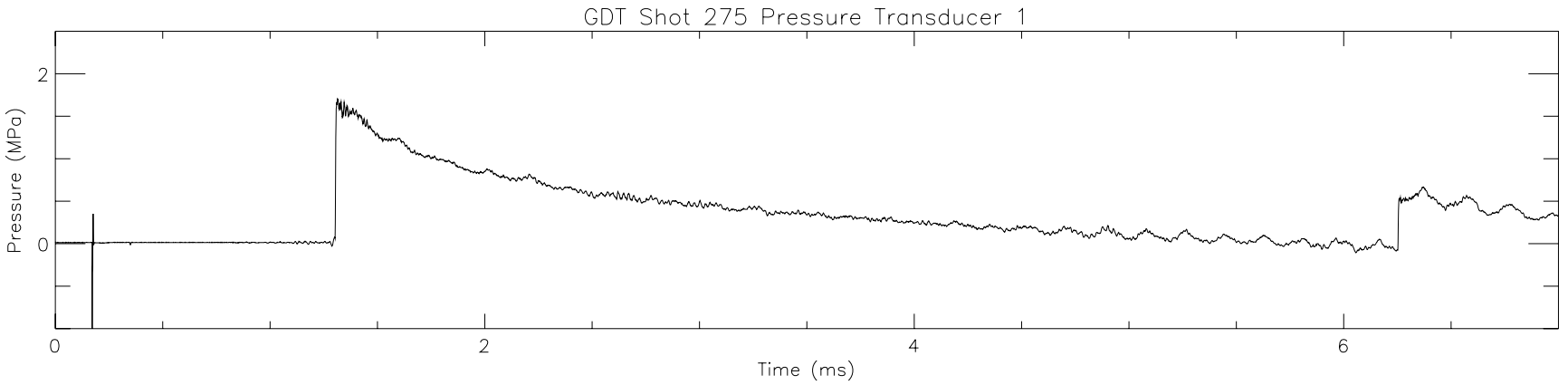
GDT Shot 275 Pressure Transducer 1
Pressure (MPa)
2
0
0
2
4
6
Time (ms)

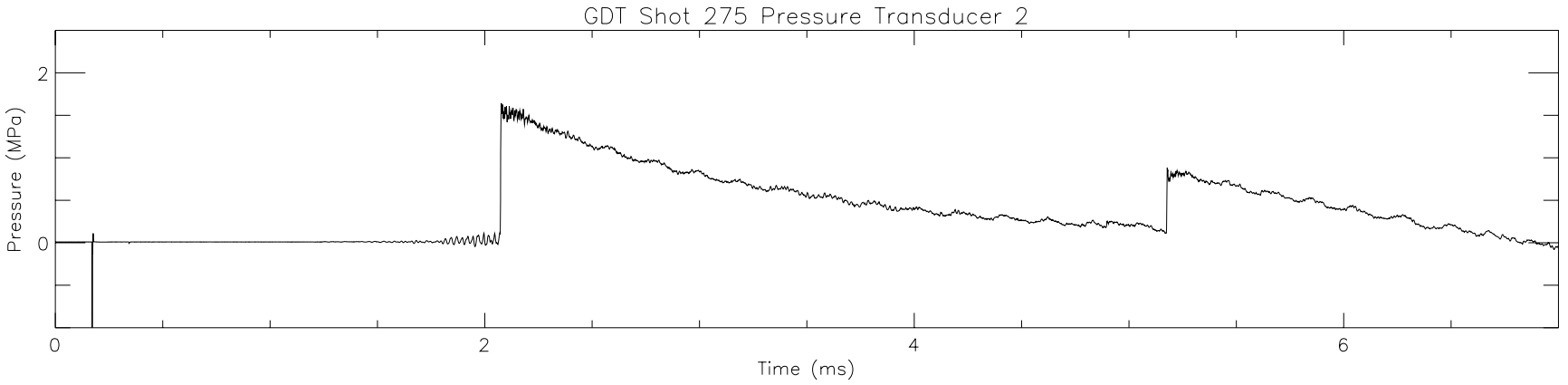
GDT Shot 275 Pressure Transducer 2
Pressure (MPa)
2
0
0
2
4
6
Time (ms)

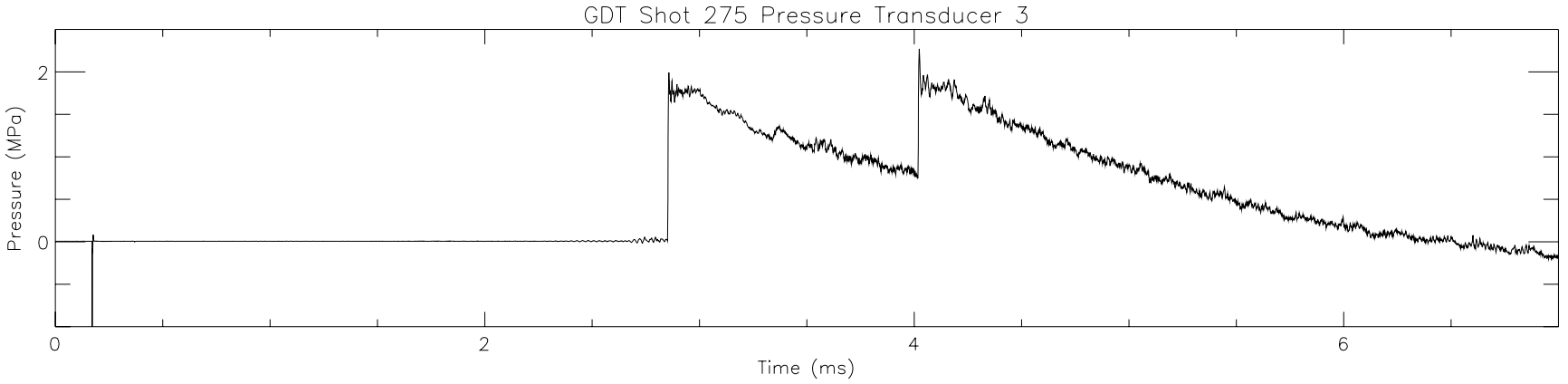
GDT Shot 275 Pressure Transducer 3
Pressure (MPa)
2
0
0
2
4
6
Time (ms)

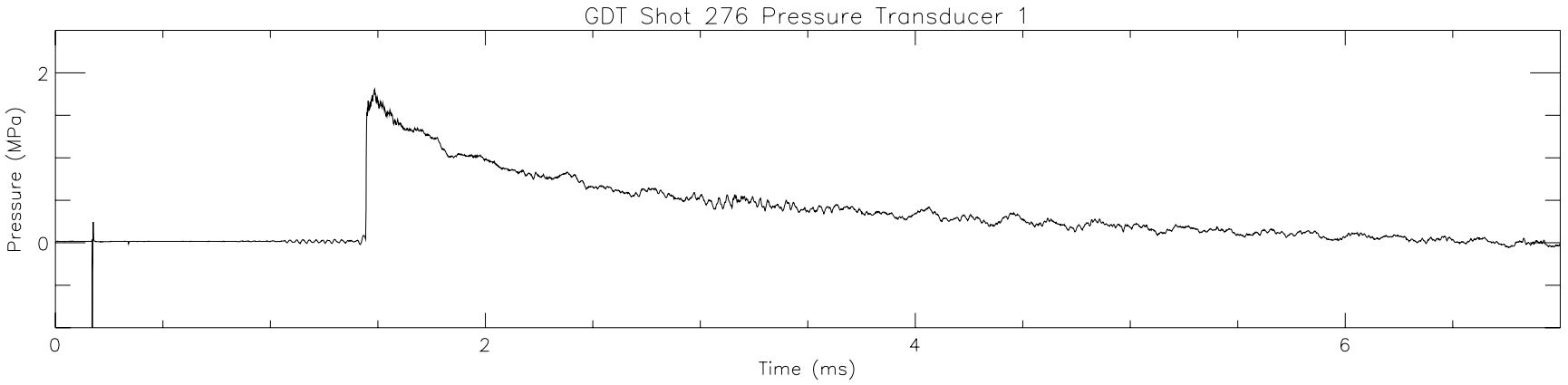
GDT Shot 276 Pressure Transducer 1
Pressure (MPa)
2
0
0
2
4
6
Time (ms)

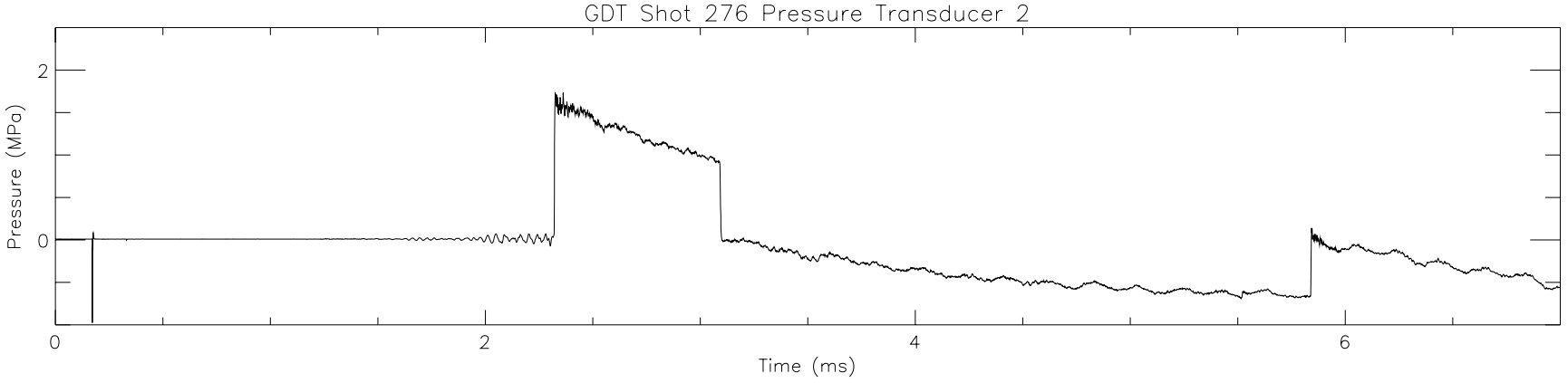
GDT Shot 276 Pressure Transducer 2
Pressure (MPa)
2
0
0
2
4
6
Time (ms)

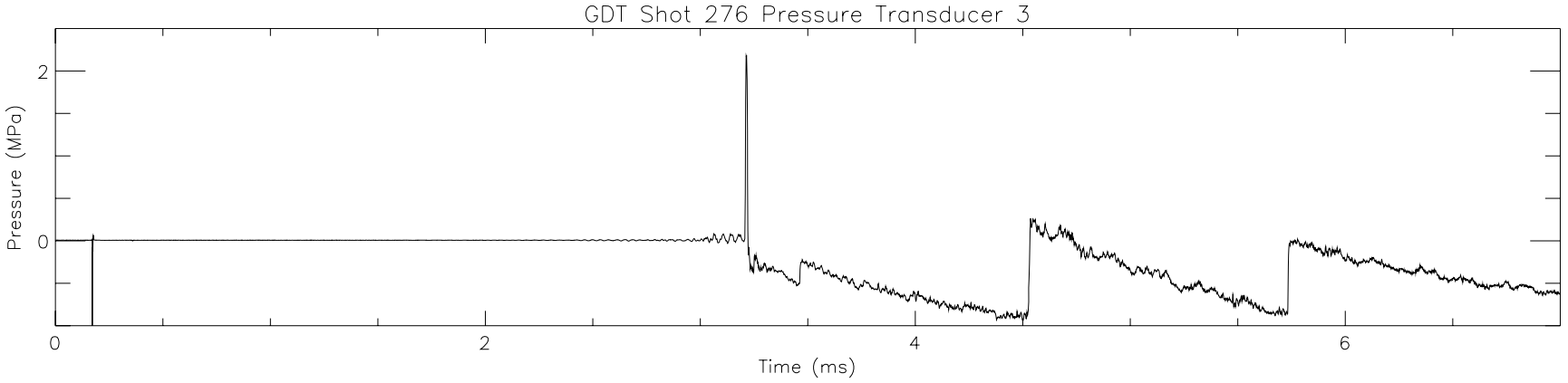
GDT Shot 276 Pressure Transducer 3
Pressure (MPa)
2
0
0
2
4
6
Time (ms)

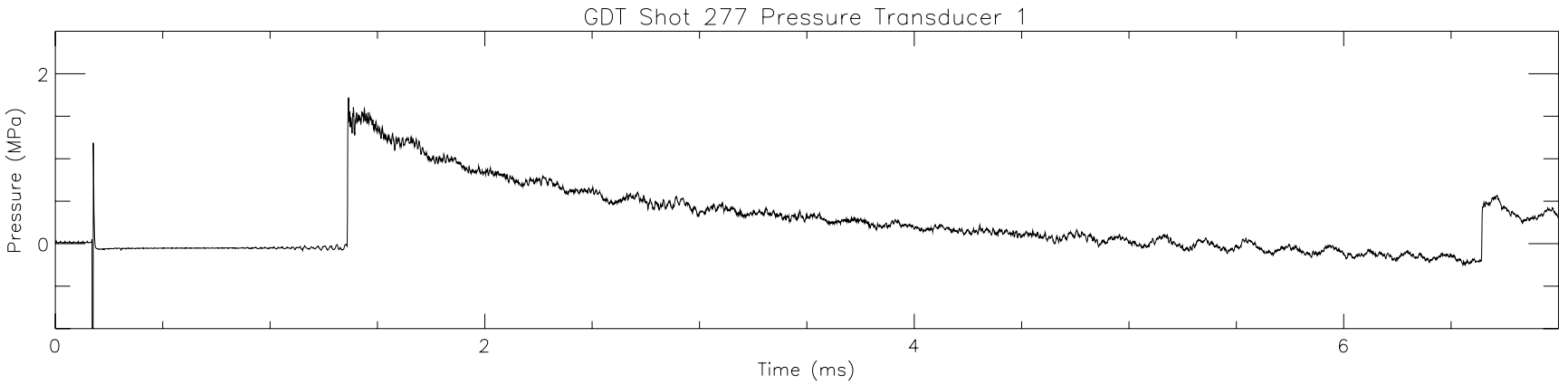
GDT Shot 277 Pressure Transducer 1
Pressure (MPa)
2
0
0
2
4
6
Time (ms)

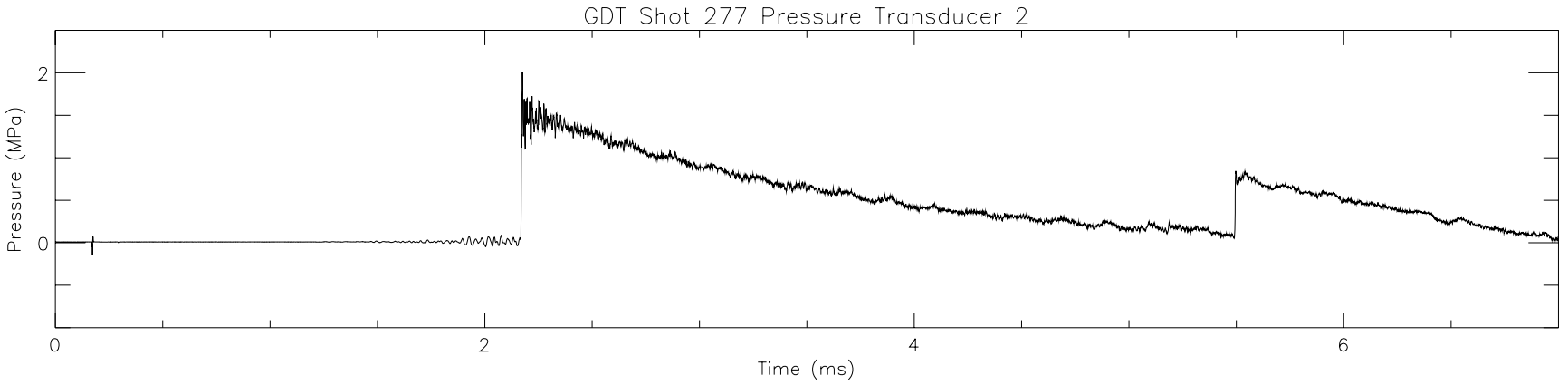
GDT Shot 277 Pressure Transducer 2
Pressure (MPa)
2
0
0
2
4
6
Time (ms)

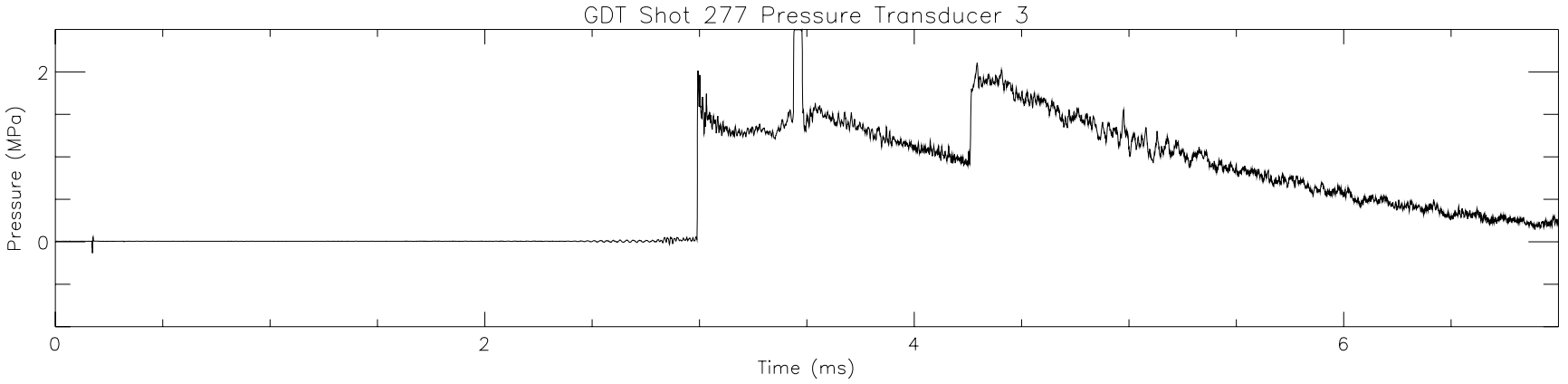
GDT Shot 277 Pressure Transducer 3
Pressure (MPa)
2
0
0
2
4
6
Time (ms)

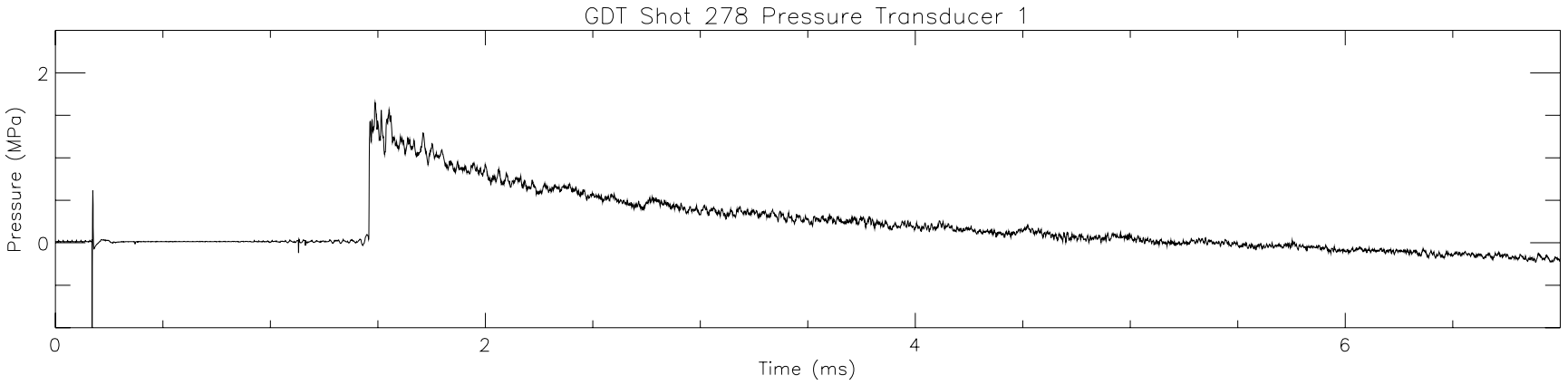
GDT Shot 278 Pressure Transducer 1
Pressure (MPa)
2
0
0
2
4
6
Time (ms)

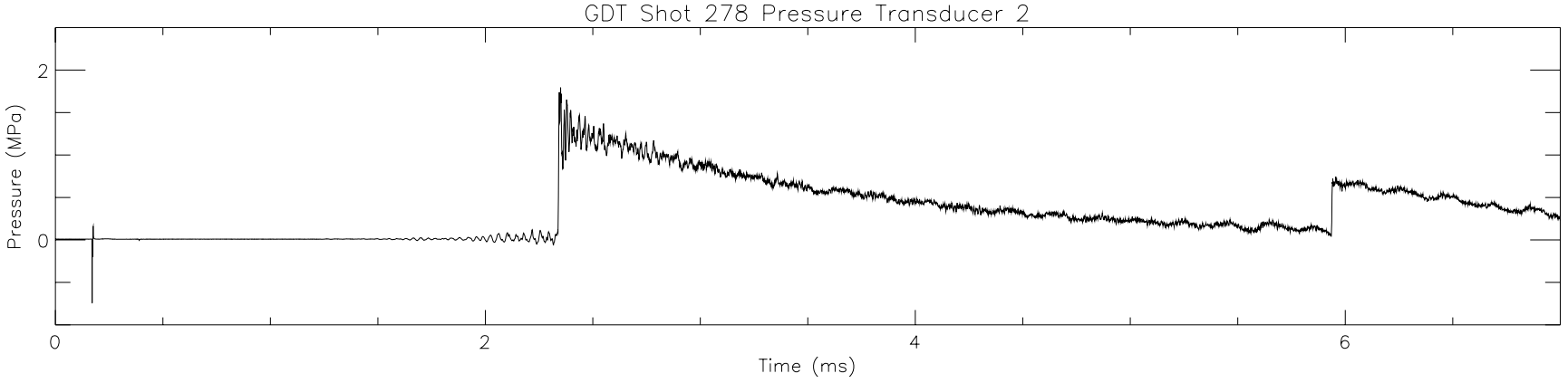
GDT Shot 278 Pressure Transducer 2
Pressure (MPa)
2
0
0
2
4
6
Time (ms)

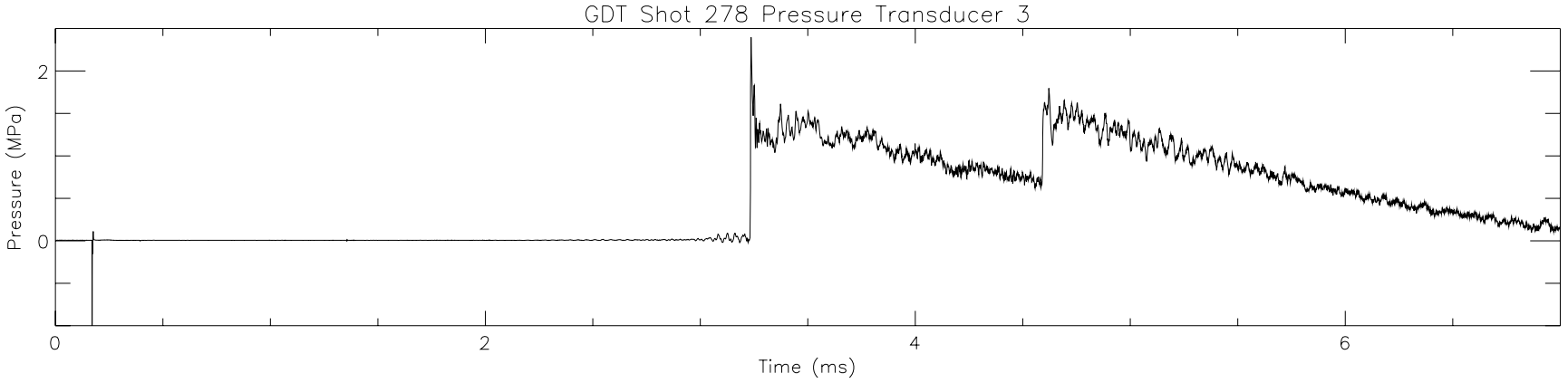
GDT Shot 278 Pressure Transducer 3
Pressure (MPa)
2
0
0
2
4
6
Time (ms)

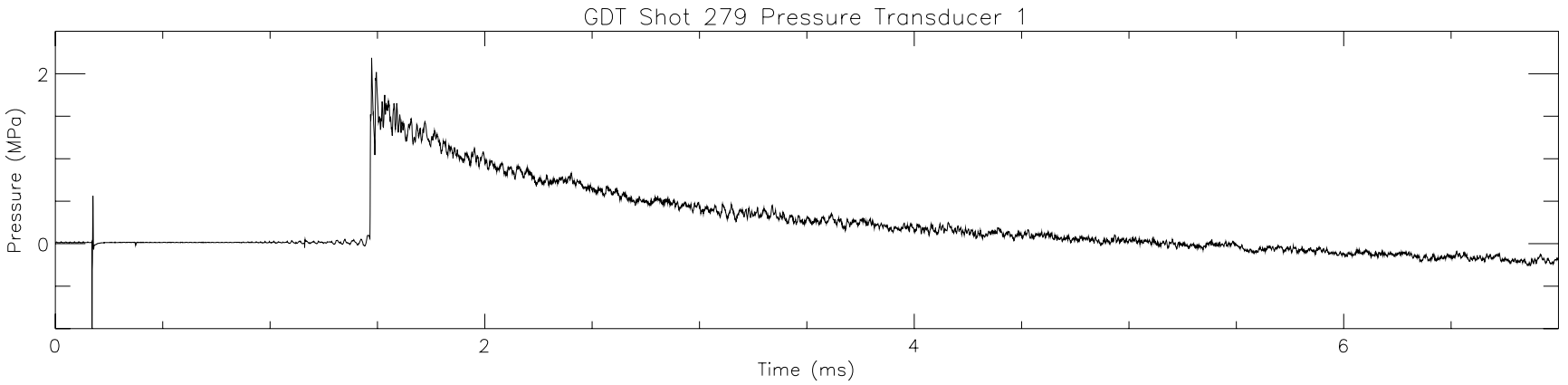
GDT Shot 279 Pressure Transducer 1
Pressure (MPa)
2
0
0
2
4
6
Time (ms)

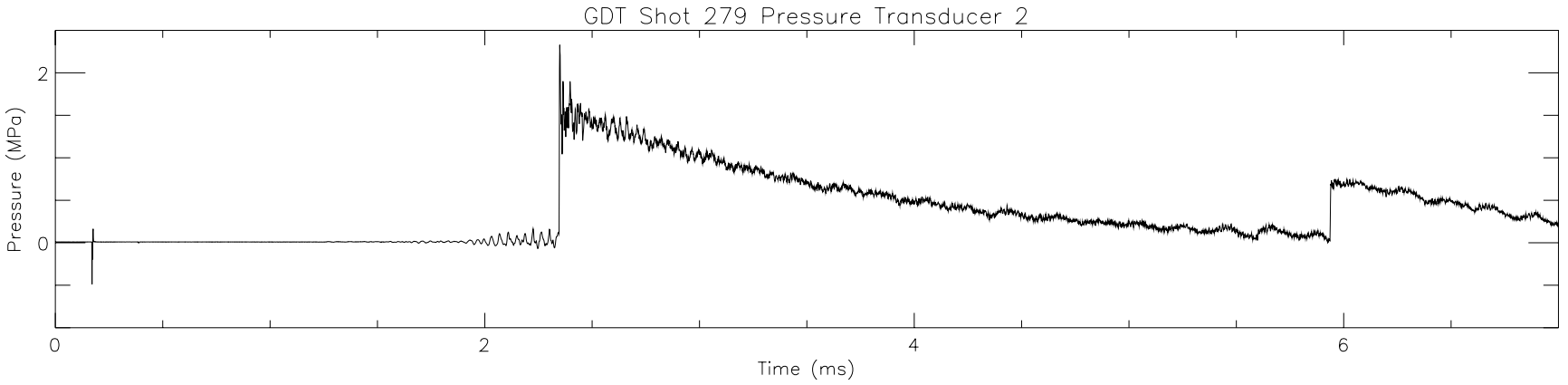
GDT Shot 279 Pressure Transducer 2
Pressure (MPa)
2
0
0
2
4
6
Time (ms)

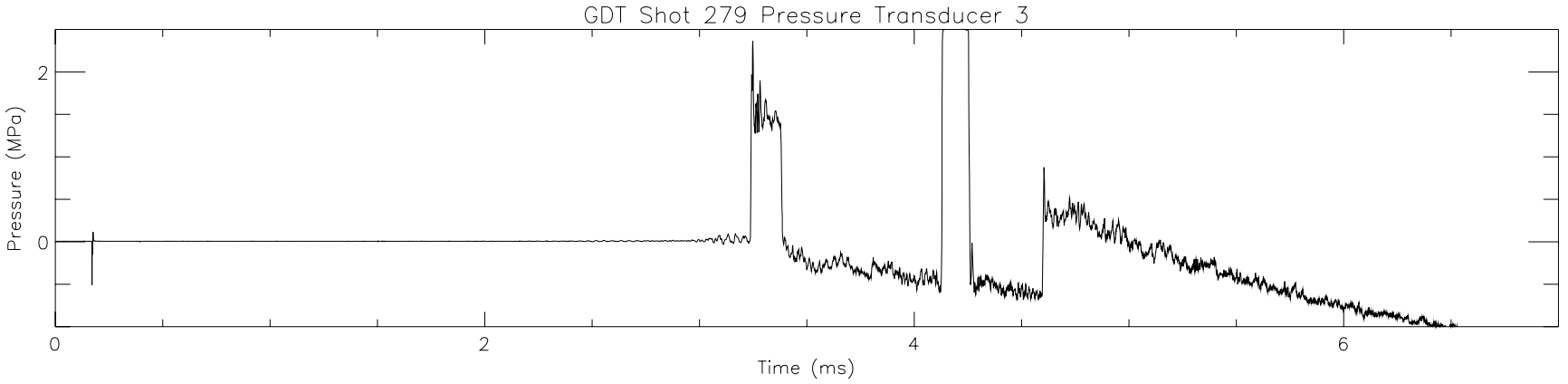
GDT Shot 279 Pressure Transducer 3
Pressure (MPa)
2
0
0
2
4
6
Time (ms)

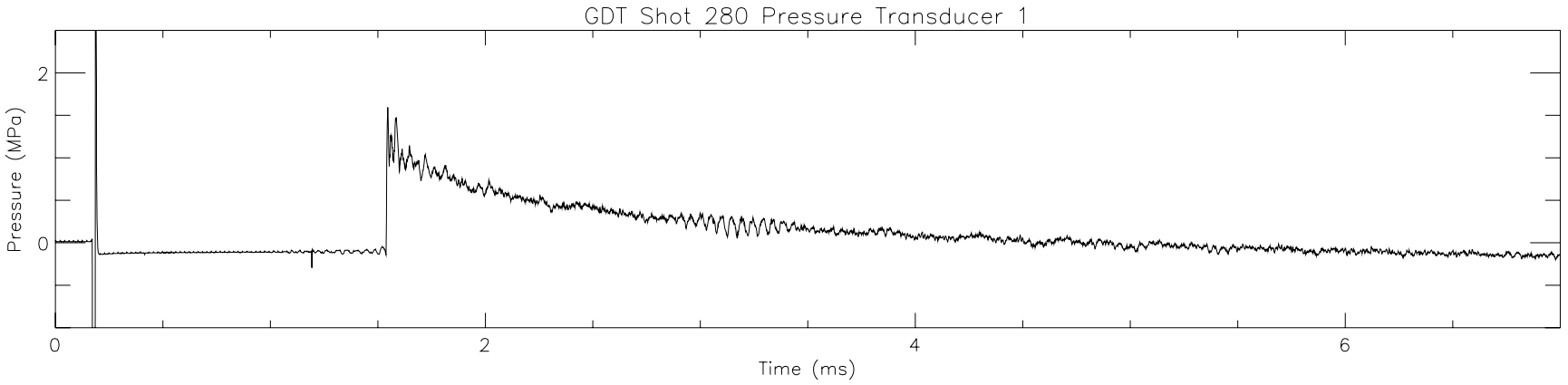
GDT Shot 280 Pressure Transducer 1
Pressure (MPa)
2
0
0
2
4
6
Time (ms)

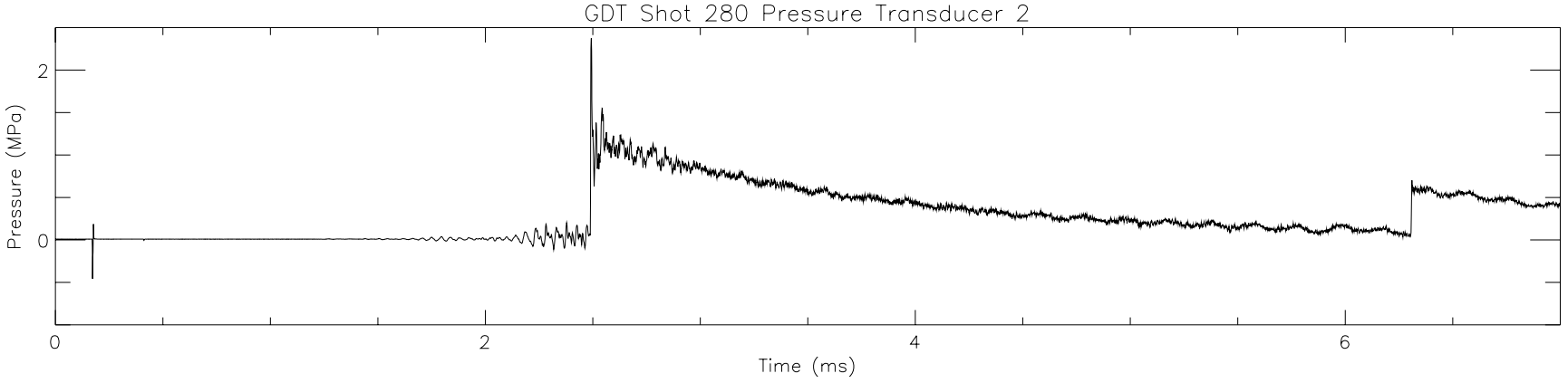
GDT Shot 280 Pressure Transducer 2
Pressure (MPa)
2
0
0
2
4
6
Time (ms)

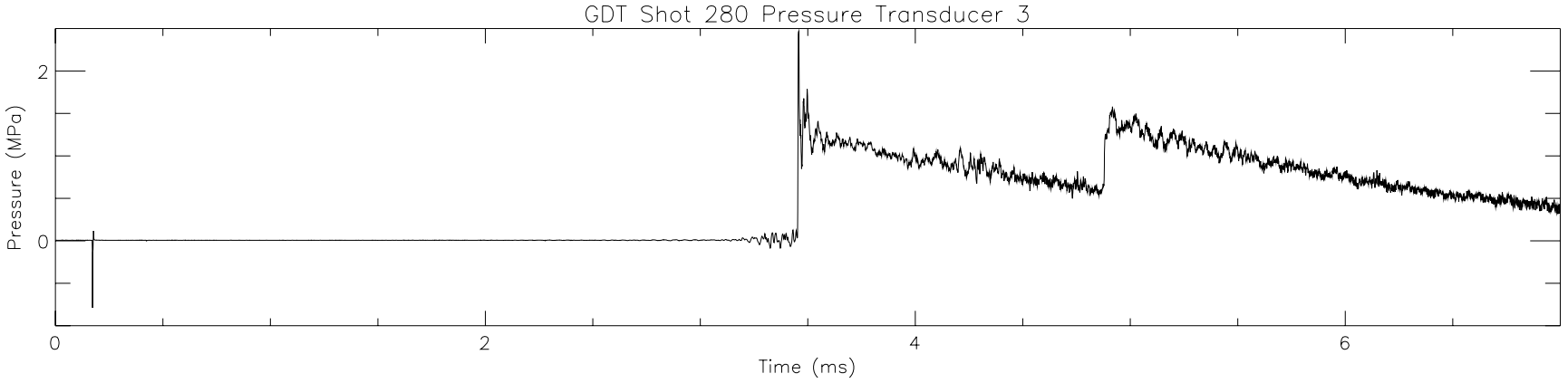
GDT Shot 280 Pressure Transducer 3
Pressure (MPa)
2
0
0
2
4
6
Time (ms)

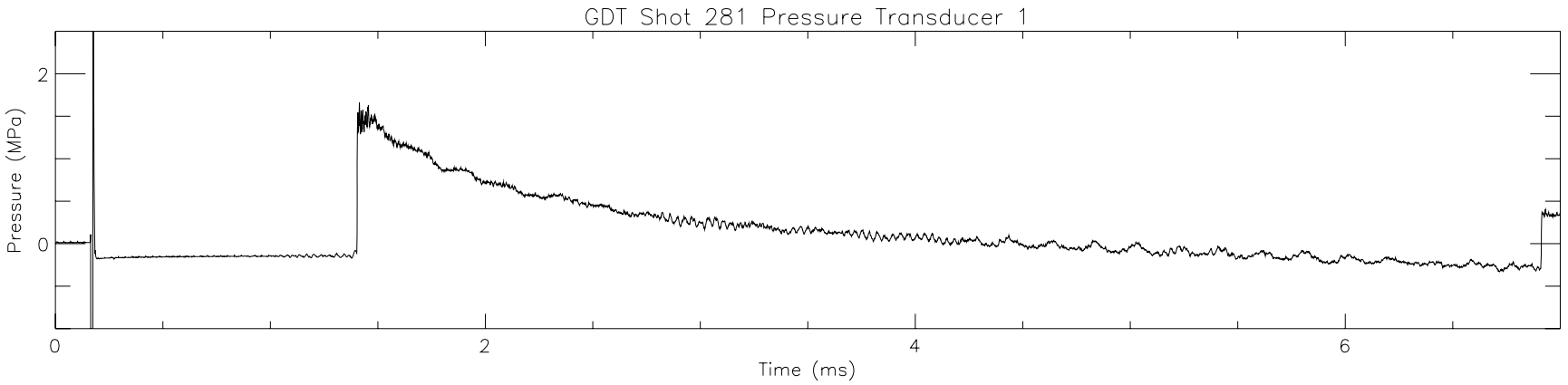
GDT Shot 281 Pressure Transducer 1
Pressure (MPa)
2
0
0
2
4
6
Time (ms)

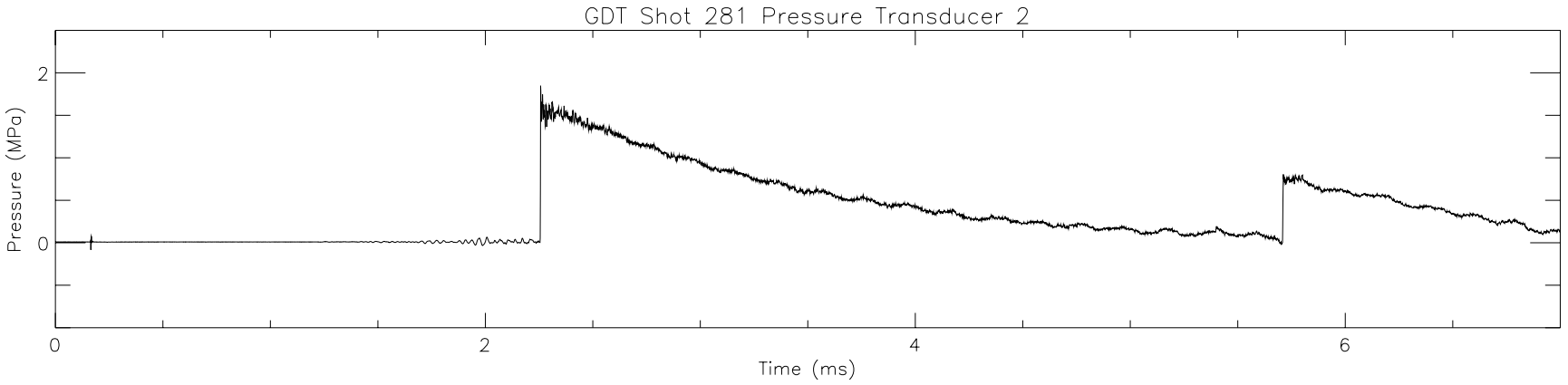
GDT Shot 281 Pressure Transducer 2
Pressure (MPa)
2
0
0
2
4
6
Time (ms)

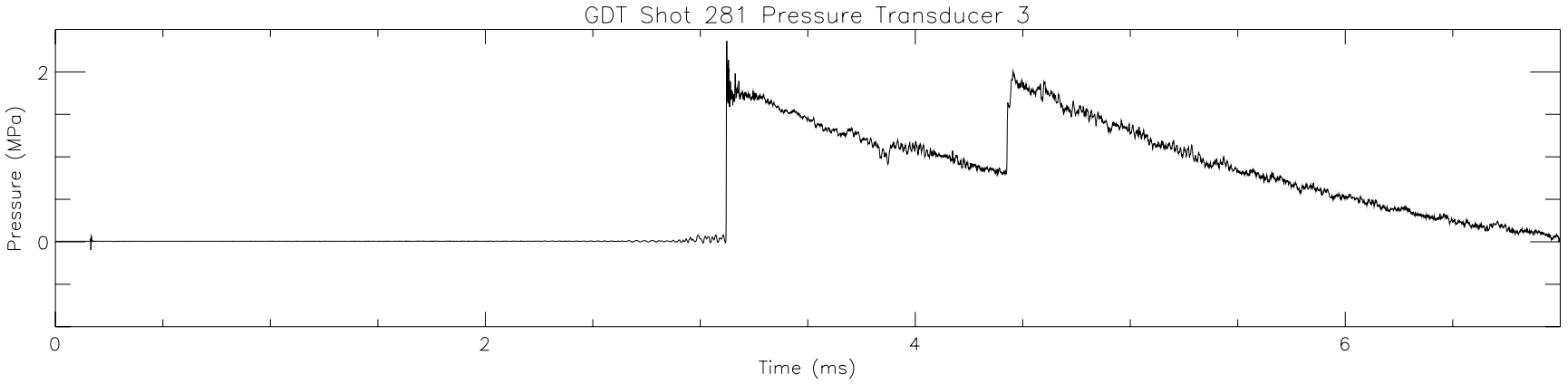
GDT Shot 281 Pressure Transducer 3
Pressure (MPa)
2
0
0
2
4
6
Time (ms)

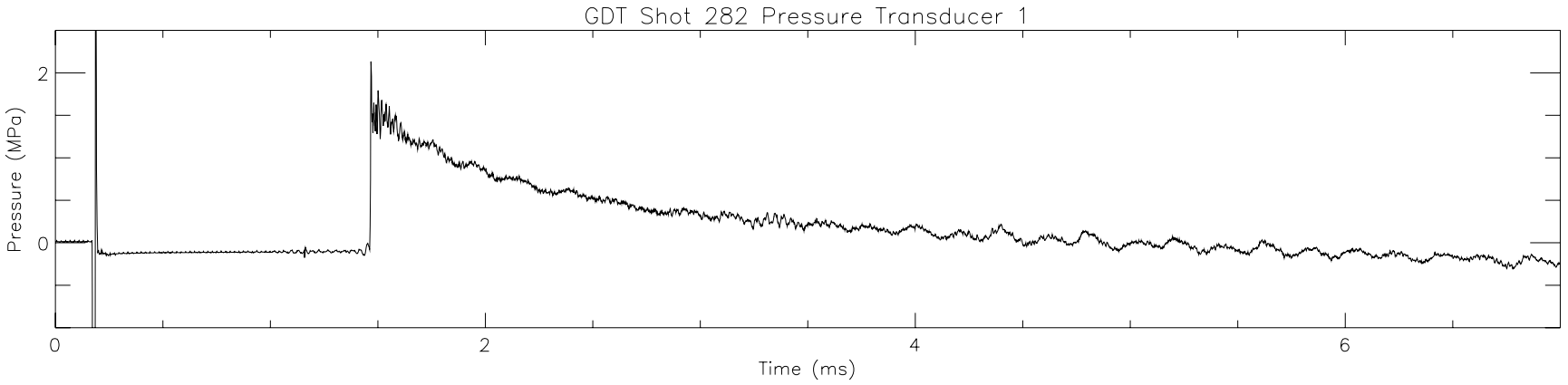
GDT Shot 282 Pressure Transducer 1
Pressure (MPa)
2
0
0
2
4
6
Time (ms)

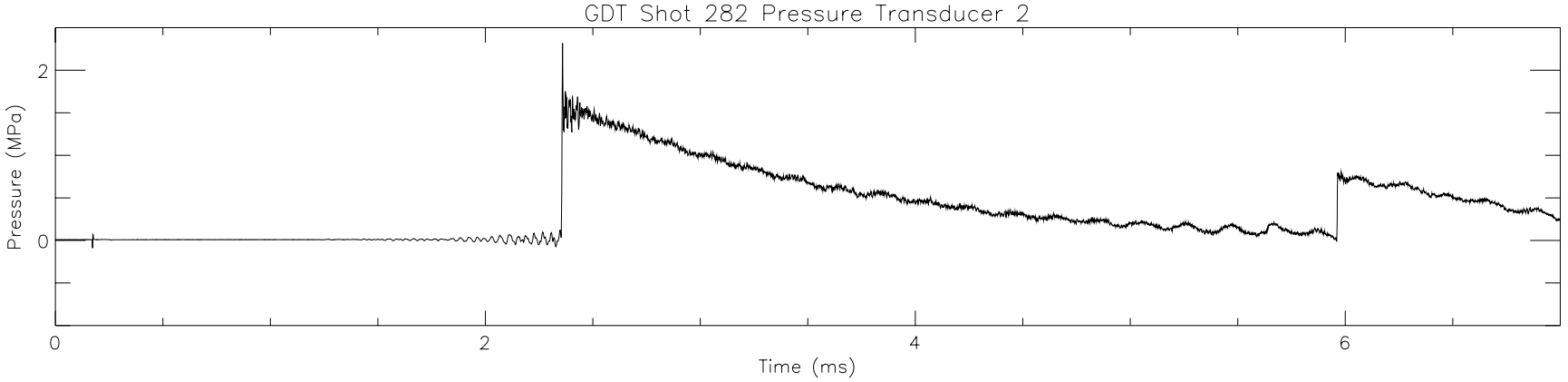
GDT Shot 282 Pressure Transducer 2
Pressure (MPa)
2
0
0
2
4
6
Time (ms)

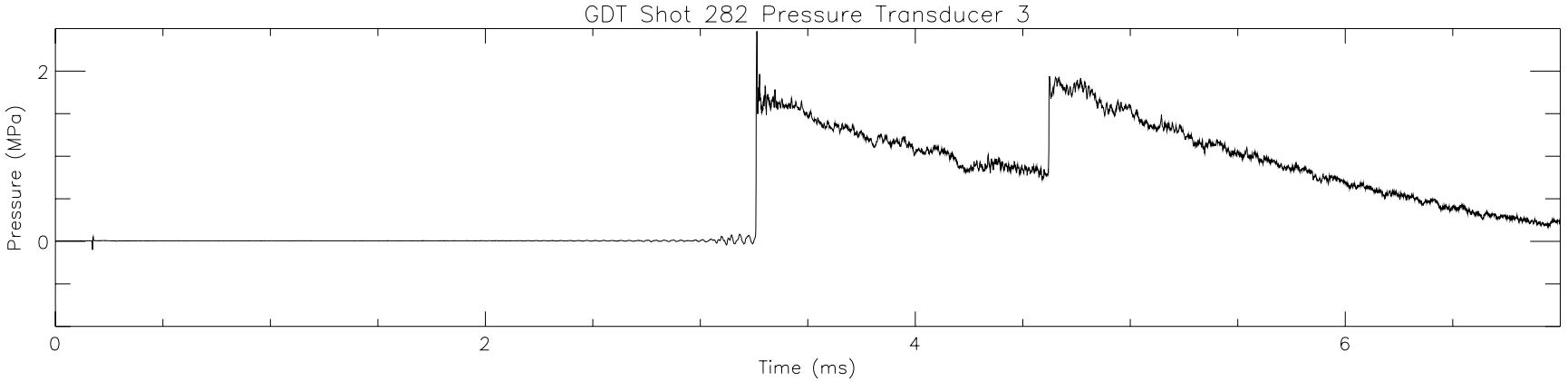
GDT Shot 282 Pressure Transducer 3
Pressure (MPa)
2
0
0
2
4
6
Time (ms)

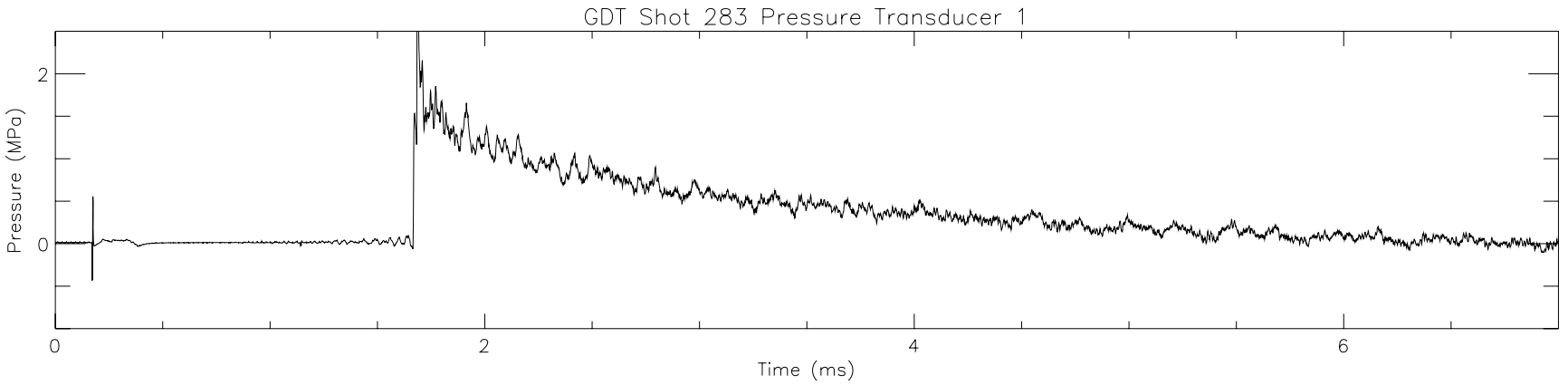
GDT Shot 283 Pressure Transducer 1
Pressure (MPa)
2
0
0
2
4
6
Time (ms)

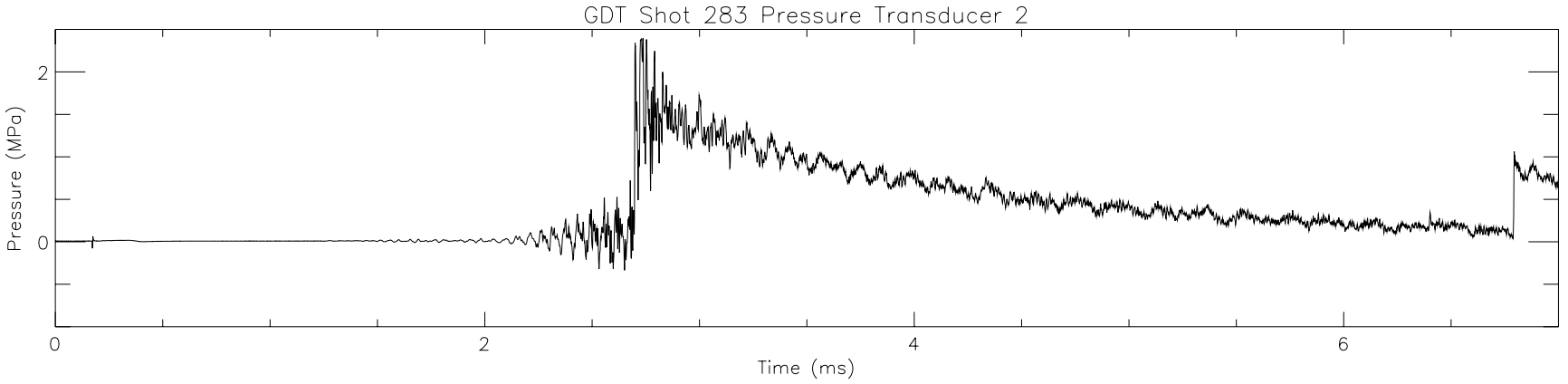
GDT Shot 283 Pressure Transducer 2
Pressure (MPa)
2
0
0
2
4
6
Time (ms)

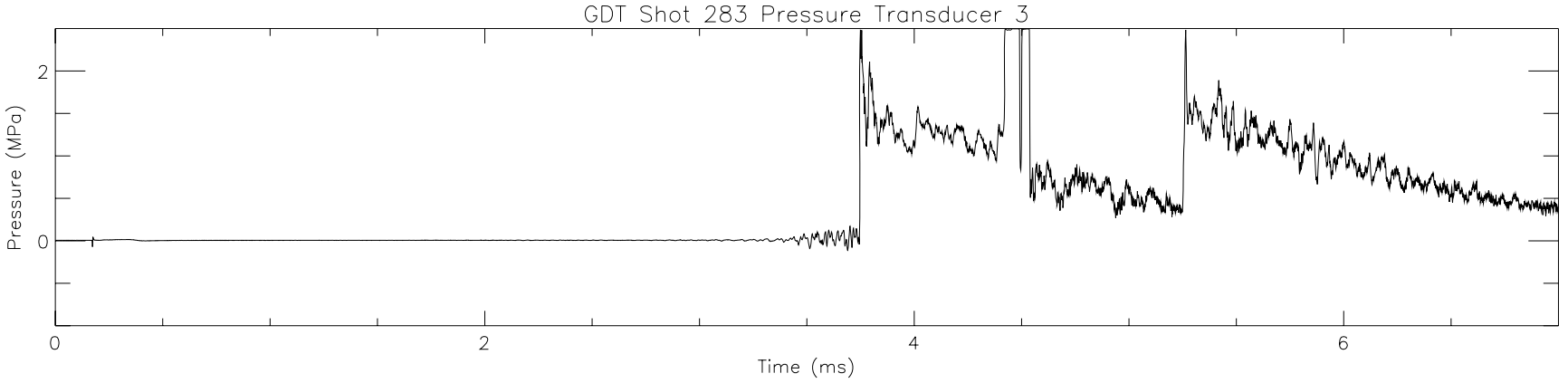
GDT Shot 283 Pressure Transducer 3
Pressure (MPa)
2
0
0
2
4
6
Time (ms)

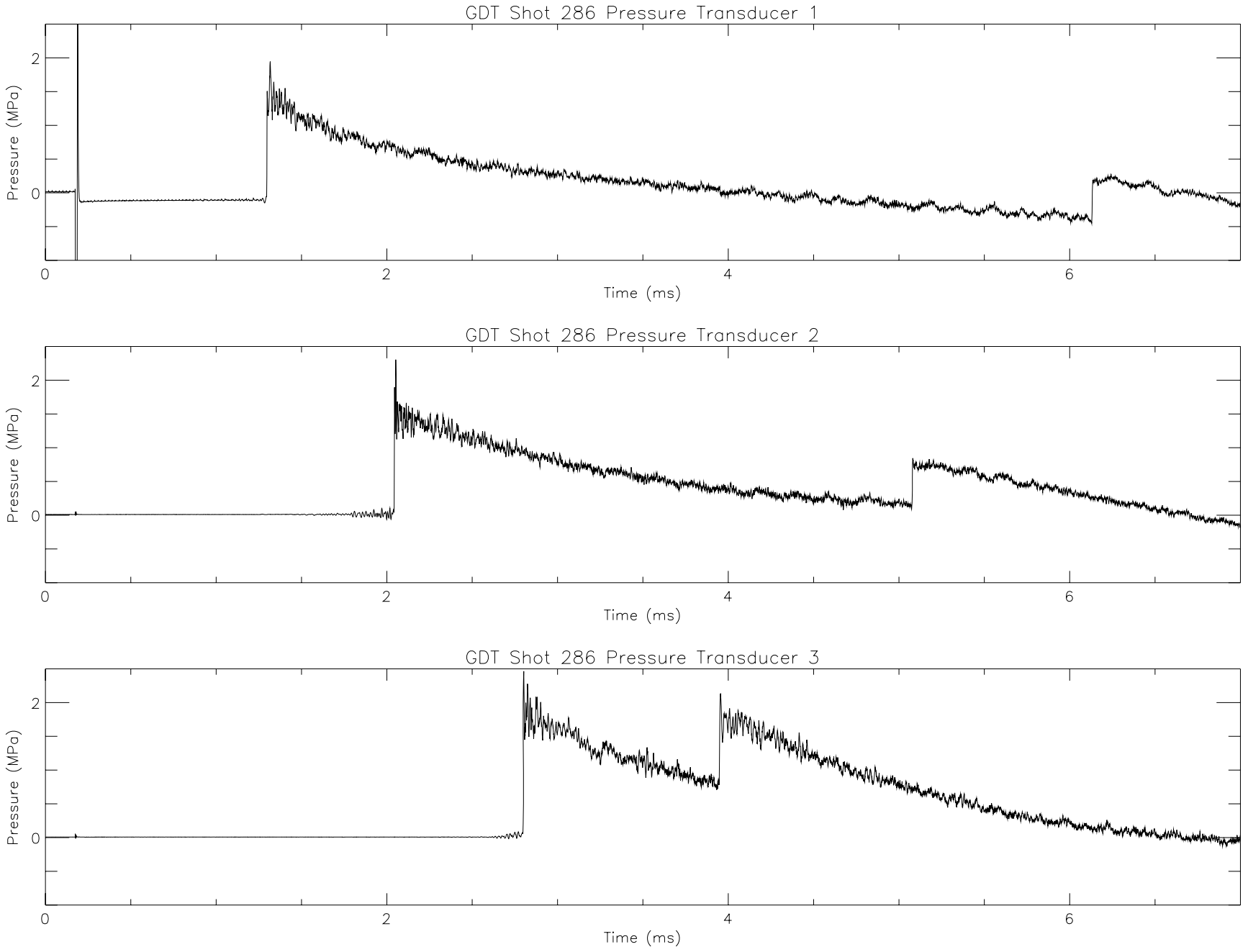
GDT Shot 286 Pressure Transducer 1
Pressure (MPa)
2
0
0
2
4
6
Time (ms)
GDT Shot 286 Pressure Transducer 2
Pressure (MPa)
2
0
0
2
4
6
Time (ms)
GDT Shot 286 Pressure Transducer 3
Pressure (MPa)
2
0
0
2
4
6
Time (ms)

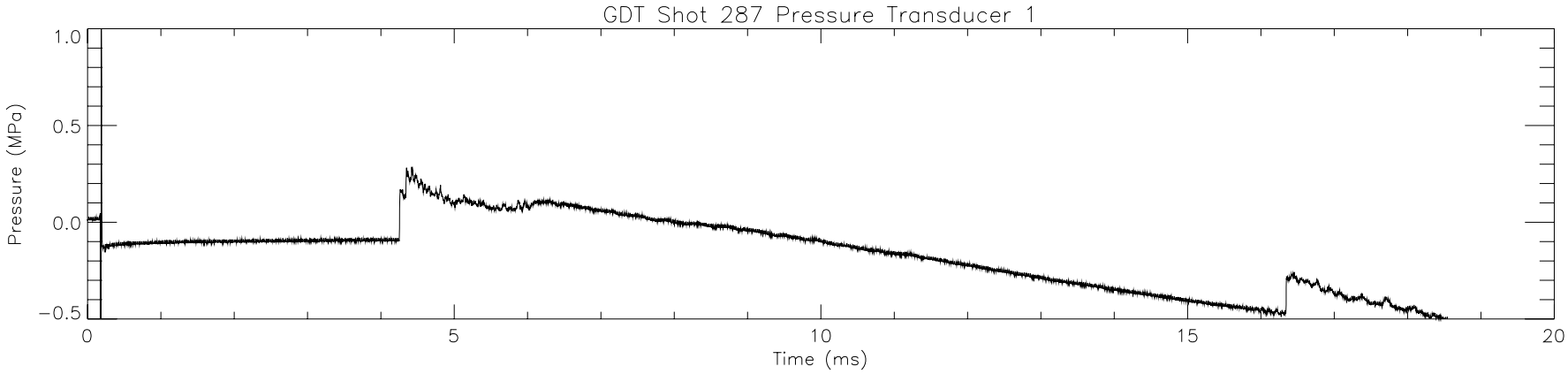
GDT Shot 287 Pressure Transducer 1
Pressure (MPa)
1.0
0.5
0.0
−0.5
0
5
10
15
20
Time (ms)

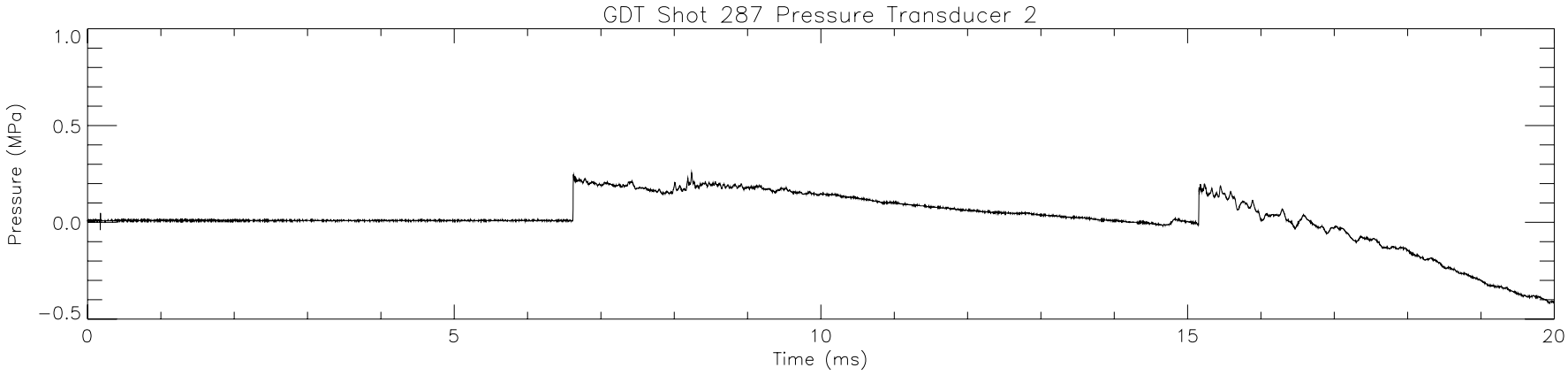
GDT Shot 287 Pressure Transducer 2
Pressure (MPa)
1.0
0.5
0.0
−0.5
0
5
10
15
20
Time (ms)

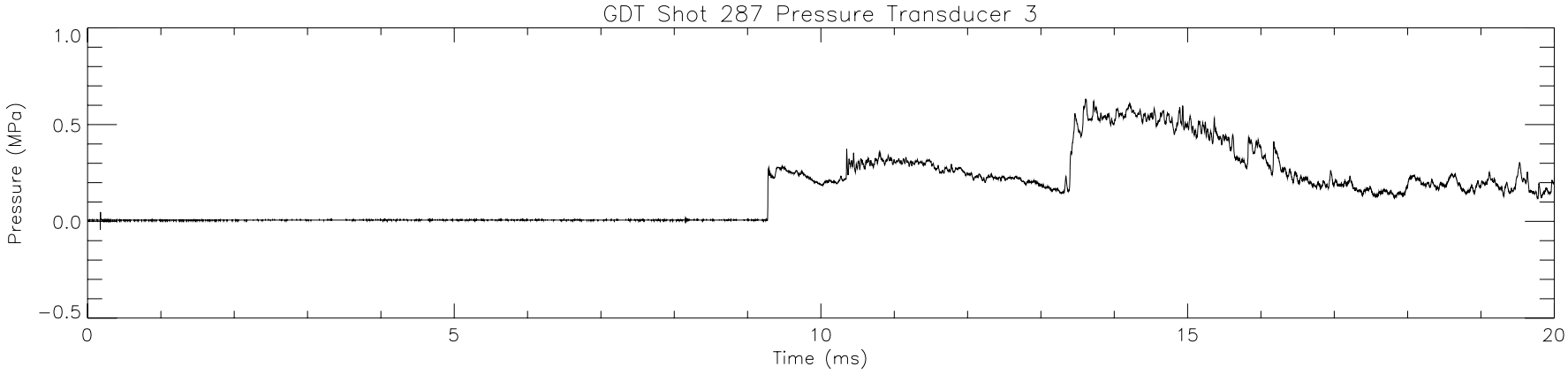
GDT Shot 287 Pressure Transducer 3
Pressure (MPa)
1.0
0.5
0.0
−0.5
0
5
10
15
20
Time (ms)

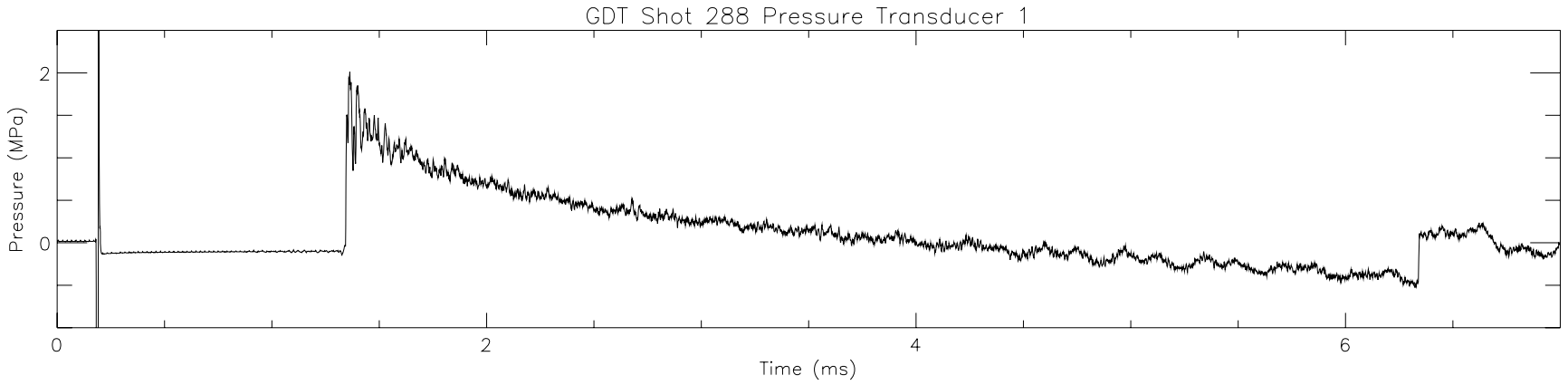
GDT Shot 288 Pressure Transducer 1
Pressure (MPa)
2
0
0
2
4
6
Time (ms)

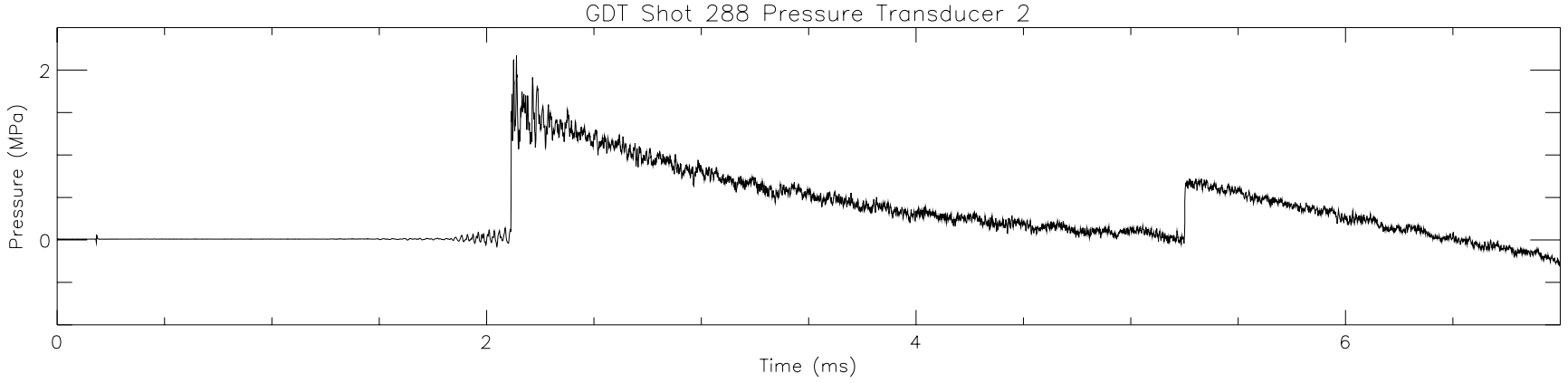
GDT Shot 288 Pressure Transducer 2
Pressure (MPa)
2
0
0
2
4
6
Time (ms)

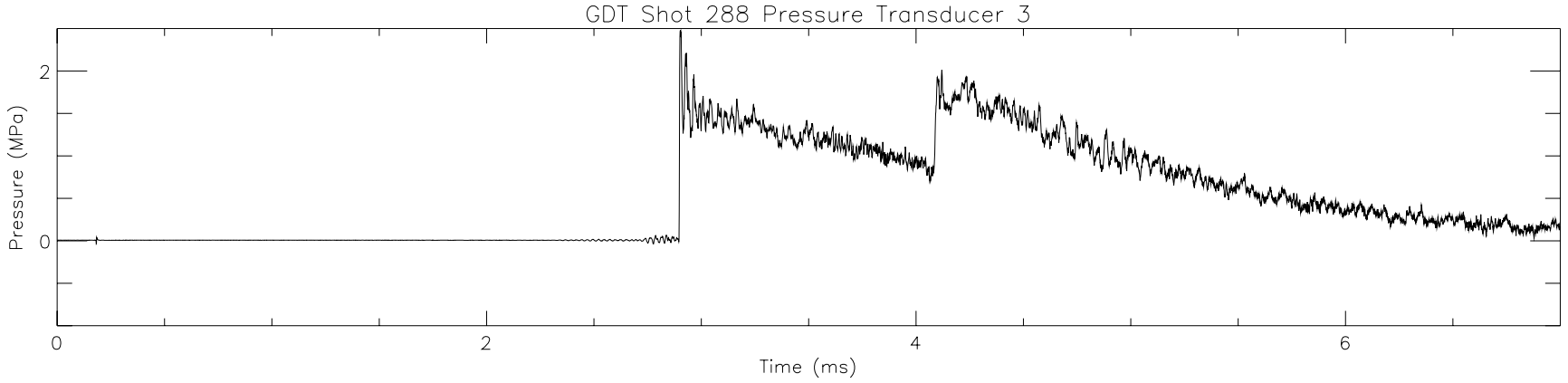
GDT Shot 288 Pressure Transducer 3
Pressure (MPa)
2
0
0
2
4
6
Time (ms)

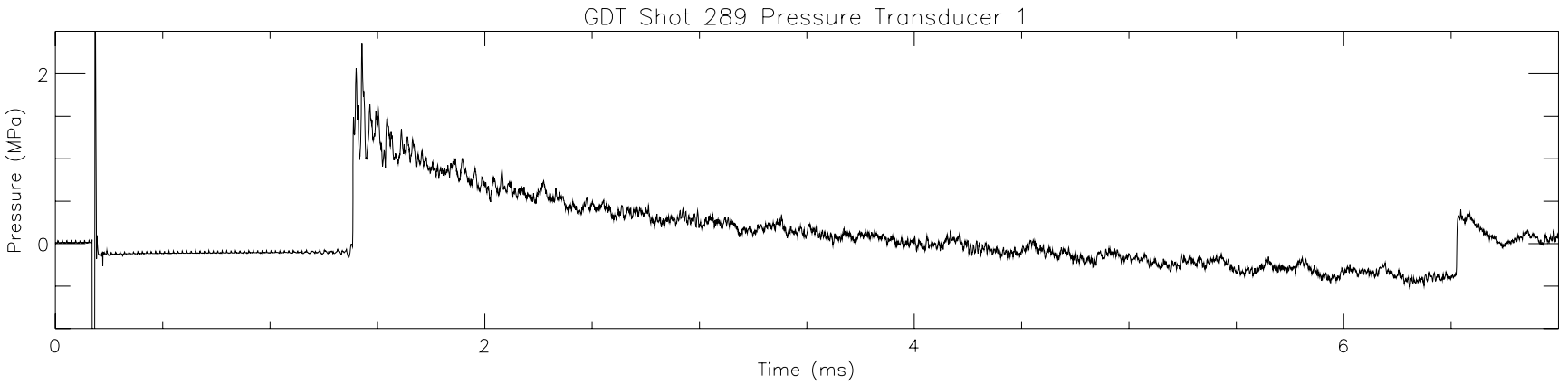
GDT Shot 289 Pressure Transducer 1
Pressure (MPa)
2
0
0
2
4
6
Time (ms)

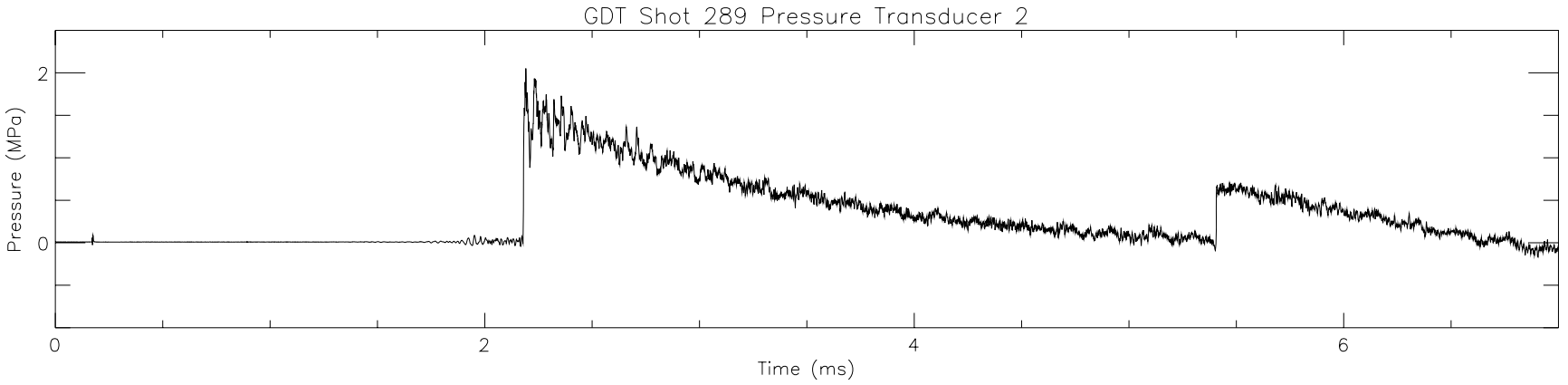
GDT Shot 289 Pressure Transducer 2
Pressure (MPa)
2
0
0
2
4
6
Time (ms)

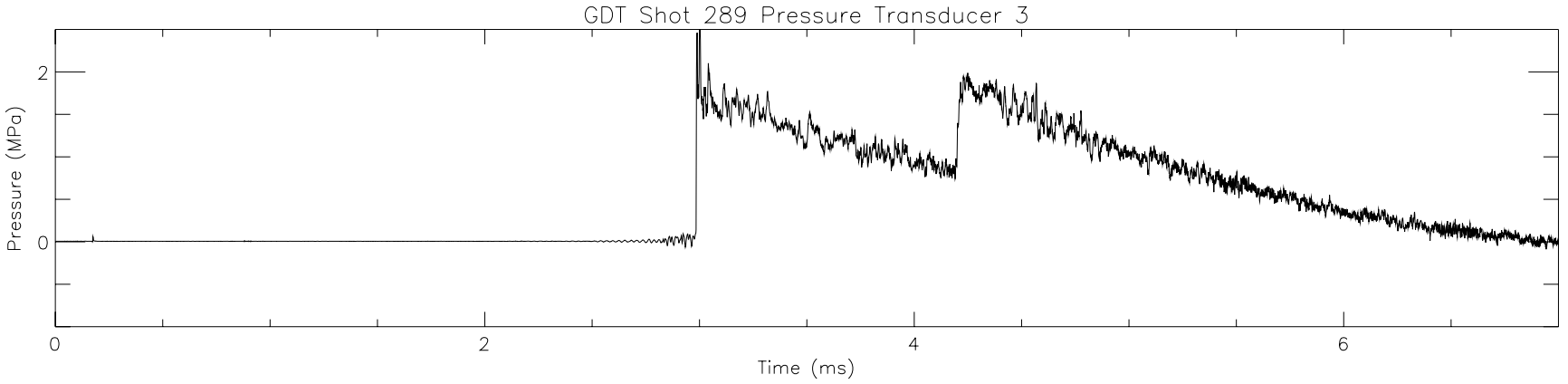
GDT Shot 289 Pressure Transducer 3
Pressure (MPa)
2
0
0
2
4
6
Time (ms)

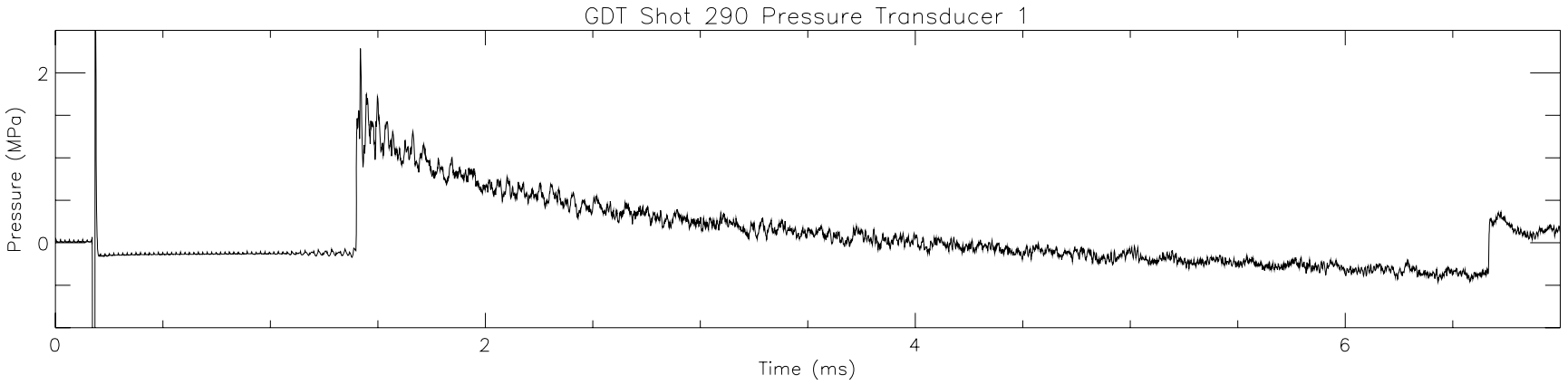
GDT Shot 290 Pressure Transducer 1
Pressure (MPa)
2
0
0
2
4
6
Time (ms)

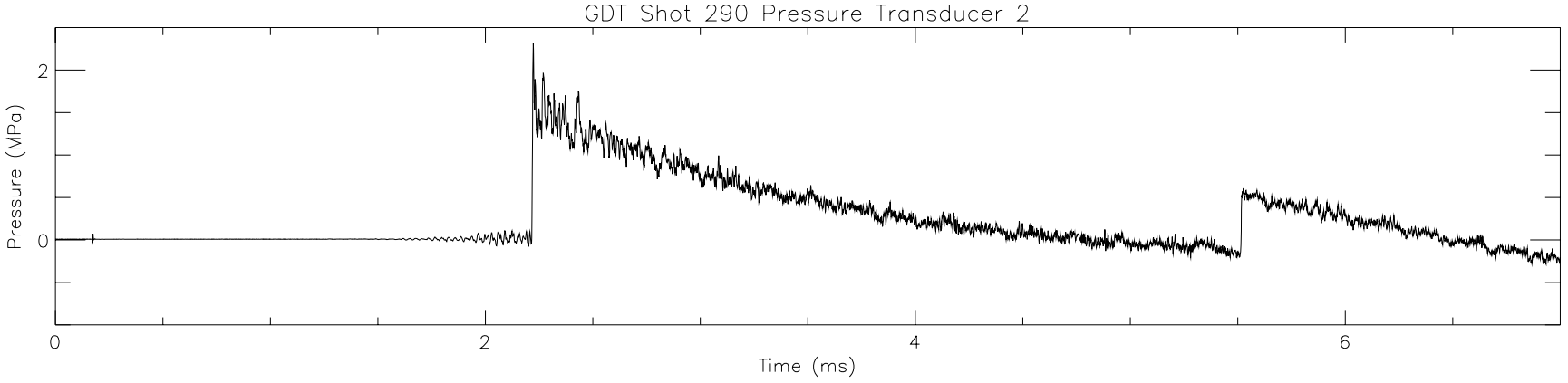
GDT Shot 290 Pressure Transducer 2
Pressure (MPa)
2
0
0
2
4
6
Time (ms)

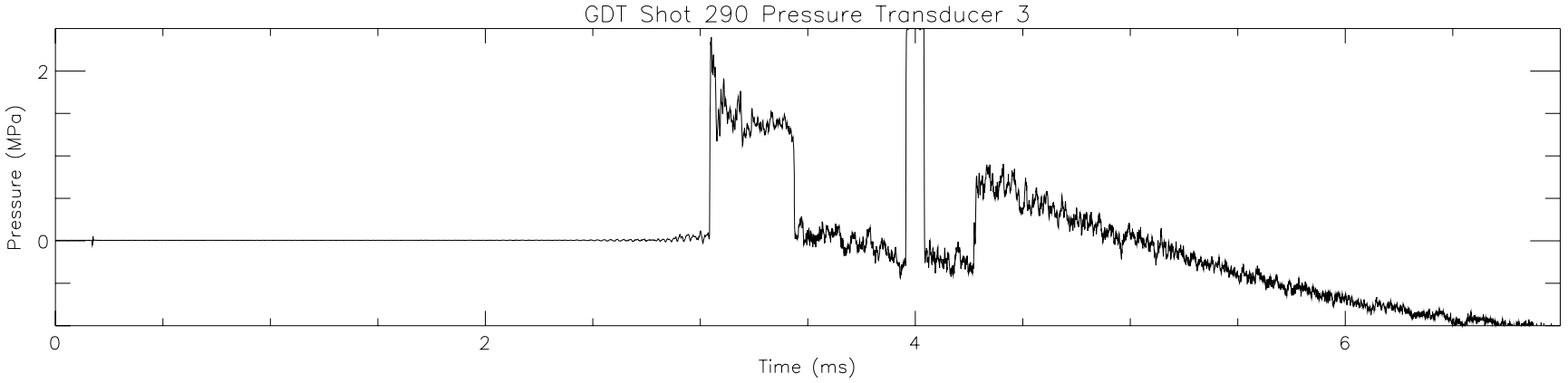
GDT Shot 290 Pressure Transducer 3
Pressure (MPa)
2
0
0
2
4
6
Time (ms)

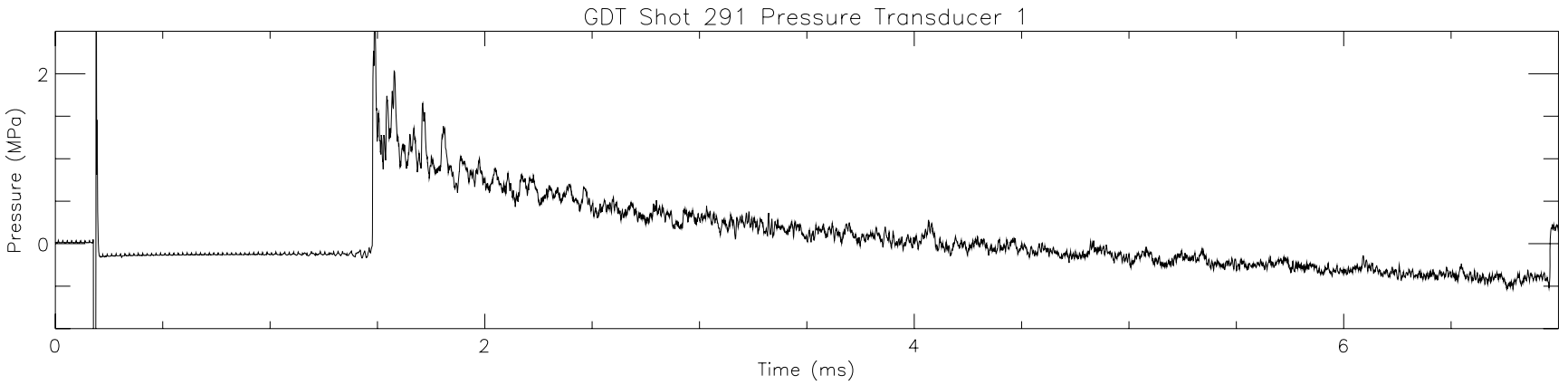
GDT Shot 291 Pressure Transducer 1
Pressure (MPa)
2
0
0
2
4
6
Time (ms)

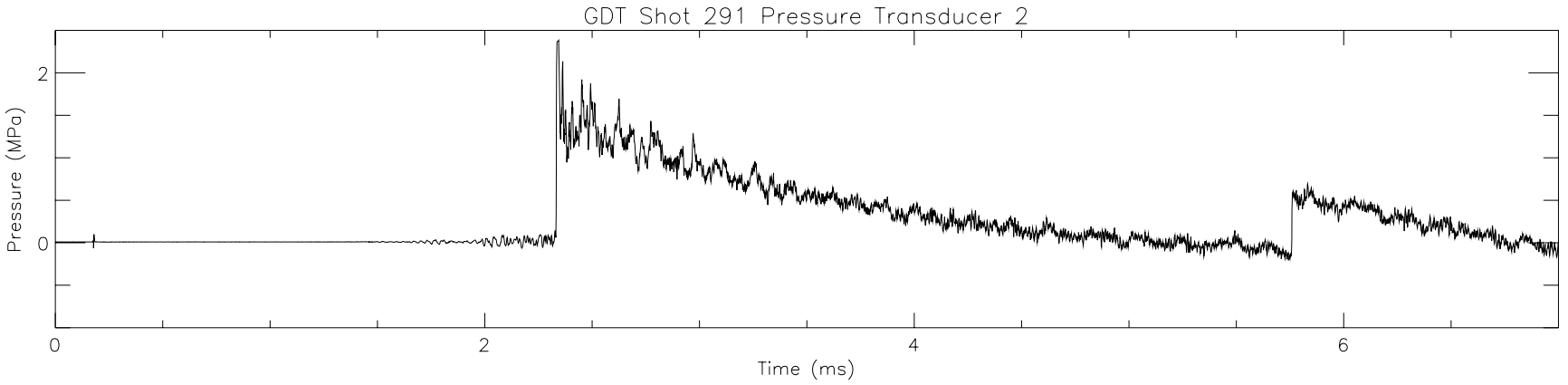
GDT Shot 291 Pressure Transducer 2
Pressure (MPa)
2
0
0
2
4
6
Time (ms)

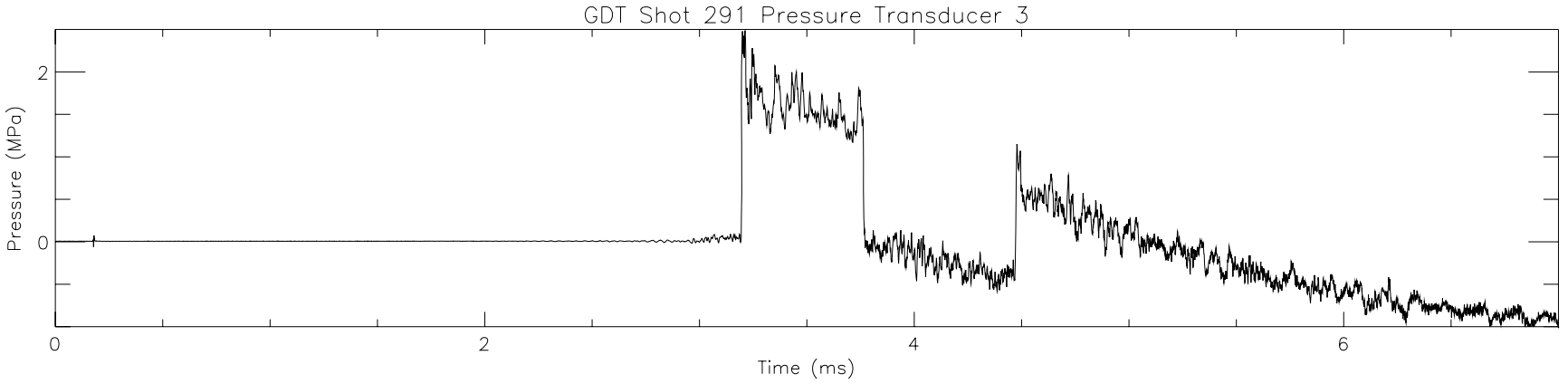
GDT Shot 291 Pressure Transducer 3
Pressure (MPa)
2
0
0
2
4
6
Time (ms)

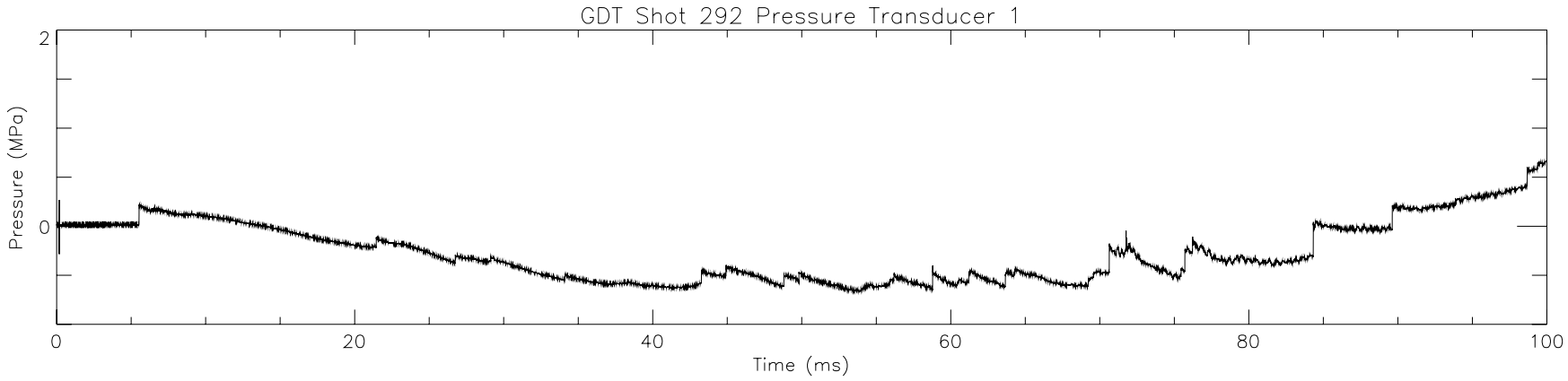
GDT Shot 292 Pressure Transducer 1
Pressure (MPa)
2
0
0
20
40
60
80
100
Time (ms)

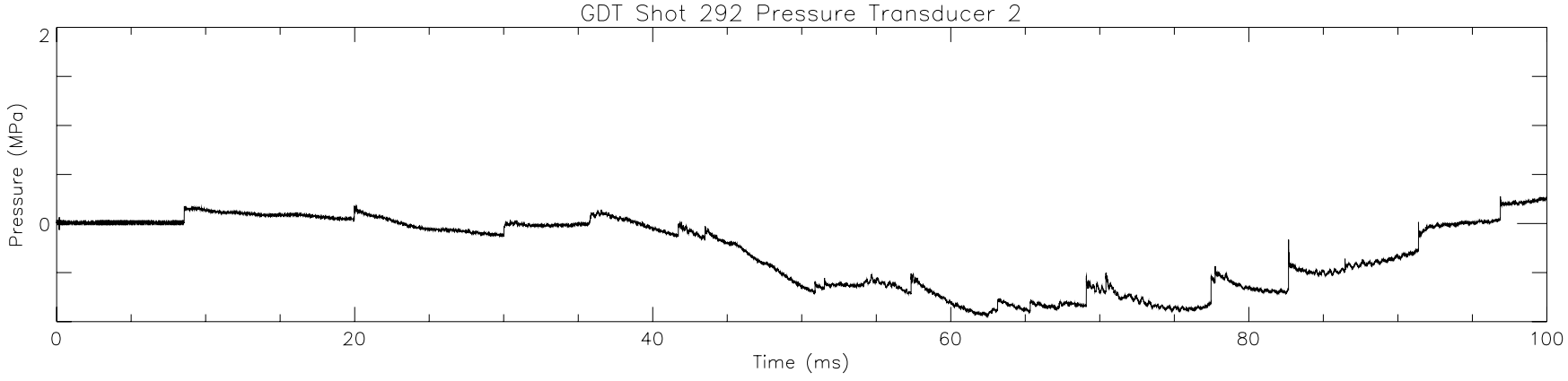
GDT Shot 292 Pressure Transducer 2
Pressure (MPa)
2
0
0
20
40
60
80
100
Time (ms)

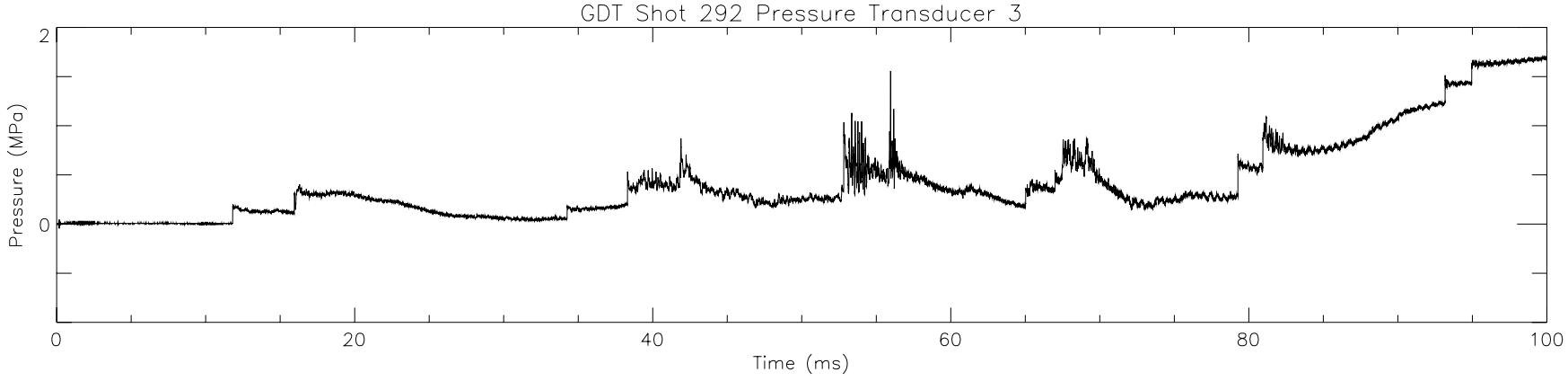
GDT Shot 292 Pressure Transducer 3
Pressure (MPa)
2
0
0
20
40
60
80
100
Time (ms)

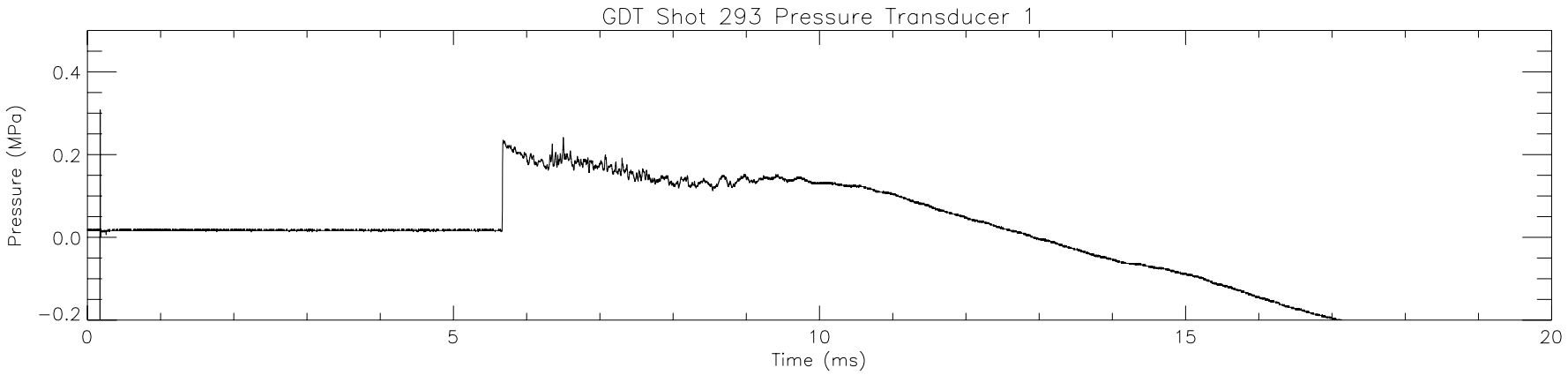
GDT Shot 293 Pressure Transducer 1
Pressure (MPa)
0.4
0.2
0.0
−0.2
0
5
10
15
20
Time (ms)

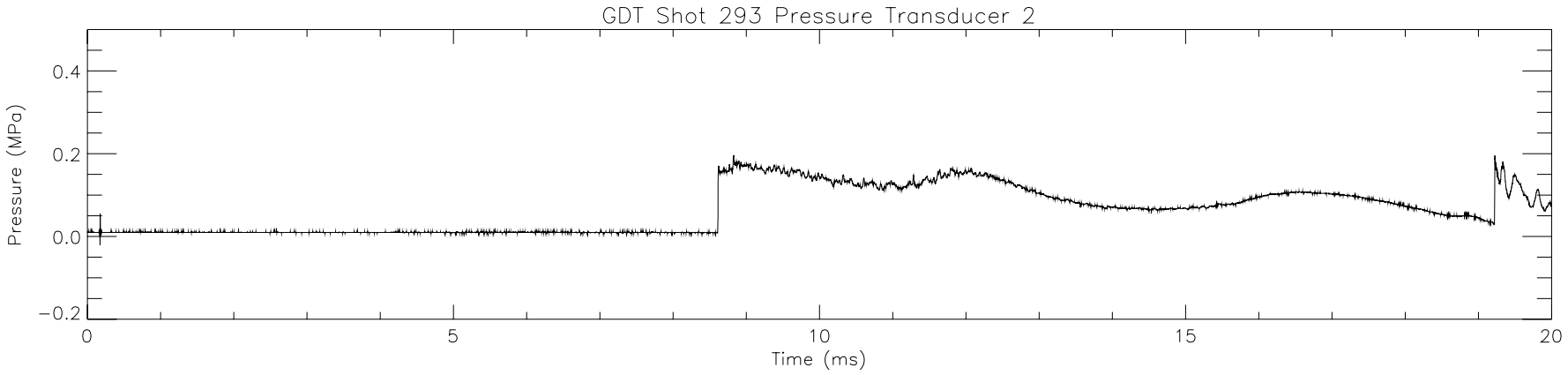
GDT Shot 293 Pressure Transducer 2
Pressure (MPa)
0.4
0.2
0.0
−0.2
0
5
10
15
20
Time (ms)

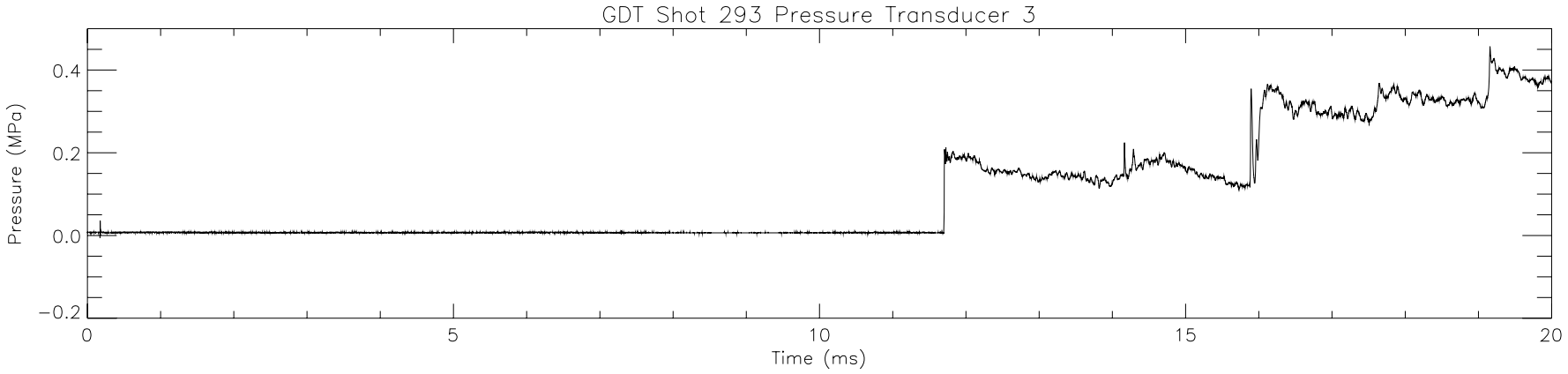
GDT Shot 293 Pressure Transducer 3
Pressure (MPa)
0.4
0.2
0.0
−0.2
0
5
10
15
20
Time (ms)

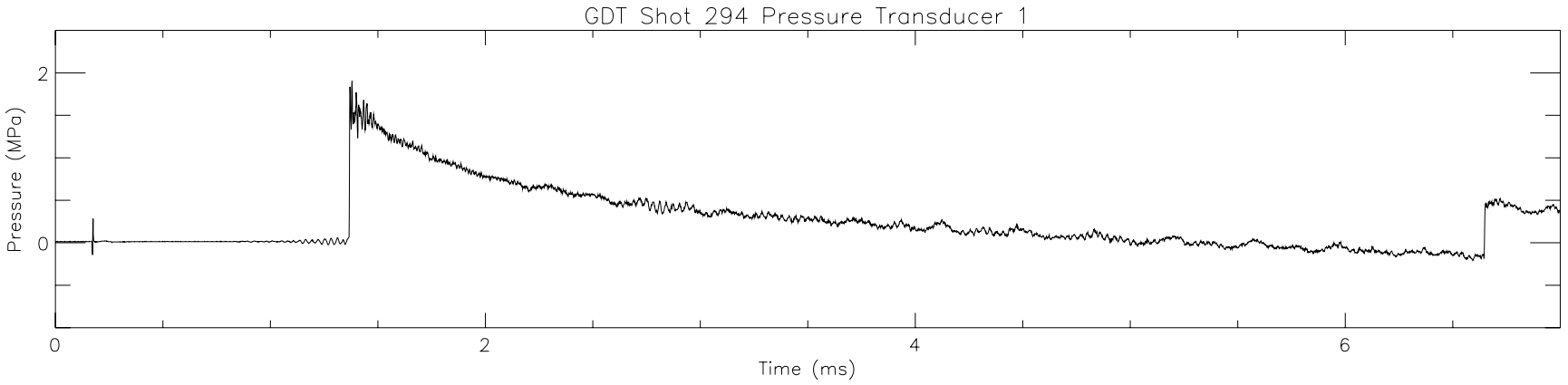
GDT Shot 294 Pressure Transducer 1
Pressure (MPa)
2
0
0
2
4
6
Time (ms)

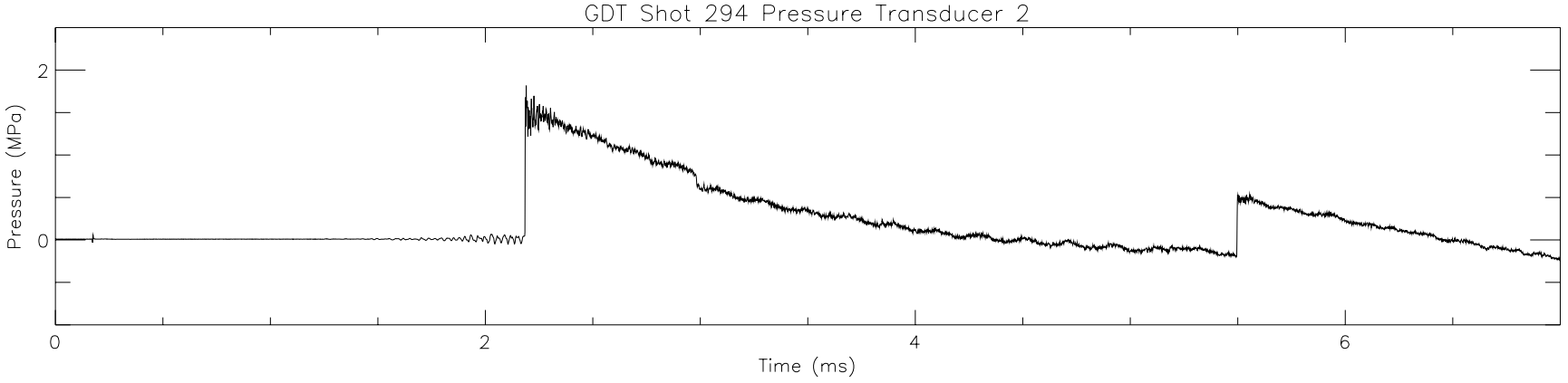
GDT Shot 294 Pressure Transducer 2
Pressure (MPa)
2
0
0
2
4
6
Time (ms)

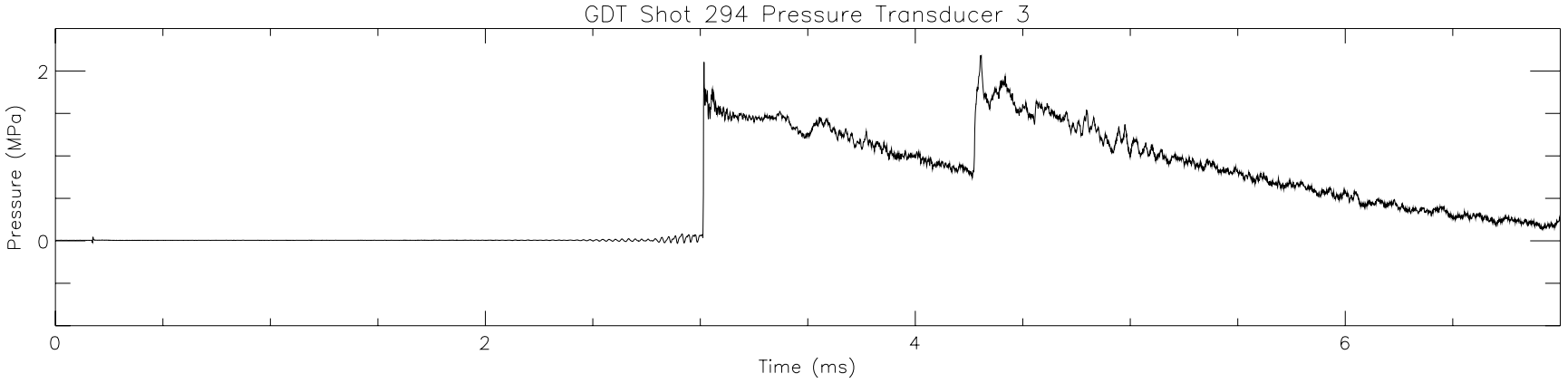
GDT Shot 294 Pressure Transducer 3
Pressure (MPa)
2
0
0
2
4
6
Time (ms)

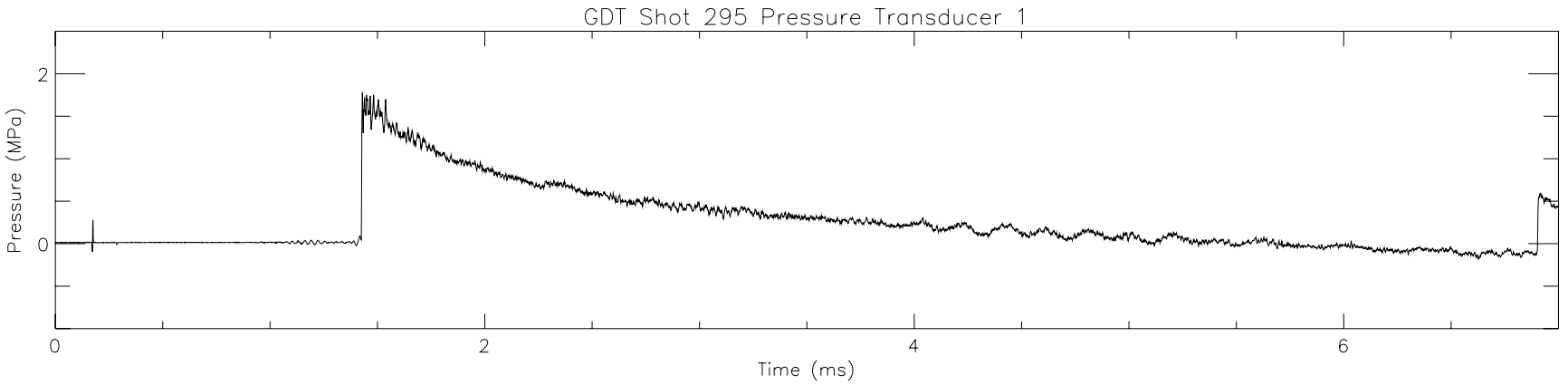
GDT Shot 295 Pressure Transducer 1
Pressure (MPa)
2
0
0
2
4
6
Time (ms)

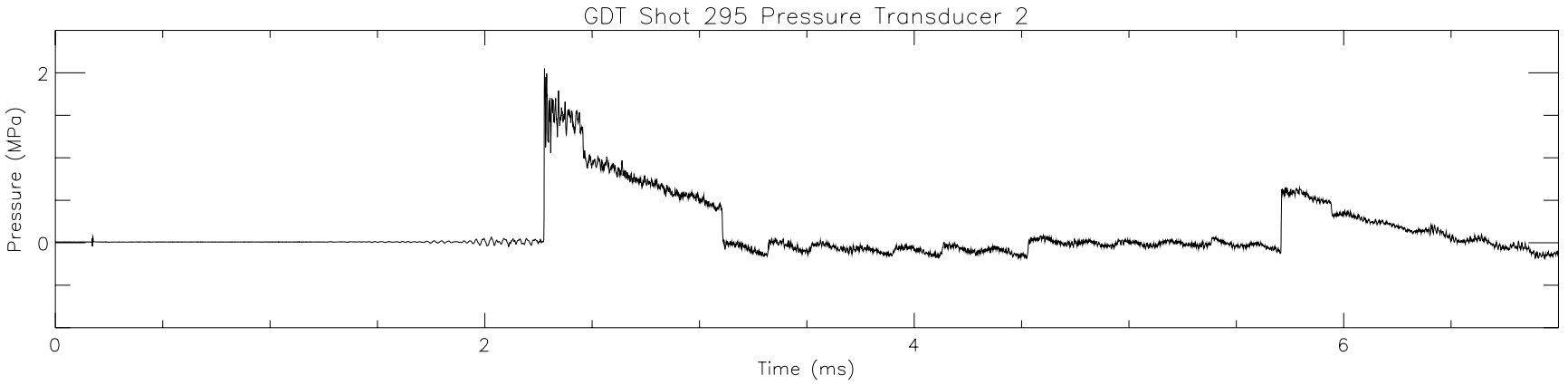
GDT Shot 295 Pressure Transducer 2
Pressure (MPa)
2
0
0
2
4
6
Time (ms)

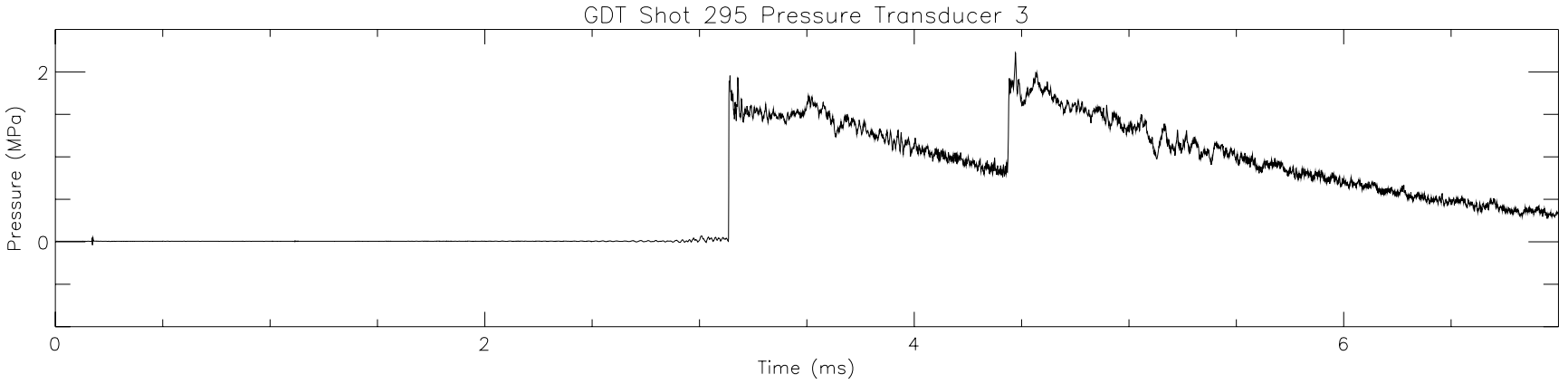
GDT Shot 295 Pressure Transducer 3
Pressure (MPa)
2
0
0
2
4
6
Time (ms)

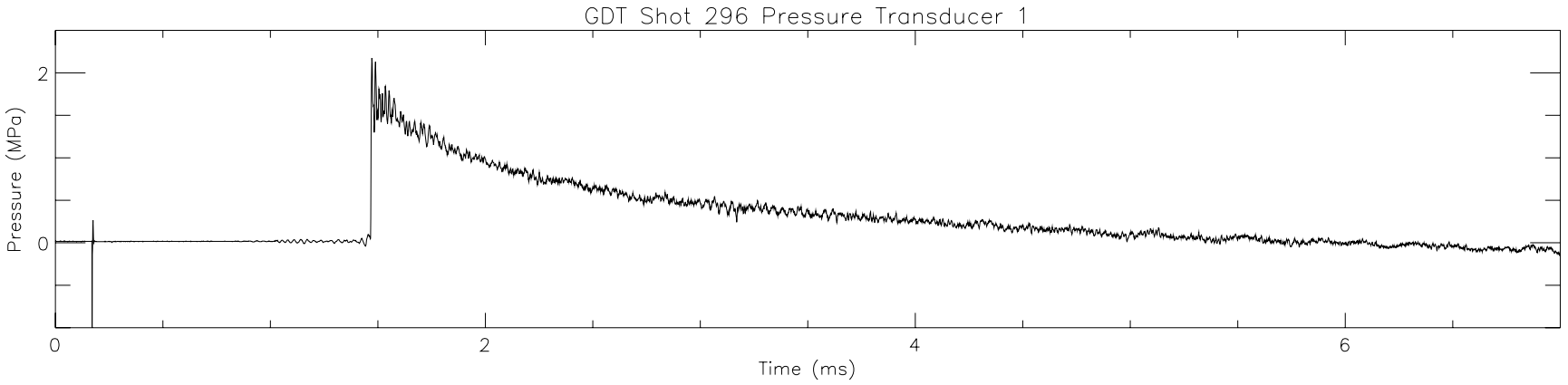
GDT Shot 296 Pressure Transducer 1
Pressure (MPa)
2
0
0
2
4
6
Time (ms)

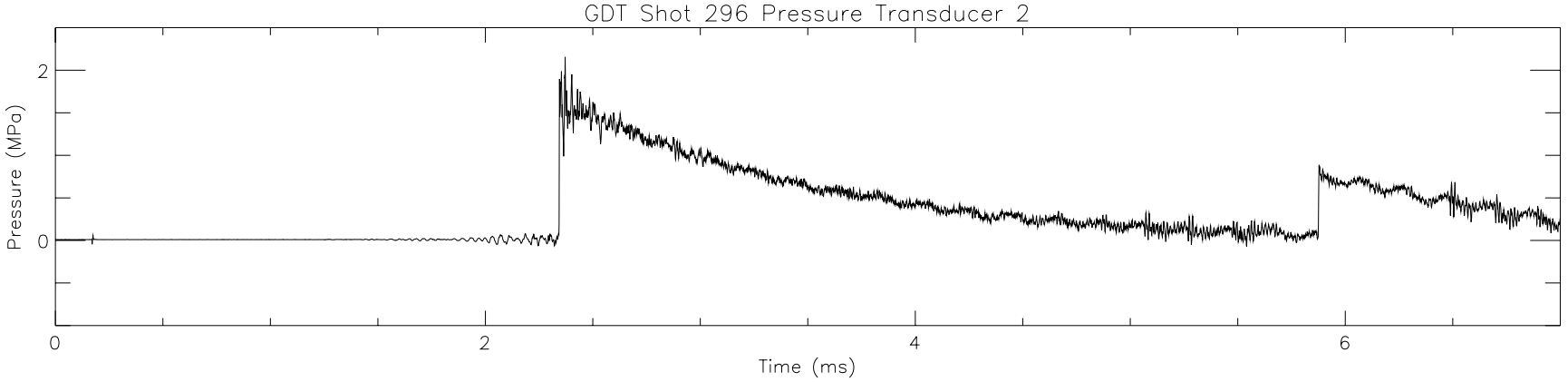
GDT Shot 296 Pressure Transducer 2
Pressure (MPa)
2
0
0
2
4
6
Time (ms)

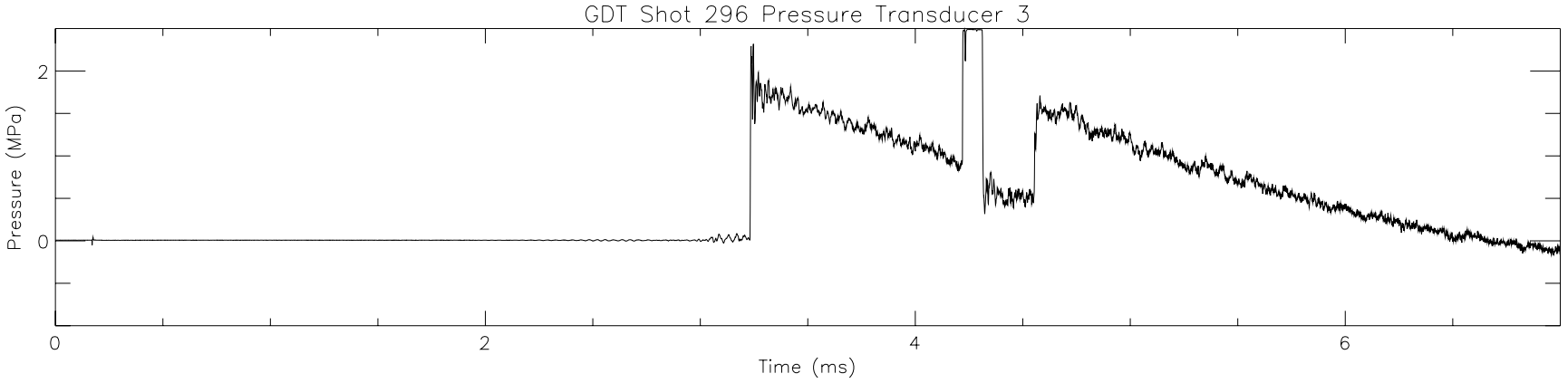
GDT Shot 296 Pressure Transducer 3
Pressure (MPa)
2
0
0
2
4
6
Time (ms)

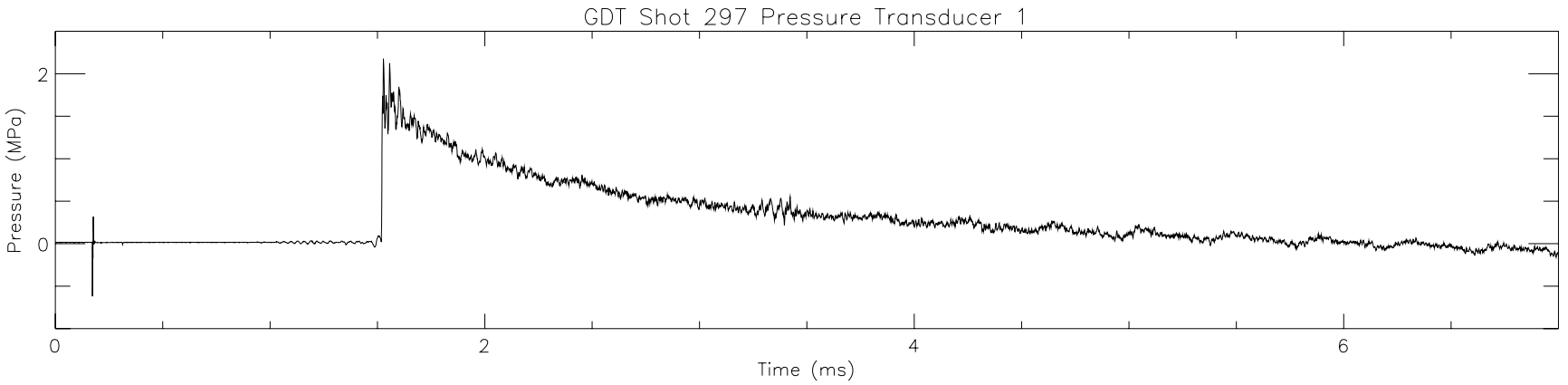
GDT Shot 297 Pressure Transducer 1
Pressure (MPa)
2
0
0
2
4
6
Time (ms)

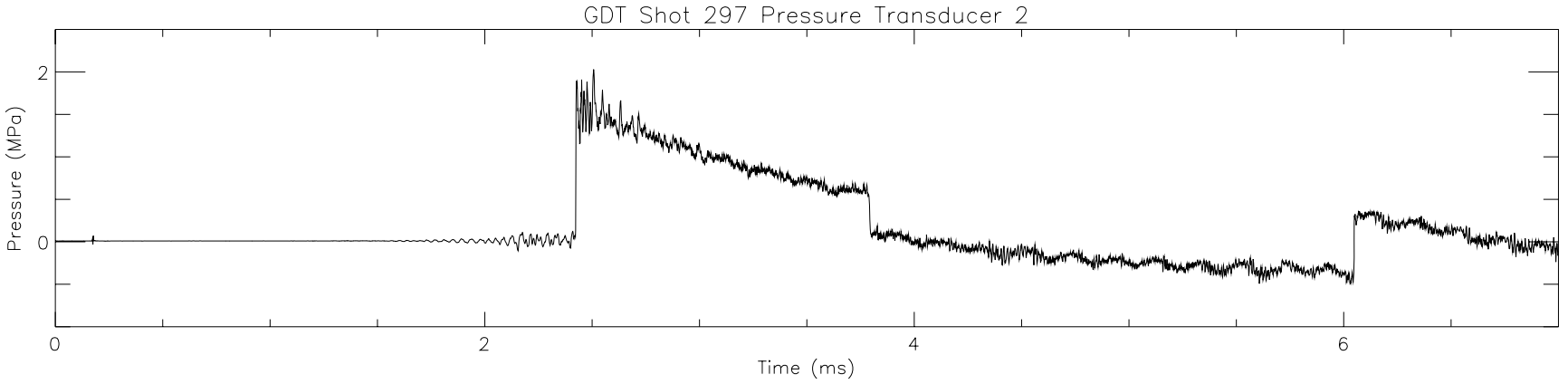
GDT Shot 297 Pressure Transducer 2
Pressure (MPa)
2
0
0
2
4
6
Time (ms)

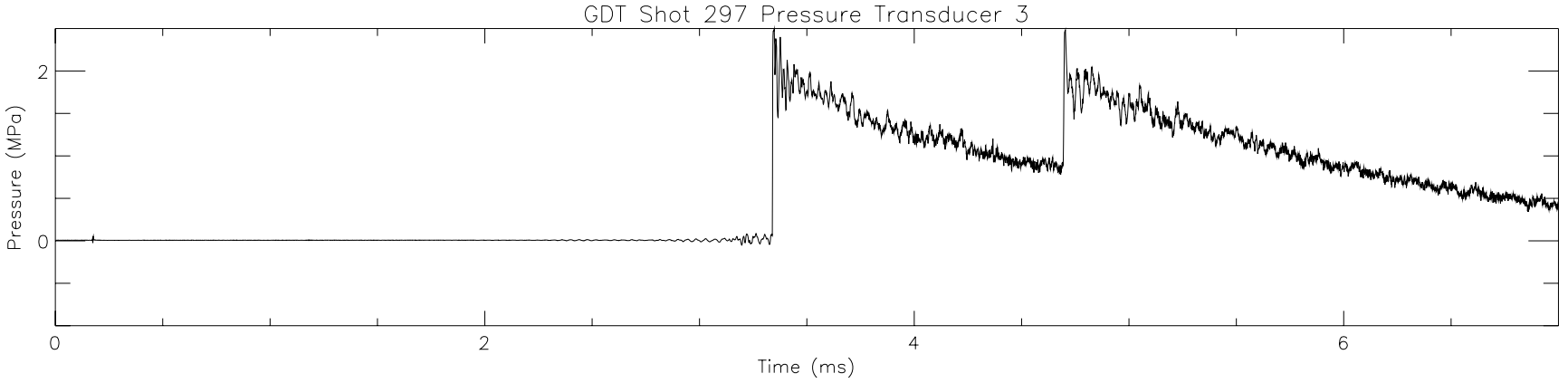
GDT Shot 297 Pressure Transducer 3
Pressure (MPa)
2
0
0
2
4
6
Time (ms)

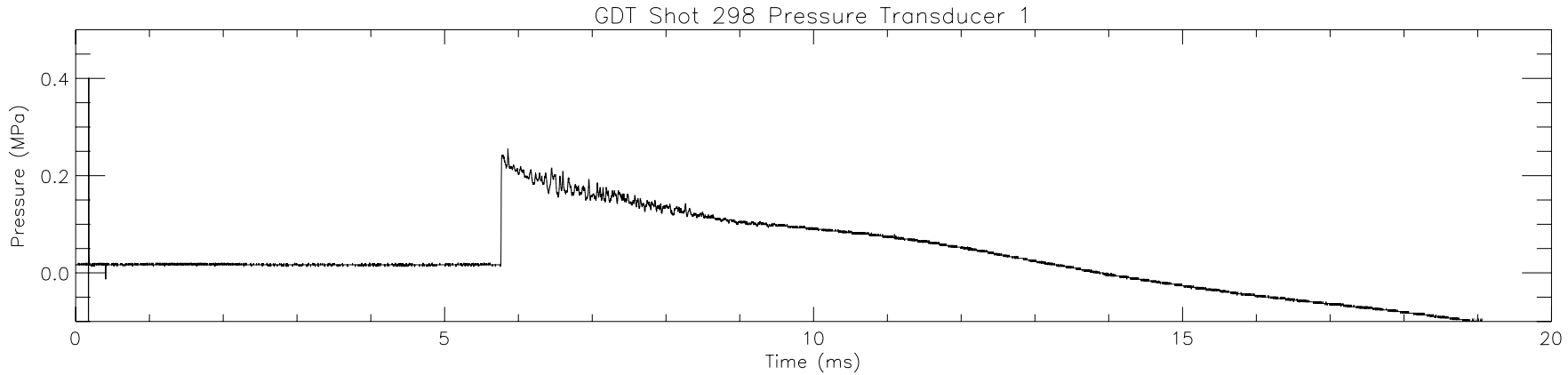
GDT Shot 298 Pressure Transducer 1
Pressure (MPa)
0.4
0.2
0.0
0
5
10
15
20
Time (ms)

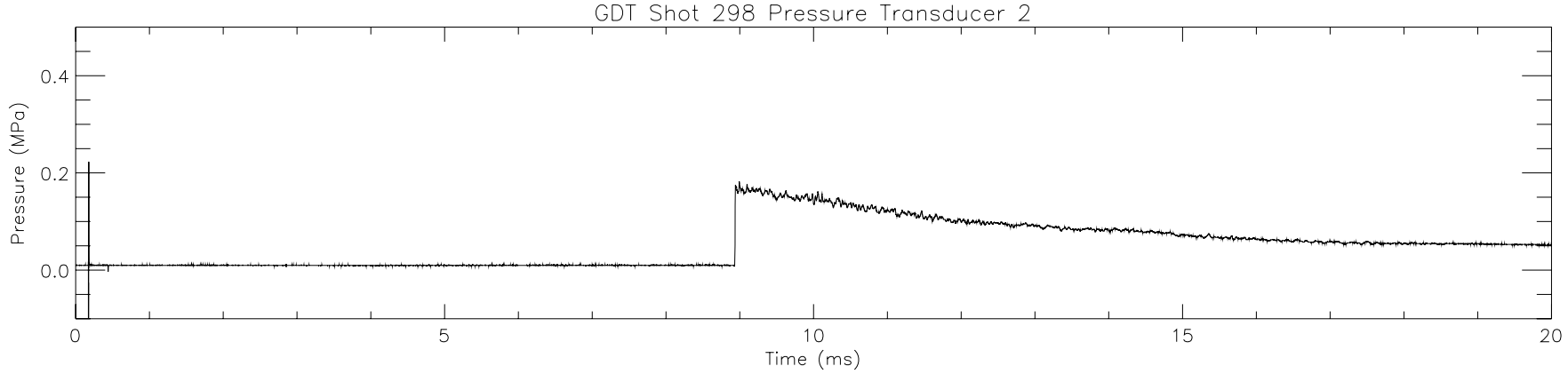
GDT Shot 298 Pressure Transducer 2
Pressure (MPa)
0.4
0.2
0.0
0
5
10
15
20
Time (ms)

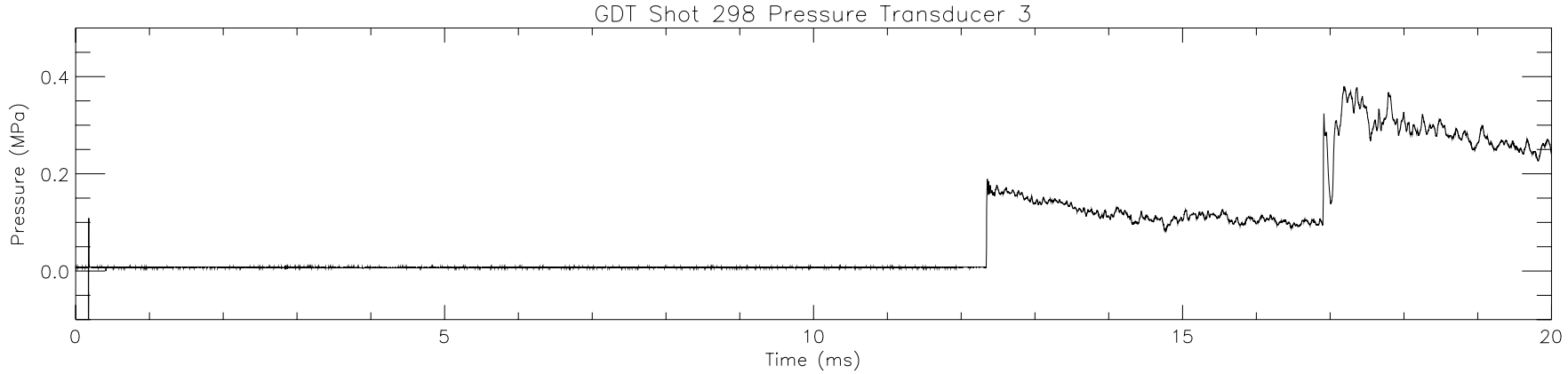
GDT Shot 298 Pressure Transducer 3
Pressure (MPa)
0.4
0.2
0.0
0
5
10
15
20
Time (ms)

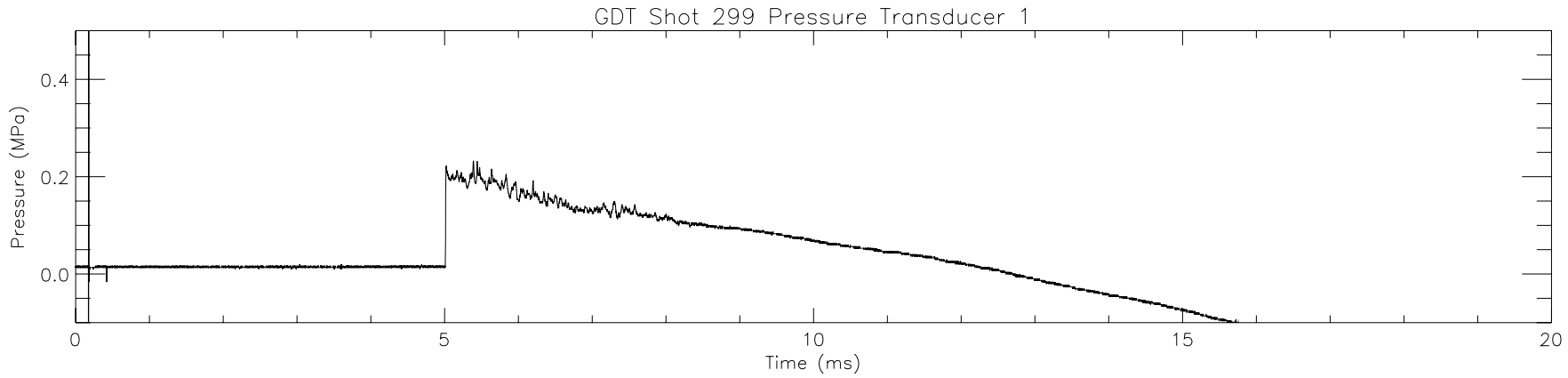
GDT Shot 299 Pressure Transducer 1
Pressure (MPa)
0.4
0.2
0.0
0
5
10
15
20
Time (ms)

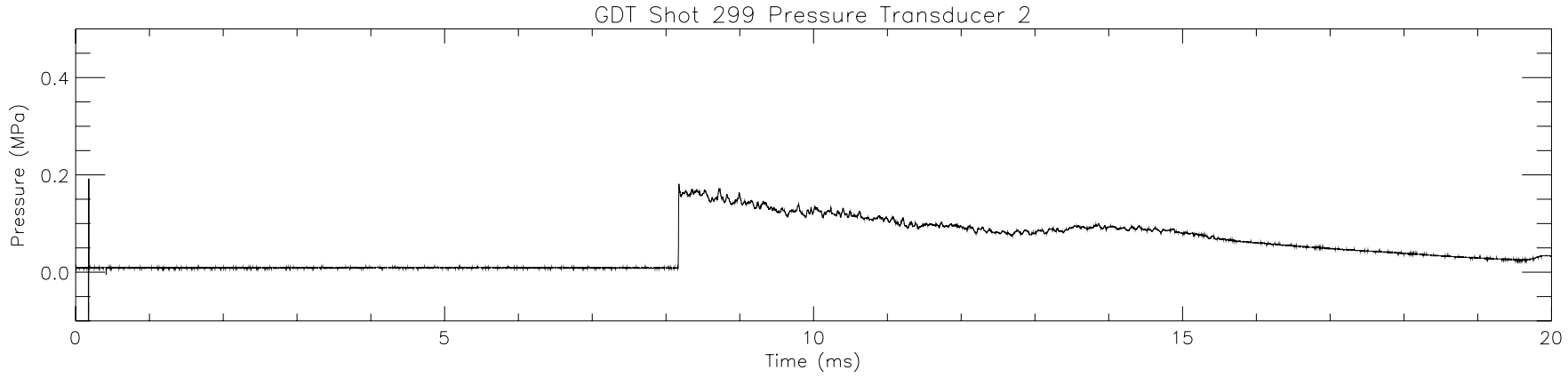
GDT Shot 299 Pressure Transducer 2
Pressure (MPa)
0.4
0.2
0.0
0
5
10
15
20
Time (ms)

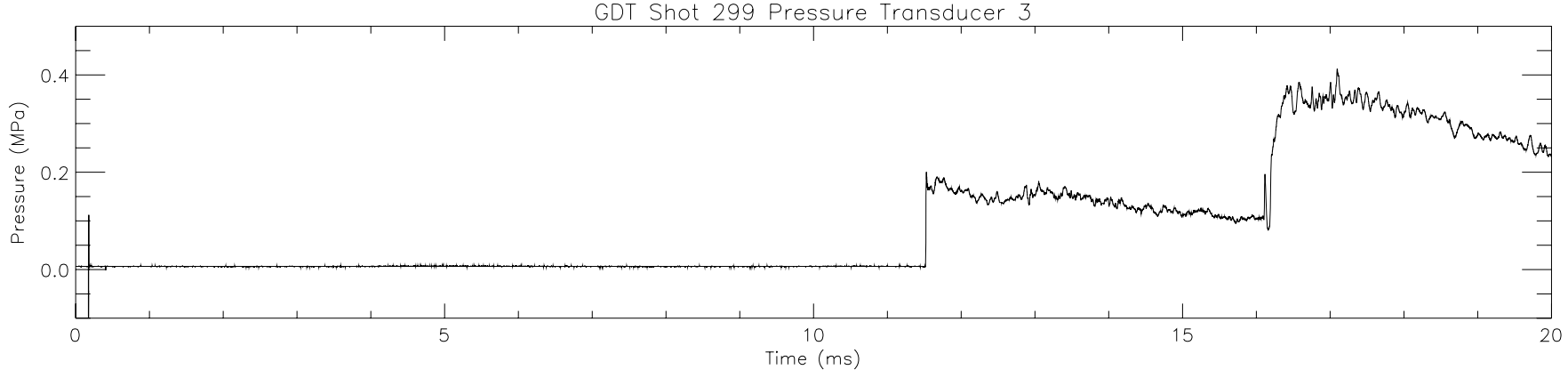
GDT Shot 299 Pressure Transducer 3
Pressure (MPa)
0.4
0.2
0.0
0
5
10
15
20
Time (ms)

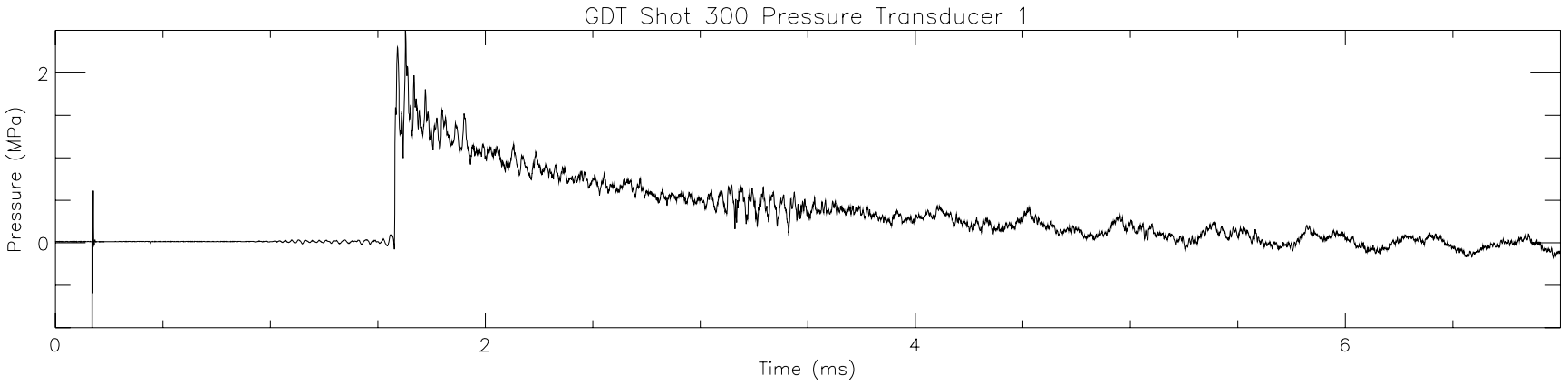
GDT Shot 300 Pressure Transducer 1
Pressure (MPa)
2
0
0
2
4
6
Time (ms)

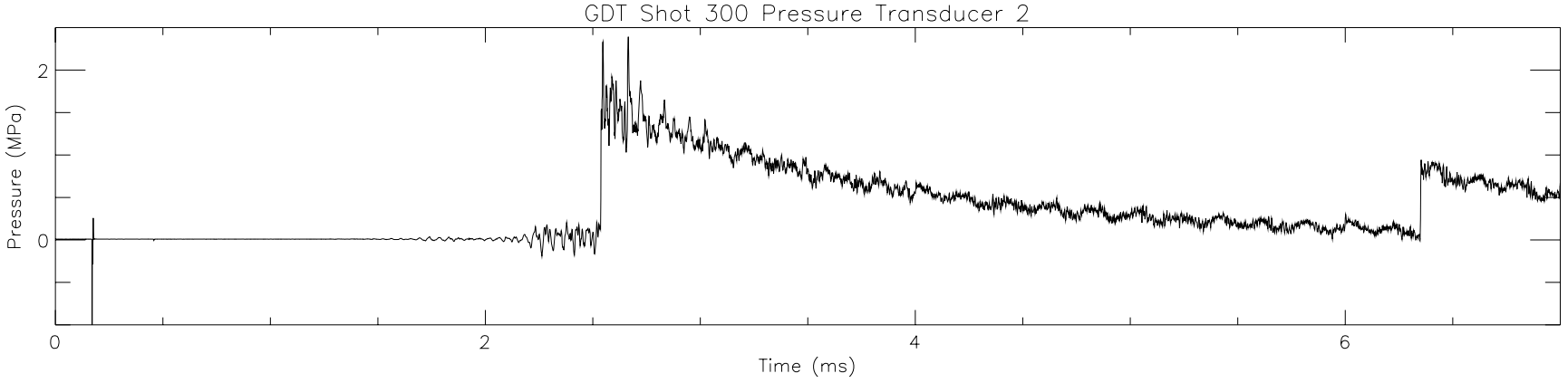
GDT Shot 300 Pressure Transducer 2
Pressure (MPa)
2
0
0
2
4
6
Time (ms)

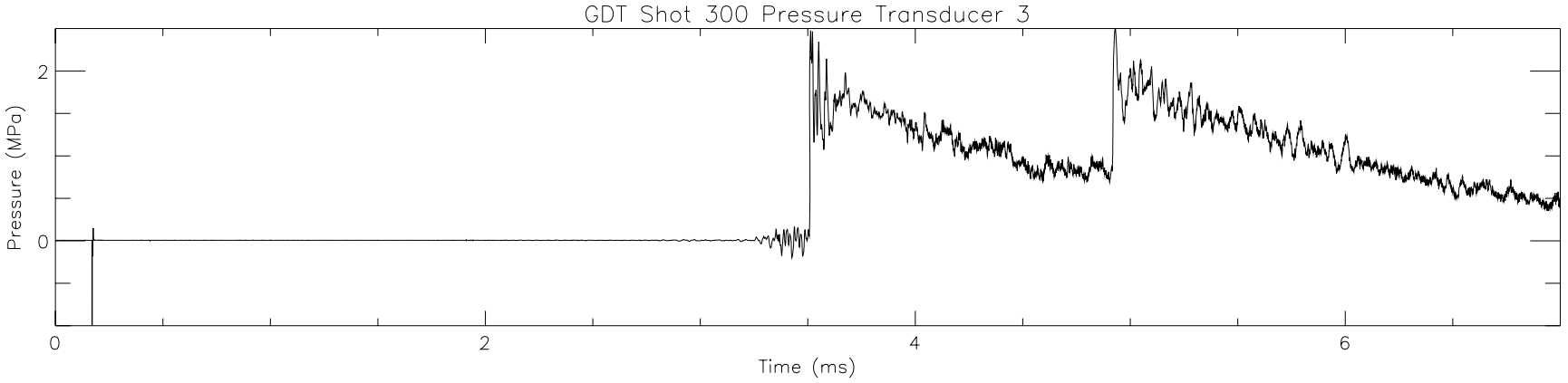
GDT Shot 300 Pressure Transducer 3
Pressure (MPa)
2
0
0
2
4
6
Time (ms)

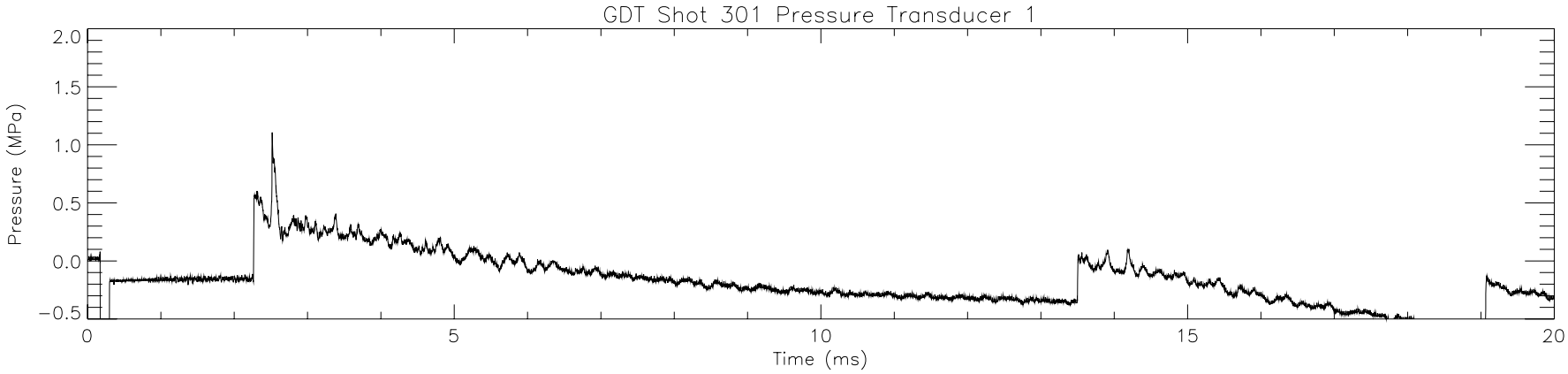
GDT Shot 301 Pressure Transducer 1
Pressure (MPa)
2.0
1.5
1.0
0.5
0.0
−0.5
0
5
10
15
20
Time (ms)

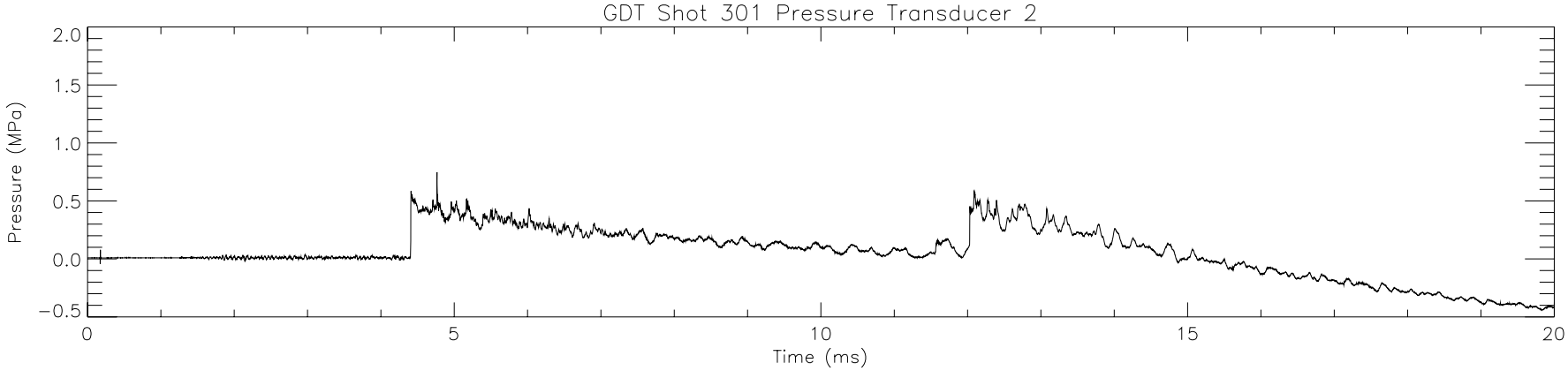
GDT Shot 301 Pressure Transducer 2
Pressure (MPa)
2.0
1.5
1.0
0.5
0.0
−0.5
0
5
10
15
20
Time (ms)

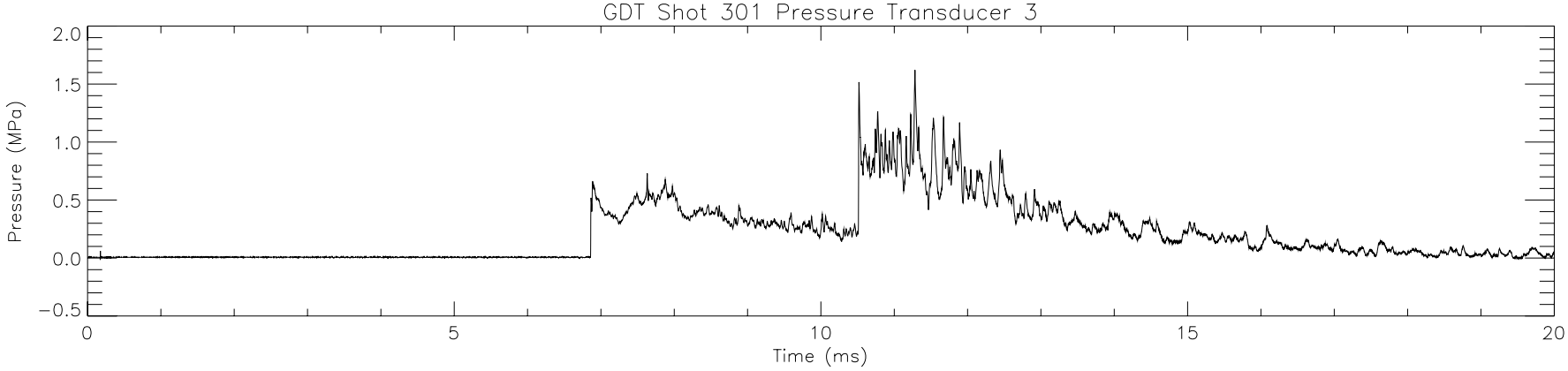
GDT Shot 301 Pressure Transducer 3
Pressure (MPa)
2.0
1.5
1.0
0.5
0.0
−0.5
0
5
10
15
20
Time (ms)

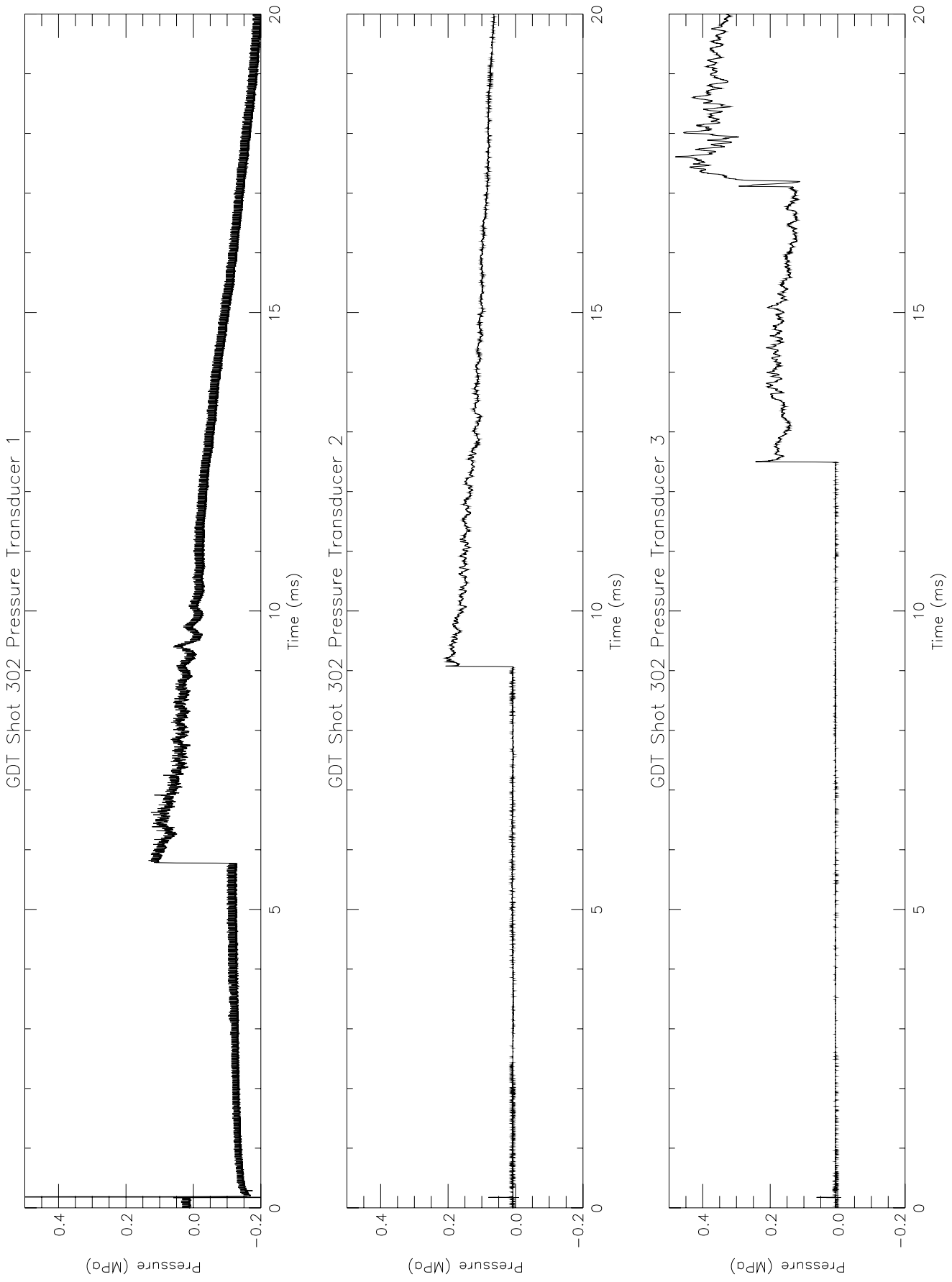
GDT Shot 302 Pressure Transducer 1
GDT Shot 302 Pressure Transducer 2
GDT Shot 302 Pressure Transducer 3
Pressure (MPa)
Time (ms)
0.4
0.2
0.0
−0.2
0
5
10
15
20

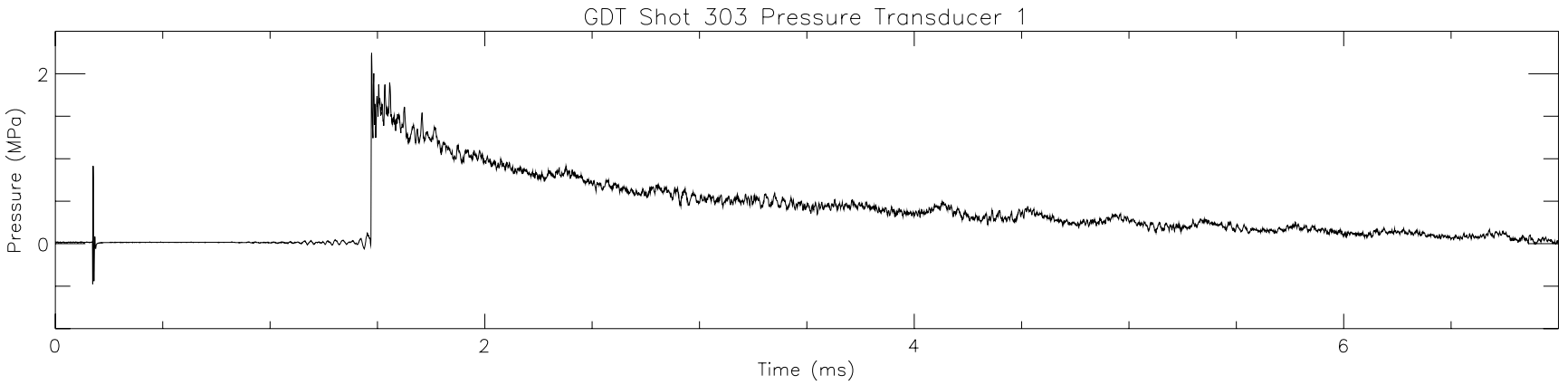
GDT Shot 303 Pressure Transducer 1
Pressure (MPa)
2
0
0
2
4
6
Time (ms)

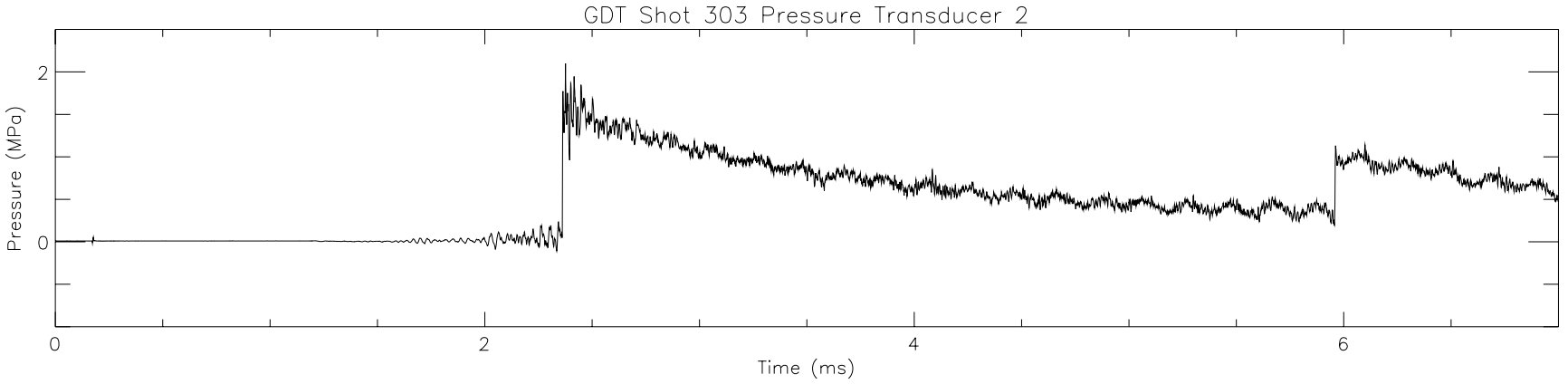
GDT Shot 303 Pressure Transducer 2
Pressure (MPa)
2
0
0
2
4
6
Time (ms)

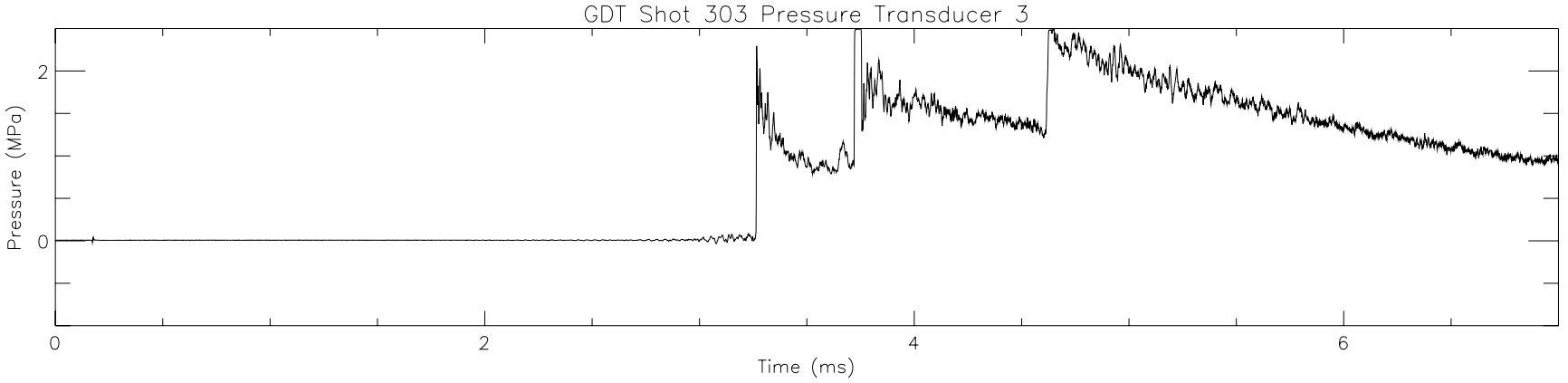
GDT Shot 303 Pressure Transducer 3
Pressure (MPa)
2
0
0
2
4
6
Time (ms)

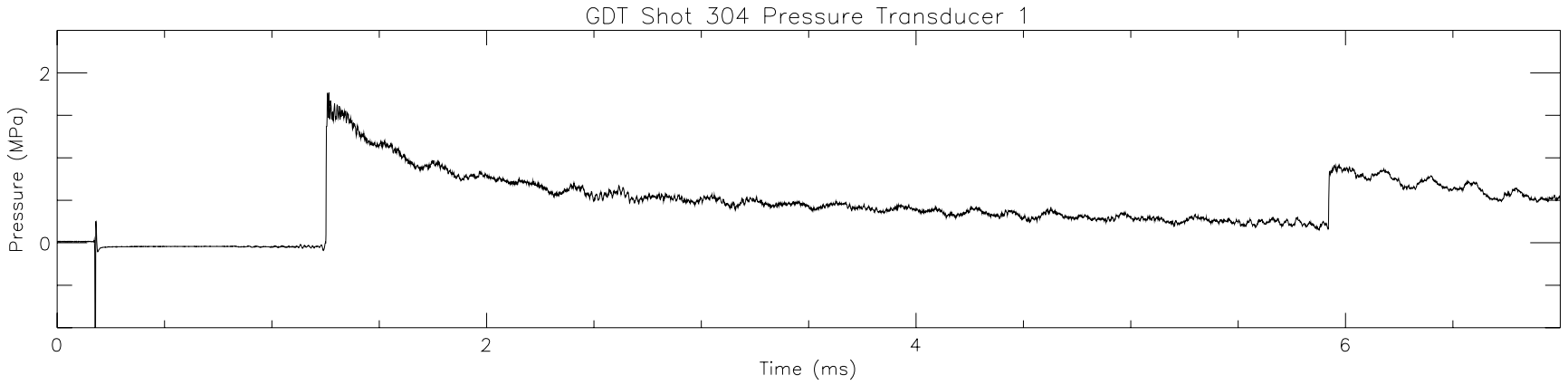
GDT Shot 304 Pressure Transducer 1
Pressure (MPa)
2
0
0
2
4
6
Time (ms)

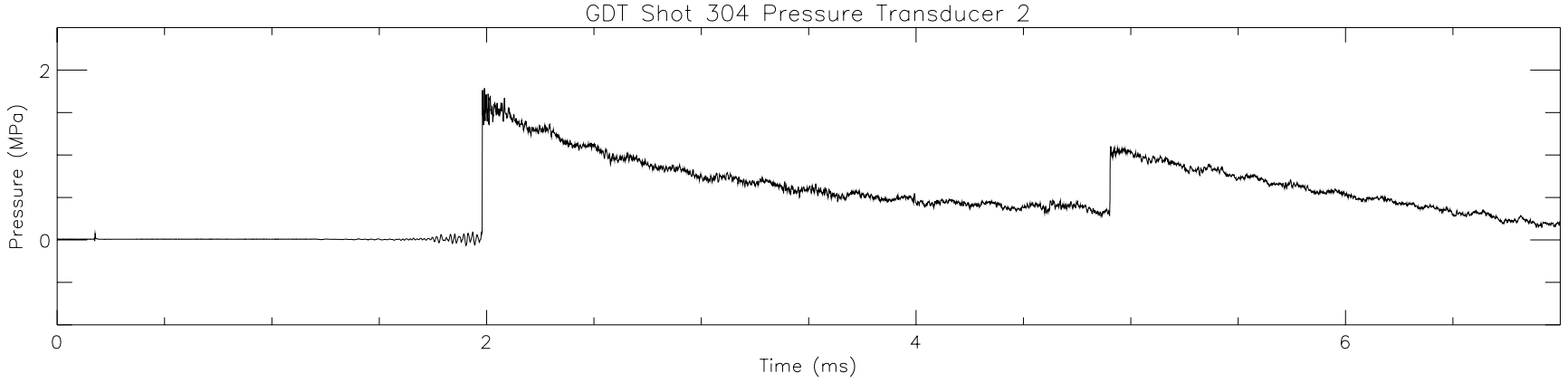
GDT Shot 304 Pressure Transducer 2
Pressure (MPa)
2
0
0
2
4
6
Time (ms)

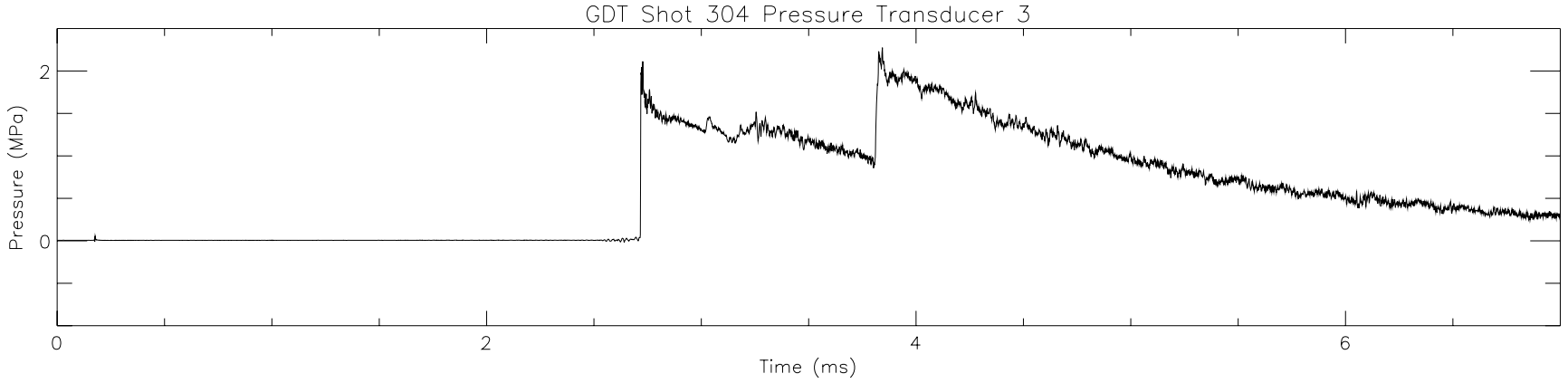
GDT Shot 304 Pressure Transducer 3
Pressure (MPa)
2
0
0
2
4
6
Time (ms)

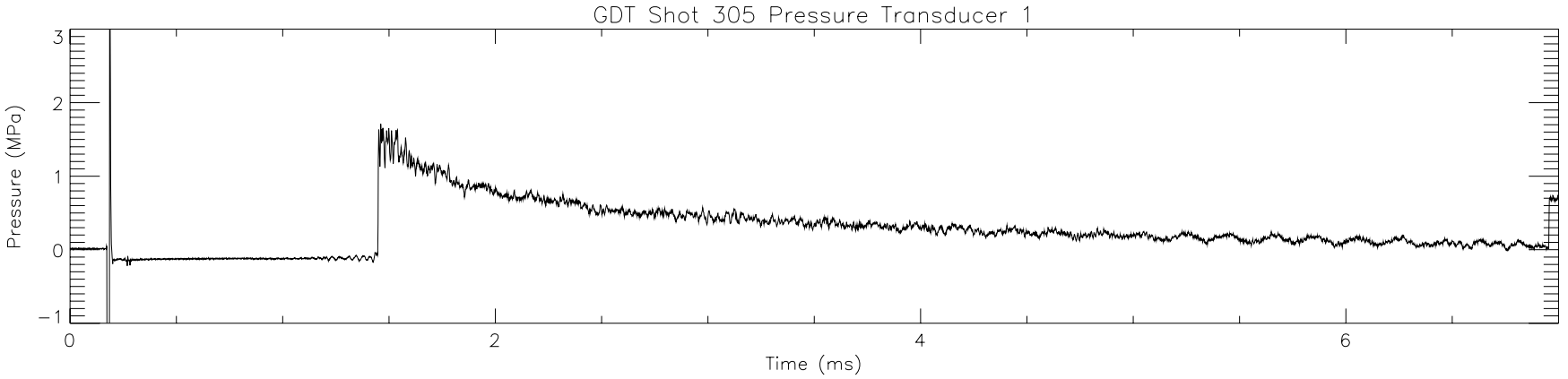
GDT Shot 305 Pressure Transducer 1
Pressure (MPa)
3
2
1
0
−1
0
2
4
6
Time (ms)

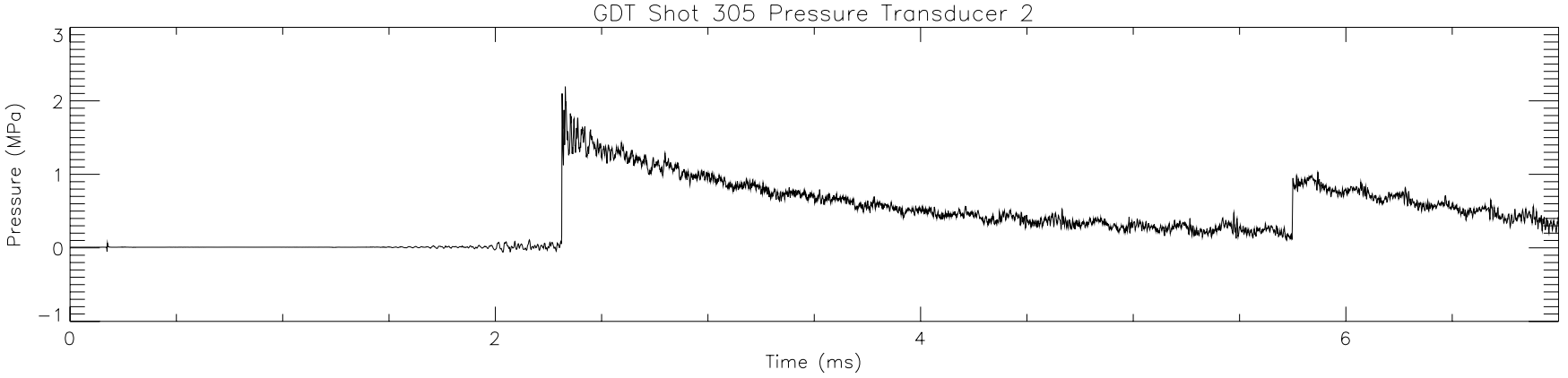
GDT Shot 305 Pressure Transducer 2
Pressure (MPa)
3
2
1
0
−1
0
2
4
6
Time (ms)

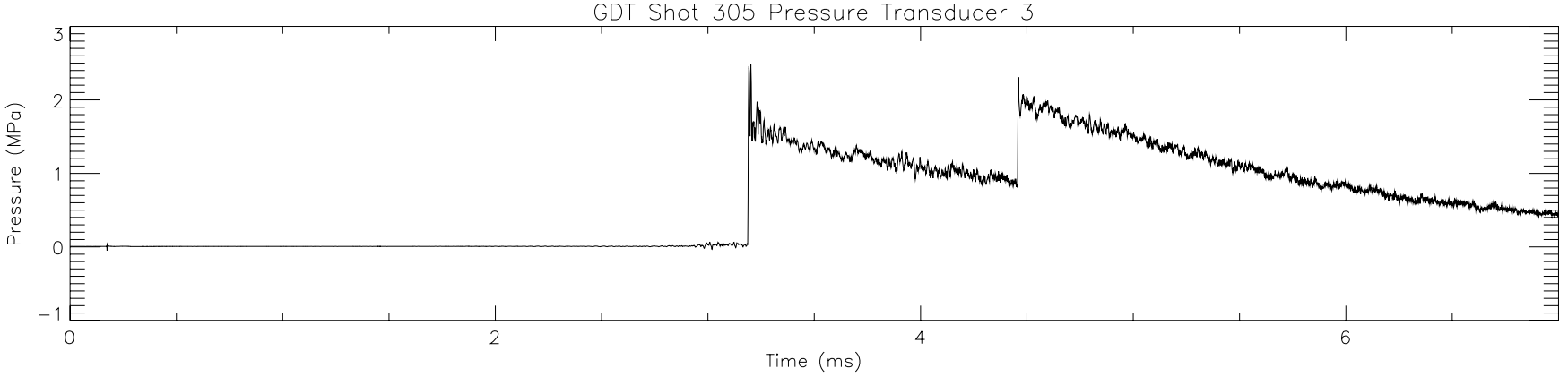
GDT Shot 305 Pressure Transducer 3
Pressure (MPa)
3
2
1
0
−1
0
2
4
6
Time (ms)

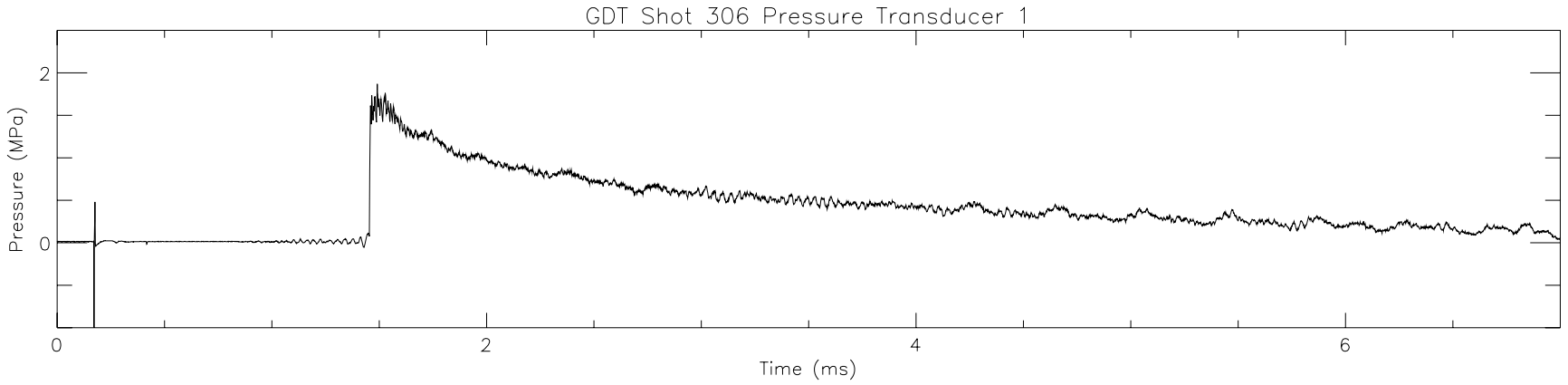
GDT Shot 306 Pressure Transducer 1
Pressure (MPa)
2
0
0
2
4
6
Time (ms)

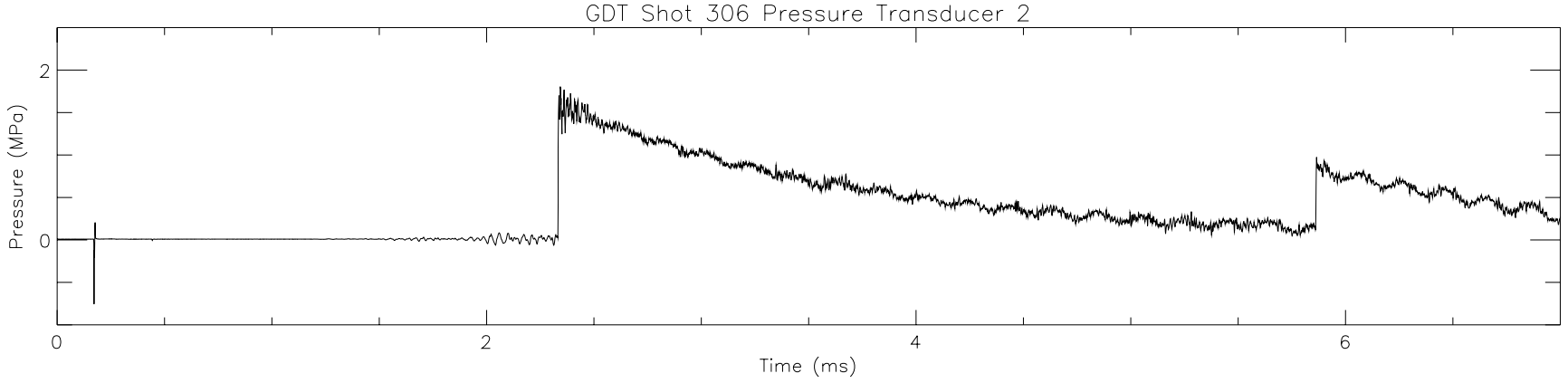
GDT Shot 306 Pressure Transducer 2
Pressure (MPa)
2
0
0
2
4
6
Time (ms)

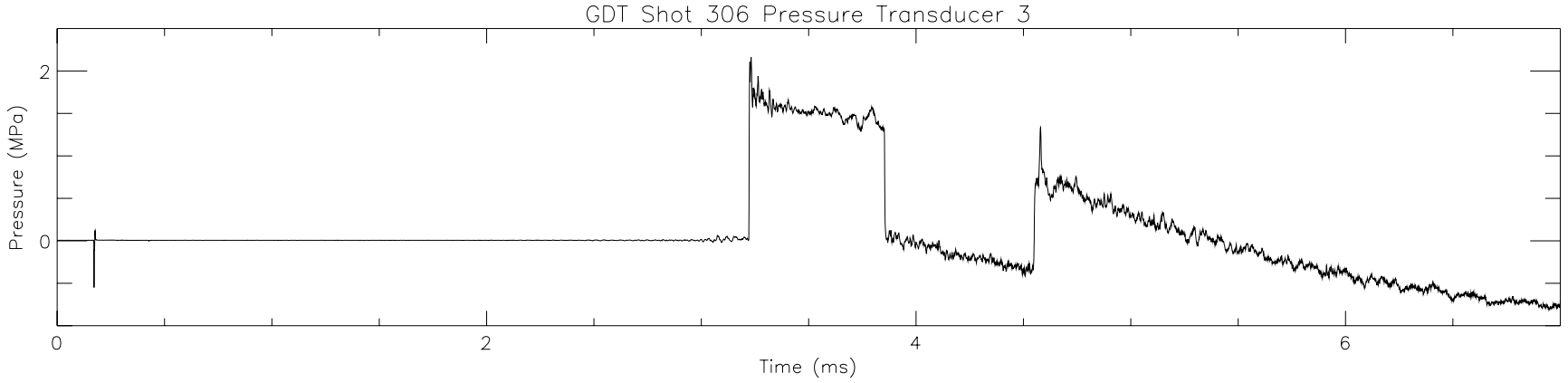
GDT Shot 306 Pressure Transducer 3
Pressure (MPa)
2
0
0
2
4
6
Time (ms)

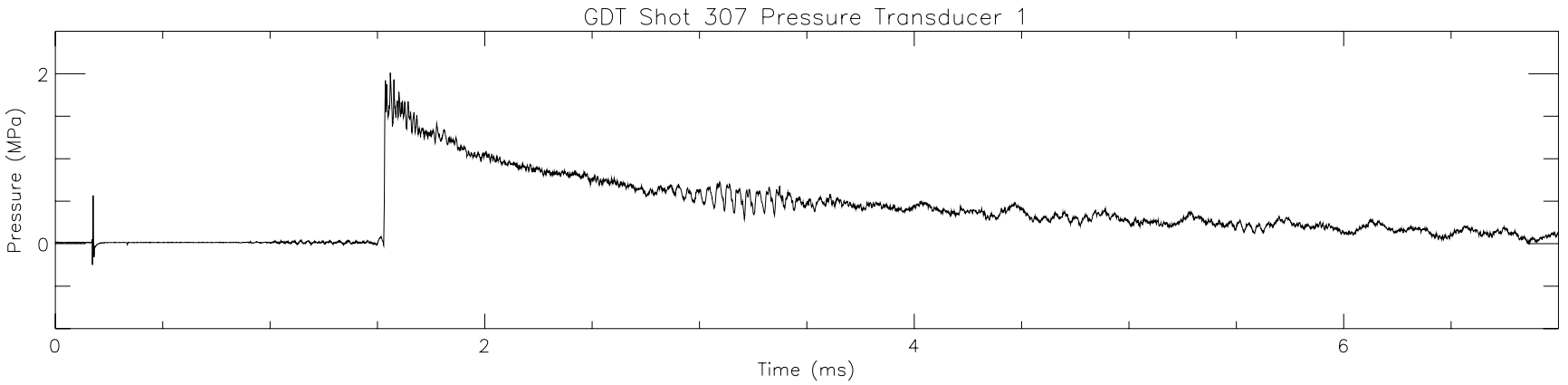
GDT Shot 307 Pressure Transducer 1
Pressure (MPa)
2
0
0
2
4
6
Time (ms)

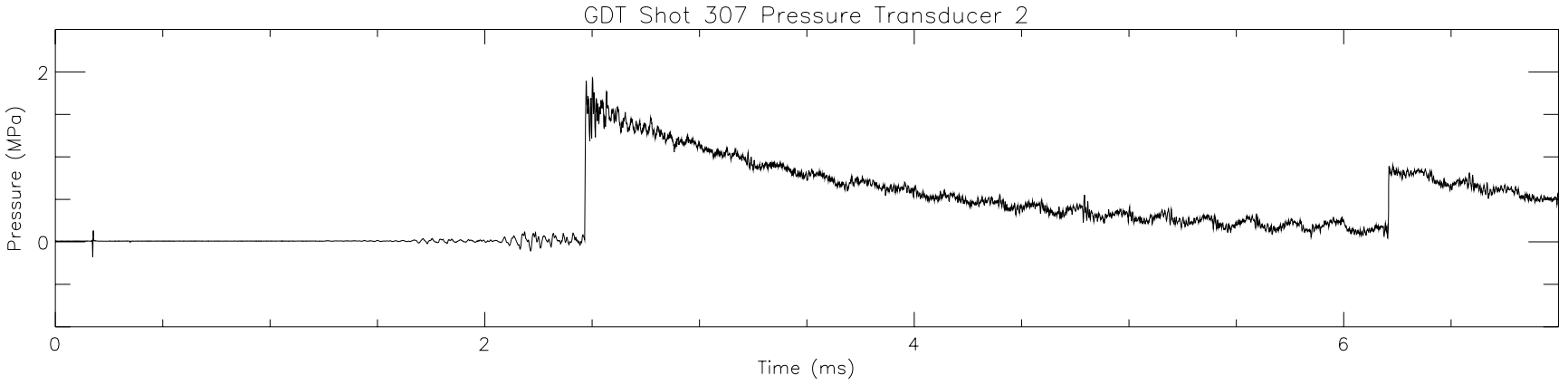
GDT Shot 307 Pressure Transducer 2
Pressure (MPa)
2
0
0
2
4
6
Time (ms)

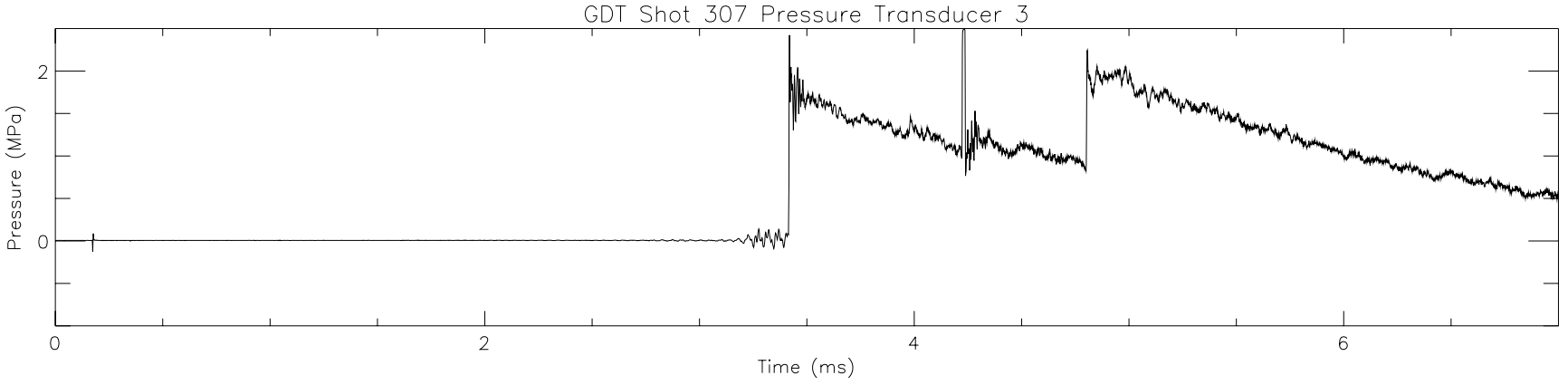
GDT Shot 307 Pressure Transducer 3
Pressure (MPa)
2
0
0
2
4
6
Time (ms)

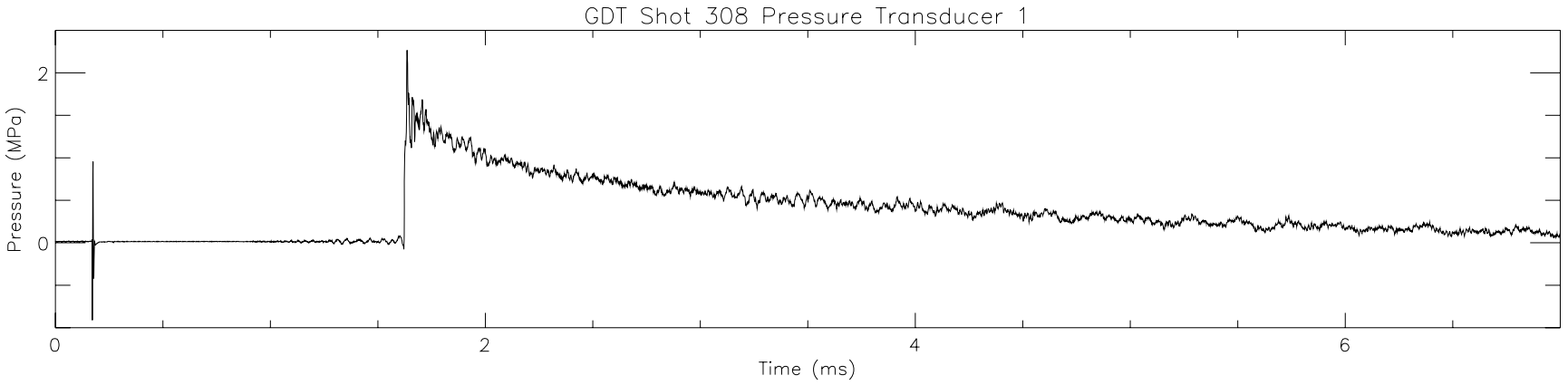
GDT Shot 308 Pressure Transducer 1
Pressure (MPa)
2
0
0
2
4
6
Time (ms)

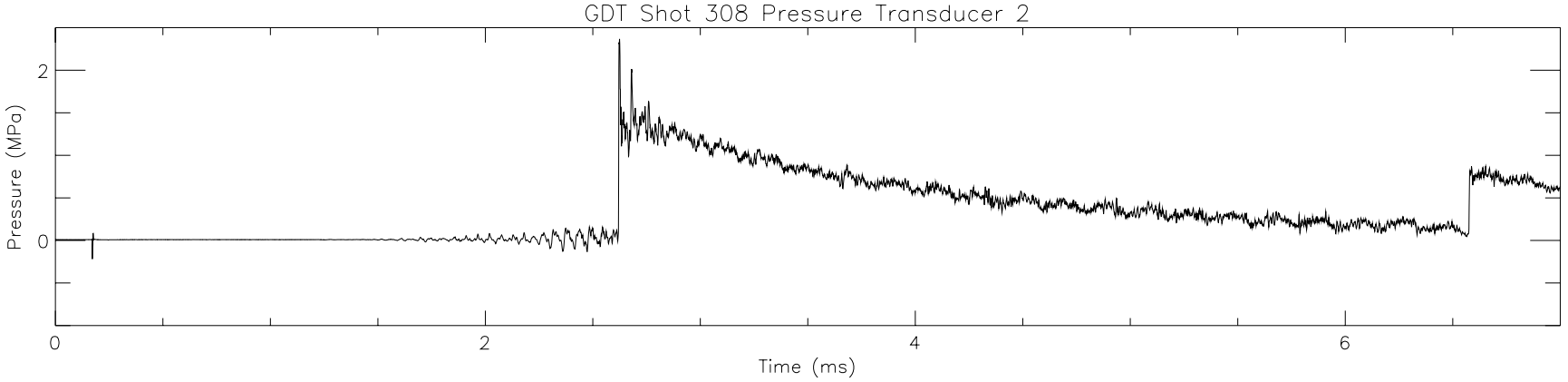
GDT Shot 308 Pressure Transducer 2
Pressure (MPa)
2
0
0
2
4
6
Time (ms)

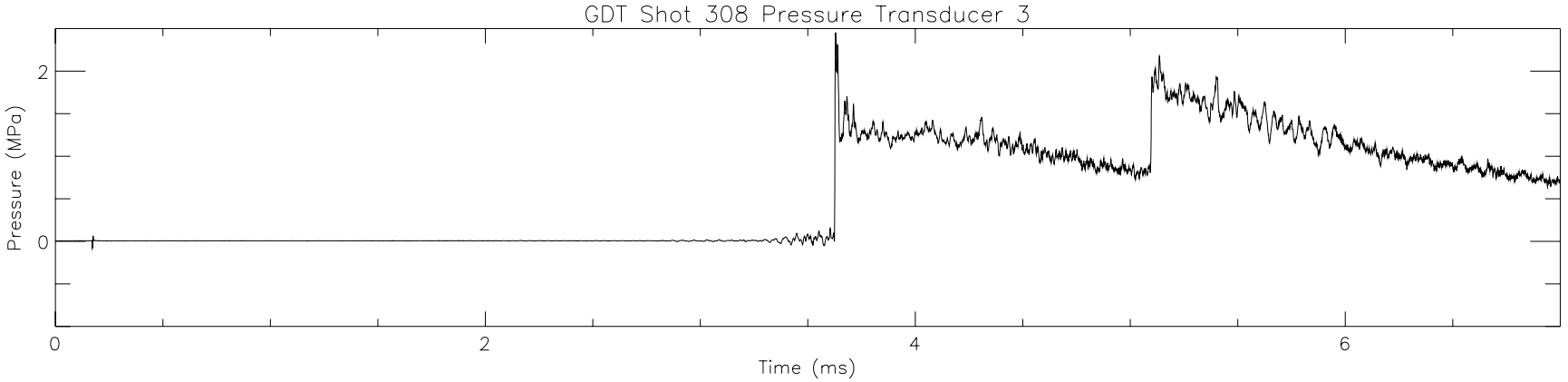
GDT Shot 308 Pressure Transducer 3
Pressure (MPa)
2
0
0
2
4
6
Time (ms)

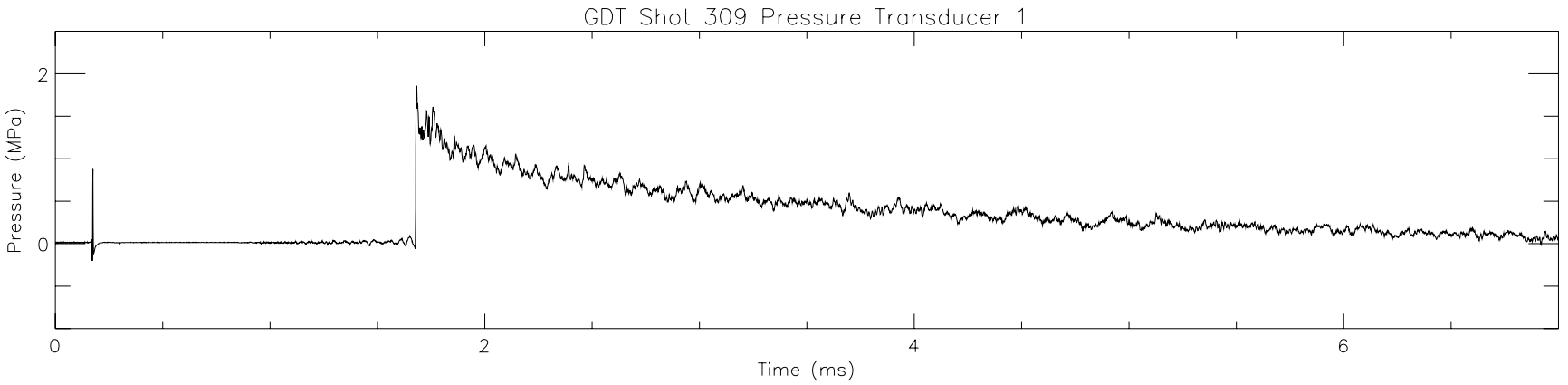
GDT Shot 309 Pressure Transducer 1
Pressure (MPa)
2
0
0
2
4
6
Time (ms)

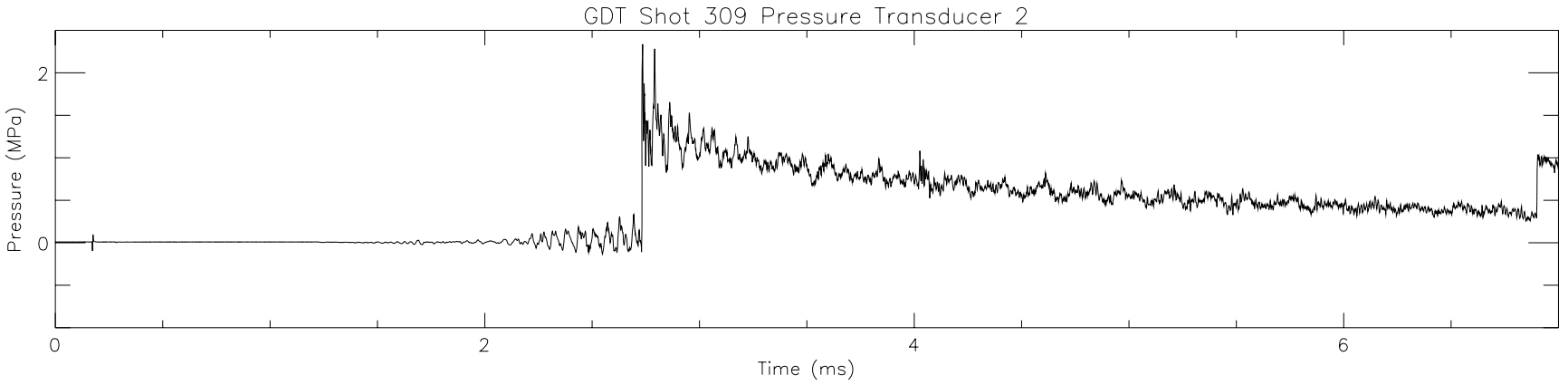
GDT Shot 309 Pressure Transducer 2
Pressure (MPa)
2
0
0
2
4
6
Time (ms)

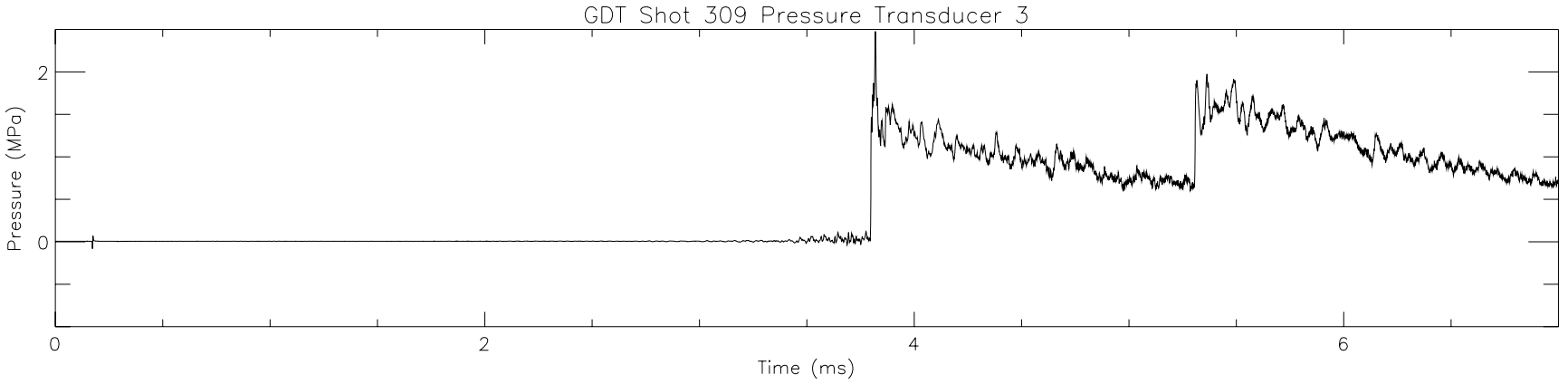
GDT Shot 309 Pressure Transducer 3
Pressure (MPa)
2
0
0
2
4
6
Time (ms)

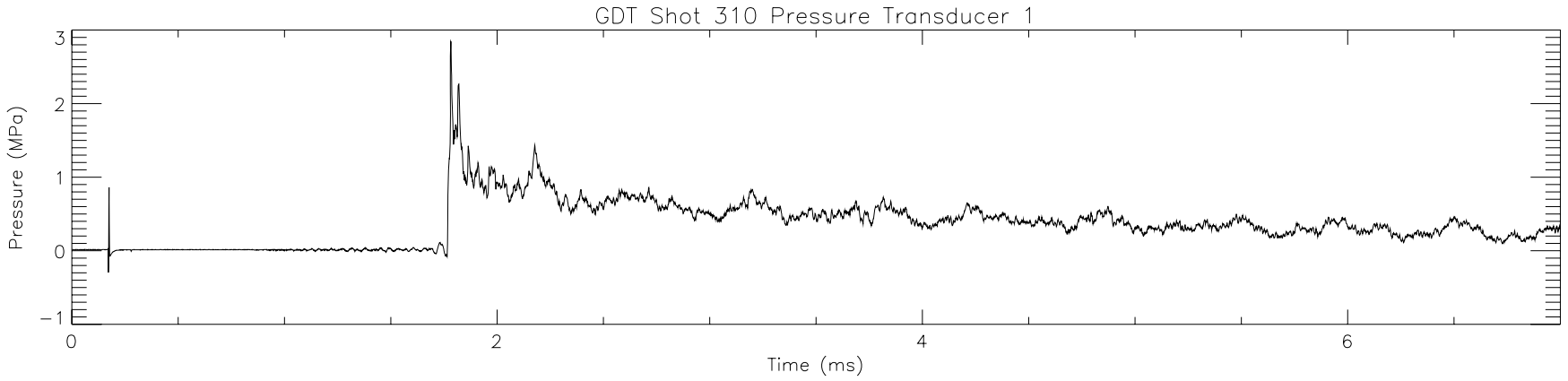
GDT Shot 310 Pressure Transducer 1
Pressure (MPa)
3
2
1
0
−1
0
2
4
6
Time (ms)

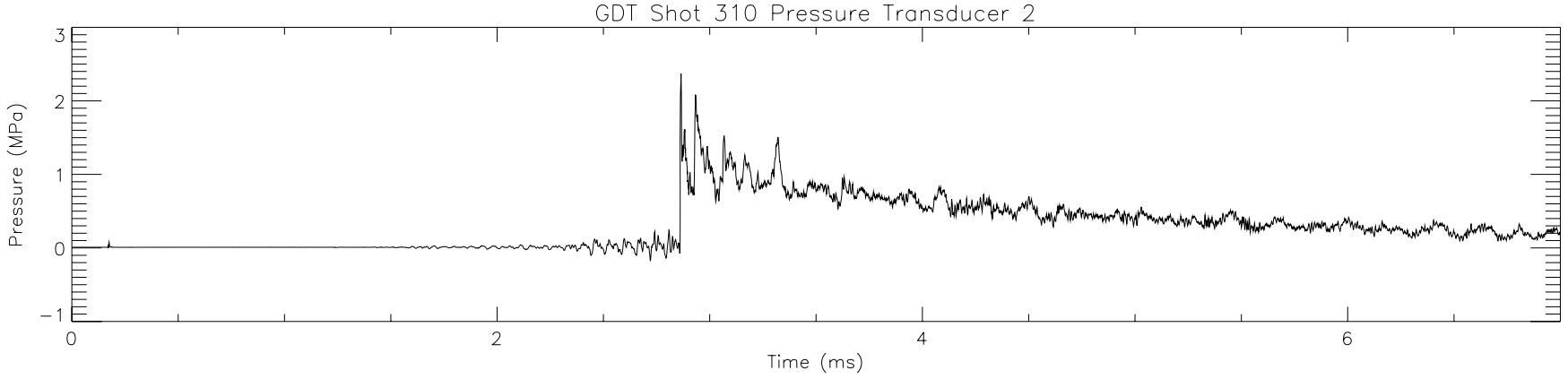
GDT Shot 310 Pressure Transducer 2
Pressure (MPa)
3
2
1
0
−1
0
2
4
6
Time (ms)

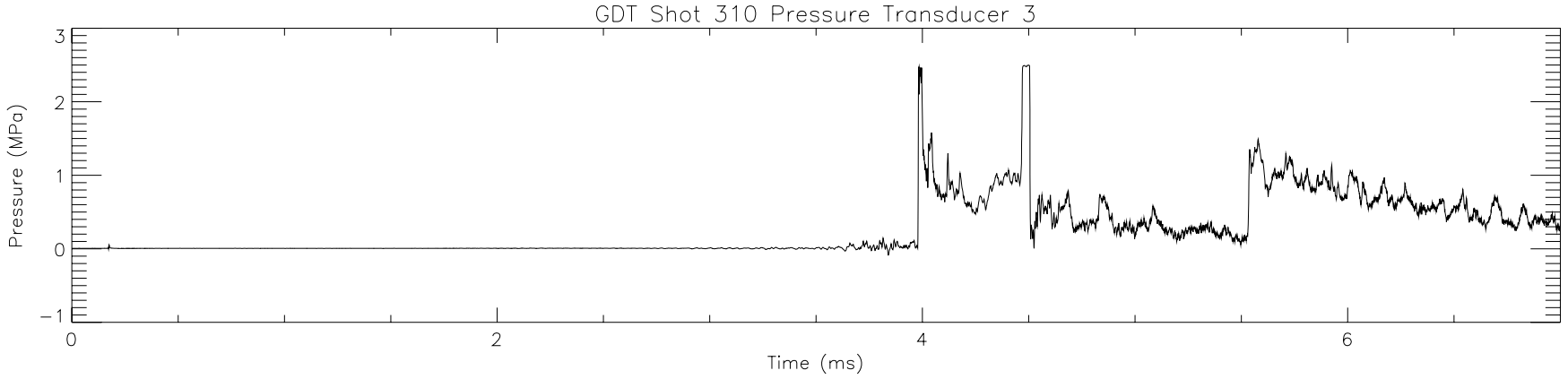
GDT Shot 310 Pressure Transducer 3
Pressure (MPa)
3
2
1
0
−1
0
2
4
6
Time (ms)

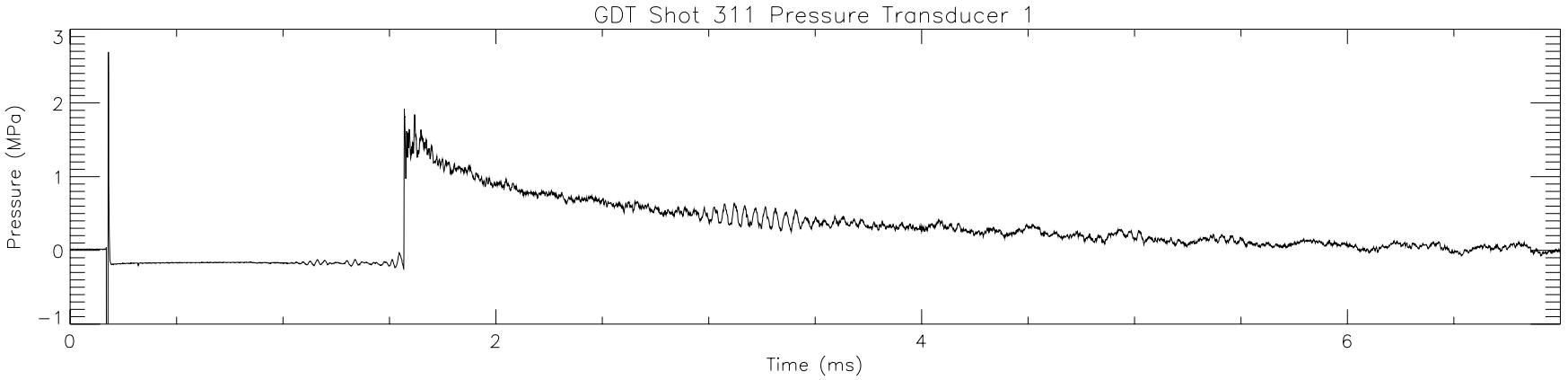
GDT Shot 311 Pressure Transducer 1
Pressure (MPa)
3
2
1
0
−1
0
2
4
6
Time (ms)

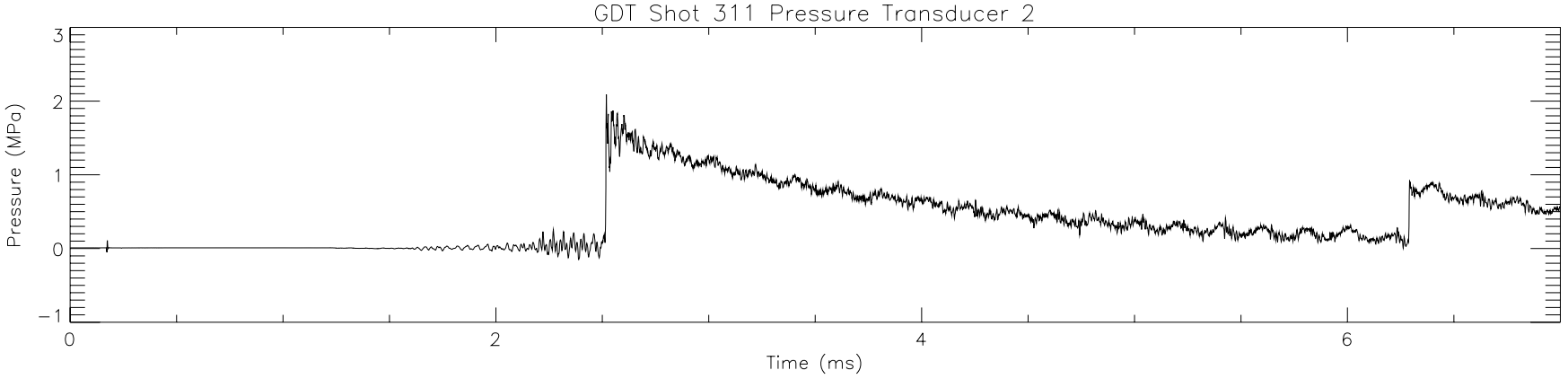
GDT Shot 311 Pressure Transducer 2
Pressure (MPa)
3
2
1
0
−1
0
2
4
6
Time (ms)

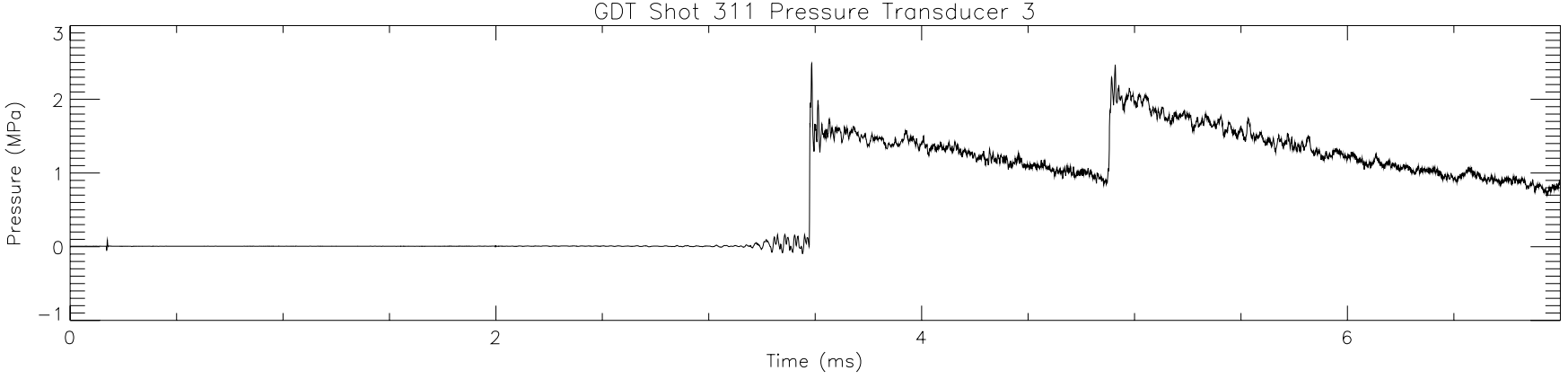
GDT Shot 311 Pressure Transducer 3
Pressure (MPa)
3
2
1
0
−1
0
2
4
6
Time (ms)

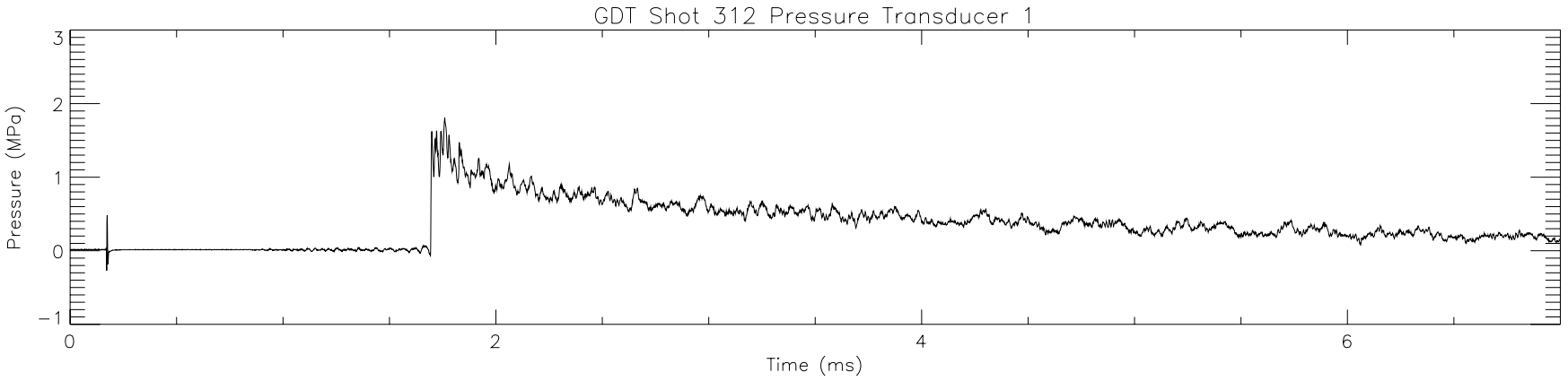
GDT Shot 312 Pressure Transducer 1
Pressure (MPa)
Time (ms)
3
2
1
0
−1
0
2
4
6

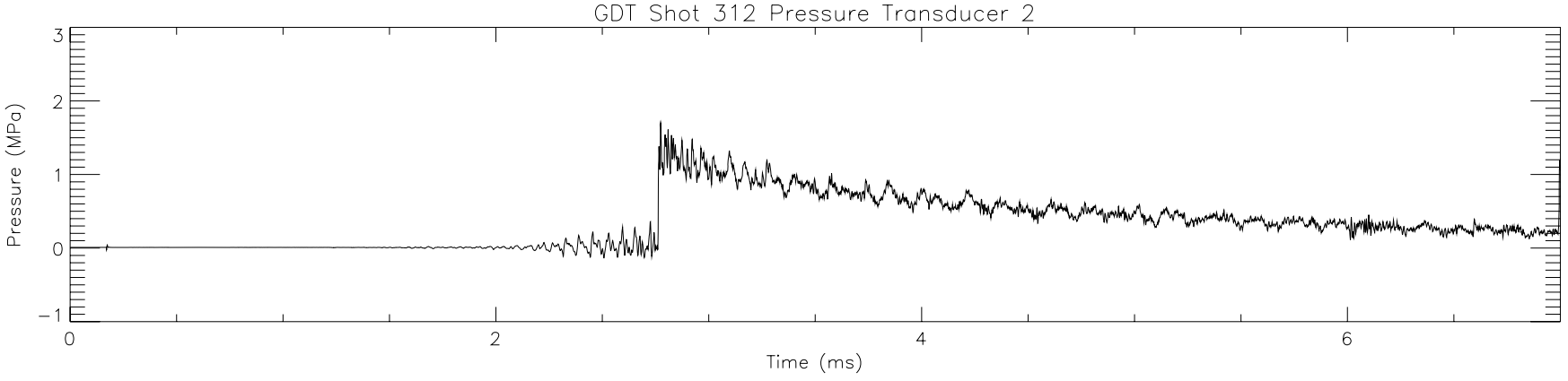
GDT Shot 312 Pressure Transducer 2
Pressure (MPa)
Time (ms)
3
2
1
0
−1
0
2
4
6

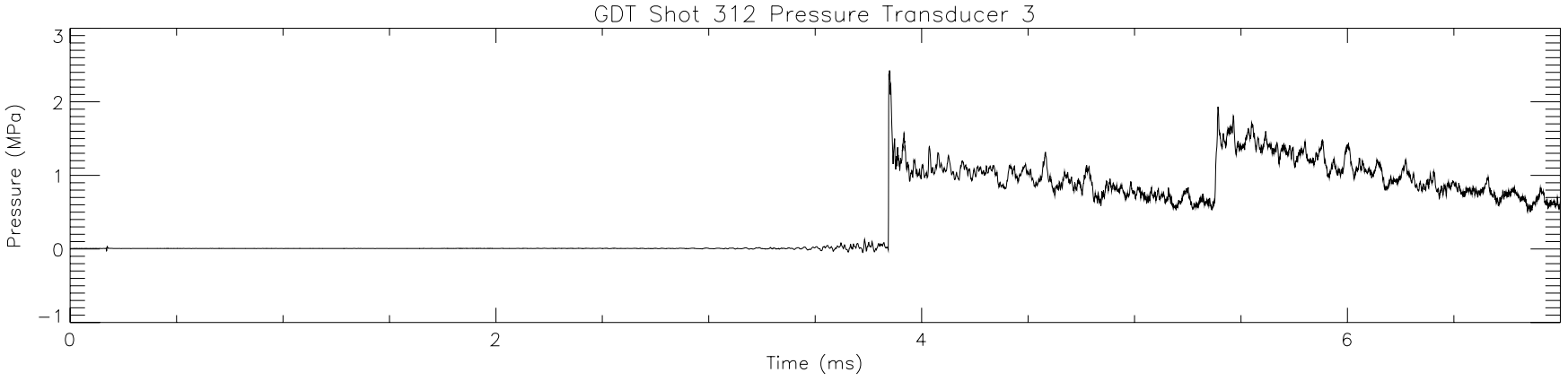
GDT Shot 312 Pressure Transducer 3
Pressure (MPa)
Time (ms)
3
2
1
0
−1
0
2
4
6

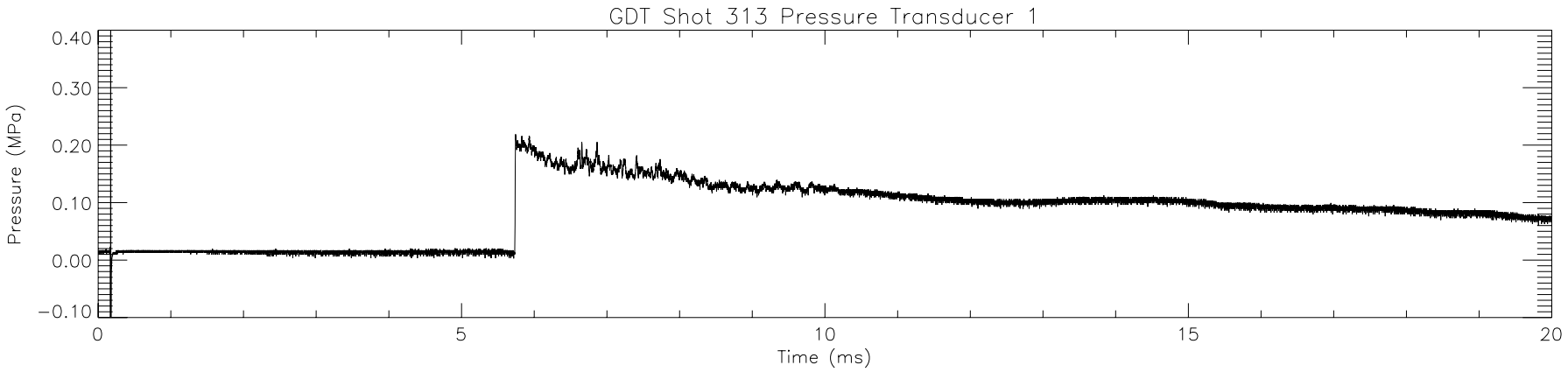
GDT Shot 313 Pressure Transducer 1
Pressure (MPa)
0.40
0.30
0.20
0.10
0.00
−0.10
0
5
10
15
20
Time (ms)

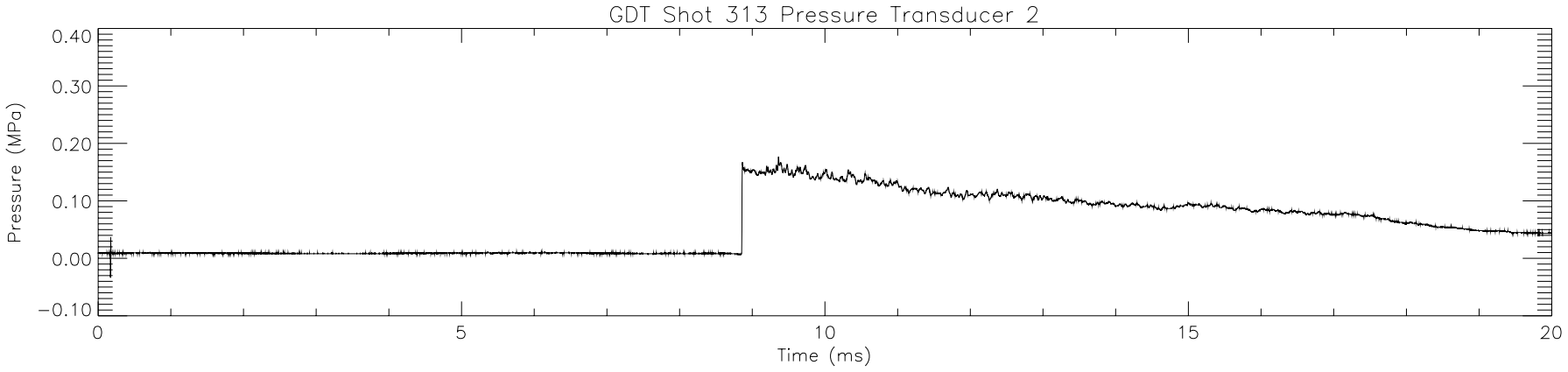
GDT Shot 313 Pressure Transducer 2
Pressure (MPa)
0.40
0.30
0.20
0.10
0.00
−0.10
0
5
10
15
20
Time (ms)

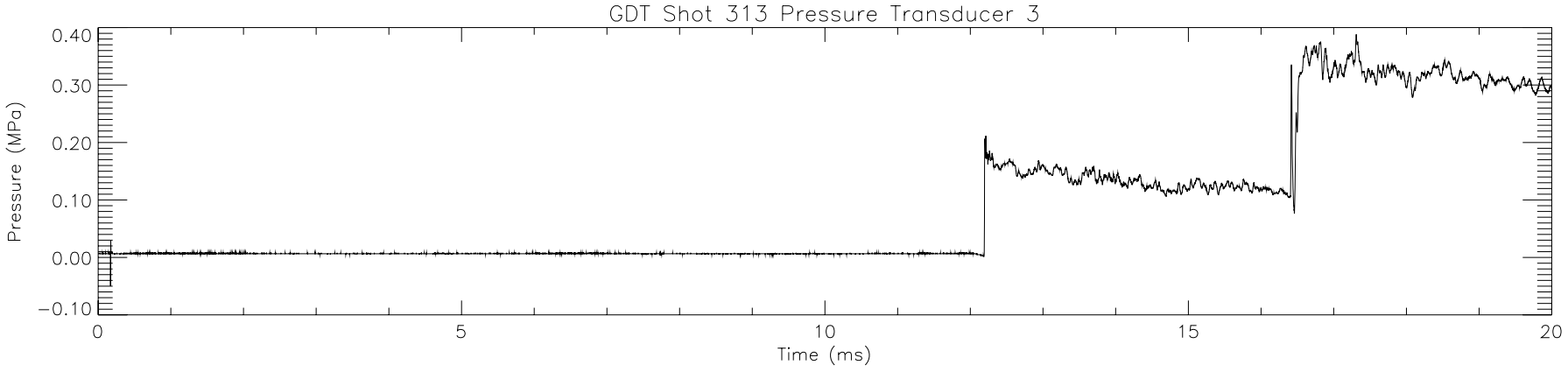
GDT Shot 313 Pressure Transducer 3
Pressure (MPa)
0.40
0.30
0.20
0.10
0.00
−0.10
0
5
10
15
20
Time (ms)

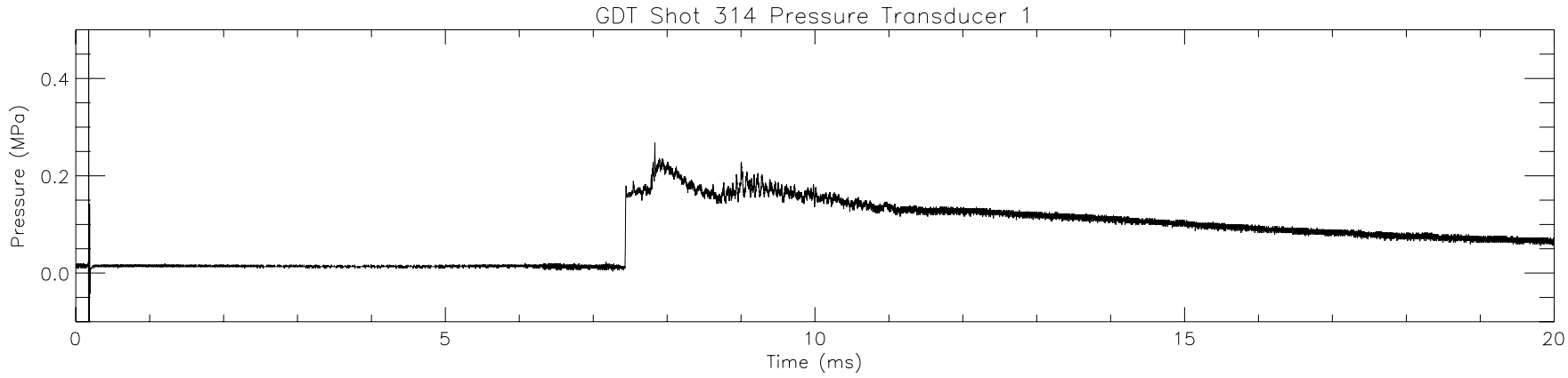
GDT Shot 314 Pressure Transducer 1
Pressure (MPa)
0.4
0.2
0.0
0
5
10
15
20
Time (ms)

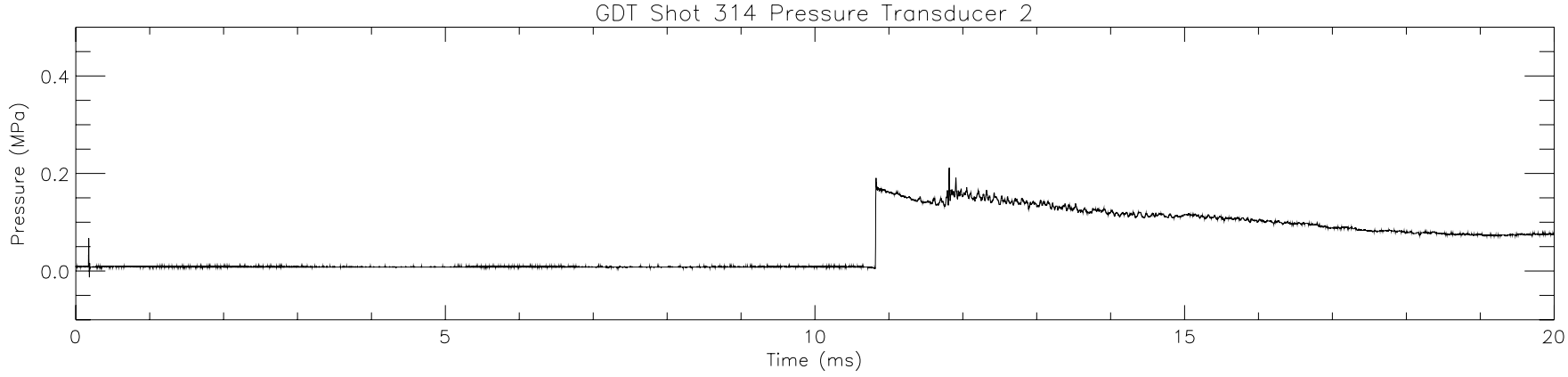
GDT Shot 314 Pressure Transducer 2
Pressure (MPa)
0.4
0.2
0.0
0
5
10
15
20
Time (ms)

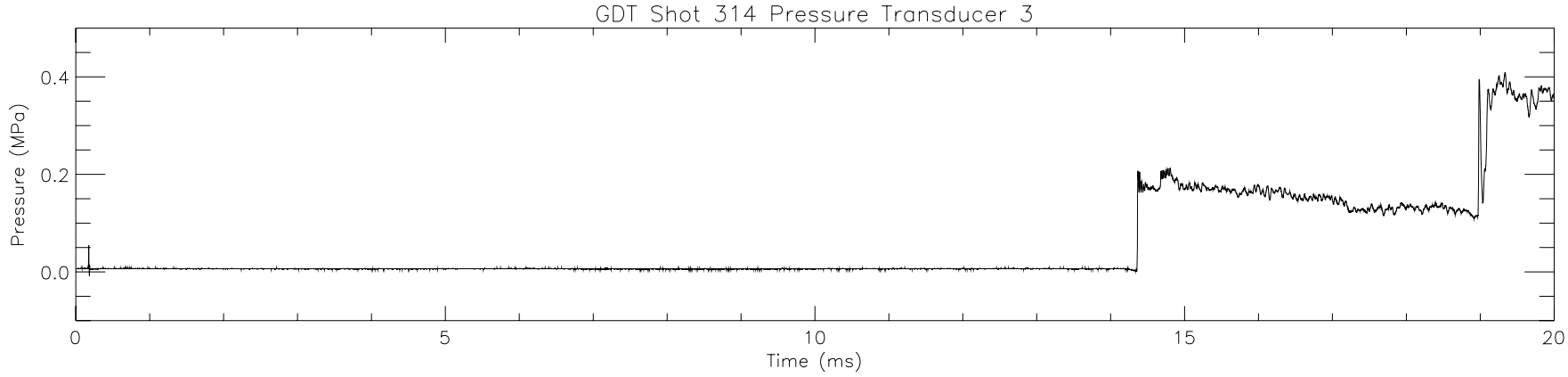
GDT Shot 314 Pressure Transducer 3
Pressure (MPa)
0.4
0.2
0.0
0
5
10
15
20
Time (ms)

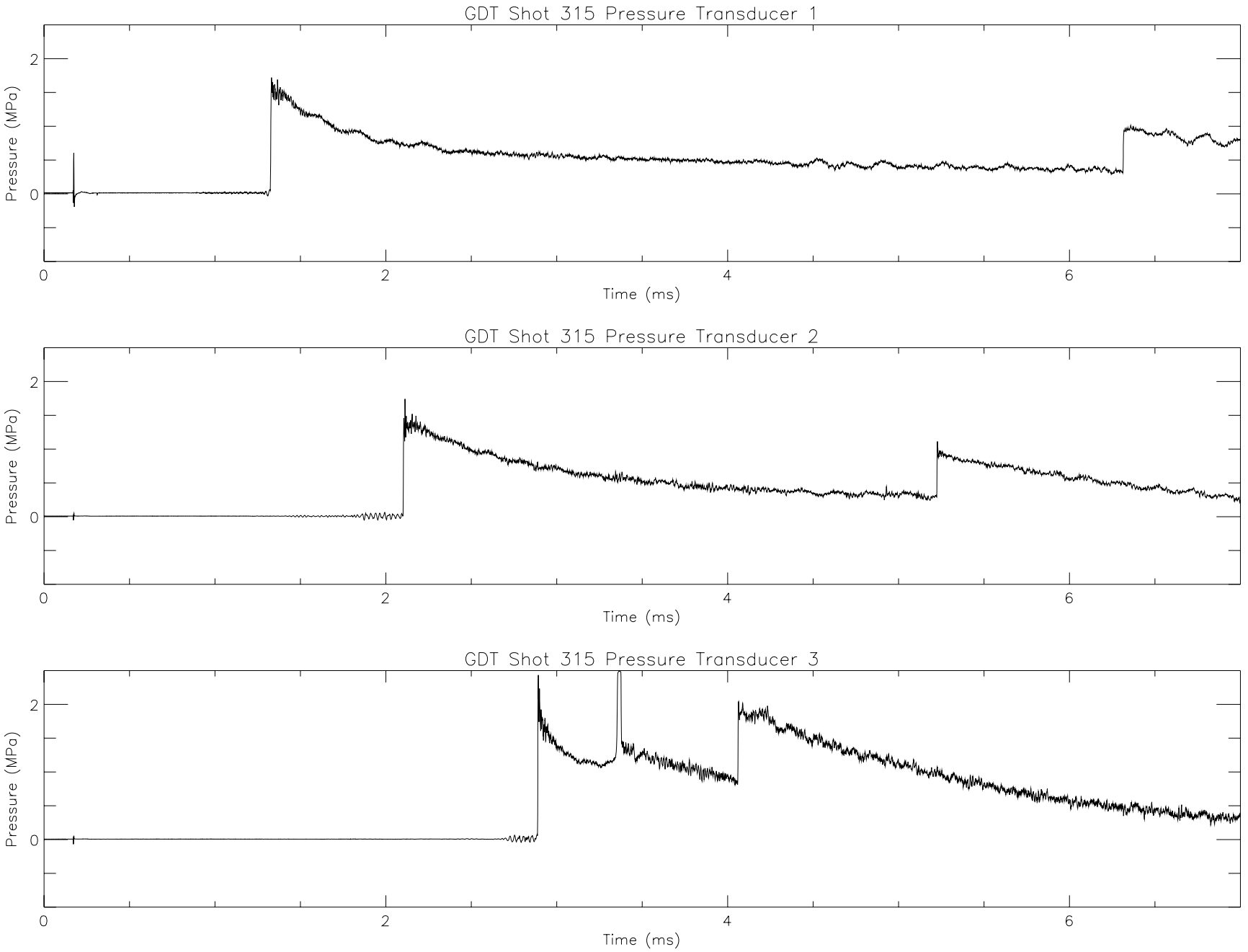
GDT Shot 315 Pressure Transducer 1
Pressure (MPa)
2
0
0
2
4
6
Time (ms)
GDT Shot 315 Pressure Transducer 2
Pressure (MPa)
2
0
0
2
4
6
Time (ms)
GDT Shot 315 Pressure Transducer 3
Pressure (MPa)
2
0
0
2
4
6
Time (ms)

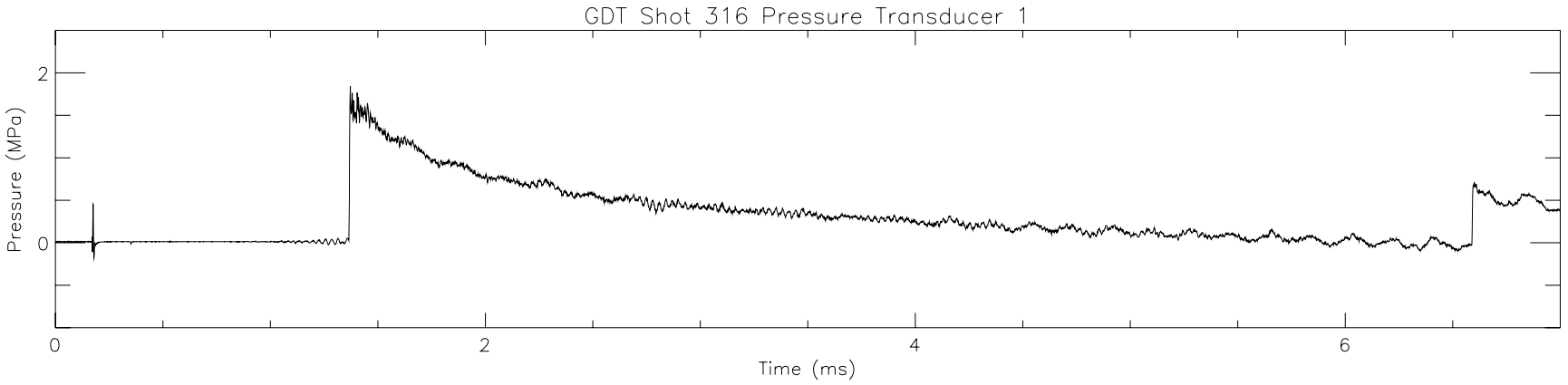
GDT Shot 316 Pressure Transducer 1
Pressure (MPa)
2
0
0
2
4
6
Time (ms)

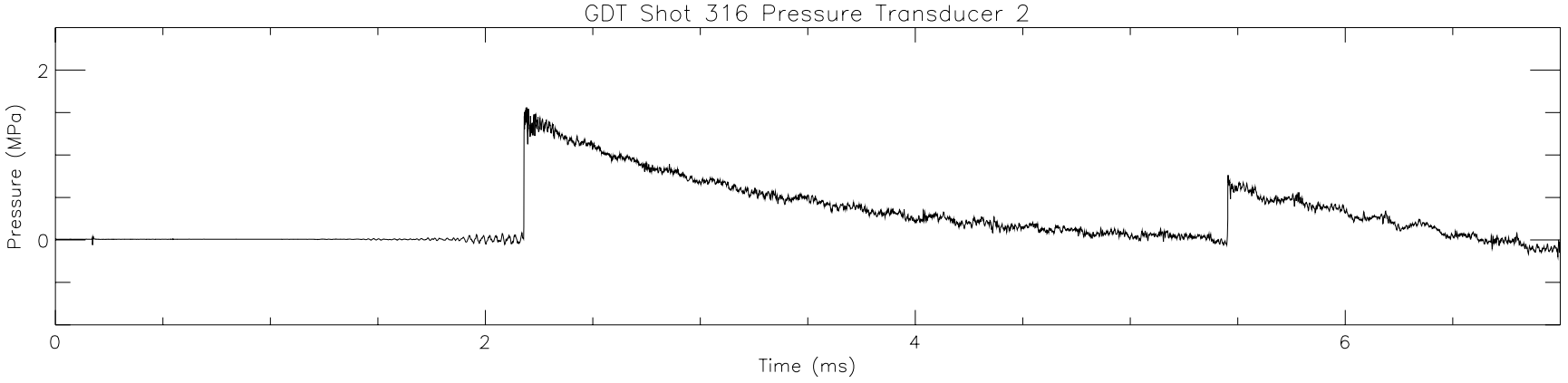
GDT Shot 316 Pressure Transducer 2
Pressure (MPa)
2
0
0
2
4
6
Time (ms)

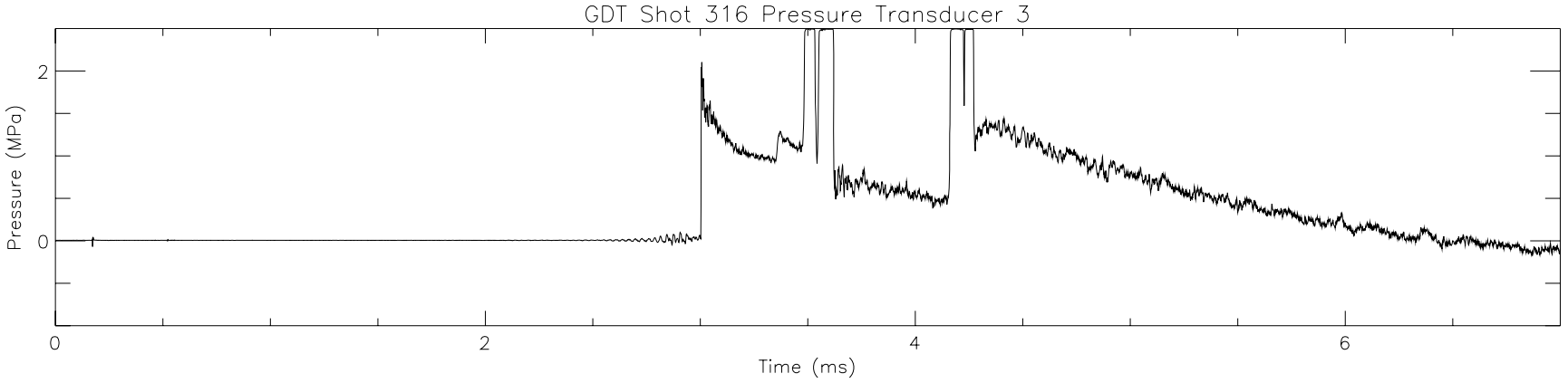
GDT Shot 316 Pressure Transducer 3
Pressure (MPa)
2
0
0
2
4
6
Time (ms)

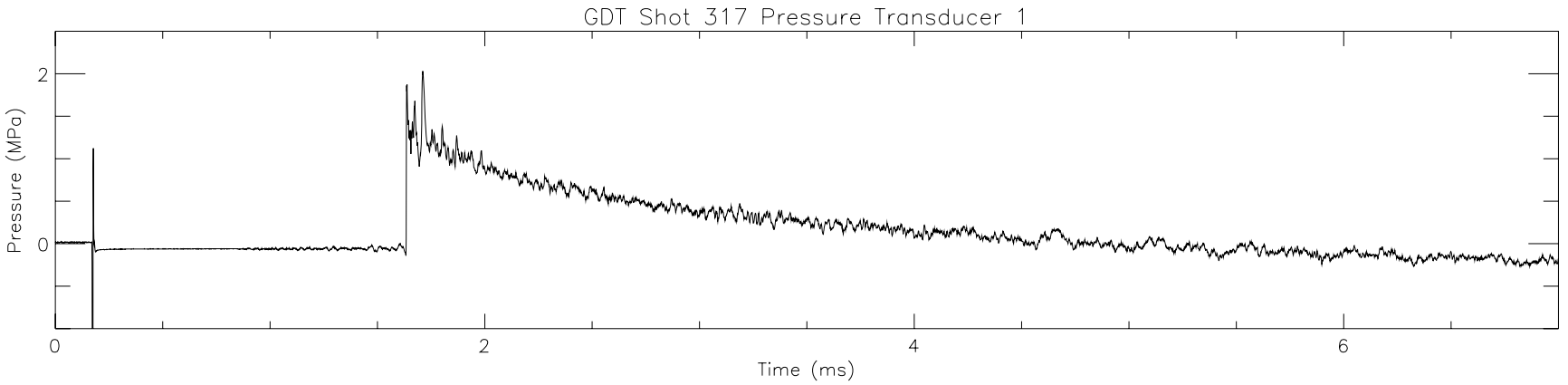
GDT Shot 317 Pressure Transducer 1
Pressure (MPa)
2
0
0
2
4
6
Time (ms)

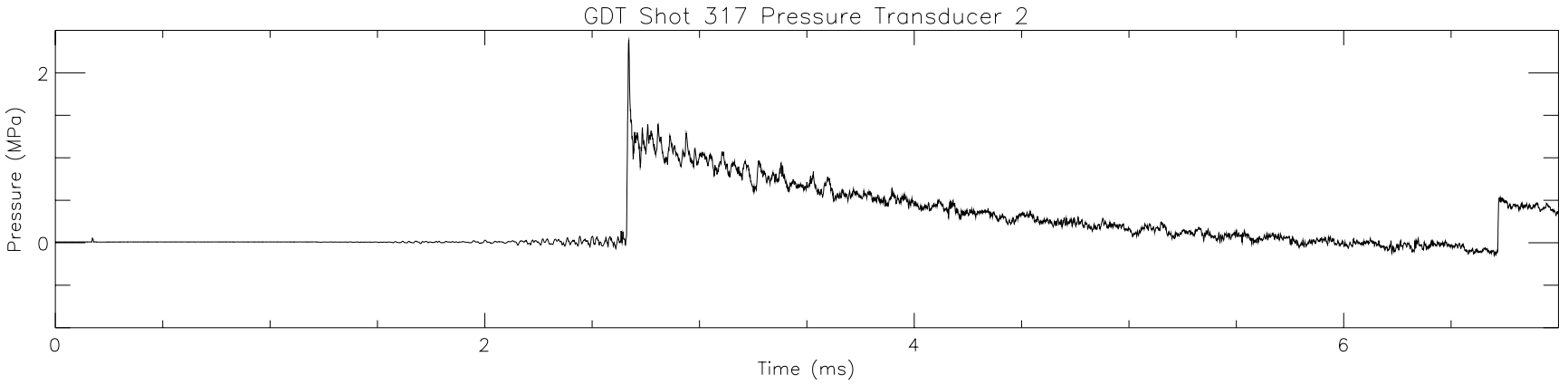
GDT Shot 317 Pressure Transducer 2
Pressure (MPa)
2
0
0
2
4
6
Time (ms)

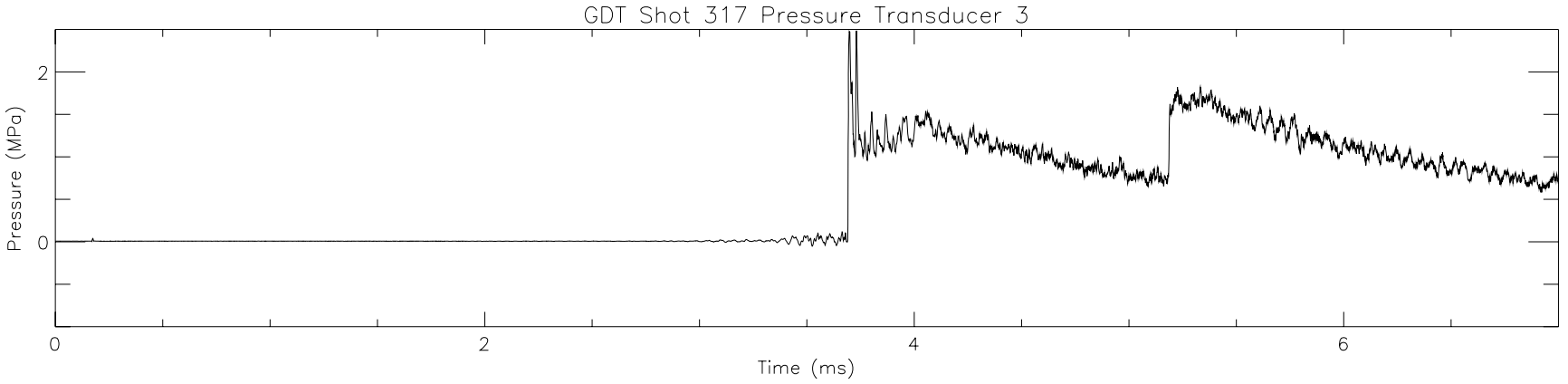
GDT Shot 317 Pressure Transducer 3
Pressure (MPa)
2
0
0
2
4
6
Time (ms)

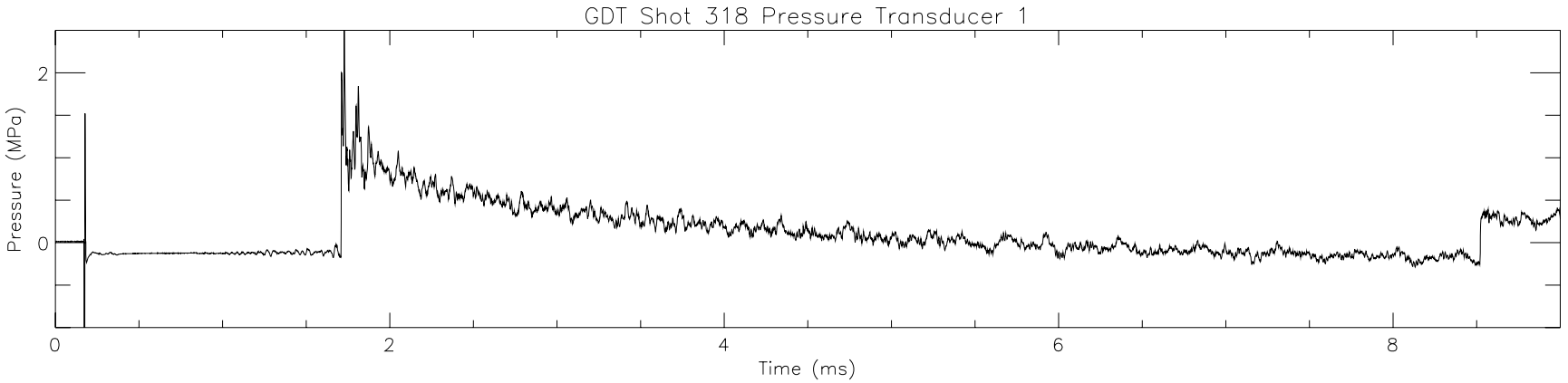
GDT Shot 318 Pressure Transducer 1
Pressure (MPa)
2
0
0
2
4
6
8
Time (ms)

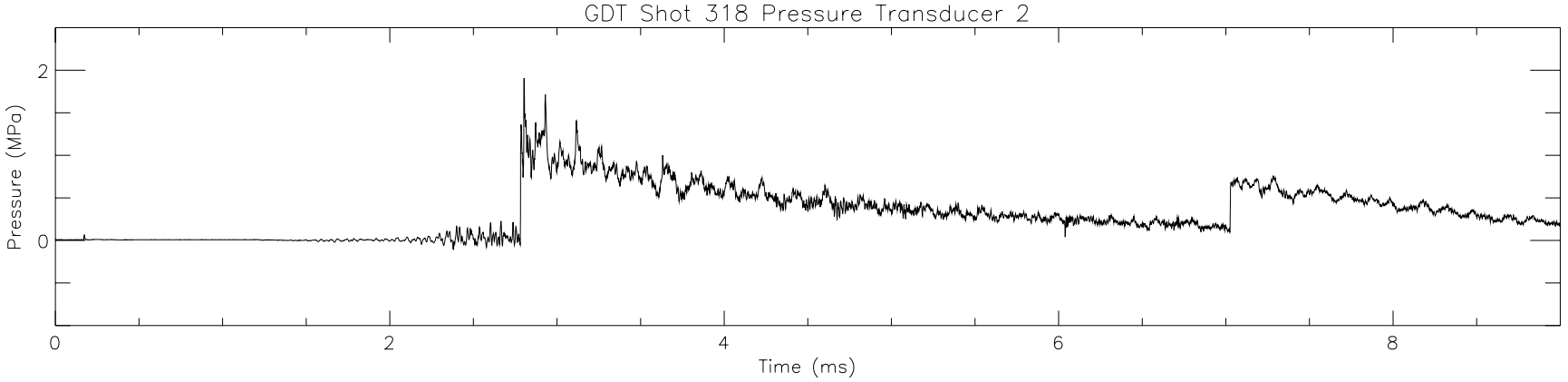
GDT Shot 318 Pressure Transducer 2
Pressure (MPa)
2
0
0
2
4
6
8
Time (ms)

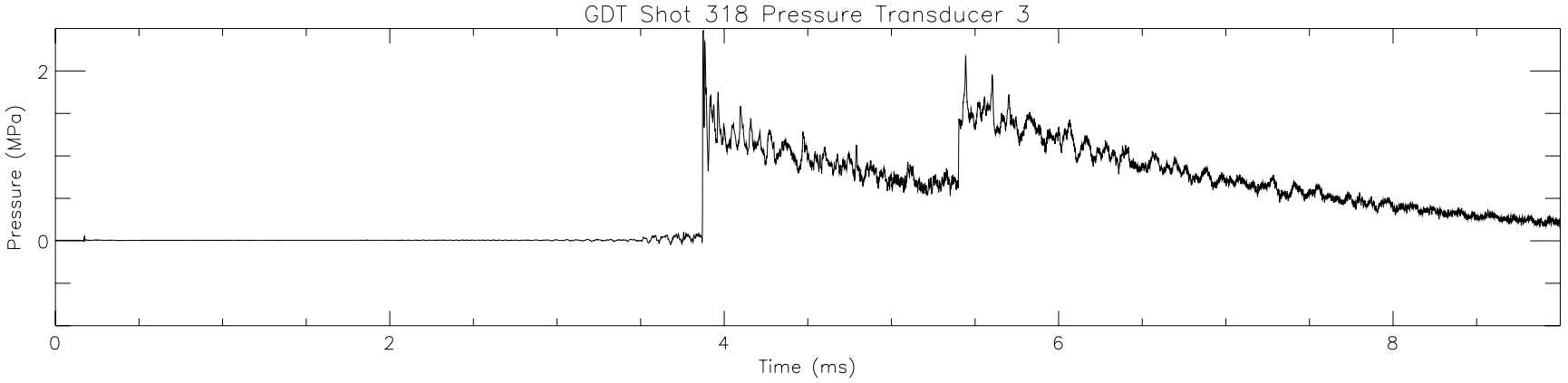
GDT Shot 318 Pressure Transducer 3
Pressure (MPa)
2
0
0
2
4
6
8
Time (ms)

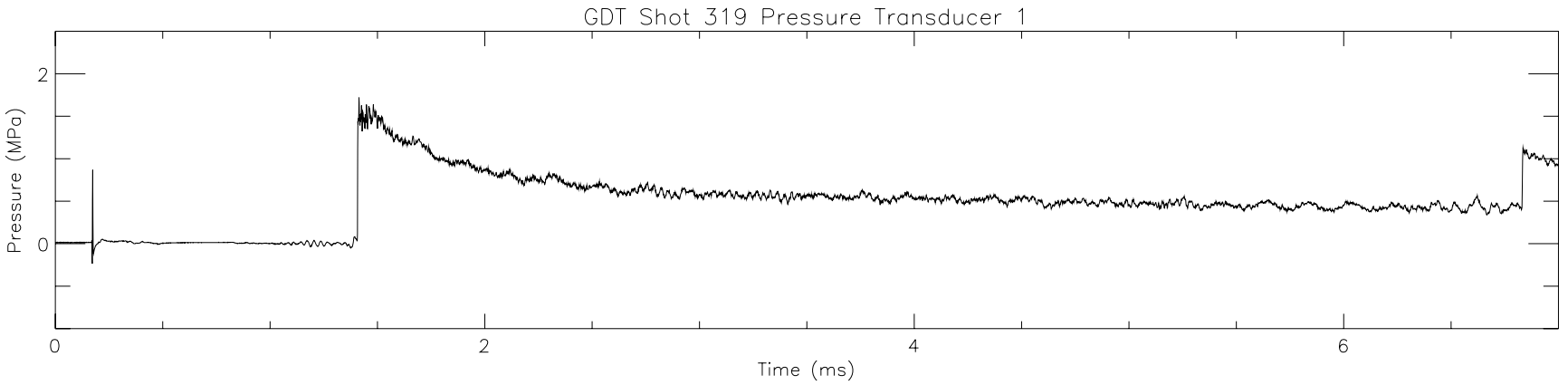
GDT Shot 319 Pressure Transducer 1
Pressure (MPa)
2
0
0
2
4
6
Time (ms)

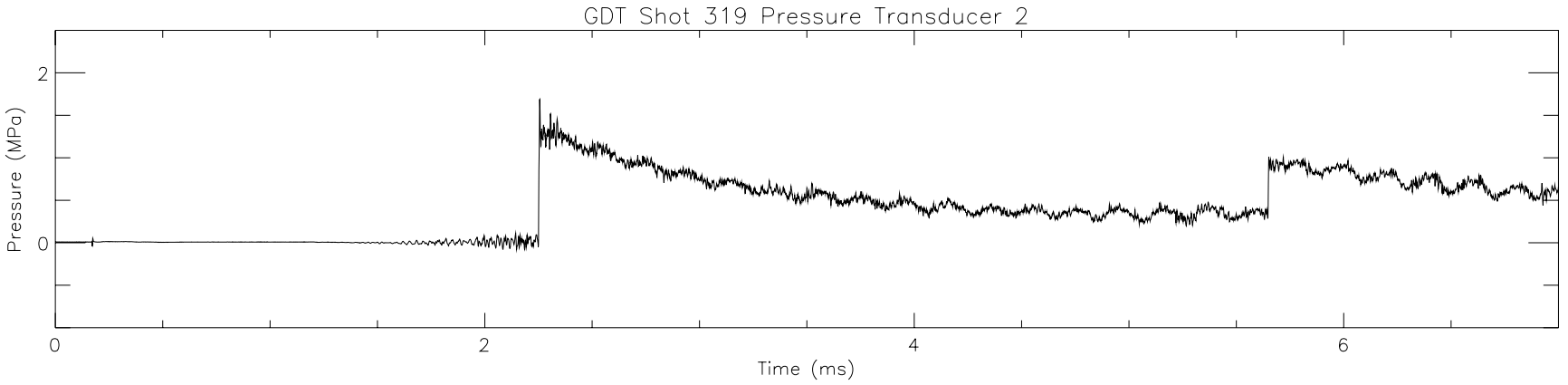
GDT Shot 319 Pressure Transducer 2
Pressure (MPa)
2
0
0
2
4
6
Time (ms)

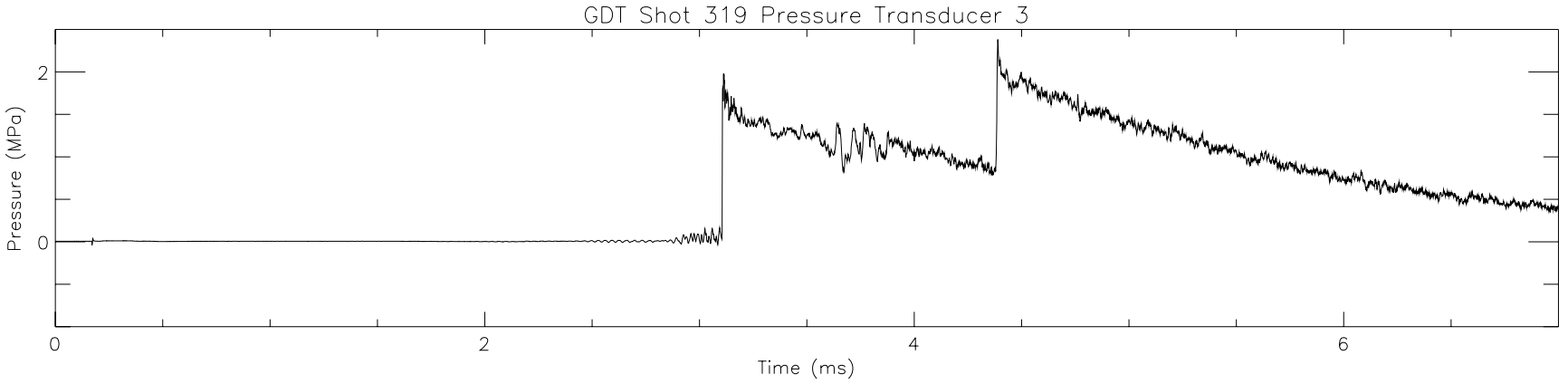
GDT Shot 319 Pressure Transducer 3
Pressure (MPa)
2
0
0
2
4
6
Time (ms)

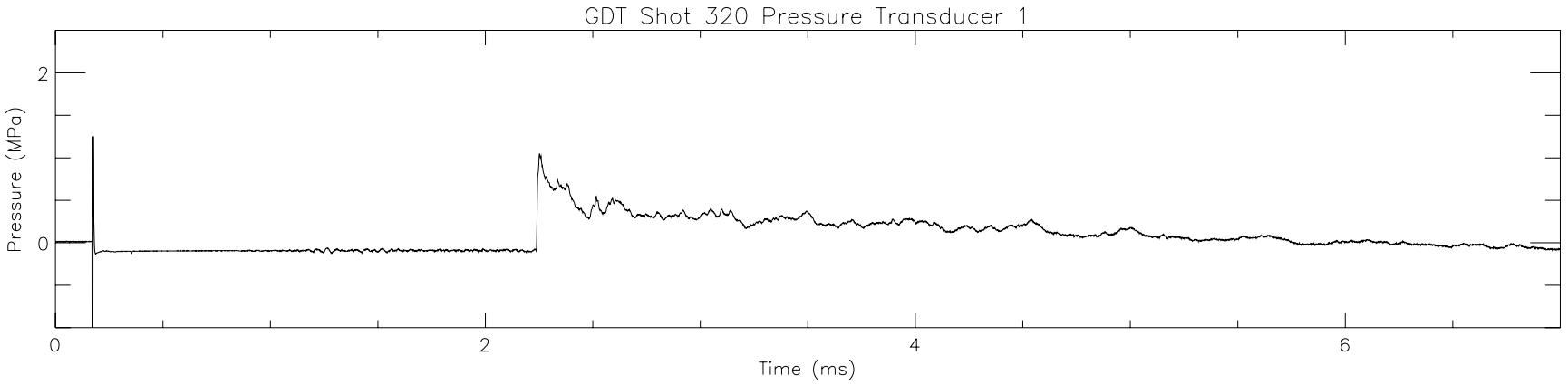
GDT Shot 320 Pressure Transducer 1
Pressure (MPa)
2
0
0
2
4
6
Time (ms)

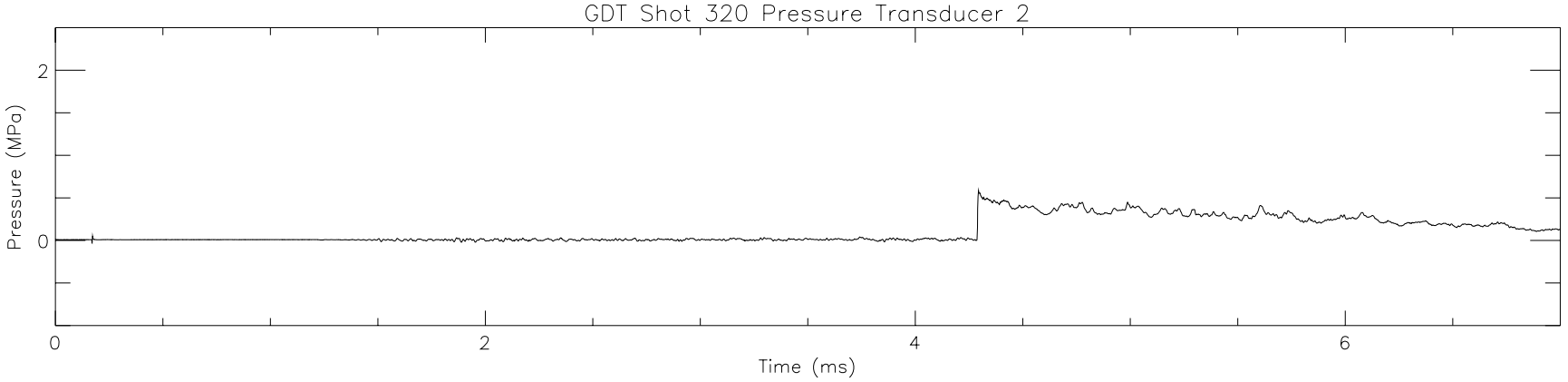
GDT Shot 320 Pressure Transducer 2
Pressure (MPa)
2
0
0
2
4
6
Time (ms)

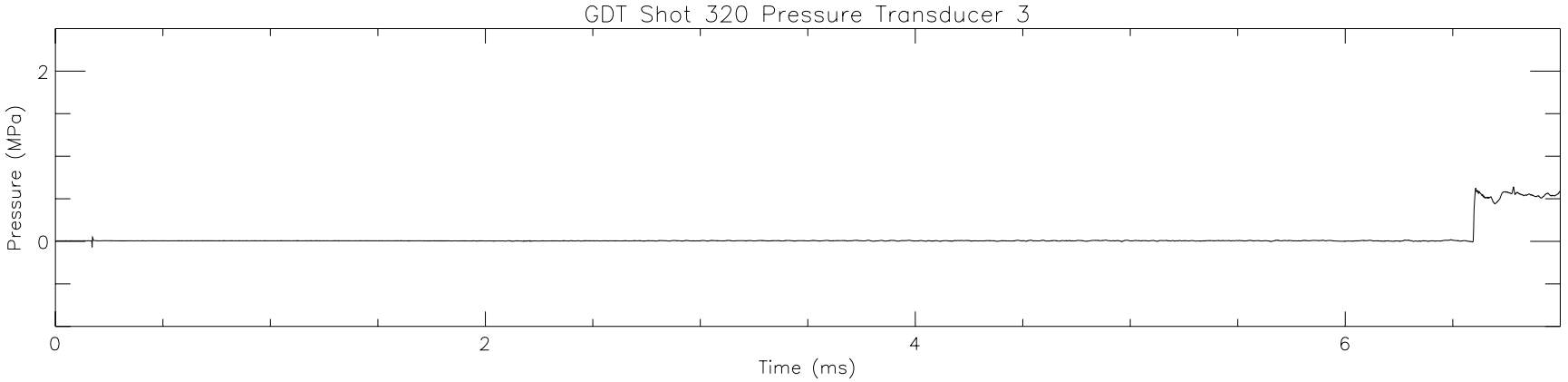
GDT Shot 320 Pressure Transducer 3
Pressure (MPa)
2
0
0
2
4
6
Time (ms)

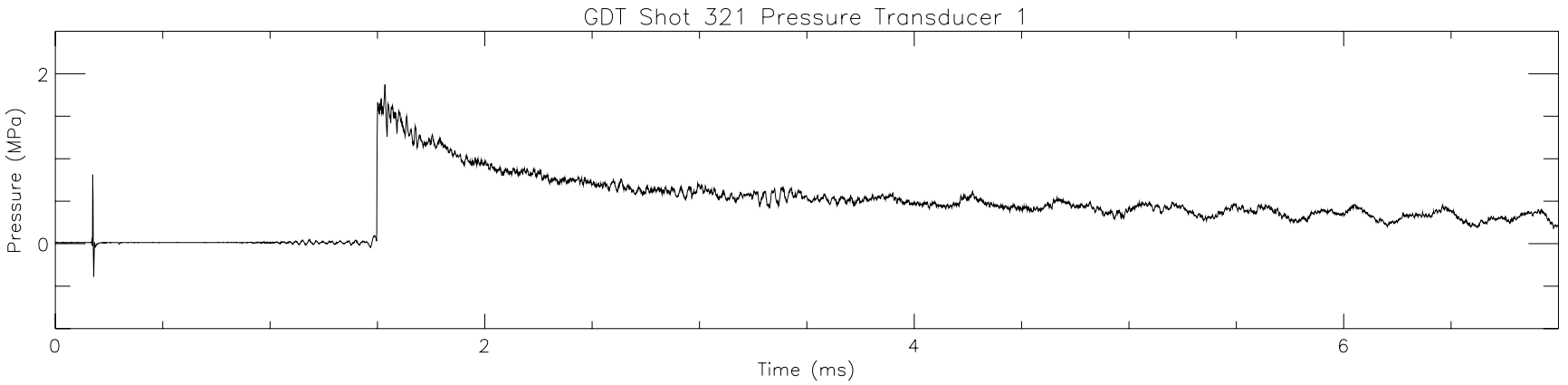
GDT Shot 321 Pressure Transducer 1
Pressure (MPa)
2
0
0
2
4
6
Time (ms)

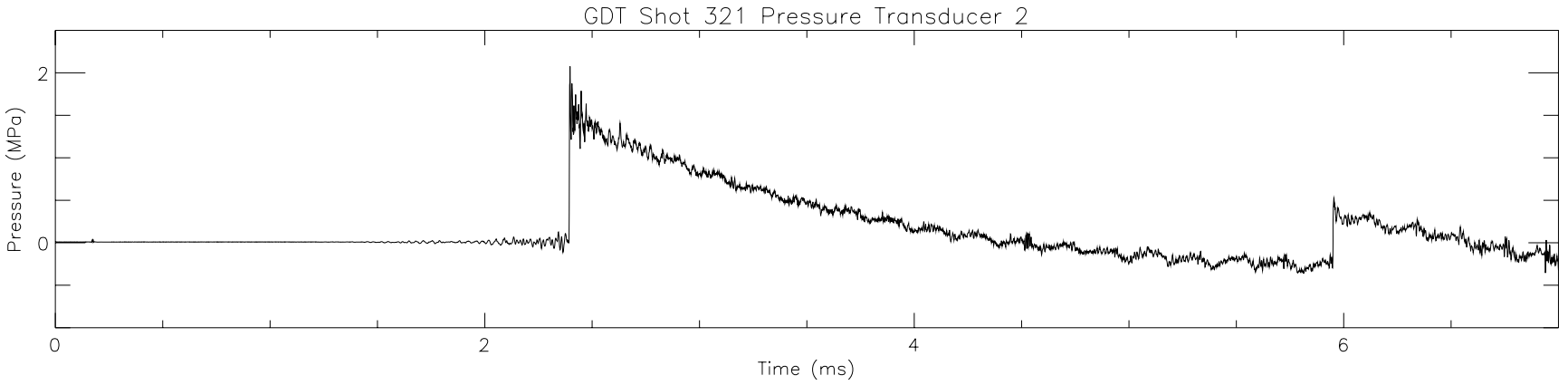
GDT Shot 321 Pressure Transducer 2
Pressure (MPa)
2
0
0
2
4
6
Time (ms)

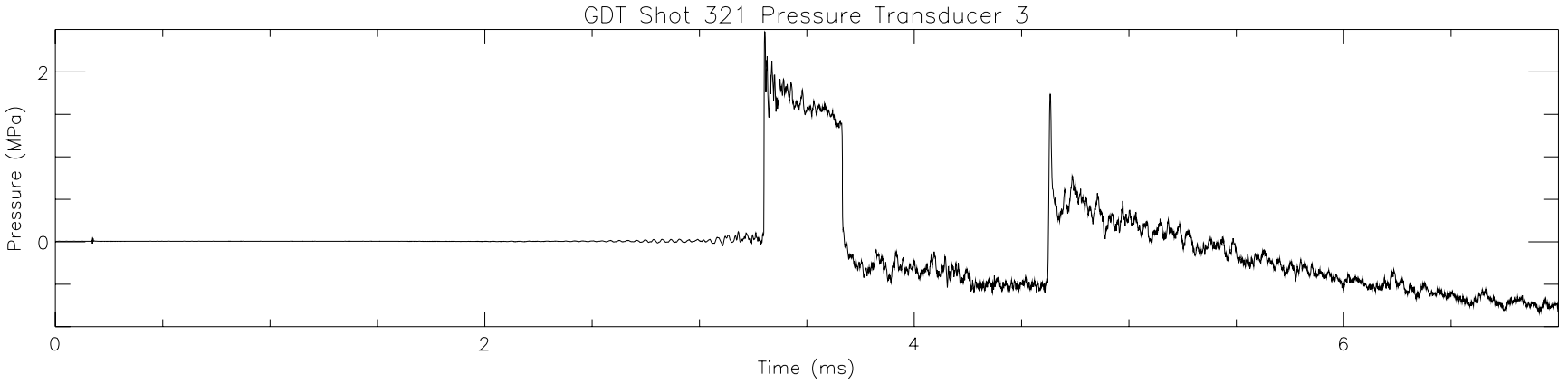
GDT Shot 321 Pressure Transducer 3
Pressure (MPa)
2
0
0
2
4
6
Time (ms)

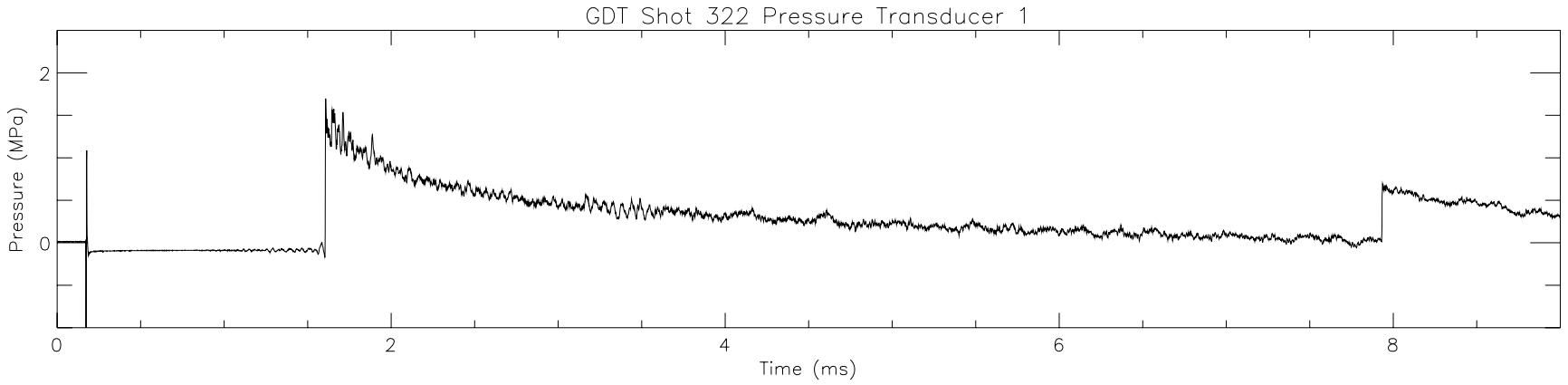
GDT Shot 322 Pressure Transducer 1
Pressure (MPa)
2
0
0
2
4
6
8
Time (ms)

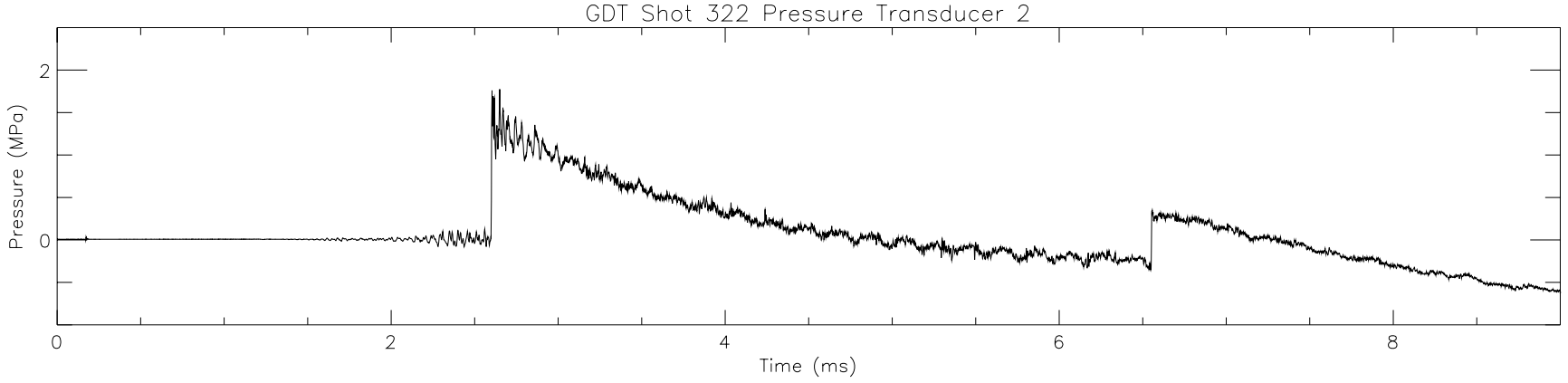
GDT Shot 322 Pressure Transducer 2
Pressure (MPa)
2
0
0
2
4
6
8
Time (ms)

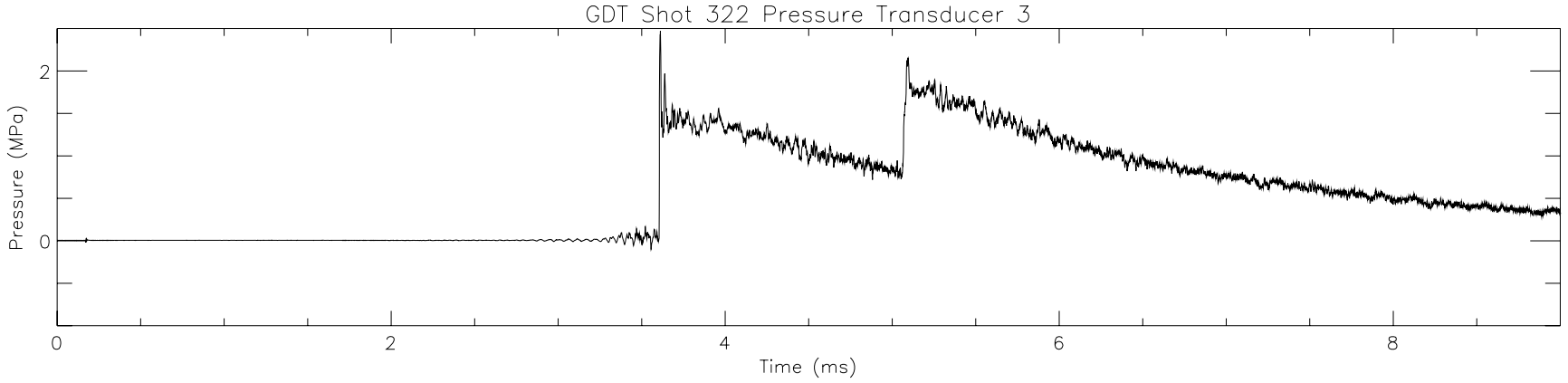
GDT Shot 322 Pressure Transducer 3
Pressure (MPa)
2
0
0
2
4
6
8
Time (ms)

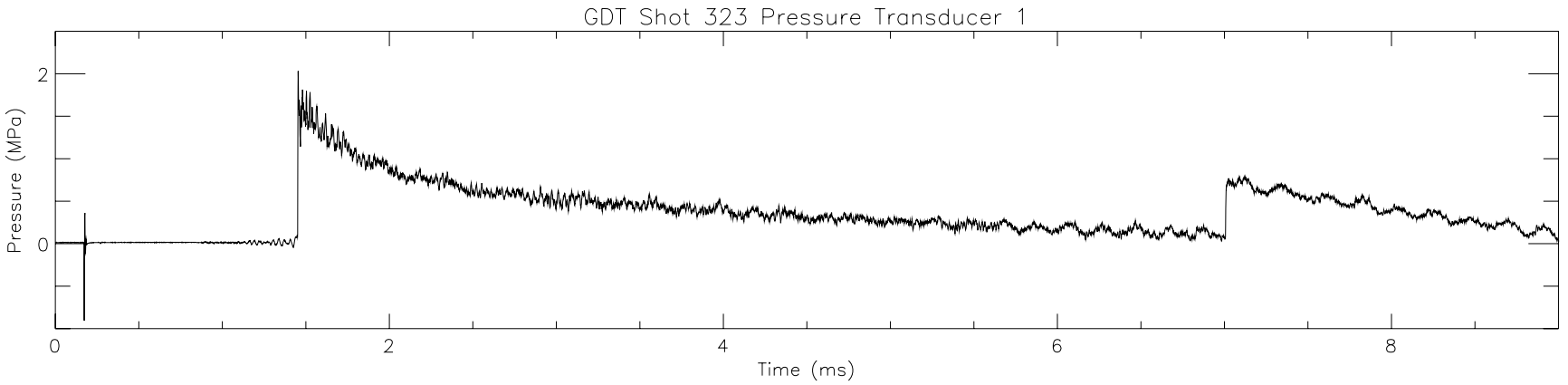
GDT Shot 323 Pressure Transducer 1
Pressure (MPa)
2
0
0
2
4
6
8
Time (ms)

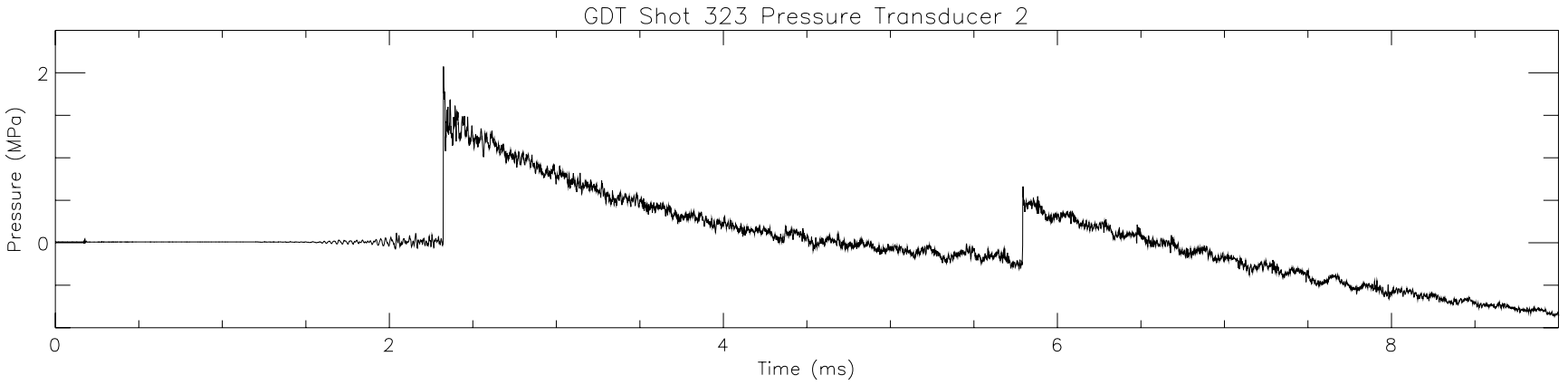
GDT Shot 323 Pressure Transducer 2
Pressure (MPa)
2
0
0
2
4
6
8
Time (ms)

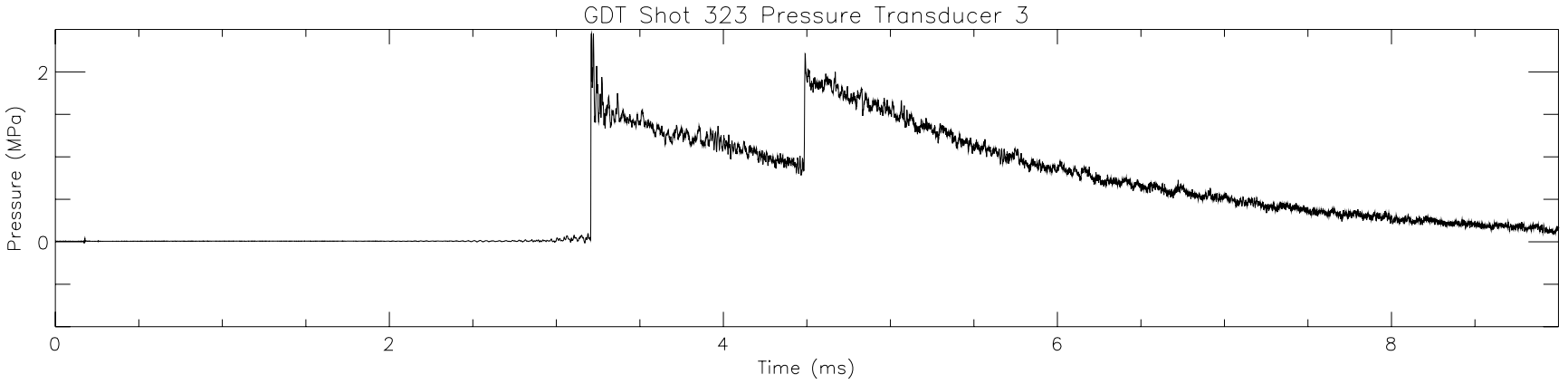
GDT Shot 323 Pressure Transducer 3
Pressure (MPa)
2
0
0
2
4
6
8
Time (ms)

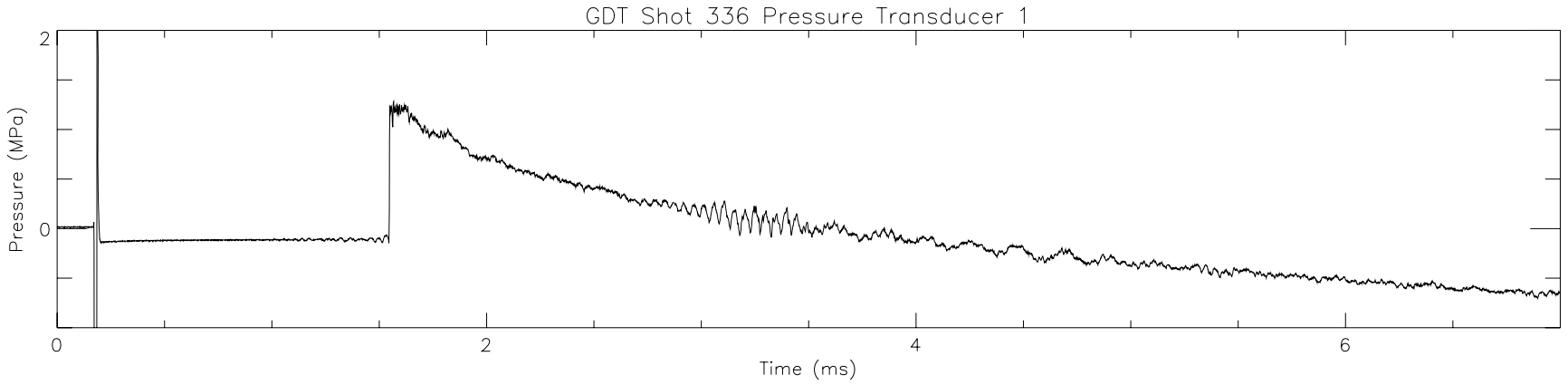
GDT Shot 336 Pressure Transducer 1
Pressure (MPa)
2
0
0
2
4
6
Time (ms)

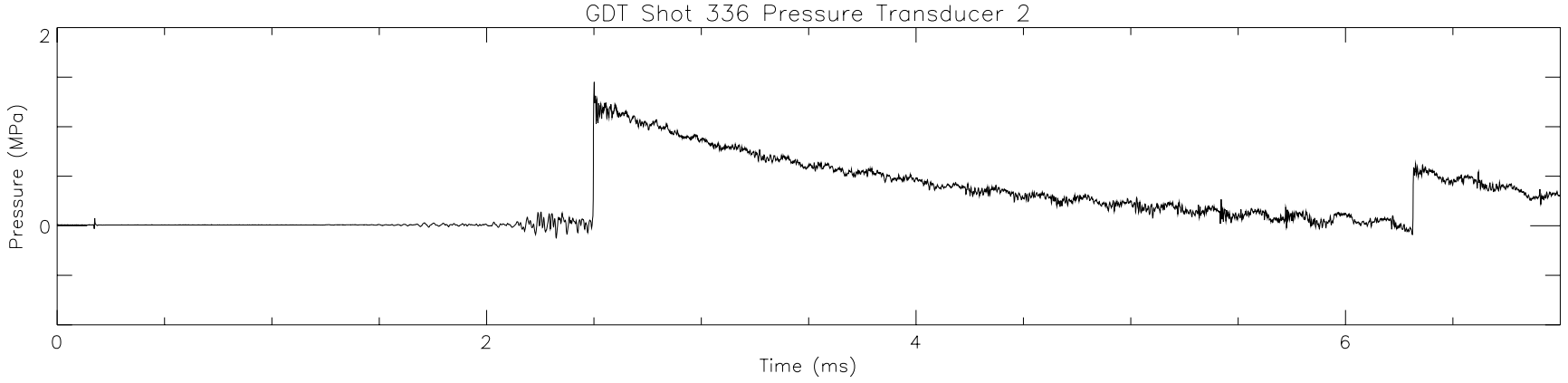
GDT Shot 336 Pressure Transducer 2
Pressure (MPa)
2
0
0
2
4
6
Time (ms)

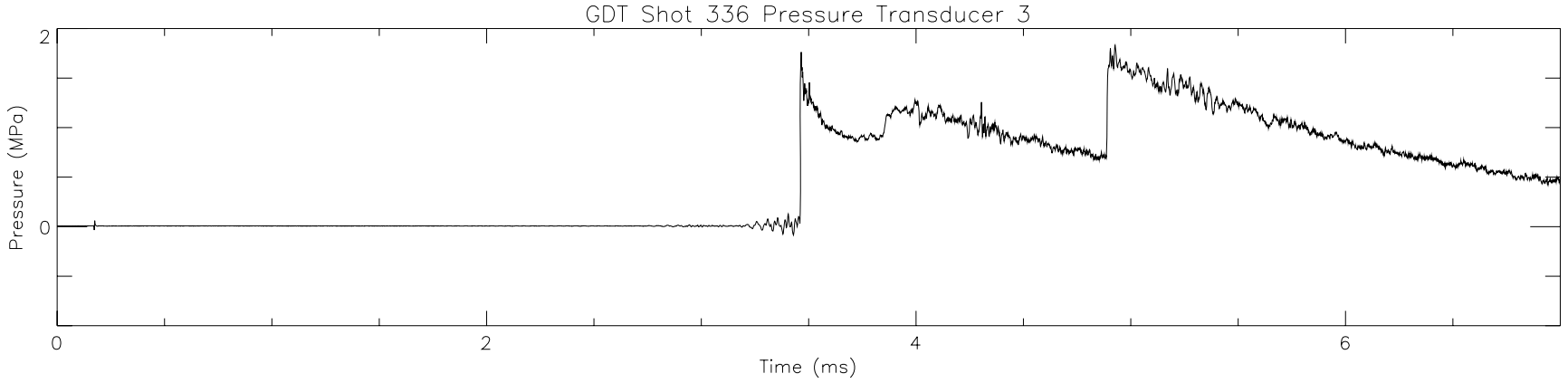
GDT Shot 336 Pressure Transducer 3
Pressure (MPa)
2
0
0
2
4
6
Time (ms)

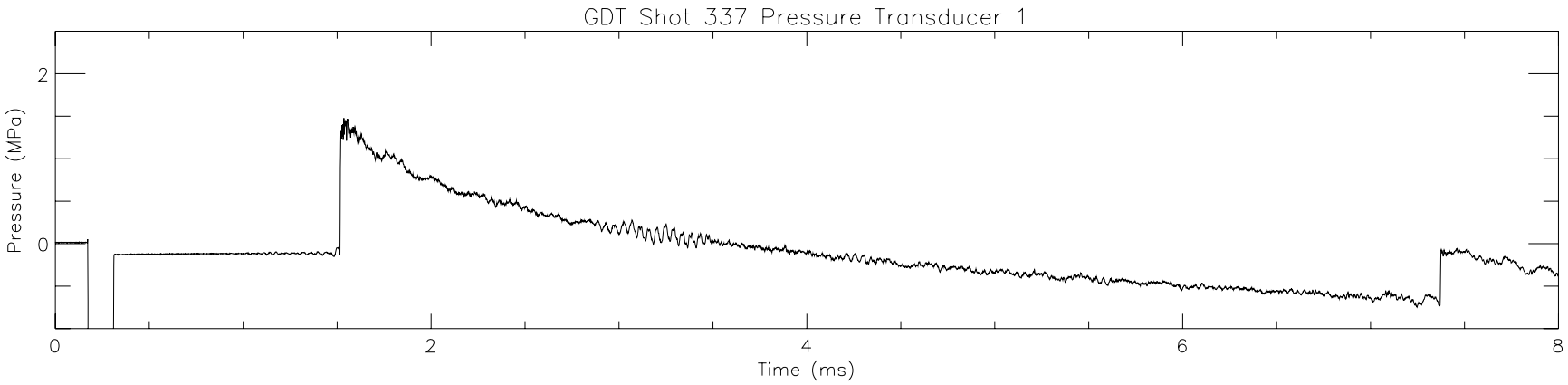
GDT Shot 337 Pressure Transducer 1
Pressure (MPa)
2
0
0
2
4
6
8
Time (ms)

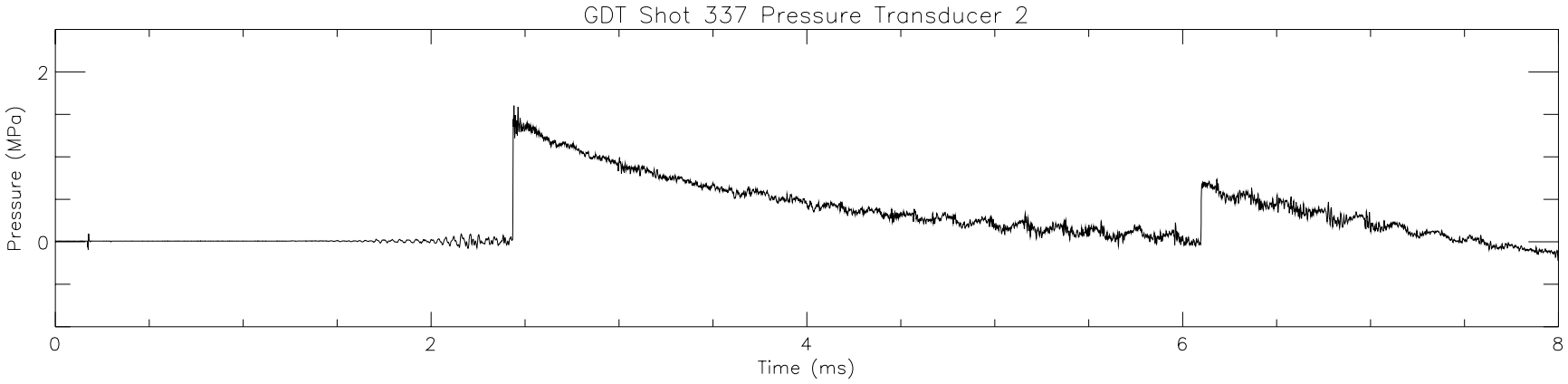
GDT Shot 337 Pressure Transducer 2
Pressure (MPa)
2
0
0
2
4
6
8
Time (ms)

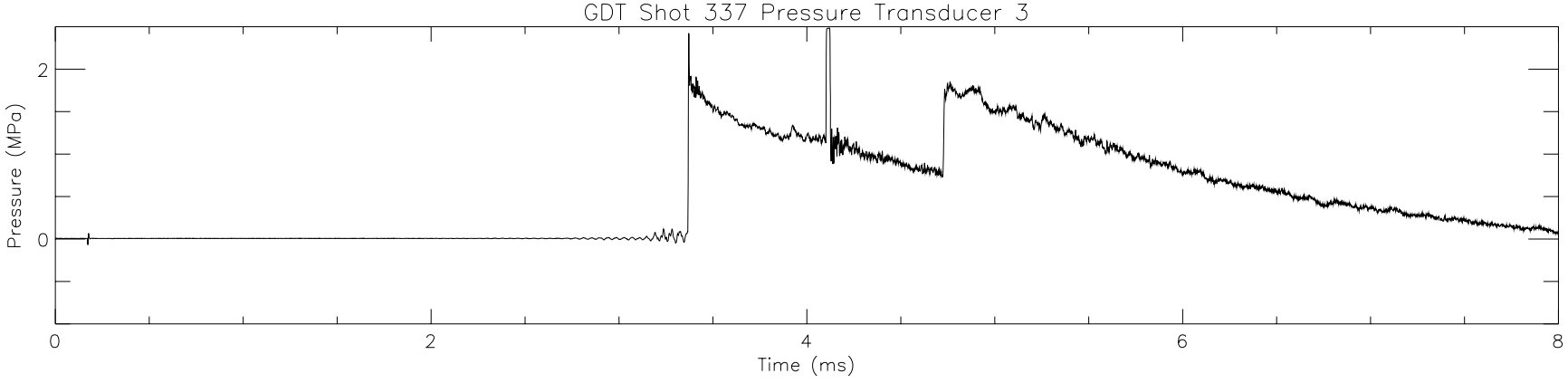
GDT Shot 337 Pressure Transducer 3
Pressure (MPa)
2
0
0
2
4
6
8
Time (ms)

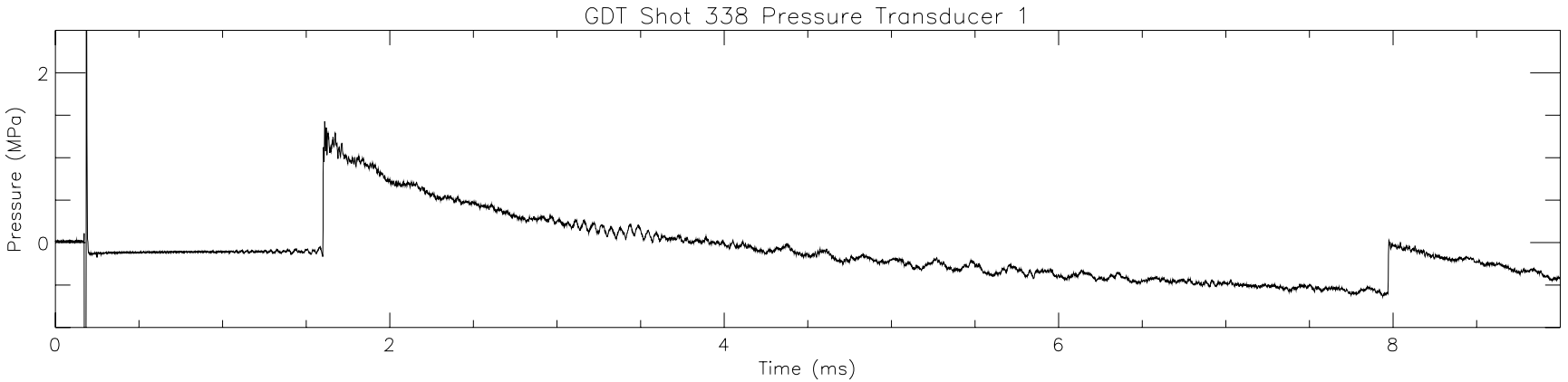
GDT Shot 338 Pressure Transducer 1
Pressure (MPa)
2
0
0
2
4
6
8
Time (ms)

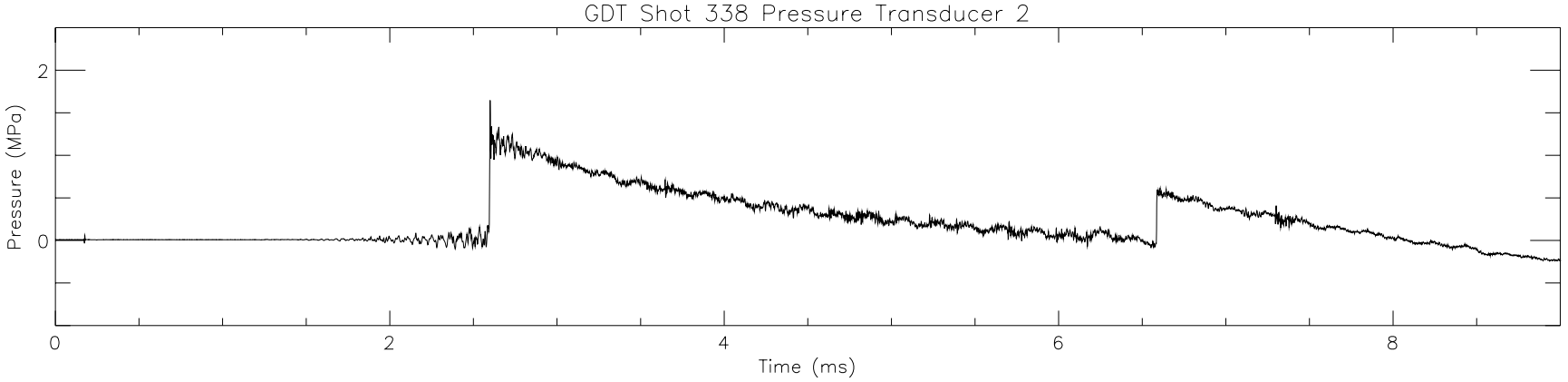
GDT Shot 338 Pressure Transducer 2
Pressure (MPa)
2
0
0
2
4
6
8
Time (ms)

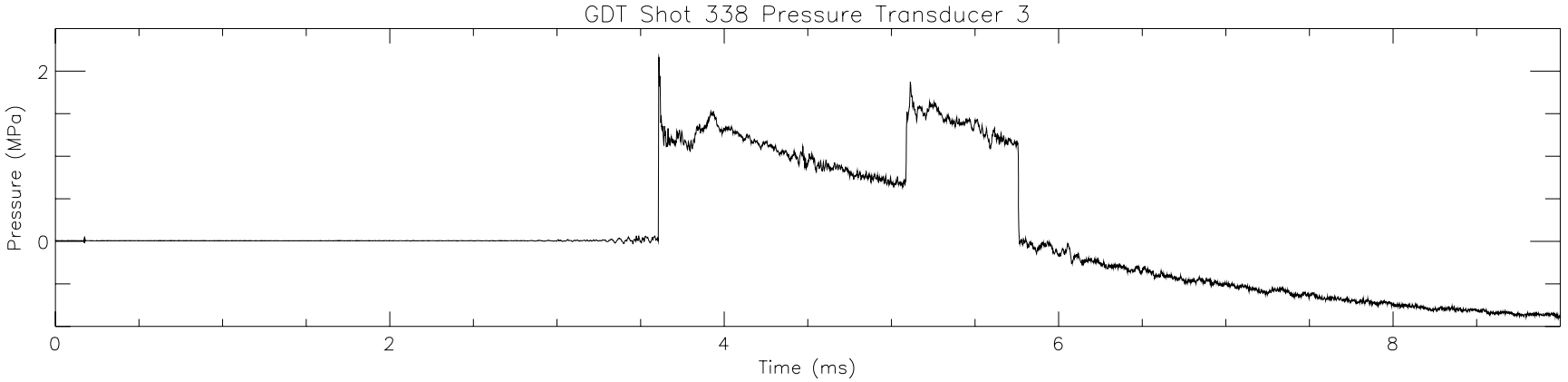
GDT Shot 338 Pressure Transducer 3
Pressure (MPa)
2
0
0
2
4
6
8
Time (ms)

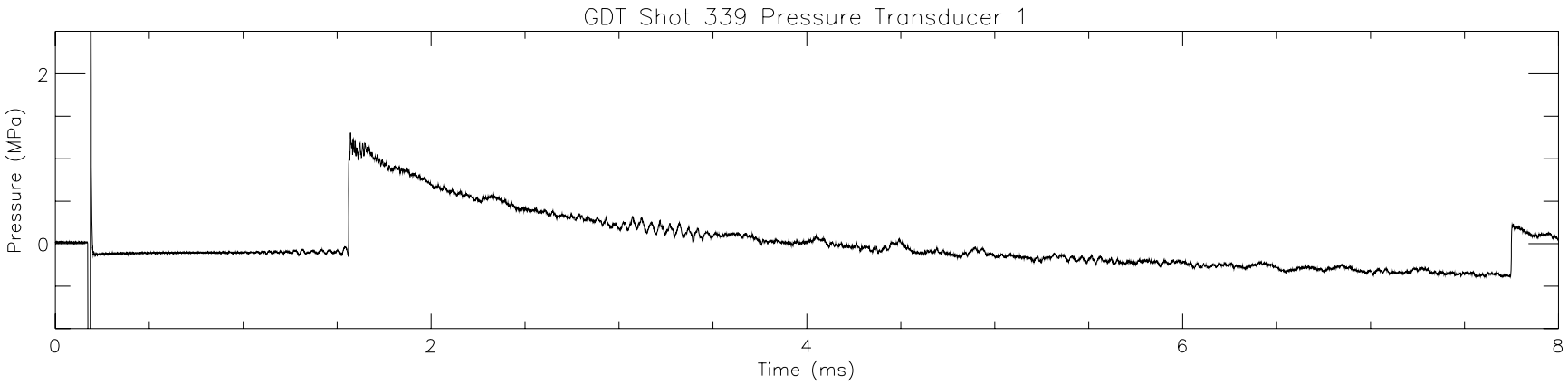
GDT Shot 339 Pressure Transducer 1
Pressure (MPa)
2
0
0
2
4
6
8
Time (ms)

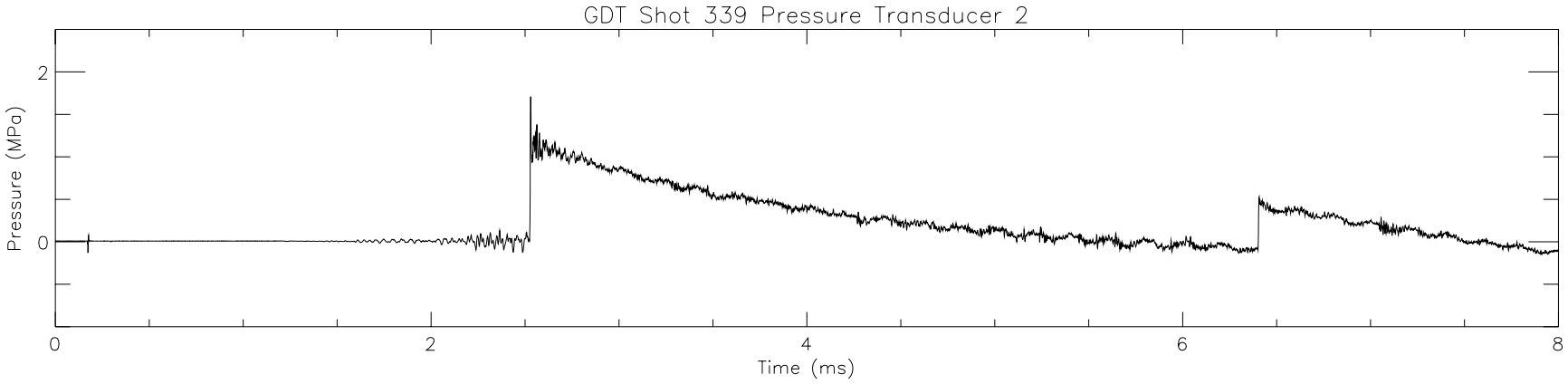
GDT Shot 339 Pressure Transducer 2
Pressure (MPa)
2
0
0
2
4
6
8
Time (ms)

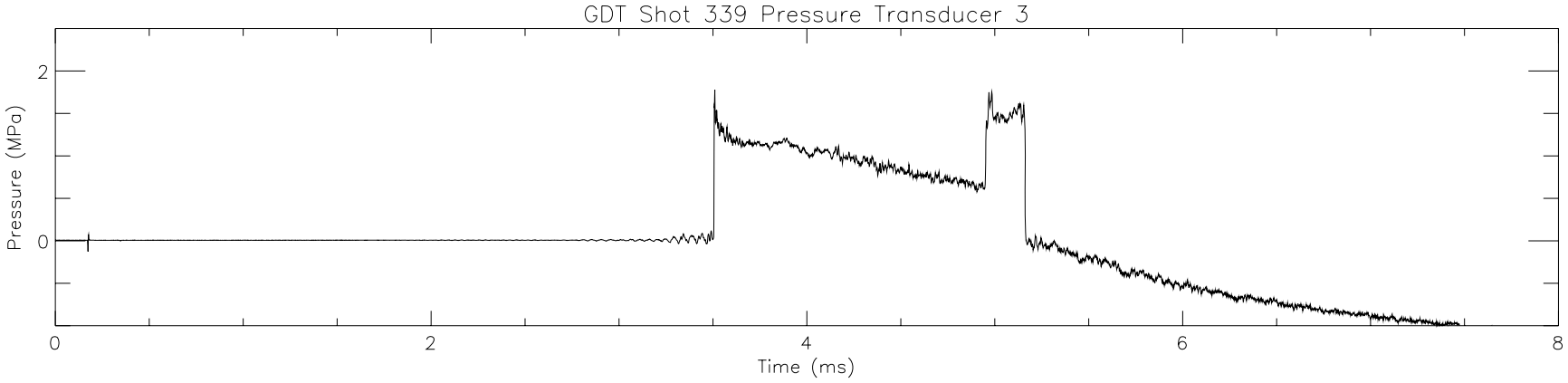
GDT Shot 339 Pressure Transducer 3
Pressure (MPa)
2
0
0
2
4
6
8
Time (ms)

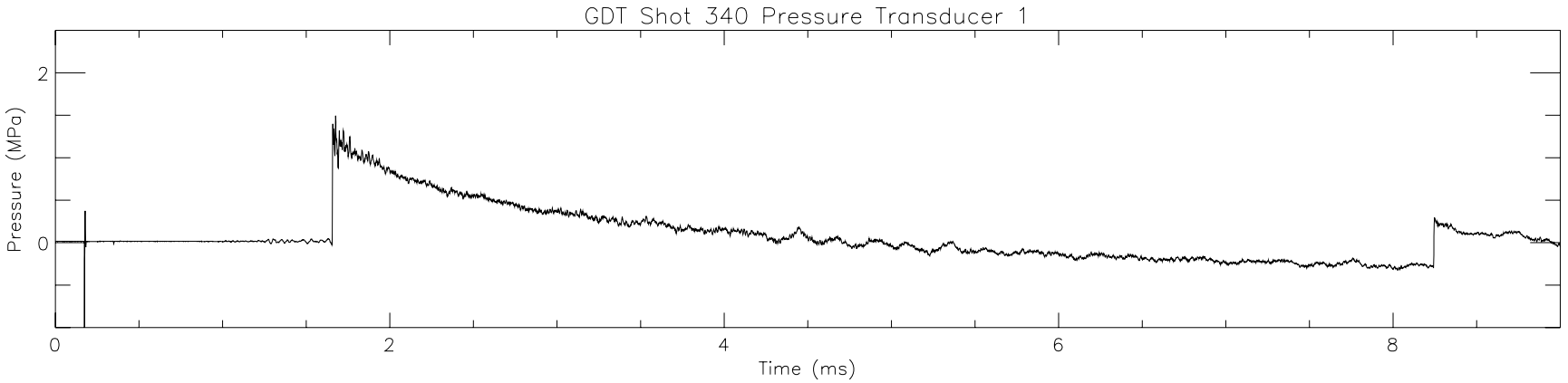
GDT Shot 340 Pressure Transducer 1
Pressure (MPa)
2
0
0
2
4
6
8
Time (ms)

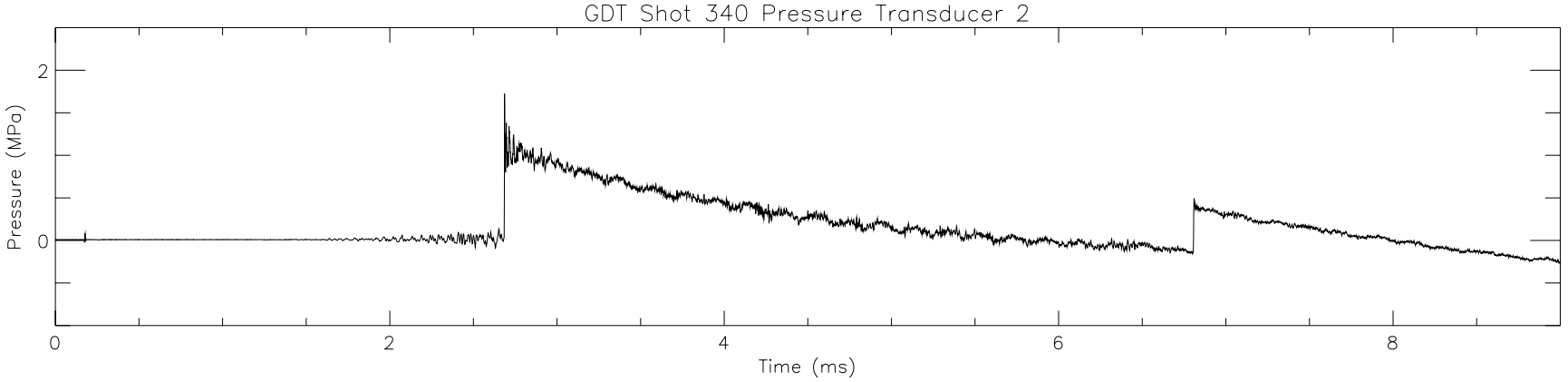
GDT Shot 340 Pressure Transducer 2
Pressure (MPa)
2
0
0
2
4
6
8
Time (ms)

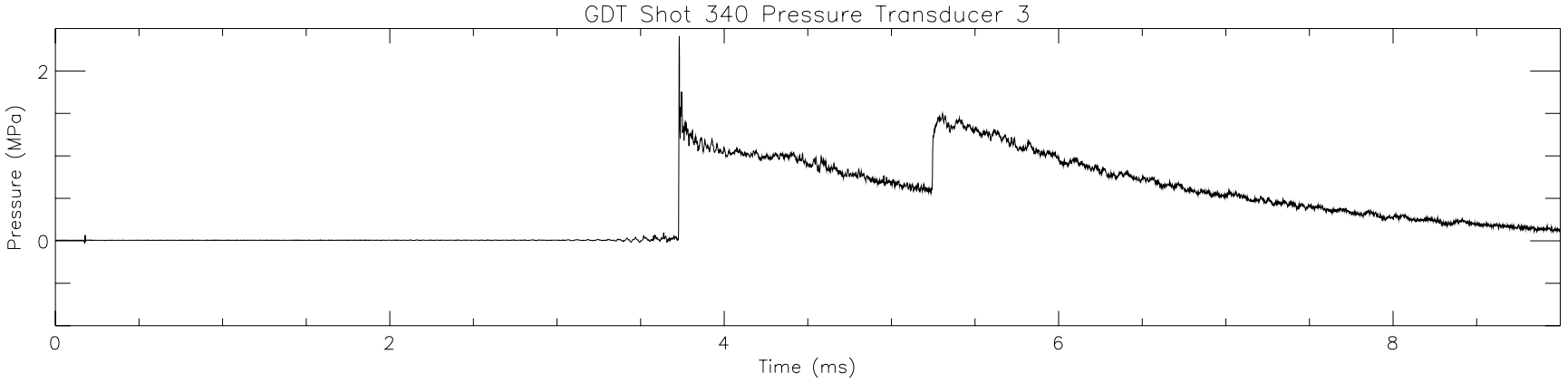
GDT Shot 340 Pressure Transducer 3
Pressure (MPa)
2
0
0
2
4
6
8
Time (ms)

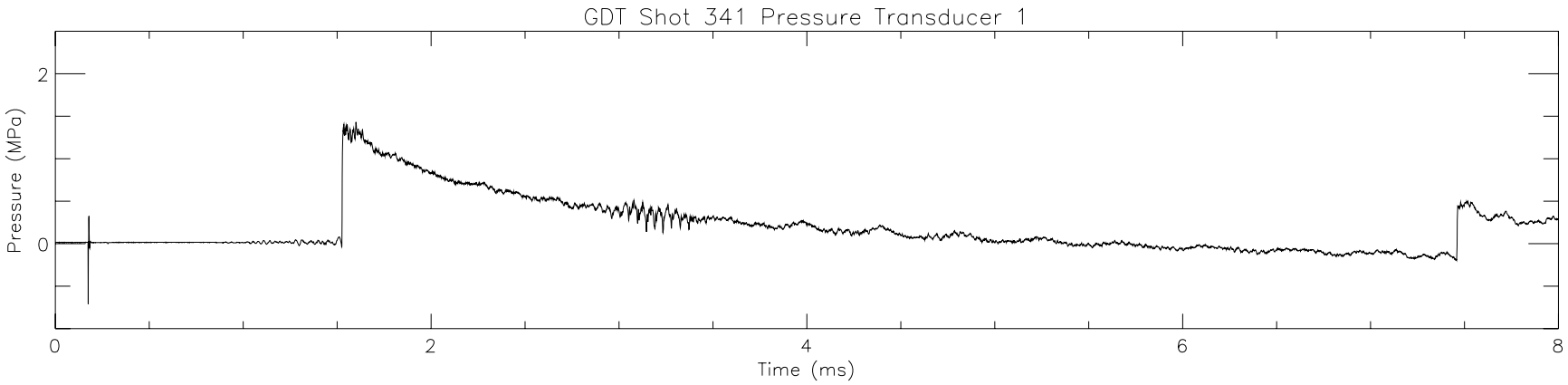
GDT Shot 341 Pressure Transducer 1
Pressure (MPa)
2
0
0
2
4
6
8
Time (ms)

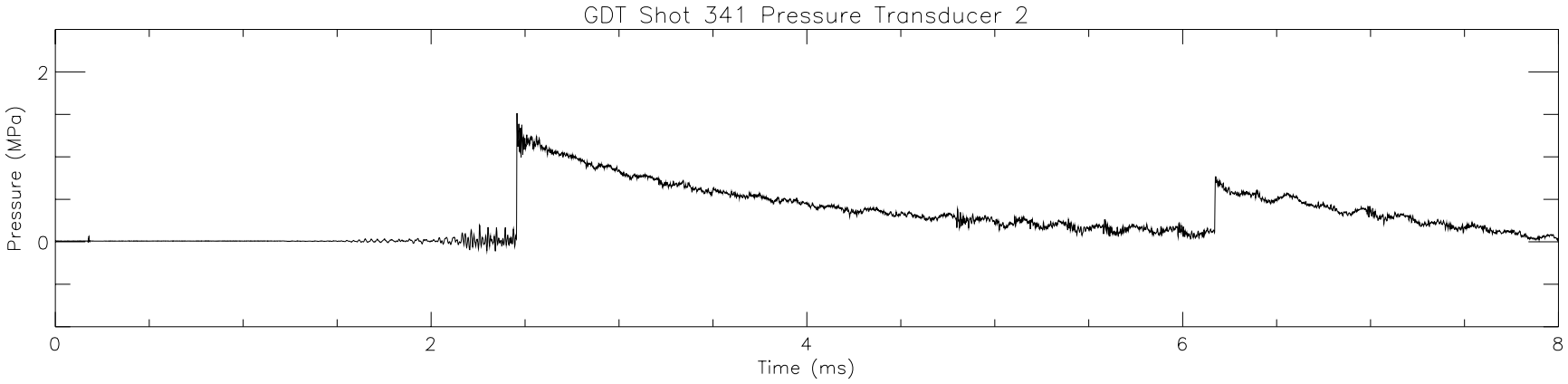
GDT Shot 341 Pressure Transducer 2
Pressure (MPa)
2
0
0
2
4
6
8
Time (ms)

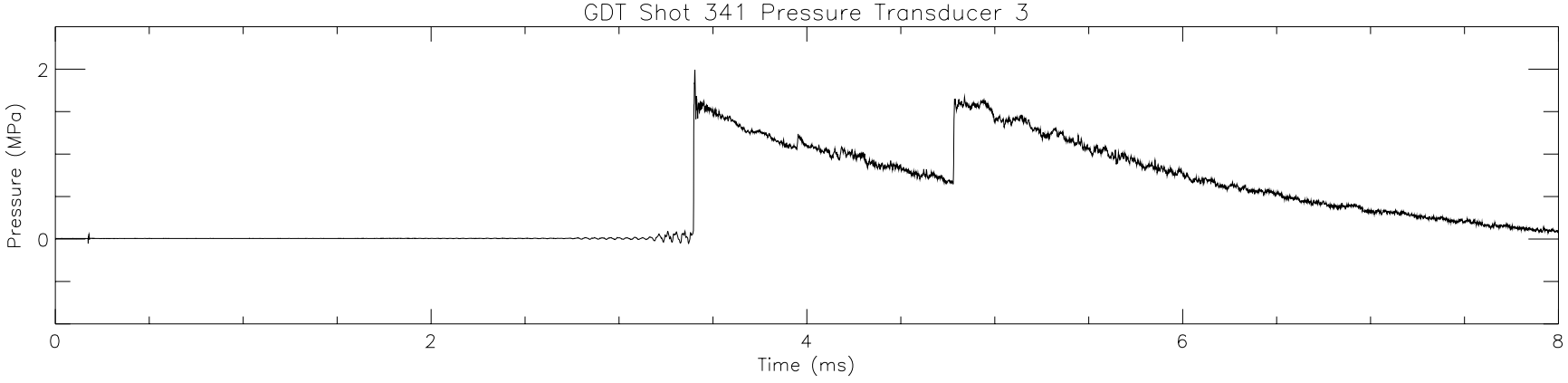
GDT Shot 341 Pressure Transducer 3
Pressure (MPa)
2
0
0
2
4
6
8
Time (ms)

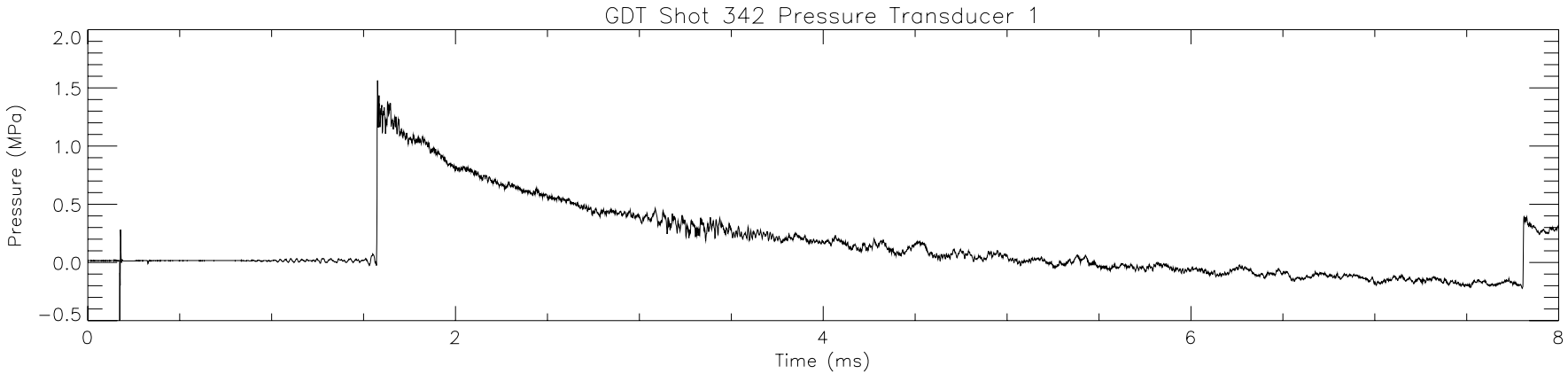
GDT Shot 342 Pressure Transducer 1
Pressure (MPa)
2.0
1.5
1.0
0.5
0.0
−0.5
0
2
4
6
8
Time (ms)

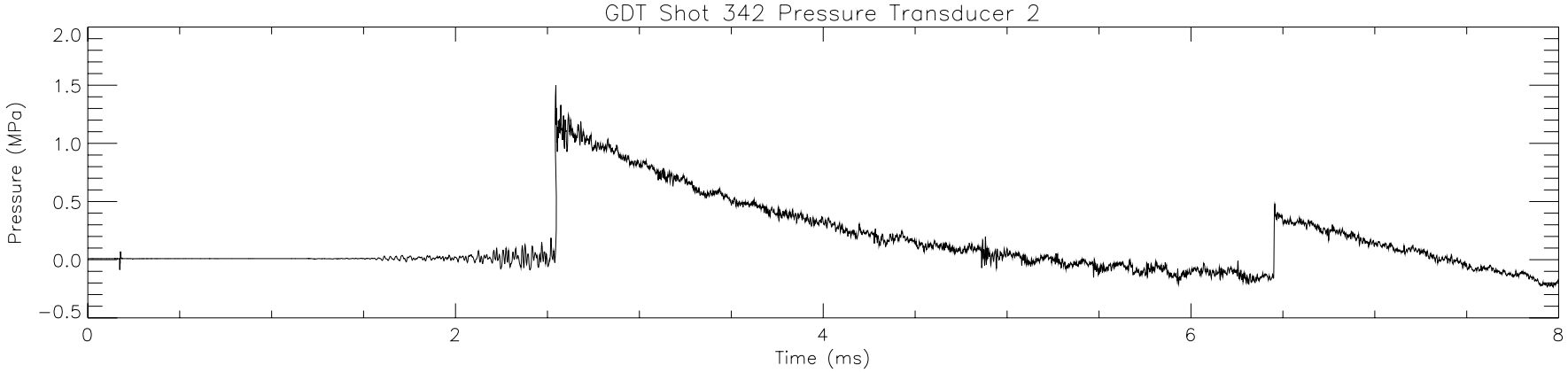
GDT Shot 342 Pressure Transducer 2
Pressure (MPa)
2.0
1.5
1.0
0.5
0.0
−0.5
0
2
4
6
8
Time (ms)

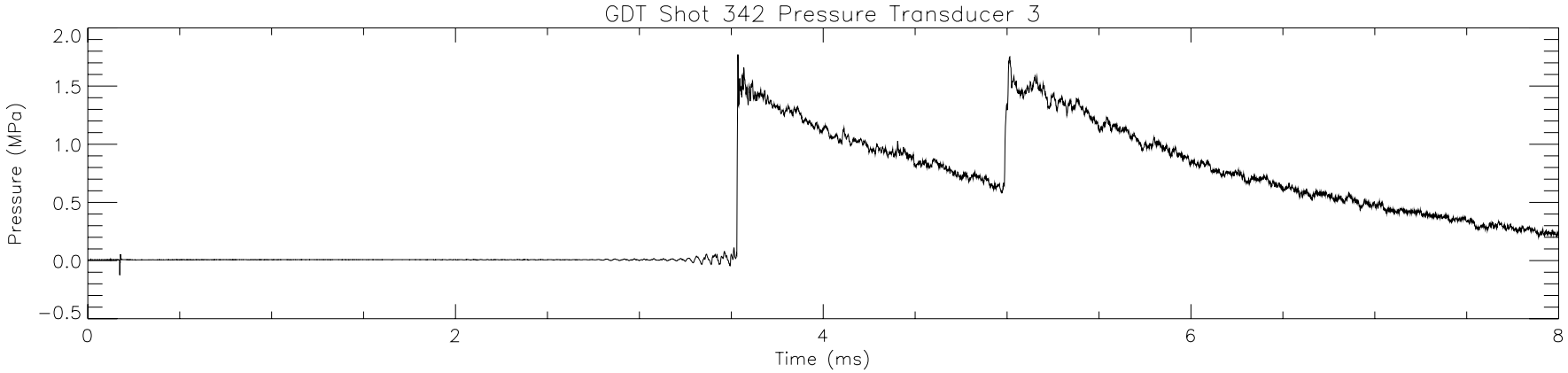
GDT Shot 342 Pressure Transducer 3
Pressure (MPa)
2.0
1.5
1.0
0.5
0.0
−0.5
0
2
4
6
8
Time (ms)